AOP ID and Title:

AOP 470: Deposition of energy leads to vascular remodeling
Short Title: Deposition of energy leads to vascular remodeling

Graphical Representation

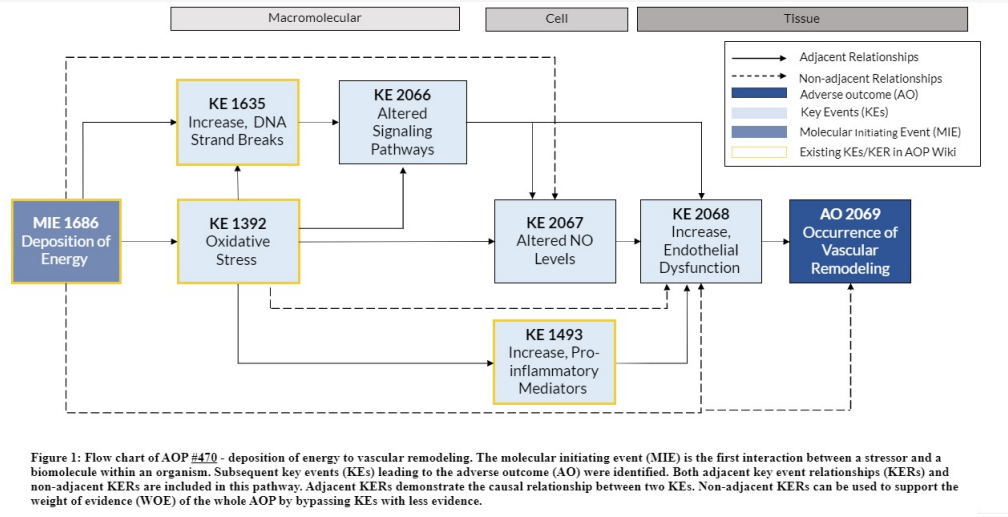

Figure 1: Flow chart of AOP #470 - deposition of energy to vascular remodeling. The molecular initiating event (MIE) is the first interaction between a stressor and a biomolecule within an organism. Subsequent key events (KEs) leading to the adverse outcome (AO) were identified. Both adjacent key event relationships (KERs) and non-adjacent KERs are included in this pathway. Adjacent KERs demonstrate the causal relationship between two KEs. Non-adjacent KERs can be used to support the weight of evidence (WOE) of the whole AOP by bypassing KEs with less evidence.

Authors

Tatiana Kozbenko[1,2], Nadine Adam, Veronica Grybas[1], Benjamin Smith[1], Dalya Alomar[1], Robyn Hocking[1], Janna Abdelaziz[3], Amanda Pace[3], Carole Yauk[2], Ruth Wilkins[1], Vinita Chauhan[1]

(1) Health Canada, Ottawa, Ontario, K1A 0K9, Canada

(2) University of Ottawa, Ottawa, Ontario K1N 6N5, Canada

(3) Carelton University, Ottawa, Ontario K1S 5B6, Canada

Consultants

Marjan Boerma[1], Omid Azimzadeh[2], Steve Blattnig[3], Nobuyuki Hamada[4]

(1) University of Arkansas for Medical Sciences, Little Rock, AR 72205, USA

(2) Federal Office for Radiation Protection (BfS), Section Radiation Biology, 85764 Neuherberg, Germany

(3) NASA Langley Research Center Hampton, VA 23681, USA

(4) Biology and Environmental Chemistry Division, Sustainable System Research Laboratory, Central Research Institute of Electric Power Industry (CRIEPI), Tokyo, Japan

Status

Author status	OECD status	OECD project	SAAOP status
Open for citation & comment			

Abstract

The present qualitative AOP (AOP#470) summarizes the evidence for a progression beginning with the deposition of energy to vascular remodeling. The pathway is initiated by ionization/excitation events from the deposition of energy (MIE: Event #1686) leading to an enviorment of reactive oxygen species (ROS), if this occurs at a rate that outpaces the antioxidant defense system, oxidative stress ensues (KE: Event #1392). Deposition of energy can concurrently induce DNA strand breaks (KE: Event #1635) either directly or through damage from ROS. Excessive ROS damages cellular compartments, thereby altering signaling pathways (KE: Event #2066), and increasing levels of pro-inflammatory mediators (KE: Event #1493). Within the vascular wall, activation of certain signaling molecules can alter nitric oxide (NO) levels (KE: Event #2067). All the upstream KEs of the pathway then converge to cause endothelial dysfunction (KE: Event #2068). Modified levels of NO can alter the blood flow within the endothelium resulting in subsequent compensatory vascular remodeling (AO: Event #2069). Vascular remodeling is an important precursor for many diverse cardiovascular pathologies and serves as an important marker for cardiovascular disease. Vascular remodeling includes

many structural changes such as increased vessel stiffness, vessel wall thickening, and decreased capillary density. Studies informing this AOP include clinical follow-up studies of radiotherapy patients, epidemiological cohort studies of atomic bomb survivors and nuclear plant workers as well as biological studies using mouse and rat models. Knowledge gaps in the weight of evidence include inconsistencies in NO evaluation, and relatively few studies exploring chronic and low dose exposures including the lack of studies focusing on female biology.

Background

Cardiovascular disease (CVD) includes any health condition affecting the heart and blood vessels. CVD is one of the leading causes of death worldwide, accounting for millions of deaths yearly and is surpassed in some countries, by only cancer (Bray et al., 2021; Tsao et al., 2022). This class of diseases includes congenital defects, as well as CVDs that can develop throughout life such as peripheral artery disease, atherosclerosis, coronary artery disease and myocardial infarction. While the progression to a CVD outcome is slow, many CVDs are often preceded by much earlier changes to vascular structure. Vascular remodeling entails various structural changes of existing vasculature arising from cell death, cell migration and changes to the endothelial cell membrane. It is important to note that changes to vascular structure are not inherently detrimental, and the cardiovascular system undergoes continuous adaptation to protect vascular health (Pries et al., 2001; Santamaría et al., 2020; Zakrzewicz et al., 2002). However, certain remodeling can also serve as an important marker and risk factor for future adverse cardiovascular events (Cohn et al., 2004; Van Varik et al., 2012). Changes to vascular structure can be triggered through perturbations such oxidative stress, inflammation, and alterations to cellular signaling pathways. Adverse remodeling of the vasculature encompasses structural and functional changes to vessel wall intima-media, elevated stiffness, and decreased lumen diameter which are all predictive of the development of and mortality and morbidity from CVD (Heald et al., 2006; Hodis et al., 1998; Polak et al., 2011; Zieman et al., 2005).

The risk of CVD increases with several factors such as age and available evidence suggests that environmental factors such as radiation can also contribute to increased risk (Belzile-Dugas & Eisenberg, 2021; Boerma et al., 2016; Francula-Zaninovic & Nola, 2018; Wang et al., 2019). The deposition of energy from radiation is a stochastic event, with adverse effects emerging years or decades after the exposure (Boerma et al., 2016; Dörr, 2015; EPRI, 2020; Menezes et al., 2018). The effects of high-dose radiation on the cardiovascular system have been well-characterized while the effects of low-dose exposure are more contended. However, growing evidence suggests that lower doses than previously thought are linked to cardiovascular outcomes (Boerma et al., 2016; EPRI, 2020; Little et al., 2021; UNSCEAR, 2008). Much of the high-dose data is from follow up studies in radiotherapy patient cohorts who have elevated risk for adverse cardiovascular events (Zou et al., 2019). In addition to clinical exposure scenarios, epidemiological studies of occupational exposures and Japanese atomic bomb survivors provide supporting evidence. Cohort studies of atomic bomb survivors show CVD risk can be modulated by factors such as age at exposure and estimated dose received (Ozasa et al., 2012; Preston et al., 2003; Shimizu et al., 2010; Takahashi et al., 2017). Long-term follow up of individuals exposed in the Chernobyl disaster also identified statistically significant elevation in CVD risk (Ivanov et al., 2006; Kashcheev et al., 2017). Occupational exposure studies have also been conducted in various countries in an effort to understand the relationship between low-dose chronic exposure and cardiovascular health of nuclear workers (Azizova et al., 2018; Gillies et al., 2017; Zielinski et al., 2009). Occupational exposure studies suggest positive associations between received dose and excessive relative risk of circulatory diseases (Zielinski et al., 2009), CVD mortality (Gillies et al., 2017) and occurrence of ischemic and cerebrovascular disease (Azizova et al., 2018).

Beyond earth, space travel presents an additional radiation exposure scenario. With future missions planned beyond low Earth orbit and the protective shield of the magnetosphere, understanding the unique challenges of space radiation is crucial for protection of travelers. In space, radiation is present in the form of high linear energy transfer (LET) particles and high mass, high energy ions (HZE) which indiscriminately impacts the whole body at a low fluence rate (Baker et al., 2011; Durante & Cucinotta, 2008; Norbury et al., 2016). While the present AOP includes an MIE focused on deposition of energy following radiation exposure, it is important to note that the space exposome contains multiple stressors to which space travelers will be exposed simultaneously. Particularly important, in the case of the cardiovascular system, is microgravity. The cardiovascular system is gravity sensitive, with the endothelial layer being responsive to changes in shear stress and blood pressure (Hughson et al., 2018; Maier et al., 2015; Versari et al., 2013). Variation to the pressure gradient throughout the body can also trigger regional adaptations to vascular structure (L. F. Zhang, 2013). While determining a mechanism for an MIE of microgravity has proven challenging, microgravity exposure has been shown to contribute to KEs in the pathway and therefore, evidence from microgravity studies has been included in the weight of evidence (WOE).

Summary of the AOP

Events

Molecular Initiating Events (MIE), Key Events (KE), Adverse Outcomes (AO)

Sequence	Type	Event ID	Title	Short name
	MIE	1686	Deposition of Energy	Energy Deposition
	KE	1392	Oxidative Stress	Oxidative Stress
	KE	1635	Increase, DNA strand breaks	Increase, DNA strand breaks

Sequence	Type	Event ID	Title	Short name
	KE	1493	Increased Pro-inflammatory mediators	Increased pro-inflammatory mediators
	KE	2066	Altered Signaling Pathways	Altered Signaling
	KE	2067	Altered, Nitric Oxide Levels	Altered, Nitric Oxide Levels
	KE	2068	Increase, Endothelial Dysfunction	Increase, Endothelial Dysfunction
	AO	2069	Occurrence, Vascular Remodeling	Occurrence, Vascular Remodeling

Key Event Relationships

Upstream Event	Relationship Type	Downstream Event	Evidence	Quantitative Understanding
Deposition of Energy	adjacent	Oxidative Stress	High	High
Deposition of Energy	adjacent	Increase, DNA strand breaks	High	High
Oxidative Stress	adjacent	Increase, DNA strand breaks	High	Moderate
Increase, DNA strand breaks	adjacent	Altered Signaling Pathways	High	Moderate
Oxidative Stress	adjacent	Altered Signaling Pathways	High	Low
Oxidative Stress	adjacent	Increased Pro-inflammatory mediators	Moderate	Moderate
Altered Signaling Pathways	adjacent	Altered, Nitric Oxide Levels	Moderate	Low
Oxidative Stress	adjacent	Altered, Nitric Oxide Levels	Moderate	Low
Altered Signaling Pathways	adjacent	Increase, Endothelial Dysfunction	Moderate	Low
Increased Pro-inflammatory mediators	adjacent	Increase, Endothelial Dysfunction	Moderate	Low
Increase, Endothelial Dysfunction	adjacent	Occurrence, Vascular Remodeling	Moderate	Low
Altered, Nitric Oxide Levels	adjacent	Increase, Endothelial Dysfunction	Moderate	Low
Deposition of Energy	non-adjacent	Altered, Nitric Oxide Levels	High	Low
Deposition of Energy	non-adjacent	Increase, Endothelial Dysfunction	Moderate	Low
Deposition of Energy	non-adjacent	Occurrence, Vascular Remodeling	High	Low
Oxidative Stress	non-adjacent	Increase, Endothelial Dysfunction	Moderate	Low

Stressors

Name	Evidence
Ionizing Radiation	

Overall Assessment of the AOP

Summary of evidence (KE & KER Relationships and evidence)

The AOP is supported by high biological plausibility and moderate empirical evidence. Research, primarily from laboratory studies, has supported dose- and temporal-concordance for each KER.

Biological Plausibility

Described below is the well-established understanding of the mechanisms underlying this AOP with supporting literature. More detailed examples of the empirical data can be found in the individual entries for each KER.

It is well accepted that when energy is deposited in the cell from ionizing radiation (IR), direct damage to cellular structures can occur (Desouky et al., 2015). When traveling through a cell, IR can induce the radiolysis of water forming reactive oxygen species (ROS). Deposition of energy can also induce feedback loops of ROS production where structures and molecules damaged by ROS including the mitochondria and NADPH oxidase (NOX) further produce ROS (Mittal et al., 2014; Soloviev & Kizub, 2019). Additionally, deposited energy can directly upregulate enzymes involved in ROS and reactive nitrogen species (RNS) (collectively RONS) production (de Jager, Cockrell and Du Plessis, 2017). If reactive nitrogen species RONS production outpaces the

antioxidant defense, a state of oxidative stress occurs (Fletcher et al., 2010; Slezak et al., 2017; Tahimic & Globus, 2017; Wang et al., 2019). Damage to macromolecules can occur due to oxidative stress, including strand breaks to DNA, oxidation of amino acid residues in proteins and peroxidation of lipids (Ping et al., 2020). Lipid peroxidation can induce further damage to cellular structures as a chain reaction is created by the lipid peroxidation radicals, attacking other lipids, proteins and nucleic acids (Ping et al., 2020). Consequently, oxidative stress can directly lead to multiple downstream KEs including altered signaling pathways, increased DNA strand breaks, increased pro-inflammatory mediators and altered nitric oxide (NO) levels.

DNA strand breaks in endothelial cells can be induced either directly through energy deposition or indirectly through oxidative stress. DNA strand breaks can recruit and activate the protein kinases ataxia telangiectasia mutated (ATM) and ATM/RAD3-related (ATR) (Nagane et al., 2021). Downstream signaling pathways involved in cell death and senescence like the p53/p21 pathway can be activated by ATM/ATR. Furthermore, DNA strand breaks induced by radiation directly or through oxidative stress can cause mutations or changes in transcription of proteins in signaling pathways (Ping et al., 2020; Schmidt-Ullrich et al., 2000). Therefore, DNA strand breaks will induce death and senescence of endothelial cells through altered signaling, resulting in endothelial dysfunction.

Oxidative stress can also induce altered signaling pathways. The effects of oxidative stress on signaling pathways occur through protein oxidation of signaling components (Ping et al., 2020; Schmidt-Ullrich et al., 2000; Valerie et al., 2007). Oxidation of cysteine and methionine residues, which are particularly sensitive to oxidation, can result in structural and functional detriments to the protein (Ping et al., 2020). RONS can influence various pathways including the Akt/PI3K/mTOR pathway, where impaired cell survival signaling can induce cellular senescence (Hassan et al., 2013; Ping et al., 2020). Additionally, inhibition of tyrosine phosphatases by ROS can increase the phosphorylation of mitogen-activated protein kinase (MAPK) pathways, resulting in various downstream effects (Schmidt-Ullrich et al., 2000; Valerie et al., 2007). A phosphorylated p53 induced by oxidative DNA damage can also activate MAPK signaling and initiates a cascade ending in apoptosis (Ashcroft et al., 1999; Gen, 2004). Through affecting cell signaling pathways, damage caused by elevated RONS affects cells beyond those that have been directly irradiated (Ramadan et al., 2021).

Excessive RONS produced by IR disrupt cellular balance and can increase pro-inflammatory mediators (Lumniczky et al., 2021; Schaue et al., 2015). Similar to activation of the immune system by damage from a pathogen, activation by oxidative stress promotes many repair mechanisms, some of which involve rapid release of pro-inflammatory cytokines (Stanojković et al., 2020). The cytokines released vary based on tissue type and radiation parameters (Di Maggio et al., 2015), but tumor necrosis factor (TNF)-α and interleukin (IL)-1 can trigger a cytokine cascade that initiates an inflammatory response (Slezak et al., 2017; Srinivasan et al., 2017). A prolonged state of inflammation in endothelial cells can lead to endothelial dysfunction (Baran et al., 2021).

Both oxidative stress and altered signaling can directly result in altered NO levels. NO is synthesized from L-arginine by the three nitric oxide synthase (NOS) enzymes, endothelial NOS (eNOS), inducible NOS (iNOS) and neuronal NOS (nNOS). ROS can directly reduce NO levels by reacting with NO to produce the RNS peroxynitrite (Deanfield et al., 2007). Furthermore, the cofactor of NOS enzymes, tetrahydrobiopterin (BH4), can be oxidized by RONS leading to inhibition of NOS dimerization, also called NOS uncoupling (Deanfield et al., 2007). Uncoupled NOS will produce superoxide instead of NO, leading to a positive feedback loop of ROS production and reduced NO (Förstermann, 2010; Förstermann & Münzel, 2006; Mitchell et al., 2019; Nagane et al., 2021; Soloviev & Kizub, 2019).

Modulation of NO through altered signaling pathways occurs through changing the activity of NOS enzymes. Phosphorylation of eNOS at Ser1177 will activate the enzyme while phosphorylation at Thr495 inhibits it (Förstermann, 2010; Nagane et al., 2021). Protein kinase B (Akt), part of the phosphoinositide 3-kinase (PI3K)/Akt pathway, can activate eNOS through phosphorylation at Ser1177 to increase NO production (Karar & Maity, 2011). In contrast, activation of the RhoA/Rho kinase (ROCK) pathway will inhibit NO production by destabilizing eNOS mRNA and preventing Ser1177 phosphorylation by Akt (Yao et al., 2010). Angiotensin II (AngII), the end product of the renin-angiotensin-aldosterone system (RAAS), is involved in both downregulating Ser1177 phosphorylation to prevent NO creation (Ding et al., 2020) and activating eNOS as a corrective measure (Millatt et al., 1999). Alterations to these pathways due to IR will result in changes in NO levels.

Each of the components of the pathway described above converge at endothelial dysfunction. Endothelial cells lining the blood vessels throughout the body are an important component for maintaining vascular homeostasis (Bonetti et al., 2003; Deanfield et al., 2007). Endothelial cells are quiescent with high levels of NO most of the time (Carmeliet & Jain, 2011). Endothelial dysfunction can occur due to prolonged activation of the endothelium, characterized by the prolonged lack of bioavailable NO, lack of endothelium-dependent vasodilation and chronic pro-thrombotic and inflammatory state (Baran et al., 2021; Bonetti et al., 2003; Deanfield et al., 2007; Krüger-Genge et al., 2019). A prolonged reduction in NO will decrease vasodilation, increase leukocyte adhesion and increase fibrous plaque formation contributing to the pro-thrombotic dysfunctional environment (Schiffrin, 2008; Senoner & Dichtl, 2019; Venkatesulu et al., 2018). Furthermore, signaling in pathways like p53/p21 or PI3K/Akt/mammalian target of rapamycin (mTOR) can induce apoptosis or premature senescence of endothelial cells as part of endothelial dysfunction due to DNA damage or oxidative stress (Borghini et al., 2013; Hughson et al., 2018; Schiffrin, 2008; Senoner & Dichtl, 2019; Soloviev & Kizub, 2019). Senescent cells have decreased levels of NO production and a pro-inflammatory secretory phenotype, which feed back to further promote endothelial dysfunction (Ungvari et al., 2013; Wang et al., 2016).

Endothelial dysfunction subsequently leads to vascular remodeling, which encompasses multiple structural changes to the vasculature. Chronic inflammation combined with impaired healing and lack of endothelium-dependent vasodilation during endothelial dysfunction increases vulnerability to damage from non-laminar flow and maladaptive repair (Sylvester et al., 2018). As compensation, vessel walls can thicken and atherosclerotic risk can increase (Hughson et al., 2018; Slezak et al., 2017; Sylvester et al., 2018). In cases of maladaptive repair of vessels, vascular remodeling can be exhibited through an increase in fibrosis (Hsu et al., 2019). The pro-thrombotic environment with increased lymphocyte adhesion induced by endothelial cell senescence can

increase the likelihood of vessel occlusion, decreasing vascular density such that the corresponding increase in vascular resistance will induce remodeling as a compensatory measure (Slezak et al., 2017). Thus, increased leukocyte adhesion during endothelial dysfunction occurs early in the development of atherosclerosis (Senoner & Dichtl, 2019). Increased arterial stiffness can also occur in response to endothelial dysfunction (Boerma et al., 2015, 2016; Patel et al., 2020), with increased collagen and smooth muscle content paired with decreased elastin and degradation of the extracellular matrix (Zieman et al., 2005). The changes to the vascular structure in response to the deposition of energy are similar to a form of accelerated age-related atherosclerosis (Boerma et al., 2016; Sylvester et al., 2018; Vernice et al., 2020).

Temporal, Dose, and Incidence Concordance

Evidence for time, dose, and incidence concordance in this AOP is moderate. It has been repeatedly shown using many study designs and systems that deposition of energy occurs immediately following irradiation, and downstream events occur at a later timepoint. Endpoints indicating oxidative stress have been observed within minutes following irradiation (Wortel et al., 2019). Studies show that oxidative stress, increased DNA strand breaks, increased pro-inflammatory mediators, and altered signaling may occur over a similar time period; however, alteration in signaling pathways, increased DNA strand breaks, and increased pro-inflammatory mediators can be observed following oxidative stress (Ramadan et al., 2020; Baselet et al., 2017; Sakata et al., 2015; Yang et al., 1998). Increases in NO levels occur in hours to weeks after irradiation (Azimzadeh et al., 2017; Sonveaux et al., 2003; Sakata et al., 2015). Then, from weeks to months following irradiation both endothelial dysfunction and vascular remodeling occur, though concordance between these events is difficult to determine, possibly due to inter-study differences in experimental design and markers (Yentrepalli et al., 2017; Soucy et al., 2007; Yu et al., 2011; Shen et al., 2018).

Overall, the majority of studies demonstrate that upstream KEs occur at the same or lower doses and earlier or the same time as downstream KEs. For example, endothelial cells show a dose-dependent increase in oxidative stress to X-ray irradiation at 0.1 and 5 Gy, while 0.1 Gy induced few changes in pro-inflammatory mediators with significant increases only observed at 5 Gy (Ramadan et al., 2020). Some studies also show that the upstream and downstream KEs can be observed at the same doses of radiation. For example, X-ray irradiation of mice resulted in oxidative stress, altered signaling and reduced NO levels at both 8 and 16 Gy (Azimzadeh et al., 2015). Dose concordance is not consistent across studies, but this may be due to differences in models, timepoints, and radiation types used.

A limited number of studies support incidence concordance. In these, the upstream KE demonstrates a greater change than the downstream KE following exposure to a stressor. For example, mice exposed to 18 Gy of X-rays showed a roughly 2-fold increases in both oxidative stress and pro-inflammatory markers. A 1.3-fold increase in markers for endothelial dysfunction was observed (Shen et al., 2018).

Uncertainties and inconsistencies

The collection of WOE identifies several important uncertainties in the literature. These include lack of quantitative understanding, low-dose or chronic-exposure studies, data from female models and consistency in measurement of NO levels.

The WOE contained data from a wide variety of interdisciplinary fields; consequently, experimental design was equally varied. Overall, studies did not use consistent doses, radiation types, time-points, or evaluation of endpoints. Since dose and type of radiation can affect biological responses, quantitative understanding of relationships could not be determined and was low overall. Additionally, most studies used single or select doses, with limited studies exploring relatively low doses (<0.5 Gy (EPRI, 2020)). Harmonized experiments evaluating changes to adjacent endpoints across a wide range of doses or time-points with consistency of radiation type would greatly benefit quantitative understanding for this AOP.

Similarly, the WOE is lacking in evidence using female models. Sex is an important modulating factor in cardiovascular changes and studies suggest vascular remodeling responses of astronauts can vary by sex (Hughson et al., 2016). The consequence of the general bias in clinical research (Rios et al., 2020; Yakerson, 2019) from which the current WOE draws, is the very large knowledge gaps in mechanistic data for the female body. Filling these knowledge gaps at all levels of biological organization will be an important step in solidifying the AOP.

Evaluation of NO levels was inconsistent between studies. According to the biological plausibility, deposition of energy and subsequent oxidative stress would lead to a decrease in NO that then contributes to impaired vascular relaxation as part of endothelial dysfunction. However, primary research concludes that NO can either increase (Abdel-Magied & Shedid, 2020; Hirakawa et al., 2002; Sakata et al., 2015; Sonveaux et al., 2003) or decrease (Baker et al., 2009; Fuji et al., 2016) following irradiation. Proxy measures used to detect NO, like NOS enzyme activities or nitrite/nitrate levels, may not directly correspond to changes in NO levels. Further standardization in NO measurement and interpretation could refine this KE to become the depletion of NO.

Domain of Applicability

Life Stage Applicability

Life Stage	Evidence
All life stages	High

Taxonomic Applicability

Term	Scientific Term	Evidence	Links

Term	Scientific Term	Evidence	Links
human	Homo sapiens	High	NCBI
rat	Rattus norvegicus	High	NCBI
mouse	Mus musculus	High	NCBI
rabbit	Oryctolagus cuniculus	Low	NCBI

Sex Applicability

Sex	Evidence
Unspecific	High

The empirical evidence supports that this AOP is relevant to human (Hong et al., 2013; Siamwala et al., 2010; Jiang et al., 2020; Lee, et al., 2020; Ramadan et al., 2020), rat (Hatoum et al., 2006; Soucy et al., 2010; Hong et al., 2013; Abdel-Magied & Shedid, 2019: Hasan et al., 2020), mouse (Yu et al., 2011; Coleman et al., 2015; Sofronova et al., 2015; Shen et al., 2018; Hamada et al., 2020), and rabbit (Soloviev et al., 2003, Hong et al., 2013) models. Biological plausibility suggests that events in this AOP are not sex specific; however, more studies used male models. Similarly, while biological plausibility suggests the pathway is not age-specific, most studies used adult models.

Essentiality of the Key Events

The essentiality of the MIE to a downstream KE is supported by a non-irradiated control. The comparison of irradiated and non-irradiated groups has shown that the effects of downstream events are enhanced or accelerated by the deposition of energy.

The essentiality of other KEs can be determined by the impact of the manipulation of the upstream KE on the resulting downstream effects. For example, the essentiality of oxidative stress is frequently assessed through antioxidant treatments, which can decrease oxidative stress markers through decreased ROS production or strengthened antioxidant defense activity. SOD administration decreased free radicals, superoxide and peroxide, and improved endothelium-dependent vasodilation, a downstream KE, which had been previously decreased due to radiation exposure (Hatoum et al., 2006). Additionally, oxypurinol treatment inhibited xanthine oxidase (XO) enzyme, which limited the enzyme's contribution to cardiac ROS and improved endothelium-dependent vasodilation and the recovery of vascular stiffness to control levels (Soucy et al., 2007, 2010, 2011).

The essentiality of DNA strand breaks was not assessed often. One study used mesenchymal stem cell conditioned media (MSC-CM) to reduce the level of ROS-mediated DNA double-stranded breaks and found decreases in signaling molecules including p53, Bax and cleaved caspase 3 (Huang et al., 2021).

The essentiality for altered signaling pathways KE was evaluated by studies using pathway inhibitors or conditioned media. Signaling pathways were shown to be suppressed by inhibitors such as ROCK inhibitor Y27632 and acid sphingomyelinase (ASM) inhibitor desipramine (dpm), which have demonstrated decreased apoptosis and recovered endothelium-dependent vasodilation (Soloviev & Kizub, 2019; Venkatesulu et al., 2018; Wang et al., 2016). Incubation of endothelial cells in MSC-CM was shown to increase cell signaling components, Akt and p-Akt, and decrease apoptosis (Chang et al., 2017). PI3K inhibitors, such as LY294002 and wortmannin, and angiotensin-converting enzyme inhibitor bradykinin-potentiating factor (BPF) were studied for their impact on NO levels. The increase in p-Akt and subsequently eNOS, p-eNOS and NO levels were reversed following PI3K inhibition (Shi et al., 2012; Siamwala et al., 2010). AngII and iNOS levels were returned to control following BPF treatment of irradiated groups (Hasan et al., 2020). Further studies are required for a better understanding of the changes in NO levels and endothelial dysfunction due to altered signaling pathways. Overall, the flexibility of signaling pathways makes it difficult to assess essentiality.

The essentiality for pro-inflammatory mediators was assessed by studies that suppress their expression. The decrease in pro-inflammatory mediators was observed following the use of TAT-Gap19 to block connexin43 hemichannels. This decrease was associated with a decrease in radiation-induced endothelial cell senescence (Ramadan et al., 2020). Additionally, MSC-CM incubation resulted in decreased pro-inflammatory cytokines, IL-1α, IL-6 and TNF-α and decreased endothelial apoptosis (Chang et al., 2017).

Changes in vascular remodeling were evaluated through vascular structure, among other endpoints. Following hindlimb unloading, ASM inhibition in the small mesenteric artery was found to reverse the changes in apoptosis and intima-media thickness (IMT) (Su et al., 2020). Comparisons between irradiated and sham or non-irradiated control groups of various studies using animal and human models have demonstrated differences in vascular structures (Hamada et al., 2020, 2021; Sárközy et al., 2019; Shen et al., 2018; Sridharan et al., 2020; Yu et al., 2011).

Essentiality of the key events

	Defining Question	High	Moderate	Low
Support for Essentiality of KEs	Are downstream KEs and/or the AO prevented if an upstream KE is blocked?	Direct evidence from specifically designed experimental studies illustrating essentiality for at least one of the important KEs	Indirect evidence that sufficient modification of an expected modulating factor attenuates or augments a KE	No or contradictory experimental evidence of the essentiality of any of the KEs
MIE: KE #1689 Deposition	Evidence for Essentiality of KE: High This event is difficult to test for essentiality as deposition of energy is a physical stressor and cannot be			

of energy	blocked/decreased using chemicals. However, studies show that control or sham-irradiated groups do not show the occurrence of downstream KEs.
KE #1392 Oxidative stress	Evidence for Essentiality of KE: High Essentiality was well supported within the literature. Antioxidant treatments led to recovery of antioxidant enzyme activity, decreases in DNA strand breaks, and decreases in pro-inflammatory mediators, while ZNO-NP also restored NO levels. Oxypurinol (Oxp) treatment was found to aid in the acetylcholine (ACh) vasodilation response and restore NO levels as it decreased xanthine oxidase (XO) activity and reactive oxygen species (ROS).
KE #1635 Increase, DNA strand breaks	Evidence for Essentiality of KE: Low Few studies use countermeasures to reduce the number of DNA strand breaks in cells. A few studies show that reducing DNA strand breaks induced by radiation restores signaling pathways and reduces endothelial dysfunction.
KE #1493 Increase, pro-inflammatory mediators	Evidence for Essentiality of KE: Low Essentiality of this event can be determined with countermeasures that limit the increase of pro-inflammatory mediators. Limited research does show essentiality, evidenced by a decrease in apoptosis of endothelial cells following treatment with MSC-CM, which contains angiogenic cytokines that have therapeutic potential for microvascular injury, and a decrease in endothelial cell senescence following treatment with TAT-Gap19, a connexin hemichannel blocker.
KE #2066 Altered signaling pathways	Evidence for Essentiality of KE: Moderate Essentiality of this relationship can be determined with the use of signaling molecule inhibitors. Signaling molecule inhibitors reduced downstream changes in eNOS, NO, p-Akt, angiotensin II (AngII) and aldosterone following stressors such as irradiation and altered gravity. Inhibitors also prevented impaired contractile response and decreased apoptosis in the arterial endothelium.
KE #2067 Altered, NO levels	Evidence for Essentiality of KE: Moderate The evidence for essentiality of this KE can be determined by using countermeasures that limit changes in NO levels, such as Oxp, L-NA (NOS inhibitor), AG (iNOS inhibitor), DAHP (Gch1 inhibitor) and losartan (AT1 receptor antagonist). Use of these countermeasures reduced NOS levels and decreased the ratio of couple-to-uncoupled eNOS. Endothelial relaxation increased after Oxp and losartan treatment after microgravity exposure, while relaxation decreased in the presence of DAHP, L-NA and AG. When treated with these countermeasures following radiation or microgravity, changes to NO were limited or restored and as a result, endothelial dysfunction was limited.
KE #2068 Increase, endothelial dysfunction	Evidence for Essentiality of KE: Moderate The essentiality of endothelial dysfunction leading to vascular remodeling is moderately supported within literature. Oxp treatment, an XO inhibitor, restored vasodilator response and reduced vascular stiffness following irradiation. Both dpm and DOX decreased apoptosis and reduced Caspase-3 protein expression. Ceramide treatment following microgravity was found to return proliferation to control levels and increase apoptosis.

Weight of Evidence Summary

	Defining Question	High	Moderate	Low
Review of Biological Plausibility for the KER	Is there a mechanistic (structural or functional) relationship between the upstream KE and downstream KE consistent with established biological knowledge	The relationship is well understood based on extensive previous documentation and has an established mechanistic basis and broad acceptance	The KER is plausible based on an analogy to accepted biological relationships but scientific understanding is not completely established	There is empirical support for a statistical association between KEs but structural or functional relationship between them is not understood
Deposition of energy (MIE: KE #1686) leads to oxidative stress (KE #1392)	Evidence for Biological Plausibility of KER: High Deposition of energy onto the water and biological components of a cell creates ROS, and as ROS production outpaces the cell's antioxidant defense system, oxidative stress is induced. Both ROS production and subsequent oxidative stress have been extensively studied and the mechanisms are well described in numerous review articles across many biological systems.			
Deposition of energy (MIE: KE #1686) leads to increase, DNA strand breaks (KE #1635)	Evidence for Biological Plausibility of KER: High The deposition of energy onto the DNA molecule will directly cause single- or double-strand breaks in the DNA. Deposited energy can induce chemical modifications to the phosphodiester backbone of both strands of the DNA, possibly resulting in breaks in one or both strands.			
Oxidative stress	Evidence for Biological Plausibility of KER: High			

(KE #1392) leads to increase, DNA strand breaks (KE #1635)	Evidence for Biological Plausibility of KER: High Increased ROS during oxidative stress can result in the oxidation of bases on the DNA strand, triggering base excision repair, which removes the oxidized bases. When multiple bases in close proximity are removed, the repair efforts cause strain which can lead to strand breaks.
Increase, DNA strand breaks (KE #1635) leads to altered signaling pathways (KE #2066)	Evidence for Biological Plausibility of KER: High Strand breaks induce the recruitment of the kinases ataxia-telangiectasia mutated (ATM) and ATM/RAD3-related (ATR). ATM and ATR can subsequently phosphorylate multiple downstream signaling molecules. High levels of DNA strand breaks can increase the recruitment of ATM and ATR, leading to greater activation of pathways like the p53/p21 pathway and subsequently greater downstream effects.
Oxidative stress (KE #1392) leads to increase, pro-inflammatory mediators (KE #1493)	Evidence for Biological Plausibility of KER: High Excess ROS during oxidative stress damages cellular structures and thus activates the immune system and repair mechanisms, many of which involve release of pro-inflammatory mediators. Cells involved with host-defense can themselves also produce ROS, further exacerbating the state of oxidative stress. The biological plausibility of the linkage between oxidative stress and increases in pro-inflammatory mediators is highly supported in literature.
Oxidative stress (KE #1392) leads to altered signaling pathways (KE #2066)	Evidence for Biological Plausibility of KER: High Oxidative stress can alter signaling pathways both directly and indirectly. Directly, oxidative stress conditions can lead to oxidation of amino acid residues. This can cause conformational changes, protein expansion, and protein degradation, leading to changes in the activity and level of signaling proteins. Oxidation of key functional amino acids can also alter the activity of signaling proteins, resulting in downstream alterations in signaling pathways. Indirectly, oxidative stress can damage DNA causing changes in the expression of signaling proteins as well as the activation of DNA damage response signaling. The mechanisms of this relationship are widely accepted.
Oxidative stress (KE #1392) leads to increase, endothelial dysfunction (KE #2068)	Evidence for Biological Plausibility of KER: High ROS can interact with NO, taking a vasodilator crucial for endothelial function and turning it into peroxynitrite, a RNS that further contributes to oxidative stress. Furthermore, cellular senescence, inhibition of vasodilation, induced inflammatory environments and cellular apoptosis are all part of endothelial dysfunction that can be indirectly caused by oxidative stress.
Increase, pro-inflammatory mediators (KE #1493) leads to increase, endothelial dysfunction (KE #2068)	Evidence for Biological Plausibility of KER: High Inflammation provides a protective effect to the endothelium but prolonged or repeated exposure to a stressor can exhaust this, leading to senescence or apoptosis in endothelial cells and subsequent leading to endothelial dysfunction. This endothelial dysfunction can also manifest as a dysregulation of vasodilation. Prolonged inflammation is a widely accepted component in the development of endothelial dysfunction.
Altered signaling pathways (KE #2066) leads to increase, endothelial dysfunction (KE #2068)	Evidence for Biological Plausibility of KER: High Signaling pathways including the PI3K/Akt/mTOR, RhoA-Rho-kinase, ASM/cer pathway, and the p53-p21 pathway have downstream effects on endothelial apoptosis, premature endothelial cell senescence and cytoskeletal proteins to impair contraction, indicators of endothelial dysfunction.
Increase, endothelial dysfunction (KE #2068) leads to occurrence, vascular remodeling (AO: KE #2069)	Evidence for Biological Plausibility of KER: High Key components of endothelial dysfunction include deficiency in bioavailable NO, impaired vasodilation, inflamed endothelium and prothrombotic environment. These events can ultimately lead to vascular remodeling to compensate for decreased capillary and vascular density and increased vascular resistance. Regional pressure changes in vessels due to microgravity can also result in regional changes to vascular structure.
Deposition of energy (MIE: KE #1686) leads to increase, endothelial	Evidence for Biological Plausibility of KER: High Irradiation can cause cellular and tissue level markers of endothelial dysfunction. Following prolonged exposure to radiation, the protective effect of the endothelium can become exhausted and lead to endothelial dysfunction. Consequently, endothelial cells may lose their integrity and become senescent or apoptotic via alterations to signaling pathways, leading to endothelial dysfunction evidenced by dysregulation of vasodilation. Endothelial

dysfunction (KE #2068)	dysfunction is commonly considered a hallmark for the development of various cardiovascular pathologies.
Deposition of energy (MIE: KE #1686) leads to occurrence, vascular remodeling (AO: KE #2069)	Evidence for Biological Plausibility of KER: High Radiation can accelerate the natural processes of vascular remodeling related to aging. An increase in ROS, produced by IR, can reduce NO bioavailability, leading to endothelial dysfunction and vascular stiffness. In addition, the low level of inflammation during early stages of radiation leads to inhibition of tissue and vessel recovery, and later results in intimal thickening and vascular remodeling. Changes in vessel composition, such as collagen content, may also occur from energy deposition and affect vascular remodeling.
Deposition of energy (MIE: KE#1686) leads to altered, NO levels (KE #2067)	Evidence for Biological Plausibility of KER: High NO is produced by NOS enzymes or by the reduction of nitrite to NO. Deposition of energy can interfere with this process in several ways. Radiolysis of water forms ROS that interacts with NO to produce peroxynitrite which reduces NO bioavailability. ROS can also cause NOS uncoupling, which can reduce NO levels. In contrast, NO can also increase as a result of IR through activation of iNOS during oxidative stress. IR can also influence various signaling pathways that control NO levels, causing radiation to indirectly affect NO levels.
Oxidative stress (KE #1392) leads to altered, NO levels (KE #2067)	Evidence for Biological Plausibility of KER: High It is thought that excessive ROS production can lead to altered NO bioavailability both through direct interaction and indirectly through decreasing its production. Elevated O2- can interact with NO converting it to peroxynitrite leading to decreased bioavailability. ROS can also oxidize the eNOS cofactor BH4, causing eNOS uncoupling inhibiting NO production. Electron leakage in uncoupled eNOS produces additional ROS, exacerbating the state of oxidative stress.
Altered signaling pathways (KE #2066) leads to altered, NO levels (KE #2067)	Evidence for Biological Plausibility of KER: High Various pathways are well known to influence NO levels. Some well-studied examples include the PI3K/Akt pathway, the RhoA/ROCK pathway, the RAAS pathway and the acidic sphingomyelinase/ceramide pathway. The PI3K/Akt, RhoA/ROCK and RAAS pathways and their components are involved in the phosphorylation of various eNOS residues affecting the enzymes activation. The activation or deactivation of eNOS affects the levels of NO production. In contrast, the acidic sphingomyelinase/ceramide pathway can activate NADPH oxidase (NOX), leading to the production of ROS that goes on to scavenge NO decreasing its bioavailability.
Altered, NO levels (KE #2067) leads to increase, endothelial dysfunction (KE #2068)	Evidence for Biological Plausibility of KER: High Lack of bioavailable NO is considered one of the key drivers of endothelial dysfunction. Under normal conditions NO binds with soluble guanylyl cyclase (sGC) creating cGMP and cAMP to activate cellular kinase cascades and Ca2+-dependent vasodilation through smooth-muscle relaxation. Lack of bioavailable NO interrupts this process, reducing the relaxation of smooth muscle cells and dilation of the blood vessels. In contrast, an increase in NO combined with simultaneous excessive ROS can drive cellular senescence through increased peroxynitrite formation. Prolonged impaired vasodilation and elevated premature endothelial cell senescence are important characteristics of endothelial dysfunction.

Quantitative Consideration

Despite biological plausibility and empirical evidence demonstrating the qualitative linkages within the AOP, quantitative understanding is low. As described above, the lack of quantitative understanding of the KERs is due to the diversity in experimental design, including doses tested and radiation types used. The evidence is primarily from laboratory studies that show dose and time response relationships for KEs; however, the strength of the response can vary with factors such as dose-rate, type of radiation, and cell type. Particularly relevant are the relative lack of low-dose studies and exposure scenarios relevant to space radiation. Future work could use the present qualitative AOP to guide experimental design and strengthen quantitative understanding. Standardized studies simultaneously measuring endpoints across several KEs, and across a range of doses and timepoints would be beneficial in filling important gaps in the quantitative understanding.

Deposition of energy (MIE: KE #1686) leads oxidative stress (KE #1392)	Evidence for Quantitative Understanding of KER: High There is a large amount of evidence supporting how much of a change in the deposition of energy is needed to produce a change in the level of oxidative stress. Several different endpoints representing oxidative stress have been used, including changes in the levels or activity of catalase, GSH, superoxide dismutase, GSH-Px, MDA, and ROS. Measurements have also been made over a large range of doses and dose rates, and changes to oxidative stress levels have been shown to depend on the nature, dose and dose rate of energy deposition.
Deposition of energy (MIE: KE #1686) leads to increase, DNA strand breaks (KE #1635)	Evidence for Quantitative Understanding of KER: High Studies examining energy deposition leading to strand breaks suggest a positive, linear relationship between these two events. The exact number of strand breaks is difficult to predict from the deposition of energy. The relationship depends on the biological model, the type of radiation, and the dose.

Oxidative stress (KE #1392) leads to increase, DNA strand breaks (KE #1635)	Evidence for Quantitative Understanding of KER: Moderate There is a considerable amount of evidence showing increased DNA strand breaks following exposure to oxidative stress. However, no model has emerged that predicts the number of DNA strand breaks following oxidative stress. Measurements of oxidative stress vary across studies.
Increase, DNA strand breaks (KE #1635) leads to altered signaling pathways (KE #2066)	Evidence for Quantitative Understanding of KER: Moderate There is much evidence showing changes in the expression or activity of signaling pathways following increased DNA strand breaks. However, no model has been developed to accurately predict the changes to signaling pathways due to increased DNA strand breaks. Furthermore, the changes to signaling pathways are very context- and cell type-dependent.
Oxidative Stress (KE #1392) leads to altered signaling pathways (KE #2066)	Evidence for Quantitative Understanding of KER: Low The quantitative understanding of oxidative stress leading to altered signaling pathways is low as a precise quantitative relationship between the key events is difficult to determine due to differences in experimental design. The exact changes to signaling pathways due to oxidative stress will depend on the cell type and species.
Oxidative stress (KE #1392) leads to increase, endothelial dysfunction (KE #2068)	Evidence for Quantitative Understanding of KER: Low Although studies quantitatively measure both oxidative stress and endothelial dysfunction following a stressor, it is difficult to compare results and identify a quantitative relationship as studies use different models, stressors, doses and time scales. In addition, many factors and pathways can contribute to endothelial dysfunction. Thus, no model has been established to predict the extent of changes in endothelial dysfunction after oxidative stress.
Oxidative stress (KE #1392) leads to increase, pro-inflammatory mediators (KE #1493)	Evidence for Quantitative Understanding of KER: Moderate Current primary research shows that an increase in oxidative stress will be followed by a more significant increase in pro-inflammatory mediators. A quantitative association between the two KEs is difficult to determine, as multiple positive feedback mechanisms exist between oxidative stress and inflammation
Increase, pro-inflammatory mediators (KE #1493) leads to increase, endothelial dysfunction (KE #2068)	Evidence for Quantitative Understanding of KER: Low Although studies reveal increases in markers for endothelial dysfunction in response to increased pro-inflammatory mediators, no quantitative understanding has been established to predict the changes in endothelial dysfunction markers. There are various pro-inflammatory mediators that may contribute to various markers of endothelial dysfunction such as apoptosis and cellular senescence. Studies investigate changes in the levels of different pro-inflammatory mediators and different measures of endothelial dysfunction; therefore, it is difficult to compare the results and identify trends.
Altered signaling pathways (KE #2066) leads to increase, endothelial dysfunction (KE #2068)	Evidence for Quantitative Understanding of KER: Low Although studies show increases in markers for endothelial dysfunction in response to altered signaling pathways, no quantitative understanding has been established to predict the changes in endothelial dysfunction markers. There are various signaling pathways that may contribute to endothelial dysfunction, including the Akt/PI3K/mTOR pathway, the RhoA-Rho-kinase pathway, and the ASM/cer pathway. Studies investigate changes to the levels of different signaling pathway molecules; therefore, it is difficult to compare the results and identify trends.
Increase, endothelial dysfunction (KE #2068) leads to occurrence, vascular remodeling (AO: KE #2069)	Evidence for Quantitative Understanding of KER: Low Vascular remodeling is consistently shown with endothelial dysfunction. However, it is difficult to compare results and identify a quantitative relationship as various models, stressors, doses and endpoint measures were used. Thus, no model has been established to accurately predict the changes in vascular remodeling.
Deposition of energy (MIE: KE #1686) leads to increase, endothelial dysfunction (KE #2068)	Evidence for Quantitative Understanding of KER: Low Studies revealed consistent increases in levels of indicators of endothelial dysfunction such as apoptosis, premature endothelial cell senescence and diminished relaxation response. There is consistent evidence that shows that as the dose increases, the maximum relaxation response decreases. However, more studies are required to quantify this association to show how this relates to levels of cellular markers of apoptosis and senescence.
Deposition of energy (MIE: KE #1686) leads to occurrence, vascular	Evidence for Quantitative Understanding of KER: Low Deposition of energy from IR is consistently demonstrated to drive vascular remodeling. However, it is difficult to compare results and quantify relationships as each study uses different models, stressors, doses and time scales. In addition, many factors and pathways contribute to the components of vascular remodeling. Thus, no

remodeling (AO: KE #2069)	model has been established to predict the changes in vascular remodeling after deposition of energy.
Deposition of energy (MIE: KE #1686) leads to altered, NO levels (KE #2067)	Evidence for Quantitative Understanding of KER: Low Altered nitric oxide levels occur consistently with deposition of energy. However, it is difficult to compare results and determine a quantitative relationship as each study uses different models, stressors, doses and endpoint measures of NO. As well, cancerous cells and normal cells can show different production of NO. Thus, no model has been established to predict the changes in nitric oxide levels at a given dose of IR.
Oxidative stress (KE #1392) leads to altered, NO levels (KE #2067)	Evidence for Quantitative Understanding of KER: Low Alterations in NO levels cannot be predicted from relevant measures of oxidative stress changes, such as increased ROS production and antioxidant enzyme activity. Nevertheless, a general decrease in NO is observed following ROS production.
Altered signaling pathways (KE #2066) leads to altered, NO levels (KE #2067)	Evidence for Quantitative Understanding of KER: Low Altered NO, iNOS and eNOS levels occur in response to altered signaling pathways; however, a model has not been established to predict the changes in NO levels. Different models, stressors, time scales, doses and dose rates make trends difficult to identify. The studies investigated the levels of different altered signaling pathway molecules and their effects on NO levels, making it difficult to compare and identify quantitative relationships across the results.
Altered, NO levels (KE #2067) leads to increase, endothelial dysfunction (KE #2068)	Evidence for Quantitative Understanding of KER: Low Increased vascular tension occurs consistently with decreased NO levels. Although many studies quantitatively measure a change in endothelial function after changes in NO levels, no model has been established. Each study cited used different models, stressors, time scales, doses and dose rates, which makes it difficult to determine if response levels are consistent between studies.

Considerations for Potential Applications of the AOP (optional)

The present AOP serves as a platform to promote broader collaborative efforts to understand non-cancer health risks from radiation exposures. It will be a foundational AOP of regulatory interest to researchers seeking areas of knowledge gaps to prioritize research in understanding mechanisms of CVD. The AOP is also relevant to space agencies and clinicians working to improve the guidance on health risks from long-term spaceflight and radiotherapy treatments, respectively. The WOE for this AOP may also inform parameters in biologically based risk models and can serve to develop countermeasures to protect the cardiovascular systems of future space travelers on deep space missions. The present qualitative AOP can be used to guide the design of experiments that will provide quantitative understanding for the KERs to support risk-model development and inform additional guidelines for radiation protection; additionally, the identified research gaps could help prioritize research needs for funding strategies.

References

Abdel-Magied, N., & Shedid, S. M. (2020). Impact of zinc oxide nanoparticles on thioredoxin-interacting protein and asymmetric dimethylarginine as biochemical indicators of cardiovascular disorders in gamma-irradiated rats. Environmental Toxicology, 35(4), 430–442. https://doi.org/10.1002/tox.22879

Ashcroft, M., Kubbutat, M. H. G., & Vousden, K. H. (1999). Regulation of p53 Function and Stability by Phosphorylation. Molecular and Cellular Biology, 19(3), 1751. https://doi.org/10.1128/MCB.19.3.1751

Azimzadeh, O., Subramanian, V., Sievert, W., Merl-Pham, J., Oleksenko, K., Rosemann, M., Multhoff, G., Atkinson, M. J., & Tapio, S. (2021). Activation of pparα by fenofibrate attenuates the effect of local heart high dose irradiation on the mouse cardiac proteome. Biomedicines, 9(12). https://doi.org/10.3390/biomedicines9121845

Azimzadeh, O. et al. (2017), “Proteome analysis of irradiated endothelial cells reveals persistent alteration in protein degradation and the RhoGDI and NO signalling pathways”, International Journal of Radiation Biology, Vol. 93/9, Informa, London, https://doi.org/10.1080/09553002.2017.1339332.

Azimzadeh, O. et al. (2015), “Integrative Proteomics and Targeted Transcriptomics Analyses in Cardiac Endothelial Cells Unravel Mechanisms of Long-Term Radiation-Induced Vascular Dysfunction”, Journal of Proteome Research, Vol. 14/2, American Chemical Society, Washington, https://doi.org/10.1021/pr501141b.

Azizova, T. V., Batistatou, E., Grigorieva, E. S., McNamee, R., Wakeford, R., Liu, H., De Vocht, F., & Agius, R. M. (2018). An Assessment of Radiation-Associated Risks of Mortality from Circulatory Disease in the Cohorts of Mayak and Sellafield Nuclear Workers. Radiation Research, 189(4), 371–388. https://doi.org/10.1667/RR14468.1

Baeyens, N., Bandyopadhyay, C., Coon, B. G., Yun, S., & Schwartz, M. A. (2016). Endothelial fluid shear stress sensing in vascular health and disease. The Journal of Clinical Investigation, 126(3), 821–828. https://doi.org/10.1172/JCI83083

Baker, J. E., Fish, B. L., Su, J., Haworth, S. T., Strande, J. L., Komorowski, R. A., Migrino, R. Q., Doppalapudi, A., Harmann, L., Allen Li, X., Hopewell, J. W., & Moulder, J. E. (2009). 10 Gy total body irradiation increases risk of coronary sclerosis, degeneration

of heart structure and function in a rat model. International Journal of Radiation Biology, 85(12), 1089–1100. https://doi.org/10.3109/09553000903264473

Baker, J. E., Moulder, J. E., & Hopewell, J. W. (2011). Radiation as a Risk Factor for Cardiovascular Disease. Antioxidant and Redox Signaling, 15(7). https://doi.org/10.1089/ars.2010.3742

Balasubramanian, D. (2000). Ultraviolet radiation and cataract. Journal of Ocular Pharmacology and Therapeutics, 16(3), 285–297. https://doi.org/10.1089/jop.2000.16.285

Baran, R., Marchal, S., Campos, S. G., Rehnberg, E., Tabury, K., Baselet, B., Wehland, M., Grimm, D., & Baatout, S. (2021). The Cardiovascular System in Space: Focus on In Vivo and In Vitro Studies. Biomedicines 2022, Vol. 10, Page 59, 10(1), 59. https://doi.org/10.3390/BIOMEDICINES10010059

Baselet, B., Belmans, N., Coninx, E., Lowe, D., Janssen, A., Michaux, A., Tabury, K., Raj, K., Quintens, R., Benotmane, M. A., Baatout, S., Sonveaux, P., & Aerts, A. (2017). Functional gene analysis reveals cell cycle changes and inflammation in endothelial cells irradiated with a single X-ray dose. Frontiers in Pharmacology, 8. https://doi.org/10.3389/fphar.2017.00213

Belzile-Dugas, E., & Eisenberg, M. J. (2021). Radiation-Induced Cardiovascular Disease: Review of an Underrecognized Pathology. Journal of the American Heart Association: Cardiovascular and Cerebrovascular Disease, 10(18), 21686. https://doi.org/10.1161/JAHA.121.021686

Berk, B. C., & Korshunov, V. A. (2006). Genetic determinants of vascular remodelling. Canadian Journal of Cardiology, 22(SUPPL. B). https://doi.org/10.1016/s0828-282x(06)70980-1

Boerma, M., Nelson, G. A., Sridharan, V., Mao, X.-W., Koturbash, I., & Hauer-Jensen, M. (2015). Space radiation and cardiovascular disease risk. World Journal of Cardiology, 7(12), 882. https://doi.org/10.4330/wjc.v7.i12.882

Boerma, M., Sridharan, V., Mao, X.-W., Nelson, G. A., Cheema, A. K., Koturbash, I., Singh, S. P., Tackett, A. J., & Hauer-Jensen, M. (2016). Effects of Ionizing Radiation on the Heart. Mutation Research - Reviews in Mutation Research, 770, 319–327. https://doi.org/10.1016/j.mrrev.2016.07.003

Bonetti, P. O., Lerman, L. O., & Lerman, A. (2003). Endothelial dysfunction: A marker of atherosclerotic risk. Arteriosclerosis, Thrombosis, and Vascular Biology, 23(2), 168–175. https://doi.org/10.1161/01.ATV.0000051384.43104.FC

Borghini, A., Luca Gianicolo, E. A., Picano, E., & Andreassi, M. G. (2013). Ionizing radiation and atherosclerosis: Current knowledge and future challenges. Atherosclerosis, 230(1), 40–47. https://doi.org/10.1016/j.atherosclerosis.2013.06.010

Bray, F., Laversanne, M., Weiderpass, E., & Soerjomataram, I. (2021). The ever-increasing importance of cancer as a leading cause of premature death worldwide. Cancer, 127(16), 3029–3030. https://doi.org/10.1002/cncr.33587

Carmeliet, P., & Jain, R. K. (2011). Molecular mechanisms and clinical applications of angiogenesis. https://doi.org/10.1038/nature10144

Cervelli, T., Panetta, D., Navarra, T., Gadhiri, S., Salvadori, P., Galli, A., Caramella, D., Basta, G., Picano, E., & Del Turco, S. (2017). A New Natural Antioxidant Mixture Protects against Oxidative and DNA Damage in Endothelial Cell Exposed to Low-Dose Irradiation. Oxidative Medicine and Cellular Longevity, 2017. https://doi.org/10.1155/2017/9085947

Chang, P. Y., Zhang, B. Y., Cui, S., Qu, C., Shao, L. H., Xu, T. K., Qu, Y. Q., Dong, L. H., & Wang, J. (2017). MSC-derived cytokines repair radiation-induced intra-villi microvascular injury. Oncotarget, 8(50). https://doi.org/10.18632/oncotarget.21236

Chauhan, V., Hamada, N., Monceau, V., Ebrahimian, T., Adam, N., Wilkins, R. C., Sebastian, S., Patel, Z. S., Huff, J. L., Simonetto, C., Iwasaki, T., Kaiser, J. C., Salomaa, S., Moertl, S., & Azimzadeh, O. (2021). Expert consultation is vital for adverse outcome pathway development: a case example of cardiovascular effects of ionizing radiation. International Journal of Radiation Biology, 97(11). https://doi.org/10.1080/09553002.2021.1969466

Cheng, Y. P., Zhang, H. J., Su, Y. T., Meng, X. X., Xie, X. P., Chang, Y. M., & Bao, J. X. (2017). Acid sphingomyelinase/ceramide regulates carotid intima-media thickness in simulated weightless rats. Pflugers Archiv European Journal of Physiology, 469(5–6). https://doi.org/10.1007/s00424-017-1969-z

Chiuve, S. E., McCullough, M. L., Sacks, F. M., & Rimm, E. B. (2006). Healthy lifestyle factors in the primary prevention of coronary heart disease among men: Benefits among users and nonusers of lipid-lowering and antihypertensive medications. Circulation, 114(2), 160–167. https://doi.org/10.1161/CIRCULATIONAHA.106.621417

Chowdhury, R., Shah, D., & Payal, A. (2017). Healthy worker effect phenomenon: Revisited with emphasis on statistical methods-A review. Indian Journal of Occupational and Environmental Medicine, 21(1), 2–8. https://doi.org/10.4103/ijoem.IJOEM_53_16

Cohn, J. N., Quyyumi, A. A., Hollenberg, N. K., & Jamerson, K. A. (2004). Surrogate markers for cardiovascular disease: Functional markers. Circulation, 109(25).

de Jager, T. L., A. E. Cockrell, S. S. Du Plessis (2017), “Ultraviolet Light Induced Generation of Reactive Oxygen Species”, in: Ultraviolet Light in Human Health, Diseases and Environment, vol 996. Springer Cham, https://doi.org/10.1007/978-3-319-56017-5_2.

Deanfield, J. E., Halcox, J. P., & Rabelink, T. J. (2007). Endothelial function and dysfunction: Testing and clinical relevance. Circulation, 115(10), 1285–1295. https://doi.org/10.1161/CIRCULATIONAHA.106.652859

Desouky, O., Ding, N., & Zhou, G. (2015). Targeted and non-targeted effects of ionizing radiation. Journal of Radiation Research and Applied Sciences, 8(2), 247–254. https://doi.org/10.1016/J.JRRAS.2015.03.003

Di Maggio, F. M., Minafra, L., Forte, G. I., Cammarata, F. P., Lio, D., Messa, C., Gilardi, M. C., & Bravatà, V. (2015). Portrait of inflammatory response to ionizing radiation treatment. In Journal of Inflammation (Vol. 12, Issue 1, pp. 1–11). BioMed Central Ltd. https://doi.org/10.1186/s12950-015-0058-3

Ding, J., Yu, M., Jiang, J., Luo, Y., Zhang, Q., Wang, S., Yang, F., Wang, A., Wang, L., Zhuang, M., Wu, S., Zhang, Q., Xia, Y., & Lu, D. (2020). Angiotensin II Decreases Endothelial Nitric Oxide Synthase Phosphorylation via AT1R Nox/ROS/PP2A Pathway. Frontiers in Physiology, 11, 1245. https://doi.org/10.3389/fphys.2020.566410

Dörr, W. (2015). Radiobiology of tissue reactions. Annals of the ICRP, 44, 58–68. https://doi.org/10.1177/0146645314560686

Durante, M., & Cucinotta, F. A. (2008). Heavy ion carcinogenesis and human space exploration. Nature Reviews Cancer, 8(6), 465–472. https://doi.org/10.1038/nrc2391

Eaton, J. W. (1994). UV-mediated cataractogenesis: A radical perspective. Documenta Ophthalmologica, 88(3–4), 233–242. https://doi.org/10.1007/BF01203677

EPRI. (2020). Cardiovascular Risks from Low Dose Radiation Exposure: Review and Scientific Appraisal of the Literature.

Fletcher, A. E. (2010). Free radicals, antioxidants and eye diseases: Evidence from epidemiological studies on cataract and age-related macular degeneration. Ophthalmic Research, 44(3), 191–198. https://doi.org/10.1159/000316476

Forrester, S. J., Kikuchi, D. S., Hernandes, M. S., Xu, Q., & Griendling, K. K. (2018). Reactive oxygen species in metabolic and inflammatory signaling. Circulation Research, 122(6), 877–902. https://doi.org/10.1161/CIRCRESAHA.117.311401

Förstermann, U. (2010). Nitric oxide and oxidative stress in vascular disease. Pflugers Archiv European Journal of Physiology, 459(6), 923–939. https://doi.org/10.1007/s00424-010-0808-2

Förstermann, U., & Münzel, T. (2006). Endothelial Nitric Oxide Synthase in Vascular Disease. Circulation, 113(13), 1708–1714. https://doi.org/10.1161/CIRCULATIONAHA.105.602532

Francula-Zaninovic, S., & Nola, I. A. (2018). Management of Measurable Variable Cardiovascular Disease' Risk Factors. Current Cardiology Reviews, 14(3), 153–163. https://doi.org/10.2174/1573403x14666180222102312

Fuji, S., Matsushita, S., Hyodo, K., Osaka, M., Sakamoto, H., Tanioka, K., Miyakawa, K., Kubota, M., Hiramatsu, Y., & Tokunaga, C. (2016). Association between endothelial function and micro-vascular remodeling measured by synchrotron radiation pulmonary micro-angiography in pulmonary arterial hypertension. General Thoracic and Cardiovascular Surgery, 64(10), 597–603. https://doi.org/10.1007/s11748-016-0684-6

Ganea, E., & Harding, J. J. (2006). Glutathione-related enzymes and the eye. In Current Eye Research (Vol. 31, Issue 1, pp. 1–11). Taylor & Francis. https://doi.org/10.1080/02713680500477347

Gen, S. W. (2004). The functional interactions between the p53 and MAPK signaling pathways. Cancer Biology and Therapy, 3(2), 156–161. https://doi.org/10.4161/cbt.3.2.614

Gillies, M., Richardson, D. B., Cardis, E., Daniels, R. D., O'Hagan, J. A., Haylock, R., Laurier, D., Leuraud, K., Moissonnier, M., Schubauer-Berigan, M. K., Thierry-Chef, I., & Kesminiene, A. (2017). Mortality from circulatory diseases and other non-cancer outcomes among nuclear workers in France, the United Kingdom and the United States (inworks). Radiation Research, 188(3), 276–290. https://doi.org/10.1667/RR14608.1

Grabham, P., & Sharma, P. (2013). The effects of radiation on angiogenesis. Vascular Cell, 5(1), 19. https://doi.org/10.1186/2045-824X-5-19

Hamada, N., Kawano, K. I., Nomura, T., Furukawa, K., Yusoff, F. M., Maruhashi, T., Maeda, M., Nakashima, A., & Higashi, Y. (2021). Vascular damage in the aorta of wild-type mice exposed to ionizing radiation: Sparing and enhancing effects of dose protraction. Cancers, 13(21). https://doi.org/10.3390/cancers13215344

Hamada, N., Kawano, K. I., Yusoff, F. M., Furukawa, K., Nakashima, A., Maeda, M., Yasuda, H., Maruhashi, T., & Higashi, Y. (2020). Ionizing irradiation induces vascular damage in the aorta of wild-type mice. Cancers, 12(10), 1–11. https://doi.org/10.3390/cancers12103030

Hasan, H. F., Radwan, R. R., & Galal, S. M. (2020). Bradykinin-potentiating factor isolated from Leiurus quinquestriatus scorpion venom alleviates cardiomyopathy in irradiated rats via remodelling of the RAAS pathway. Clinical and Experimental Pharmacology and Physiology, 47(2), 263–273. https://doi.org/10.1111/1440-1681.13202

Hassan, B., Akcakanat, A., Holder, A. M., & Meric-Bernstam, F. (2013). Targeting the PI3-Kinase/Akt/mTOR Signaling Pathway. Surgical Oncology Clinics of North America, 22(4), 641–664. https://doi.org/10.1016/j.soc.2013.06.008

Hatoum, O. A., Otterson, M. F., Kopelman, D., Miura, H., Sukhotnik, I., Larsen, B. T., Selle, R. M., Moulder, J. E., & Gutterman, D. D. (2006). Radiation induces endothelial dysfunction in murine intestinal arterioles via enhanced production of reactive oxygen species. Arteriosclerosis, Thrombosis, and Vascular Biology, 26(2), 287–294. https://doi.org/10.1161/01.ATV.0000198399.40584.8c

Heald, C. L., Fowkes, F. G. R., Murray, G. D., & Price, J. F. (2006). Risk of mortality and cardiovascular disease associated with the ankle-brachial index: Systematic review. Atherosclerosis, 189(1), 61–69. https://doi.org/10.1016/J.ATHEROSCLEROSIS.2006.03.011

Hemmings, B. A., & Restuccia, D. F. (2012). PI3K-PKB/Akt pathway. Cold Spring Harbor Perspectives in Biology, 4(9). https://doi.org/10.1101/cshperspect.a011189

Hirakawa, M., Oike, M., Masuda, K., & Ito, Y. (2002). Tumor cell apoptosis by irradiation-induced nitric oxide production in vascular endothelium. Cancer Research, 62(5), 1450–1457.

Hladik, D., & Tapio, S. (2016). Effects of ionizing radiation on the mammalian brain. Mutation Research - Reviews in Mutation Research, 770, 219–230. https://doi.org/10.1016/j.mrrev.2016.08.003

Hodis, H. N., Mack, W. J., LaBree, L., Selzer, R. H., Liu, C. R., Liu, C. H., & Azen, S. P. (1998). The role of carotid arterial intima - Media thickness in predicting clinical coronary events. Annals of Internal Medicine, 128(4), 262–269. https://doi.org/10.7326/0003-4819-128-4-199802150-00002

Hong, C. W., Kim, Y. M., Pyo, H., Lee, J. H., Kim, S., Lee, S., & Noh, J. M. (2013). Involvement of inducible nitric oxide synthase in radiation-Induced vascular endothelial damage. Journal of Radiation Research, 54(6), 1036–1042. https://doi.org/10.1093/jrr/rrt066

Hsu, T., Nguyen-Tran, H. H., & Trojanowska, M. (2019). Active roles of dysfunctional vascular endothelium in fibrosis and cancer. Journal of Biomedical Science, 26(1), 1–12. https://doi.org/10.1186/s12929-019-0580-3

Huang, Y. et al. (2021), “Mesenchymal Stem Cell-Conditioned Medium Protects Hippocampal Neurons From Radiation Damage by Suppressing Oxidative Stress and Apoptosis”, Dose-response, Vol. 19/1, Sage Publishing, https://doi.org/10.1177/1559325820984944

Hughson, R. L., Helm, A., & Durante, M. (2018). Heart in space: Effect of the extraterrestrial environment on the cardiovascular system. In Nature Reviews Cardiology (Vol. 15, Issue 3). https://doi.org/10.1038/nrcardio.2017.157

Hughson, R. L., Robertson, A. D., Arbeille, P., Shoemaker, J. K., Rush, J. W. E., Fraser, K. S., & Greaves, D. K. (2016). Increased postflight carotid artery stiffness and inflight insulin resistance resulting from 6-mo spaceflight in male and female astronauts. American Journal of Physiology - Heart and Circulatory Physiology, 310(5), H628–H638. https://doi.org/10.1152/ajpheart.00802.2015

Ismail, A. F. M., & El-Sonbaty, S. M. (2016). Fermentation enhances Ginkgo biloba protective role on gamma-irradiation induced neuroinflammatory gene expression and stress hormones in rat brain. Journal of Photochemistry and Photobiology B: Biology, 158, 154–163. https://doi.org/10.1016/j.jphotobiol.2016.02.039

Ivanov, V. K., Maksioutov, M. A., Chekin, S. Y., Petrov, A. V., Biryukov, A. P., Kruglova, Z. G., Matyash, V. A., Tsyb, A. F., Manton, K. G., & Kravchenko, J. S. (2006). The risk of radiation-induced cerebrovascular disease in chernobyl emergency workers. Health Physics, 90(3), 199–207. https://doi.org/10.1097/01.HP.0000175835.31663.EA

Karam, H. M., & Radwan, R. R. (2019). Metformin modulates cardiac endothelial dysfunction, oxidative stress and inflammation in irradiated rats: A new perspective of an antidiabetic drug. Clinical and Experimental Pharmacology and Physiology, 46(12), 1124–1132. https://doi.org/10.1111/1440-1681.13148

Karar, J., & Maity, A. (2011). PI3K/AKT/mTOR Pathway in Angiogenesis. Frontiers in Molecular Neuroscience, 4, 51. https://doi.org/10.3389/fnmol.2011.00051

Karimi, N., Monfared, A., Haddadi, G., Soleymani, A., Mohammadi, E., Hajian-Tilaki, K., & Borzoueisileh, S. (2017). Radioprotective effect of hesperidin on reducing oxidative stress in the lens tissue of rats. International Journal of Pharmaceutical Investigation, 7(3), 149. https://doi.org/10.4103/jphi.jphi_60_17

Kashcheev, V. V., Chekin, S. Y., Karpenko, S. V., Maksioutov, M. A., Menyaylo, A. N., Tumanov, K. A., Kochergina, E. V., Kashcheeva, P. V., Gorsky, A. I., Shchukina, N. V., Lovachev, S. S., Vlasov, O. K., & Ivanov, V. K. (2017). Radiation Risk of Cardiovascular Diseases in the Cohort of Russian Emergency Workers of the Chernobyl Accident. Health Physics, 113(1), 23–29. https://doi.org/10.1097/HP.0000000000000670

Kessler, E. L., Rivaud, M. R., Vos, M. A., & Van Veen, T. A. B. (2019). Sex-specific influence on cardiac structural remodeling and therapy in cardiovascular disease. Biology of Sex Differences, 10(1). https://doi.org/10.1186/s13293-019-0223-0

Konukoglu, D., & Uzun, H. (2016). Endothelial dysfunction and hypertension. In Advances in Experimental Medicine and Biology (Vol. 956, pp. 511–540). Adv Exp Med Biol. https://doi.org/10.1007/5584_2016_90

Korpela, E., & Liu, S. K. (2014). Endothelial perturbations and therapeutic strategies in normal tissue radiation damage. Radiation Oncology, 9(1). https://doi.org/10.1186/s13014-014-0266-7

Kozbenko, T., Adam, N., Lai, V., Sandhu, S., Kuan, J., Flores, D., Appleby, M., Parker, H., Hocking, R., Tsaioun, K., Yauk, C., Wilkins, R., & Chauhan, V. (2022). Deploying elements of scoping review methods for adverse outcome pathway development: a space travel case example. International Journal of Radiation Biology, 1–12. https://doi.org/10.1080/09553002.2022.2110306

Krüger-Genge, A., Blocki, A., Franke, R.-P., & Jung, F. (2019). Vascular Endothelial Cell Biology: An Update. International Journal of Molecular Sciences, 20(18), 4411. https://doi.org/10.3390/ijms20184411

Lee, M. S., Finch, W., & Mahmud, E. (2013). Cardiovascular complications of radiotherapy. American Journal of Cardiology, 112(10), 1688–1696. https://doi.org/10.1016/j.amjcard.2013.07.031

Li, J., De Leon, H., Ebato, B., Cui, J., Todd, J., Chronos, N. A. F., & Robinson, K. A. (2002). Endovascular irradiation impairs vascular functional responses in noninjured pig coronary arteries. Cardiovascular Radiation Medicine, 152–162. https://doi.org/10.1016/S1522-1865(03)00096-9

Little, M. P., Azizova, T. V., & Hamada, N. (2021). Low- and moderate-dose non-cancer effects of ionizing radiation in directly exposed individuals, especially circulatory and ocular diseases: a review of the epidemiology. International Journal of Radiation Biology, 97(6), 782–803. https://doi.org/10.1080/09553002.2021.1876955

Luiking, Y. C., Engelen, M. P. K. J., & Deutz, N. E. P. (2010). Regulation of nitric oxide production in health and disease. Current Opinion in Clinical Nutrition and Metabolic Care, 13(1), 97–104. https://doi.org/10.1097/MCO.0B013E328332F99D

Lumniczky, K., Impens, N., Armengol, G., Candéias, S., Georgakilas, A. G., Hornhardt, S., Martin, O. A., Rödel, F., & Schaue, D. (2021). Low dose ionizing radiation effects on the immune system. Environment International, 149, 106212. https://doi.org/10.1016/j.envint.2020.106212

Maier, J. A. M., Cialdai, F., Monici, M., & Morbidelli, L. (2015). The impact of microgravity and hypergravity on endothelial cells. BioMed Research International, 2015. https://doi.org/10.1155/2015/434803

Matsubara, K., Higaki, T., Matsubara, Y., & Nawa, A. (2015). Nitric oxide and reactive oxygen species in the pathogenesis of preeclampsia. International Journal of Molecular Sciences, 16(3), 4600–4614. https://doi.org/10.3390/ijms16034600

Menezes, K. M., Wang, H., Hada, M., & Saganti, P. B. (2018). Radiation Matters of the Heart: A Mini Review. Frontiers in Cardiovascular Medicine, 5, 83. https://doi.org/10.3389/FCVM.2018.00083

Millatt, L. J., Abdel-Rahman, E. M., & Siragy, H. M. (1999). Angiotensin II and nitric oxide: A question of balance. Regulatory Peptides, 81(1–3), 1–10. https://doi.org/10.1016/S0167-0115(99)00027-0

Mitchell, A., Pimenta, D., Gill, J., Ahmad, H., & Bogle, R. (2019). Cardiovascular effects of space radiation: implications for future human deep space exploration. European Journal of Preventive Cardiology, 26(16), 1707–1714. https://doi.org/10.1177/2047487319831497

Mittal, M., Siddiqui, M. R., Tran, K., Reddy, S. P., & Malik, A. B. (2014). Reactive oxygen species in inflammation and tissue injury. Antioxidants and Redox Signaling, 20(7), 1126–1167. https://doi.org/10.1089/ars.2012.5149

Mosca, L., Barrett-Connor, E., & Kass Wenger, N. (2011). Sex/gender differences in cardiovascular disease prevention: What a difference a decade makes. Circulation, 124(19), 2145–2154. https://doi.org/10.1161/CIRCULATIONAHA.110.968792

Mozaffarian, D., Wilson, P. W. F., & Kannel, W. B. (2008). Beyond Established and Novel Risk Factors. Circulation, 117(23), 3031–3038. https://doi.org/10.1161/CIRCULATIONAHA.107.738732

Nagane, M., Yasui, H., Kuppusamy, P., Yamashita, T., & Inanami, O. (2021). DNA damage response in vascular endothelial senescence: Implication for radiation-induced cardiovascular diseases. Journal of Radiation Research, 62(4), 564–573. https://doi.org/10.1093/jrr/rrab032

Nathan, C., & Xie, Q. wen. (1994). Nitric oxide synthases: Roles, tolls, and controls. Cell, 78(6), 915–918. https://doi.org/10.1016/0092-8674(94)90266-6

Norbury, J. W., Schimmerling, W., Slaba, T. C., Azzam, E. I., Badavi, F. F., Baiocco, G., Benton, E., Bindi, V., Blakely, E. A., Blattnig, S. R., Boothman, D. A., Borak, T. B., Britten, R. A., Curtis, S., Dingfelder, M., Durante, M., Dynan, W. S., Eisch, A. J., Robin Elgart, S., … Zeitlin, C. J. (2016). Galactic cosmic ray simulation at the NASA Space Radiation Laboratory. Life Sciences in Space Research, 8, 38–51. https://doi.org/10.1016/j.lssr.2016.02.001

North, B. J., & Sinclair, D. A. (2012). The intersection between aging and cardiovascular disease. Circulation Research, 110(8), 1097–1108. https://doi.org/10.1161/CIRCRESAHA.111.246876

Ozasa, K., Shimizu, Y., Suyama, A., Kasagi, F., Soda, M., Grant, E. J., Sakata, R., Sugiyama, H., & Kodama, K. (2012). Studies of the mortality of atomic bomb survivors, report 14, 1950-2003: An overview of cancer and noncancer diseases. In Radiation Research (Vol. 177, Issue 3). https://doi.org/10.1667/RR2629.1

Padgaonkar, V. A., Leverenz, V. R., Bhat, A. V., Pelliccia, S. E., & Giblin, F. J. (2015). Thioredoxin reductase activity may be more important than GSH level in protecting human lens epithelial cells against UVA light. Photochemistry and Photobiology, 91(2), 387–396. https://doi.org/10.1111/php.12404

Patel, Z. S., Brunstetter, T. J., Tarver, W. J., Whitmire, A. M., Zwart, S. R., Smith, S. M., & Huff, J. L. (2020). Red risks for a journey to the red planet: The highest priority human health risks for a mission to Mars. Npj Microgravity, 6(1), 1–13. https://doi.org/10.1038/s41526-020-00124-6

Ping, Z., Peng, Y., Lang, H., Xinyong, C., Zhiyi, Z., Xiaocheng, W., Hong, Z., & Liang, S. (2020). Oxidative Stress in Radiation-Induced Cardiotoxicity. Oxidative Medicine and Cellular Longevity, 2020. https://doi.org/10.1155/2020/3579143

Polak, J. F., Pencina, M. J., Pencina, K. M., O'Donnell, C. J., Wolf, P. A., & Ralph B. D'Agostino, S. (2011). Carotid-Wall Intima–Media Thickness and Cardiovascular Events. The New England Journal of Medicine, 365(3), 213. https://doi.org/10.1056/NEJMOA1012592

Preston, D. L., Shimizu, Y., Pierce, D. A., Suyama, A., & Mabuchi, K. (2003). Studies of Mortality of Atomic Bomb Survivors. Report 13: Solid Cancer and Noncancer Disease Mortality: 1950–1997. Https://Doi.Org/10.1667/RR3049, 160(4), 381–407. https://doi.org/10.1667/RR3049

Pries, A. R., Reglin, B., & Secomb, T. W. (2001). Structural adaptation of microvascular networks: Functional roles of adaptive responses. American Journal of Physiology - Heart and Circulatory Physiology, 281(3). https://doi.org/10.1152/ajpheart.2001.281.3.h1015

Ramadan, R., Baatout, S., Aerts, A., & Leybaert, L. (2021). The role of connexin proteins and their channels in radiation-induced atherosclerosis. Cellular and Molecular Life Sciences, 78(7), 3087–3103. https://doi.org/10.1007/s00018-020-03716-3

Ramadan, R., Vromans, E., Anang, D. C., Goetschalckx, I., Hoorelbeke, D., Decrock, E., Baatout, S., Leybaert, L., & Aerts, A. (2020). Connexin43 Hemichannel Targeting With TAT-Gap19 Alleviates Radiation-Induced Endothelial Cell Damage. Frontiers in Pharmacology, 11. https://doi.org/10.3389/fphar.2020.00212

Rehman, M. U., Jawaid, P., Uchiyama, H., & Kondo, T. (2016). Comparison of free radicals formation induced by cold atmospheric plasma, ultrasound, and ionizing radiation. Archives of Biochemistry and Biophysics, 605, 19–25. https://doi.org/10.1016/j.abb.2016.04.005

Rios, A., Joshi, R., & Shin, H. (2020). Quantifying 60 Years of Gender Bias in Biomedical Research with Word Embeddings. 1–13. https://doi.org/10.18653/v1/2020.bionlp-1.1

Rodgers, J. L., Jones, J., Bolleddu, S. I., Vanthenapalli, S., Rodgers, L. E., Shah, K., Karia, K., & Panguluri, S. K. (2019). Cardiovascular risks associated with gender and aging. Journal of Cardiovascular Development and Disease, 6(2). https://doi.org/10.3390/jcdd6020019

Sadhukhan, R., Leung, J. W. C., Garg, S., Krager, K. J., Savenka, A. V., Basnakian, A. G., & Pathak, R. (2020). Fractionated radiation suppresses Kruppel-like factor 2 pathway to a greater extent than by single exposure to the same total dose. Scientific Reports, 10(1), 1–13. https://doi.org/10.1038/s41598-020-64672-3

Sakata, K., Kondo, T., Mizuno, N., Shoji, M., Yasui, H., Yamamori, T., Inanami, O., Yokoo, H., Yoshimura, N., & Hattori, Y. (2015). Roles of ROS and PKC-βII in ionizing radiation-induced eNOS activation in human vascular endothelial cells. Vascular Pharmacology, 70, 55–65. https://doi.org/10.1016/j.vph.2015.03.016

Santamaría, R., González-Álvarez, M., Delgado, R., Esteban, S., & Arroyo, A. G. (2020). Remodeling of the Microvasculature: May the Blood Flow Be With You. Frontiers in Physiology, 11, 1256. https://doi.org/10.3389/FPHYS.2020.586852/XML/NLM

Sárközy, M., Gáspár, R., Zvara, A., Kiscsatári, L., Varga, Z., Kővári, B., Kovács, M. G., Szűcs, G., Fabian, G., Diószegi, P., Cserni, G., Puskás, L. G., Thum, T., Kahán, Z., Csont, T., & Batkai, S. (2019). Selective heart irradiation induces cardiac overexpression of the pro-hypertrophic miR-212. Frontiers in Oncology, 9(JUN), 598. https://doi.org/10.3389/fonc.2019.00598

Schaue, D., Micewicz, E. D., Ratikan, J. A., Xie, M. W., Cheng, G., & McBride, W. H. (2015). Radiation and Inflammation. In Seminars in Radiation Oncology (Vol. 25, Issue 1, pp. 4–10). W.B. Saunders. https://doi.org/10.1016/j.semradonc.2014.07.007

Schiffrin, E. L. (2008). Oxidative stress, nitric oxide synthase, and superoxide dismutase: A matter of imbalance underlies endothelial dysfunction in the human coronary circulation. Hypertension, 51(1), 31–32. https://doi.org/10.1161/HYPERTENSIONAHA.107.103226

Schmidt-Ullrich, R. K., Dent, P., Grant, S., Mikkelsen, R. B., & Valerie, K. (2000). Signal transduction and cellular radiation responses. Radiation Research, 153(3), 245–257. https://doi.org/10.1667/0033-7587(2000)153[0245:STACRR]2.0.CO;2

Schultz, W. M., Kelli, H. M., Lisko, J. C., Varghese, T., Shen, J., Sandesara, P., Quyyumi, A. A., Taylor, H. A., Gulati, M., Harold, J. G., Mieres, J. H., Ferdinand, K. C., Mensah, G. A., & Sperling, L. S. (2018). Socioeconomic Status and Cardiovascular Outcomes: Challenges and Interventions. Circulation, 137(20). https://doi.org/10.1161/circulationaha.117.029652

Senoner, T., & Dichtl, W. (2019). Oxidative stress in cardiovascular diseases: Still a therapeutic target? Nutrients, 11(9). https://doi.org/10.3390/nu11092090

Shen, Y., Jiang, X., Meng, L., Xia, C., Zhang, L., & Xin, Y. (2018). Transplantation of bone marrow mesenchymal stem cells prevents radiation-induced artery injury by suppressing oxidative stress and inflammation. Oxidative Medicine and Cellular Longevity, 2018. https://doi.org/10.1155/2018/5942916

Shi, F., Wang, Y. C., Zhao, T. Z., Zhang, S., Du, T. Y., Yang, C. Bin, Li, Y. H., & Sun, X. Q. (2012). Effects of simulated microgravity on human umbilical vein endothelial cell angiogenesis and role of the PI3K-Akt-eNOS signal pathway. PLoS ONE, 7(7). https://doi.org/10.1371/journal.pone.0040365

Shimizu, Y., Kodama, K., Nishi, N., Kasagi, F., Suyama, A., Soda, M., Grant, E. J., Sugiyama, H., Sakata, R., Moriwaki, H., Hayashi, M., Konda, M., & Shore, R. E. (2010). Radiation exposure and circulatory disease risk: Hiroshima and Nagasaki atomic bomb survivor data, 1950-2003. The BMJ, 340(7739), 193. https://doi.org/10.1136/BMJ.B5349

Siamwala, J. H., Reddy, S. H., Majumder, S., Kolluru, G. K., Muley, A., Sinha, S., & Chatterjee, S. (2010). Simulated microgravity perturbs actin polymerization to promote nitric oxide-associated migration in human immortalized Eahy926 cells. Protoplasma, 242(1), 3–12. https://doi.org/10.1007/s00709-010-0114-z

Slezak, J., Kura, B., Babal, P., Barancik, M., Ferko, M., Frimmel, K., Kalocayova, B., Kukreja, R. C., Lazou, A., Mezesova, L., Okruhlicova, L., Ravingerova, T., Singal, P. K., Bacova, B. S., Viczenczova, C., Vrbjar, N., & Tribulova, N. (2017). Potential markers and metabolic processes involved in the mechanism of Radiation-Induced heart injury. Canadian Journal of Physiology and Pharmacology, 95(10), 1190–1203. https://doi.org/10.1139/cjpp-2017-0121

Soloviev, A. I., & Kizub, I. V. (2019). Mechanisms of vascular dysfunction evoked by ionizing radiation and possible targets for its pharmacological correction. Biochemical Pharmacology, 159, 121–139. https://doi.org/10.1016/j.bcp.2018.11.019

Sonveaux, P., Brouet, A., Havaux, X., Grégoire, V., Dessy, C., Balligand, J. L., & Feron, O. (2003). Irradiation-induced angiogenesis through the up-regulation of the nitric oxide pathway: Implications for tumor radiotherapy. Cancer Research, 63(5), 1012–1019. https://doi.org/10.1016/s0167-8140(03)80572-8

Soucy, K. G., Lim, H. K., Attarzadeh, D. O., Santhanam, L., Kim, J. H., Bhunia, A. K., Sevinc, B., Ryoo, S., Vazquez, M. E., Nyhan, D., Shoukas, A. A., & Berkowitz, D. E. (2010). Dietary inhibition of xanthine oxidase attenuates radiation-induced endothelial dysfunction in rat aorta. Journal of Applied Physiology, 108(5), 1250–1258. https://doi.org/10.1152/japplphysiol.00946.2009

Soucy, K. G., Lim, H. K., Benjo, A., Santhanam, L., Ryoo, S., Shoukas, A. A., Vazquez, M. E., & Berkowitz, D. E. (2007). Single exposure gamma-irradiation amplifies xanthine oxidase activity and induces endothelial dysfunction in rat aorta. Radiation and Environmental Biophysics, 46(2), 179–186. https://doi.org/10.1007/s00411-006-0090-z

Soucy, K. G., Lim, H. K., Kim, J. H., Oh, Y., Attarzadeh, D. O., Sevinc, B., Kuo, M. M., Shoukas, A. A., Vazquez, M. E., & Berkowitz, D. E. (2011). HZE 56Fe-ion irradiation induces endothelial dysfunction in rat aorta: Role of xanthine oxidase. Radiation Research, 176(4), 474–485. https://doi.org/10.1667/RR2598.1

Sridharan, V., Seawright, J. W., Landes, R. D., Cao, M., Singh, P., Davis, C. M., Mao, X. W., Singh, S. P., Zhang, X., Nelson, G. A., & Boerma, M. (2020). Effects of single-dose protons or oxygen ions on function and structure of the cardiovascular system in male Long Evans rats. Life Sciences in Space Research, 26, 62–68. https://doi.org/10.1016/j.lssr.2020.04.002

Srinivasan, L., Harris, M. C., & Kilpatrick, L. E. (2017). Cytokines and Inflammatory Response in the Fetus and Neonate. In Fetal and Neonatal Physiology, 2-Volume Set (pp. 1241–1254). https://doi.org/10.1016/B978-0-323-35214-7.00128-1

Stanojković, T. P., Matić, I. Z., Petrović, N., Stanković, V., Kopčalić, K., Besu, I., Đorđić Crnogorac, M., Mališić, E., Mirjačić-Martinović, K., Vuletić, A., Bukumirić, Z., Žižak, Ž., Veldwijk, M., Herskind, C., & Nikitović, M. (2020). Evaluation of cytokine expression and circulating immune cell subsets as potential parameters of acute radiation toxicity in prostate cancer patients. Scientific Reports, 10(1). https://doi.org/10.1038/s41598-020-75812-0

Su, Y. T., Cheng, Y. P., Zhang, X., Xie, X. P., Chang, Y. M., & Bao, J. X. (2020). Acid sphingomyelinase/ceramide mediates structural remodeling of cerebral artery and small mesenteric artery in simulated weightless rats. Life Sciences, 243. https://doi.org/10.1016/j.lfs.2019.117253

Summers, S. M., Nguyen, S. V., & Purdy, R. E. (2008). Hindlimb unweighting induces changes in the RhoA-Rho-kinase pathway of the rat abdominal aorta. Vascular Pharmacology, 48(4–6), 208–214. https://doi.org/10.1016/j.vph.2008.03.006

Sylvester, C. B., Abe, J. I., Patel, Z. S., & Grande-Allen, K. J. (2018). Radiation-Induced Cardiovascular Disease: Mechanisms and Importance of Linear Energy Transfer. Frontiers in Cardiovascular Medicine, 5, 1. https://doi.org/10.3389/FCVM.2018.00005

Tahimic, C. G. T., & Globus, R. K. (2017). Redox signaling and its impact on skeletal and vascular responses to spaceflight. International Journal of Molecular Sciences, 18(10). https://doi.org/10.3390/ijms18102153

Takahashi, I., Shimizu, Y., Grant, E. J., Cologne, J., Ozasa, K., & Kodama, K. (2017). Heart disease mortality in the life span study, 1950-2008. In Radiation Research (Vol. 187, Issue 3). https://doi.org/10.1667/RR14347.1

Tapio, S. (2016). Pathology and biology of radiation-induced cardiac disease. Journal of Radiation Research, 57(5), 439–448. https://doi.org/10.1093/jrr/rrw064

Tsao, C. W., Aday, A. W., Almarzooq, Z. I., Alonso, A., Beaton, A. Z., Bittencourt, M. S., Boehme, A. K., Buxton, A. E., Carson, A. P., Commodore-Mensah, Y., Elkind, M. S. V., Evenson, K. R., Eze-Nliam, C., Ferguson, J. F., Generoso, G., Ho, J. E., Kalani, R., Khan, S. S., Kissela, B. M., … Martin, S. S. (2022). Heart Disease and Stroke Statistics-2022 Update: A Report From the American Heart Association. Circulation, 145(8), e153–e639. https://doi.org/10.1161/CIR.0000000000001052/FORMAT/EPUB

Ungvari, Z., Podlutsky, A., Sosnowska, D., Tucsek, Z., Toth, P., Deak, F., Gautam, T., Csiszar, A., & Sonntag, W. E. (2013). Ionizing radiation promotes the acquisition of a senescence-associated secretory phenotype and impairs angiogenic capacity in cerebromicrovascular endothelial cells: Role of increased dna damage and decreased dna repair capacity in microvascular radiosens. Journals of Gerontology - Series A Biological Sciences and Medical Sciences, 68(12 A), 1443–1457. https://doi.org/10.1093/gerona/glt057

UNSCEAR. (2008). UNSCEAR 2006 report. Annex B. Epidemiological evaluation of cardiovascular disease and other non_cancer diseases following radiation exposure.

Valerie, K., Yacoub, A., Hagan, M. P., Curiel, D. T., Fisher, P. B., Grant, S., & Dent, P. (2007). Radiation-induced cell signaling: Inside-out and outside-in. Molecular Cancer Therapeutics, 6(3), 789–801. https://doi.org/10.1158/1535-7163.MCT-06-0596

Van Varik, B. J., Rennenberg, R. J. M. W., Reutelingsperger, C. P., Kroon, A. A., De Leeuw, P. W., & Schurgers, L. J. (2012). Mechanisms of arterial remodeling: Lessons from genetic diseases. Frontiers in Genetics, 3(DEC), 290. https://doi.org/10.3389/FGENE.2012.00290/BIBTEX

Varma, S. D., Kovtun, S., & Hegde, K. R. (2011). Role of ultraviolet irradiation and oxidative stress in cataract formation-medical prevention by nutritional antioxidants and metabolic agonists. Eye and Contact Lens, 37(4), 233–245. https://doi.org/10.1097/ICL.0b013e31821ec4f2

Venkatesulu, B. P., Mahadevan, L. S., Aliru, M. L., Yang, X., Bodd, M. H., Singh, P. K., Yusuf, S. W., Abe, J. ichi, & Krishnan, S. (2018). Radiation-Induced Endothelial Vascular Injury: A Review of Possible Mechanisms. JACC: Basic to Translational Science, 3(4), 563–572. https://doi.org/10.1016/j.jacbts.2018.01.014

Verma, S., Buchanan, M. R., & Anderson, T. J. (2003). Endothelial Function Testing as a Biomarker of Vascular Disease. Circulation, 108(17), 2054–2059. https://doi.org/10.1161/01.CIR.0000089191.72957.ED

Vernice, N. A., Meydan, C., Afshinnekoo, E., & Mason, C. E. (2020). Long-term spaceflight and the cardiovascular system. Precision Clinical Medicine, 3(4), 284–291. https://doi.org/10.1093/PCMEDI/PBAA022

Versari, S., Longinotti, G., Barenghi, L., Maier, J. A. M., & Bradamante, S. (2013). The challenging environment on board the International Space Station affects endothelial cell function by triggering oxidative stress through thioredoxin interacting protein overexpression: the ESA-SPHINX experiment. FASEB Journal, 27(11), 4466–4475. https://doi.org/10.1096/fj.13-229195

Wang, H., Wei, J., Zheng, Q., Meng, L., Xin, Y., Yin, X., & Jiang, X. (2019). Radiation-induced heart disease: a review of classification, mechanism and prevention. International Journal of Biological Sciences, 15(10), 2128. https://doi.org/10.7150/IJBS.35460

Wang, Y., Boerma, M., & Zhou, D. (2016). Ionizing Radiation-Induced Endothelial Cell Senescence and Cardiovascular Diseases. Radiation Research, 186(2), 153–161. https://doi.org/10.1667/RR14445.1

Winham, S. J., de Andrade, M., & Miller, V. M. (2014). Genetics of cardiovascular disease: Importance of sex and ethnicity. Atherosclerosis, 241(1), 219–228. https://doi.org/10.1016/j.atherosclerosis.2015.03.021

Yakerson, A. (2019). Women in clinical trials: A review of policy development and health equity in the Canadian context. International Journal for Equity in Health, 18(1), 56. https://doi.org/10.1186/s12939-019-0954-x

Yan, T., Zhang, T., Mu, W., Qi, Y., Guo, S., Hu, N., Zhao, W., Zhang, S., Wang, Q., Shi, L., & Liu, L. (2020). Ionizing radiation induces BH4 deficiency by downregulating GTP-cyclohydrolase 1, a novel target for preventing and treating radiation enteritis. Biochemical Pharmacology, 180, 114102. https://doi.org/10.1016/j.bcp.2020.114102

Yang, Y. et al. (1998), “The Effect of Catalase Amplification on Immortal Lens Epithelial Cell Lines”, Experimental Eye Research, Vol. 67/6, Elsevier, Amsterdam https://doi.org/10.1006/exer.1998.0560

Yang, E. H., Marmagkiolis, K., Balanescu, D. V., Hakeem, A., Donisan, T., Finch, W., Virmani, R., Herrman, J., Cilingiroglu, M., Grines, C. L., Toutouzas, K., & Iliescu, C. (2021). Radiation-Induced Vascular Disease—A State-of-the-Art Review. Frontiers in Cardiovascular Medicine, 8, 223. https://doi.org/10.3389/FCVM.2021.652761/XML/NLM

Yao, L., Romero, M. J., Toque, H. A., Yang, G., Caldwell, R. B., & Caldwell, R. W. (2010). The role of RhoA/Rho kinase pathway in endothelial dysfunction. Journal of Cardiovascular Disease Research, 1(4), 165–170. https://doi.org/10.4103/0975-3583.74258

Yentrapalli, R., Azimzadeh, O., Barjaktarovic, Z., Sarioglu, H., Wojcik, A., Harms-Ringdahl, M., Atkinson, M. J., Haghdoost, S., & Tapio, S. (2013). Quantitative proteomic analysis reveals induction of premature senescence in human umbilical vein endothelial cells exposed to chronic low-dose rate gamma radiation. Proteomics, 13(7), 1096–1107. https://doi.org/10.1002/pmic.201200463

Yentrapalli, R., Azimzadeh, O., Sriharshan, A., Malinowsky, K., Merl, J., Wojcik, A., Harms-Ringdahl, M., Atkinson, M. J., Becker, K. F., Haghdoost, S., & Tapio, S. (2013). The PI3K/Akt/mTOR Pathway Is Implicated in the Premature Senescence of Primary Human Endothelial Cells Exposed to Chronic Radiation. PLoS ONE, 8(8). https://doi.org/10.1371/journal.pone.0070024

Yu, T., Parks, B. W., Yu, S., Srivastava, R., Gupta, K., Wu, X., Khaled, S., Chang, P. Y., Kabarowski, J. H., & Kucik, D. F. (2011). Iron-ion radiation accelerates atherosclerosis in apolipoprotein E-Deficient mice. Radiation Research, 175(6), 766–773. https://doi.org/10.1667/RR2482.1

Zakrzewicz, A., Secomb, T. W., & Pries, A. R. (2002). Angioadaptation: Keeping the vascular system in shape. News in Physiological Sciences, 17(5). https://doi.org/10.1152/nips.01395.2001

Zhang, L. F. (2013). Region-specific vascular remodeling and its prevention by artificial gravity in weightless environment. European Journal of Applied Physiology, 113(12), 2873–2895. https://doi.org/10.1007/S00421-013-2597-8

Zhang, R., Bai, Y. G., Lin, L. J., Bao, J. X., Zhang, Y. Y., Tang, H., Cheng, J. H., Jia, G. L., Ren, X. L., & Jin, M. (2009). Blockade of at 1 receptor partially restores vasoreactivity, NOS expression, and superoxide levels in cerebral and carotid arteries of hindlimb unweighting rats. Journal of Applied Physiology, 106(1), 251–258. https://doi.org/10.1152/japplphysiol.01278.2007

Zielinski, J. M., Ashmore, P. J., Band, P. R., Jiang, H., Shilnikova, N. S., Tait, V. K., & Krewski, D. (2009). Low dose ionizing radiation exposure and cardiovascular disease mortality: Cohort study based on Canadian national dose registry of radiation workers. International Journal of Occupational Medicine and Environmental Health, 22(1), 27–33. https://doi.org/10.2478/v10001-009-0001-z

Zieman, S. J., Melenovsky, V., & Kass, D. A. (2005). Mechanisms, Pathophysiology, and Therapy of Arterial Stiffness. Arteriosclerosis, Thrombosis, and Vascular Biology, 25(5), 932–943. https://doi.org/10.1161/01.ATV.0000160548.78317.29

Zigman, S., McDaniel, T., Schultz, J., & Reddan, J. (2000). Effects of intermittent UVA exposure on cultured lens epithelial cells. Current Eye Research, 20(2), 95–100. https://doi.org/10.1076/0271-3683(200002)2021-DFT095

Zou, B., Schuster, J. P., Niu, K., Huang, Q., Rühle, A., & Huber, P. E. (2019). Radiotherapy-induced heart disease: a review of the literature. Precision Clinical Medicine, 2(4), 270–282. https://doi.org/10.1093/pcmedi/pbz025

Appendix 1

List of MIEs in this AOP

Event: 1686: Deposition of Energy

Short Name: Energy Deposition

AOPs Including This Key Event

AOP ID and Name	Event Type
Aop:272 - Deposition of energy leading to lung cancer	MolecularInitiatingEvent
Aop:432 - Deposition of Energy by Ionizing Radiation leading to Acute Myeloid Leukemia	MolecularInitiatingEvent
Aop:386 - Deposition of ionizing energy leading to population decline via inhibition of photosynthesis	MolecularInitiatingEvent
Aop:387 - Deposition of ionising energy leading to population decline via mitochondrial dysfunction	MolecularInitiatingEvent
Aop:388 - Deposition of ionising energy leading to population decline via programmed cell death	MolecularInitiatingEvent
Aop:435 - Deposition of ionising energy leads to population decline via pollen abnormal	MolecularInitiatingEvent
Aop:216 - Deposition of energy leading to population decline via DNA strand breaks and follicular atresia	MolecularInitiatingEvent
Aop:238 - Deposition of energy leading to population decline via DNA strand breaks and oocyte apoptosis	MolecularInitiatingEvent
Aop:311 - Deposition of energy leading to population decline via DNA oxidation and oocyte apoptosis	MolecularInitiatingEvent
Aop:299 - Deposition of energy leading to population decline via DNA oxidation and follicular atresia	MolecularInitiatingEvent
Aop:441 - Ionizing radiation-induced DNA damage leads to microcephaly via apoptosis and premature cell differentiation	MolecularInitiatingEvent
Aop:444 - Ionizing radiation leads to reduced reproduction in Eisenia fetida via reduced spermatogenesis and cocoon hatchability	MolecularInitiatingEvent
Aop:470 - Deposition of energy leads to vascular remodeling	MolecularInitiatingEvent
Aop:473 - Energy deposition from internalized Ra-226 decay lower oxygen binding capacity of hemocyanin	MolecularInitiatingEvent
Aop:478 - Deposition of energy leading to occurrence of cataracts	MolecularInitiatingEvent
Aop:482 - Deposition of energy leading to occurrence of bone loss	MolecularInitiatingEvent
Aop:483 - Deposition of Energy Leading to Learning and Memory Impairment	MolecularInitiatingEvent

Stressors

Name
Ionizing Radiation

Biological Context

Level of Biological Organization
Molecular

Evidence for Perturbation by Stressor

Overview for Molecular Initiating Event

It is well documented that ionizing radiation((eg. X-rays, gamma, photons, alpha, beta, neutrons, heavy ions) leads to energy deposition on the atoms and molecules of the substrate. Many studies, have demonstrated that the type of radiation and distance from source has an impact on the pattern of energy deposition (Alloni, et al. 2014). High linear energy transfer (LET) radiation has been associated with higher-energy deposits (Liamsuwan et al., 2014) that are more densely-packed and cause more complex effects within the particle track (Hada and Georgakilas, 2008; Okayasu, 2012ab; Lorat et al., 2015; Nikitaki et al., 2016) in comparison to low LET radiation. Parameters such as mean lineal energy, dose mean lineal energy, frequency mean specific energy and dose mean specific energy can impact track structure of the traversed energy into a medium (Friedland et al., 2017). The detection of energy deposition by ionizing radiation can be demonstrated with the use of fluorescent nuclear track detectors (FNTDs). FNTDs used in conjunction with fluorescent microscopy, are able to visualize radiation tracks produced by ionizing radiation (Niklas et al., 2013; Kodaira et al., 2015; Sawakuchi and Akselrod, 2016). In addition, these FNTD chips can quantify the LET of primary and secondary radiation tracks up to 0.47 keV/um (Sawakuchi and Akselrod, 2016). This co-visualization of the radiation tracks and the cell markers enable the mapping of the radiation trajectory to specific cellular compartments, and the identification of accrued damage (Niklas et al., 2013; Kodaira et al., 2015). There are no known chemical initiators or prototypes that can mimic the MIE.

Domain of Applicability

Taxonomic Applicability

Term	Scientific Term	Evidence	Links
human	Homo sapiens	Moderate	NCBI
rat	Rattus norvegicus	Moderate	NCBI
mouse	Mus musculus	Moderate	NCBI
nematode	Caenorhabditis elegans	High	NCBI
zebrafish	Danio rerio	High	NCBI
thale-cress	Arabidopsis thaliana	High	NCBI
Scotch pine	Pinus sylvestris	Moderate	NCBI
Daphnia magna	Daphnia magna	High	NCBI
Chlamydomonas reinhardtii	Chlamydomonas reinhardtii	Moderate	NCBI
common brandling worm	eisenia fetida	Moderate	NCBI
Lemna minor	Lemna minor	High	NCBI
Salmo salar	Salmo salar	Low	NCBI

Life Stage Applicability

Life Stage	Evidence
All life stages	High

Sex Applicability

Sex	Evidence
Unspecific	Low

Energy can be deposited into any substrate, both living and non-living; it is independent of age, taxa, sex, or life-stage.

Taxonomic applicability: This MIE is not taxonomically specific.

Life stage applicability: This MIE is not life stage specific.

Sex applicability: This MIE is not sex specific.

Key Event Description

Deposition of energy refers to events where energetic subatomic particles, nuclei, or electromagnetic radiation deposit energy in the media through which they transverse. The energy may either be sufficient (e.g. ionizing radiation) or insufficient (e.g. non-ionizing radiation) to ionize atoms or molecules (Beir et al.,1999).

Ionizing radiation can cause the ejection of electrons from atoms and molecules, thereby resulting in their ionization and the breakage of chemical bonds. The energy of these subatomic particles or electromagnetic waves mostly range from 124 KeV to 5.4 MeV and is dependent on the source and type of radiation (Zyla et al., 2020). To be ionizing the incident radiation must have sufficient energy to free electrons from atomic or molecular electron orbitals. The energy deposited can induce direct and indirect ionization events and this can be via internal (injections, inhalation, or absorption of radionuclides) or external exposure from radiation fields -- this also applies to non-ionizing radiation.

Direct ionization is the principal path where charged particles interact with biological structures such as DNA, proteins or membranes to cause biological damage. Photons, which are electromagnetic waves can also deposit energy to cause direct ionization. Ionization of water, which is a major constituent of tissues and organs, produces free radical and molecular species, which themselves can indirectly damage critical targets such as DNA (Beir et al., 1999; Balagamwala et al., 2013) or alter cellular processes. Given the fundamental nature of energy deposition by radioactive/unstable nuclei, nucleons or elementary particles in material, this process is universal to all biological contexts.

The spatial structure of ionizing energy deposition along the resulting particle track is represented as linear energy transfer (LET) (Hall and Giaccia, 2018 UNSCEAR, 2020). High LET refers to energy mostly above 10 keV μm^{-1} which produces more complex, dense structural damage than low LET radiation (below 10 keV μm^{-1}). Low-LET particles produce sparse ionization events such as photons (X- and gamma rays), as well as high-energy protons. Low LET radiation travels farther into tissue but deposits smaller amounts of energy, whereas high LET radiation, which includes heavy ions, alpha particles and high-energy neutrons, does not travel as far but deposits larger amounts of energy into tissue at the same absorbed dose. The biological effect of the deposition of energy can be modulated by varying dose and dose rate of exposure, such as acute, chronic, or fractionated exposures (Hall and Giaccia, 2018).

Non-ionizing radiation is electromagnetic waves that does not have enough energy to break bonds and induce ion formation but it can cause molecules to excite and vibrate faster resulting in biological effects. Examples of non-ionizing radiation include radio waves (wavelength: 100 km-1m), microwaves (wavelength: 1m-1mm), infrared radiation (wavelength: 1mm- 1 um), visible light (wavelengths: 400-700 nm), and ultraviolet radiation of longer wavelengths such as UVB (wavelengths: 315-400nm) and UVA (wavelengths: 280-315 nm). UVC radiation (X-X nm) is, in contrast to UVB and UVA, considered to be a type of ionizing radiation.

How it is Measured or Detected

Radiation type	Assay Name	References	Description	OECD Approved Assay
Ionizing radiation	Monte Carlo Simulations (Geant4)	Douglass et al., 2013; Douglass et al. 2012; Zyla et al., 2020	Monte Carlo simulations are based on a computational algorithm that mathematically models the deposition of energy into materials.	No
Ionizing radiation	Fluorescent Nuclear Track Detector (FNTD)	Sawakuchi, 2016; Niklas, 2013; Koaira & Konishi, 2015	FNTDs are biocompatible chips with crystals of aluminium oxide doped with carbon and magnesium; used in conjuction with fluorescent microscopy, these FNTDs allow for the visualization and the linear energy transfer (LET) quantification of tracks produced by the deposition of energy into a material.	No
Ionizing radiation	Tissue equivalent proportional counter (TEPC)	Straume et al, 2015	Measure the LET spectrum and calculate the dose equivalent.	No
Ionizing radiation	alanine dosimeters/NanoDots	Lind et al. 2019; Xie et al., 2022		No
Non-ionizing radiation	UV meters or radiameters	Xie et at., 2020	UVA/UVB (irradiance intensity), UV dosimeters (accumulated irradiance over time), Spectrophoto meter (absorption of UV by a substance or material)	No

References

Balagamwala, E. H. et al. (2013), “Introduction to radiotherapy and standard teletherapy techniques”, *Dev Ophthalmol*, Vol. 52, Karger, Basel, https://doi.org/10.1159/000351045

Beir, V. et al. (1999), “The Mechanistic Basis of Radon-Induced Lung Cancer”, in *Health Risks of Exposure to Radon: BEIR VI*, National Academy Press, Washington, D.C., https://doi.org/10.17226/5499

Douglass, M. et al. (2013), “Monte Carlo investigation of the increased radiation deposition due to gold nanoparticles using kilovoltage and megavoltage photons in a 3D

randomized cell model", *Medical Physics*, Vol. 40/7, American Institute of Physics, College Park, https://doi.org/10.1118/1.4808150

Douglass, M. et al. (2012), "Development of a randomized 3D cell model for Monte Carlo microdosimetry simulations.", *Medical Physics*, Vol. 39/6, American Institute of Physics, College Park, https://doi.org/10.1118/1.4719963

Hall, E. J. and Giaccia, A.J. (2018), *Radiobiology for the Radiologist*, 8th edition, Wolters Kluwer, Philadelphia.

Kodaira, S. and Konishi, T. (2015), "Co-visualization of DNA damage and ion traversals in live mammalian cells using a fluorescent nuclear track detector.", *Journal of Radiation Research*, Vol. 56/2, Oxford University Press, Oxford, https://doi.org/10.1093/jrr/rru091

Lind, O.C., D.H. Oughton and Salbu B. (2019), "The NMBU FIGARO low dose irradiation facility", *International Journal of Radiation Biology*, Vol. 95/1, Taylor & Francis, London, https://doi.org/10.1080/09553002.2018.1516906.

Sawakuchi, G.O. and Akselrod, M.S. (2016), "Nanoscale measurements of proton tracks using fluorescent nuclear track detectors.", *Medical Physics*, Vol. 43/5, American Institute of Physics, College Park, https://doi.org/10.1118/1.4947128

Straume, T. et al. (2015), "Compact Tissue-equivalent Proportional Counter for Deep Space Human Missions.", *Health physics,* Vol. 109/4, Lippincott Williams & Wilkins, Philadelphia, https://doi.org/10.1097/HP.0000000000000334

Niklas, M. et al. (2013), "Engineering cell-fluorescent ion track hybrid detectors.", *Radiation Oncology*, Vol. 8/104, BioMed Central, London, https://doi.org/10.1186/1748-717X-8-141

UNSCEAR (2020), *Sources, effects and risks of ionizing radiation*, United Nations.

Xie, Li. et al. (2022), "Ultraviolet B Modulates Gamma Radiation-Induced Stress Responses in Lemna Minor at Multiple Levels of Biological Organisation", *SSRN*, Elsevier, Amsterdam, http://dx.doi.org/10.2139/ssrn.4081705 .

Zyla, P.A. et al. (2020), *Review of particle physics: Progress of Theoretical and Experimental Physics,* 2020 Edition, Oxford University Press, Oxford.

List of Key Events in the AOP

Event: 1392: Oxidative Stress

Short Name: Oxidative Stress

Key Event Component

Process	Object	Action
oxidative stress		increased

AOPs Including This Key Event

AOP ID and Name	Event Type
Aop:220 - Cyp2E1 Activation Leading to Liver Cancer	KeyEvent
Aop:17 - Binding of electrophilic chemicals to SH(thiol)-group of proteins and /or to seleno-proteins involved in protection against oxidative stress during brain development leads to impairment of learning and memory	KeyEvent
Aop:284 - Binding of electrophilic chemicals to SH(thiol)-group of proteins and /or to seleno-proteins involved in protection against oxidative stress leads to chronic kidney disease	KeyEvent
Aop:377 - Dysregulated prolonged Toll Like Receptor 9 (TLR9) activation leading to Multi Organ Failure involving Acute Respiratory Distress Syndrome (ARDS)	KeyEvent
Aop:411 - Oxidative stress Leading to Decreased Lung Function	MolecularInitiatingEvent
Aop:424 - Oxidative stress Leading to Decreased Lung Function via CFTR dysfunction	MolecularInitiatingEvent
Aop:425 - Oxidative Stress Leading to Decreased Lung Function via Decreased FOXJ1	MolecularInitiatingEvent
Aop:429 - A cholesterol/glucose dysmetabolism initiated Tau-driven AOP toward memory loss (AO) in sporadic Alzheimer's Disease with plausible MIE's plug-ins for environmental neurotoxicants	KeyEvent
Aop:437 - Inhibition of mitochondrial electron transport chain (ETC) complexes leading to kidney toxicity	KeyEvent
Aop:452 - Adverse outcome pathway of PM-induced respiratory toxicity	KeyEvent
Aop:464 - Calcium overload in dopaminergic neurons of the substantia nigra leading to parkinsonian	

AOP ID and Name	Event Type
motor deficits	KeyEvent
Aop:470 - Deposition of energy leads to vascular remodeling	KeyEvent
Aop:478 - Deposition of energy leading to occurrence of cataracts	KeyEvent
Aop:479 - Mitochondrial complexes inhibition leading to heart failure via increased myocardial oxidative stress	KeyEvent
Aop:481 - AOPs of amorphous silica nanoparticles: ROS-mediated oxidative stress increased respiratory dysfunction and diseases.	KeyEvent
Aop:482 - Deposition of energy leading to occurrence of bone loss	KeyEvent
Aop:483 - Deposition of Energy Leading to Learning and Memory Impairment	KeyEvent

Stressors

Name
Acetaminophen
Chloroform
furan
Platinum
Aluminum
Cadmium
Mercury
Uranium
Arsenic
Silver
Manganese
Nickel
Zinc
nanoparticles

Biological Context

Level of Biological Organization
Molecular

Evidence for Perturbation by Stressor

Platinum

Kruidering et al. (1997) examined the effect of platinum on pig kidneys and found that it was able to induce significant dose-dependant ROS formation within 20 minutes of treatment administration.

Aluminum

In a study of the effects of aluminum treatment on rat kidneys, Al Dera (2016) found that renal GSH, SOD, and GPx levels were significantly lower in the treated groups, while lipid peroxidation levels were significantly increased.

Cadmium

Belyaeva et al. (2012) investigated the effect of cadmium treatment on human kidney cells. They found that cadmium was the most toxic when the sample was treated with 500 µM for 3 hours (Belyaeva et al., 2012). As this study also looked at mercury, it is worth noting that mercury was more toxic than cadmium in both 30-minute and 3-hour exposures at low concentrations (10-100 µM) (Belyaeva et al., 2012).

Wang et al. (2009) conducted a study evaluating the effects of cadmium treatment on rats and found that the treated group showed a significant increase in lipid peroxidation. They also assessed the effects of lead in this study, and found that cadmium can achieve a very similar level of lipid peroxidation at a much lower concentration than lead can, implying that cadmium is a much more toxic metal to the kidney mitochondria than lead is (Wang et al., 2009). They also found that when lead and cadmium were applied together they had an additive effect in increasing lipid peroxidation content in the renal cortex of rats (Wang et al., 2009).

Jozefczak et al. (2015) treated *Arabidopsis thaliana* wildtype, *cad2-1* mutant, and *vtc1-1* mutant plants with cadmium to determine the effects of heavy metal exposure to plant mitochondria in the roots and leaves. They found that total GSH/GSG ratios were significantly increased after cadmium exposure in the leaves of all sample varieties and that GSH content was most significantly decreased for the wildtype plant roots (Jozefczak et al., 2015).

Andjelkovic et al. (2019) also found that renal lipid peroxidation was significantly increased in rats treated with 30 mg/kg of cadmium.

Mercury

Belyaeva et al. (2012) conducted a study which looked at the effects of mercury on human kidney cells, they found that mercury was the most toxic when the sample was treated with 100 µM for 30 minutes.

Buelna-Chontal et al. (2017) investigated the effects of mercury on rat kidneys and found that treated rats had higher lipid peroxidation content and reduced cytochrome c content in their kidneys.

Uranium

In Shaki et al.'s article (2012), they found rat kidney mitochondria treated with uranyl acetate caused increased formation of ROS, increased lipid peroxidation, and decreased GSH content when exposed to 100 µM or more for an hour.

Hao et al. (2014), found that human kidney proximal tubular cells (HK-2 cells) treated with uranyl nitrate for 24 hours with 500 µM showed a 3.5 times increase in ROS production compared to the control. They also found that GSH content was decreased by 50% of the control when the cells were treated with uranyl nitrate (Hao et al., 2014).

Arsenic

Bhadauria and Flora (2007) studied the effects of arsenic treatment on rat kidneys. They found that lipid peroxidation levels were increased by 1.5 times and the GSH/GSSG ratio was decreased significantly (Bhadauria and Flora, 2007).

Kharroubi et al. (2014) also investigated the effect of arsenic treatment on rat kidneys and found that lipid peroxidation was significantly increased, while GSH content was significantly decreased.

In their study of the effects of arsenic treatment on rat kidneys, Turk et al. (2019) found that lipid peroxidation was significantly increased while GSH and GPx renal content were decreased.

Silver

Miyayama et al. (2013) investigated the effects of silver treatment on human bronchial epithelial cells and found that intracellular ROS generation was increased significantly in a dose-dependant manner when treated with 0.01 to 1.0 µM of silver nitrate.

Manganese

Chtourou et al. (2012) investigated the effects of manganese treatment on rat kidneys. They found that manganese treatment caused significant increases in ROS production, lipid peroxidation, urinary H_2O_2 levels, and PCO production. They also found that intracellular GSH content was depleted in the treated group (Chtourou et al., 2012).

Nickel

Tyagi et al. (2011) conducted a study of the effects of nickel treatment on rat kidneys. They found that the treated rats showed a significant increase in kidney lipid peroxidation and a significant decrease in GSH content in the kidney tissue (Tyagi et al., 2011).

Zinc

Yeh et al. (2011) investigated the effects of zinc treatment on rat kidneys and found that treatment with 150 µM or more for 2 weeks or more caused a time- and dose-dependant increase in lipid peroxidation. They also found that renal GSH content was decreased in the rats treated with 150 µM or more for 8 weeks (Yeh et al., 2011).

It should be noted that Hao et al. (2014) found that rat kidneys exposed to lower concentrations of zinc (such as 100 µM) for short time periods (such as 1 day), showed a protective effect against toxicity induced by other heavy metals, including uranium. Soussi,

Gargouri, and El Feki (2018) also found that pre-treatment with a low concentration of zinc (10 mg/kg treatment for 15 days) protected the renal cells of rats were from changes in varying oxidative stress markers, such as lipid peroxidation, protein carbonyl, and GPx levels.

nanoparticles

Huerta-García et al. (2014) conducted a study of the effects of titanium nanoparticles on human and rat brain cells. They found that both the human and rat cells showed time-dependant increases in ROS when treated with titanium nanoparticles for 2 to 6 hours (Huerta-García et al., 2014). They also found elevated lipid peroxidation that was induced by the titanium nanoparticle treatment of human and rat cell lines in a time-dependant manner (Huerta-García et al., 2014).

Liu et al. (2010) also investigated the effects of titanium nanoparticles, however they conducted their trials on rat kidney cells. They found that ROS production was significantly increased in a dose dependant manner when treated with 10 to 100 µg/mL of titanium nanoparticles (Liu et al., 2010).

Pan et al. (2009) treated human cervix carcinoma cells with gold nanoparticles (Au1.4MS) and found that intracellular ROS content in the treated cells increased in a time-dependant manner when treated with 100 µM for 6 to 48 hours. They also compared the treatment with Au1.4MS gold nanoparticles to treatment with Au15MS treatment, which are another size of gold nanoparticle (Pan et al., 2009). The Au15MS nanoparticles were much less toxic than the Au1.4MS gold nanoparticles, even when the Au15MS nanoparticles were applied at a concentration of 1000 µM (Pan et al., 2009). When investigating further markers of oxidative stress, Pan et al. (2009) found that GSH content was greatly decreased in cells treated with gold nanoparticles.

Ferreira et al. (2015) also studied the effects of gold nanoparticles. They exposed rat kidneys to GNPs-10 (10 nm particles) and GNPs-30 (30 nm particles), and found that lipid peroxidation and protein carbonyl content in the rat kidneys treated with GNPs-30 and GNPs-10, respectively, were significantly elevated.

Domain of Applicability

Taxonomic Applicability

Term	Scientific Term	Evidence	Links
rodents	rodents	High	NCBI
Homo sapiens	Homo sapiens	High	NCBI

Life Stage Applicability

Life Stage	Evidence
All life stages	High

Sex Applicability

Sex	Evidence
Mixed	High

Taxonomic applicability: Occurrence of oxidative stress is not species specific.

Life stage applicability: Occurrence of oxidative stress is not life stage specific.

Sex applicability: Occurrence of oxidative stress is not sex specific.

Evidence for perturbation by prototypic stressor: There is evidence of the increase of oxidative stress following perturbation from a variety of stressors including exposure to ionizing radiation and altered gravity (Bai et al., 2020; Ungvari et al., 2013; Zhang et al., 2009).

Key Event Description

Oxidative stress is defined as an imbalance in the production of reactive oxygen species (ROS) and antioxidant defenses. High levels of oxidizing free radicals can be very damaging to cells and molecules within the cell. As a result, the cell has important defense mechanisms to protect itself from ROS. For example, Nrf2 is a transcription factor and master regulator of the oxidative stress response. During periods of oxidative stress, Nrf2-dependent changes in gene expression are important in regaining cellular homeostasis (Nguyen, et al. 2009) and can be used as indicators of the presence of oxidative stress in the cell.

In addition to the directly damaging actions of ROS, cellular oxidative stress also changes cellular activities on a molecular level. Redox sensitive proteins have altered physiology in the presence and absence of ROS, which is caused by the oxidation of sulfhydryls to disulfides (2SH àSS) on neighboring amino acids (Antelmann and Helmann 2011). Importantly Keap1, the negative regulator of Nrf2, is regulated in this manner (Itoh, et al. 2010).

ROS also undermine the mitochondrial defense system from oxidative damage. The antioxidant systems consist of superoxide dismutase, catalase, glutathione peroxidase and glutathione reductase, as well as antioxidants such as α-tocopherol and ubiquinol,

or antioxidant vitamins and minerals including vitamin E, C, carotene, lutein, zeaxanthin, selenium, and zinc (Fletcher, 2010). The enzymes, vitamins and minerals catalyze the conversion of ROS to non-toxic molecules such as water and O_2. However, these antioxidant systems are not perfect and endogenous metabolic processes and/or exogenous oxidative influences can trigger cumulative oxidative injuries to the mitochondria, causing a decline in their functionality and efficiency, which further promotes cellular oxidative stress (Balasubramanian, 2000; Ganea & Harding, 2006; Guo et al., 2013; Karimi et al., 2017).

However, an emerging viewpoint suggests that ROS-induced modifications may not be as detrimental as previously thought, but rather contribute to signaling processes (Foyer et al., 2017).

Protection against oxidative stress is relevant for all tissues and organs, although some tissues may be more susceptible. For example, the brain possesses several key physiological features, such as high O2 utilization, high polyunsaturated fatty acids content, presence of autooxidable neurotransmitters, and low antioxidant defenses as compared to other organs, that make it highly susceptible to oxidative stress (Halliwell, 2006; Emerit and al., 2004; Frauenberger et al., 2016).

Sources of ROS Production

Direct Sources: Direct sources involve the deposition of energy onto water molecules, breaking them into active radical species. When ionizing radiation hits water, it breaks it into hydrogen (H*) and hydroxyl (OH*) radicals by destroying its bonds. The hydrogen will create hydroxyperoxyl free radicals (HO_2*) if oxygen is available, which can then react with another of itself to form hydrogen peroxide (H_2O_2) and more O_2 (Elgazzar and Kazem, 2015). Antioxidant mechanisms are also affected by radiation, with catalase (CAT) and peroxidase (POD) levels rising as a result of exposure (Seen et al. 2018; Ahmad et al. 2021).

Indirect Sources: An indirect source of ROS is the mitochondria, which is one of the primary producers in eukaryotic cells (Powers et al., 2008). As much as 2% of the electrons that should be going through the electron transport chain in the mitochondria escape, allowing them an opportunity to interact with surrounding structures. Electron-oxygen reactions result in free radical production, including the formation of hydrogen peroxide (H_2O_2) (Zhao et al., 2019). The electron transport chain, which also creates ROS, is activated by free adenosine diphosphate (ADP), O_2, and inorganic phosphate (P_i) (Hargreaves et al. 2020; Raimondi et al. 2020; Vargas-Mendoza et al. 2021). The first and third complexes of the transport chain are the most relevant to mammalian ROS production (Raimondi et al., 2020). The mitochondria have its own set of DNA and it is a prime target of oxidative damage (Guo et al., 2013). ROS are also produced through nicotinamide adenine dinucleotide phosphate oxidase (NOX) stimulation, an event commenced by angiotensin II, a product/effector of the renin-angiotensin system (Nguyen Dinh Cat et al. 2013; Forrester et al. 2018). Other ROS producers include xanthine oxidase, immune cells (macrophage, neutrophils, monocytes, and eosinophils), phospholipase A_2 (PLA_2), monoamine oxidase (MAO), and carbon-based nanomaterials (Powers et al. 2008; Jacobsen et al. 2008; Vargas-Mendoza et al. 2021).

How it is Measured or Detected

Oxidative Stress. Direct measurement of ROS is difficult because ROS are unstable. The presence of ROS can be assayed indirectly by measurement of cellular antioxidants, or by ROS-dependent cellular damage. Listed below are common methods for detecting the KE, however there may be other comparable methods that are not listed

- Detection of ROS by chemiluminescence (https://www.sciencedirect.com/science/article/abs/pii/S0165993606001683)
- Detection of ROS by chemiluminescence is also described in OECD TG 495 to assess phototoxic potential.
- Glutathione (GSH) depletion. GSH can be measured by assaying the ratio of reduced to oxidized glutathione (GSH:GSSG) using a commercially available kit (e.g., http://www.abcam.com/gshgssg-ratio-detection-assay-kit-fluorometric-green-ab138881.html).
- TBARS. Oxidative damage to lipids can be measured by assaying for lipid peroxidation using TBARS (thiobarbituric acid reactive substances) using a commercially available kit.
- 8-oxo-dG. Oxidative damage to nucleic acids can be assayed by measuring 8-oxo-dG adducts (for which there are a number of ELISA based commercially available kits),or HPLC, described in Chepelev et al. (Chepelev, et al. 2015).

Molecular Biology: Nrf2. Nrf2's transcriptional activity is controlled post-translationally by oxidation of Keap1. Assay for Nrf2 activity include:

- Immunohistochemistry for increases in Nrf2 protein levels and translocation into the nucleus
- Western blot for increased Nrf2 protein levels
- Western blot of cytoplasmic and nuclear fractions to observe translocation of Nrf2 protein from the cytoplasm to the nucleus
- qPCR of Nrf2 target genes (e.g., Nqo1, Hmox-1, Gcl, Gst, Prx, TrxR, Srxn), or by commercially available pathway-based qPCR array (e.g., oxidative stress array from SABiosciences)
- Whole transcriptome profiling by microarray or RNA-seq followed by pathway analysis (in IPA, DAVID, metacore, etc.) for enrichment of the Nrf2 oxidative stress response pathway (e.g., Jackson et al. 2014)
- OECD TG422D describes an ARE-Nrf2 Luciferase test method
- In general, there are a variety of commercially available colorimetric or fluorescent kits for detecting Nrf2 activation

Assay Type & Measured	Description	Dose Range	Assay Characteristics (Length

Content		Studied	/ Ease of use/Accuracy)
ROS Formation in the Mitochondria assay (Shaki et al., 2012)	"The mitochondrial ROS measurement was performed flow cytometry using DCFH-DA. Briefly, isolated kidney mitochondria were incubated with UA (0, 50, 100 and 200 µM) in respiration buffer containing (0.32 mM sucrose, 10 mM Tris, 20 mM Mops, 50 µM EGTA, 0.5 mM MgCl2, 0.1 mM KH2PO4 and 5 mM sodium succinate) [32]. In the interval times of 5, 30 and 60 min following the UA addition, a sample was taken and DCFH-DA was added (final concentration, 10 µM) to mitochondria and was then incubated for 10 min. Uranyl acetate-induced ROS generation in isolated kidney mitochondria were determined through the flow cytometry (Partec, Deutschland) equipped with a 488-nm argon ion laser and supplied with the Flomax software and the signals were obtained using a 530-nm bandpass filter (FL-1 channel). Each determination is based on the mean fluorescence intensity of 15,000 counts."	0, 50, 100 and 200 µM of Uranyl Acetate	Long/ Easy High accuracy
Mitochondrial Antioxidant Content Assay Measuring GSH content (Shaki et al., 2012)	"GSH content was determined using DTNB as the indicator and spectrophotometer method for the isolated mitochondria. The mitochondrial fractions (0.5 mg protein/ml) were incubated with various concentrations of uranyl acetate for 1 h at 30 °C and then 0.1 ml of mitochondrial fractions was added into 0.1 mol/l of phosphate buffers and 0.04% DTNB in a total volume of 3.0 ml (pH 7.4). The developed yellow color was read at 412 nm on a spectrophotometer (UV-1601 PC, Shimadzu, Japan). GSH content was expressed as µg/mg protein."	0, 50, 100, or 200 μM Uranyl Acetate	
H_2O_2 Production Assay Measuring H_2O_2 Production in isolated mitochondria (Heyno et al., 2008)	"Effect of $CdCl_2$ and antimycin A (AA) on H_2O_2 production in isolated mitochondria from potato. H_2O_2 production was measured as scopoletin oxidation. Mitochondria were incubated for 30 min in the measuring buffer (see the Materials and Methods) containing 0.5 mM succinate as an electron donor and 0.2 µM mesoxalonitrile 3-chlorophenylhydrazone (CCCP) as an uncoupler, 10 U horseradish peroxidase and 5 µM scopoletin." (	0, 10, 30 μM Cd^{2+} 2 μM antimycin A	
Flow Cytometry ROS & Cell Viability (Kruiderig et al., 1997)	"For determination of ROS, samples taken at the indicated time points were directly transferred to FACScan tubes. Dih123 (10 mM, final concentration) was added and cells were incubated at 37°C in a humidified atmosphere (95% air/5% CO2) for 10 min. At *t* 5 9, propidium iodide (10 mM, final concentration) was added, and cells were analyzed by flow cytometry at 60 ml/min. Nonfluorescent Dih123 is cleaved by ROS to fluorescent R123 and detected by the FL1 detector as described above for Dc (Van de Water 1995)"		Strong/easy medium
DCFH-DA Assay Detection of hydrogen peroxide production (Yuan et al., 2016)	Intracellular ROS production was measured using DCFH-DA as a probe. Hydrogen peroxide oxidizes DCFH to DCF. The probe is hydrolyzed intracellularly to DCFH carboxylate anion. No direct reaction with H_2O_2 to form fluorescent production.	0-400 µM	Long/ Easy High accuracy
H2-DCF-DA Assay Detection of superoxide production (Thiebault et al., 2007)	This dye is a stable nonpolar compound which diffuses readily into the cells and yields H2-DCF. Intracellular OH or ONOO- react with H2-DCF when cells contain peroxides, to form the highly fluorescent compound DCF, which effluxes the cell. Fluorescence intensity of DCF is measured using a fluorescence spectrophotometer.	0–600 µM	Long/ Easy High accuracy
CM-H2DCFDA Assay	**Come back and explain the flow cytometry determination of oxidative stress from Pan et al. (2009)**		

Direct Methods of Measurement

Method of Measurement	References	Description	OECD-Approved Assay
Chemiluminescence	(Lu, C. et	ROS can induce electron transitions in	No

	al., 2006; Griendling, K. K., et al., 2016)	molecules, leading to electronically excited products. When the electrons transition back to ground state, chemiluminescence is emitted and can be measured. Reagents such as uminol and lucigenin are commonly used to amplify the signal.	
Spectrophotometry	(Griendling, K. K., et al., 2016)	NO has a short half-life. However, if it has been reduced to nitrite (NO2-), stable azocompounds can be formed via the Griess Reaction, and further measured by spectrophotometry.	No
Direct or Spin Trapping-Based Electron Paramagnetic Resonance (EPR) Spectroscopy	(Griendling, K. K., et al., 2016)	The unpaired electrons (free radicals) found in ROS can be detected with EPR, and is known as electron paramagnetic resonance. A variety of spin traps can be used.	No
Nitroblue Tetrazolium Assay	(Griendling, K. K., et al., 2016)	The Nitroblue Tetrazolium assay is used to measure $O_2^{\bullet -}$ levels. $O_2^{\bullet -}$ reduces nitroblue tetrazolium (a yellow dye) to formazan (a blue dye), and can be measured at 620 nm.	No
Fluorescence analysis of dihydroethidium (DHE) or Hydrocyans	(Griendling, K. K., et al., 2016)	Fluorescence analysis of DHE is used to measure $O_2^{\bullet -}$ levels. $O_2^{\bullet -}$ is reduced to O2 as DHE is oxidized to 2-hydroxyethidium, and this reaction can be measured by fluorescence. Similarly, hydrocyans can be oxidized by any ROS, and measured via fluorescence.	No
Amplex Red Assay	(Griendling, K. K., et al., 2016)	Fluorescence analysis to measure extramitochondrial or extracellular H_2O_2 levels. In the presence of horseradish peroxidase and H_2O_2, Amplex Red is oxidized to resorufin, a fluorescent molecule measurable by plate reader.	No
Dichlorodihydrofluorescein Diacetate (DCFH-DA)	(Griendling, K. K., et al., 2016)	An indirect fluorescence analysis to measure intracellular H_2O_2 levels. H_2O_2 interacts with peroxidase or heme proteins, which further react with DCFH, oxidizing it to dichlorofluorescein (DCF), a fluorescent product.	No
HyPer Probe	(Griendling, K. K., et al., 2016)	Fluorescent measurement of intracellular H_2O_2 levels. HyPer is a genetically encoded fluorescent sensor that can be used for *in vivo* and *in situ* imaging.	No
Cytochrome c Reduction Assay	(Griendling, K. K., et al., 2016)	The cytochrome c reduction assay is used to measure $O_2^{\bullet -}$ levels. $O_2^{\bullet -}$ is reduced to O2 as ferricytochrome c is oxidized to ferrocytochrome c, and this reaction can be measured by an absorbance increase at 550 nm.	No
Proton-electron double-resonance imagine (PEDRI)	(Griendling, K. K., et al., 2016)	The redox state of tissue is detected through nuclear magnetic resonance/magnetic resonance imaging, with the use of a nitroxide spin probe or biradical molecule.	No

Glutathione (GSH) depletion	(Biesemann, N. et al., 2018)	A downstream target of the Nrf2 pathway is involved in GSH synthesis. As an indication of oxidation status, GSH can be measured by assaying the ratio of reduced to oxidized glutathione (GSH:GSSG) using a commercially available kit (e.g., http://www.abcam.com/gshgssg-ratio-detection-assay-kit-fluorometric-green-ab138881.html).	No
Thiobarbituric acid reactive substances (TBARS)	(Griendling, K. K., et al., 2016)	Oxidative damage to lipids can be measured by assaying for lipid peroxidation with TBARS using a commercially available kit.	No
Protein oxidation (carbonylation)	(Azimzadeh et al., 2017; Azimzadeh etal., 2015; Ping et al., 2020)	Can be determined with enzyme-linked immunosorbent assay (ELISA) or a commercial assay kit. Protein oxidation can indicate the level of oxidative stress.	No
Seahorse XFp Analyzer	Leung et al. 2018	The Seahorse XFp Analyzer provides information on mitochondrial function, oxidative stress, and metabolic dysfunction of viable cells by measuring respiration (oxygen consumption rate; OCR) and extracellular pH (extracellular acidification rate; ECAR).	No

Molecular Biology: Nrf2. Nrf2's transcriptional activity is controlled post-translationally by oxidation of Keap1. Assays for Nrf2 activity include:

Method of Measurement	References	Description	OECD-Approved Assay
Immunohistochemistry	(Amsen, D., de Visser, K. E., and Town, T., 2009)	Immunohistochemistry for increases in Nrf2 protein levels and translocation into the nucleus	No
Quantitative polymerase chain reaction (qPCR)	(Forlenza et al., 2012)	qPCR of Nrf2 target genes (e.g., Nqo1, Hmox-1, Gcl, Gst, Prx, TrxR, Srxn), or by commercially available pathway-based qPCR array (e.g., oxidative stress array from SABiosciences)	No
Whole transcriptome profiling via microarray or via RNA-seq followed by a pathway analysis	(Jackson, A. F. et al., 2014)	Whole transcriptome profiling by microarray or RNA-seq followed by pathway analysis (in IPA, DAVID, metacore, etc.) for enrichment of the Nrf2 oxidative stress response pathway	No

References

Ahmad, S. et al. (2021), "60Co-γ Radiation Alters Developmental Stages of Zeugodacus cucurbitae (Diptera: Tephritidae) Through Apoptosis Pathways Gene Expression", *Journal Insect Science,* Vol. 21/5, Oxford University Press, Oxford, https://doi.org/10.1093/jisesa/ieab080

Antelmann, H. and J. D. Helmann (2011), "Thiol-based redox switches and gene regulation.", *Antioxidants & Redox Signaling*, Vol. 14/6, Mary Ann Leibert Inc., Larchmont, https://doi.org/10.1089/ars.2010.3400

Amsen, D., de Visser, K. E., and Town, T. (2009), "Approaches to determine expression of inflammatory cytokines", in

Inflammation and Cancer, Humana Press, Totowa, https://doi.org/10.1007/978-1-59745-447-6_5

Azimzadeh, O. et al. (2015), "Integrative Proteomics and Targeted Transcriptomics Analyses in Cardiac Endothelial Cells Unravel Mechanisms of Long-Term Radiation-Induced Vascular Dysfunction", *Journal of Proteome Research*, Vol. 14/2, American Chemical Society, Washington, https://doi.org/10.1021/pr501141b

Azimzadeh, O. et al. (2017), "Proteome analysis of irradiated endothelial cells reveals persistent alteration in protein degradation and the RhoGDI and NO signalling pathways", *International Journal of Radiation Biology*, Vol. 93/9, Informa, London, https://doi.org/10.1080/09553002.2017.1339332

Azzam, E. I. et al. (2012), "Ionizing radiation-induced metabolic oxidative stress and prolonged cell injury", Cancer Letters, Vol. 327/1-2, Elsevier, Ireland, https://doi.org/10.1016/j.canlet.2011.12.012

Bai, J. et al. (2020), "Irradiation-induced senescence of bone marrow mesenchymal stem cells aggravates osteogenic differentiation dysfunction via paracrine signaling", *American Journal of Physiology - Cell Physiology*, Vol. 318/5, American Physiological Society, Rockville, https://doi.org/10.1152/ajpcell.00520.2019.

Balasubramanian, D (2000), "Ultraviolet radiation and cataract", *Journal of ocular pharmacology and therapeutics*, Vol. 16/3, Mary Ann Liebert Inc., Larchmont, https://doi.org/10.1089/jop.2000.16.285.

Biesemann, N. et al., (2018), "High Throughput Screening of Mitochondrial Bioenergetics in Human Differentiated Myotubes Identifies Novel Enhancers of Muscle Performance in Aged Mice", *Scientific Reports,* Vol. 8/1, Nature Portfolio, London, https://doi.org/10.1038/s41598-018-27614-8.

Elgazzar, A. and N. Kazem. (2015), "Chapter 23: Biological effects of ionizing radiation" in *The Pathophysiologic Basis of Nuclear Medicine*, Springer, New York, pp. 540-548

Fletcher, A. E (2010), "Free radicals, antioxidants and eye diseases: evidence from epidemiological studies on cataract and age-related macular degeneration", *Ophthalmic Research*, Vol. 44, Karger International, Basel, https://doi.org/10.1159/000316476.

Forlenza, M. et al. (2012), "The use of real-time quantitative PCR for the analysis of cytokine mRNA levels" in *Cytokine Protocols,* Springer, New York, https://doi.org/10.1007/978-1-61779-439-1_2

Forrester, S.J. et al. (2018), "Angiotensin II Signal Transduction: An Update on Mechanisms of Physiology and Pathophysiology", *Physiological Reviews,* Vol. 98/3**,** American Physiological Society, Rockville, https://doi.org/10.1152/physrev.00038.201

Foyer, C. H., A. V. Ruban, and G. Noctor (2017), "Viewing oxidative stress through the lens of oxidative signalling rather than damage", Biochemical Journal, Vol. 474/6, Portland Press, England, https://doi.org/10.1042/BCJ20160814

Ganea, E. and J. J. Harding (2006), "Glutathione-related enzymes and the eye", *Current eye research*, Vol. 31/1, Informa, London, https://doi.org/10.1080/02713680500477347.

Griendling, K. K. et al. (2016), "Measurement of reactive oxygen species, reactive nitrogen species, and redox-dependent signaling in the cardiovascular system: a scientific statement from the American Heart Association", *Circulation research*, Vol. 119/5, Lippincott Williams & Wilkins, Philadelphia, https://doi.org/10.1161/RES.0000000000000110

Guo, C. et al. (2013), "Oxidative stress, mitochondrial damage and neurodegenerative diseases", *Neural regeneration research*, Vol. 8/21, Publishing House of Neural Regeneration Research, China, https://doi.org/10.3969/j.issn.1673-5374.2013.21.009

Hargreaves, M., and L. L. Spriet (2020), "Skeletal muscle energy metabolism during exercise.", *Nature Metabolism*, Vol. 2, Nature Portfolio, London, https://doi.org/10.1038/s42255-020-0251-4

Hladik, D. and S. Tapio (2016), "Effects of ionizing radiation on the mammalian brain", *Mutation Research/Reviews in Mutation Research*, Vol. 770, Elsevier, Amsterdam, https://doi.org/10.1016/j.mrrev.2016.08.003

Itoh, K., J. Mimura and M. Yamamoto (2010), "Discovery of the negative regulator of Nrf2, Keap1: a historical overview", *Antioxidants & Redox Signaling*, Vol. 13/11, Mary Ann Leibert Inc., Larchmont, https://doi.org/10.1089/ars.2010.3222

Jackson, A.F. et al. (2014), "Case study on the utility of hepatic global gene expression profiling in the risk assessment of the carcinogen furan.", *Toxicology and Applied Pharmacology,* Vol. 274/11, Elsevier, Amsterdam, https://doi.org/10.1016/j.taap.2013.10.019

Jacobsen, N.R. et al. (2008), "Genotoxicity, cytotoxicity, and reactive oxygen species induced by single-walled carbon nanotubes and C_{60} fullerenes in the FE1-Muta^{TM} Mouse lung epithelial cells", *Environmental and Molecular Mutagenesis,* Vol. 49/6, John Wiley & Sons, Inc., Hoboken, https://doi.org/10.1002/em.20406

Karimi, N. et al. (2017), "Radioprotective effect of hesperidin on reducing oxidative stress in the lens tissue of rats", *International Journal of Pharmaceutical Investigation*, Vol. 7/3, Phcog Net, Bengaluru, https://doi.org/10.4103/jphi.JPHI_60_17.

Leung, D.T.H., and Chu, S. (2018), “Measurement of Oxidative Stress: Mitochondrial Function Using the Seahorse System” In: Murthi, P., Vaillancourt, C. (eds) Preeclampsia. Methods in Molecular Biology, vol 1710. Humana Press, New York, NY. https://doi.org/10.1007/978-1-4939-7498-6_22

Lu, C., G. Song, and J. Lin (2006), “Reactive oxygen species and their chemiluminescence-detection methods”, *TrAC Trends in Analytical Chemistry*, Vol. 25/10, Elsevier, Amsterdam, https://doi.org/10.1016/j.trac.2006.07.007

Nguyen Dinh Cat, A. et al. (2013), “Angiotensin II, NADPH oxidase, and redox signaling in the vasculature”, *Antioxidants & redox signaling,* Vol. 19/10**,** Mary Ann Liebert, Larchmont, https://doi.org/10.1089/ars.2012.4641

Ping, Z. et al. (2020), “Oxidative Stress in Radiation-Induced Cardiotoxicity”, *Oxidative Medicine and Cellular Longevity*, Vol. 2020, Hindawi, https://doi.org/10.1155/2020/3579143

Powers, S.K. and M.J. Jackson. (2008), “Exercise-Induced Oxidative Stress: Cellular Mechanisms and Impact on Muscle Force Production”, *Physiological Reviews,* Vol. 88/4**,** American Physiological Society, Rockville, https://doi.org/10.1152/physrev.00031.2007

Raimondi, V., F. Ciccarese and V. Ciminale. (2020), “Oncogenic pathways and the electron transport chain: a dangeROS liason”, *British Journal of Cancer,* Vol. 122/2, Nature Portfolio, London, https://doi.org/10.1038/s41416-019-0651-y

Seen, S. and L. Tong. (2018), “Dry eye disease and oxidative stress”, *Acta Ophthalmologica,* Vol. 96/4**,** John Wiley & Sons, Inc., Hoboken, https://doi.org/10.1111/aos.13526

Ungvari, Z. et al. (2013), “Ionizing Radiation Promotes the Acquisition of a Senescence-Associated Secretory Phenotype and Impairs Angiogenic Capacity in Cerebromicrovascular Endothelial Cells: Role of Increased DNA Damage and Decreased DNA Repair Capacity in Microvascular Radiosensitivity”, *The Journals of Gerontology Series A: Biological Sciences and Medical Sciences*, Vol. 68/12, Oxford University Press, Oxford, https://doi.org/10.1093/gerona/glt057.

Vargas-Mendoza, N. et al. (2021), “Oxidative Stress, Mitochondrial Function and Adaptation to Exercise: New Perspectives in Nutrition”, *Life,* Vol. 11/11, Multidisciplinary Digital Publishing Institute, Basel, https://doi.org/10.3390/life11111269

Wang, H. et al. (2019), “Radiation-induced heart disease: a review of classification, mechanism and prevention”, *International Journal of Biological Sciences,* Vol. 15/10, Ivyspring International Publisher, Sydney, https://doi.org/10.7150/ijbs.35460

Zhang, R. et al. (2009), “Blockade of AT1 receptor partially restores vasoreactivity, NOS expression, and superoxide levels in cerebral and carotid arteries of hindlimb unweighting rats”, *Journal of applied physiology*, Vol. 106/1, American Physiological Society, Rockville, https://doi.org/10.1152/japplphysiol.01278.2007.

Zhao, R. Z. et al. (2019), “Mitochondrial electron transport chain, ROS generation and uncoupling”, *International journal of molecular medicine*, Vol. 44/1, Spandidos Publishing Ltd., Athens, https://doi.org/10.3892/ijmm.2019.4188

Event: 1635: Increase, DNA strand breaks

Short Name: Increase, DNA strand breaks

AOPs Including This Key Event

AOP ID and Name	Event Type
Aop:296 - Oxidative DNA damage leading to chromosomal aberrations and mutations	KeyEvent
Aop:272 - Deposition of energy leading to lung cancer	KeyEvent
Aop:322 - Alkylation of DNA leading to reduced sperm count	KeyEvent
Aop:216 - Deposition of energy leading to population decline via DNA strand breaks and follicular atresia	KeyEvent
Aop:238 - Deposition of energy leading to population decline via DNA strand breaks and oocyte apoptosis	KeyEvent
Aop:478 - Deposition of energy leading to occurrence of cataracts	KeyEvent
Aop:483 - Deposition of Energy Leading to Learning and Memory Impairment	KeyEvent
Aop:470 - Deposition of energy leads to vascular remodeling	KeyEvent

Stressors

Name
Ionizing Radiation
Topoisomerase inhibitors
Radiomimetic compounds

Biological Context

Level of Biological Organization

Molecular

Domain of Applicability

Taxonomic Applicability

Term	Scientific Term	Evidence	Links
human and other cells in culture	human and other cells in culture		NCBI

Life Stage Applicability

Life Stage	Evidence
All life stages	High

Sex Applicability

Sex	Evidence
Unspecific	High

Taxonomic applicability: DNA strand breaks are relevant to all species, including vertebrates such as humans, that contain DNA (Cannan & Pederson, 2016).

Life stage applicability: This key event is not life stage specific as all life stages display strand breaks. However, there is an increase in baseline levels of DNA strand breaks seen in older individuals though it is unknown whether this change due to increased break induction or a greater retention of breaks due to poor repair (White & Vijg, 2016).

Sex applicability: This key event is not sex specific as both sexes display evidence of strand breaks. In some cell types, such as peripheral blood mononuclear cells, males show higher levels of single strand breaks than females (Garm et al., 2012).

Evidence for perturbation by a stressor: There are studies demonstrating that increased DNA strand breaks can result from exposure to multiple stressor types including ionizing & non-ionizing radiation, chemical agents, and oxidizing agents (EPRI, 2014; Hamada, 2014; Cencer et al., 2018; Cannan & Pederson, 2016; Yang et al., 1998).

Key Event Description

DNA strand breaks can occur on a single strand (SSB) or both strands (double strand breaks; DSB). SSBs arise when the phosphate backbone connecting adjacent nucleotides in DNA is broken on one strand. DSBs are generated when both strands are simultaneously broken at sites that are sufficiently close to one another that base-pairing and chromatin structure are insufficient to keep the two DNA ends juxtaposed. As a consequence, the two DNA ends generated by a DSB can physically dissociate from one another, becoming difficult to repair and increasing the chance of inappropriate recombination with other sites in the genome (Jackson, 2002). SSB can turn into DSB if the replication fork stalls at the lesion leading to fork collapse.

Strand breaks are intermediates in various biological events, including DNA repair (e.g., excision repair), V(D)J recombination in developing lymphoid cells and chromatin remodeling in both somatic cells and germ cells. The spectrum of damage can be complex, particularly if the stressor is from large amounts of deposited energy which can result in complex lesions and clustered damage defined as two or more oxidized bases, abasic sites or starnd breaks on opposing DNA strands within a few helical turns. These lesions are more difficult to repair and have been studied in many types of models (Barbieri et al., 2019 and Asaithamby et al., 2011). DSBs and complex lesions are of particular concern, as they are considered the most lethal and deleterious type of DNA lesion. If misrepaired or left unrepaired, DSBs may drive the cell towards genomic instability, apoptosis or tumorigenesis (Beir, 1999).

How it is Measured or Detected

Please refer to the table below for details regarding these and other methodologies for detecting DNA DSBs.

Assay Name	References	Description	OECD Approved Assay
Comet Assay	Collins, 2004;	To detect SSBs or DSBs, single cells are	Yes (No. 489)

(Single Cell Gel Eletrophoresis - Alkaline)	Olive and Banath, 2006; Platel et al., 2011; Nikolova et al., 2017	encapsulated in agarose on a slide, lysed, and subjected to gel electrophoresis at an alkaline pH (pH >13); DNA fragments are forced to move, forming a "comet"-like appearance	
Comet Assay (Single Cell Gel Eltrophoresis - Neutral)	Collins, 2014; Olive and Banath, 2006; Anderson and Laubenthal, 2013; Nikolova et al., 2017	To detect DSBs, single cells are encapsulated in agarose on a slide, lysed, and subjected to gel electrophoresis at a neutral pH; DNA fragments, which are not denatured at the neutral pH, are forced to move, forming a "comet"-like appearance	N/A
γ-H2AX Foci Quantification - Flow Cytometry	Rothkamm and Horn, 2009; Bryce et al., 2016	Measurement of γ-H2AX immunostaining in cells by flow cytometry, normalized to total levels of H2AX	N/A
γ-H2AX Foci Quantification - Western Blot	Burma et al., 2001; Revet et al., 2011	Measurement of γ-H2AX immunostaining in cells by Western blotting, normalized to total levels of H2AX	N/A
γ-H2AX Foci Quantification - Microscopy	Redon et al., 2010; Mah et al., 2010; Garcia-Canton et al., 2013	Quantification of γ-H2AX immunostaining by counting γ- H2AX foci visualized with a microscope	N/A
γ-H2AX Foci Detection - ELISA and flow cytometry	Ji et al., 2017; Bryce et al., 2016	Detection of γ-H2AX in cells by ELISA, normalized to total levels of H2AX; γH2AX foci detection can be high-throughput and automated using flow cytometry-based immunodetection.	N/A
Pulsed Field Gel Electrophoresis (PFGE)	Ager et al., 1990; Gardiner et al., 1985; Herschleb et al., 2007; Kawashima et al., 2017	To detect DSBs, cells are embedded and lysed in agarose, and the released DNA undergoes gel electrophoresis in which the direction of the voltage is periodically alternated; Large DNA fragments are thus able to be separated by size	N/A
The TUNEL (Terminal Deoxynucleotidyl Transferase dUTP Nick End Labeling) Assay	Loo, 2011	To detect strand breaks, dUTPs added to the 3'OH end of a strand break by the DNA polymerase terminal deoxynucleotidyl transferase (TdT) are tagged with a fluorescent dye or a reporter enzyme to allow visualization (We note that this method is typically used to measure apoptosis)	N/A
In Vitro DNA Cleavage Assays using Topoisomerase	Nitiss, 2012	Cleavage of DNA can be achieved using purified topoisomerase; DNA strand breaks can then be separated and quantified using gel electrophoresis	N/A
PCR assay	**Figueroa-González & Pérez-Plasencia, 2017**	**Assay of strand breaks through the observation of DNA amplification prevention. Breaks block Taq polymerase, reducing the number of DNA templates, preventing amplification**	N/A
Sucrose density gradient centrifuge	**Raschke et al. 2009**	**Division of DNA pieces by density, increased fractionation leads to lower density pieces, with the use of a sucrose cushion**	N/A
Alkaline Elution Assay	**Kohn, 1991**	**Cells lysed with detergent-solution, filtered through membrane to remove all but intact DNA**	N/A
Unwinding Assay	**Nacci et al. 1992**	**DNA is stored in alkaline solutions with DNA-specific dye and allowed to unwind following removal from tissue, increased strand damage associated with increased unwinding**	N/A

References

Ager, D. D. et al. (1990). "Measurement of Radiation- Induced DNA Double-Strand Breaks by Pulsed-Field Gel Electrophoresis." Radiat Res. 122(2), 181-7.

Anderson, D. & Laubenthal J. (2013), "Analysis of DNA Damage via Single-Cell Electrophoresis. In: Makovets S, editor. DNA Electrophoresis. Totowa.", NJ: Humana Press. p 209-218.

Asaithamby, A., B. Hu and D.J. Chen. (2011) Unrepaired clustered DNA lesions induce chromosome breakage in human cells. Proc Natl Acad Sci U S A 108(20): 8293-8298 .

Barbieri, S., G. Babini, J. Morini et a l (2019). . Predicting DNA damage foci and their experimental readout with 2D microscopy: a

unified approach applied to photon and neutron exposures. Scientific Reports 9(1): 14019

Bryce, S. et al. (2016), “Genotoxic mode of action predictions from a multiplexed flow cytometric assay and a machine learning approach.”, Environ Mol Mutagen. 57:171-189. Doi: 10.1002/em.21996.

Burma, S. et al. (2001), “ATM phosphorylates histone H2AX in response to DNA double-strand breaks.”, J Biol Chem, 276(45): 42462-42467. doi:10.1074/jbc.C100466200

Cannan, W.J. and D.S. Pederson (2016), "Mechanisms and Consequences of Double-Strand DNA Break Formation in Chromatin.", Journal of Cellular Physiology, Vol.231/1, Wiley, New York, https://doi.org/10.1002/jcp.25048.

Cencer, C. et al. (2018), “PARP-1/PAR Activity in Cultured Human Lens Epithelial Cells Exposed to Two Levels of UVB Light”, Photochemistry and Photobiology, Vol.94/1, Wiley-Blackwell, Hoboken, https://doi.org/10.1111/php.12814.

Charlton, E. D. et al. (1989), “Calculation of Initial Yields of Single and Double Stranded Breaks in Cell Nuclei from Electrons, Protons, and Alpha Particles.”, Int. J. Radiat. Biol. 56(1): 1-19. doi: 10.1080/09553008914551141.

Collins, R. A. (2004), “The Comet Assay for DNA Damage and Repair. Molecular Biotechnology.”, Mol Biotechnol. 26(3): 249-61. doi:10.1385/MB:26:3:249

EPRI (2014), Epidemiology and mechanistic effects of radiation on the lens of the eye: Review and scientific appraisal of the literature, EPRI, California.

Figueroa-González, G. and C. Pérez-Plasencia. (2017), “Strategies for the evaluation of DNA damage and repair mechanisms in cancer”, Oncology Letters, Vol.13/6, Spandidos Publications, Athens, https://doi.org/10.3892/ol.2017.6002.

Garcia-Canton, C. et al. (2013), “Assessment of the in vitro p-H2AX assay by High Content Screening asa novel genotoxicity test.”, Mutat Res. 757:158-166. Doi: 10.1016/j.mrgentox.2013.08.002

Gardiner, K. et al. (1986), “Fractionation of Large Mammalian DNA Restriction Fragments Using Vertical Pulsed-Field Gradient Gel Electrophoresis.”, Somatic Cell and Molecular Genetics. 12(2): 185-95.Doi: 10.1007/bf01560665.

Garm, C. et al. (2012), “Age and gender effects on DNA strand break repair in peripheral blood mononuclear cells”, Aging Cell, Vol.12/1, Blackwell Publishing Ltd, Oxford, https://doi.org/10.1111/acel.12019.

Hamada, N. (2014), “What are the intracellular targets and intratissue target cells for radiation effects?”, Radiation research, Vol. 181/1, The Radiation Research Society, Indianapolis, https://doi.org/10.1667/RR13505.1.

Herschleb, J. et al. (2007), “Pulsed-field gel electrophoresis.”, Nat Protoc. 2(3): 677-684. doi:10.1038/nprot.2007.94

Iliakis, G. et al. (2015), “Alternative End-Joining Repair Pathways Are the Ultimate Backup for Abrogated Classical Non-Homologous End-Joining and Homologous Recombination Repair: Implications for the Formation of Chromosome Translocations.”, Mutation Research/Genetic Toxicology and Environmental Mutagenesis. 2(3): 677-84. doi: 10.1038/nprot.2007.94

Jackson, S. (2002). “Sensing and repairing DNA double-strand breaks.”, Carcinogenesis. 23:687-696. Doi:10.1093/carcin/23.5.687.

Ji, J. et al. (2017), “Phosphorylated fraction of H2AX as a measurement for DNA damage in cancer cells and potential applications of a novel assay.”, PLoS One. 12(2): e0171582. doi:10.1371/journal.pone.0171582

Kawashima, Y.(2017), “Detection of DNA double-strand breaks by pulsed-field gel electrophoresis.”, Genes Cells 22:84-93. Doi: 10.1111/gtc.12457.

Khoury, L. et al. (2013), “Validation of high-throughput genotoxicity assay screening using cH2AX in-cell Western assay on HepG2 cells.”, Environ Mol Mutagen, 54:737-746. Doi: 10.1002/em.21817.

Khoury, L. et al. (2016), “Evaluation of four human cell lines with distinct biotransformation properties for genotoxic screening.”, Mutagenesis, 31:83-96. Doi: 10.1093/mutage/gev058.

Kohn, K.W. (1991), “Principles and practice of DNA filter elution”, Pharmacology & Therapeutics, Vol.49/1, Elsevier, Amsterdam, https://doi.org/10.1016/0163-7258(91)90022-E.

Loo, DT. (2011), “In Situ Detection of Apoptosis by the TUNEL Assay: An Overview of Techniques. In: Didenko V, editor. DNA Damage Detection In Situ, Ex Vivo, and In Vivo. Totowa.”, NJ: Humana Press. p 3-13.doi: 10.1007/978-1-60327-409-8_1.

Mah, L. J. et al. (2010), “Quantification of gammaH2AX foci in response to ionising radiation.”, J Vis Exp(38). doi:10.3791/1957.

Nacci, D. et al. (1992), “Application of the DNA alkaline unwinding assay to detect DNA strand breaks in marine bivalves”, Marine Environmental Research, Vol.33/2, Elsevier BV, Amsterdam, https://doi.org/10.1016/0141-1136(92)90134-8.

Nikolova, T., F. et al. (2017), “Genotoxicity testing: Comparison of the γH2AX focus assay with the alkaline and neutral comet assays.”, Mutat Res 822:10-18. Doi: 10.1016/j.mrgentox.2017.07.004.

Nitiss, J. L. et al. (2012), “Topoisomerase assays. ”, Curr Protoc Pharmacol. Chapter 3: Unit 3 3.

OECD. (2014). Test No. 489: “In vivo mammalian alkaline comet assay.” OECD Guideline for the Testing of Chemicals, Section 4 .

Olive, P. L., & Banáth, J. P. (2006), “The comet assay: a method to measure DNA damage in individual cells.”, Nature Protocols. 1(1): 23-29. doi:10.1038/nprot.2006.5.

Platel A. et al. (2011), “Study of oxidative DNA damage in TK6 human lymphoblastoid cells by use of the thymidine kinase gene-mutation assay and the *in vitro* modified comet assay: Determination of No-Observed-Genotoxic-Effect-Levels.”, Mutat Res 726:151-159. Doi: 10.1016/j.mrgentox.2011.09.003.

Raschke, S., J. Guan and G. Iliakis. (2009), “Application of alkaline sucrose gradient centrifugation in the analysis of DNA replication after DNA damage”, Methods in Molecular Biology, Vol.521, Humana Press, Totowa, https://doi.org/10.1007/978-1-60327-815-7_18.

Redon, C. et al. (2010), “The use of gamma-H2AX as a biodosimeter for total-body radiation exposure in non-human primates.”, PLoS One. 5(11): e15544. doi:10.1371/journal.pone.0015544

Revet, I. et al. (2011), “Functional relevance of the histone γH2Ax in the response to DNA damaging agents.” Proc Natl Acad Sci USA.108:8663-8667. Doi: 10.1073/pnas.1105866108

Rogakou, E.P. et al. (1998), “DNA Double-stranded Breaks Induce Histone H2AX Phosphorylation on Serine 139.” , J Biol Chem, 273:5858-5868. Doi: 10.1074/jbc.273.10.5858

Rothkamm, K. & Horn, S. (2009), “γ-H2AX as protein biomarker for radiation exposure.”, Ann Ist Super Sanità, 45(3): 265-71.

White, R.R. and J. Vijg. (2016), “Do DNA Double-Strand Breaks Drive Aging?”, Molecular Cell, Vol.63, Elsevier, Amsterdam, http://doi.org/10.1016/j.molcel.2016.08.004.

Yang, Y. et al. (1998), “The effect of catalase amplification on immortal lens epithelial cell lines”, Experimental Eye Research, Vol.67/6, Academic Press Inc, Cambridge, https://doi.org/10.1006/exer.1998.0560.

Event: 1493: Increased Pro-inflammatory mediators

Short Name: Increased pro-inflammatory mediators

Key Event Component

Process	Object	Action
acute inflammatory response		increased

AOPs Including This Key Event

AOP ID and Name	Event Type
Aop:17 - Binding of electrophilic chemicals to SH(thiol)-group of proteins and /or to seleno-proteins involved in protection against oxidative stress during brain development leads to impairment of learning and memory	KeyEvent
Aop:38 - Protein Alkylation leading to Liver Fibrosis	KeyEvent
Aop:144 - Endocytic lysosomal uptake leading to liver fibrosis	KeyEvent
Aop:293 - Increased DNA damage leading to increased risk of breast cancer	KeyEvent
Aop:294 - Increased reactive oxygen and nitrogen species (RONS) leading to increased risk of breast cancer	KeyEvent
Aop:377 - Dysregulated prolonged Toll Like Receptor 9 (TLR9) activation leading to Multi Organ Failure involving Acute Respiratory Distress Syndrome (ARDS)	KeyEvent
Aop:432 - Deposition of Energy by Ionizing Radiation leading to Acute Myeloid Leukemia	KeyEvent
Aop:470 - Deposition of energy leads to vascular remodeling	KeyEvent

Biological Context

Level of Biological Organization

Tissue

Domain of Applicability

Taxonomic Applicability

Term	Scientific Term	Evidence	Links
human	Homo sapiens		NCBI
Vertebrates	Vertebrates		NCBI

Life Stage Applicability

Life Stage	Evidence
All life stages	

Sex Applicability

Sex	Evidence
Unspecific	

LIVER:

Human [Santibañez et al., 2011]

Rat [Luckey and Petersen, 2001]

Mouse [Nan et al., 2013]

BRAIN:

Falsig 2004; Lund 2006 ; Kuegler 2010; Monnet-Tschudi et al., 2011; Sandström et al., 2014; von Tobel et al., 2014

Taxonomic applicability: The inflammatory response and increase of the pro-inflammatory mediators has been observed across species from simple invertebrates such as Daphnia to higher order vertebrates (Weavers & Martin, 2020).

Life stage applicability: This key event is not life stage specific (Kalm et al., 2013; Veeraraghan et al., 2011; Hladik & Tapio, 2016).

Sex applicability: Most studies conducted were on male models, although sex-dependent differences in pro-inflammatory markers have been previously reported (Cekanaviciute et al., 2018; Parihar et al., 2020).

Evidence for perturbation by a prototypic stressor: There is evidence of the increase of pro-inflammatory mediators following perturbation from a variety of stressors including exposure to ionizing radiation. (Abdel-Magied et al., 2019; Cho et al., 2017; Gaber et al., 2003; Ismail et al., 2016; Kim et al. 2002; Lee et al., 2010; Parihar et al., 2018).

Key Event Description

Inflammatory mediators are soluble, diffusible molecules that act locally at the site of tissue damage and infection, and at more distant sites. They can be divided into exogenous and endogenous mediators.

Exogenous mediators of inflammation are bacterial products or toxins like endotoxin or LPS. Endogenous mediators of inflammation are produced from within the (innate and adaptive) immune system itself, as well as other systems. They can be derived from molecules that are normally present in the plasma in an inactive form, such as peptide fragments of some components of complement, coagulation, and kinin systems. Or they can be released at the site of injury by a number of cell types that either contain them as preformed molecules within storage granules, e.g. histamine, or which can rapidly switch on the machinery required to synthesize the mediators.

Table1: a non-exhaustive list of examples for pro-inflammatory mediators

Classes of inflammatory mediators	**Examples**
Pro-inflammatory cytokines	TNF-a, Interleukins (IL-1, IL-6, IL-8), Interferons (IFN-g), chemokines (CXCL, CCL, GRO-α, MCP-1), GM-CSF
Prostaglandins	PGE2
Bradykinin	
Vasoactive amines	histamine, serotonin
Reactive oxygen species (ROS)	O^{2-}, H_2O_2
Reactive nitrogen species (RNS)	NO, iNOS

The increased production of pro-inflammatory mediators can have negative consequences on the parenchymal cells leading even to cell death, as described for TNF-a or peroxynitrite on neurons (Chao et al., 1995; Brown and Bal-Price, 2003). Along with TNF-α, IL-1β and IL-6 have been shown to exhibit negative consequences on neurogenesis and neuronal precursor cell proliferation when overexpressed. IFN-γ is also associated with neuronal damage, although it is not as extensively studied compared to TNF-α, IL-1β and IL-6. In addition, via a feedback loop, they can act on the reactive resident cells thus maintaining or exacerbating their reactive state; and by modifying elements of their signalling pathways, they can favour the M1 phenotypic polarization and the chronicity of the inflammatory process (Taetzsch et al., 2015).

Basically, this event occurs equally in various tissues and does not require tissue-specific descriptions. Nevertheless, there are some specificities such as the release of glutamate by brain reactive glial cells (Brown and Bal-Price, 2003; Vesce et al., 2007).The differences may rather reside in the type of insult favouring the increased expression and/or release of a specific class of inflammatory mediators, as well the time after the insult reflecting different stages of the inflammatory process. For these reasons, the analyses of the changes of a battery of inflammatory mediators rather than of a single one is a more adequate measurement of this KE.

Regulatory examples using the KE

CD54 and CD 86 as well as IL-8 expression is used to assess skin sensitization potential (OECD TG 442E). IL-2 expression is used to assess immunotoxicity (and will become an OECD test guideline); for the latter see also doi: 10.1007/s00204-018-2199-7.

LIVER:

When activated, resident macrophages (Kupffer cells) release inflammatory mediators including cytokines, chemokines, lysosomal, and proteolytic enzymes and are a main source of TGF-β1 - the most potent pro-fibrogenic cytokine. Following the role of TGF-β is described in more detail.

Transforming growth factor β (TGF-β) is a pleiotropic cytokine with potent regulatory and

inflammatory activity [Sanjabi et al., 2009; Li and Flavell, 2008a;2008b]. The multi-faceted effects of TGF-β on numerous immune functions are cellular and environmental context dependent [Li et al., 2006]. TGF-β binds to TGF-β receptor II (TGF-βRII) triggering the kinase activity of the cytoplasmic domain that in turn activates TGF-βRI. The activated receptor complex leads to nuclear translocation of Smad molecules,

and transcription of target genes [Li et al., 2006a]. The role of TGF-β as an immune modulator of T cell activity is best exemplified by the similarities between TGF-β1 knockout and T cell specific

TGF-β receptor II knockout mice [Li et al., 2006b; Marie et al., 2006;Shull et al., 1992]. The animals in both of these models develop severe multi-organ autoimmunity and succumb to death within a few weeks after birth [Li et al., 2006b; Marie et al., 2006; Shull et al., 1992]. In addition, in mice where TGF-β signaling is blocked specifically in T cells, the development of natural killer T (NKT) cells, natural regulatory T (nTreg) cells, and CD8+ T cells was shown to be dependent on TGF-β signaling in the thymus [Li et al., 2006b; Marie et al., 2006].

TGF-β plays a major role under inflammatory conditions. TGF-β in the presence of IL-6 drives the differentiation of T helper 17 (Th17) cells, which can promote further inflammation and augment autoimmune conditions [Korn et al., 2009]. TGF-β orchestrates the differentiation of both Treg and Th17 cells in a concentration-dependent manner [Korn et al., 2008]. In addition, TGF-β in combination with IL-4, promotes the differentiation of IL-9- and IL-10-producing T cells, which lack

suppressive function and also promote tissue inflammation [Dardalhon et al., 2008; Veldhoen et al., 2008]. The biological effects of TGF-β under inflammatory conditions on effector and memory CD8+ T cells are much less understood. In a recent study, it was shown that TGF-β has a drastically opposing role on naïve compared to antigen-experienced/memory CD8+ T cells [Filippi et al., 2008]. When cultured *in vitro*, TGF-β suppressed naïve CD8+ T cell activation and IFN-γ production, whereas TGF-β enhanced survival of memory CD8+ T cells and increased the production of IL-17 and IFN-γ [Filippi et al., 2008]. TGF-β also plays an important role in suppressing the cells of the innate immune system.

The transforming growth factor beta (TGF-β) family of cytokines are ubiquitous, multifunctional, and essential to survival. They play important roles in growth and development, inflammation and repair, and host immunity. The mammalian TGF-β isoforms (TGF-β1, β2 and β3) are secreted as latent precursors and have multiple cell surface receptors of which at least two mediate signal transduction. Autocrine and paracrine effects of TGF-βs can be modified by extracellular matrix, neighbouring cells and other cytokines. The vital role of the TGF-β family is illustrated by the fact that approximately 50% of TGF-1 gene knockout mice die in utero and the remainder succumb to uncontrolled inflammation after birth. The role of TGF-β in homeostatic and pathogenic processes suggests numerous applications in the diagnosis and treatment of various diseases characterised by inflammation and fibrosis. [Clark and Coker, 1998; Santibañez et al., 2011; Pohlers et al., 2009] Abnormal TGF-β regulation and function are implicated in a growing number of fibrotic and inflammatory pathologies, including pulmonary fibrosis, liver cirrhosis, glomerulonephritis and diabetic nephropathy, congestive heart failure, rheumatoid arthritis, Marfan syndrome, hypertrophic scars, systemic sclerosis, myocarditis, and Crohn's disease. [Gordon and Globe,2008] TGF-β1 is a polypeptide member of the TGF-β superfamily of cytokines. TGF-β is synthesized as a non-active pro-form, forms a complex with two latent associated proteins latency-associated protein (LAP) and latent TGF- β binding protein (LTBP) and undergoes protolithic cleavage by the endopeptidase furin to generate the mature TGF-β dimer. Among the TGF-βs, six distinct isoforms have been discovered although

only the TGF-β1, TGF-β2 and TGF-β3 isoforms are expressed in mammals, and their human genes are located on chromosomes 19q13, 1q41 and 14q24, respectively. Out of the three TGF-β isoforms (β1, β2 and β3) only TGF-β1 was linked to fibrogenesis and is the most potent fibrogenic factor for hepatic stellate cells. [Roberts, 1998; Govinden and Bhoola, 2003]. During fibrogenesis, tissue and blood levels of active TGF-β are elevated and overexpression of TGF-β1 in transgenic mice can induce fibrosis. Additionally, experimental fibrosis can be inhibited by anti-TGF-β treatments with neutralizing antibodies or soluble TGF-β receptors [Qi et al.; 1999; Shek and Benyon , 2004; De Gouville et al., 2005; Chen et al., 2009]. TGF-β1 induces its own mRNA to sustain high levels in local sites of injury. The effects of TGF-β1 are classically mediated by intracellular signalling via Smad proteins. Smads 2 and 3 are stimulatory whereas Smad 7 is inhibitory. [Parsons et al., 2013; Friedman, 2008; Kubiczkova et al., 2012] Smad1/5/8, MAP kinase (mitogen-activated protein) and PI3 kinase are further signalling pathways in different cell types for TGF-β1 effects.

TGF-β is found in all tissues, but is particularly abundant in bone, lung, kidney and placental tissue. TGF-β is produced by many, but not all parenchymal cell types, and is also produced or released by infiltrating cells such as lymphocytes, monocytes/macrophages, and platelets. Following wounding or inflammation, all these cells are potential sources of TGF-β. In general, the release and activation of TGF-β stimulates the production of various extracellular matrix proteins and inhibits the degradation of these matrix proteins. [Branton and Kopp, 1999]

TGF-β 1 is produced by every leukocyte lineage, including lymphocytes, macrophages, and dendritic cells, and its expression serves in both autocrine and paracrine modes to control the differentiation, proliferation, and state of activation of these immune cells. [Letterio and Roberts; 1998]

In the liver TGF-β1 is released by activated Kupffer cells, liver sinusoidal endothelial cells, and platelets; in the further course of events also activated hepatic stellate cells express TGF-β1. Hepatocytes do not produce TGF-β1 but are implicated in intracellular activation of latent TGF-β1. [Roth et al., 1998; Kisseleva and Brenner, 2007; Kisseleva and Brenner, 2008; Poli, 2000; Liu et al., 2006]

TGF-β1 is the most established mediator and regulator of epithelial-mesenchymal-transition (EMT) which further contributes to the production of extracellular matrix. It has been shown that TGF-β1 mediates EMT by inducing snail-1 transcription factor and tyrosine phosphorylation of Smad2/3 with subsequent recruitment of Smad4. [Kolios et al., 2006; Bataller and Brenner, 2005; Guo and Friedman,2007; Brenner,2009; Kaimori et al., 2007; Gressner et al., 2002; Kershenobich Stalnikowitz and Weisssbrod, 2003; Li et al., 2008; Matsuoka and Tsukamoto, 1990; Kisseleva and Brenner, 2008; Poli, 200; Parsons et al., 2007; Friedman 2008; Liu et al., 2006]

TGF-β1 induces apoptosis and angiogenesis in vitro and in vivo through the activation of vascular endothelial growth factor (VEGF) High levels of VEGF and TGF-β1 are present in many tumors. Crosstalk between the signalling pathways activated by these growth factors controls endothelial cell apoptosis and angiogenesis. [Clark and Coker; 1998]

How it is Measured or Detected

The specific type of measurement(s) might vary with tissue, environment and context and will need to be described for different tissue contexts as used within different AOP descriptions.

In general, quantification of inflammatory markers can be done by:

- qRT-PCR (mRNA expression)
- ELISA
- Immunocytochemistry
- Immunoblotting

For descriptions of techniques, see Falsig 2004; Lund 2006 ; Kuegler 2010; Monnet-Tschudi et al., 2011; Sandström et al., 2014; von Tobel et al., 2014

LIVER:

There are several assays for TGB-β1 measurement available.

e.g. Human TGF-β1 ELISA Kit. The Human TGF-β 1 ELISA (Enzyme –Linked Immunosorbent Assay) kit is an in vitro enzyme-linked immunosorbent assay for the quantitative measurement of human TGF-β1 in serum, plasma, cell culture supernatants, and urine. This assay employs an antibody specific for human TGF-β1 coated on a 96-well plate. Standards and samples are pipetted into the wells and TGF-β1 present in a sample is bound to the wells by the immobilized antibody. The wells are washed and biotinylated anti-human TGF-β1 antibody is added. After washing away unbound biotinylated antibody, HRP- conjugated streptavidin is pipetted to the wells. The wells are again washed, a TMB substrate solution is added to the wells and colour develops in proportion to the amount of TGF-β1 bound. The StopSolution changes the colour from blue to yellow, and the intensity of the colour is measured at 450 nm [Mazzieri et al., 2000]

Listed below are common methods for detecting the KE, however there may be other comparable methods that are not listed.

			OECD

Assay	Reference	Description	Approved Assay
• RT-qPCR • Q-PCR	(Veremeyko et al., 2012; Alwine et al, 1977; Forlenza et al., 2012)	Measures mRNA expression of cytokines, chemokines and inflammatory markers	No
Immunoblotting (western blotting)	(Lee et al., 2008)	Uses antibodies specific to proteins of interest, can used to detect presence of pro-inflammatory mediators in samples of cell or tissue lysate	No
Whole blood stimulation assay	(Thurm & Halsey, 2005)	Detects inflammatory cytokines in blood	No
Imaging tests	(Rollins & Miskolci, 2014)	A qualitative technique using a cytokine specific antibodies and fluorophores can be used to visualize expression patterns, subcellular location of the target and protein-protein interactions. Common examples include double immunofluorescence confocal microscopy or other molecular imaging modalities.	No
Flow-cytometry	(Karanikas et al., 2000)	Detects the intracellular cytokines with stimulation.	No
Immunoassays (ex. enzyme-linked immunosorbent assay (ELISA), enzyme-linked immunospot (ELISpot), radioimmunoassay)	(Amsen et al., 2009; Engvall & Perlmann, 1972; Ji & Forsthuber, 2016; Goldsmith, 1975)	Plate based assay technique using antibodies to detect presence of a protein in a liquid sample. Can be used to identify presence of an inflammatory cytokine of interest especially when in low concentrations.	No
Inflammatory cytokine arrays	(Amsen et al., 2009)	Similar to the ELISA, except using a membrane-based rather than plate-based approach. Can be used to measure multiple cytokine targets concurrently.	No
Immunohistochemistry (IHC)	(Amsen et al., 2009; Coons et al., 1942)	Immobilized tissue or cell cultures are stained using antibodies for specificity of ligands of interest. Versions of the assays can be used to visualize localization of inflammatory cytokines.	No

References

Brown GC, Bal-Price A (2003) Inflammatory neurodegeneration mediated by nitric oxide, glutamate, and mitochondria. Mol Neurobiol 27: 325-355

Dong Y, Benveniste EN (2001) Immune Function of Astrocytes. Glia 36: 180-190

Falsig J, Latta M, Leist M. Defined inflammatory states in astrocyte cultures correlation with susceptibility towards CD95-driven apoptosis. J Neurochem. 2004 Jan;88(1):181-93.

Falsig J, Pörzgen P, Lund S, Schrattenholz A, Leist M. The inflammatory transcriptome of reactive murine astrocytes and implications for their innate immune function. J Neurochem. 2006 Feb;96(3):893-907.

Falsig J, van Beek J, Hermann C, Leist M. Molecular basis for detection of invading pathogens in the brain. J Neurosci Res. 2008 May 15;86(7):1434-47.

Hamadi N, Sheikh A, Madjid N, Lubbad L, Amir N, Shehab SA, Khelifi-Touhami F, Adem A: Increased pro-inflammatory cytokines, glial activation and oxidative stress in the hippocampus after short-term bilateral adrenalectomy. BMC Neurosci 2016, **17:**61.

Kuegler PB, Zimmer B, Waldmann T, Baudis B, Ilmjärv S, Hescheler J, Gaughwin P, Brundin P, Mundy W, Bal-Price AK, Schrattenholz A, Krause KH, van Thriel C, Rao MS, Kadereit S, Leist M. Markers of murine embryonic and neural stem cells, neurons and astrocytes: reference points for developmental neurotoxicity testing. ALTEX. 2010;27(1):17-42

Lund S, Christensen KV, Hedtjärn M, Mortensen AL, Hagberg H, Falsig J, Hasseldam H, Schrattenholz A, Pörzgen P, Leist M. The dynamics of the LPS triggered inflammatory response of murine microglia under different culture and in vivo conditions. J Neuroimmunol. 2006 Nov;180(1-2):71-87.

Monnet-Tschudi, F., A. Defaux, et al. (2011). "Methods to assess neuroinflammation." Curr Protoc Toxicol Chapter 12: Unit12 19.

Sandstrom von Tobel, J., D. Zoia, et al. (2014). "Immediate and delayed effects of subchronic Paraquat exposure during an early differentiation stage in 3D-rat brain cell cultures." Toxicol Lett. DOI : 10.1016/j.toxlet.2014.02.001

Taetzsch T, Levesque S, McGraw C, Brookins S, Luqa R, Bonini MG, Mason RP, Oh U, Block ML (2015) Redox regulation of NF-kappaB p50 and M1 polarization in microglia. Glia 5, **63:**423-440.

Vesce S, Rossi D, Brambilla L, Volterra A (2007) Glutamate release from astrocytes in physiological conditions and in neurodegenerative disorders characterized by neuroinflammation. Int Rev Neurobiol. 82 :57-71.

LIVER:

- Bataller, R. and D.A. Brenner (2005), Liver Fibrosis, J.Clin. Invest, vol. 115, no. 2, pp. 209-218.
- Branton, M.H. and J.B. Kopp (1999), TGF-beta and fibrosis, Microbes Infect, vol. 1, no. 15, pp. 1349-1365.
- Brenner, D.A. (2009), Molecular Pathogenesis of Liver Fibrosis, Trans Am Clin Climatol Assoc, vol. 120, pp. 361–368.
- Cheng, K., N.Yang and R.I. Mahato (2009), TGF-beta1 gene silencing for treating liver fibrosis, Mol Pharm, vol. 6, no. 3, pp. 772–779.
- Clark, D.A. and R.Coker (1998), Transforming growth factor-beta (TGF-beta), Int J Biochem Cell Biol, vol. 30, no. 3, pp. 293-298.
- Dardalhon V, Awasthi A, Kwon H, Galileos G, Gao W, Sobel RA, Mitsdoerffer M, Strom TB,
- De Gouville, A.C. et al. (2005), Inhibition of TGF-beta signaling by an ALK5 inhibitor protects rats from dimethylnitrosamine-induced liver fibrosis, Br J Pharmacol, vol. 145, no. 2, pp. 166–177.
- Filippi CM, Juedes AE, Oldham JE, Ling E, Togher L, Peng Y, Flavell RA, von Herrath MG, Transforming growth factor-beta suppresses the activation of CD8+ T-cells when naive but promotes their survival and function once antigen experienced: a two-faced impact on autoimmunity. Diabetes 2008;57:2684–2692.
- Friedman, S.L. (2008), Mechanisms of Hepatic Fibrogenesis, Gastroenterology, vol. 134, no. 6, pp. 1655–1669.
- Gordon, K.J. and G.C. Blobe (2008), Role of transforming growth factor-β superfamily signalling pathways in human disease, Biochim Biophys Acta, vol. 1782, no. 4, pp. 197–228.
- Govinden, R. and K.D. Bhoola (2003), Genealogy, expression, and cellular function of transforming growth factor-β, Pharmacol. Ther, vol. 98, no. 2, pp. 257–265.
- Gressner, A.M. et al. (2002), Roles of TGF-β in hepatic fibrosis. Front Biosci, vol. 7, pp. 793-807.
- Guo, J. and S.L. Friedman (2007), Hepatic fibrogenesis, Semin Liver Dis, vol. 27, no. 4, pp. 413-426.
- Kaimori, A. et al. (2007), Transforming growth factor-beta1 induces an epithelial-to-mesenchymal transition state in mouse hepatocytes in vitro, J Biol Chem, vol. 282, no. 30, pp. 22089-22101.
- Kershenobich Stalnikowitz, D. and A.B. Weisssbrod (2003), Liver Fibrosis and Inflammation. A Review, Annals of Hepatology, vol. 2, no. 4, pp.159-163.
- Kisseleva T and Brenner DA, (2008), Mechanisms of Fibrogenesis, Exp Biol Med, vol. 233, no. 2, pp. 109-122.
- Kisseleva, T. and Brenner, D.A. (2007), Role of hepatic stellate cells in fibrogenesis and the reversal of fibrosis, Journal of Gastroenterology and Hepatology, vol. 22, Suppl. 1; pp. S73–S78.
- Kolios, G., V. Valatas and E. Kouroumalis (2006), Role of Kupffer cells in the pathogenesis of liver disease, World J.Gastroenterol, vol. 12, no. 46, pp. 7413-7420.
- Korn T, Mitsdoerffer M, Croxford AL, Awasthi A, Dardalhon VA, Galileos G, Vollmar P, Stritesky GL, Kaplan MH, Waisman A, Kuchroo VK, Oukka M., IL-6 controls Th17 immunity in vivo by inhibiting the conversion of conventional T cells into Foxp3+ regulatory T cells, Proceedings of the National Academy of Sciences Nov 2008, 105 (47) 18460-18465; DOI: 10.1073/pnas.0809850105
- Korn T, Bettelli E, Oukka M, Kuchroo VK. IL-17 and Th17 Cells. Annu Rev Immunol. 2009
- Kubiczkova, L. et al, (2012), TGF-β - an excellent servant but a bad master, J Transl Med, vol. 10, p. 183.
- Letterio, J.J. and A.B. Roberts (1998), Regulation of immune responses by TGF-beta, Annu Rev Immunol, vol.16, pp. 137-161.
- Li MO, Flavell RA. Contextual regulation of inflammation: a duet by transforming growth factor-beta and interleukin-10. Immunity 2008a;28:468–476.
- Li MO, Flavell RA. TGF-beta: a master of all T cell trades. Cell 2008b;134:392–404.
- Li MO, Sanjabi S, Flavell RA. Transforming growth factor-beta controls development, homeostasis, and tolerance of T cells by regulatory T cell-dependent and -independent mechanisms. Immunity 2006b;25:455–471.
- Li MO, Wan YY, Sanjabi S, Robertson AK, Flavell RA. Transforming growth factor-beta regulation of immune responses. Annu Rev Immunol 2006a;24:99–146.
- Li, Jing-Ting et al. (2008), Molecular mechanism of hepatic stellate cell activation and antifibrotic therapeutic strategies, J Gastroenterol, vol. 43, no. 6, pp. 419–428.
- Liu, Xingjun et al. (2006), Therapeutic strategies against TGF-beta signaling pathway in hepatic fibrosis. Liver Int, vol.26, no.1, pp. 8-22.
- Luckey, S.W., and D.R. Petersen (2001), Activation of Kupffer cells during the course of carbon tetrachloride-induced liver injury and fibrosis in rats, Exp Mol Pathol, vol. 71, no. 3, pp. 226-240.
- Marie JC, Liggitt D, Rudensky AY. Cellular mechanisms of fatal early-onset autoimmunity in mice with the T cell-specific targeting of transforming growth factor-beta receptor. Immunity 2006;25:441–454.
- Matsuoka, M. and H. Tsukamoto, (1990), Stimulation of hepatic lipocyte collagen production by Kupffer cell-derived transforming growth factor beta: implication for a pathogenetic role in alcoholic liver fibrogenesis, Hepatology, vol. 11, no. 4, pp. 599-605.
- Mazzieri, R .et al. (2000), Measurements of Active TGF-β Generated by Culture Cells, Methods in Molecular Biology, vol. 142, pp. 13-27.
- Nan, Y.M. et al. (2013), Activation of peroxisome proliferator activated receptor alpha ameliorates ethanol mediated liver fibrosis in mice, Lipids Health Dis, vol. 12, p.11.
- Parsons, C.J., M.Takashima and R.A. Rippe (2007), Molecular mechanisms of hepatic fibrogenesis. J Gastroenterol Hepatol, vol. 22, Suppl.1, pp. S79-S84.
- Pohlers , D. et al. (2009), TGF-β and fibrosis in different organs – molecular pathway imprints, Biochim. Biophys. Acta, vol. 1792, no. 8, pp.746–756.
- Poli, G. (2000), Pathogenesis of liver fibrosis: role of oxidative stress, Mol Aspects Med, vol. 21, no. 3, pp. 49 – 98.
- Qi Z et al.(1999),Blockade of type beta transforming growth factor signalling prevents liver fibrosis and dysfunction in the rat, Proc Natl Acad Sci USA, vol. 96, no. 5, pp. 2345-2349.
- Roberts, A.B. (1998), Molecular and cell biology of TGF-β, Miner Electrolyte Metab, vol. 24, no. 2-3, pp. 111-119.
- Roth, S., K. Michel and A.M. Gressner (1998), (Latent) transforming growth factor beta in liver parenchymal cells, its injury-dependent release, and paracrine effects on rat HSCs, Hepatology, vol. 27, no. 4, pp. 1003-1012.
- Sanjabi S, Zenewicz LA, Kamanaka M, Flavell RA. Anti- and Pro-inflammatory Roles of TGF-β, IL-10, and IL-22 In Immunity and Autoimmunity. Current opinion in pharmacology. 2009;9(4):447-453.
- Santibañez J.F., M. Quintanilla and C. Bernabeu (2011), TGF-β/TGF-β receptor system and its role in physiological and pathological

conditions, Clin Sci (Lond), vol. 121, no. 6, pp. 233-251.
- Shek, F.W. and R.C. Benyon (2004), How can transforming growth factor beta be targeted usefully to combat liver fibrosis? Eur J Gastroenterol Hepatol, vol. 16, no. 2, pp.123-126.
- Shull MM, Ormsby I, Kier AB, Pawlowski S, Diebold RJ, Yin M, Allen R, Sidman C, Proetzel G, Calvin D, et al. Targeted disruption of the mouse transforming growth factor-beta 1 gene results in multifocal inflammatory disease. Nature. 1992 Oct 22;359(6397):693-9.
- Veldhoen M, Uyttenhove C, van Snick J, Helmby H, Westendorf A, Buer J, Martin B, Wilhelm C, Stockinger B. Transforming growth factor-beta 'reprograms' the differentiation of T helper 2 cells and promotes an interleukin 9-producing subset. Nat Immunol 2008;9:1341–1346.

Abdel-Magied, N., S. M., Shedid and Ahmed, A. G. (2019), “Mitigating effect of biotin against irradiation-induced cerebral cortical and hippocampal damage in the rat brain tissue”, Environmental Science and Pollution Research, Vol. 26/13, Springer, London, https://doi.org/10.1007/S11356-019-04806-X.

Alwine, J. C., D. J. Kemp and G. R. Stark (1977), “Method for detection of specific RNAs in agarose gels by transfer to diazobenzyloxymethyl-paper and hybridization with DNA probes”, Proceedings of the National Academy of Sciences of the United States of America, Vol. 74/12, United States National Academy of Sciences, Washington, D.C., https://doi.org/10.1073/pnas.74.12.5350

Amsen, D., de Visser, K. E., and Town, T. (2009), “Approaches to determine expression of inflammatory cytokines”, in Inflammation and Cancer, Humana Press, Totowa, https://doi.org/10.1007/978-1-59745-447-6_5

Cekanaviciute, E., S. Rosi and S. Costes. (2018), "Central Nervous System Responses to Simulated Galactic Cosmic Rays", International Journal of Molecular Sciences, Vol. 19/11, Multidisciplinary Digital Publishing Institute (MDPI) AG, Basel, https://doi.org/10.3390/ijms19113669.

Cho, H. J. et al. (2017), “Role of NADPH Oxidase in Radiation-induced Pro-oxidative and Pro-inflammatory Pathways in Mouse Brain”, International Journal of Radiation Biology, Vol. 93/11, Informa, London, https://doi.org/10.1080/09553002.2017.1377360.

Coons, A. H. et al. (1942), “The Demonstration of Pneumococcal Antigen in Tissues by the Use of Fluorescent Antibody”, The Journal of Immunology, Vol. 45/3, American Association of Immunologists, Minneapolis, pp. 159-169

Engvall, E., and P. Perlmann (1972), “Enzyme-Linked Immunosorbent Assay, Elisa”, The Journal of Immunology, Vol. 109/1, American Association of Immunologists, Minneapolis, pp. 129-135

Fan, L. W. and Y. Pang. (2017), "Dysregulation of neurogenesis by neuroinflammation: Key differences in neurodevelopmental and neurological disorders", Neural Regeneration Research, Vol. 12/3, Wolters Kluwer, Alphen aan den Rijn, https://doi.org/10.4103/1673-5374.202926.

Forlenza, M. et al. (2012), “The use of real-time quantitative PCR for the analysis of cytokine mRNA levels” in Cytokine Protocols, Springer, New York, https://doi.org/10.1007/978-1-61779-439-1_2

Gaber, M. W. et al. (2003), “Differences in ICAM-1 and TNF-alpha expression between large single fraction and fractionated irradiation in mouse brain”, International Journal of Radiation Biology, Vol. 79/5, Informa, London, https://doi.org/10.1080/0955300031000114738.

Goldsmith, S. J. (1975), "Radioimmunoassay: Review of basic principles", Seminars in Nuclear Medicine, Vol. 5/2, https://doi.org/10.1016/S0001-2998(75)80028-6.

Hladik, D. and S. Tapio. (2016), "Effects of ionizing radiation on the mammalian brain", Mutation Research/Reviews in Mutation Research, Vol. 770, Elsevier B. b., Amsterdam, https://doi.org/10.1016/j.mrrev.2016.08.003.

Ismail, A. F. M., A.A.M. Salem and M.M.T. Eassawy (2016), “Modulation of gamma-irradiation and carbon tetrachloride induced oxidative stress in the brain of female rats by flaxseed oil”, Journal of Photochemistry and Photobiology B: Biology, Vol. 161, Elsevier, Amsterdam, https://doi.org/10.1016/J.JPHOTOBIOL.2016.04.031.

Ji, N. and T. G. Forsthuber. (2014), "ELISPOT Techniques" (pp. 63–71), https://doi.org/10.1007/7651_2014_111.

Kalm, M., K. Roughton and K. Blomgren. (2013), "Lipopolysaccharide sensitized male and female juvenile brains to ionizing radiation", Cell Death & Disease, Vol. 4/12, Nature Publishing Group, Berlin, https://doi.org/10.1038/cddis.2013.482.

Karanikas, V. et al. (2000), “Flow cytometric measurement of intracellular cytokines detects immune responses in MUC1 immunotherapy”, Clinical Cancer Research, Vol. 6/3, American Association for Cancer Research, Philadelphia, pp. 829–837

Kim, S. H. et al. (2002), “Expression of TNF-alpha and TGF-beta 1 in the rat brain after a single high-dose irradiation”, Journal of Korean Medical Science, Vol. 17/2, Korean Medical Association, Seoul, https://doi.org/10.3346/JKMS.2002.17.2.242.

Lee, J. W. et al. (2008), “Neuro-inflammation induced by lipopolysaccharide causes cognitive impairment through enhancement of beta-amyloid generation”, Journal of Neuroinflammation, Vol. 5/1, BioMed Central, London, https://doi.org/10.1186/1742-2094-5-37

Lee, W. H. et al. (2010), “Irradiation induces regionally specific alterations in pro-inflammatory environments in rat brain”, International Journal of Radiation Biology, Vol. 86/2, Informa, London, https://doi.org/10.3109/09553000903419346.

Parihar, V. K. et al. (2018), “Persistent nature of alterations in cognition and neuronal circuit excitability after exposure to simulated cosmic radiation in mice”, Experimental Neurology, Vol. 305, Elsevier, Amsterdam, https://doi.org/10.1016/J.EXPNEUROL.2018.03.009.

Parihar, V. K. et al. (2020), "Sex-Specific Cognitive Deficits Following Space Radiation Exposure", Frontiers in Behavioral Neuroscience, Vol.

14, https://doi.org/10.3389/fnbeh.2020.535885.

Rollins, J. and V. Miskolci (2014), “Immunofluorescence and subsequent confocal microscopy of intracellular TNF in human neutrophils” in Cytokines Bioassays, Springer, London, https://doi.org/10.1007/978-1-4939-0928-5_24

Thurm, C. W. and J. F. Halsey (2005), “Measurement of Cytokine Production Using Whole Blood”, in Current Protocols in Immunology, John Wiley & Sons, Inc., Hoboken, https://doi.org/10.1002/0471142735.im0718bs66

Veeraraghavan, J. et al. (2011), "Low-dose γ-radiation-induced oxidative stress response in mouse brain and gut: Regulation by NFκB–MnSOD cross-signaling", Mutation Research/Genetic Toxicology and Environmental Mutagenesis, Vol. 718/1–2, Elsevier, Amsterdam, https://doi.org/10.1016/j.mrgentox.2010.10.006.

Veremeyko, T. et al. (2012), “Detection of microRNAs in microglia by real-time PCR in normal CNS and during neuroinflammation”, Journal of Visualized Experiments: JoVE, Vol. 65, MyJove Corporation, Cambridge, https://doi.org/10.3791/4097

Weavers, H. and P. Martin (2020), “The cell biology of inflammation: From common traits to remarkable immunological adaptations”, Journal of Cell Biology, Vol. 219, Rockefeller University Press, New York, https://doi.org/10.1083/jcb.202004003

Event: 2066: Altered Signaling Pathways

Short Name: Altered Signaling

AOPs Including This Key Event

AOP ID and Name	Event Type
Aop:470 - Deposition of energy leads to vascular remodeling	KeyEvent
Aop:482 - Deposition of energy leading to occurrence of bone loss	KeyEvent
Aop:483 - Deposition of Energy Leading to Learning and Memory Impairment	KeyEvent

Biological Context

Level of Biological Organization

Molecular

Domain of Applicability

Taxonomic Applicability

Term	Scientific Term	Evidence	Links
human	Homo sapiens	Moderate	NCBI
rat	Rattus norvegicus	Moderate	NCBI
mouse	Mus musculus	Moderate	NCBI

Life Stage Applicability

Life Stage	Evidence
All life stages	Moderate

Sex Applicability

Sex	Evidence
Unspecific	Low

Taxonomic applicability: Altered signaling is applicable to all animals as cell signaling occurs among animal cells. This includes vertebrates such as humans, mice and rats (Nair et al., 2019).

Life stage applicability: This key event is not life stage specific.

Sex applicability: This key event is not sex specific.

Evidence for perturbation by a stressor: Multiple studies show that signaling pathways can be disrupted by many types of stressors including ionizing radiation and altered gravity (Cheng et al., 2020; Coleman et al., 2021; Su et al., 2020; Yentrapalli et al., 2013).

Key Event Description

Cells receive, process, and transmit signals to respond to their environment via signaling pathways. Signaling pathways are groups of molecules that work together in a cell to control physiological and metabolic processes. Kinases, for example, are important signaling molecules that can phosphorylate other proteins (Svoboda & Reenstra, 2002). Initiation of signaling pathways is an important component of cellular homeostasis including normal cell development and the response to cellular damage from exposure to external stressors (Esbenshade & Duzic, 2006). Signaling pathways are themselves activated by signals and the same signal can lead to different responses depending on the tissue type (Hamada, et al. 2011; Svoboda & Reenstra, 2002). Examples of signals include the activation of receptors to activate transcriptional targets, induction of receptor-ligand interactions and the initiation of cell-cell contact, or cell-extracellular matrix contact (Hunter, 2000). Many signalling pathways are crucial to intercellular communication via membrane receptors that transduce signals into the cell, while others are activated in an intracellular manner (Svoboda & Reenstra, 2002). Altered signalling (i.e., increase/decrease) can lead to different physiological outcomes, meaning that the directionality of the signaling response, determines the end outcome. For example, increase of the PI3K/Akt/mTOR pathway, which under physiological conditions is responsible for regulating the cell cycle, can lead to increased proliferation and decreased apoptosis. However, a decrease expression of this pathway can lead to an increase in apoptosis and decreased proliferation (Porta et al., 2014; Venkatesulu et al., 2018).

How it is Measured or Detected

Method of Measurement	Reference	Description	OECD Approved Assay
Kinase assays	(Svoboda & Reenstra, 2002)	Block kinase with inhibitors to monitor the activity of a kinase of interest.	No
Cell behaviour assays	(Svoboda & Reenstra, 2002)	Signal transduction events of cells are monitored. Cells are exposed to varying levels of signaling proteins and the resulting actions of a cell are observed (changes in structure, cell shape, matrix binding etc.).	No
Ratiometric or single-wavelength dyes	(Svoboda & Reenstra, 2002)	Detects alterations in signal-transduction activities via monitoring changes in detectable wavelengths.	No
Fluorescence microscopy/spectroscopy	(Oksvold et al., 2002)	Measures cell localization, protein interactions, signal propagation, amplification, and integration in the cell in real-time, or upon stimulation.	Yes
Green Fluorescent Protein (GFP)	(Zaccolo and Pozzan, 2000)	GFP assays act as fluorescent reporters but also as a marker of intracellular signalling events i.e. second messengers Ca2+ and cAMP, or for pH in different various cell compartments	No
Fluorescence Resonance Energy Transfer (FRET)	(Bunt and Wouters, 2017)	Assay helps illuminate the interactions between biological molecules	No
Fluorescence recovery after photobleaching (FRAP)	(Svoboda & Reenstra, 2002)	Determines mobility and diffusion of small molecules.	No
Immunoprecipitation	(Svoboda & Reenstra, 2002)	Involves isolating and concentrating a particular protein from mixed	Chromatin immunoprecipitation approved for

		samples to detect changes in signalling molecule activity.	analyzing histone modifications
Immunohistochemistry	(Kurien et al., 2011; Svoboda & Reenstra, 2002)	Northern, western and southern blotting techniques can be used to visualize signal transduction events. For example, antibodies with recognition epitopes can be used to locate active configurations or phosphorylated proteins within a cell or cell lysate.	No
Reverse transcription-quantitative polymerase chain reaction (RT-qPCR)	(Veremeyko et al., 2012; Alwine et al, 1977)	Measures mRNA expression of the gene of interest.	No
Enzyme-linked immunosorbent assay (ELISA)	(Amsen et al., 2009; Engvall & Perlmann, 1972)	Plate-based assay technique using antibodies to detect presence of a protein in a liquid sample. Can be used to identify presence of a protein of interest especially in when in low concentrations	No

References

Alwine, J. C., D. J. Kemp and G. R. Stark (1977), “Method for detection of specific RNAs in agarose gels by transfer to diazobenzyloxymethyl-paper and hybridization with DNA probes”, *Proceedings of the National Academy of Sciences of the United States of America*, Vol. 74/12, United States National Academy of Sciences, Washington, D.C., https://doi.org/10.1073/pnas.74.12.5350

Amsen, D., de Visser, K. E., and Town, T. (2009), “Approaches to determine expression of inflammatory cytokines”, in *Inflammation and Cancer*, Humana Press, Totowa, https://doi.org/10.1007/978-1-59745-447-6_5

Bunt, G., and F. S. Wouters (2017), “FRET from single to multiplexed signaling events”, *Biophysical reviews*, Vol. 9, Springer, London, https://doi.org/10.1007/s12551-017-0252-z

Cheng, Y. P. et al. (2017), “Acid sphingomyelinase/ceramide regulates carotid intima-media thickness in simulated weightless rats”, *Pflugers Archiv European Journal of Physiology*, Vol. 469, Springer, New York, https://doi.org/10.1007/s00424-017-1969-z

Coleman, M. A. et al. (2015), “Low-dose radiation affects cardiac physiology: gene networks and molecular signaling in cardiomyocytes”, *American Journal of Physiology - Heart and Circulatory Physiology*, Vol. 309/11, American Physiological Society, Rockville, https://doi.org/10.1152/ajpheart.00050.2015

Engvall, E., and P. Perlmann (1972), “Enzyme-Linked Immunosorbent Assay, Elisa”, *The Journal of Immunology*, Vol. 109/1, American Association of Immunologists, Minneapolis, pp. 129-135

Esbenshade, T. A., and E. Duzic (2006), “Overview of signal transduction”, *Current Protocols in Pharmacology*, Vol. 31/1, John Wiley & Sons, Ltd., Hoboken, https://doi.org/10.1002/0471141755.ph0201s31

Hamada, N. et al. (2011), “Signaling pathways underpinning the manifestations of ionizing radiation-induced bystander effects”, *Current Molecular Pharmacology*, Vol. 4/2, Bentham Science Publishers, Sharjah UAE, https://doi.org/10.2174/1874467211104020079

Hunter, T. (2000), “Signaling - 2000 and beyond”, *Cell*, Vol. 100/1, Cell Press, Cambridge, https://doi.org/10.1016/s0092-8674(00)81688-8

Kurien, B. T. et al. (2011), “An overview of Western blotting for determining antibody specificities for immunohistochemistry”, in *Signal Transduction Immunohistochemistry Methods and Protocols*, Springer, London, https://doi.org/10.1007/978-1-61779-024-9_3

Nair, A. et al. (2019), “Conceptual Evolution of Cell Signaling”, *International journal of molecular sciences*, Vol. 20/13, Multidisciplinary Digital Publishing Institute, Basel, https://doi.org/10.3390/ijms20133292

Oksvold, M. P. et al. (2002), “Fluorescent histochemical techniques for analysis of intracellular signaling”, *The Journal of*

Histochemistry and Cytochemistry, Vol. 50/3, SAGE Publications, Thousand Oaks, https://doi.org/10.1177/002215540205000301

Porta, C., C. Paglino and A. Mosca (2014), “Targeting PI3K/Akt/mTOR Signaling in Cancer”, *Frontiers in Oncology*, Vol. 4, Frontiers Media SA, Lausanne, https://doi.org/10.3389/fonc.2014.00064

Su, Y. T. et al. (2020), “Acid sphingomyelinase/ceramide mediates structural remodeling of cerebral artery and small mesenteric artery in simulated weightless rats”, *Life Sciences*, Vol. 243, Elsevier, Amsterdam, https://doi.org/10.1016/j.lfs.2019.117253

Svoboda, K. K. and W. R. Reenstra (2002), “Approaches to studying cellular signaling: a primer for morphologists”, *The Anatomical record*, Vol. 269/2, John Wiley & Sons, Ltd., Hoboken, https://doi.org/10.1002/ar.10074

Venkatesulu, B. P. et al. (2018), “Radiation-Induced Endothelial Vascular Injury: A Review of Possible Mechanisms”, *JACC: Basic to Translational Science*, Vol. 3/4, Elsevier, Amsterdam, https://doi.org/10.1016/j.jacbts.2018.01.014

Veremeyko, T. et al. (2012), “Detection of microRNAs in microglia by real-time PCR in normal CNS and during neuroinflammation”, *Journal of Visualized Experiments: JoVE*, Vol. 65, MyJove Corporation, Cambridge, https://doi.org/10.3791/4097

Yentrapalli, R. et al. (2013), “The PI3K/Akt/mTOR pathway is implicated in the premature senescence of primary human endothelial cells exposed to chronic radiation”, *PloS one*, Vol. 8/8, PLOS, San Francisco, https://doi.org/10.1371/journal.pone.0070024

Zaccolo, M. and T. Pozzan (2000), “Imaging signal transduction in living cells with GFP-based probes”, *IUBMB life*, Vol. 49/5, John Wiley & Sons, Ltd., Hoboken, https://doi.org/10.1080/152165400410218

Event: 2067: Altered, Nitric Oxide Levels

Short Name: Altered, Nitric Oxide Levels

Key Event Component

Process	Object	Action
nitric oxide homeostasis	endothelium	functional change

AOPs Including This Key Event

AOP ID and Name	Event Type
Aop:470 - Deposition of energy leads to vascular remodeling	KeyEvent

Biological Context

Level of Biological Organization

Cellular

Domain of Applicability

Taxonomic Applicability

Term	Scientific Term	Evidence	Links
human	Homo sapiens	High	NCBI
rat	Rattus norvegicus	High	NCBI
mouse	Mus musculus	Moderate	NCBI
rabbit	Oryctolagus cuniculus	Moderate	NCBI

Life Stage Applicability

Life Stage	Evidence
Adult	Moderate

Life Stage	Evidence
Not Otherwise Specified	Moderate

Sex Applicability

Sex	Evidence
Male	High
Female	Low
Unspecific	Moderate

Taxonomic applicability: Altered nitric oxide is applicable to vertebrates only, as endothelial NO synthase (eNOS) is required for the formation of NO from the amino acid, L-arginine, and only vertebrates have a true endothelial lining (Yano et al., 2007).

Life stage applicability: This key event is not life stage specific.

Sex applicability: This key event is not sex specific (Soucy et al., 2011; Takeda et al., 2003).

Evidence for perturbation by a stressor: Current literature provides ample evidence of external stressors, including ionizing radiation exposure and altered gravity, inducing significant changes to levels of nitric oxide, nitrate, and NO synthase (Soucy et al., 2011; Zhang et al., 2009).

Key Event Description

Nitric oxide (NO) is a diffusible molecule produced by many cell types, including endothelial cells, and is responsible for vasodilation (Schulz, Gori & Münzel, 2011; Soloviev & Kizub, 2019). The source of endogenous NO is L-arginine (Burov et al., 2022). Production of NO in the body can occur through nitric oxide synthase (NOS), an enzyme that degrades L-arginine in the presence of oxygen and nicotinamide adenine dinucleotide phosphate (NADPH) (Luiking, Engelen & Deutz, 2010). Tetrahydrobiopterin (BH4) is an important cofactor of NOS, allowing the enzymatic production of NO. A non-enzymatic method to produce NO includes the reduction of nitrite (Luiking, Engelen & Deutz, 2010). NO is constitutively produced by endothelial nitric oxide synthase (eNOS) and neuronal NOS (nNOS), and can be increased by inducible NOS (iNOS) (Powers & Jackson, 2008). Changes in the expression or activity of NOS enzymes can cause changes in NO levels. For example, iNOS is mainly regulated through transcription and its upregulation can result in increased production of NO (Farah, Michel & Balligand, 2018). Also, eNOS can be regulated by Ca2+ concentrations and blood flow shear stress through phosphorylation at Ser1177 (activating) and Thr495 (inhibiting) (Förstermann, 2010).

How it is Measured or Detected

Without measuring NO levels directly, NOS levels can be used as a proxy to measure NO production. eNOS and iNOS are common points for assessing NO levels indirectly. Decreased NOS protein expression often corresponds to a decrease in NO. However, it is important to note that NOS levels do not perfectly correlate with NO levels. Increased NOS can also decrease NO if paired with a simultaneous increase in ROS, which, through oxidizing the enzyme's cofactor BH4, causes NOS uncoupling (Forstermann, 2010; Zhang et al., 2009). Uncoupled NOS produces additional ROS that react with NO and reduce its overall abundance. Therefore, in this case, higher levels of NOS correlate to increased quantity of uncoupled NOS and a subsequent drop in NO bioavailability (Soloviev & Kizub, 2019).

Assay	Reference	Description	OECD Approved Assay
Western blotting/immunoblotting	(Hong et al., 2013; Baker et al., 2009; Yan et al., 2020; Zhang et al., 2009; Zhang et al., 2008; Shi et al., 2012; Azimzadeh et al., 2017; Azimzadeh et al., 2015)	Western blotting/immunoblotting is used to determine levels of inducible and endothelial NOS (NO synthesizing enzyme) in its phosphorylated and unphosphorylated forms, as well as nitrotyrosine (an indicator of NO). NOS and nitrotyrosine are detected by antibodies of each protein, visualized using chemiluminescence, and quantified using densitometry.	No
Nitric oxide/nitrate/nitrate (NOx) assay kit (Griess assay)	(Azimzadeh et al., 2017; Adbel-Magied & Shedid, 2019; Yan et al., 2020; Cervelli et al., 2017; Siamwala et al., 2010)	Levels of nitrite/nitrate (NOx) are determined using the NO assay kit. Nitrate reductase is used to convert nitrate into nitrite and the Griess reagent is then used to quantify levels of nitrite.	No
Immunohistochemical staining	(Fuji et al., 2016)	Uses an antibody to detect and measure levels of eNOS.	No
Immunofluorescence	(Hamada et al., 2019)	Uses fluorescent dye-labeled eNOS antibodies to visualize and determine eNOS levels.	No
ELISA kit	(Hasan et al., 2020; Azimzadeh et al., 2015)	Used to determine levels of NO and iNOS in serum by immobilizing the target antigen and binding it to associated antibodies linked to reporter enzymes. The activity of the reporter	

		enzymes is then measured to determine levels of NO and iNOS.	
4-amino-5-methylamino-2′,7′-difluorofluorescein diacetate (DAF-FM) fluorescent probe	(Soucy et al., 2011; Soucy et al., 2010)	Used to detect low concentrations of NO by reacting with it to become a fluorescent benzotriazole that can then be visualized and measured.	No

References

Abdel-Magied, N. and S. M. Shedid (2019), “Impact of zinc oxide nanoparticles on thioredoxin-interacting protein and asymmetric dimethylarginine as biochemical indicators of cardiovascular disorders in gamma-irradiated rats”, *Environmental Toxicology*, Vol. 35/4, John Wiley & Sons, Inc., Hoboken, https://doi.org/10.1002/tox.22879

Azimzadeh, O. et al. (2015), “Integrative Proteomics and Targeted Transcriptomics Analyses in Cardiac Endothelial Cells Unravel Mechanisms of Long-Term Radiation-Induced Vascular Dysfunction”, *Journal of Proteome Research*, Vol. 14/2, American Chemical Society, Washington, https://doi.org/10.1021/pr501141b

Azimzadeh, O. et al. (2017), “Proteome analysis of irradiated endothelial cells reveals persistent alteration in protein degradation and the RhoGDI and NO signalling pathways”, *International Journal of Radiation Biology*, Vol. 93/9, Informa, London, https://doi.org/10.1080/09553002.2017.1339332

Baker, J. E. et al. (2009), “10 Gy total body irradiation increases risk of coronary sclerosis, degeneration of heart structure and function in a rat model”, *International Journal of Radiation Biology*, Vol. 85/12, Informa, London, https://doi.org/10.3109/09553000903264473

Burov, O. N. et al. (2022), “Mechanisms of nitric oxide generation in living systems”, *Nitric Oxide*, Vol. 118, Elsevier, Amsterdam, https://doi.org/10.1016/j.niox.2021.10.003.

Cervelli, T. et al. (2017), “A new natural antioxidant mixture protects against oxidative and DNA damage in endothelial cell exposed to low-dose irradiation”, *Oxidative Medicine and Cellular Longevity*, Vol. 2017, Hindawi, London, https://doi.org/10.1155/2017/9085947

Farah, C., L. Y. M. Michel and J.-L. Balligand. (2018), "Nitric oxide signalling in cardiovascular health and disease", *Nature Reviews Cardiology*, Vol. 15/5, Springer Nature, London, https://doi.org/10.1038/nrcardio.2017.224.

Förstermann, U. (2010), "Nitric oxide and oxidative stress in vascular disease", *Pflügers Archiv - European Journal of Physiology*, Vol. 459, Springer Nature, London, https://doi.org/10.1007/S00424-010-0808-2.

Fuji, S. et al. (2016), “Association between endothelial function and micro-vascular remodeling measured by synchrotron radiation pulmonary micro-angiography in pulmonary arterial hypertension”, *General Thoracic and Cardiovascular Surgery*, Vol. 64/10, Springer, London, https://doi.org/10.1007/s11748-016-0684-6

Hamada, N. et al. (2020), “Ionizing Irradiation Induces Vascular Damage in the Aorta of Wild-Type Mice”, *Cancers*, Vol. 12/10, Multidisciplinary Digital Publishing Institute, Basel, https://doi.org/10.3390/CANCERS12103030

Hamada, N. et al. (2022), “Temporal Changes in Sparing and Enhancing Dose Protraction Effects of Ionizing Irradiation for Aortic Damage in Wild-Type Mice”, *Cancers*, Vol. 14/14, Multidisciplinary Digital Publishing Institute, Basel, https://doi.org/10.3390/cancers1414331

Hasan, H. F., R. R. Radwan and S. M. Galal (2020), “Bradykinin-potentiating factor isolated from Leiurus quinquestriatus scorpion venom alleviates cardiomyopathy in irradiated rats via remodelling of the RAAS pathway”, *Clinical and Experimental Pharmacology and Physiology*, Vol. 47/2, Wiley-Blackwell, Hoboken, https://doi.org/10.1111/1440-1681.13202

Hong, C. W. et al. (2013), “Involvement of inducible nitric oxide synthase in radiation-induced vascular endothelial damage”, *Journal of Radiation Research*, Vol. 54/6, Oxford University Press, Oxford, https://doi.org/10.1093/JRR/RRT066

Powers, S. K. and M. J. Jackson. (2008), "Exercise-Induced Oxidative Stress: Cellular Mechanisms and Impact on Muscle Force Production", *Physiological Reviews*, Vol. 88/4, The American Physiological Society, Rockville, https://doi.org/10.1152/physrev.00031.2007.

Schulz, E., T. Gori and T. Münzel. (2011), "Oxidative stress and endothelial dysfunction in hypertension", *Hypertension Research*, Vol. 34/6, Nature Portfolio, London, https://doi.org/10.1038/hr.2011.39.

Shi, F. et al. (2012), “Effects of Simulated Microgravity on Human Umbilical Vein Endothelial Cell Angiogenesis and Role of the PI3K-Akt-eNOS Signal Pathway”, *PLoS ONE*, Vol. 7/7, PLOS, San Francisco, https://doi.org/10.1371/journal.pone.0040365

Siamwala, J. H. et al. (2010), “Simulated microgravity perturbs actin polymerization to promote nitric oxide-associated migration in human immortalized Eahy926 cells”, *Protoplasma*, Vol. 242/1, Springer, London, https://doi.org/10.1007/S00709-010-0114-Z

Soloviev, A. I. and I. V. Kizub. (2019), "Mechanisms of vascular dysfunction evoked by ionizing radiation and possible targets for its pharmacological correction", *Biochemical Pharmacology*, Vol. 159, Elsevier, Amsterdam, https://doi.org/10.1016/J.BCP.2018.11.019

Soucy, K. G. et al. (2010), “Dietary inhibition of xanthine oxidase attenuates radiation-induced endothelial dysfunction in rat aorta”, *Journal of Applied Physiology*, Vol. 108/5, American Physiological Society, Rockville, https://doi.org/10.1152/japplphysiol.00946.2009.

Soucy, K. G. et al. (2011), “HZE 56Fe-ion irradiation induces endothelial dysfunction in rat aorta: Role of xanthine oxidase”, *Radiation Research*, Vol. 176/4, Radiation Research Society, Bozeman, https://doi.org/10.1667/RR2598.1.

Yan, T., et al. (2020), “Ionizing radiation induces BH4 deficiency by downregulating GTP-cyclohydrolase 1, a novel target for preventing and treating radiation enteritis”, *Biochemical Pharmacology*, Vol. 180, Elsevier, Amsterdam, https://doi.org/10.1016/J.BCP.2020.114102

Takeda, I., et al. (2013), “Possible Role of Nitric Oxide in Radiation-Induced Salivary Gland Dysfunction”, *Radiation Research*, Vol. 159/4, BioOne, https://doi.org/10.1667/0033-7587(2003)159[0465:PRONOI]2.0.CO;2

Yano, K., et al. (2007), “Phenotypic heterogeneity is an evolutionarily conserved feature of the endothelium”, *Blood*, Vol. 109/2, American Society of Hematology, Washington, D.C., https://doi.org/10.1182/blood-2006-05-026401

Yao, L. et al. (2010), "The role of RhoA/Rho kinase pathway in endothelial dysfunction", *Journal of Cardiovascular Disease Research*, Vol. 1/4, Elsevier, Amsterdam, https://doi.org/10.4103/0975-3583.74258

Zhang, R. et al. (2009), “Blockade of AT1 receptor partially restores vasoreactivity, NOS expression, and superoxide levels in cerebral and carotid arteries of hindlimb unweighting rats”, *Journal of Applied Physiology*, Vol. 106, American Physiological Society, Rockville, https://doi.org/10.1152/japplphysiol.01278.2007

Event: 2068: Increase, Endothelial Dysfunction

Short Name: Increase, Endothelial Dysfunction

AOPs Including This Key Event

AOP ID and Name	Event Type
Aop:470 - Deposition of energy leads to vascular remodeling	KeyEvent

Biological Context

Level of Biological Organization

Tissue

Organ term

Organ term

endothelium

Domain of Applicability

Taxonomic Applicability

Term	Scientific Term	Evidence	Links
human	Homo sapiens	Moderate	NCBI
rat	Rattus norvegicus	Moderate	NCBI
mouse	Mus musculus	Moderate	NCBI

Life Stage Applicability

Life Stage	Evidence
All life stages	Moderate

Sex Applicability

Sex	Evidence
Unspecific	Moderate

Taxonomic applicability: Endothelial dysfunction is applicable to vertebrates as only vertebrates have a true endothelial lining (Yano et al., 2007).

Life stage applicability: Although endothelial dysfunction may occur due to aging (Hererra et al., 2010), this key event can occur at any life stage (Chang et al., 2017; Lee et al., 2020).

Sex applicability: This key event is not sex specific (Hughson et al., 2018; Lee et al., 2020).

Evidence for perturbation by a stressor: Multiple studies show that endothelial dysfunction can be triggered by many types of stressors including ionizing radiation and altered gravity (Cheng et al., 2017; Soucy et al., 2011; Su et al., 2020; Yentrapalli et al., 2013).

Key Event Description

The endothelium is the innermost lining of blood vessels consisting of a single layer of endothelial cells. As the layer separating blood and vessel walls, the endothelium controls the flow of molecules, fluid, and circulating blood cells between the two. However, the specific functions and even the structure of endothelial cells vary greatly depending on the organ (Ricard et al., 2021). Dysfunction to the vascular endothelium can age arteries and is the result of increased proliferation and apoptotic behaviour of cells including an increased response to endothelial constrictors. It is also represented by an imbalance between vasodilators and vasoconstrictors which are produced by the endothelium. The dysfunction can encompass vasospasm, thrombosis, penetration of immune cells (i.e macrophage) and an increase in cyclooxygenase. These processes can activate the endothelium and a prolonged state of activation is problematic and is referred to as endothelial dysfunction (Sitia et al., 2010; Deanfield et al., 2005; Konukoglu & Uzun, 2017; Korpela & Liu, 2014). Other factors leading to endothelial dysfunction are loss in endothelial function leading to cell senescence and a low proliferative capacity of endothelial progenitor cells.

How it is Measured or Detected

Endothelial cell senescence

Assay	Reference	Description	OECD Approved Assay
Senescence-associated beta-galactosidase staining (SA-beta-gal)	(Farhat et al., 2008; González-Gualda et al., 2021; Hooten et al., 2017)	Can be used to measure senescence-associated β-galactosidase activity, a marker for senescent cells.	No
Bromodeoxyuridine (BrdU) detected with staining incorporation	(González-Gualda et al., 2021)	Reduced BrdU incorporation can indicate a lack of DNA synthesis.	No
Immunohistochemistry to detect senescence markers.	(González-Gualda et al., 2021)	Markers include Ki67 and Lamin B1. Reduced Ki67 can indicate reduced proliferation. Reduced Lamin B1 indicates impaired structural integrity of the nucleus.	No
Cell morphology and size measured with light microscopy or flow cytometry.	(González-Gualda et al., 2021)	Senescent cells exhibit an enlarged and flattened morphology.	No

Cell death:

See the increase, cell death KE for methods to measure endothelial cell death.

Impaired vasomotion

Assay	Reference	Description	OECD Approved Assay
Concentration-response curves to vasodilators/vasoconstrictors	(Deanfield et al., 2005; Verma et	Measurement of endothelial relaxation/contraction of blood vessels can give insight into endothelial dysfunction. This can be induced by endothelium-independent stimuli to stimulate vasodilation or vasoconstriction. A decreased stimuli response can be indicative of endothelial dysfunction.	No

	al., 2003)		
Detection of contractile factors (eg. endothelin) using enzyme-linked immunosorbent assay (ELISA).	(Abdel-Sayed et al., 2003)	Endothelin is an endothelium-derived vasoconstrictor.	No

References

Abdel-Sayed, S. et al. (2003), “Measurement of plasma endothelin-1 in experimental hypertension and in healthy subjects”, *American Journal of Hypertension*, Vol. 16/7, Oxford University Press, Oxford, https://doi.org/10.1016/S0895-7061(03)00903-8

Chang, P. Y. et al. (2017), “MSC-derived cytokines repair radiation-induced intra-villi microvascular injury”, *Oncotarget*, Vol. 8/50, Impact Journals, Orchard Park, https://doi.org/10.18632/oncotarget.21236

Cheng, Y. P. et al. (2017), “Acid sphingomyelinase/ceramide regulates carotid intima-media thickness in simulated weightless rats”, *Pflugers Archiv European Journal of Physiology*, Vol. 469, Springer, New York, https://doi.org/10.1007/s00424-017-1969-z

Deanfield, J. et al. (2005), “Endothelial function and dysfunction”, *Journal of hypertension*, Vol. 23/1, Lippincott Williams & Wilkins, Philadelphia, https://doi.org/10.1097/00004872-200501000-00004

Farhat, N. et al. (2008), “Stress-induced senescence predominates in endothelial cells isolated from atherosclerotic chronic smokers”, *Canadian Journal of Physiology and Pharmacology*, Vol. 86/11, Canadian Science Publishing, Ottawa, https://doi.org/10.1139/Y08-082

González-Gualda, E. et al. (2021), “A guide to assessing cellular senescence in vitro and in vivo”, *The FEBS Journal*, Vol. 288, FEBS press, https://doi.org/10.1111/febs.15570

Herrera, M. D. et al. (2010), “Endothelial dysfunction and aging: An update”, *Ageing Research Reviews*, Vol 9/2, Elsevier, Amsterdam, https://doi.org/10.1016/j.arr.2009.07.002

Hooten, N. N. and M. K. Evans (2017), “Techniques to Induce and Quantify Cellular Senescence”, *Journal of Visualized Experiments: JoVE*, Vol. 123, MyJove Corporation, Cambridge, https://doi.org/10.3791/55533

Hughson, R. L., A. Helm and M. Durante (2018), “Heart in space: effect of the extraterrestrial environment on the cardiovascular system”, *Nature Reviews Cardiology*, Vol. 15/3, Nature Portfolio, London, https://doi.org/10.1038/nrcardio.2017.157

Konukoglu, D., and H. Uzun (2017), “Endothelial Dysfunction and Hypertension”, in *Hypertension: from basic research to clinical practice*, Springer, London, https://doi.org/10.1007/5584_2016_90

Korpela, E., and S. K. Liu (2014), “Endothelial perturbations and therapeutic strategies in normal tissue radiation damage”, *Radiation Oncology,* Vol. 9, BioMed Central, London, https://doi.org/10.1186/s13014-014-0266-7

Lee, S. et al. (2020), “Arterial structure and function during and after long-duration spaceflight”, *Journal of Applied Physiology,* Vol. 129/1, American Physiological Society, Rockville, https://doi.org/10.1152/japplphysiol.00550.2019

Ricard, N. et al. (2021), “The quiescent endothelium: signalling pathways regulating organ-specific endothelial normalcy”, Nature reviews cardiology, Vol. 18/8, Springer Nature, https://doi.org/10.1038/s41569-021-00517-4

Sitia, S. et al. (2010), “From endothelial dysfunction to atherosclerosis”, Autoimmunity Reviews, Vol. 9/12, Elsevier, Amsterdam, https://doi.org/10.1016/j.autrev.2010.07.016

Soucy, K. G. et al. (2011), “HZE ^{56}Fe-ion irradiation induces endothelial dysfunction in rat aorta: Role of xanthine oxidase”, *Radiation Research*, Vol. 176/4, Radiation Research Society, Bozeman, https://doi.org/10.1667/RR2598.1

Su, Y. T. et al. (2020), “Acid sphingomyelinase/ceramide mediates structural remodeling of cerebral artery and small mesenteric artery in simulated weightless rats”, *Life Sciences*, Vol. 243, Elsevier, Amsterdam, https://doi.org/10.1016/j.lfs.2019.117253

Verma, S., M. R. Buchanan and T. J. Anderson (2003), “Endothelial function testing as a biomarker of vascular disease”, *Circulation*, Vol. 108/17, Lippincott Williams & Wilkins, Philadelphia, https://doi.org/10.1161/01.CIR.0000089191.72957.ED

Yano, K. et al. (2007), “Phenotypic heterogeneity is an evolutionarily conserved feature of the endothelium”, *Blood*, Vol. 109/2, American Society of Hematology, Washington, D.C., https://doi.org/10.1182/blood-2006-05-026401

Yentrapalli, R. et al. (2013), “The PI3K/Akt/mTOR pathway is implicated in the premature senescence of primary human endothelial cells exposed to chronic radiation”, *PloS one*, Vol. 8/8, PLOS, San Francisco, https://doi.org/10.1371/journal.pone.0070024

List of Adverse Outcomes in this AOP

Event: 2069: Occurrence, Vascular Remodeling

Short Name: Occurrence, Vascular Remodeling

Key Event Component

Process	Object	Action
blood vessel remodeling	blood vessel	occurrence

AOPs Including This Key Event

AOP ID and Name	Event Type
Aop:470 - Deposition of energy leads to vascular remodeling	AdverseOutcome

Biological Context

Level of Biological Organization
Organ

Organ term

Organ term
blood vessel

Domain of Applicability

Taxonomic Applicability

Term	Scientific Term	Evidence	Links
human	Homo sapiens	Moderate	NCBI
rat	Rattus norvegicus	Moderate	NCBI
mouse	Mus musculus	Moderate	NCBI

Life Stage Applicability

Life Stage	Evidence
Adult	Moderate
Not Otherwise Specified	Moderate

Sex Applicability

Sex	Evidence
Male	Moderate
Female	Low
Unspecific	Moderate

Taxonomic applicability: Vascular remodelling is applicable to all species with a closed circulatory system where blood is transported throughout the body via blood vessels with corresponding vessel walls (Renna, Heras & Miatello, 2013). Closed circulatory systems are present in most vertebrates and some invertebrates.

Life stage applicability: This key event is not life stage specific. However, advancing age is a risk factor for vascular remodeling (Harvey, Montezano & Touyz, 2015).

Sex applicability: This key event is not sex specific. However, men are shown to develop vascular remodeling younger than women (Kessler et al., 2019).

Evidence for perturbation by a stressor: Current literature provides ample evidence of vascular remodelling being induced by stressors including ionizing radiation exposure and altered gravity (Shen et al. 2018; Su et al., 2020; Delp et al., 2000, Cheng et al., 2017, Yu et al., 2011; Soucy et al., 2007; Soucy et al., 2010; Soucy et al., 2011).

Key Event Description

The vascular wall is composed of endothelial, smooth muscle and fibroblast cell interactions (Gibbons & Dzau, 1994; Renna, Heras & Miatello, 2013). The vasculature is capable of detecting changes in its surroundings and maintaining homeostasis (Gibbons & Dzau, 1994; Renna, Heras & Miatello, 2013). The functionality of blood vessels is highly dependent on their structure, with changes in arterial morphology being associated with downstream impacts (Gibbons & Dzau, 1994). Vascular remodeling is a term for many histological changes, including increased vascular stiffness, wall shear stress, intima-media thickening (IMT), increased intima-media section area, and increased vessel diameter (Herity et al., 1999). As blood vessels stiffen, this impacts systolic and diastolic pressure and pulse which can be indicators of vascular remodeling. Cellular level changes characterized by processes of growth, death, migration and production or degradation of the extracellular matrix (ECM) result in inflammation (increase in VCAM, ICAM, cytokines, chemokines) and calcification (changes in ratios of collagen and elastin) (Gibbons & Dzau, 1994). Initial tissue injury and resulting remodeling can also lead to turbulent blood flow causing further structural changes like increased vessel fibrosis. Increased vascular remodelling is often associated with a build-up of plaque in the arteries (known as atherosclerosis) due to impaired healing, which forces the vessel walls to attempt to remodel to maintain blood flow (Sylvester et al., 2018).

How it is Measured or Detected

Assay	Reference	Description	OECD Approved Assay
Pulse wave velocity (PWV)	(Soucy et al., 2007; Soucy et al., 2010; Soucy et al., 2011)	Used to measure blood vessel stiffness. Calculated using measurements from a Doppler probe and electrocardiogram (ECG).	No
NIS-Elements image analysis software (Nikon)	(Soucy et al., 2011)	Used to measure intraluminal perimeter (which in turn is used to calculate circular luminal diameter) and vessel wall thickness.	No
Hematoxylin-eosin (HE) staining	(Shen et al., 2018; Su et al., 2020; Delp et al., 2000, Cheng et al., 2017, Yu et al., 2011)	Used to measure aortic wall thickness, intima-media wall thickness (IMT), wall shear stress, outer media perimeter, and media cross section area (CSA).	No
Wire myography	(Tarasova et al., 2020)	Blood vessels are mounted in wire myograph systems and the relaxed inner diameter is estimated from the passive length-tension relationship between each artery.	No
Verhoeff-van Gieson staining	(Sofronova et al., 2015)	Measures elastin-collagen content in blood vessels, with Verhoeff stain highlighting elastin and van Gieson highlighting collagen. The higher the ratio of elastin to collagen, the greater the distensibility of the vessel. A higher collagen ratio is associated with increased vascular stiffness.	No
Sonography	(Lee et al., 2020; Sarkozy et al., 2019; Sridharan et al., 2020)	Uses ultrasound waves to measure IMT and intima-media area, both of which are markers of vascular structure and are used to calculate vascular stiffness.	No

References

Cheng, Y. P. et al. (2017), "Acid sphingomyelinase/ceramide regulates carotid intima-media thickness in simulated weightless rats", *Pflugers Archiv European Journal of Physiology*, Vol. 469, Springer Nature, London, https://doi.org/10.1007/s00424-017-1969-z

Delp, M.D. et al. (2000), “Structural and functional remodeling of skeletal muscle microvasculature is induced by simulated microgravity”, *American Journal of Physiology - Heart and Circulatory Physiology*, Vol. 278, American Physiological Society, Rockville, https://doi.org/10.1152/ajpheart.2000.278.6.h1866

Gibbons, G. H., and V. J. Dzau (1994), “The Emerging Concept of Vascular Remodeling”, *New England Journal of Medicine*, Vol. 330/20, Massachusetts Medical Society, Waltham, https://doi.org/10.1056/NEJM199405193302008

Harvey, A., A. C. Montezano, & R. M. Touyz. (2015), “Vascular biology of ageing-Implications in hypertension”, *Journal of molecular and cellular cardiology*, Vol. 83, Elsevier, Amsterdam, https://doi.org/10.1016/j.yjmcc.2015.04.011

Herity, N.A. et al. (1999), “Review: Clinical Aspects of Vascular Remodeling”, *Journal of Cardiovascular Electrophysiology*, Vol.10/7, Wiley, https://doi.org/10.1111/j.1540-8167.1999.tb01273.x

Kessler, E. L. et al. (2019), “Sex-specific influence on cardiac structural remodeling and therapy in cardiovascular disease”, *Biology of Sex Differences*, Vol. 10, Springer Nature, https://doi.org/10.1186/s13293-019-0223-0

Lee, S. M. C. et al. (2020), “Arterial structure and function during and after long-duration spaceflight”, *Journal of Applied Physiology*, Vol. 129, American Physiological Society, Rockville, https://doi.org/10.1152/japplphysiol.00550.2019

Patel, S. (2020), "The effects of microgravity and space radiation on cardiovascular health: From low-Earth orbit and beyond", *IJC Heart and Vasculature*, Vol. 30, Elsevier, Amsterdam, https://doi.org/10.1016/j.ijcha.2020.100595.

Renna, N. F., N. Heras, R. M. Miatello (2013), “Pathophysiology of Vascular Remodeling in Hypertension”, *International Journal of Hypertension,* Vol. 2013, Hindawi, London, http://doi.org/10.1155/2013/808353

Sárközy, M. et al. (2019), "Selective heart irradiation induces cardiac overexpression of the pro-hypertrophic miR-212", *Frontiers in Oncology*, Vol. 9, Frontiers Media S.A., Lausanne, https://doi.org/10.3389/FONC.2019.00598/FULL

Shen, Y. et al. (2018), “Transplantation of bone marrow mesenchymal stem cells prevents radiation-induced artery injury by suppressing oxidative stress and inflammation”, *Oxidative Medicine and Cellular Longevity*, Vol. 2018, Hindawi, London, https://doi.org/10.1155/2018/5942916.

Sofronova, S. I. et al. (2015), “Spaceflight on the Bion-M1 biosatellite alters cerebral artery vasomotor and mechanical properties in mice”, *Journal of Applied Physiology*, Vol. 118/7, American Physiological Society, Rockville, https://doi.org/10.1152/japplphysiol.00976.2014.

Soucy, K. G. et al. (2011), “HZE 56Fe-ion irradiation induces endothelial dysfunction in rat aorta: Role of xanthine oxidase”, *Radiation Research*, Vol. 176/4, Radiation Research Society, Bozeman, https://doi.org/10.1667/RR2598.1.

Soucy, K. G. et al. (2010), “Dietary inhibition of xanthine oxidase attenuates radiation-induced endothelial dysfunction in rat aorta”, *Journal of Applied Physiology*, Vol. 108/5, American Physiological Society, Rockville, https://doi.org/10.1152/japplphysiol.00946.2009.

Soucy, K. G. et al. (2007), “Single exposure gamma-irradiation amplifies xanthine oxidase activity and induces endothelial dysfunction in rat aorta”, *Radiation and Environmental Biophysics*, Vol. 46, Springer, New York, https://doi.org/10.1007/s00411-006-0090-z.

Sridharan, V. et al. (2020), "Effects of single-dose protons or oxygen ions on function and structure of the cardiovascular system in male Long Evans rats", *Life Sciences in Space Research*, Vol. 26, Elsevier, Amsterdam, https://doi.org/10.1016/j.lssr.2020.04.002.

Su, Y. T. et al. (2020), "Acid sphingomyelinase/ceramide mediates structural remodeling of cerebral artery and small mesenteric artery in simulated weightless rats", *Life Sciences*, Vol. 243, Elsevier, Amsterdam, https://doi.org/10.1016/j.lfs.2019.117253.

Sylvester, C. B. et al. (2018), "Radiation-Induced Cardiovascular Disease: Mechanisms and Importance of Linear Energy Transfer", *Frontiers in Cardiovascular Medicine*, Vol. 5, Frontiers Media SA, Lausanne, https://doi.org/10.3389/fcvm.2018.00005.

Tarasova, O. S. et al. (2020), "Simulated Microgravity Induces Regionally Distinct Neurovascular and Structural Remodeling of Skeletal Muscle and Cutaneous Arteries in the Rat", *Frontiers in Physiology*, Vol. 1, Frontiers Media SA, Lausanne, https://doi.org/10.3389/fphys.2020.00675.

Yu, T. et al. (2011), "Iron-ion radiation accelerates atherosclerosis in apolipoprotein E-Deficient mice", *Radiation Research*, Vol. 175/6, Radiation Research Society, Bozeman, https://doi.org/10.1667/RR2482.1.

Appendix 2

List of Key Event Relationships in the AOP

List of Adjacent Key Event Relationships

Relationship: 2769: Energy Deposition leads to Oxidative Stress

AOPs Referencing Relationship

AOP Name	Adjacency	Weight of Evidence	Quantitative Understanding
Deposition of energy leads to vascular remodeling	adjacent	High	High
Deposition of Energy Leading to Learning and Memory Impairment	adjacent	High	Moderate
Deposition of energy leading to occurrence of bone loss	adjacent	High	Moderate
Deposition of energy leading to occurrence of cataracts	adjacent	High	High

Evidence Supporting Applicability of this Relationship

Taxonomic Applicability

Term	Scientific Term	Evidence	Links
human	Homo sapiens	Moderate	NCBI
mouse	Mus musculus	Moderate	NCBI
rat	Rattus norvegicus	High	NCBI
rabbit	Oryctolagus cuniculus	Low	NCBI

Life Stage Applicability

Life Stage	Evidence
Juvenile	High
Adult	Moderate

Sex Applicability

Sex	Evidence
Male	High
Female	Moderate
Unspecific	High

Most evidence is derived from in vitro studies, predominately using rabbit models. Evidence in humans and mice is moderate, while there is considerable available data using rat models. The relationship is applicable in both sexes, however, males are used more often in animal studies. No studies demonstrate the relationship in preadolescent animals, while adolescent animals were used very often, and adults were used occasionally in in vivo studies.

Key Event Relationship Description

Energy deposited onto biomolecules stochastically in the form on ionizing and non-ionizing radiation can cause direct and indirect molecular-level damage. As energy is deposited in an aqueous solution, water molecules can undergo radiolysis, breaking bonds to produce reactive oxygen species (ROS) (Ahmadi et al., 2021; Karimi et al., 2017) or directly increase function of enzymes involved in ROS generation (i.e. catalaze). Various species of ROS can be generated with differing degrees of biological effects. For example, singlet oxygen, superoxide, and hydroxyl radical are highly unstable, with short half-lives and react close to where they are produced, while species like H_2O_2 are much more stable and membrane permeable, meaning they can travel from the site of production, reacting elsewhere as a much weaker oxidant (Spector, 1990). In addition, enzymes involved in reactive oxygen and nitrogen species (RONS) production can be directly upregulated following the deposition of energy (de Jager, Cockrell and Du Plessis, 2017). Although less common than ROS, reactive nitrogen species (RNS) can also be produced by energy deposition resulting in oxidative stress (Cadet et al., 2012; Tangvarasittichai & Tangvarasittichai, 2019), a state in which the amount of ROS and RNS, collectively known as RONS, overwhelms the cell's antioxidant defense system. This loss in redox homeostasis can lead

to oxidative damage to macromolecules including proteins, lipids, and nucleic acids (Schoenfeld et al., 2012; Tangvarasittichai & Tangvarasittichai, 2019; Turner et al., 2002).

Evidence Supporting this KER

Overal weight of evidence: High

Biological Plausibility

A large body of literature supports the linkage between the deposition of energy and oxidative stress. Multiple reviews describe the relationship in the context of ROS production (Marshall, 1985; Balasubramanian, 2000; Jurja et al., 2014), antioxidant depletion (Cabrera et al., 2011; Fletcher, 2010; Ganea & Harding, 2006; Hamada et al., 2014; Spector, 1990; Schoenfeld et al., 2012; Wegener, 1994), and overall oxidative stress (Eaton, 1994, Tangvarasittichai & Tangvarasittichain, 2019). This includes investigations into the mechanism behind the relationship (Ahmadi et al., 2021; Balasubramanian, 2000; Cencer et al., 2018; Eaton, 1994; Fletcher, 2010; Jiang et al., 2006; Jurja et al., 2014; Padgaonkar et al., 2015; Quan et al., 2021; Rong et al., 2019; Slezak et al., 2015; Soloviev & Kizub, 2019; Tian et al., 2017; Tahimic & Globus, 2017; Varma et al., 2011; Venkatesulu et al., 2018; Wang et al., 2019a; Yao et al., 2008; Yao et al., 2009; Zigman et al., 2000).

Water radiolysis is a main source of free radicals. Energy ionizes water and free radicals are produced that combine to create more stable ROS, such as hydrogen peroxide, hydroxide, superoxide, and hydroxyl (Eaton, 1994; Rehman et al., 2016; Tahimic & Globus, 2017; Tian et al., 2017; Varma et al., 2011; Venkatesulu et al., 2018). ROS formation causes ensuing damage to the body, as ~80% of tissues are comprised of water (Wang et al., 2019a). Ionizing radiation (IR) is a source of energy deposition, it can also interact with molecules, such as nitric oxide (NO), to produce less common free radicals, including RNS (Slezak et al., 2015; Tahimic & Globus, 2017; Wang et al., 2019a). Free radicals can diffuse throughout the cell and damage vital cellular components, such as proteins, lipids, and DNA, as well as dysregulate cellular processes, such as cell signalling (Slezak et al., 2015; Tian et al., 2017).

ROS are also commonly produced by nicotinamide adenine dinucleotide phosphate (NADPH) oxidase (NOX). Deposition of energy can activate NOX and induce expression of its catalytic and cytosolic components, resulting in increased intracellular ROS (Soloviev & Kizub, 2019). Intracellular ROS production can also be initiated through the expression of protein kinase C, which in turn activates NOX through phosphorylation of its cytosolic components (Soloviev & Kizub, 2019). Alternatively, ROS are often formed at the electron transport chain (ETC) of the mitochondria, due to IR-induced electron leakage leading to ionization of the surrounding O_2 to become superoxide (Soloviev & Kizub, 2019). Additionally, energy reaching a cell can be absorbed by an unstable molecule, often NADPH, known as a chromophore, which leads to the production of ROS (Balasubramanian, 2000; Cencer et al., 2018; Jiang et al., 2006; Jurja et al., 2014; Padgaonkar et al., 2015; Yao et al., 2009; Zigman et al., 2000).

Energy deposition can also weaken a cell's antioxidant defense system through the depletion of certain antioxidant enzymes, such as superoxide dismutase (SOD) and catalase (CAT). Antioxidants are consumed during the process of neutralizing ROS, so as energy deposition stimulates the formation of ROS it begins to outpace the rate at which antioxidants are replenished; this results in an increased risk of oxidative stress when their concentrations are low (Belkacémi et al., 2001; Giblin et al., 2002; Ji et al., 2014; Kang et al., 2020; Karimi et al., 2017; Padgaonkar et al., 2015; Rogers et al., 2004; Slezak et al., 2015; Tahimic & Globus, 2017; Wang et al., 2019a; Wegener, 1994; Weinreb & Dovrat, 1996; Zhang et al., 2012; Zigman et al., 1995; Zigman et al., 2000). When the amount of ROS overwhelms the antioxidant defense system, the cell will enter oxidative stress leading to macromolecular and cellular damage (Tangvarasittichai & Tangvarasittichai, 2019).

Empirical Evidence

The relationship between energy deposition and oxidative stress is strongly supported by primary research on the effects of IR on ROS and antioxidant levels (Bai et al., 2020; Cervelli et al., 2017; Hatoum et al., 2006; Huang et al., 2018; Huang et al., 2019; Karam & Radwan, 2019; Kook et al., 2015; Liu et al., 2018; Liu et al., 2019; Mansour, 2013; Philipp et al., 2020; Ramadan et al., 2020; Sharma et al., 2018; Shen et al., 2018; Soltani et al., 2016; Soucy et al., 2010; Soucy et al., 2011; Ungvari et al., 2013; Wang et al., 2016; Wang et al., 2019b; Zhang et al., 2018; Zhang et al., 2020). Of note is that the relationship is demonstrated across studies conducted using various cell types, models and using broad dose-ranges as summarized below. Much evidence is available and described to help discern the quantitative understanding of the relationship, since it is well established.

Dose Concordance

It is well-accepted that any dose of radiation will deposit energy onto matter. Doses as low as 1 cGy support this relationship (Tseung et al., 2014). Following the deposition of energy, markers of oxidative stress are observed in the form of RONS, a change in levels of antioxidants, and oxidative damage to macromolecules. These effects have been shown across various organs/tissues and cell types as described below.

<u>RONS</u>

Cardiovascular tissue:

There is a considerable amount of evidence to support this relationship in cell types and tissues of relevance to the cardiovascular system. Recent studies have shown a linear increase in ROS in human umbilical vein endothelial cells (HUVECs) following 0-5 Gy gamma irradiation (Wang et al., 2019b). HUVECs irradiated with 0.25 Gy X-rays (Cervelli et al., 2017) and 9 Gy 250kV photons (Sharma et al., 2018) show increased ROS. Gamma ray irradiated rats at 5 Gy display increased ROS levels in the aorta (Soucy et al., 2010). A study using cerebromicrovascular endothelial cell (CMVECs) showed a dose-dependent increase in ROS from 0-8 Gy gamma irradiation (Ungvari et al., 2013). Additionally, telomerase-immortalized coronary artery endothelial (TICAE) and telomerase-immortalized microvascular endothelial (TIME) cells irradiated with 0.1 and 5 Gy of X-rays displayed increased ROS production (Ramadan et al., 2020). Gut arterioles of rats showed increased ROS following multiple fractions of 2.5 Gy X-ray rat irradiation (Hatoum et al., 2006). Additionally, rats irradiated with 1 Gy of 56Fe expressed increased ROS levels in the aorta (Soucy et al., 2011).

Brain tissue:

Markers of oxidative stress have also been consistently observed in brain tissue. Human neural stem cells subjected to 1, 2 or 5 Gy gamma rays showed a dose-dependent increase in RONS production (Acharya et al., 2010). A dose-dependent increase in ROS was observed in rat brains following 1-10 Gy gamma rays (Collins-Underwood et al., 2008). Neural precursor cells exposed to 0-10 Gy of X-irradiation showed increased ROS levels (Giedzinski et al., 2005; Limoli et al., 2004). Mice brain tissue displayed increased ROS following proton irradiation (Baluchamy et al., 2012; Giedzinski et al., 2005). Neural processor cells expressed linearly increased ROS levels following doses of 56Fe (Limoli et al., 2007). A dose-dependent increase in RONS was also observed after exposure to 1-15 cGy 56Fe irradiation in mice neural stem/precursor cell (Tseng et al., 2014). Human neural stem cells exposed to 5-100 cGy of various ions demonstrated a dose-dependent increase in RONs (Baulch et al., 2015).

Eye tissue:

The eye is also sensitive to the accumulation of free radicals, in a state of antioxidant decline. It has been shown in human lens epithelial cells (HLECs) and HLE-B3 following gamma irradiation of 0.25 and 0.5 Gy that ROS levels are markedly increased (Ahmadi et al., 2021). Exposure to non-ionizing radiation, such as ultraviolet (UV)-B, has also led to increased ROS in HLECs and mice lenses (Ji et al., 2015; Kubo et al., 2010; Rong et al., 2019; Yang et al., 2020)

Bone tissue:

Rat bone marrow-derived mesenchymal stem cell (bmMSCs) irradiated with 2, 5 and 10 Gy gamma rays and Murine MC3T3-E1 osteoblast cells irradiated with 2, 4, and 8 Gy of X-rays have shown a dose-dependent increase in ROS levels (Bai et al., 2020; Kook et al., 2015). Murine RAW264.7 cells and rat bmMSC irradiated with 2 Gy of gamma rays displayed increased ROS levels (Huang et al., 2019; Huang et al., 2018; hang et al., 2020). Human bone marrow-derived mesenchymal stem cell (hBMMSCs) irradiated with 2 or 8 Gy X-rays showed increased ROS (Liu et al., 2018; Zhang et al., 2018). Similarly, murine MC3T3-E1 osteoblast-like cells irradiated with 6 Gy of X-rays also displayed increased ROS (Wang et al., 2016). Finally, whole-body irradiation of mice with 2 Gy of 31.6 keV/mm LET 12C heavy ions showed increased ROS (Liu et al., 2019)

Antioxidants

Blood:

Workers exposed to X-rays at less than 1 mSv/year for an average of 15 years showed around 20% decreased antioxidant activity compared to unexposed controls (Klucinski et al., 2008). Similarly, adults exposed to high background irradiation of 260 mSv/year showed about 50% lower antioxidant activity power compared to controls (Attar, Kondolousy and Khansari, 2007).

Cardiovascular tissue:

Heart tissue of rats following gamma irradiation of rats at 5 and 6 Gy resulted in a decrease in antioxidant levels (Karam & Radwan, 2019; Mansour, 2013). Similarly, HUVECs (Soltani, 2016) and TICAE cells (Philipp et al., 2020) irradiated at 2 Gy and 0.25-10 Gy gamma rays, respectively, displayed decreased antioxidant levels. Mice exposed to 18 Gy of X-ray irradiation showed decreased antioxidants in the aorta (Shen et al., 2018).

Brain tissue:

Mice brain tissue following 2, 10 and 50 cGy whole-body gamma irradiation revealed a dose-dependent change in SOD2 activity (Veeraraghan et al., 2011). Mice brain tissue showed decreased glutathione (GSH) and SOD levels following proton irradiation (Baluchamy et al., 2012)

Eye tissue:

Rats exposed to 15 Gy gamma rays demonstrated decreased antioxidants in the lens tissue (Karimi et al, 2017). Neutron irradiation of rats at 3.6 Sv resulted in a decrease in antioxidants in lens (Chen et al., 2021). A few studies found a dose concordance between UV irradiation and decreased antioxidant levels (Hua et al, 2019; Ji et al, 2015; Zigman et al., 2000; Zigman et al, 1995). HLECs following UVB exposure from 300 J/m2 to 14,400 J/m2 in HLECs showed linear decreases in antioxidant activity (Ji et al., 2015). Similarly, HLEC exposed to 4050, 8100 and 12,150 J/m2 found decreased antioxidant levels (Hua et al., 2019). Following UV irradiation of rabbit and squirrel lens epithelial cells (LECs) showed a linear decrease of antioxidant level, CAT (Zigman et al., 2000; Zigman et al., 1995). Mice exposed to UV irradiation found decreased antioxidant levels in lens (Zhang et al., 2012). Similarly, SOD levels decreased following 0.09 mW/cm 2 UVB exposure of HLECs (Kang et al., 2020).

Bone tissue:

Rat bmMSCs irradiated with 2, 5 and 10 Gy gamma rays and Murine MC3T3-E1 osteoblast cells irradiated with 2, 4, and 8 Gy of X-rays showed a dose-dependent decrease in antioxidant levels (Bai et al., 2020; Kook et al., 2015). hBMMSCs irradiated with 8 Gy X-rays also showed a decrease in antioxidant, SOD, levels (Liu et al., 2018).

Oxidative Damage

Cardiovascular tissue:

HUVECs and rat hearts irradiated by gamma rays at 2 and 6 Gy, respectively, resulted in increased levels of oxidative stress markers, such as malondialdehyde (MDA), and thiobarbituric reactive substances (TBARS) (Mansour, 2013; Soltani, 2016).

Brain tissue:

Mice brain tissue were shown to have increased lipid peroxidation (LPO) as determined by MDA measurements, following proton irradiation at 1 and 2 Gy (Baluchamy et al., 2012). Neural precursor cells from rat hippocampus exposed to 0, 1, 5 and 10 Gy of X-irradiation resulted in increased lipid peroxidation (Limoli et al., 2004).

Eye tissue:

Rats exposed to 15 Gy gamma rays demonstrated increased MDA in lens tissue (Karimi et al, 2017). Neutron irradiation of rats at 3.6 Sv resulted in an initial decrease, followed by an increase in MDA in lens (Chen et al., 2021). Following UV irradiation at 300 4050, 8100 and 12,150 J/m2, there was an increase in LPO in in human lens (Chitchumroonchokchai et al, 2004; Hua et al, 2019). Similarly, LPO increased following 0.09 mW/cm 2 UVB exposure of HLECs (Kang et al., 2020).

Time Concordance

It is well-accepted that deposition of energy into matter results in immediate vibrational changes to molecules or ionization events. Deposition of energy is therefore an upstream event to all follow-on latent events like oxidative stress.

RONS

Cardiovascular tissue:

In TICAE and TIME cells, ROS increased at 45 mins after X-ray irradiation (Ramadan et al., 2020). Superoxide and peroxide production were increased 1 day after 2-8 Gy of gamma irradiation in CMVECs (Unvari et al., 2013).

Bone tissue:

hBMMSCs irradiated with X-rays at 2 Gy showed peak ROS production at 2-8h post-irradiation (Zhang et al., 2018). Murine RAW264.7 cells (can undergo osteoclastogenesis) irradiated with 2 Gy of gamma rays showed increased ROS at 2-8h post-irradiation (Huang et al., 2018).

Brain tissue:

In human lymphoblast cells exposed to 2 Gy of X-rays, ROS were increased at various times between 13 and 29 days post-

irradiation (Rugo and Schiestl, 2004). RONS were increased in human neural stem cells at 12-48h post-irradiation with 2 and 5 Gy of gamma rays (Acharya et al., 2010). ROS levels were increased in rat neural precursor cells at 6-24h after irradiation with 1-10 Gy of protons (Giedzinksi et al., 2005). Both 56Fe (1.3 Gy) and gamma ray (2 Gy) irradiation of mice increased ROS levels after 2 months post-irradiation in the cerebral cortex (Suman et al., 2013). ROS were also increased 12 months after 56Fe irradiation (Suman et al., 2013). RONS increased as early as 12h post-irradiation continuing to 8 weeks with 2-200 cGy doses of 56Fe irradiation of mouse neural stem/precursor cells (Tseng et al., 2014). The same cell type irradiated with 1 and 5 Gy of 56Fe irradiation showed increased ROS at 6h post-irradiation, with the last increase observed 25 days post-irradiation (Limoli et al., 2004).

Eye tissue:

Mice exposed to 11 Gy of X-rays showed increased ROS at 9 months post-irradiation in lenses (Pendergrass et al., 2010). In human lens cells, ROS were found increased at 1h after 0.25 Gy gamma ray irradiation (Ahmadi et al., 2021), 15 minutes after 30 mJ/cm2 UV radiation (Jiang et al., 2006), 2.5-120 minutes after 0.014 and 0.14 J/cm2 UV radiation (Cencer et al., 2018), and 24h after 30 mJ/cm2 UVB radiation (Yang et al., 2020).

Antioxidants

Cardiovascular tissue:

CAT antioxidant enzyme was decreased in mice aortas as early as 3 days post-irradiation, remaining decreased until 84 days after irradiation with 18 Gy of X-rays (Shen et al., 2018). The antioxidant enzymes peroxiredoxin 5 (PRDX5) and SOD were both shown to have the greatest decrease at 24h after 2 Gy gamma irradiation of TICAE cells (Philipp et al., 2020).

Eye tissue:

Bovine lenses irradiated with 44.8 J/cm2 of UVA radiation showed decreased CAT levels at 48-168h post-irradiation (Weinreb and Dovrat, 1996). UV irradiation of mice at 20.6 kJ/m2 led to decreased GSH at both 1 and 16 months post-irradiation in the lens (Zhang et al., 2012). Bovine lens cells exposed to 10 Gy of X-rays showed decreased levels of the antioxidant GSH at 24 and 120h after exposure (Belkacemi et al., 2001).

Oxidative damage markers

Cardiovascular tissue:

Oxidative damage markers 4-hydroxynonemal (4-HNE) and 3-Nitrotyosine (3-NT) were both significantly increased in the aorta of mice at 3 days post-irradiation, remaining increased until 84 days after irradiation with 18 Gy of X-rays (Shen et al., 2018).

Essentiality

Radiation has been found to induce oxidative stress above background levels. Many studies have shown that lower doses of ionizing radiation resulted in decreased levels in markers of oxidative stress in multiple cell types (Acharya et al., 2010; Ahmadi et al., 2021; Bai et al., 2020; Baluchamy et al., 2012 Chen et al., 2021; Collins-Underwood et al., 2008; Giedzinski et al., 2005; Kook et al., 2015; Kubo et al., 2010; Philipp et al., 2020; Ramadan et al., 2020; Ungvari et al., 2013; Veeraraghan et al., 2011; Wang et al., 2019b; Zigman et al., 2000; Zigman et al., 1995). The essentiality of deposition of energy can be assessed through the removal of deposited energy, a physical stressor that does not require to be metabolized in order to elicit downstream effects on a biological system. Studies that do not deposit energy are observed to have no downstream effects.

Uncertainties and Inconsistencies

There are several uncertainties and inconsistencies in this KER.

- Chen et al. (2021) found that radiation can have adaptive responses. The study used three neutron radiation doses, 0.4 and 1.2 Sv, and 3.6 Sv. After 0.4 and 1.2 Sv, the activity of antioxidant enzymes GSH and SOD increased, and the concentration of malondialdehyde, a product of oxidative stress, decreased. After 3.6 Sv, the opposite was true.
- While the concentration of most antioxidant enzymes decreases after energy deposition, there is some uncertainty with SOD. Certain papers have found that its concentration decreases with dose (Chen et al., 2021; Hua et al., 2019; Ji et al., 2015; Kang et al., 2020) while others found no difference after irradiation (Rogers et al., 2004; Zigman et al., 1995). Several studies have also found that higher levels of SOD do not increase resistance to UV radiation (Eaton, 1994; Hightower, 1995).
- At 1-week post-irradiation with 10 Gy of 60Co gamma rays, TICAE cells experienced a significant increase in levels of the antioxidant, PRDX5, contrary to the decrease generally seen in antioxidant levels following radiation exposure (Philipp et al.,

2020).

- Various studies found an increase in antioxidant SOD levels within the brain after radiation exposure (Acharya et al., 2010; Baluchamy et al., 2012; Baulch et al., 2015; Veeraraghan et al., 2011).

Quantitative Understanding of the Linkage

The table below provides some representative examples of quantitative linkages between the two key events. It was difficult to identify a general trend across all the studies due to differences in experimental design and reporting of the data. All data is statistically significant unless otherwise stated.

Response-response relationship

Dose Concordance

Reference	Experiment Description	Result
Attar, Kondolousy and Khansari, 2007	In vivo. One hundred individuals between 20 and 50 years old in two villages in Iran exposed to background IR at 260 mSv/year had antioxidant levels measured. The control group was from two villages not exposed to the high background radiation. The total antioxidant levels in the blood were determined by the ferric reducing/antioxidant power assay.	The total antioxidant level was significantly reduced from 1187±199 µmol in the control to 686±170 µmol in the exposed group.
Klucinski et al., 2008	In vivo. A group of 14 men and 31 women aged 25–54 years working X-ray equipment (receiving doses of less than 1 mSv/year) for an average of 15.3 years (range of 2-33 years) were compared to a control group for antioxidant activity. Antioxidant activity of SOD, glutathione peroxidase (GSH-Px), and CAT in erythrocytes were measured in U/g of hemoglobin.	All three enzymes showed significantly decreased antioxidant activity in the workers. In the controls (U/g of Hb): • SOD: 1200 ± 300 • GSH-Px: 39 ± 7 • CAT: 300 ± 60 In the workers (U/g of Hb): • SOD: 1000 ± 200 • GSH-Px: 29 ± 4 • CAT: 270 ± 50
Limoli et al., 2007	In vitro. Neural precursor cells isolated from rat hippocampi was exposed to 0.25-5 Gy of 56Fe irradiation at dose rates of 0.5-1.0 Gy/min. ROS were measured 6h post-irradiation.	At a low dose of 0.25 Gy and 0.5 Gy, relative ROS levels were significantly elevated and showed a linear dose response (from ~1 to ~2.25 relative ROS levels) until 1 Gy, where it reached its peak (~3 relative ROS levels). At higher doses, the relative ROS levels decreased.
Tseng et al., 2014	In vitro. Neural stem/precursor cells isolated from mouse subventricular and hippocampal dentate subgranular zones were exposed to 1-15 cGy of 56Fe irradiation at dose rates ranging from 5-50 cGy/min. RONS levels were measured.	A dose-dependent and significant rise in RONS levels was detected after 56Fe irradiation. 12 h post-irradiation, a steady rise was observed and reached a 6-fold peak after 15 cGy.
Limoli et al., 2004	In vitro. Neural precursor cells from rat hippocampus were exposed to 0, 1, 5 and 10 Gy of X-irradiation at a dose rate of 4.5 Gy/min. ROS levels were measured. In vivo. MDA was used to quantify	A dose-dependent increase in ROS levels was seen in the first 12 h post-irradiation, with relative maximums at 12 h after 5 Gy (35% increase) and 24 h after 1 Gy (31% increase). ROS levels measured 1 week after 5 Gy were increased by 180% relative to sham-irradiated controls. MDA levels increased significantly (approximately 1.3-fold)

	oxidative stress.	after exposure to 10 Gy.
Collins-Underwood et al., 2008	In vitro. Immortalized rat brain microvascular endothelial cells were exposed to 1-10 Gy of 137Cs-irradiation at a dose rate of 3.91 Gy/min. Intracellular ROS and O2- production were both measured.	Irradiation resulted in a significant dose-dependent increase in intracellular ROS generation from 1-10 Gy. At 5 Gy, there was an approximate 10-fold increase in ROS levels, and at 10 Gy there was an approximate 20-fold increase.
Giedzinski et al., 2005	In vitro. Neural precursor cells were irradiated with 1, 2, 5 and 10 Gy of 250 MeV protons (1.7-1.9 Gy/min) and X-irradiation (4.5 Gy/min). ROS levels were measured.	There was a rapid increase in ROS at 6, 12, 18 and 24h after proton irradiation, with an exception at the 1 Gy 18h point. Most notably, at 6h post-irradiation, a dose-dependent increase in relative ROS levels from 1 to 10 Gy was seen that ranged from 15% (at 1 Gy) to 65% (at 10 Gy). Linear regression analysis showed that at ≤2 Gy, ROS levels increased by 16% per Gy. The linear dose response obtained at 24h showed that proton irradiation increased the relative ROS levels by 3% per Gy.
Veeraraghan et al., 2011	In vivo. Adult mice were exposed to 2, 10 or 50 cGy of whole-body gamma irradiation at 0.81 Gy/min. Brain tissues were harvested 24h post-irradiation. SOD2 levels and activity were measured.	Compared to the controls, the levels of SOD2 expression increased in the brain after 2, 10 and 50 cGy. Analysis revealed a significant and dose-dependent change in SOD2 activity. More specifically, SOD2 activity showed significant increases after 10 (~25% increase above control) and 50 cGy (~60% increase above control), but not 2 cGy.
Baluchamy et al., 2012	In vivo. Male mice were exposed to whole-body irradiation with 250 MeV protons at 0.01, 1 and 2 Gy and the whole brains were dissected out. ROS, LPO, GSH and total SOD were measured.	Dose-dependent increases in ROS levels was observed compared to controls, with a two-fold increase at 2 Gy. A 2.5 to 3-fold increase in LPO levels was also seen at 1 and 2 Gy, respectively, which was directly correlated with the increase in ROS levels. Additionally, results showed a significant reduction in GSH (~70% decrease at 2 Gy) and SOD activities (~2-fold decrease) following irradiation that was dose-dependent.
Acharya et al., 2010	In vitro. Human neural stem cells were subjected to 1, 2 or 5 Gy of gamma irradiation at a dose rate of 2.2 Gy/min. RONS and superoxide levels were determined.	Intracellular RONS levels increased by approximately 1.2 to 1.3-fold compared to sham-irradiated controls and was found to be reasonable dose-responsive. At 12h, levels of superoxide increased 2 and 4-fold compared to control for 2 and 5 Gy, respectively. At 24h and 48h, there was a dose-dependent increase in RONS levels. At 7 days, levels of RONS increased approximately 3 to 7-fold for 2 and 5 Gy, respectively.
Baulch et al., 2015	In vitro. Human neural stem cells were exposed to 5-100 cGy of 16O, 28Si, 48Ti or 56Fe particles (600 MeV) at 10-50 cGy/min. RONS and superoxide levels were determined.	3 days post-irradiation, oxidative stress was found to increase after particle irradiation. Most notably, exposure to 56Fe resulted in a dose-dependent increase with 100% increase in RONS levels at 100 cGy. Dose-dependent increase was also seen in superoxide levels after 56Fe irradiation. At 7 days post-irradiation, 56Fe irradiation induced significantly lower nitric oxide levels by 47% (5 cGy), 55% (25 cGy) and 45% (100 cGy).
Bai et al., 2020	In vitro. bmMSCs were taken from 4-week-old, male Sprague-Dawley rats. After extraction, cells were then irradiated with 2, 5, and 10 Gy of 137Cs gamma rays. Intracellular ROS levels and relative mRNA expression of the antioxidants, SOD1, SOD2, and CAT2, were measured to assess the extent of oxidative stress induced by IR.	Cellular ROS levels increased significantly in a dose-dependent manner from 0-10 Gy. Compared to sham-irradiated controls, ROS levels increased by ~15%, ~55%, and ~105% after exposure to 2, 5, and 10 Gy, respectively. Antioxidant mRNA expression decreased in a dose-dependent manner from 0-10 Gy, with significant increases seen at doses 2 Gy for SOD1 and CAT2 and 5 Gy for SOD2. Compared to sham-irradiated controls, SOD1 expression decreased by ~9%, ~18%, and ~27% after exposure to 2, 5, and 10 Gy, respectively. SOD2 expression decreased by ~31% and ~41% after exposure to 5 and 10 Gy, respectively. CAT2 expression decreased by ~15%, ~33%, and ~58% after exposure to 2, 5, and 10 Gy, respectively.
Liu et al., 2018	In vitro. hBMMSCs were irradiated with 8 Gy of X-rays at a rate of 1.24 Gy/min. Intracellular ROS levels and SOD activity were measured to analyze IR-induced oxidative stress.	Compared to sham-irradiated controls, hBMMSCs irradiated with 8 Gy of X-rays experienced a significant increase to intracellular ROS levels. hBMMSCs irradiated with 8 Gy of X-rays experienced a ~46% reduction in SOD activity.
	In vitro. Murine MC3T3-E1	Compared to sham-irradiated controls, irradiated MC3T3-E1 cells

Kook et al., 2015	osteoblast cells were irradiated with 2, 4, and 8 Gy of X-rays at a rate of 1.5 Gy/min. Intracellular ROS levels and the activity of antioxidant enzymes, including GSH, SOD, CAT, were measured to assess the extent of oxidative stress induced by IR exposure.	experienced a dose-dependent increase in ROS levels, with significant increases at 4 and 8 Gy (~26% and ~38%, respectively). Antioxidant enzyme activity initially increased by a statistically negligible amount from 0-2 Gy and then decreased in a dose-dependent manner from 2-8 Gy. SOD activity decreased significantly at 4 and 8 Gy by ~29% and ~59%, respectively. GSH activity similarly decreased significantly at 4 and 8 Gy by ~30% and ~48%, respectively. CAT activity did not change by a statistically significant amount.
Liu et al., 2019	In vivo. 8–10-week-old, juvenile, female SPF BALB/c mice underwent whole-body irradiation with 2 Gy of 31.6 keV/µm 12C heavy ions at a rate of 1 Gy/min. ROS levels were measured from femoral bone marrow mononuclear cells of the irradiated mice to analyze IR-induced oxidative stress.	Compared to sham-irradiated controls, irradiated mice experienced a ~120% increase in ROS levels.
Zhang et al., 2020	In vitro. Murine RAW264.7 osteoclast precursor cells were irradiated with 2 Gy of 60Co gamma rays at a rate of 0.83 Gy/min. ROS levels were measured to determine the extent of oxidative stress induced by IR exposure.	Compared to sham-irradiated controls, ROS levels in irradiated RAW264.7 cells increased by ~100%.
Wang et al., 2016	In vitro. Murine MC3T3-E1 osteoblast-like cells were irradiated with 6 Gy of X-rays. Intracellular ROS production was measured to assess oxidative stress from IR exposure.	Compared to sham-irradiated controls, Intracellular ROS production increased by ~81%.
Huang et al., 2018	In vitro. Murine RAW264.7 osteoblast-like cells were irradiated with 2 Gy of gamma rays at a rate of 0.83 Gy/min. ROS levels were measured to analyze IR-induced oxidative stress.	Compared to sham-irradiated controls, ROS levels in RAW264.7 cells increased by ~138% by 2 h post-irradiation.
Zhang et al., 2018	In vitro. hBMMSCs were irradiated with 2 Gy of X-rays at a rate of 0.6 Gy/min. Relative ROS concentration was measured to assess the extent of oxidative stress induced by IR.	Compared to sham-irradiated controls, irradiated hBMMSCs experienced a maximum increase of ~90% to ROS levels at 3 h post-irradiation.
Huang et al., 2019	In vitro. Rat bmMSC were irradiated with 2 Gy of 60Co gamma rays at a rate of 0.83 Gy/min. ROS levels were measured to assess IR-induced oxidative stress.	Compared to sham-irradiated controls, ROS levels in irradiated bone marrow stromal cells increased by approximately 2-fold.
Soucy et al., 2011	In vivo. 7- to 12-month-old, adult, male Wistar rats underwent whole-body irradiation with 1 Gy of 56Fe heavy ions. ROS production in the aorta was measured along with changes in activity of the ROS-producing enzyme xanthine oxidase (XO) to assess IR-induced oxidative stress.	Compared to sham-irradiated controls, irradiated mice experienced a 74.6% increase in ROS production (from 4.84 to 8.45) and XO activity increased by 36.1% (6.12 to 8.33).
Soucy et al., 2010	In vivo. 4-month-old, adult, male Sprague-Dawley rats underwent whole-body irradiation with 5 Gy of 137Cs gamma rays. Changes in XO activity and ROS production were measured in the aortas of	Compared to sham-irradiated controls, irradiated mice experienced a ~68% increase in ROS production and a ~46% increase in XO activity.

	the mice to assess IR-induced oxidative stress.	
Karam & Radwan, 2019	In vivo. Adult male Albino rats underwent irradiation with 5 Gy of 137Cs gamma rays at a rate of 0.665 cGy/s. Activity levels of the antioxidants, SOD and CAT, present in the heart tissue were measured to assess IR-induced oxidative stress.	Compared to the sham-irradiated controls, SOD and CAT activity decreased by 57% and 43%, respectively, after irradiation.
Cervelli et al., 2017	In vitro. HUVECs were irradiated with 0.25 Gy of X-rays at a rate of 91 mGy/min. ROS production was measured to analyze IR-induced oxidative stress.	Compared to the sham-irradiated controls, irradiated mice experienced a ~171% increase in ROS production (not significant).
Mansour, 2013	In vivo. Male Wistar rats underwent whole-body irradiation with 6 Gy of 137Cs gamma rays at a rate of 0.012 Gy/s. MDA was measured from heart homogenate, along with the antioxidants: SOD, GSH, and GSH-Px.	Compared to sham-irradiated controls, MDA increased by 65.9%. SOD, GSH-Px, and GSH decreased by 33.8%, 42.4%, and 50.0%, respectively.
Soltani, 2016	In vitro. HUVECs were irradiated with 2 Gy of ^{60}Co gamma rays at a dose rate of 0.6 Gy/min. Markers of oxidative stress, including reduced GSH and TBARS, were measured to assess GSH depletion and LPO, respectively.	Compared to non-irradiated controls, sham-irradiated cells experienced a ~28% decrease in GSH and a ~433% increase in TBARS.
Wang et al., 2019b	In vitro. HUVECs were irradiated with 0.2, 0.5, 1, 2, and 5 Gy of 137Cs gamma rays. ROS production was measured to assess IR-induced oxidative stress.	Compared to sham-irradiated controls, ROS production saw a significant, ~32% increase at 5 Gy. While changes to ROS production were insignificant at doses <2 Gy, they followed a linear increase from 0-5 Gy.
Sharma et al., 2018	In vitro. HUVECs were irradiated with 9 Gy of photons. ROS production was measured to determine the effects of IR on oxidative stress.	Compared to sham-irradiated controls, irradiated HUVECs saw a significant, ~133% increase in ROS production.
Hatoum et al., 2006	In vivo. Sprague-Dawley rats were irradiated with 9 fractions of 2.5 Gy of X-rays for a cumulative dose of 22.5 Gy at a rate of 2.43 Gy/min. Production of the ROS superoxide and peroxide in gut arterioles were measured to determine the level of oxidative stress caused by irradiation.	ROS production started increasing compared to the sham-irradiated control after the second dose and peaked at the fifth dose. By the ninth dose, superoxide production increased by 161.4% and peroxide production increased by 171.3%.
Phillip et al., 2020	In vitro. Human TICAE cells were irradiated with 0.25, 0.5, 2, and 10 Gy of 60Co gamma rays at a rate of 0.4 Gy/min. Levels of the antioxidants, SOD1 and PRDX5 were measured to assess oxidative stress from IR exposure.	While SOD1 levels did not follow a dose-dependent pattern. At 2 Gy, SOD1 decreased about 0.5-fold. At 1-week post-irradiation, PRDX5 remained at approximately control levels for doses <2 Gy but increased by ~60% from 2-10 Gy. PRDX5 only decreased at 2 Gy and 24h post-irradiation.
Ramadan et al., 2020	In vitro. Human TICAE/TIME cells were irradiated with 0.1 and 5 Gy of X-rays at a dose rate of 0.5 Gy/min. Intracellular ROS production was measured to determine the extent of IR-induced oxidative stress.	ROS production saw a dose-dependent increase in both TICAE and TIME cells. By 45 mins post-irradiation, 0.1 Gy of IR had induced increases to ROS production of ~3.6-fold and ~8-fold in TICAE and TIME cells, respectively, compared to sham-irradiated controls. 5 Gy of IR caused more significant increases to ROS production of ~18-fold and ~17-fold in TICAE and TIME cells, respectively, compared to sham-irradiated controls.

Shen et al., 2018	In vivo. 8-week-old, female, C57BL/6 mice were irradiated with 18 Gy of X-rays. Levels of the oxidative markers, 4-HNE and 3-NT, and the antioxidants, CAT and heme oxygenase 1 (HO-1) were measured in the aortas of the mice.	Compared to sham-irradiated controls, irradiated mice saw maximum increases of ~1.75-fold on day 14 and ~2.25-fold on day 7 to 4-HNE and 3-NT levels, respectively. While CAT levels decreased up to 0.33-fold on day 7, HO-1 levels increased by ~1.9-fold on day 7.
Ungvari et al., 2013	In vitro. The CMVECs of adult male rats were irradiated with 2, 4, 6, and 8 Gy of 137Cs gamma rays. Production of the reactive oxygen species, peroxide and O2.-, were measured to assess the extent of IR-induced oxidative stress.	Compared to sham-irradiated controls, production of peroxide in CMVECs of irradiated mice 1 day-post exposure increased in a dose-dependent manner from 0-8 Gy, with significant changes observed at doses >4 Gy. At 8 Gy, peroxide production had increased ~3.25-fold. Production of O2.- followed a similar dose-dependent increase with significant observed at doses >6 Gy. At 8 Gy, O2.- production increased ~1.6-fold. 14 days post-exposure, IR-induced changes to ROS production were not significant for either peroxide or O2.- and did not show a dose-dependent pattern. ROS production progressively decreased from 0-4 Gy and then recovered from 6-8 Gy back to control levels.
Ahmadi et al., 2021	In vitro. HLEC and HLE-B3 cells were exposed to 0.1, 0.25 and 0.5 Gy of gamma irradiation at 0.3 and 0.065 Gy/min. Intracellular ROS levels were measured.	In HLE-B3 cells, there were about 7 and 17% ROS-positive cells 1 h after exposure to 0.25 and 0.5 Gy respectively at 0.3 Gy/min. 24 h after exposure there were about 10% ROS-positive cells after 0.5 Gy at 0.3 Gy/min. 1 h after exposure there were about 13 and 17% ROS-positive cells at 0.25 and 0.5 Gy and 0.065 Gy/min. 24 h after exposure there were 8% ROS-positive cells after 0.5 Gy and 0.065 Gy/min. In human lens epithelial cells 1 h after exposure there were about 10 and 19% ROS-positive cells after 0.25 and 0.5 Gy at 0.3 Gy/min. After exposure to 0.5 Gy at 0.065 Gy/min there were about 16 and 9% ROS-positive cells one and 24 h after exposure.
Ji et al, 2015	In vitro. HLECs were exposed to UVB-irradiation (297 nm; 2 W/m2) for 0 – 120 min. Total antioxidative capability (T-AOC), ROS levels, MDA, and SOD were measured at various time points at 5-120 min.	HLECs exposed to 1 W/m2 UVB for 0 - 120 min (representative of dose) showed a gradual increase in ROS levels that began to plateau 105 min post-irradiation at an ROS level 750 000x control.
Hua et al, 2019	In vitro. HLECs were exposed to 4050, 8100 and 12,150 J/m2 of UVB-irradiation at 1.5, 3.0 and 4.5 W/m2. MDA, SOD, GSH-Px, and GSH were measured.	MDA activity as a ratio of the control increased about 1.5 at 3.0 W/m2 and about 3 at 4.5 W/m2. SOD activity as a ratio of the control decreased about 0.1 at 1.5 W/m2, 0.2 at W/m2, and 0.3 at 4.5 W/m2. GSH-Px activity as a ratio of the control decreased about 0.02 at 3.0 W/m2 and 0.2 at 4.5 W/m2. GSH activity .as a ratio of the control decreased about 0.2 at 3.0 W/m2 and 0.7 at 4.5 W/m2.
Chen et al, 2021	In vivo. Male rats were irradiated with 0, 0.4, 1.2 and 3.6 Sv of neutron-irradiation at 14, 45 and 131 mSv/h. In rat lenses, MDA, GSH, and SOD, were measured.	MDA concentration decreased by about 1.5 nmol/mg protein at 1.2 Sv and increased by about 7.5 nmol/mg protein relative to the control at 3.6 Sv. GSH concentration increased by about 3.5 µg/mg protein and decreased by about 1 µg/mg protein relative to the control at 3.6 Sv (neutron radiation). SOD activity decreased by about 0.08 U/mg protein relative to the control at 3.6 Sv. It should be noted that Sv is not the correct unit when investigating

		animals and cultured cells, radiation should have been measured in Gy (ICRU, 1998).
Zigman et al., 2000	In vitro. Rabbit LECs were exposed to 3-12 J/cm2 of UVA-irradiation (300-400 nm range, 350 nm peak). CAT activity was assayed to demonstrate oxidative stress.	Rabbit LECs exposed to 3 – 12 J/cm2 UVA showed an approximately linear decrease in catalase activity (indicative of increased oxidative stress) with the maximum dose displaying a 3.8x decrease.
Chitchumroonchokchai et al, 2004	In vitro. HLECs were exposed to 300 J/m2 of UVB-irradiation at 3 mW/cm2. MDA and HAE were used to measure oxidative stress.	The concentration of MDA and HAE increased by about 900 pmol/mg protein compared to the control after irradiation with 300 J/m2 UVB.
Zigman et al, 1995	In vitro. Rabbit and squirrel LECs were exposed to 6, 9, 12, 15 and 18 J/m2 of UV-irradiation at 3 J/cm2/h (300-400 nm range, 350 nm peak). CAT was used to measure oxidative stress levels.	The CAT activity was 10% of the control activity at 6 J/cm2, and then decreased to 0% of the control activity at 18 J/cm2 (99.9% UV-A and 0.1% UV-B).
Karimi et al, 2017	In vivo. Adult rats were exposed to 15 Gy of gamma 60Co-irradiation at a dose rate of 98.5 cGy/min. In lens tissue, MDA, thiobarbituric acid (TBA), and GSH levels were used to indicate oxidative stress.	MDA concentration increased from 0.37 +/- 0.03 to 1.60 +/- 0.16 nmol/g of lens after irradiation. GSH concentration decreased from 0.99 +/- 0.06 to 0.52 +/- 0.16 µmol/g of lens after exposure.
Rong et al., 2019	In vitro. HLECs were exposed to UVB-irradiation (297 nm; 2 W/m^2 for 10 min). Intracellular H_2O_2 and superoxide levels were measured.	The amount of ROS was measured as the dicholofluoroscein (DCFH-DA) fluorescence density, which increased about 10-fold relative to the control. A similar test but with dihydroethidium (DHE) staining showed a fluorescence density increase of about 3-fold relative to the control.
Kubo et al., 2010	In vitro. Lenses isolated from mice were exposed to 400 or 800 J/m2 of UVB-irradiation. ROS levels were measured.	The ratio of ROS level/survived LECs increased from about 175 to 250% after exposure to 400 and 800 J/m2 UVB respectively.
Kang et al., 2020	In vitro. HLECs were exposed to 0.09 mW/cm2 UVB-irradiation (275-400 nm range, 310 nm peak) for 15 mins. MDA and SOD activity were measured.	MDA activity increased about 30% compared to control after 15 mins of 0.09 mW/cm2 UVB exposure. SOD activity decreased about 50% compared to control under the same conditions.
Yang et al., 2020	In vitro. HLECs were irradiated with 30 mJ/cm2 of UVB-irradiation. ROS levels were determined.	The level of ROS production in HLECs increased approximately 5-fold as determined by 2',7'-dichlorofluorescein diacetate after exposure to 30 mJ/cm2 UVB.
Zhang et al., 2012	In vivo. Adult mice were exposed to 20.6 kJ/m2 UV-irradiation (313 nm peak; 1.6 mW/cm2). GSH levels were measured in lens homogenates.	Decrease in GSH of about 1 and 2 µmol/g wet weight compared to control after 1 and 16 months respectively after 20.6 kJ/m2 UV (313 nm peak) at 1.6 mW/cm2.

Time-scale

Time Concordance

Reference	Experiment Description	Result
Tseng et al., 2014	In vitro. Neural stem/precursor cells isolated from mouse subventricular and hippocampal dentate subgranular zones were exposed to 1-200 cGy of 56Fe irradiation at dose rates ranging from 5-50 cGy/min. RONS were measured from 1 to 8 weeks post-irradiation.	Compared to sham-irradiated controls, a trend toward increasing oxidative stress was seen, particularly at 1- and 4-weeks post-irradiation where RONS levels showed dose-responsive increases. The greatest rise was also seen at 10 cGy where relative RONS levels increased ~2-fold from 1 to 4 weeks, ~3-fold from 4 to 6 weeks and ~2 fold from 6 to 8 weeks. RONS were also found increased at doses as low as 2 cGy at 12 and 24h post-irradiation.
	In vivo. Female mice were exposed to	ROS levels showed statistically significant increases after 56Fe

Suman et al., 2013	either 1.3 Gy of 56Fe irradiation (1 GeV/nucleon; dose rate of 1 Gy/min) or 2 Gy of gamma irradiation (dose rate of 1 Gy/min). ROS were measured in cerebral cortical cells at 2 and 12 months.	irradiation at both 2 and 12 months, while gamma irradiation led to an increase at only 2 months. The percent fluorescence intensity of ROS levels for control, gamma irradiated and 56Fe-irradiated were approximately 100, 115 and 140 at 2 months, and 100, 90 and 125 at 12 months, respectively.
Limoli et al., 2004	In vitro. Neural stem/precursor cells isolated from mouse subventricular and hippocampal dentate subgranular zones were exposed to 1 or 5 Gy of 56Fe irradiation at dose rates ranging from 4.5 Gy/min. RONS were measured at various time points until 33 days post-exposure.	ROS levels exhibited statistically significant fluctuations, increasing over the first 12h before dropping at 18h and rising again at 24h. At 5 Gy, ROS levels fluctuated with a peak at 7 days, a decrease at 13 days, an increase at 25 days, and a decrease below control levels at 33 days. At 1 Gy, ROS levels peaked at 25 days and also decreased below control at 33 days.
Gledzinski et al., 2005	In vitro. Neural precursor cells derived from rats were irradiated with 1, 2, 5 and 10 Gy of proton (1.7-1.9 Gy/min). ROS levels were determined at 5-25h post-irradiation.	Proton irradiation led to a rapid rise in ROS levels, with the increase most marked at 6h (approximately 10-70% for 1 and 10 Gy, respectively). The increase in ROS persisted for 24h, mainly for 10 Gy where the ROS levels were around 30% above control at the 12, 18 and 24h mark.
Acharya et al., 2010	In vitro. Human neural stem cells were subjected to 1, 2 or 5 Gy of gamma irradiation at a dose rate of 2.2 Gy/min. RONS and superoxide levels were measured at various time points until 7 days.	Intracellular RONS and superoxide levels showed significant increase from 2- to 4-fold at 12h. At 7 days, levels of RONS increased and were dose-responsive, elevated by ~3- to 7-fold and 3- to 5-fold, respectively, over sham-irradiated controls.
Rugo and Schiestl, 2004	In vitro. Human lymphoblast cell lines (TK6 and TK6 E6) were irradiated with 2 Gy of X-irradiation at a dose rate of 0.72 Gy/min. ROS levels were measured at various time points until 29 days.	In the TK6 E6 clones, there was only a significant ROS increase at day 29 (45.7 DCF fluorescence units). In the TK6 clones, there were significant ROS increases at days 13 (26.0 DCF fluorescence units), 15 (26.3 DCF fluorescence units) and 20 (38.1 DCF fluorescence units), with a strong trend of increased ROS in the treated group at day 25. On day 18, ROS levels decreased in the irradiated group, and there was no significant difference at day 29.
Huang et al., 2018	In vitro. Murine RAW264.7 cells were irradiated with 2 Gy of gamma rays at a rate of 0.83 Gy/min. ROS levels were measured at 2 and 8 h post-irradiation.	ROS levels in irradiated RAW264.7 cells decreased by ~10% from 2 h post-exposure to 8 h post-exposure (from ~138% above control at 2 h to ~98% above control at 8).
Zhang et al., 2018	In vitro. hBMMSCs were irradiated with 2 Gy of X-rays at a rate of 0.6 Gy/min. Relative ROS concentration was measured at 0, 0.5, 2, 3, 6, 8, and 12 h post-irradiation.	ROS levels increased in time dependent manner until a peak of ~90% above control level at 3 h-post irradiation, and then steadily declined back to approximately control levels at 12 h post-irradiation.
Phillip et al., 2020	In vitro. Human TICAE cells were irradiated with 0.25, 0.5, 2, and 10 Gy of 60Co gamma rays at a rate of 400 mGy/min. Levels of the antioxidants, SOD1 and PRDX5 were measured at 4 h, 24 h, 48 h, and 1-week post-irradiation to assess oxidative stress from IR exposure.	SOD1 levels did not follow a time-dependent pattern. However, SOD1 decreased at 2 Gy for every timepoint post-irradiation. While PRDX5 levels stayed at approximately baseline levels for the first two days after exposure to 10 Gy of radiation, levels elevated by ~1.6-fold after 1 week.
Ramadan et al., 2020	In vitro. Human TICAE/TIME cells were irradiated with 0.1 and 5 Gy of X-rays at a rate of 0.5 Gy/min. Intracellular ROS production was measured at 45 mins, 2 h, and 3 h post-irradiation.	After irradiation, ROS production saw time-dependent decreases in both TICAE and TIME cells from 45 mins to 3 h post-exposure. ROS production was elevated at 45 mins but returned to approximately baseline levels at 2 and 3 h.
Shen et al., 2018	In vivo. 8-week-old, female, C57BL/6 mice were irradiated with 18 Gy of X-rays. Levels of the oxidative markers, 4-HNE and 3-NT, and the antioxidants, CAT and heme HO-1 were measured the aortas of the mice at 3, 7, 14, 28, and 84 days post-irradiation.	Significant changes were observed in 4-HNE, 3-NT, CAT, and HO-1 levels of irradiated mice after 3 days. 3-NT and HO-1 levels increased from days 3 to 7 and then progressively decreased, while 4-HNE levels followed the same pattern but with a peak at day 14. CAT levels were at their lowest at day 3 and followed a time dependent increase until day 84.
Ungvari et al., 2013	In vitro. The CMVECs of adult male rats were irradiated with 2, 4, 6, and 8 Gy of 137Cs gamma rays. Production of the reactive oxygen species, peroxide and superoxide, were measured at 1- and 14-days post-irradiation.	ROS production was generally higher at day 1 than day 14, with the difference becoming progressively more significant from 2-8 Gy. Peroxide production was reduced from a ~3.25-fold increase compared to controls at day 1 back to baseline levels at day 14. Superoxide production had a ~1.6-fold increase at day 1 recover to baseline levels at day 14.
	In vitro. HLEC and HLE-B3 cells were exposed to 0.1, 0.25 and 0.5 Gy of gamma	

Ahmadi et al., 2021	irradiation at 0.3 and 0.065 Gy/min. ROS levels were measured.	In human LECs immediately exposed to 0.25 Gy gamma rays, the level of ROS positive cells increased by 5%, relative to control, 1 h post-irradiation.
Jiang et al., 2006	In vitro. HLECs were exposed to UV-irradiation at a wavelength over 290 nm (30 mJ/cm2). ROS levels were measured.	Approximately 10-fold increase in ROS generation 15 mins after exposure to 30 mJ/cm2 UV.
Pendergrass et al., 2010	In vivo. Female mice were irradiated with 11 Gy of X-irradiation at a dose rate of 2 Gy/min. ROS levels in the lenses were used to represent oxidative stress.	9 months after irradiation with 11 Gy X-rays at 2 Gy/min there's 2250% cortical ROS relative to the control. 3 months after there was no significant change.
Belkacemi et al., 2001	In vitro. Bovine lens cells were exposed to 10 Gy of X-irradiation at 2 Gy/min. GSH levels were measured.	The intracellular GSH pool was measured by a decrease of about 15% monobromobimane fluorescence relative to the control 24 h after exposure to 10 Gy X-rays at 2 Gy/min and there was a decrease of about 40% relative to the control by 120 h.
Weinreb and Dovrat, 1996	In vitro. Bovine lenses were irradiated with 22.4 J/cm2 (10 min) and 44.8 J/cm2 (100 min) of UVA-irradiation at 8.5 mW/cm2. CAT levels were determined.	CAT activity decreased from 1.75 (control) to 0.5 U/mg protein at 48-168 h after exposure to 44.8 J/cm2 UV-A.
Cencer et al., 2018	In vitro. HLECs were exposed to 0.014 and 0.14 J/cm^2 of UVB-irradiation at 0.09, 0.9 mW/cm^2 for 2 and 5 min. ROS levels (mainly H_2O_2) were measured.	About 5 min after exposure to both 0.09 and 0.9 mW/cm2 UVB for 2.5 mins there is an increase of about 4 average brightness minus control (densitometric fluorescence scanning for ROS, mostly indicating H_2O_2). About 90 and 120 min after exposure to 0.9 mW/cm^2 the average brightness minus control is about 35 and 20 respectively.
Yang et al., 2020	In vitro. HLECs were irradiated with 30 mJ/cm2 of UVB-irradiation. Intracellular ROS levels were measured.	The level of ROS production in HLECs increased approximately 5-fold as determined by 2',7'-dichlorofluorescein diacetate 24 h after exposure to 30 mJ/cm2 UVB.
Zhang et al., 2012	In vivo. Adult mice were exposed to 20.6 kJ/m2 UV-irradiation (313 nm peak; 1.6 mW/cm2). GSH levels were measured in lens homogenates.	Decrease in GSH of about 1 and 2 µmol/g wet weight compared to control after 1 and 16 months respectively after 20.6 kJ/m2 UV (313 nm peak) at 1.6 mW/cm2.

Known modulating factors

Modulating Factors	MF details	Effects on the KER	References
Antioxidants	CAT, GSH-Px, SOD, PRDX, vitamin E, C, carotene, lutein, zeaxanthin, selenium, zinc, alpha-lipoic acid, melatonin, gingko biloba leaf, fermented gingko biloba leaf, Nigella sativa oil, thymoquinone, and ferulic acid	Adding or withholding antioxidants will decrease or increase the level of oxidative stress respectively	Zigman et al., 1995; Belkacémi et al., 2001; Chitchumroonchokchai et al., 2004; Fatma et al., 2005; Jiang et al., 2006; Fletcher, 2010; Karimi et al., 2017; Hua et al., 2019; Kang et al., 2020; Yang et al., 2020; Manda et al., 2008; Limoli et al., 2007; Manda et al., 2007; Taysi et al., 2012;

			Ismail et al., 2016; Demir et al., 2020; Chen et al., 2021
Age	Increased age	Antioxidant levels are lower and show a greater decrease after radiation in older organisms. This compromises their defense system, resulting in ROS increases and therefore, an increased likelihood of oxidative stress	Marshall, 1985; Spector, 1990; Giblin et al., 2002; Kubo et al., 2010; Pendergrass et al., 2010; Zhang et al., 2012; Hamada et al., 2014; Tangvarasittichai & Tangvarasittichai, 2019
Oxygen	Increased oxygen levels	Higher oxygen concentrations increase sensitivity to ROS	Hightower et al., 1992; Eaton, 1994; Huang et al., 2006; Zhang et al., 2010; Schoenfeld et al., 2012

Known Feedforward/Feedback loops influencing this KER

The relationship between deposition of energy and increased oxidative stress leads to several feedforward loops. Firstly, ROS activates the transforming growth factor beta (TGF)-β, which increases the production of ROS. This process is modulated in normal cells containing PRDX-6, or cells with added MnTBAP, which will both prevent TGF-β from inducing ROS formation (Fatma et al., 2005). Secondly, ROS can damage human mitochondrial DNA (mtDNA), this can then cause changes to the cellular respiration mechanisms, leading to increased ROS production (Turner et al., 2002; Zhang et al., 2010; Tangvarasittichai & Tangvarasittichai, 2019, Ahmadi et al., 2021; Yves, 2000). Some other feedback loops through which deposition of energy causes oxidative stress are discussed by Soloviev & Kizub (2019).

References

Acharya, M. M. et al. (2010), “Consequences of ionizing radiation-induced damage in human neural stem cells”, Free radical biology & medicine, Vol. 49/12, Elsevier, Amsterdam, https://doi.org/10.1016/j.freeradbiomed.2010.08.021.

Ahmadi, M. et al. (2021), “Early responses to low-dose ionizing radiation in cellular lens epithelial models”, Radiation research, Vol. 197/1, Radiation Research Society, Bozeman, https://doi.org/10.1667/RADE-20-00284.1

Attar, M., Y. M. Kondolousy, N. Khansari, (2007), “Effect of High Dose Natural Ionizing Radiation on the Immune System of the Exposed Residents of Ramsar Town, Iran”, Iranian Journal of Allergy, Asthma and Immunology, Vol. 6/2, pp. 73-78.

Bai, J. et al. (2020), “Irradiation-induced senescence of bone marrow mesenchymal stem cells aggravates osteogenic differentiation dysfunction via paracrine signaling”, American Journal of Physiology - Cell Physiology, Vol. 318/5, American Physiological Society, Rockville, https://doi.org/10.1152/ajpcell.00520.2019.

Balasubramanian, D (2000), “Ultraviolet radiation and cataract”, Journal of ocular pharmacology and therapeutics, Vol. 16/3, Mary Ann Liebert Inc., Larchmont, https://doi.org/10.1089/jop.2000.16.285.

Baluchamy, S. et al. (2012), “Reactive oxygen species mediated tissue damage in high energy proton irradiated mouse brain”, Molecular and cellular biochemistry, Vol. 360/1-2, Springer, London, https://doi.org/10.1007/s11010-011-1056-2.

Baulch, J. E. et al. (2015), “Persistent oxidative stress in human neural stem cells exposed to low fluences of charged particles Redox biology, Vol. 5, Elsevier, Amsterdam, https://doi.org/10.1016/j.redox.2015.03.001.

Belkacémi, Y. et al. (2001), “Lens epithelial cell protection by aminothiol WR-1065 and anetholedithiolethione from ionizing radiation”, International journal of cancer, Vol. 96, John Wiley & Sons, Ltd., Hoboken, https://doi.org/10.1002/ijc.10346.

Cabrera M., R. Chihuailaf and F. Wittwer Menge (2011), “Antioxidants and the integrity of ocular tissues”, Veterinary medicine international, Vol. 2011, Hindawi, London, https://doi.org/10.4061/2011/905153.

Cadet, J. et al. (2012), “Oxidatively generated complex DNA damage: tandem and clustered lesions”, Cancer letters, Vol. 327, Elsevier, Amsterdam, https://doi.org/10.1016/j.canlet.2012.04.005.

Cencer, C. et al. (2018), “PARP-1/PAR activity in cultured human lens epithelial cells exposed to tow levels of UVB light”, Photochemistry and photobiology, Vol. 94, John Wiley & Sons, Ltd., Hoboken, https://doi.org/10.1111/php.12814.

Cervelli, T. et al. (2017), “A New Natural Antioxidant Mixture Protects against Oxidative and DNA Damage in Endothelial Cell Exposed to Low-Dose Irradiation”, Oxidative medicine and cellular longevity, Vol. 2017, Hindawi, London, https://doi.org/10.1155/2017/9085947.

Chen, Y. et al. (2021), “Effects of neutron radiation on Nrf2-regulated antioxidant defense systems in rat lens”, Experimental and therapeutic medicine, Vol. 21/4, Spandidos Publishing Ltd, Athens, https://doi.org/10.3892/etm.2021.9765.

Chitchumroonchokchai, C. et al. (2004), “Xanthophylls and α-tocopherol decrease UVB-induced lipid peroxidation and stress signaling in human lens epithelial cells”, The Journal of Nutrition, Vol. 134/12, American Society for Nutritional Sciences, Bethesda, https://doi.org/10.1093/jn/134.12.3225.

Collins-Underwood, J. R. et al. (2008), “NADPH oxidase mediates radiation-induced oxidative stress in rat brain microvascular endothelial cells”, Free radical biology & medicine, Vol. 45/6, Elsevier, Amsterdam, https://doi.org/10.1016/j.freeradbiomed.2008.06.024.

de Jager, T.L., Cockrell, A.E., Du Plessis, S.S. (2017), “Ultraviolet Light Induced Generation of Reactive Oxygen Species”, in Ultraviolet Light in Human Health, Diseases and Environment. Advances in Experimental Medicine and Biology, Springer, Cham, https://doi.org/10.1007/978-3-319-56017-5_2

Demir, E. et al. (2020), “Nigella sativa oil and thymoquinone reduce oxidative stress in the brain tissue of rats exposed to total head irradiation”, International journal of radiation biology, Vol. 96/2, Informa, London, https://doi.org/10.1080/09553002.2020.1683636.

Eaton, J. W. (1994), “UV-mediated cataractogenesis: A radical perspective”, Documenta ophthalmologica, Vol. 88, Springer, London, https://doi.org/10.1007/BF01203677.

Fatma, N. et al. (2005), “Impaired homeostasis and phenotypic abnormalities in Prdx6-/- mice lens epithelial cells by reactive oxygen species: Increased expression and activation of TGFβ”, Cell death and differentiation, Vol. 12, Nature Portfolio, London, https://doi.org/10.1038/sj.cdd.4401597.

Fletcher, A. E (2010), “Free radicals, antioxidants and eye diseases: evidence from epidemiological studies on cataract and age-related macular degeneration”, Ophthalmic Research, Vol. 44, Karger International, Basel, https://doi.org/10.1159/000316476.

Ganea, E. and J. J. Harding (2006), “Glutathione-related enzymes and the eye”, Current eye research, Vol. 31/1, Informa, London, https://doi.org/10.1080/02713680500477347.

Giblin, F. J. et al. (2002), “UVA light in vivo reaches the nucleus of the guinea pig lens and produces deleterious, oxidative effects”, Experimental eye research, Vol. 75/4, Elsevier, Amsterdam, https://doi.org/10.1006/exer.2002.2039.

Giedzinski, E. et al. (2005), “Efficient production of reactive oxygen species in neural precursor cells after exposure to 250 MeV protons”, Radiation research, Vol. 164/4, Radiation Research Society, Bozeman, https://doi.org/10.1667/rr3369.1.

Hamada, N. et al. (2014), “Emerging issues in radiogenic cataracts and cardiovascular disease”, Journal of radiation research, Vol. 55/5, Oxford University Press, Oxford, https://doi.org/10.1093/jrr/rru036.

Hatoum, O. A. et al. (2006), “Radiation induces endothelial dysfunction in murine intestinal arterioles via enhanced production of reactive oxygen species”, Arteriosclerosis, Thrombosis, and Vascular Biology, Vol. 26/2, Lippincot Williams & Wilkins, Philadelphia, https://doi.org/10.1161/01.ATV.0000198399.40584.8C.

Hightower, K. and J. McCready (1992), “Mechanisms involved in cataract development following near-ultraviolet radiation of cultured lenses”, Current eye research, Vol. 11/7, Informa, London, https://doi.org/10.3109/02713689209000741.

Hightower, K. R. (1995), “The role of the lens epithelium in development of UV cataract”, Current eye research, Vol. 14/1, Informa, London, https://doi.org/10.3109/02713689508999916.

Hua, H. et al. (2019), “Protective effects of lanosterol synthase up-regulation in UV-B-induced oxidative stress”, Frontiers in pharmacology, Vol. 10, Frontiers Media SA, Lausanne, https://doi.org/10.3389/fphar.2019.00947.

Huang, L. et al. (2006), “Oxidation-induced changes in human lens epithelial cells 2. Mitochondria and the generation of reactive oxygen species”, Free radical biology & medicine, Vol. 41/6, Elsevier, Amsterdam, https://doi.org/10.1016/j.freeradbiomed.2006.05.023.

Huang, B. et al. (2019), “Amifostine suppresses the side effects of radiation on BMSCs by promoting cell proliferation and reducing ROS production”, Stem Cells International, Vol. 2019, Hindawi, London, https://doi.org/10.1155/2019/8749090.

Huang, B. et al. (2018), “Sema3a inhibits the differentiation of raw264.7 cells to osteoclasts under 2gy radiation by reducing inflammation”, PLoS ONE, Vol. 13/7, PLOS, San Francisco, https://doi.org/10.1371/journal.pone.0200000.

ICRU (1998), “ICRU report 57: conversion coefficients for use in radiological protection against external radiation”, Journal of the ICRU, Vol. 29/2, SAGE Publishing

Ismail, A. F. and S. M. El-Sonbaty (2016), “Fermentation enhances Ginkgo biloba protective role on gamma-irradiation induced neuroinflammatory gene expression and stress hormones in rat brain”, Journal of photochemistry and photobiology. B, Biology, Vol. 158, Elsevier, Amsterdam, https://doi.org/10.1016/j.jphotobiol.2016.02.039.

Ji, Y. et al. (2015), “The mechanism of UVB irradiation induced-apoptosis in cataract”, Molecular and cellular biochemistry, Vol. 401, Springer, London, https://doi.org/10.1007/s11010-014-2294-x.

Jiang, Q. et al. (2006), “UV radiation down-regulates Dsg-2 via Rac/NADPH oxidase-mediated generation of ROS in human lens epithelial cells”, International Journal of Molecular Medicine, Vol. 18/2, Spandidos Publishing Ltd, Athens, https://doi.org/10.3892/ijmm.18.2.381.

Jurja, S. et al. (2014), “Ocular cells and light: harmony or conflict?”, Romanian Journal of Morphology & Embryology, Vol. 55/2, Romanian Academy Publishing House, Bucharest, pp. 257–261.

Kang, L. et al. (2020), “Ganoderic acid A protects lens epithelial cells from UVB irradiation and delays lens opacity”, Chinese journal of natural medicines, Vol. 18/12, Elsevier, Amsterdam, https://doi.org/10.1016/S1875-5364(20)60037-1.

Karam, H. M. and R. R. Radwan (2019), “Metformin modulates cardiac endothelial dysfunction, oxidative stress and inflammation in irradiated rats: A new perspective of an antidiabetic drug”, Clinical and Experimental Pharmacology and Physiology, Vol. 46/12, Wiley-Blackwell, Hoboken, https://doi.org/10.1111/1440-1681.13148.

Karimi, N. et al. (2017), “Radioprotective effect of hesperidin on reducing oxidative stress in the lens tissue of rats”, International Journal of Pharmaceutical Investigation, Vol. 7/3, Phcog Net, Bengaluru, https://doi.org/10.4103/jphi.JPHI_60_17.

Kłuciński, P. et al. (2008), “Erythrocyte antioxidant parameters in workers occupationally exposed to low levels of ionizing radiation”, Annals of Agricultural and Environmental Medicine, Vol. 15/1, pp. 9-12.

Kook, S. H. et al. (2015), “Irradiation inhibits the maturation and mineralization of osteoblasts via the activation of Nrf2/HO-1 pathway”, Molecular and Cellular Biochemistry, Vol. 410/1-2, Springer, London, https://doi.org/10.1007/s11010-015-2559-z.

Kozbenko, T. et al. (2022), “Deploying elements of scoping review methods for adverse outcome pathway development: a space travel case example”, International Journal of Radiation Biology, 1–12. https://doi.org/10.1080/09553002.2022.2110306

Kubo, E. et al. (2010), “Protein expression profiling of lens epithelial cells from Prdx6-depleted mice and their vulnerability to UV radiation exposure”, American Journal of Physiology, Vol. 298/2, American Physiological Society, Rockville, https://doi.org/10.1152/ajpcell.00336.2009.

Lee, J. et al. (2004), “Reactive oxygen species, aging, and antioxidative nutraceuticals”, Comprehensive reviews in food science and food safety, Vol. 3/1, Blackwell Publishing Ltd, Oxford, http://doi.org/10.1111/j.1541-4337.2004.tb00058.x.

Limoli, C. L. et al. (2007), “Redox changes induced in hippocampal precursor cells by heavy ion irradiation”, Radiation and environmental biophysics, Vol. 46/2, Springer, London, https://doi.org/10.1007/s00411-006-0077-9.

Limoli, C. L. et al. (2004), “Radiation response of neural precursor cells: linking cellular sensitivity to cell cycle checkpoints, apoptosis and oxidative stress”, Radiation research, Vol. 161/1, Radiation Research Society, Bozeman, https://doi.org/10.1667/rr3112.

Liu, F. et al. (2019), “Transcriptional response of murine bone marrow cells to total-body carbon-ion irradiation”, Mutation Research - Genetic Toxicology and Environmental Mutagenesis, Vol. 839, Elsevier, Amsterdam, https://doi.org/10.1016/j.mrgentox.2019.01.014.

Liu, Y. et al. (2018), “Protective effects of α2macroglobulin on human bone marrow mesenchymal stem cells in radiation injury”, Molecular Medicine Reports, Vol. 18/5, Spandidos Publishing Ltd, Athens, https://doi.org/10.3892/mmr.2018.9449.

Manda, K. et al. (2007), “Melatonin attenuates radiation-induced learning deficit and brain oxidative stress in mice”, Acta neurobiologiae experimentalis, Vol. 67/1, Nencki Institute of Experimental Biology, Warsaw, pp. 63 –70.

Manda, K., M. Ueno and K. Anzai (2008), “Memory impairment, oxidative damage and apoptosis induced by space radiation: ameliorative potential of alpha-lipoic acid”, Behavioural brain research, Vol. 187/2, Elsevier, Amsterdam, https://doi.org/10.1016/j.bbr.2007.09.033.

Mansour, H. H. (2013), “Protective effect of ginseng against gamma-irradiation-induced oxidative stress and endothelial dysfunction in rats”, EXCLI Journal, Vol. 12, Leibniz Research Centre for Working Environment and Human Factors, Dortmund, pp. 766-777.

Marshall, J. (1985), “Radiation and the ageing eye”, Ophthalmic & physiological optics, Vol. 5, Wiley-Blackwell, Hoboken, https://doi.org.10.1111/j.1475-1313.1985.tb00666.x.

Padgaonkar, V. A. et al. (2015) “Thioredoxin reductase activity may be more important than GSH level in protecting human lens epithelial cells against UVA light”, Photochemistry and photobiology, Vol. 91/2, Wiley-Blackwell, Hoboken, https://doi.org/10.1111/php.12404.

Pendergrass, W. et al. (2010), “X-ray induced cataract is preceded by LEC loss, and coincident with accumulation of cortical DNA, and ROS; similarities with age-related cataracts”, Molecular Vision, Vol. 16, Emory University, Atlanta, pp. 1496-513.

Philipp, J. et al. (2020), “Radiation Response of Human Cardiac Endothelial Cells Reveals a Central Role of the cGAS-STING Pathway in the Development of Inflammation”, Proteomes, Vol. 8/4, Multidisciplinary Digital Publishing Institute, Basel, https://doi.org/10.3390/proteomes8040030.

Quan, Y. et al. (2021), “Connexin hemichannels regulate redox potential via metabolite exchange and protect lens against cellular oxidative damage”, Redox biology, Vol. 46, Elsevier, Amsterdam, https://doi.org/10.1016/j.redox.2021.102102.

Ramadan, R. et al. (2020), “Connexin43 Hemichannel Targeting With TAT-Gap19 Alleviates Radiation-Induced Endothelial Cell Damage”, Frontiers in Pharmacology, Vol. 11, Frontiers Media SA, Lausanne, https://doi.org/10.3389/fphar.2020.00212

Rehman, M. U. et al. (2016), “Comparison of free radicals formation induced by cold atmospheric plasma, ultrasound, and ionizing radiation”, Archives of biochemistry and biophysics, Vol. 605, Elsevier, Amsterdam, https://doi.org/10.1016/j.abb.2016.04.005.

Rogers, C. S. et al. (2004), “The effects of sub-solar levels of UV-A and UV-B on rabbit corneal and lens epithelial cells”, Experimental eye research, Vol. 78, Elsevier, Amsterdam, https://doi.org/10.1016/j.exer.2003.12.011.

Rong, X. et al. (2019), “TRIM69 inhibits cataractogenesis by negatively regulating p53”, Redox biology, Vol. 22, Elsevier, Amsterdam, https://doi.org/10.1016/j.redox.2019.101157.

Rugo, R. E. and R. H. Schiestl (2004), “Increases in oxidative stress in the progeny of X-irradiated cells”, Radiation research, Vol. 162/4, Radiation Research Society, Bozeman, https://doi.org/10.1667/rr3238.

Santos, A. L., S. Sinha, and A. B. Linder (2018), “The good, the bad, and the ugly of ROS: New insights on aging and aging-related diseases from eukaryotic and prokaryotic model organisms”, Oxidative medicine and cellular longevity, Vol. 2018, Hindawi, London, https://doi.org/10.1155/2018/1941285.

Schoenfeld, M. P. et al. (2012), “A hypothesis on biological protection from space radiation through the use of new therapeutic gases as medical counter measures”, Medical gas research, Vol. 2/8, BioMed Central Ltd, London, https://doi.org/10.1186/2045-9912-2-8.

Sharma, U. C. et al. (2018), “Effects of a novel peptide Ac-SDKP in radiation-induced coronary endothelial damage and resting myocardial blood flow”, Cardio-oncology, Vol. 4, BioMed Central Ltd, London, https://doi.org/10.1186/s40959-018-0034-1.

Shen, Y. et al. (2018), “Transplantation of bone marrow mesenchymal stem cells prevents radiation-induced artery injury by suppressing oxidative stress and inflammation”, Oxidative Medicine and Cellular Longevity, Vol. 2018, Hindawi, London, https://doi.org/10.1155/2018/5942916.

Slezak, J. et al. (2017), “Potential markers and metabolic processes involved in the mechanism of radiation-induced heart injury”, Canadian journal of physiology and pharmacology, Vol. 95/10, Canadian Science Publishing, Ottawa, https://doi.org/10.1139/cjpp-2017-0121.

Soloviev, A. I. and I.V. Kizub (2019), “Mechanisms of vascular dysfunction evoked by ionizing radiation and possible targets for its pharmacological correction”, Biochemical pharmacology, Vol. 159, Elsevier, Amsterdam, https://doi.org/10.1016/j.bcp.2018.11.019.

Soltani, B. (2016), “Nanoformulation of curcumin protects HUVEC endothelial cells against ionizing radiation and suppresses their adhesion to monocytes: potential in prevention of radiation-induced atherosclerosis”, Biotechnology Letters, Vol. 38, Springer, London, https://doi.org/10.1007/s10529-016-2189-x.

Soucy, K. G. et al. (2011), “HZE 56Fe-Ion Irradiation Induces Endothelial Dysfunction in Rat Aorta: Role of Xanthine Oxidase”, Radiation Research, Vol. 176/4, Radiation Research Society, Bozeman, https://doi.org/10.1667/RR2598.1.

Soucy, K. G. et al. (2010), “Dietary inhibition of xanthine oxidase attenuates radiation-induced endothelial dysfunction in rat aorta”, Journal of Applied Physiology, Vol. 108/5, American Physiological Society, Rockville, https://doi.org/10.1152/japplphysiol.00946.2009.

Spector, A. (1990), “Oxidation and aspects of ocular pathology”, The CLAO journal, Vol. 16, Contact Lens Association of Ophthalmologists, Colorado, pp. S8-10.

Stohs, S. (1995), “The role of free radicals in toxicity and disease”, Journal of Basic and Clinical Physiology and Pharmacology, Vol. 6/3-4, Walter de Gruyter GmbH, Berlin, pp. 205-228.

Suman, S. et al. (2013), “Therapeutic and space radiation exposure of mouse brain causes impaired DNA repair response and premature senescence by chronic oxidant production”, Aging, Vol. 5/8, Impact Journals, Orchard Park, https://doi.org/10.18632/aging.100587.

Tahimic, C. G. T., and R. K. Globus (2017), “Redox signaling and its impact on skeletal and vascular responses to spaceflight”, International Journal of Molecular Sciences, Vol. 18/10, Multidisciplinary Digital Publishing Institute, Basel, https://doi.org/10.3390/ijms18102153.

Tangvarasittichai, O. and S. Tangvarasittichai (2018), “Oxidative stress, ocular disease and diabetes retinopathy”, Current pharmaceutical design, Vol. 24/40, Bentham Science Publishers, Sharjah, https://doi.org/10.2174/1381612825666190115121531.

Taysi, S. et al. (2012), “Zinc administration modulates radiation-induced oxidative injury in lens of rat”, Pharmacognosy Magazine, Vol. 8/2, https://doi.org/10.4103/0973-1296.103646

Tian, Y. et al. (2017), “The Impact of Oxidative Stress on the Bone System in Response to the Space Special Environment”, International Journal of Molecular Sciences, Vol. 18/10, Multidisciplinary Digital Publishing Institute, Basel, https://doi.org/10.3390/ijms18102132.

Tseng, B. P. et al. (2014), “Functional consequences of radiation-induced oxidative stress in cultured neural stem cells and the

brain exposed to charged particle irradiation", Antioxidants & redox signaling, Vol. 20/9, Mary Ann Leibert Inc., Larchmont, https://doi.org/10.1089/ars.2012.5134.

Turner, N. D. et al. (2002), "Opportunities for nutritional amelioration of radiation-induced cellular damage", Nutrition, Vol. 18/10, Elsevier Inc, New York, http://doi.org/10.1016/S0899-9007(02)00945-0.

Ungvari, Z. et al. (2013), "Ionizing Radiation Promotes the Acquisition of a Senescence-Associated Secretory Phenotype and Impairs Angiogenic Capacity in Cerebromicrovascular Endothelial Cells: Role of Increased DNA Damage and Decreased DNA Repair Capacity in Microvascular Radiosensitivity", The Journals of Gerontology Series A: Biological Sciences and Medical Sciences, Vol. 68/12, Oxford University Press, Oxford, https://doi.org/10.1093/gerona/glt057.

Varma, S. D. et al. (2011), "Role of ultraviolet irradiation and oxidative stress in cataract formation-medical prevention by nutritional antioxidants and metabolic agonists", Eye & contact lens, Vol. 37/4, Lippincot Williams & Wilkins, Philadelphia, https://doi.org/10.1097/ICL.0b013e31821ec4f2.

Venkatesulu, B. P. et al. (2018), "Radiation-Induced Endothelial Vascular Injury: A Review of Possible Mechanisms", JACC: Basic to Translational Science, Vol. 3/4, Elsevier, Amsterdam, https://doi.org/10.1016/j.jacbts.2018.01.014.

Veeraraghavan, J. et al. (2011), "Low-dose gamma-radiation-induced oxidative stress response in mouse brain and gut: regulation by NFκB-MnSOD cross-signaling", Mutation research, Vol. 718/1-2, Elsevier, Amsterdam, https://doi.org/10.1016/j.mrgentox.2010.10.006.

Wang, C. et al. (2016), "Protective effects of cerium oxide nanoparticles on MC3T3-E1 osteoblastic cells exposed to X-ray irradiation", Cellular Physiology and Biochemistry, Vol. 38/4, Karger International, Basel, https://doi.org/10.1159/000443092.

Wang, H. et al. (2019a), "Radiation-induced heart disease: a review of classification, mechanism and prevention", International Journal of Biological Sciences, Vol. 15/10, Ivyspring International Publisher, Sydney, https://doi.org/10.7150/ijbs.35460.

Wang, H. et al. (2019b), "Gamma Radiation-Induced Disruption of Cellular Junctions in HUVECs Is Mediated through Affecting MAPK/NF-κB Inflammatory Pathways", Oxidative Medicine and Cellular Longevity, Vol. 2019, Hindawi, London, https://doi.org/10.1155/2019/1486232.

Wegener, A. R. (1994), "In vivo studies on the effect of UV-radiation on the eye lens in animals", Documenta ophthalmologica, Vol. 88, Springer, London, https://doi.org/10.1007/BF01203676.

Weinreb O. and A. Dovrat (1996), "Transglutaminase involvement in UV-A damage to the eye lens", Experimental eye research, Vol. 63/5, Elsevier, London, https://doi.org/10.1006/exer.1996.0150.

Yang, H. et al. (2020), "Cytoprotective role of humanin in lens epithelial cell oxidative stress-induced injury", Molecular medicine reports, Vol. 22/2, Spandidos Publishing Ltd, Athens, https://doi.org/10.3892/mmr.2020.11202.

Yao, K. et al. (2008), "The flavonoid, fisetin, inhibits UV radiation-induced oxidative stress and the activation of NF-κB and MAPK signaling in human lens epithelial cells", Molecular Vision, Vol. 14, Emory University, Atlanta, pp. 1865-1871.

Yao, J. et al. (2009), "UVB radiation induces human lens epithelial cell migration via NADPH oxidase-mediated generation of reactive oxygen species and up-regulation of matrix metalloproteinases", International Journal of Molecular Medicine, Vol. 24/2, Spandidos Publishing Ltd, Athens, https://doi.org/10.3892/ijmm_00000218.

Yves, C. (2000), "Oxidative stress and Alzheimer disease", The American Journal of Clinical Nutrition, Vol. 71/2, https://doi.org/10.1093/ajcn/71.2.621s.

Zhang, J. et al. (2012), "Ultraviolet radiation-induced cataract in mice: The effect of age and the potential biochemical mechanism", Investigative ophthalmology & visual science, Vol. 53, Association for Research in Vision and Ophthalmology, Rockville, https://doi.org/10.1167/iovs.12-10482.

Zhang, L. et al. (2020), "Amifostine inhibited the differentiation of RAW264.7 cells into osteoclasts by reducing the production of ROS under 2 Gy radiation", Journal of Cellular Biochemistry, Vol. 121/1, John Wiley & Sons, Ltd., Hoboken, https://doi.org/10.1002/jcb.29247.

Zhang, L. et al. (2018), "Astragalus polysaccharide inhibits ionizing radiation-induced bystander effects by regulating MAPK/NF-κB signaling pathway in bone mesenchymal stem cells (BMSCs)", Medical Science Monitor, Vol. 24, International Scientific Information, Inc., Melville, https://doi.org/10.12659/MSM.909153.

Zigman, S. et al. (2000), "Effects of intermittent UVA exposure on cultured lens epithelial cells", Current Eye Research, Vol. 20/2, Informa UK Limited, London, https://doi.org/10.1076/0271-3683(200002)2021-DFT095.

Zigman, S. et al. (1995), "Damage to cultured lens epithelial cells of squirrels and rabbits by UV-A (99.9%) plus UV-B (0.1%) radiation and alpha tocopherol protection", Molecular and cellular biochemistry, Vol. 143, Springer, London, https://doi.org/10.1007/BF00925924.

Relationship: 1977: Energy Deposition leads to Increase, DNA strand breaks

AOPs Referencing Relationship

AOP Name	Adjacency	Weight of Evidence	Quantitative Understanding
Deposition of energy leading to lung cancer	adjacent	High	High
Deposition of energy leading to population decline via DNA strand breaks and follicular atresia	adjacent	High	
Deposition of energy leading to population decline via DNA strand breaks and oocyte apoptosis	adjacent		
Deposition of energy leading to occurrence of cataracts	adjacent	High	High
Deposition of energy leads to vascular remodeling	adjacent	High	High
Deposition of Energy Leading to Learning and Memory Impairment	adjacent	High	High

Evidence Supporting Applicability of this Relationship

Taxonomic Applicability

Term	Scientific Term	Evidence	Links
mouse	Mus musculus	High	NCBI
human	Homo sapiens	High	NCBI
rat	Rattus norvegicus	High	NCBI
bovine	Bos taurus	Low	NCBI
rabbit	Oryctolagus cuniculus	Low	NCBI
Pig	Pig	Low	NCBI

Life Stage Applicability

Life Stage	Evidence
All life stages	High

Sex Applicability

Sex	Evidence
Unspecific	High

This KER is plausible in all life stages, sexes, and organisms with DNA. The majority of the evidence is from In vivo adult mice and human In vitro models that do not specify the sex.

Key Event Relationship Description

Direct deposition of ionizing energy refers to imparted energy interacting directly with the DNA double helix and producing randomized damage. This can be in the form of double strand breaks (DSBs), single-strand breaks, base damage, or the crosslinking of DNA to other molecules (Smith et al., 2003; Joiner, 2009; Christensen, 2014; Sage and Shikazono, 2017). Among these, the most detrimental type of DNA damage to a cell is DSBs. They are caused by the breaking of the sugar-phosphate backbone on both strands of the DNA double helix molecule, either directly across from each other or several nucleotides apart (Ward, 1988; Iliakis et al., 2015). This occurs when high-energy subatomic particles interact with the orbital electrons of the DNA causing ionization (where electrons are ejected from atoms) and excitation (where electrons are raised to higher energy levels) (Joiner, 2009). The number of DSBs produced and the complexity of the breaks is highly dependent on the amount of energy deposited on and absorbed by the cell. This can vary as a function of the dose-rate (Brooks et al., 2016) and the radiation quality which is a function of its linear energy transfer (LET) (Sutherland et al., 2000; Nikjoo et al., 2001; Jorge et al., 2012). LET describes the amount of energy that an ionizing particle transfers to media per unit distance (Smith et al., 2003; Okayasu, 2012a; Christensen et al., 2014). High LET radiation, such as alpha particles, heavy ion particles, and neutrons can deposit larger quantities of energy within a single track than low LET radiation, such as γ-rays, X-rays, electrons, and protons (Kadhim et al., 2006; Franken et al., 2012; Frankenberg et al., 1999; Rydberg et al., 2002; Belli et al., 2000; Antonelli et al., 2015). As such, radiation with higher LETs tends to produce more complex, dense structural damage, particularly in the form of clustered damage, in comparison to lower LET radiation (Nikjoo et al., 2001; Terato and Ide, 2005; Hada and Georgakilas, 2008; Okayasu, 2012a; Lorat et al., 2015; Nikitaki et al., 2016). Thus, the complexity and yield of clustered DNA damage increases with ionizing density (Ward, 1988; Goodhead, 2006). However, clustered damage can also be induced even by a single radiation track through a cell.

While the amount of DSBs produced depends on the radiation dose (see dose concordance), it also depends on several other factors. As the LET increases, the complexity of DNA damage increases, decreasing the repair rate, and increasing toxicity (Franken et al., 2012; Antonelli et al., 2015).

Evidence Supporting this KER

Overall Weight of Evidence for this KER: High

Biological Plausibility

The biological rationale linking the direct deposition of energy on DNA with an increase in DSB formation is strongly supported by numerous literature reviews that are available on this topic (J .F. Ward, 1988; Lipman, 1988; Hightower, 1995; Terato & Ide, 2005; Goodhead, 2006; Kim & Lee, 2007; Asaithamby et al., 2008; Hada & Georgakilas, 2008; Jeggo, 2009; Clement, 2012; Okayasu, 2012b; Stewart, 2012; M. E. Lomax et al., 2013; EPRI, 2014; Hamada, 2014; Moore et al., 2014; Desouky et al., 2015; Ainsbury, 2016; Foray et al., 2016; Hamada & Sato, 2016; Hamada, 2017a; Sage & Shikazono, 2017; Chadwick, 2017; Wang et al., 2021; Nagane et al., 2021; Sylvester et al., 2018; Baselet et al., 2019). Ionizing radiation can be in the form of high energy particles (such as alpha particles, beta particles, or charged ions) or high energy photons (such as gamma-rays or X-rays). Ionizing radiation can break the DNA within chromosomes both directly and indirectly, as shown through using velocity sedimentation of DNA through neutral and alkaline sucrose gradients. The most direct path entails a collision between a high-energy particle or photon and a strand of DNA.

Additionally, excitation of secondary electrons in the DNA allows for a cascade of ionization events to occur, which can lead to the formation of multiple damage sites (Joiner, 2009). As an example, high-energy electrons will traverse a DNA molecule in a mammalian cell within 10^{-18} s and 10^{-14} s, resulting in 100,000 ionizing events per 1 Gy dose in a 10 µm cell (Joiner, 2009). The amount of damage can be influenced by factors such as the cell cycle stage and chromatin structure. It has been shown that in more condensed, packed chromatin structures such as those present in intact cells and heterochromatin, it is more difficult for the DNA to be damaged (Radulescu et al., 2006; Agrawala et al., 2008; Falk et al., 2008; Venkatesh et al., 2016). In contrast, DNA damage is more easily induced in lightly-packed chromatin such as euchromatin and nucleoids, (Radulescu et al., 2006; Falk et al., 2008; Venkatesh et al., 2016).

Of the possible radiation-induced DNA damage types, DSB is considered to be the most harmful to the cell, as there may be severe consequences if this damage is not adequately repaired (Khanna & Jackson, 2001; Smith et al., 2003; Okayasu, 2012a; M. E. Lomax et al., 2013; Rothkamm et al., 2015).

A considerable fraction of DSBs can also be formed in cells through indirect mechanisms. In this case, deposited energy can split water molecules near DNA, which can generate a significant quantity of reactive oxygen species in the form of hydroxyl free radicals (Ward, 1988; Wolf, 2008; Desouky et al., 2015; Maier et al., 2016, Cencer et al., 2018; Bains, 2019; Ahmadi et al., 2021). Estimates using models and experimental results suggest that hydroxyl radicals may be present within nanoseconds of energy deposition by radiation (Yamaguchi et al., 2005). These short-lived but highly reactive hydroxyl radicals may react with nearby DNA. This will produce DNA damage, including single-strand breaks and DSBs (Ward, 1988; Sasaki, 1998; Desouky et al., 2015; Maier et al., 2016). DNA breaks are especially likely to be produced if the sugar moiety is damaged, and DSBs occur when two single-strand breaks are in close proximity to each other (Ward, 1988).

Empirical Evidence

Empirical data strongly supports this KER. The evidence presented below is summarized in table 1. The types of DNA damage produced by ionizing radiation and the associated mechanisms, including the induction of DSBs, are reviewed by Lomax et al. (2013) and documents produced by international radiation governing frameworks (Valentin, 1998; UNSCEAR, 2000). Other reviews also highlight the relationship between the deposition of energy by radiation and DSB induction, and discuss the various methods available to detect these DSBs (Terato & Ide, 2005; Rothkamm et al., 2015; Sage & Shikazono, 2017). A visual representation of the time frames and dose ranges probed by the dedicated studies discussed here is shown in Figures 1 & 2 below.

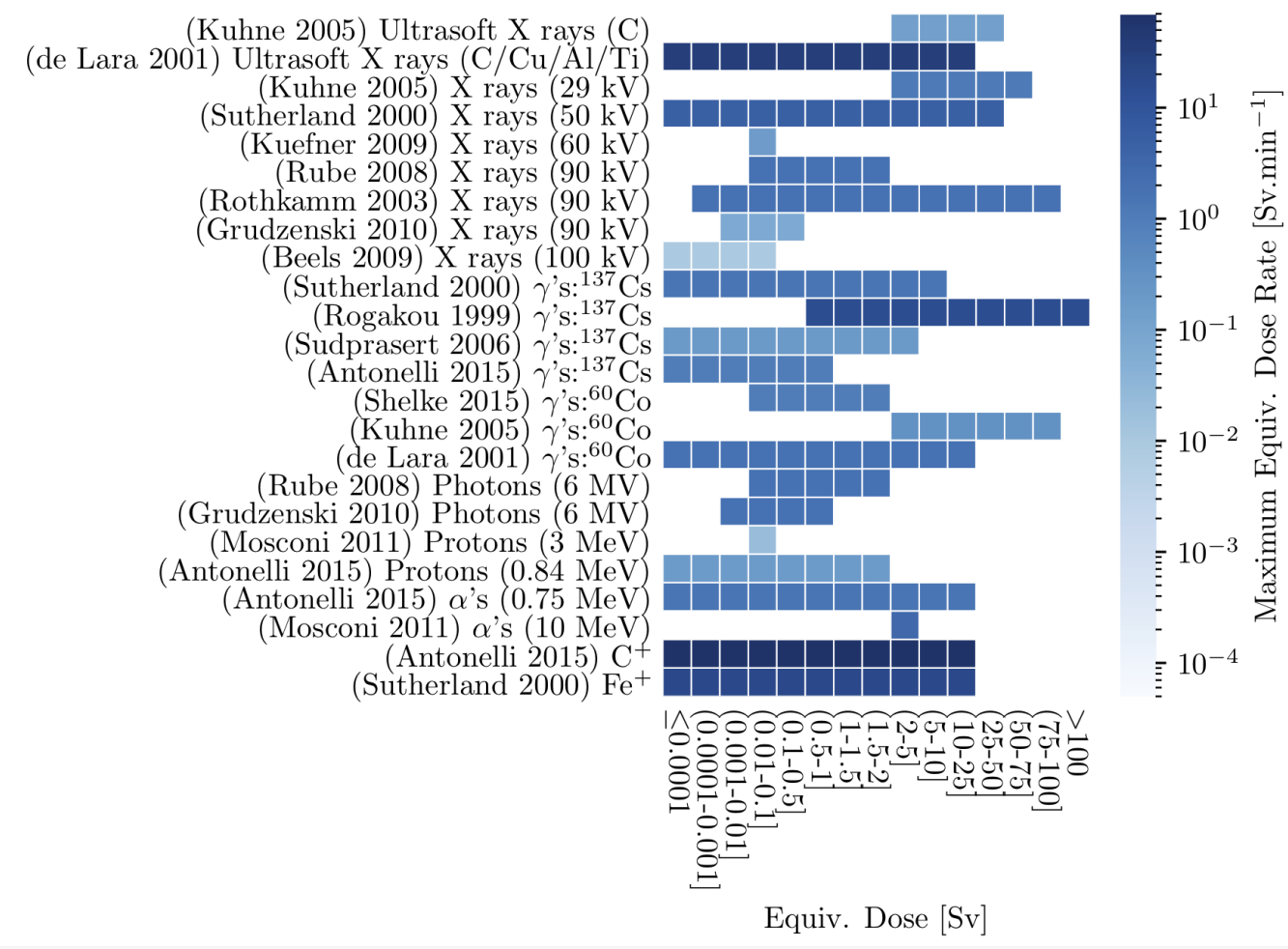

Figure 1: Plot of example studies (y-axis) against equivalent dose (Sv) used to determine the empirical link between direct deposition of energy and DSBs. The z-axis

denotes the equivalent dose rate used in each study. The y-axis is ordered from low LET to high LET from top to bottom.

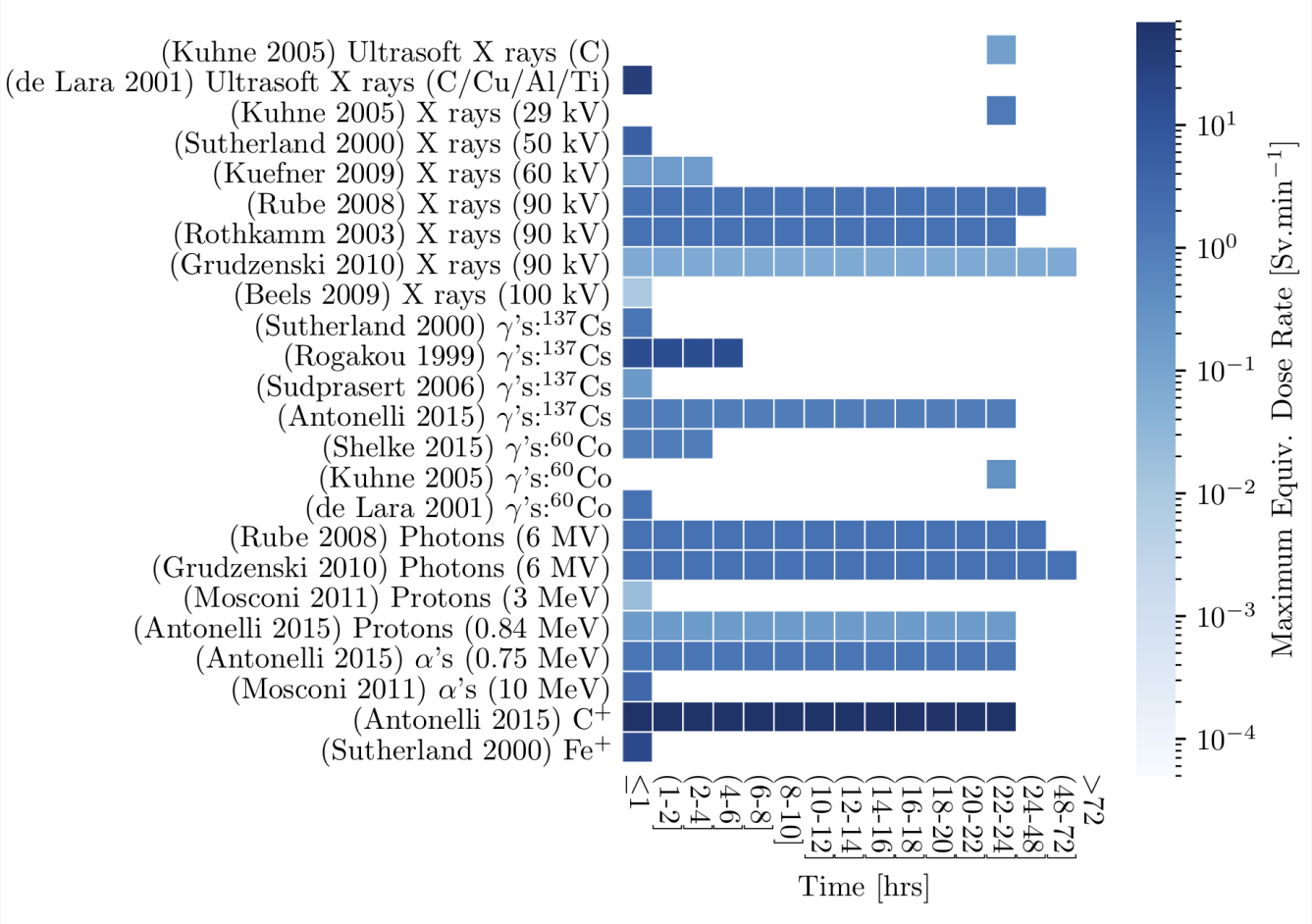

Figure 2: Plot of example studies (y-axis) against time scales used to determine the empirical link between direct deposition of energy and DSBs. The z-axis denotes the equivalent dose rate used in each study. The y-axis is ordered from low LET to high LET from top to bottom.

Dose Concordance

There is evidence in the literature suggesting a dose concordance between the direct deposition of energy by ionizing radiation and the incidence (Grudzenski et al., 2010) of DNA DSBs. Results from in vitro (Aufderheide et al., 1987; Sidjanin, 1993; Bucolo, 1994; Frankenberg et al., 1999; Rogakou et al., 1999; Belli et al., 2000; Sutherland et al., 2000; Lara et al., 2001; Rydberg et al., 2002; Baumstark-Kham et al., 2003; Rothkamm and Lo, 2003; Long, 2004; Kuhne et al., 2005; Sudprasert et al., 2006; Beels et al., 2009; Grudzenski et al., 2010; Liao, 2011; Franken et al., 2012; Bannik et al., 2013; Shelke & Das, 2015; Antonelli et al., 2015; Markiewicz et al., 2015; Allen, 2018; Dalke, 2018; Bains, 2019; Ahmadi et al., 2021; Sabirzhanov et al., 2020; Ungvari et al., 2013; Rombouts et al., 2013; Baselet et al., 2017), in vivo (Reddy, 1998; Sutherland et al., 2000; Rube et al., 2008; Beels et al., 2009; Grudzenski et al., 2010; Markiewicz et al., 2015; Barnard, 2018; Barnard, 2019; Barnard, 2022; Schmal et al., 2019; Barazzuol et al., 2017; Geisel et al., 2012), ex vivo (Rube et al., 2008; Flegal et al., 2015) and simulation studies (Charlton et al., 1989) suggest that there is a positive, linear, dose-dependent increase in DSBs with increasing deposition of energy across a wide range of radiation types (iron ions, X-rays, ultrasoft X-rays, gamma-rays, photons, UV light, and alpha particles) and radiation doses (1 mGy - 100 Gy) (Aufderheide et al., 1987; Sidjanin, 1993; Frankenberg et al., 1999; Sutherland et al., 2000; de Lara et al., 2001; Baumstark-Khan et al., 2003; Rothkamm & Lo, 2003; Kuhne et al., 2005; Rube et al., 2008; Grudzenski et al., 2010; Bannik et al., 2013; Shelke & Das, 2015; Antonelli et al., 2015; Dalke, 2018; Barazzuol et al., 2017; Ungvari et al., 2013; Rombouts et al., 2013; Baselet et al., 2017; Geisel et al., 2012). DSBs have been predicted to occur at energy deposition levels as low as 75 eV (Charlton et al., 1989).

Time Concordance

There is evidence suggesting a time concordance between the direct deposition of energy and the incidence of DSBs. A number of different models and experiments have provided evidence of ionizing radiation-induced foci (IRIF), which can be used to infer DSB formation seconds (Mosconi et al., 2011) or minutes after radiation exposure (Rogakou et al., 1999; Rothkamm and Lo, 2003; Rube et al., 2008; Beels et al., 2009; Kuefner et al., 2009; Grudzenski et al., 2010; Antonelli et al., 2015; Acharya et al., 2010; Sabirzhanov et al., 2020; Rombouts et al., 2013; Nübel et al., 2006; Baselet et al., 2017; Zhang et al., 2017).

Essentiality

Deposition of energy is essential for DNA strand breaks. They can also be caused through other routes, such as oxidative stress (Cadet et al., 2012), but under normal physiological conditions deposition of energy is necessary. This was tested through many studies using various indicators such as 53BP1 foci/cell, γH2AX foci/cell, DNA migration, and the amount of DNA in tails for the comet assay. Various organisms such as humans, mice, rabbits, guinea pigs, and cattle were used. They showed that without the deposition of energy, there was only a negligible amount of DNA strand breaks (Aufderheide et al., 1987; Sidjanin, 1993; Bucolo, 1994; Reddy, 1998; Rogers, 2004; Bannik et al., 2013; Dalke, 2018; Bains, 2019; Barnard, 2019; Barnard, 2021).

Uncertainties and Inconsistencies

Uncertainties and inconsistencies in this KER are as follows:

- Studies have shown that dose-rates (Brooks et al., 2016) and radiation quality (Sutherland et al., 2000; Nikjoo et al., 2001; Jorge et al., 2012) are factors that can influence the dose-response relationship.
- Low-dose radiation has been observed to have beneficial effects and may even invoke protection against spontaneous genomic damage (Feinendegen, 2005; Day et al., 2007; Feinendegen et al., 2007; Shah et al., 2012; Nenoi et al., 2015; Dalke, 2018). This protective effect has been documented in in vivo and in vitro, as reviewed by ICRP (2007) and UNSCEAR (2008) and can vary depending on the cell type, the tissue, the organ, or the entire organism (Brooks et al., 2016).
- Depositing ionizing energy is a stochastic event; as such this can influence the location, degree and type of DNA damage imparted on a cell. As an example, studies have shown that mitochondrial DNA may also be an important target for genotoxic effects of ionizing radiation (Wu et al., 1999).

Quantitative Understanding of the Linkage

Quantitative understanding of this linkage suggests that DSBs can be predicted upon exposure to ionizing radiation. This is dependent on the biological model, the type of radiation and the radiation dose. In general, 1 Gy of radiation is thought to result in 3000 damaged bases (Maier et al., 2016), 1000 single-strand breaks, and 40 DSBs (Ward, 1988; Foray et al., 2016; Maier et al., 2016) . The table below provides representative examples of the calculated DNA damage rates across different model systems, most of which are examining DNA DSBs.

Dose Concordance

The following tables provide representative examples of the relationship, unless otherwise indicated, all data is significantly significant.

Reference	Experiment Description	Result
Ward, 1988	In vitro. Cells containing approximately 6 pg of DNA were exposed to 1 Gy.	Under the assumption of 6 pg of DNA per cell. 60 eV of energy deposited per event over a total of 1 Gy. Deoxyribose (2.3 pg/cell): 14,000 eV deposited, 235 events. Bases (2.4 pg/cell): 14.7 keV deposited, 245 events. Phosphate (1.2 pg/cell): 7,300 eV deposited, 120 events. Bound water (3.1 pg/cell): 19 keV deposited, 315 events. Inner hydration shell (4.2 pg/cell): 25,000 eV deposited 415 events.
Charlton, 1989	In-silico. A computer simulation/model was used to test various types of radiation with doses from 0 to 400 eV (energy deposited) on the amount of DNA damage produced.	Simulated dose-concordance prediction of increase in number of DSBs/54 nucleotide pairs as direct deposition of energy increases in the range 75-400 eV. In the range 100 - 150 eV: 0.38 DSBs/54 nucleotide pairs and at 400 eV: ~0.80 DSBs per 64 nucleotide pairs.
Sutherland, 2000	In vitro. Human cells were exposed to ^{137}Cs γ-rays (0 – 100 Gy, 0.16 – 1.6 Gy/min). The frequency of DSBs was determined using gel electrophoresis.	Using isolated bacteriophage T7 DNA and 0-100 Gy of γ radiations, observed a response of 2.4 DSBs per megabase pair per Gy.
Rogakou et al., 1999	In vitro. Normal human fibroblasts (IMR90) and human breast cancer cells (MCF7 were exposed to 0.6 and 2 Gy ^{137}Cs γ-rays delivered at 15.7 Gy/min. The number of DSBs were determined by immunoblotting for γ-H2AX.	Radiation doses of 0.6 Gy & 2 Gy to normal human fibroblasts (IMR90) and MCF7 cells resulted in 10.1 & 12.2 DSBs per nucleus on average (0.6 Gy), respectively; increasing to 24 & 27.1 DSBs per nucleus (2 Gy).
Kuhne et al., 2005	In vitro. Primary human skin fibroblasts (HSF2) were exposed to 0 – 70 Gy ^{60}Co γ-rays (0.33 Gy/min), X-rays (29 kVp, 1.13 Gy/min), and CKX-rays (0.14 Gy/min). The number of DSBs were determined with pulsed-field gel electrophoresis.	γ-ray and X-ray irradiation of primary human skin fibroblasts (HSF2) at 0 - 70 Gy. γ-rays: (6.1 ± 0.2) x 10-9 DSBs per base pair per Gy, X-rays: (7.0 ± 0.2) x 10-9 DSBs per base pair per Gy. CKX -rays: (12.1 ± 1.9) x 10-9 DSBs per base pair per Gy.
Rothkamm, 2003	In vitro. Primary human fibroblast cell lines MRC-5 (lung), HSF1 and HSF2 (skin), and180BR (deficient in DNA ligase IV) were exposed to 1 mGy – 100 Gy X-rays (90 kV). Low doses were delivered at 6 – 60 mGy/min and high doses were delivered at 2 Gy/min. The number of DSBs were determined with pulsed-field gel electrophoresis.	X-ray irradiation of primary human fibroblasts (MRC-5) in the range 1 mGy - 100 Gy, 35 DSBs per cell per Gy.
Grudzenski et al, 2010	In vitro. Primary human fibroblasts (HSF1) and C57BL/6NCrl adult mice were exposed to X-rays (2.5 – 200 mGy, 70 mGy/min), and photons (10 mGy – 1 Gy, 2 Gy/min (100 mGy and 1 Gy), and 0.35 Gy/min (10 mGy)). γ-H2AX immunofluorescence was observed to determine DSBs.	X-rays irradiating primary human fibroblasts (HSF1) in the range 2.5 - 100 mGy yielded a response of 21 foci per Gy. When irradiating adult C57BL/6NCrl mice with photons a response of 0.07 foci per cell at 10 mGy was found. At 100 mGy the response was 0.6 foci per cell and finally, at 1 Gy; 8 foci per cell.
de Lara, 2001	In vitro. Chinese hamster cells (V79-4) were exposed to 0 – 20 Gy of ^{60}Co γ-rays (2 Gy/min), and ultrasoft X-rays (0.7 – 35 Gy/min): carbon-K shell (0.28 keV), copper L-shell (0.96 keV), aluminum K-shell (1.49 keV), and titanium K-shell (4.55 keV). The number of DSBs were determined with pulsed-field gel electrophoresis.	V79-4 cells irradiated with γ-rays and ultrasoft X-rays (carbon K-shell, copper L-shell, aluminium K-shell and titanum K-shell) in the range 0 - 20 Gy. Response (DSBs per Gy per cell): γ-rays: 41, carbon K-shell: 112, copper L-shell: 94, aluminum K-shell: 77, titanium K-shell: 56.
	In vivo. Brain, lung, heart and small intestine tissue from adult SCID, A-T,	

Rübe et al., 2008	BALB/c and C57BL/6NCrl mice; Whole blood and isolated lymphocytes from BALB/c and C57BL/6NCrl mice were exposed to 0.1 – 2 Gy of photons (whole body irradiation, 6 MV, 2 Gy/min) and X-rays (whole body irradiation, 90 kV, 2 Gy/min). γ-H2AX foci were determined with immunochemistry to measure DSBs.	Linear dose-dependent increase in DSBs in the brain, small intestine, lung and heart of C57BL/6CNrl mice after whole-body irradiation with 0.1 - 1.0 Gy of radiation. 0.8 foci per cell (0.1 Gy) and 8 foci per cell (1 Gy).
Antonelli et al., 2015	In vitro. Primary human foreskin fibroblasts (AG01522) were exposed to 0 – 1 Gy of ^{136}Cs γ-rays (1 Gy/min), protons (0.84 MeV, 28.5 keV/um), carbon ions (58 MeV/u, 39.4 keV/um), and alpha particles (americium-241, 0.75 MeV/u, 0.08 Gy/min, 125.2 keV/um). γ-H2AX foci were determined with immunochemistry to measure DSBs.	Linear dose-dependent increase in the number of DSBs from 0 - 1 Gy for γ-rays and alpha particles as follows: γ-rays: 24.1 foci per Gy per cell nucleus, alpha particles: 8.8 foci per Gy per cell nucleus.
Barnard et al., 2019	In vivo. 10-week-old female C57BL/6 mice were whole-body exposed to 0.5, 1, and 2 Gy of 60Co γ-rays at 0.3, 0.063, and 0.014 Gy/min. p53 binding protein 1 (53BP1) foci were determined via immunofluorescence.	Central LECs showed a linear increase in mean 53BP1 foci/cell with the maximum dose and dose-rate displaying a 78x increase compared to control. Peripheral LECs and lower dose rates displayed similar results, with slightly fewer foci.
Ahmadi et al., 2021	In vitro. Human LEC cells were exposed to 137Cs γ-rays at doses of 0, 0.1, 0.25, and 0.5 Gy and dose rates of 0.065 and 0.3 Gy/min. DNA strand breaks were measured using the comet assay.	Human LECs showed a gradual increase in the tail from the comet assay with the maximum dose and dose-rate displaying a 3.7x increase compared to control. Lower dose-rates followed a similar pattern with a lower amount of strand breaks.
Hamada et al., 2006	In vitro. Primary normal human diploid fibroblast (HE49) cells were exposed to 0.1, 0.5, and 4 Gy X-rays at 240 kV with a dose rate of 0.5 Gy/min. The number of H2AX foci/cell, which represented DNA strand breaks, was determined 6 – 7 minutes after irradiation through fluorescence microscopy.	Cells displayed a linear increase in the number of H2AX foci/cell, with the maximum dose displaying a 125x increase compared to control.
Dubrova & Plumb, 2002		At 1 Gy observe 70 DSBs, 1000 single-strange breaks and 2000 damaged DNA bases per cell per Gy.
Sabirzhanov et al., 2020	In vitro. Rat cortical neurons were exposed to 2, 8 or 32 Gy of X rays (320 kV) at a dose rate of 1.25 Gy/min. Western blot was used to measure γ-H2AX, p-ataxia telangiectasia mutated (ATM) and p- ATM/RAD3-related (ATR) levels.	In rat cortical neurons, p-ATM increased at 2, 8, and 32 Gy, with a 15-fold increase at 8 and 32 Gy. γ-H2AX levels increased at 8 and 32 Gy.
Geisel et al., 2012	In vivo. Patients with suspected coronary artery disease receiving X-rays from computed tomography or conventional coronary angiography had levels of DSBs assessed in blood lymphocytes by γ-H2AX fluorescence.	There was a correlation between effective dose (in mSv) and DSBs. For both conventional coronary angiography and computed tomography, a dose of 10 mSv produced about 2-fold more DNA DSBs than a dose of 5 mSv.
Ungvari et al., 2013	In vitro. Rat cerebromicrovascular endothelial cells and hippocampal neurons were irradiated with 2-10 Gy of ^{137}Cs gamma rays. DNA strand breaks were assessed with the comet assay.	DNA damage increased at all doses (2-10 Gy). In the control, less than 5% of DNA was in the tail, while by 6 Gy, 35% of the DNA was in the tail in cerebromicrovascular endothelial cells and 25% was in the tail in neurons.
Rombouts et al., 2013	In vitro. EA.hy926 cells and human umbilical vein endothelial cells were irradiated with various doses of X-rays (0.25 Gy/min). γ-H2AX foci were assessed with immunofluorescence.	More γ-H2AX foci were observed at higher doses in both cell types. In human umbilical vein endothelial cells, few foci/nucleus were observed at 0.05 Gy, with about 23 at 2 Gy. In EA.hy926 cells, few foci/nucleus were observed at 0.05 Gy, with about 37 at 2 Gy.
Baselet et al., 2017	In vitro. Human telomerase-immortalized coronary artery endothelial cells were irradiated with various doses of X-rays (0.5 Gy/min). Immunocytochemical staining was performed for γ-H2AX and 53BP1 foci.	Doses of 0.05 and 0.1 Gy did not increase the number of γ-H2AX foci, but 0.5 Gy increased foci number by 5-fold and 2 Gy by 15-fold. A dose of 0.05 Gy did not increase the number of 53BP1 foci, but 0.1 Gy, 0.5 Gy and 2 Gy increased levels by 3-fold, 7-fold and 8-fold, respectively.

Time Concordance

Reference	Experiment Description	Result
Rogakou et al., 1999	In vitro. Normal human fibroblasts (IMR90), human breast cancer cells (MCF7), human astrocytoma cells (SF268), Indian muntjac Muntiacus muntjak normal skin fibroblasts, Xenopus laevisA6 normal kidney cells, Drosophila melanogaster epithelial cells, and Saccharomyces cerevisiae were exposed to 0.6, 2, 20, 22, 100, and 200 Gy 137Cs γ-rays. Doses below 20 Gy were delivered at 15.7 Gy/min and other doses were delivered in 1 minute. DNA breaks were visualized using γ-H2AX antibodies and microscopy.	DSBs were present at 3 min and persisted from 15 - 60 min.
Hamada & Woloschak, 2017	In vitro. human LECs were exposed to 0.025 Gy X-rays at 0.42 – 0.45 Gy/min. 53BP1 foci were measured via indirect immunofluorescence.	In cells immediately exposed to 0.025 Gy, the level of 53BP1 foci/cell increased to 3.3x relative to control 0.5 h post-irradiation.
Hamada et al., 2006	In vitro. Primary normal human diploid fibroblast (HE49) cells were exposed to 0.1, 0.5, and 4 Gy (deposition of energy) at 240 kV with a dose rate of 0.5 Gy/min. The number of H2AX foci/cell, which represented DNA strand breaks, was determined through fluorescence microscopy.	In cells immediately exposed to 0.5 Gy, 11% of cells had 18 foci six min post-irradiation, compared to 90% of controls having 0 foci.
Acharya et al., 2010	In vitro. Human neural stem cells were exposed to 1, 2 and 5 Gy of γ-rays at a dose rate of 2.2 Gy/min. The levels of γ-H2AX phosphorylation post irradiation were assessed by immunocytochemistry, fluorescence-activated cell sorting (FACS) analysis and γ-H2AX foci enumeration.	The number of cells positive for nuclear γ-H2AX foci peaked at 20 min post-irradiation. After 1h, this level quickly declined.
Schmal et al., 2019	In vivo. Juvenile and adult C57BL/6 mice were exposed to whole body 6-MV photons at 2 Gy/min. Irradiations were done in 5x, 10x, 15x and 20x fractions of 0.1 Gy. Double staining for NeuN and 53BP1 was used to quantify DNA damage foci and the possible accumulation in the hippocampal dentate gyrus.	To assess possible accumulation of persisting 53BP1-foci during fractionated radiation, juvenile and adult mice were examined 72 h after exposure to 5×, 10×, 15×, or 20× fractions of 0.1 Gy, compared to controls. The number of persisting 53BP1-foci increased significantly in both juvenile and adult mice during fractionated irradiation (maximum at 1 m post-IR).
Dong et al., 2015	In vivo. C57BL/6J mice were exposed to 2 Gy of X-rays at 2 Gy/min using a 6 MV source. γ-H2AX foci were assessed with immunofluorescence in the brain.	At 0.5 h, about 14 γ-H2AX foci/cell were present. This decreased linearly to about 2 foci/cell at 24 h, with no foci/cell from 48 h to 6 weeks.
Barazzuol et	In vivo. C57BL/6 mice were exposed to 0.1 or 2 Gy of X-rays (250 kV) at a rate of 0.5	At both 0.5 and 6 h post-irradiation, increased 53BP1 foci were

al., 2017	Gy/min. 53BP1 foci were quantified with immunofluorescence in neural stem cells and neuron progenitors in the lateral ventricle.	observed, with the highest level at 0.5 h.
Sabirzhanov et al., 2020	In vitro. Rat cortical neurons were exposed to 2, 8 or 32 Gy of X rays (320 kV) at a dose rate of 1.25 Gy/min. Western blot was used to measure γ-H2AX, p-ATM and p-ATR levels.	In rat cortical neurons, γ-H2AX, p-ATM and p-ATR all increased at 30 minutes post-irradiation, with a sustained increase until 6 h.
Zhang et al., 2017	In vitro. HT22 hippocampal neuronal cellsT were irradiated with X-rays (320 kVp) at 8 or 12 Gy at a dose rate of 4 Gy/min. The comet assay was preformed to assess the DNA double strand breaks in HT22 cells. Western blot was used to measure γ-H2AX and p-ATM.	At 8 Gy, the comet assay showed an increased tail moment at both 30 minutes and 24 h post-irradiation. At 12 Gy, p-ATM was increased over 4-fold at both 30 minutes and 1 h post-irradiation. γ-H2AX was increased over 3-fold at 30 minutes post-irradiation and almost 2-fold at 1 and 24 h.
Geisel et al., 2012	In vivo. Patients with suspected coronary artery disease receiving X-rays from computed tomography or conventional coronary angiography had levels of DSBs assessed in blood lymphocytes by γ-H2AX fluorescence.	DSBs were increased at 1 h post-irradiation and returned to pre-irradiation levels by 24 h.
Park et al., 2022	In vitro. Human aortic endothelial cells were irradiated with 137Cs gamma rays at 4 Gy (3.5 Gy/min). γ-H2AX was measured with western blot. p-ATM and 53BP1 were determined with immunofluorescence.	γ-H2AX, p-ATM, and 53BP1 were shown increased at 1 h post-irradiation and slightly decreased for the rest of the 6 h but remained elevated above the control.
Kim et al., 2014	In vitro. Human umbilical vein endothelial cells were irradiated with 4 Gy of 137Cs gamma rays. γ-H2AX levels were determined with immunofluorescence.	γ-H2AX foci greatly increased at 1 and 6 h post-irradiation, with the greatest increase at 1 h.
Dong et al., 2014	In vitro. Human umbilical vein endothelial cells were irradiated with 2 Gy of 137Cs gamma rays. γ-H2AX levels were determined with immunofluorescence.	γ-H2AX foci increased 8-fold at 3 h, 7-fold at 6 h, and 2-fold at 12 and 24 h post-irradiation.
Rombouts et al., 2013	In vitro. EA.hy926 cells and human umbilical vein endothelial cells were irradiated with X-rays (0.25 Gy/min). γ-H2AX foci were assessed with immunofluorescence.	The greatest increase in γ-H2AX foci was observed 30 minutes post-irradiation, while levels were still slightly elevated at 24 h.
Nübel et al., 2006	In vitro. Human umbilical vein endothelial cells were irradiated with gamma rays at 20 Gy. DNA strand breaks were assessed with the comet assay and western blot for γ-H2AX.	The olive tail moment increased 5-fold immediately after irradiation and returned to control levels by 4 h. A large increase in γ-H2AX was observed at 0.5 h post-irradiation, with lower levels at 4 h but still above the control.
Baselet et al., 2017	In vitro. Human telomerase-immortalized coronary artery endothelial cells were irradiated with various doses of X-rays (0.5 Gy/min). Immunocytochemical staining was performed for γ-H2AX and 53BP1 foci.	Increased γ-H2AX and 53BP1 foci were observed at 0.5 h post-irradiation, remaining elevated at 4 h but returning to control levels at 24 h.
Gionchiglia et al., 2021	In vivo. Male CD1 and B6/129 mice were irradiated with X-rays at 10 Gy. Brain sections were single or double-stained with antibodies against γ-H2AX and p53BP1.	In the forebrain, cerebral cortex, hippocampus and subventricular zone (SVZ)/ rostral migratory stream (RMS)/ olfactory bulb (OB), γH2AX and p53BP1 positive cells increased at both 15 and 30 minutes post-irradiation, with the greatest increase at 30 minutes.

Response-response relationship

There is evidence of a response-response relationship between the deposition of energy and the frequency of DSBs. In studies encompassing a variety of biological models, radiation types and radiation doses, a positive, linear relationship was found between the radiation dose and the number of DSBs (Aufderheide et al., 1987; Sidjanin, 1993; Frankenberg et al., 1999; Sutherland et al., 2000; de Lara et al., 2001; Baumstark-Khan et al., 2003; Rothkamm & Lo, 2003; Kuhne et al., 2005; Rube et al., 2008; Grudzenski et al., 2010; Bannik et al., 2013; Shelke & Das, 2015; Antonelli et al., 2015; Hamada, 2017b; Dalke, 2018; Barazzuol et al., 2017; Geisel et al., 2012; Ungvari et al., 2013; Rombouts et al., 2013; Baselet et al., 2017). There were, however, at least four exceptions reported. When human blood lymphocytes were irradiated with X-rays in vitro, a linear relationship was only found for doses ranging from 6 - 500 mGy; at low doses from 0 - 6 mGy, there was a quadratic relationship reported (Beels et al., 2009). Secondly, simulation studies predicted that there would be a non-linear increase in DSBs as energy deposition increased, with a saturation point at higher LETs (Charlton et al., 1989). Furthermore, primary normal human fibroblasts exposed to 1.2 – 5 mGy X-rays at 5.67 mGy/min showed a supralinear relationship, indicating at low doses, the DSBs are mostly due to radiation-induced bystander effects. Doses above 10 mGy showed a positive linear relationship (Ojima et al., 2008). Finally, in the human lens epithelial cell line SRA01/04, DNA strand breaks appeared immediately after exposure to UVB (0.14 J/cm2) and were repaired after 30 minutes. They then reappeared after 60 and 90 minutes. Both were once again repaired within 30 minutes. However, the two subsequent stages of DNA strand breaks did not occur when exposed to a lower dose of UVB (0.014 J/cm2) (Cencer et al., 2018).

Time-scale

Data from temporal response studies suggests that DSBs likely occur within seconds to minutes of energy deposition by ionizing radiation. In a variety of biological models, the presence of DSBs has been well documented within 10 - 30 minutes of radiation exposure (Rogakou et al., 1999; Rube et al., 2008; Beels et al., 2009; Kuefner et al., 2009; Grudzenski et al., 2010; Antonelli et al., 2015; Acharya et al., 2010; Dong et al., 2015; Barazzuol et al., 2017; Sabirzhanov et al., 2020; Rombouts et al., 2013; Nübel et al., 2006; Baselet et al., 2017; Zhang et al., 2017; Gionchiglia et al., 2021); there is also evidence that DSBs may actually be present within 3 - 5 minutes of irradiation (Kleiman, 1990; Rogakou et al., 1999; Rothkamm & Lo, 2003; Rube et al., 2008; Grudzenski et al., 2010; Cencer et al., 2018). Interestingly, one study that focussed on monitoring the cells before, during and after irradiation by taking photos every 5, 10 or 15 seconds found that foci indicative of DSBs were present 25 and 40 seconds after collision of the alpha particles and protons with the cell, respectively. The number of foci were found to increase over time until plateauing at approximately 200 seconds after alpha particle exposure and 800 seconds after proton exposure (Mosconi et al., 2011).

After the 30 minute mark, DSBs have been shown to rapidly decline in number. By 24 hours post-irradiation, DSB numbers had declined substantially in systems exposed to radiation doses between 40 mGy and 80 Gy (Aufderheide et al., 1987; Baumstark-Khan et al., 2003; Rothkamm & Lo, 2003; Rube et al., 2008; Grudzenski et al., 2010; Bannik et al., 2013; Markiewicz et al., 2015; Russo et al., 2015; Antonelli et al., 2015; Dalke, 2018; Bains, 2019; Barnard, 2019; Ahmadi et al., 2021; Dong et al., 2015; Dong et al., 2014; Sabirzhanov et al., 2020; Rombouts et al., 2013; Baselet et al., 2017; Gionchiglia et al., 2021), with the sharpest decrease documented within the first 5 h (Kleiman, 1990; Sidjanin, 1993; Rogakou et al., 1999; Rube et al., 2008; Kuefner et al., 2009; Grudzenski et al., 2010; Bannik, 2013; Markiewicz et al., 2015; Shelke and Das, 2015; Cencer et al., 2018; Acharya et al., 2010; Park et al., 2022; Kim et al., 2014; Nübel et al., 2006). Interestingly, DSBs were found to be more persistent when they were induced by higher LET radiation (Aufderheide et al., 1987, Baumstark-Khan et al., 2003; Antonelli et al., 2015).

Known modulating factors

Modulating Factor	Details	Effects on the KER	References
Nitroxides	Increased concentration	Decreased DNA strand breaks.	DeGraff et al., 1992; Citrin & Mitchel, 2014
5-fluorouracil	Increased concentration	Increased DNA strand breaks.	De Angelis et al., 2006; Citrin & Mitchel, 2014
Thiols	Increased concentration	Decreased DNA strand breaks.	Milligan et al., 1995; Citrin & Mitchel, 2014
Cisplatin	Increased concentration	Decreased DNA break repair.	Sears & Turchi; Citrin & Mitchel, 2014

Known Feedforward/Feedback loops influencing this KER

Not identified.

References

Agrawala, P.K. et al. (2008), "Induction and repairability of DNA damage caused by ultrasoft X-rays: Role of core events.", Int. J. Radiat. Biol., 84(12):1093–1103. doi:10.1080/09553000802478083.

Ahmadi, M. et al. (2021), “Early responses to low-dose ionizing radiation in cellular lens epithelial models”, Radiation research, Vol.197/1, *Radiation Research Society*, United States, https://doi.org/10.1667/RADE-20-00284.1

Ainsbury, E. A. et al. (2016), “Ionizing radiation induced cataracts: Recent biological and mechanistic developments and perspectives for future research”, *Mutation research. Reviews in mutation research*, Vol. 770, Elsevier B.V., Amsterdam, https://doi.org/10.1016/j.mrrev.2016.07.010

Alexander, J. L. and Orr-Weaver, T. L. (2016), “Replication fork instability and the consequences of fork collisions from replication”, *Genes & Development*, Vol. 30/20, Cold Spring Harbor Laboratory Press, https://doi.org/ 10.1101/gad.288142.116

Allen, C. H. et al. (2018), “Raman micro-spectroscopy analysis of human lens epithelial cells exposed to a low-dose-range of ionizing radiation”, *Physics in medicine & biology*, Vol. 63/2, IOP Publishing, Bristol, https://doi.org/10.1088/1361-6560/aaa176

Antonelli, A.F. et al. (2015), "Induction and Repair of DNA DSB as Revealed by H2AX Phosphorylation Foci in Human Fibroblasts Exposed to Low- and High-LET Radiation: Relationship with Early and Delayed Reproductive Cell Death", Radiat. Res. 183(4):417-31, doi:10.1667/RR13855.1.

Acharya, M. et al. (2010), “Consequences of ionizing radiation-induced damage in human neural stem cells”, Free Radical Biology and Medicine. 49(12):1846-1855, doi:10.1016/j.freeradbiomed.2010.08.021.

Asaithamby, A. et al. (2008), "Repair of HZE-Particle-Induced DNA Double-Strand Breaks in Normal Human Fibroblasts.", Radiat Res. 169(4):437–446. doi:10.1667/RR1165.1.

Aufderheide, E. et al. (1987), “Heavy ion effects on cellular DNA: Strand break induction and repair in cultured diploid lens epithelial cells”, *International journal of radiation biology and related studies in physics, chemistry and medicin*e, Vol. 51/5, Taylor & Francis, London, https://doi.org/10.1080/09553008714551071

Bannik, K. et al. (2013), “Are mouse lens epithelial cells more sensitive to γ-irradiation than lymphocytes?”, *Radiation and environmental biophysics*, Vol. 52/2, Springer-Verlag, Berlin/Heidelberg, https://doi.org/10.1007/s00411-012-0451-8

Bains, S. K. et al. (2019), “Effects of ionizing radiation on telomere length and telomerase activity in cultured human lens epithelium cells”, I*nternational journal of radiation biology*, Vol. 95/1, Taylor & Francis, Abingdon, https://doi.org/10.1080/09553002.2018.1466066

Barazzuol, L et al. (2017), “A coordinated DNA damage response promotes adult quiescent neural stem cell activation. PLOS Biology, 15(5). https://doi.org/10.1371/journal.pbio.2001264

Barnard, S. G. R. et al. (2018), “Dotting the eyes: mouse strain dependency of the lens epithelium to low dose radiation-induced DNA damage”, *International journal of radiation biology*, Vol. 94/12, Taylor & Francis, Abingdon, https://doi.org/10.1080/09553002.2018.1532609

Barnard, S. G. R. et al. (2019), “Inverse dose-rate effect of ionising radiation on residual 53BP1 foci in the eye lens”, *Scientific Reports*, Vol. 9/1, Nature Publishing Group, England, https://doi.org/10.1038/s41598-019-46893-3

Barnard, S. G. R. et al. (2022), “Radiation-induced DNA damage and repair in lens epithelial cells of both Ptch1 (+/-) and Ercc2 (+/-) mutated mice”, *Radiation Research*, Vol. 197/1, Radiation Research Society, United States, https://doi.org/10.1667/RADE-20-00264.1

Baselet, B. et al. (2019), “Pathological effects of ionizing radiation: endothelial activation and dysfunction”, Cellular and molecular life sciences, Vol. 76/4, Springer Nature, https://doi.org/10.1007/s00018-018-2956-z

Baselet, B. et al. (2017), “Functional Gene Analysis Reveals Cell Cycle Changes and Inflammation in Endothelial Cells Irradiated with a Single X-ray Dose”, Frontiers in pharmacology, Vol. 8, Frontiers, https://doi.org/10.3389/fphar.2017.00213

Baumstark-Khan, C., J. Heilmann, and H. Rink (2003), ‘Induction and repair of DNA strand breaks in bovine lens epithelial cells after high LET irradiation”, *Advances in space research*, Vol. 31/6, Elsevier Ltd, England, https://doi.org/10.1016/S0273-1177(03)00095-4

Beels, L. et al. (2009), "g-H2AX Foci as a Biomarker for Patient X-Ray Exposure in Pediatric Cardiac Catheterization", Are We Underestimating Radiation Risks?":1903–1909. doi:10.1161/CIRCULATIONAHA.109.880385.

Belli M, Cherunbini R, Vecchia MD, Dini V, Moschini G, Signoretti C, Simon G, Tabocchini MA, Tiveron P. 2000. DNA DSB induction and rejoining in V79 cells irradiated with light ions: a constant field gel electrophoresis study. Int J Radiat Biol. 76(8):1095-1104.

Brooks, A.L., D.G. Hoel & R.J. Preston (2016), "The role of dose rate in radiation cancer risk: evaluating the effect of dose rate at the molecular, cellular and tissue levels using key events in critical pathways following exposure to low LET radiation.", Int. J. Radiat. Biol. 92(8):405–426. doi:10.1080/09553002.2016.1186301.

Bucolo, C. et al. (1994), “The effect of ganglioside on oxidation-induced permeability changes in lens and in epithelial cells of lens and retina”, *Experimental eye research,* Vol. 58/6, Elsevier Ltd, London, https://doi.org/10.1006/exer.1994.1067

Cabrera et al. (2011), “Antioxidants and the integrity of ocular tissues”, in Veterinary medicine international, SAGE-Hindawi Access to Research, United States. DOI:

10.4061/2011/905153

Cadet, J. et al. (2012), “Oxidatively generated complex DNA damage: tandem and clustered lesions”, Cancer letters, Vol. 327/1, Elsevier Ireland Ltd, Ireland. https://doi.org/10.1016/j.canlet.2012.04.005

Cannan, W.J. & D.S. Pederson (2016), "Mechanisms and Consequences of Double-Strand DNA Break Formation in Chromatin.", J. Cell Physiol. 231(1):3–14. doi:10.1002/jcp.25048.

Cencer, C. S. et al. (2018), “PARP-1/PAR activity in cultured human lens epithelial cells exposed to two levels of UVB light”, Photochemistry and photobiology, Vol. 94/1, Wiley, Hoboken, https://doi.org/10.1111/php.12814

Chadwick, K.H., (2017), Towards a new dose and dose-rate effectiveness factor (DDREF)? Some comments., J Radiol Prot., 37:422-433. doi: 10.1088/1361-6498/aa6722.

Charlton, D.E., H. Nikjoo & J.L. Humm (1989), "Calculation of initial yields of single- and double-strand breaks in cell nuclei from electrons, protons and alpha particles.", Int. J. Rad. Biol., 53(3):353-365, DOI: 10.1080/09553008814552501

Christensen, D.M. (2014), "Management of Ionizing Radiation Injuries and Illnesses, Part 3: Radiobiology and Health Effects of Ionizing Radiation.", 114(7):556–565. doi:10.7556/jaoa.2014.109.

Citrin, D.E. & J.B. Mitchel (2014), "Public Access NIH Public Access.", 71(2):233–236. doi:10.1038/mp.2011.182.doi.

Dalke, C. et al. (2018), “Lifetime study in mice after acute low-dose ionizing radiation: a multifactorial study with special focus on cataract risk”, Radiation and environmental biophysics, Vol. 57/2, Springer Berlin Heidelberg, Berling/Heidelberg, https://doi.org/10.1007/s00411-017-0728-z

Day, T.K. et al. (2007), "Adaptive Response for Chromosomal Inversions in pKZ1 Mouse Prostate Induced by Low Doses of X Radiation Delivered after a High Dose.", Radiat Res. 167(6):682–692. doi:10.1667/rr0764.1.

De Angelis, P. M. et al. (2006), “Cellular response to 5-fluorouracil (5-FU) in 5-FU-resistant colon cancer cell lines during treatment and recovery”, Molecular Cancer, Vol. 5/20, BioMed Central, https://doi.org/10.1186/1476-4598-5-20

DeGraff, W. G. et al. (1992), “Nitroxide-mediated protection against X-ray- and neocarzinostatin-induced DNA damage”, Free Radical Biology and Medicine, Vol. 13/5, Elsevier, https://doi.org/10.1016/0891-5849(92)90142-4

Desouky, O., N. Ding & G. Zhou (2015), "ScienceDirect Targeted and non-targeted effects of ionizing radiation.", J. Radiat. Res. Appl. Sci. 8(2):247–254. doi:10.1016/j.jrras.2015.03.003.

Dong et al. (2015), “Relationship between irradiation-induced neuro-inflammatory environments and impaired cognitive function in the developing brain of Mice. International Journal of Radiation Biology, 91(3):224–239. https://doi.org/10.3109/09553002.2014.988895

Dong, X. et al. (2014), “NEMO modulates radiation-induced endothelial senescence of human umbilical veins through NF-κB signal pathway”, Radiation Research, Vol. 183/1, BioOne, https://doi.org/10.1667/RR13682.1

Dubrova, Y.E. & M.A. Plumb (2002), "Ionising radiation and mutation induction at mouse minisatellite loci The story of the two generations", Mutat. Res. 499(2):143–150.

EPRI (2014), Epidemiology and mechanistic effects of radiation on the lens of the eye: Review and scientific appraisal of the literature, EPRI, California

Falk, M., E. Lukášová & S. Kozubek (2008), "Chromatin structure influences the sensitivity of DNA to γ-radiation.", Biochim. Biophys. Acta. - Mol. Cell. Res. 1783(12):2398–2414. doi:10.1016/j.bbamcr.2008.07.010.

Feinendegen, L.E. (2005), "UKRC 2004 debate Evidence for beneficial low level radiation effects and radiation hormesis. Radiology.", 78:3–7. doi:10.1259/bjr/63353075.

Feinendegen, L.E., M. Pollycove & R.D. Neumann (2007), "Whole-body responses to low-level radiation exposure: New concepts in mammalian radiobiology.", Exp. Hematol. 35(4 SUPPL.):37–46. doi:10.1016/j.exphem.2007.01.011.

Flegal, M. et al. (2015), "Measuring DNA Damage and Repair in Mouse Splenocytes After Chronic In Vivo Exposure to Very Low Doses of Beta- and γ-Radiation.", (July):1–9. doi:10.3791/52912.

Foray, N., M. Bourguignon and N. Hamada (2016), “Individual response to ionizing radiation”, Mutation research. Reviews in mutation research, Vol. 770, Elsevier B.V., Amsterdam, https://doi.org/10.1016/j.mrrev.2016.09.001

Franken NAP, Hovingh S, Cate RT, Krawczyk P, Stap J, Hoebe R, Aten J, Barendsen GW. 2012. Relative biological effectiveness of high linear energy transfer alpha-particles for the induction of DNA-double-strand breaks, chromosome aberrations and reproductive cell death in SW-1573 lung tumour cells. Oncol reports. 27:769-774.

Frankenberg D, Brede HJ, Schrewe UJ, Steinmetz C, Frankenberg-Scwager M, Kasten G, Pralle E. 1999. Induction of DNA Double-Strand Breaks by 1H and 4He Ions in Primary Human Skin Fibroblasts in the LET range of 8 to 124 keV/µm. Radiat Res. 151:540-549.

Geisel, D. et al. (2012), “DNA double-strand breaks as potential indicators for the biological effects of ionising radiation exposure from cardiac CT and conventional coronary angiography: a randomised, controlled study”, European Radiology, Vol. 22/8, Springer Nature, https://doi.org/10.1007/s00330-012-2426-1

Gionchiglia, N. et al. (2021), “Association of Caspase 3 Activation and H2AX γ Phosphorylation in the Aging Brain: Studies on Untreated and Irradiated Mice,” Biomedicines. 9(9):1166. doi: 10.3390/biomedicines9091166.

Goodhead, D.T. (2006), "Energy deposition stochastics and track structure: What about the target?", Radiat. Prot. Dosimetry. 122(1–4):3–15. doi:10.1093/rpd/ncl498.

Grudzenski, S. et al. (2010), "Inducible response required for repair of low-dose radiation damage in human fibroblasts.", Proc. Natl. Acad. Sci. USA. 107(32): 14205-14210, doi:10.1073/pnas.1002213107.

Hada, M. & A.G. Georgakilas (2008), "Formation of Clustered DNA Damage after High-LET Irradiation: A Review.", J. Radiat. Res., 49(3):203–210. doi:10.1269/jrr.07123.

Hamada, N. et al. (2006), “Histone H2AX phosphorylation in normal human cells irradiated with focused ultrasoft X rays: evidence for chromatin movement during repair”,

Radiation Research, Vol. 166/1, Radiation Research Society, United States, https://doi.org/10.1667/RR3577.1

Hamada, N. (2014), “What are the intracellular targets and intratissue target cells for radiation effects?”, Radiation research, Vol. 181/1, The Radiation Research Society, Lawrence, https://doi.org/10.1667/RR13505.1

Hamada, N. and T. Sato (2016), “Cataractogenesis following high-LET radiation exposure”, Mutation Research. Reviews in mutation research, Vol. 770, Elsevier B.V., Amsterdam, https://doi.org/10.1016/j.mrrev.2016.08.005

Hamada, N. (2017a), “Ionizing radiation sensitivity of the ocular lens and its dose rate dependence”, International journal of radiation biology, Vol. 93/10, Taylor & Francis, Abingdon, https://doi.org/10.1080/09553002.2016.1266407

Hamada, N. and G. E. Woloschak (2017), “Ionizing radiation response of primary normal human lens epithelial cells”, PloS ONE, Vol. 12/7, Public Library Science, San Francisco, https://doi.org/10.1371/journal.pone.0181530

Havas, M. (2017), “When theory and observation collide: Can non-ionizing radiation cause cancer?”, Environmental pollution, Vol. 221, Elsevier Ltd, England. https://doi.org/10.1016/j.envpol.2016.10.018

Hightower, K. R. (1995), “The role of the lens epithelium in development of UV cataract”, Current eye research, Vol. 14/1, Informal UK Ltd, Philadelphia, https://doi.org/10.3109/02713689508999916

Iliakis, G., T. Murmann & A. Soni (2015), "Alternative end-joining repair pathways are the ultimate backup for abrogated classical non-homologous end-joining and homologous recombination repair: Implications for the formation of chromosome translocations.", Mutat. Res. - Genet. Toxicol. Environ. Mutagen. 793:166–175. doi:10.1016/j.mrgentox.2015.07.001.

Joiner, M. (2009), "Basic Clinical Radiobiology", Edited by. [1] P.J. Sadler, Next-Generation Met Anticancer Complexes Multitargeting via Redox Modul Inorg Chem 52 21.:375. doi:10.1201/b13224.

Jorge, S.-G. et al. (2012), "Evidence of DNA double strand breaks formation in Escherichia coli bacteria exposed to alpha particles of different LET assessed by the SOS response.", Appl. Radiat. Isot. 71(SUPPL.):66–70. doi:10.1016/j.apradiso.2012.05.007.

Kadhim, M.A., M.A. Hill & S.R. Moore, (2006), "Genomic instability and the role of radiation quality.", Radiat. Prot. Dosimetry. 122(1–4):221–227. doi:10.1093/rpd/ncl445.

Khanna, K.K. & S.P. Jackson (2001), "DNA double-strand breaks: signaling, repair and the cancer connection.", Nature Genetics. 27(3):247-54. doi:10.1038/85798.

Kim, K. S. et al. (2014), “Characterization of DNA damage-induced cellular senescence by ionizing radiation in endothelial cells”, International Journal of Radiation Biology, Vol. 90/1, Informa, London, https://doi.org/10.3109/09553002.2014.859763

Kim, J. N. and B. M. Lee (2007), “Risk factors, health risks, and risk management for aircraft personnel and frequent flyers”, Journal of toxicology and environmental health. Part B, Critical reviews, Vol. 10/3, Taylor & Francis Group, Philadelphia, https://doi.org/10.1080/10937400600882103

Kleiman, N. J., R. Wang and A. Spector (1990), “Ultraviolet light induced DNA damage and repair in bovine lens epithelial cells”, Current eye research, Vol. 9/12, Informa UK Ltd, Oxford, https://doi.org/10.3109/02713689009003475

Kozbenko, T. et al. (2022), “Deploying elements of scoping review methods for adverse outcome pathway development: a space travel case example”, International Journal of Radiation Biology, 1–12. https://doi.org/10.1080/09553002.2022.2110306

Kuefner, M.A. et al. (2009), "DNA Double-Strand Breaks and Their Repair in Blood Lymphocytes of Patients Undergoing Angiographic Procedures.", Investigative radiology. 44(8):440-6. doi:10.1097/RLI.0b013e3181a654a5.

Kuefner, M.A. et al. (2015), "Chemoprevention of Radiation-Induced DNA Double-Strand Breaks with Antioxidants.", Curr Radiol Rep (2015) 3: 81. https://doi.org/10.1007/s40134-014-0081-9

Kuhne, M., G. Urban & M. Lo, (2005), "DNA Double-Strand Break Misrejoining after Exposure of Primary Human Fibroblasts to CK Characteristic X Rays, 29 kVp X Rays and Co γ-Rays.", Radiation Research. 164(5):669-676. doi:10.1667/RR3461.1.

de Lara, C.M. et al. (2001), "Dependence of the Yield of DNA Double-Strand Breaks in Chinese Hamster V79-4 Cells on the Photon Energy of Ultrasoft X Rays.", Radiation Research. 155(3):440-8. doi:10.1667/0033-7587(2001)155[0440:DOTYOD]2.0.CO;2.

Liao, J. et al. (2011), “Anti-UVC irradiation and metal chelation properties of 6-benzoyl-5,7-dihydroxy-4-phenyl-chromen-2-one: An implications for anti-cataract agent”, International journal of molecular sciences, Vol. 12/10, MDPI, Basel. https://doi.org/10.3390/ijms12107059

Lipman, R. M., B. J. Tripathi, R. C. Tripathi (1998), “Cataracts induced by microwave and ionizing radiation”, Survey of ophthalmology, Vol. 33/3, Elsevier Inc, United States, https://doi.org/10.1016/0039-6257(88)90088-4

Lomax, M.E., L.K. Folkes & P.O. Neill (2013). "Biological Consequences of Radiation-induced DNA Damage: Relevance to Radiotherapy", Statement of Search Strategies Used and Sources of Information Why Radiation Damage is More Effective than Endogenous Damage at Killing Cells Ionising Radiation-induced Do. 25:578–585. doi:10.1016/j.clon.2013.06.007.

Long, A. C., C. M. H. Colitz, and J. A. Bomser (2001), “Apoptotic and necrotic mechanisms of stress-induced human lens epithelial cell death”, Experimental biology and medicine, SAGE Publications, London, https://doi.org/10.1177/153537020422901012

Lorat, Y. et al. (2015), "Nanoscale analysis of clustered DNA damage after high-LET irradiation by quantitative electron microscopy – The heavy burden to repair.", DNA Repair (Amst). 28:93–106. doi:10.1016/j.dnarep.2015.01.007.

Maier, P. et al. (2016), "Cellular Pathways in Response to Ionizing Radiation and Their Targetability for Tumor Radiosensitization.", Int. J. Mol. Sci., 14;17(1), pii:E102, doi:10.3390/ijms17010102.

Markiewicz, E. et al. (2015), “Nonlinear ionizing radiation-induced changes in eye lens cell proliferation, cyclin D1 expression and lens shape”, Open biology, Vol. 5/4, Royal society, London, https://doi.org/10.1098/rsob.150011

Milligan, J. R. et al. (1995), « DNA repair by thiols in air shows two radicals make a double-strand break”, Radiation Research, Vol 143/3, pp. 273-280

Moore, S., F.K.T. Stanley & A.A. Goodarzi (2014), "The repair of environmentally relevant DNA double strand breaks caused by high linear energy transfer irradiation – No simple task.", DNA repair (Amst), 17:64–73. doi: 10.1016/j.dnarep.2014.01.014.

Mosconi, M., U. Giesen & F. Langner (2011), "53BP1 and MDC1 foci formation in HT-1080 cells for low- and high-LET microbeam irradiations.", Radiat. Envrion. Biophys. 50(3):345–352. doi:10.1007/s00411-011-0366-9.

Nagane, M. et al. (2021), “DNA damage response in vascular endothelial senescence: Implication for radiation-induced cardiovascular disease”, Journal of Radiation Research, Vol. 62/4, https://doi.org/10.1093/jrr/rrab032

Nenoi, M., B. Wang & G. Vares (2015), "In vivo radioadaptive response: A review of studies relevant to radiation-induced cancer risk.", Hum. Exp. Toxicol. 34(3):272–283. doi:10.1177/0960327114537537.

Nikitaki, Z. et al. (2016), "Measurement of complex DNA damage induction and repair in human cellular systems after exposure to ionizing radiations of varying linear energy transfer (LET).", Free Radiac. Res. 50(sup1):S64-S78, doi:10.1080/10715762.2016.1232484.

Nikjoo, H. et al. (2001), "Computational approach for determining the spectrum of DNA damage induced by ionizing radiation.", Radiat. Res. 156(5 Pt 2):577–83.

Nübel, T. et al. (2006), “Lovastatin protects human endothelial cells from killing by ionizing radiation without impairing induction and repair of DNA double-strand breaks”, Clinical Cancer Research, Vol. 12/3, American Association for Cancer Research, https://doi.org/10.1158/1078-0432.CCR-05-1903

Ojima, M., N. Ban, and M. Kai (2008), “DNA double-strand breaks induced by very low X-ray doses are largely due to bystander effects”, Radiation Research, Vol. 170/3, Radiation Research Society, United States, https://doi.org/10.1667/RR1255.1

Okayasu, R. (2012a), "Repair of DNA damage induced by accelerated heavy ions-A mini review.", Int. J. Cancer. 130(5):991–1000. doi:10.1002/ijc.26445.

Okayasu, R. (2012b), "Heavy ions — a mini review.", 1000:991–1000. doi:10.1002/ijc.26445.

Park, J. W. et al. (2022), “Metformin alleviates ionizing radiation-induced senescence by restoring BARD1-mediated DNA repair in human aortic endothelial cells”, Experimental Gerontology, Vol. 160, Elsevier, Amsterdam, https://doi.org/10.1016/j.exger.2022.111706

Parris, C.N. et al. (2015), "Enhanced γ-H2AX DNA damage foci detection using multimagnification and extended depth of field in imaging flow cytometry.", Cytom. Part A. 87(8):717–723. doi:10.1002/cyto.a.22697.

Radulescu I., K. Elmroth & B. Stenerlöw (2006), "Chromatin Organization Contributes to Non-randomly Distributed Double-Strand Breaks after Exposure to High-LET Radiation.", Radiat. Res. 161(1):1–8. doi:10.1667/rr3094.

Rastogi, R. P. et al. (2010), “Molecular mechanisms of ultraviolet radiation-induced DNA damage and repair”, Journal of nucleic acids, Hindawi Ltd, United States. https://doi.org/10.4061/2010/592980

Reddy, V. N. et al. (1998), “The effect of aqueous humor ascorbate on ultraviolet-B-induced DNA damage in lens epithelium”, Investigative ophthalmology & visual science, Vol. 39/2, Arvo, pp. 344-350

Rogakou, E.P. et al. (1999), "Megabase Chromatin Domains Involved in DNA Double-Strand Breaks In Vivo.", J. Cell Biol, 146(5):905-16. doi: 10.1083/jcb.146.5.905.

Rogers, C. S. et al. (2004), “The effects of sub-solar levels of UV-A and UV-B on rabbit corneal and lens epithelial cells”, Experimental eye research, Vol. 78/5, Elsevier Ltd, London, https://doi.org/10.1016/j.exer.2003.12.011

Rombouts, C. et al. (2013), “Differential response to acute low dose radiation in primary and immortalized endothelial cells”, International Journal of Radiation Biology, Vol. 89/10, Informa, London, https://doi.org/10.3109/09553002.2013.806831

Rothkamm, K. et al. (2015), "Review DNA Damage Foci: Meaning and Significance.", Environ. Mol. Mutagen., 56(6):491-504, doi: 10.1002/em.21944.

Rothkamm, K. & M. Lo (2003), "Evidence for a lack of DNA double-strand break repair in human cells exposed to very low x-ray doses.", PNAS, 100(9):5057-62. doi:10.1073/pnas.0830918100.

Rübe, C.E. et al. (2008), "Cancer Therapy: Preclinical DNA Double-Strand Break Repair of Blood Lymphocytes and Normal Tissues Analysed in a Preclinical Mouse Model: Implications for Radiosensitivity Testing.", Clin. Cancer Res., 14(20):6546–6556. doi:10.1158/1078-0432.CCR-07-5147.

Russo, A. et al. (2015), "Review Article Genomic Instability: Crossing Pathways at the Origin of Structural and Numerical Chromosome Changes.", Envrion. Mol. Mutagen. 56(7):563-580. doi:10.1002/em.

Rydberg B, Heilbronn L, Holley WR, Lobrich M, Zeitlin C et al. 2002. Spatial Distribution and Yield of DNA Double-Strand Breaks Induced by 3-7 MeV Helium Ions in Human Fibroblasts. Radiat Res. 158(1):32-42.

Sabirzhanov, et al. (2020), “Irradiation-Induced Upregulation of miR-711 Inhibits DNA Repair and Promotes Neurodegeneration Pathways.”, Int J Mol Sci. 21(15):5239. doi: 10.3390/ijms21155239.

Sage, E. & N. Shikazono (2017), "Free Radical Biology and Medicine Radiation-induced clustered DNA lesions: Repair and mutagenesis.", Free Radic. Biol. Med. 107(December 2016):125–135. doi:10.1016/j.freeradbiomed.2016.12.008.

Sasaki, H. et al. (1998), “TEMPOL protects against lens DNA strand breaks and cataract in the x-rayed rabbit”, Investigative ophthalmology & visual sciences, Vol. 39/3, Arvo, Rockville, pp. 544-552

Schmal, Z. et al. (2019), “DNA damage accumulation during fractionated low-dose radiation compromises hippocampal neurogenesis”, Radiotherapy and Oncology. 137:45-54. doi:10.1016/j.radonc.2019.04.021.

Sears, C. R. and J. J. Turchi (2012), “Complex cisplatin-double strand break (DSB) lesions directly impair cellular non-homologous end-joining (NHEJ) independent of downstream damage response (DDR) pathways”, Journal of biological chemistry, Vol 287/29, The American Society for Biochemistry and Molecular Biology, Inc, USA, https://doi.org/ 10.1074/jbc.M112.344911

Shah, D.J., R.K. Sachs & D.J. Wilson (2012), "Radiation-induced cancer: A modern view." Br. J. Radiol. 85(1020):1166–1173. doi:10.1259/bjr/25026140.

Shelke, S. & B. Das (2015), "Dose response and adaptive response of non- homologous end joining repair genes and proteins in resting human peripheral blood mononuclear cells exposed to γ radiation.", (December 2014):365–379. doi:10.1093/mutage/geu081.

Sidjanin, D., S. Zigman and J. Reddan (1993), “DNA damage and repair in rabbitlens epithelial cells following UVA radiation”, Current eye research, Vol. 12/9, Informa UK Ltd, Oxford, https://doi.org/10.3109/02713689309020382

Smith, J. et al. (2003), "Impact of DNA ligase IV on the delity of end joining in human cells.", Nucleic Acids Research. 31(8):2157-2167.doi:10.1093/nar/gkg317.

Smith, T.A. et al. (2017), "Radioprotective agents to prevent cellular damage due to ionizing radiation." Journal of Translational Medicine.15(1).doi:10.1186/s12967-017-1338-x.

Stewart, F. A. et al. (2012), "ICRP publication 118: ICRP statement on tissue reactions and early and late effects of radiation in normal tissues and organs – threshold doses for tissue reactions in a radiation protection context", Annals of the ICRP, Vol, 41/1-2, Elsevier Ltd, London, https://doi.org/10.1016/j.icrp.2012.02.001

Sudprasert, W., P. Navasumrit & M. Ruchirawat (2006), "Effects of low-dose γ radiation on DNA damage, chromosomal aberration and expression of repair genes in human blood cells.", Int. J. Hyg. Envrion. Health, 209:503–511. doi:10.1016/j.ijheh.2006.06.004.

Sutherland, B.M. et al. (2000), "Clustered DNA damages induced in isolated DNA and in human cells by low doses of ionizing radiation.", J. of Rad. Res. 43 Suppl(S):S149-52. doi: 10.1269/jrr.43.S149

Sylvester, C. B. et al. (2018), "Radiation-Induced Cardiovascular Disease: Mechanisms and Importance of Linear Energy Transfer", Frontiers in cardiovascular medicine, Vol. 5, Frontiers, https://doi.org/10.3389/fcvm.2018.00005

Terato, H. & H. Ide (2005), "Clustered DNA damage induced by heavy ion particles.", Biol. Sci. Sp. 18(4):206–215. doi:10.2187/bss.18.206.

Ungvari, Z. et al. (2013), "Ionizing radiation promotes the acquisition of a senescence-associated secretory phenotype and impairs angiogenic capacity in cerebromicrovascular endothelial cells: role of increased DNA damage and decreased DNA repair capacity in microvascular radiosensitivity", The journals of gerontology. Series A, Biological sciences and medical sciences, Vol. 68/12, Oxford University Press, Oxford, https://doi.org/10.1093/gerona/glt057

Valentin, J.D.J (1998), "Chapter 1. Ann ICRP.", 28(4):5–7. doi:10.1016/S0146-6453(00)00002-6. http://www.ncbi.nlm.nih.gov/pubmed/10882804.

Venkatesh, P. et al. (2016), "Effect of chromatin structure on the extent and distribution of DNA double strand breaks produced by ionizing radiation; comparative study of hESC and differentiated cells lines.", Int J. Mol. Sci. 17(1). doi:10.3390/ijms17010058.

Wang, et al. (2021), "Ionizing Radiation-Induced Brain Cell Aging and the Potential Underlying Molecular Mechanisms.", Cells. 10(12):3570. doi: 10.3390/cells10123570

Ward, J. F. (1988), "DNA Damage Produced by Ionizing Radiation in Mammalian Cells: Identities, Mechanisms of Formation, and Reparability.", Prog. Nucleic Acid Res. Mol. Biol. 35(C):95–125. doi:10.1016/S0079-6603(08)60611-X.

Wolf, N. et al. (2008), "Radiation cataracts: Mechanisms involved in their long delayed occurrence but then rapid progression", Molecular vision, Vol. 14/34-35, Molecular Vision, Atlanta, pp. 274-285

Wu, L.J. et al. (1999), "Targeted cytoplasmic irradiation with alpha particles induces mutations in mammalian cells.", Proc. Natl. Acad. Sci. 96(9):4959–4964. doi:10.1073/pnas.96.9.4959.

Yamaguchi, H. et al. (2005), "Estimation of Yields of OH Radicals in Water Irradiated by Ionizing Radiation.", J. of Rad. Res. 46(3):333-41. doi: 10.1269/jrr.46.333.

Zhang, L. et al. (2017), "The inhibitory effect of minocycline on radiation-induced neuronal apoptosis via AMPKα1 signaling-mediated autophagy.", Sci Rep.7(1):16373. doi: 10.1038/s41598-017-16693-8.

Relationship: 2811: Oxidative Stress leads to Increase, DNA strand breaks

AOPs Referencing Relationship

AOP Name	Adjacency	Weight of Evidence	Quantitative Understanding
Deposition of energy leading to occurrence of cataracts	adjacent	Moderate	Low
Deposition of Energy Leading to Learning and Memory Impairment	adjacent	Moderate	Moderate
Deposition of energy leads to vascular remodeling	adjacent	High	Moderate

Evidence Supporting Applicability of this Relationship

Taxonomic Applicability

Term	Scientific Term	Evidence	Links
human	Homo sapiens	Low	NCBI
rat	Rattus norvegicus	Low	NCBI
rabbit	Oryctolagus cuniculus	Low	NCBI
bovine	Bos taurus	Low	NCBI
mouse	Mus musculus	Low	NCBI

Life Stage Applicability

Life Stage	Evidence
Adult	Low

Life Stage	Evidence
Not Otherwise Specified	Low

Sex Applicability

Sex	Evidence
Unspecific	Low
Male	Low

This KER is plausible in all life stages, sexes, and organisms with DNA. The evidence is from human, rodent, rabbit and bovine in vitro studies that do not specify the sex, as well as an adult rat in vivo study.

Key Event Relationship Description

Oxidative stress is an event that involves both a reduction in free radical scavengers and enzymes, and an increase in free radicals (Brennan et al., 2012). Oxidative stress needs to be maintained within an organism to avoid an excess of damage to biological structures, such as DNA. A redox homeostasis between the radicals and the scavengers is necessary. Between reactive oxygen species (ROS) and reactive nitrogen species (RNS), collectively known as RONS, ROS is particularly significant to oxidative damage and disease states. Radicals such as singlet oxygen and hydroxyl radical are highly unstable and will react with molecules near their generation point, while radicals such as H_2O_2 are more stable and membrane permeable, meaning they can travel further to find electrons (Spector, 1990). Since DNA is mainly found in nucleus, ROS needs to reach the nucleus to induce breaks. Hydroxyl radicals, in addition to being highly reactive, are capable of causing DNA damage (Halliwell et al., 2021; Engwa et al., 2020). The regulation of these radicals is achieved by the antioxidant defense response (ADR), which includes enzymatic and non-enzymatic processes. The ADR is recruited to manage RONS levels, with antioxidants such as superoxide dismutase (SOD) functioning as the first line of defense (Engwa et al., 2020). These antioxidants act as scavengers to oxidants, reacting with them before reaching other structures within the cell such as DNA strands (Cabrera et al., 2011; Engwa et al., 2020). The backbone of DNA can fragment upon sustained exposure to ROS (Uwineza et al., 2019; Cannan et al., 2016). Due to low oxidation potentials, adenine and guanine are the DNA bases more prone to oxidation, with oxidation potentials (normal hydrogen electrode) at pH 7 of 1.3 eV and 1.42 eV compared to the 1.6 eV and 1.7 eV of cytosine and thymine (Fong, 2016; Halliwell et al., 2021; Poetsch, 2020). In fact, certain radicals even target guanine in a selective fashion, including carbonate anion radical ($CO_3^{\bullet-}$) and singlet oxygen ($^1O_2$) (Halliwell et al., 2021).

Evidence Supporting this KER

Overall Weight of Evidence: Moderate

Biological Plausibility

The biological plausibility of the relationship between increased oxidative stress leading to increased DNA double strand breaks (DSBs) is highly supported by the literature. Evidence was collected from studies conducted using in vitro lens epithelial cell models and derived from humans, bovine and germ line cells (Spector, 1990; Stohs, 1995; Aitken et al., 2001; Spector, 1995). As this evidence is derived from studies using a human cell model it limits the ability to compare between different taxonomies (Ahmadi et al., 2022; Cencer et al., 2018; Liu et al., 2013; Meng et al., 2021; Smith et al., 2015; Zhou et al., 2016). Other evidence comes from human-derived and rodent models of neuronal and endothelial cells (Cervelli et al., 2014; El-Missiry et al., 2018; Huang et al., 2021; Sakai et al., 2017; Ungvari et al., 2013; Zhang et al., 2017).

ROS that are generated specifically as a result of radiation are highly localized, increasing the likelihood of clustered regions of damage. Naturally generated ROS are more widespread and as a result less capable of generating clusters of damage. ROS will act on DNA bases to oxidize or delete them from the sequence, which create nicks on the strand (Cannan et al., 2016). This damage can occur to any DNA base but bases such as guanine and adenine are most vulnerable due to their low oxidation potentials (Fong, 2016). The mechanism through which the strand break occurs is a result of base excision repair (BER) happening at multiple sites that are too close together, resulting in the spontaneous conversion to DSBs prior to completion of repair. ROS damage to bases clustered together means that multiple sites of BER are happening very close together and while the strand may be able to support the damaged area for one repair, concurrent repairs make surrounding areas more fragile and the strand breaks at the nick sites are under added strain (Cannan et al., 2016). Endogenous damage to DNA as a result of radicals appears over time and mainly as isolated lesions, a pattern understood to be due to the diffusion of the radicals resulting in homogenous distribution patterns. This differs from the specific situations where radiation acts as the stressor to increase oxidative stress, as the radiation track will be highly localized and form radicals within that hit space. This leads to non-homologous lesions and clustered damage to the DNA (Ward et al., 1985).

Empirical Evidence

This relationship is well supported through empirical evidence from studies using stressors such as H_2O_2, photons, γ- and X-ray, which cause an increase in markers of oxidative stress such as ROS-generating enzymes (lactate dehydrogenase, LDH), and a decrease in free radical scavengers, resulting in DNA strand fragmentation. These studies include both in vivo and in vitro human lens epithelial cells (LECs), mouse, rat and rabbit models, including neuronal cells lines and endothelial cells (Ahmadi et al., 2022; Cencer et al., 2018; Cervelli et al., 2014; El-Missiry et al., 2018; Huang et al., 2021; Liu et al., 2013; Meng et al., 2021; Spector et al., 1997; Ungvari et al., 2013; Zhang et al., 2017; Zhou et al., 2016; Sakai et al., 2017).

Dose/Incidence Concordance

There is high evidence to support a dose concordance between oxidative stress and DNA strand breaks. One in vitro study demonstrated that when ROS levels in LECs are 10% above control following 0.5 Gy gamma ray exposure, DNA strand breaks increased 15-20% above control (Ahmadi et al., 2021). Another study with ultraviolet (UV)B radiation demonstrated higher ROS levels after exposure to 0.14 J/cm^2 on in vitro LECs as compared to a lower dose exposure (0.014 J/cm^2) for the same time. This corresponded to DNA strand break levels also increasing following high dose rate exposure, but not with the low dose exposure (Cencer et al., 2018).

A 30 µM of H_2O_2 treatment of in vitro LECs is associated with a 1.4x increase in lactate dehydrogenase (LDH) and 55% more DNA strand breaks (Liu et al., 2013; Smith et al., 2015). Following exposure of in vitro LECs to 50 µM H_2O_2, increased ROS levels, 4x for LDH, and decreased antioxidant levels, 2x control for GSH-Px and SOD, are associated with a 3x increase in γ-H2AX, a marker of DNA strand breaks (Meng et al., 2021). SOD and GSH decreased by 2-fold following 100 µM H_2O_2 exposure on LECs with an in vitro model (Zhou et al., 2016). At 125 µM H_2O_2 intact DNA can be reduced to near 1% of pre-treatment levels for in vitro LECs (Spector et al., 1997). Following 400 µM H_2O_2 LDH increased to 1200% of control in neuroblastoma cells (Feng et al., 2016) and DNA strand breaks increased to over 150% of control in in vitro LECs (Li et al., 1998).

Exposure of in vitro mouse hippocampal neuronal cells (HT22 cell line) to 10 Gy of X-irradiation resulted in a 5x increase in ROS generation and 3x increase in γ-H2AX (Huang et al., 2021). Another study exposed the same cell line to 8 and 12 Gy of X-irradiation and found a ~2x increase in ROS at 8 Gy and a 4.4x and 3.2x increase in

phosphorylation of ataxia telangiectasia mutated (ATM) and γ-H2AX, respectively, 30 minutes after 12 Gy (Zhang et al., 2017). A separate study exposed adult male rats to 4 Gy of γ-irradiation and found 2x increase in 4-hydroxy-2-nonenal (4-HNE) (lipid peroxidation marker) and 3x increase in protein carbonylation. Glutathione reductase decreased by approximately 5x, whereas glutathione and glutathione peroxidase levels decreased by approximately 3x each. Tail DNA %, tail length and tail moment (DNA strand break parameters) increased by approximately 2x, 3x and 6x, respectively (El-Missiry et al., 2018).

Endothelial cells exposed to irradiation also demonstrated the relation between oxidative stress and DNA strand breaks. Rat cerebromicrovascular endothelial cells (CMVECs) exposed to 8 Gy ^{137}Cs gamma rays showed increased cellular peroxide production and mitochondrial oxidative stress. Tail DNA content indicating DNA damage was also increased from 0 to 45% (Ungvari et al., 2013). Human umbilical vein endothelial cells (HUVECs) were irradiated with single (0.125, 0.25, 0.5 Gy), or fractionated (2 × 0.125 Gy, 2 × 0.250 Gy) doses of X-rays. Intracellular ROS production increased in a dose-dependent manner following 0.125, 0.25, 0.5 Gy, and γ-H2AX foci positive cells were observed at all doses (Cervelli et al., 2014). Human aortic endothelial cells (HAECs) exposed to 100μM H_2O_2 showed 3.7-fold increase in intracellular ROS and a 3.4- and 4.7-fold increase in γ-H2AX and p-ATM, respectively (Sakai et al., 2017).

Time Concordance

There is low evidence to support a time concordance between oxidative stress to strand breaks on DNA. Non-protein-thiol levels, an antioxidant, in in vitro LECs decreased to near zero by 30 min post-exposure to 300 μM H_2O_2, before recovering to 70% of control by 120 min. At 60 min post-exposure to 125 μM H_2O_2 there was a start to a divergence from control level DNA fragmentation, one that increased logarithmically, with the treated group having a 14~18% reduction in intact DNA by 9 h post-exposure (Yang et al., 1998). Time response information is difficult to monitor for DNA strand breaks because repair will occur, reducing the number of breaks over time. At 0 minutes post in vitro exposure to 40 μM H_2O_2 LECs had ~145% of control level DNA strand breaks but that number dropped to ~105% by 30 minutes post-exposure (Li et al., 1998).

Essentiality

Oxidative stress has been found to increase levels of DNA strand breaks above background levels (Li et al., 1998; Liu et al., 2013; Cencer et al., 2018; Ahmadi et al., 2022; El-Missiry et al., 2018; Huang et al., 2021; Cervelli et al., 2017; Sakai et al., 2017). It has been shown that inhibition of oxidative stress leads to a reduction in DNA strand breaks. Sulforaphane (SFN) is an isothiocyanate, which provides chemical protection against ROS by activating the release of enzymatic scavengers. When SFN was added to in vitro LECs exposed to 30 μM H_2O_2, LDH decreased to near unexposed cell levels from the 1.4x control level without SFN. This LDH drop was associated with reducing the levels of DNA strand breaks induced by oxidative stress almost 3-fold as compared to cells without SFN (Liu et al., 2013). In another study, intact DNA levels were returned to control when treated with μPx-11 (peroxidase that breaks down H_2O_2), following exposure to 125 μM H_2O_2. This was a near 100% recovery compared to the drop seen in LECs that did not contain μPx-11 (Spector et al., 1997).

Within the brain of Wistar rats, epigallocatechin-3-gallate (EGCG) ameliorated radiation-induced increases in lipid peroxidation and protein carbonylation, as well as decreases in glutathione (GSH), glutathione peroxidase (GPx) and glutathione reductase (GR) and reverted the levels back to those similar to controls. DNA strand break parameters also returned to those similar to controls after treatment with EGCG (El-Missiry et al., 2018). Similar effects were also shown in another study using treatment mesenchymal stem cell-conditioned medium in mouse hippocampal cells exposed to 10 Gy of X-irradiation (Huang et al., 2021).

HUVECs pretreated with the antioxidant mixture RiduROS blunted ROS generation in a concentration-dependent manner by 65% ± 5.6% and 98% ± 2%, at 0.1 and 1 μg/mL, respectively, compared with cells irradiated without pretreatment. Low-dose irradiation also increased DSB-induced γ-H2AX foci compared with control cells and 24 h of RiduROS pretreatment reduced the γ-H2AX foci number by 41% (Cervelli et al., 2017). Additionally, HAECs treated with eicosapentaenoic acid (EPA) and docosahexaenoic acid (DHA) found significantly reduced intracellular ROS at 100μM, as well as reduced γ-H2AX foci formation by 47% and 48% following EPA and DHA treatment respectively. (Sakai et al., 2017).

Uncertainties and Inconsistencies

N/A

Quantitative Understanding of the Linkage

The following tables provide representative examples of the relationship, unless otherwise indicated, all data is significantly significant.

Dose Concordance

Reference	Experiment Description	Result
Cencer et al., 2018	In vitro, human LECs exposed to UVB and tested for 120 min post exposure with fluorescent probes to detect ROS production and mitochondrial superoxide, and tetramethylrhodamine-dUTP (TMR) red assay to detect strand breaks.	Both ROS and DNA strand breaks were increased by both 0.014 J/cm^2 and 0.14 J/cm^2 UVB radiation. At 0.014 J/cm^2, cellular ROS increased a maximum of 15 fluorescence units above the control at 5 minutes post-UVB, while DNA strand breaks increased about 115 fluorescence units above the control at this time. At 0.14 J/cm^2, cellular ROS increased a maximum of about 35 fluorescence units above the control at 90 minutes post-UVB, while mitochondrial superoxide increased about 30 fluorescence units above the control and DNA strand breaks increased about 125 fluorescence units above the control at this time.
Ahmadi et al., 2021	In vitro, human LECs exposed to 0.065-0.3 Gy/min gamma radiation, with dihydroethdium (DHE) fluorescent probes to measure ROS levels and comet assay to measure strand breaks.	Human LECs exposed in vitro to 0.1 - 0.5 Gy gamma rays showed a gradual increase in ROS levels and a corresponding gradual increase in DNA in the tail from the comet assay (indicative of increased DNA strand breaks) with the maximum dose displaying a 10% increase in ROS levels and a 17% increase in DNA strand damage.
Li et al., 1998	In vitro, bovine LECs were exposed to 40 and 400 μM H_2O_2 with an alkaline unwinding assay to determine strand break levels.	Immediately after LECs were exposed to 40 μM and 400 μM H_2O_2, there were ~145% and ~150% DNA strand breaks compared to the unexposed control level, respectively. The amounts of DNA strand breaks in cells exposed to both concentrations were reduced to ~105% of the unexposed control level after 30 mins. After 400 μM H_2O_2, oxidative stress as measured by LDH was 1200% of control in neuroblastoma cells.
Spector et	In vitro, rat LECs exposed to 100 and 125 μM H_2O_2 with alkaline elution assay to determine single strand break	Exposure to 125 μM of H_2O_2 to lens epithelial cells resulted in reduction of intact DNA to near

al., 1997	level.	1% by 9 hr post-exposure. Exposure to 100 µM H_2O_2 reduced SOD and GSH levels by 2-fold.
El-Missiry et al., 2018	In vivo, albino Wistar rats were exposed to 4 Gy of γ radiation (^{137}Cs source) at 0.695 rad/s. Kits were used to measure 4-HNE (secondary product of lipid peroxidation) and protein carbonyl group levels as markers of oxidative stress. Antioxidants including GSH, GPx and GR were also assessed. The comet assay was used to analyze DNA strand breaks by visualizing DNA tail %, tail length and tail moment.	4-HNE and protein carbonyl levels increased by approximately 2- and 3-fold after radiation exposure. GSH and GPx levels decreased by approximately 3-fold each, whereas GR levels decreased by approximately 5-fold. Tail DNA %, tail length and tail moment increased by approximately 2-, 3- and 6-fold after exposure to 4 Gy.
Ungvari et al., 2013	In vitro. CMVECs and rat hippocampal neurons were irradiated with 2-8 Gy ^{137}Cs gamma rays. 5(and 6)-chloromethyl-2′,7′-dichlorodihydrofluorescein diacetate acetyl ester (CM-H2DCFDA) staining, and flow cytometry were used to measure ROS production. DNA damage was quantified by measuring the tail DNA content (as a percentage of total DNA) using the Comet Assay-IV software.	Day 1 post-irradiation showed increased cellular peroxide production and increased mitochondrial oxidative stress in CMVECs in a dose-dependent manner, increasing a maximum of ~3-fold at 8 Gy. Tail DNA content also increased in a dose-dependent manner with an approximate increase from 0 to 45% at 8 Gy.
Huang et al., 2021	In vitro, HT22 cells (mouse hippocampal neuronal cell line) were exposed to 10 Gy of X-irradiation at 6 Gy/min. ROS levels were measured using H2-DCFDA staining and fluorescence microscope analysis, whereas western blotting was used to detect γ-H2AX.	At 10 Gy, intracellular ROS generation increased by 5-fold and γ-H2AX increased by 3-fold.
Zhang et al., 2017	In vitro. HT22 cells were exposed to 8 and 12 Gy X-rays. Relative intracellular ROS levels were determined by DCFDA. p-ATM, γ-H2AX were measured with Western blot.	Following 8 Gy irradiation, intracellular ROS levels increased ~1.8-fold. Phosphorylation of ATM and γ-H2AX were increased 4.4-fold and 3.2-fold, respectively, 30 minutes after 12 Gy.
Cervelli et al., 2014	In vitro. HUVECs were irradiated with single doses (0.125, 0.25, 0.5 Gy), or fractionated doses (2 × 0.125 Gy, 2 × 0.250 Gy) of X-rays. Intracellular ROS generation was measured with a fluorescent dye, C-DCFDA, using a spectrofluorometer. Immunofluorescence microscopy was used to measure γ-H2AX foci.	Intracellular ROS production was significantly increased in a dose-dependent manner (1.6-, 2- and 2.8-fold at 0.125, 0.25, 0.5 Gy, respectively). When HUVECs were exposed to fractionated doses, no increase in ROS generation was observed, compared with respective single doses. 24h post-irradiation the percentage of foci-positive cells exposed to 0.125 Gy, 2 × 0.125 Gy, 0.250 Gy, 2 × 0.250 Gy and 0.5 Gy, was 1.68, 1.48, 3.53, 2.59, 8.74-fold over the control, respectively.
Sakai et al., 2017	In vitro. HAECs were exposed to 100uM H_2O_2. Intracellular ROS was measured by CM-H2DCFDA. DNA DSBs were detected by immunofluorescent analysis with γ-H2AX as a marker.	Intracellular ROS increased by ~3.7-fold p-ATM increased by ~4.7-fold. γ-H2AX increased by ~3.4-fold.

Incidence Concordance

Reference	Experiment Description	Result
Meng et al., 2021	In vitro, human LECs exposed to 50 µM H_2O_2 with DCFH-DA fluorescent probe to detect ROS levels and immunofluorescence and western blot assay to detect γ-H2AX.	50 µM H_2O_2 exposure to lens epithelial cells increased oxidative stress, with ROS measured by LDH, by 4-fold and decreased the level of antioxidants by 2-fold as measured by SOD and GSH-PX. This resulted in 3-fold increase in γ-H2AX.
Smith et al., 2015	In vitro, human LECs exposed to 30 µM H_2O_2 with alkaline comet assay to determine amount of strand breaks.	Treatment of lens epithelial cells to 30 µM H_2O_2 induced DNA strand breaks by 55% at 0.5 hr after exposure and increased the level of LDH by ~1.4 fold at 24 hr post-exposure.
Liu et al. 2013	In vitro, human LECs exposed to 30 µM H_2O_2 with alkaline comet assay determination of strand breaks.	LDH increased by ~1.4 fold at 24 hr post-exposure, with a 5x increase from control levels in DNA strand breaks.

Time Concordance

Reference	Experiment Description	Result
Yang et al., 1998	In vitro, rabbit LECs exposed to H_2O_2 with TCA addition and thiol assay to determine non-protein thiol (NP-SH) level and alkaline elusion assay to determine strand breaks.	In rabbit LECs exposed in vitro to 125 µM H_2O_2, non-protein thiol levels decreased to <5% control (indicates oxidative stress) 30 min post-irradiation, and % DNA retained using alkaline elution decreased by 1.6 log (indicates increased DNA fragmentation) within the next 8.5 h.

Known modulating factors

There is limited evidence demonstrating this relationship across different life stages/ages or sexes (Cencer et al., 2018; Li et al., 1998).

Modulating Factors	MF Details	Effects on the KER	References
Age	Reduced antioxidant capacities have been linked to aged lenses (in humans >30 years old). The development of a chemical barrier between the cortex and the nucleus is partially responsible, as it prevents GSH from protecting aged lens cells from ROS.	Prevention of RONS-mediated damage is primarily achieved by antioxidants, so a lowered capacity would likely lead to reduced damage mitigation abilities. 78% of lens over 30 had a low level of GSH in the center compared to 14% of lens under 30. Lens epithelial cells have an associated 3-fold increase in γ-H2AX (marker of DNA damage) when GSH-PX decreases by 2-fold.	Taylor & Davies, 1987; Cabrera & Chihuailaf, 2011; Quinlan & Hogg, 2018; Sweeney & Truscott, 1998; Meng & Fang, 2021
	ROS-scavengers are essential components of	Isothiocyanates, such as sulforaphane (SFN), activate the release of more	

Free radical scavengers	the body's natural defense against oxidative damage. Increased ROS production leads to increased incidence of electron donation by scavengers, thus reducing the overall level of free radical scavengers available to deal with ROS.	isothiocyanates, such as sulforaphane (SFN), activate the release of more enzymatic scavengers. When SFN was added to in vitro LECs, LDH decreased to near unexposed cell levels and was associated with 3.3x less DNA strand breaks compared to the non-SFN cells following stressor exposure. Epigallocatechin-3-gallate (EGCG) also has antioxidant properties and was shown to alleviate radiation-induced increases in oxidative stress and DNA strand breaks within rat hippocampi.	Taylor et al., 1987; Cabrera et al., 2011; Liu et al., 2013; El-Missiry et al., 2018
Media	Mesenchymal stem cell-conditioned medium (MSC-CM), which has self-renewal, differential and proliferation capacities.	MSC-CM treatment has also been shown to improve ROS levels and decrease radiation-induced DNA strand breaks within mouse hippocampal neuronal cells.	Huang et al., 2021

Known Feedforward/Feedback loops influencing this KER

N/A

References

Ahmadi, M. et al. (2021), "Early Responses to Low-Dose Ionizing Radiation in Cellular Lens Epithelial Models", Radiation Research, Vol.197, Radiation Research Society, Indianapolis, https://doi.org/10.1667/RADE-20-00284.1.

Aitken, R.J. and C. Krausz. (2001), "Oxidative stress, DNA damage and the Y chromosome", Reproduction, Vol.122/2001, Bioscientifica, Bristol, https://doi.org/10.1530/rep.0.1220497.

Annesley, S.J. and P.R. Fisher. (2019), "Mitochondria in Health and Disease", Cells, Vol.8/7, MDPI, Basel, https://doi.org/10.3390/cells8070680.

Brennan, L., R. McGreal and M. Kantorow. (2012), "Oxidative stress defense and repair systems of the ocular lens", Frontiers in Bioscience – Elite, Vol.4/E(1), Frontiers in Bioscience, Singapore, https://doi.org/10.2741/365.

Britton, S. et al. (2020), "ATM antagonizes NHEJ proteins assembly and DNA-ends synapsis at single-ended DNA double strand breaks", Nucleic Acids Research, Vol.48/17, Oxford University Press, Oxford, https://doi.org/10.1093/nar/gkaa723.

Cabrera, M. and R. Chihuailaf. (2011), "Antioxidants and the integrity of ocular tissues", Veterinary Medicine International, Vol.2011, Hindawi Limited, London, https://doi.org/10.4061/2011/905153.

Cannan, W. and D. Pederson. (2016), "Mechanisms and consequences of double-strand DNA break formation in chromatin", Journal of Cell Physiology, Vol.231/1, Wiley, Hoboken, https://doi.org/10.1002/jcp.25048.

Cencer, C. et al. (2018), "PARP-1/PAR Activity in Cultured Human Lens Epithelial Cells Exposed to Two Levels of UVB Light", Photochemistry and Photobiology, Vol.94/1, Wiley-Blackwell, Hoboken, https://doi.org/10.1111/php.12814.

Cervelli, T.et al. (2014), "Effects of single and fractionated low-dose irradiation on vascular endothelial cells", Atherosclerosis, Vol.235/2, Elsevier, Amsterdam, https://doi.org/10.1016/j.atherosclerosis.2014.05.932.

Cervelli, T. et al. (2017), "A New Natural Antioxidant Mixture Protects against Oxidative and DNA Damage in Endothelial Cell Exposed to Low-Dose Irradiation", Oxidative medicine and cellular longevity, Vol. 2017, Hindawi, London, https://doi.org/10.1155/2017/9085947.

Climent, M. et al. (2020), "MicroRNA and ROS Crosstalk in Cardiac and Pulmonary Diseases", International Journal of Molecular Science, Vol.21/12, MDPI, Basel, https://doi.org/10.3390/ijms21124370.

Dahm-Daphie, J., C. Sass, and W. Alberti. (2000), "Comparison of biological effects of DNA damage induced by ionizing radiation and hydrogen peroxide in CHO cells", International Journal Radiation Biology, Vol.76/1, Informa, London, https://doi.org/10.1080/095530000139023.

El-Missiry, M. A. et al. (2018), "Neuroprotective effect of epigallocatechin-3-gallate (EGCG) on radiation-induced damage and apoptosis in the rat hippocampus", International Journal of Radiation Biology, Vol. 94/9, https://doi.org/10.1080/09553002.2018.1492755.

Engwa, G.A., F.N. Nweke and B.N. Nkeh-Chungag. (2020), "Free Radicals, Oxidative Stress-Related Diseases and Antioxidant Supplementation", Alternative therapies in health and medicine, Vol.28/1, InnoVision Health Media, Eagan, pp.114-128.

Feng, C. et al. (2016), "Lycopene protects human SH-SY5Y neuroblastoma cells against hydrogen peroxide-induced death via inhibition of oxidative stress and mitochondria-associated apoptotic pathways", Molecular Medicine Reports, Vol.13/5, Spandidos Publications, Athens, https://doi.org/10.3892/mmr.2016.5056.

Fong, C.W. (2016), "Platinum anti-cancer drugs: Free radical mechanism of Pt-DNA adduct formation and anti-neoplastic effect", Free Radical Biology and Medicine, Vol.95/June 2016, Elsevier, Amsterdam, https://doi.org/10.1016/j.freeradbiomed.2016.03.006.

Halliwell, B. et al. (2021), "Hydroxyl radical is a significant player in oxidative DNA damage in vivo", Chemical Society Reviews, Vol.50, Royal Society of Chemistry, London, https://doi.org/10.1039/d1cs00044f.

Huang, Y. et al. (2021), "Mesenchymal Stem Cell-Conditioned Medium Protects Hippocampal Neurons From Radiation Damage by Suppressing Oxidative Stress and Apoptosis", Dose-Response, Vol. 19/1, https://doi.org/10.1177/1559325820984944.

Kay, J. et al. (2019), "Inflammation-induced DNA damage, mutations and cancer", DNA Repair, Vol.83, Elsevier, Amsterdam, https://doi.org/10.1016/j.dnarep.2019.102673.

Jeggo, P.A., V. Geuting and M. Löbrich. (2011), "The role of homologous recombination in radiation-induced double-strand break repair", Radiotherapy and Oncology, Vol.101/1, Elsevier, Amsterdam, https://doi.org/10.1016/j.radonc.2011.06.019.

Kurutas E. B. (2016), "The importance of antioxidants which play the role in cellular response against oxidative/nitrosative stress: current state", Nutrition journal, Vol.15/1, Biomed Central, London, https://doi.org/10.1186/s12937-016-0186-5.

Kruk, J., K. Kubasik-Kladna and H. Aboul-Enein. (2016), "The Role Oxidative Stress in the Pathogenesis of Eye Diseases: Current Status and a Dual Role of Physical Activity", Mini-Review in Medicinal Chemistry, Vol.16/3, Bentham Science Publishers, Sharjah, https://doi.org/10.2174/1389557516666151120114605.

Li, Y. et al. (1998), “Response of lens epithelial cells to hydrogen peroxide stress and the protective effect of caloric restriction”, Experimental Cell Research, Vol.239/2, Elsevier, Amsterdam, https://doi.org/10.1006/excr.1997.3870.

Liu, H. et al. (2013), “Sulforaphane can protect lens cells against oxidative stress: Implications for cataract prevention”, Investigative Ophthalmology and Visual Science, Vol.54/8, Association for Research in Vision and Ophthalmology, Rockville, https://doi.org/10.1167/iovs.13-11664.

Meng, K. and C. Fang. (2021), “Knockdown of Tripartite motif-containing 22 (TRIM22) relieved the apoptosis of lens epithelial cells by suppressing the expression of TNF receptor-associated factor 6 (TRAF6)”, Bioengineered, Vol.12/1, Taylor & Francis, Oxfordshire, https://doi.org/10.1080/21655979.2021.1980645.

Nishida, M. et al. (2005), “Ga12/13- and Reactive Oxygen Species-dependent Activation of c-Jun NH2-terminal Kinase and p38 Mitogen-activated Protein Kinase by Angiotensin Receptor Stimulation in Rat Neonatal Cardiomyocytes”, Journal of Biological Chemistry, Vol.280/18, American Society for Biochemistry and Molecular Biology, Rockville, https://doi.org/10.1074/jbc.M409710200.

Poetsch, A.R. (2020), “The genomics of oxidative DNA damage, repair, and resulting mutagenesis”, Computational and Structural Biotechnology Journal, Vol.18, Elsevier, Amsterdam, https://doi.org/10.1016/j.csbj.2019.12.013.

Quinlan, R.A., and P.J. Hogg. (2018), “γ-Crystallin redox–detox in the lens”, Journal of Biological Chemistry, Vol.293/46, American Society for Biochemistry and Molecular Biology, Rockville, https://doi.org/10.1074/jbc.H118.006240.

Sakai, C. et al. (2017), “Fish oil omega-3 polyunsaturated fatty acids attenuate oxidative stress-induced DNA damage in vascular endothelial cells”, PloS one, Vol.12/11, https://doi.org/10.1371/journal.pone.0187934.

Scully, R. and A. Xie. (2013), “Double strand break repair functions of histone H2AX”, Mutation Research, Vol.750/1-2, Elsevier, Amsterdam, https://doi.org/10.1016/j.mrfmmm.2013.07.007.

Smith, A. et al. (2015), “Ku80 counters oxidative stress-induced DNA damage and cataract formation in the human lens”, Investigative Ophthalmology and Visual Science, Vol.56/13, Association for Research in Vision and Ophthalmology, Rockville, https://doi.org/10.1167/iovs.15-18309.

Spector, A. et al. (1997), “Microperoxidases catalytically degrade reactive oxygen species and may be anti-cataract agents”, Experimental Eye Research, Vol.65/4, Academic Press Inc, Cambridge, https://doi.org/10.1006/exer.1997.0336.

Spector, A. et al. (1996), “Variation in cellular glutathione peroxidase activity in lens epithelial cells, transgenics and knockouts does not significantly change the response to H2O2 stress”, Experimental Eye Research, Vol.62/5, Academic Press Inc, Cambridge, https://doi.org/10.1006/exer.1996.0063.

Spector, A. (1995), “Oxidative stress-induced cataract: mechanism of action”, The FASEB Journal, Vol.9/12, Federation of American Societies for Experimental Biology, Bethesda, https://doi.org/10.1096/fasebj.9.12.7672510.

Spector, A. (1990), “Oxidation and Aspects of Ocular Pathology”, CLAO Journal, Vol.16/1, Lippincott, Williams and Wilkins Ltd, Philadelphia, S8-S10.

Stohs, S. (1995), “The role of free radicals in toxicity and disease”, Journal of Basic Clinical Physiology and Pharmacology, Vol.6/3-4, Walter de Gruyter GmbH, Berlin, https://doi.org/10.1515/jbcpp.1995.6.3-4.205.

Sweeney, M.H.J. and R.J.W. Truscott. (1998), “An Impediment to Glutathione Diffusion in Older Normal Human Lenses: a Possible Precondition for Nuclear Cataract”, Experimental Eye Research, Vol.67, Academic Press Inc, Cambridge, https://doi.org/10.1006/exer.1998.0549.

Taylor, A. and K. J. A. Davies (1987), “Protein oxidation and loss of protease activity may lead to cataract formation in the aged lens”, Free Radical Biology & Medicine, Vol. 3, Pergamon Journals Ltd, United States of America, pp. 371-377

Ungvari, Z. et al. (2013), "Ionizing Radiation Promotes the Acquisition of a Senescence-Associated Secretory Phenotype and Impairs Angiogenic Capacity in Cerebromicrovascular Endothelial Cells: Role of Increased DNA Damage and Decreased DNA Repair Capacity in Microvascular Radiosens", The Journals of Gerontology Series A: Biological Sciences and Medical Sciences, Vol. 68/12, https://doi.org/10.1093/gerona/glt057.

Uwineza, A. et al. (2019), “Cataractogenic load – A concept to study the contribution of ionizing radiation to accelerated aging in the eye lens”, Mutation Research - Reviews in Mutation Research, Vol.779, Elsevier, Amsterdam, https://doi.org/10.1016/j.mrrev.2019.02.004.

Ward, J.F., W.F. Blakely & E.I. Joner. (1985), “Mammalian Cells Are Not Killed by DNA Single-Strand Breaks Caused by Hydroxyl Radicals from Hydrogen Peroxide”, Radiation Research, Vol.103/3, Radiation Research Society, Indianapolis, hptts://doi.org/10.2307/3576760.

Wu, H. et al. (2021), “Lactate dehydrogenases amplify reactive oxygen species in cancer cells in response to oxidative stimuli”, Signal Transduction and Targeted Therapy, Vol.6/1, Nature Portfolio, Berlin, https://doi.org/10.1038/s41392-021-00595-3.

Yang, Y. et al. (1998), “The effect of catalase amplification on immortal lens epithelial cell lines”, Experimental Eye Research, Vol.67/6, Academic Press Inc, Cambridge, https://doi.org/10.1006/exer.1998.0560.

Yuan, J., R. Adamski and J. Chen. (2010), “Focus on histone variant H2AX: To be or not to be”, FEBS Letters, Vol.584/17, Wiley, Hoboken, https://doi.org/10.1016/j.febslet.2010.05.021.

Zhang, L. et al. (2017), "The inhibitory effect of minocycline on radiation-induced neuronal apoptosis via AMPKα1 signaling-mediated autophagy", Scientific Reports, Vol. 7/1, https://doi.org/10.1038/s41598-017-16693-8.

Zhou, Y. et al. (2016), “Protective Effect of Rutin Against H2O2-Induced Oxidative Stress and Apoptosis in Human Lens Epithelial Cells”, Current Eye Research, Vol.41/7, Taylor & Francis, Oxfordshire, https://doi.org/10.3109/02713683.2015.1082186.

Relationship: 2856: Increase, DNA strand breaks leads to Altered Signaling

AOPs Referencing Relationship

AOP Name	Adjacency	Weight of Evidence	Quantitative Understanding
Deposition of energy leads to vascular remodeling	adjacent	High	Moderate
Deposition of Energy Leading to Learning and Memory Impairment	adjacent	Moderate	Low

Evidence Supporting Applicability of this Relationship

Taxonomic Applicability

Term	Scientific Term	Evidence	Links
human	Homo sapiens	Low	NCBI
mouse	Mus musculus	Moderate	NCBI
rat	Rattus norvegicus	Moderate	NCBI

Life Stage Applicability

Life Stage	Evidence
Juvenile	Low
Adult	Moderate

Sex Applicability

Sex	Evidence
Male	Moderate
Female	Low

Evidence for this relationship is predominantly from studies using rat- and mouse-derived cells, with some in vivo evidence in mice and rats. There is in vivo evidence in male animals, but no in vivo studies specify the use of female animals. In vivo evidence is from adult models.

Key Event Relationship Description

DNA strand breaks can lead to altered signaling of various pathways through the DNA damage response. DNA strand breaks, which are a form of DNA damage, can induce ataxia telangiectasia mutated (ATM) and ATM/RAD3-related (ATR), two phosphoinositide 3-kinase (PI3K)-related serine/threonine kinases (PIKKs) (Abner and McKinnon, 2004; Lee and McKinnon, 2007; Nagane et al., 2021; Sylvester et al., 2018; Thadathil et al., 2019; Wang et al., 2020; Wang et al., 2017). Following DNA strand breaks, DNA damage response cellular signaling can phosphorylate downstream proteins and activate several transcription factors and pathways (Wang et al., 2017). Spontaneous DNA strand breaks from endogenous sources will induce signaling as a normal response to facilitate DNA repair. However, excessive DNA damage induced by a stressor will result in increased activation of these pathways and subsequent harmful downstream effects. Signaling pathways induced by DNA strand breaks include p53/p21 (Abner and McKinnon, 2004; Baselet et al., 2018; Lee and McKinnon, 2007; Nagane et al., 2021; Sylvester et al., 2018; Thadathil et al., 2019; Wang et al., 2020; Wang et al., 2017), caspase (Abner and McKinnon, 2004; Baselet et al., 2019; Wang et al., 2020; Wang et al., 2016) and mitogen-activated protein kinase (MAPK) family pathways (Ghahremani et al., 2002; Nagane et al., 2021).

Evidence Supporting this KER

Overall weight of evidence: Moderate

Biological Plausibility

There is strong evidence supporting the link between DNA strand breaks leading to altered signaling pathways. Single strand breaks (SSBs) or double strand breaks (DSBs) in DNA from both endogenous and exogenous sources can induce the DNA damage response, which can result in the induction of various signaling pathways (Baselet et al., 2019). DNA strand breaks are well known to lead to the activation of ATM and ATR as part of the normal DNA damage response (Abner and McKinnon, 2004; Baselet et al., 2019; Lee and McKinnon, 2007; Nagane et al., 2021; Sylvester et al., 2018; Thadathil et al., 2019; Wang et al., 2020; Wang et al., 2017; Wang et al., 2016). While ATM tends to be recruited to DSBs, ATR is recruited by many types of DNA damage including both DSBs and SSBs (Maréchal and Zou, 2013; Wang et al., 2017). Following a DNA DSB, the Mre11-Rad50-Nbs1 (MRN) complex senses and directly binds to the DNA ends at the site of the break, which subsequently activates ATM (Lee and McKinnon, 2007; Maréchal and Zou, 2013). Following a DNA SSB, resection of the damaged strand by apurinic/apyrimidinic endonuclease (APE)1/APE2 is followed by coating the single-stranded DNA with replication protein A (RPA), where the recruitment of the ATR-ATR interacting protein (ATRIP) complex and the activation of ATR occurs (Caldecott, 2022; Maréchal and Zou, 2013).

ATM and ATR can phosphorylate over 700 proteins (Nagane et al., 2021), and phosphorylation of key signaling proteins by

ATM/ATR will alter signaling in their respective pathways. High levels of DNA strand breaks induced by exogenous stressors will enhance ATM/ATR activation and subsequently further activate downstream signaling, leading to downstream consequences. The extracellular signal-regulated kinase (ERK), c-Jun N-terminal kinase (JNK) and p38 MAPK subfamily pathways can be phosphorylated and activated by ATM/ATR (Ghahremani et al., 2002; Nagane et al., 2021). Additionally, ATM/ATR can phosphorylate p53 on serine 15 to enhance the stability of p53, leading to activation of the p53 pathway and changes in the transcriptional activity of p53 (Abner and McKinnon, 2004; Baselet et al., 2019; Lee and McKinnon, 2007; Nagane et al., 2021; Sylvester et al., 2018; Thadathil et al., 2019; Wang et al., 2020; Wang et al., 2017; Wang et al., 2016). The apoptosis pathway downstream of p53 can also be activated by DNA strand breaks (Abner and McKinnon, 2004; Baselet et al., 2019; Lee and McKinnon, 2007; Thadathil et al., 2019; Wang et al., 2020).

Empirical Evidence

Evidence for this relationship was collected from studies using in vivo mouse and rat models as well as in vitro mouse-derived, rat-derived and human-derived cell models. The stressors used to support this relationship include ^{137}Cs gamma rays and X rays. Markers of DNA strand breaks in this KER include p53 binding protein 1 (53BP1), phosphorylation of H2AX (γ-H2AX), phosphorylation of ATR (p-ATR) and phosphorylation of ATM (p-ATM). Altered signaling was measured mostly by the protein expression of the p53/p21 and apoptosis pathways.

Dose Concordance

A few studies have indicated a dose concordance between the increase in DNA strand breaks and altered signaling pathways. X-ray irradiation of rat cortical neurons showed increased DNA damage markers, γ-H2AX, p-ATM and p-ATR and increased levels of signaling proteins, including p21, p-p53 and cleaved caspase 3 at both doses of 8 and 32 Gy (Sabirzhanov et al., 2020). ^{137}Cs gamma irradiated cerebromicrovascular endothelial cells (CMVECs) and rat hippocampal neurons showed increased DNA strand breaks, measured by comet assay, at 2-10 Gy, and increased caspase 3/7 activity at 2, 4 and 6 Gy (Ungvari et al., 2013).

Time Concordance

Many studies demonstrate that DNA strand breaks occur before altered signaling in a time course. Although both KEs can occur quickly, Gionchiglia et al. (2021) showed in mice that γ-H2AX and p53BP1 foci were increased as early as 15 minutes after 10 Gy of X-ray irradiation while cleaved caspase 3 did not increase until 30 minutes after irradiation. In HT22 hippocampal neurons irradiated with 12 Gy of X-rays, γ-H2AX and p-ATM were increased at 30 minutes post-irradiation while p53 was increased after 1 h and caspase 3 was increased after 48 h (Zhang et al., 2017). Similarly, rat cortical neurons irradiated with 8 Gy of X-rays showed increased p-ATM, γ-H2AX and p-ATR after 30 minutes, while p-p53, p21 and cleaved caspase 3 did not increase until 3 or 6 h post-irradiation (Sabirzhanov et al., 2020). Multiple studies using human- and rat-derived endothelial cells irradiated with 4 Gy of ^{137}Cs gamma rays show increased DNA strand breaks at 1 h post-irradiation, with altered signaling to p53 and p21 at 6 h and to caspase 3/7 at 18 h post-irradiation (Kim et al., 2014; Park et al., 2022; Ungvari et al., 2013). In a longer-term study irradiating human lung microvascular endothelial cells (HMVEC-L) with 15 Gy of X-rays, increased DNA strand breaks were observed at 14 days post-irradiation, while altered signaling in the p53 pathway was observed at 21 days post-irradiation (Lafargue et al., 2017).

Incidence concordance

A few studies have demonstrated an incidence concordance between DNA strand breaks and altered signaling at equivalent doses. Following X-ray irradiation of mice, DNA damage markers, γ-H2AX and p53BP1, increased by 10, 15 and 5-fold in different region of the brain, while cleaved caspase 3 signaling molecule increased by 1.4 and 2.6-fold (Gionchiglia et al., 2021). Gamma ray irradiation of Wistar rats showed a 6-fold increase in DNA damage marker compared to a 0.2-fold decrease in (B-cell lymphoma 2) Bcl-2 and a 2- to 4-fold increase in signaling proteins p53, Bcl-2-associated protein X (Bax) and caspase 3/8/9 (El-Missiry et al., 2018).

Essentiality

Some studies show that preventing an increase in DNA strand breaks will restore signaling. Treatment with mesenchymal stem cell-conditioned medium (MSC-CM) reduced γ-H2AX, decreased the levels of p53, Bax, cleaved caspase 3 and increased the levels of Bcl-2 in HT22 cells irradiated with 10 Gy of X-rays (Huang et al., 2021). The inhibition of microRNA (miR)-711 decreased levels of DNA damage markers, p-ATM, p-ATR and γ-H2AX, and decreased signaling molecules including p-p53, p21 and cleaved caspase 3 (Sabirzhanov et al., 2020).

Uncertainties and Inconsistencies

None identified

Quantitative Understanding of the Linkage

The tables below provide some representative examples of quantitative linkages between the two key events. All data that is represented is statistically significant unless otherwise indicated.

Response-response relationship

Dose Concordance

Reference	Experiment Description	Result
Sabirzhanov et al., 2020	*In vitro*. Rat cortical neurons were exposed to 2, 8 and 32 Gy X-rays. DNA damage was determined by γ-H2AX staining and western blot analysis of p-ATM and p-ATR. Altered signaling was determined by levels of p-p53, p21, cleaved caspase 3, measured by Western blot.	Irradiated primary cortical neurons showed increased γ-H2AX by 30-fold at both 8 and 32 Gy but not at 2 Gy. p-ATM was increased at all doses, increasing about 15-fold at 8 and 32 Gy. Signaling molecules including p-p53, p21, and cleaved caspase 3 were increased at all doses.
Ungvari et al., 2013	*In vitro*. CMVECs and rat hippocampal neurons were irradiated with ^{137}Cs gamma rays. DNA strand breaks were assessed with the comet assay. Caspase 3/7 activity was determined by an assay kit.	DNA damage increased at all doses (2-10 Gy). In the control, less than 5% of DNA was in the tail while by 6 Gy 35% of the DNA was in the tail in CMVECs and 25% was in the tail in neurons. In CMVECs, 2, 4, and 6 Gy increased caspase 3/7 activity 5- to 6-fold.

Incidence Concordance

Reference	Experiment Description	Result
El-Missiry et al., 2018	*In vivo*. Wistar rats were irradiated with 4 Gy of ^{137}Cs gamma rays (0.695 cGy/s). DNA damage was assessed with a comet assay. Multiple signaling proteins were assessed with assay kits.	The tail moment increased 6-fold while signaling proteins including p53, Bax, and caspases 3/8/9 increased 2- to 4-fold, and Bcl-2 decreased 0.2-fold.
Gionchiglia et al., 2021	*In vivo*. CD1 and B6/129 mice were irradiated with 10 Gy of X-rays. γ-H2AX and 53BP1 foci were quantified with immunofluorescence. Cleaved caspase 3 positive cells were measured with immunofluorescence.	γ-H2AX and p53BP1 foci increased about 10-fold in the forebrain and cerebral cortex, about 15-fold in the hippocampus and about 5-fold in the subventricular zone (SVZ)/ rostral migratory stream (RMS)/ olfactory bulb (OB). Cleaved caspase 3 increased 1.4-fold in the cerebral cortex and hippocampus and 2.6-fold in the SVZ/RMS/OB.

Time-scale

Time Concordance

Reference	Experiment Description	Result
Zhang et al., 2017	*In vitro*. HT22 cells were irradiated with 12 Gy of X-rays (1.16 Gy/min). p-ATM, γ-H2AX, cleaved caspase 3 and p53 were measured with Western blot.	p-ATM and γ-H2AX were increased 4.4-fold and 3.2-fold, respectively, 30 minutes after 12 Gy. p53 was increased 4.6-fold at 1 h post-irradiation. A 9-fold increase in cleaved caspase 3 was observed 48 h post-irradiation.
Gionchiglia et al., 2021	*In vivo*. CD1 and B6/129 mice were irradiated with 10 Gy of X-rays. γ-H2AX and 53BP1 foci were quantified with immunofluorescence in neurons. Cleaved caspase 3 positive neurons were measured with immunofluorescence.	At both 15 and 30 minutes post-irradiation, γ-H2AX and p53BP1 foci increased. However, cleaved caspase 3 increased at 30 minutes but not at 15 minutes.
Sabirzhanov et al., 2020	*In vitro*. Rat cortical neurons were exposed to 2, 8 and 32 Gy X-rays. DNA damage was determined by γ-H2AX staining and western blot analysis of p-ATM and p-ATR. Altered signaling was determined by levels of p-p53, p21, cleaved caspase 3, measured by Western blot.	DNA damage occurred as early as 30 min post 8 Gy irradiation, indicated by increased p-ATM, γ-H2AX and p-ATR. Signaling molecules p-p53, p21 and cleaved caspase 3 increased at 3 or 6h post-irradiation.
Park et al., 2022	*In vitro*. Human aortic endothelial cells (HAECs) were irradiated with 4 Gy of ^{137}Cs gamma rays (3.5 Gy/min). γ-H2AX was measured with western blot. p-ATM and 53BP1 were determined with immunofluorescence. p-p53 and p21 were measured with Western blot.	γ-H2AX, p-ATM, and 53BP1 were shown increased at 1 h post-irradiation, while p-p53 and p21 were increased at 6 h post-irradiation.
Kim et al., 2014	*In vitro*. Human umbilical vein endothelial cells (HUVECs) were irradiated with 4 Gy ^{137}Cs gamma rays. DNA damage was determined by γ-H2AX. p21 and p53 were measured by Western blot.	γ-H2AX foci greatly increased at 1 and 6 h post-irradiation, while p-p53 and p21 were increased at 6 h post-irradiation.
[illegible]	*In vitro*. CMVECs and rat hippocampal neurons were	DNA damage in neurons and CMVECs increased at 1

Ungvari et al., 2013	irradiated with 2-6 Gy of ^{137}Cs gamma rays. DNA strand breaks were assessed with the comment assay. Caspase 3/7 activity was determined by an assay kit.	h post-irradiation, while caspase 3/7 activity increased the greatest at 18 h post-irradiation in CMVECs.
Lafargue et al., 2017	*In vitro*. HMVEC-L were irradiated with 15 Gy of X-rays. γ-H2AX foci were assessed with immunofluorescence. p-ATM and ATM were assessed with Western blot. Signaling proteins including p53, p21 and p16 were assessed with western blot.	Without irradiation, most cells had 0 or 1 γ-H2AX foci, while 14 days after 15 Gy, most cells had 2-6 γ-H2AX foci. The ratio of p-ATM/ATM was also increased 14 days after 15 Gy. p53, p21, and p16 were all increased at 21 days after 15 Gy.

Known modulating factors

Modulating factor	Details	Effects on the KER	References
Media	MSC-CM	Treatment decreased γ-H2AX, p53, the Bax/Bcl-2 ratio and cleaved caspase 3 in irradiated neurons.	Huang et al., 2021
Genetic	miR-711	miR-711 inhibition reduced the DNA damage response including p-ATM, p-ATR, and γ-H2AX. It also decreased signaling molecules including p-p53, p21, and cleaved caspase 3.	Sabirzhanov et al., 2020
Drug	Minocycline	Treatment with minocycline in irradiated neurons reduced the DNA damage response through reduced γ-H2AX and p-ATM. Caspase 3 was also inhibited by minocycline, but p53 was not changed.	Zhang et al., 2017
Drug	Metformin	Treatment reduced p-ATM, p-p53 and p21 levels, but did not change the level of 53BP1 in irradiated HAECs.	Park et al., 2022

Known Feedforward/Feedback loops influencing this KER

None identified

References

Abner, C. W. and P. J. McKinnon. (2004), "The DNA double-strand break response in the nervous system", *DNA Repair*, Vol. 3/8–9, Elsevier, Amsterdam, https://doi.org/10.1016/j.dnarep.2004.03.009.

Baselet, B. et al. (2019), "Pathological effects of ionizing radiation: endothelial activation and dysfunction", *Cellular and Molecular Life Sciences*, Vol. 76/4, Springer Nature, https://doi.org/10.1007/s00018-018-2956-z.

Caldecott, K. W. (2022), “DNA single-strand break repair and human genetic disease”, *Trends in Cell Biology*, 32(9), Elsevier, Amsterdam, https://doi.org/10.1016/j.tcb.2022.04.010

El-Missiry, M. A. et al. (2018), "Neuroprotective effect of epigallocatechin-3-gallate (EGCG) on radiation-induced damage and apoptosis in the rat hippocampus", *International Journal of Radiation Biology*, Vol. 94/9, Informa, London, https://doi.org/10.1080/09553002.2018.1492755.

Ghahremani, H. et al. (2002), “Interaction of the c-Jun/JNK Pathway and Cyclin-dependent Kinases in Death of Embryonic Cortical Neurons Evoked by DNA Damage”, *Journal of Biological Chemistry*, Vol. 277/38, Elsevier, Amsterdam, https://doi.org/10.1074/jbc.M204362200

Gionchiglia, N. et al. (2021), "Association of Caspase 3 Activation and H2AX γ Phosphorylation in the Aging Brain: Studies on Untreated and Irradiated Mice", *Biomedicines*, Vol. 9/9, MDPI, Basel, https://doi.org/10.3390/biomedicines9091166.

Huang, Y. et al. (2021), "Mesenchymal Stem Cell-Conditioned Medium Protects Hippocampal Neurons From Radiation Damage by Suppressing Oxidative Stress and Apoptosis", *Dose-Response*, Vol. 19/1, SAGE publications, https://doi.org/10.1177/1559325820984944.

Kozbenko, T. et al. (2022), “Deploying elements of scoping review methods for adverse outcome pathway development: a space travel case example”, *International Journal of Radiation Biology*, Vol. 98/12. https://doi.org/10.1080/09553002.2022.2110306

Kim, K. S. et al. (2014), "Characterization of DNA damage-induced cellular senescence by ionizing radiation in endothelial cells", *International Journal of Radiation* Biology, Vol. 90/1, Informa, London, https://doi.org/10.3109/09553002.2014.859763.

Lafargue, A. et al. (2017), "Ionizing radiation induces long-term senescence in endothelial cells through mitochondrial respiratory complex II dysfunction and superoxide generation", *Free Radical Biology and Medicine*, Vol. 108, Elsevier, Amsterdam, https://doi.org/10.1016/j.freeradbiomed.2017.04.019.

Lee, Y. and P. J. McKinnon. (2007), "Responding to DNA double strand breaks in the nervous system", *Neuroscience*, Vol. 145/4, Elsevier, Amsterdam, https://doi.org/10.1016/j.neuroscience.2006.07.026.

Maréchal, A. and L. Zou. “DNA damage sensing by the ATM and ATR kinases”, *Cold Spring Harbor Perspectives in Biology*, 5(9), Cold Spring Harbor Laboratory Press, https://doi.org/10.1101/cshperspect.a012716

Nagane, M. et al. (2021), "DNA damage response in vascular endothelial senescence: Implication for radiation-induced cardiovascular diseases", *Journal of Radiation Research*, Vol. 62/4, Oxford University Press, Oxford, https://doi.org/10.1093/jrr/rrab032.

Park, J.-W. et al. (2022), "Metformin alleviates ionizing radiation-induced senescence by restoring BARD1-mediated DNA repair in human aortic endothelial cells", *Experimental Gerontology*, Vol. 160, Elsevier, Amsterdam, https://doi.org/10.1016/j.exger.2022.111706.

Sabirzhanov, B. et al. (2020), "Irradiation-Induced Upregulation of miR-711 Inhibits DNA Repair and Promotes Neurodegeneration Pathways", *International Journal of Molecular Sciences*, Vol. 21/15, MDPI, Basel, https://doi.org/10.3390/ijms21155239.

Sylvester, C. B. et al. (2018), "Radiation-Induced Cardiovascular Disease: Mechanisms and Importance of Linear Energy Transfer", *Frontiers in Cardiovascular Medicine*, Vol. 5, Fronteirs, https://doi.org/10.3389/fcvm.2018.00005.

Thadathil, N. et al. (2019), "DNA double-strand breaks: a potential therapeutic target for neurodegenerative diseases", *Chromosome Research*, Vol. 27/4, Springer Nature, https://doi.org/10.1007/s10577-019-09617-x.

Ungvari, Z. et al. (2013), "Ionizing Radiation Promotes the Acquisition of a Senescence-Associated Secretory Phenotype and Impairs Angiogenic Capacity in Cerebromicrovascular Endothelial Cells: Role of Increased DNA Damage and Decreased DNA Repair Capacity in Microvascular Radiosensitivity", *The journals of gerontology. Series A, Biological sciences and medical sciences*, Vol. 68/12, Oxford University Press, Oxford, https://doi.org/10.1093/gerona/glt057.

Wang, Q. et al. (2020), "Radioprotective Effect of Flavonoids on Ionizing Radiation-Induced Brain Damage", *Molecules*, Vol. 25/23, MDPI, Basel, https://doi.org/10.3390/molecules25235719.

Wang, H. et al. (2017), "Chronic oxidative damage together with genome repair deficiency in the neurons is a double whammy for neurodegeneration: Is damage response signaling a potential therapeutic target?", *Mechanisms of Ageing and Development*, Vol. 161, Elsevier, Amsterdam, https://doi.org/10.1016/j.mad.2016.09.005.

Wang, Y., M. Boerma and D. Zhou. (2016), "Ionizing Radiation-Induced Endothelial Cell Senescence and Cardiovascular Diseases", *Radiation Research*, Vol. 186/2, BioOne, https://doi.org/10.1667/RR14445.1.

Zhang, L. et al. (2017), "The inhibitory effect of minocycline on radiation-induced neuronal apoptosis via AMPKα1 signaling-mediated autophagy", *Scientific Reports*, Vol. 7/1, Springer Nature, https://doi.org/10.1038/s41598-017-16693-8.

Relationship: 2771: Oxidative Stress leads to Altered Signaling

AOPs Referencing Relationship

AOP Name	Adjacency	Weight of Evidence	Quantitative Understanding
Deposition of energy leads to vascular remodeling	adjacent	High	Low
Deposition of Energy Leading to Learning and Memory Impairment	adjacent	High	Low
Deposition of energy leading to occurrence of bone loss	adjacent	High	Low

Evidence Supporting Applicability of this Relationship

Taxonomic Applicability

Term	Scientific Term	Evidence	Links
human	Homo sapiens	Low	NCBI
mouse	Mus musculus	High	NCBI
rat	Rattus norvegicus	High	NCBI
Pig	Pig	Moderate	NCBI

Life Stage Applicability

Life Stage	Evidence
Adult	Moderate
Juvenile	Moderate

Sex Applicability

Sex	Evidence

Sex	Evidence
Male	High
Female	Low
Unspecific	Low

Based on the prioritized studies presented here, the evidence of taxonomic applicability is low for humans despite there being strong plausibility as the evidence only includes *in vitro* human cell-derived models. The taxonomic applicability for mice and rats is considered high as there is much available data using *in vivo* rodent models that demonstrate the concordance of the relationship. The taxonomic applicability was determined to be moderate for pigs as only one *in vivo* study provided meaningful support to the relationship. In terms of sex applicability, all *in vivo* studies that indicated the sex of the animals used male animals, therefore, the evidence for males is high and females is considered to be low for this KER. The majority of studies used adolescent animals, with a few using adult animals. Preadolescent animals were not used to support the KER; however, the relationship in preadolescent animals is still plausible.

Key Event Relationship Description

Oxidative stress occurs when the production of free radicals exceeds the capacity of cellular antioxidant defenses (Cabrera & Chihuailaf, 2011). Reactive oxygen species (ROS) and reactive nitrogen species (RNS) are both free radicals that can contribute to oxidative stress (Ping et al., 2020); however, ROS are more commonly studied than RNS (Nagane et al., 2021). ROS can mediate oxidative damage to biomacromolecules as they react with DNA, proteins and lipids, resulting in functional changes to these molecules (Ping et al., 2020). For example, ROS acting on lipids creates lipid peroxidation (Cabrera & Chihuailaf, 2011).

Many signaling pathways control and maintain physiological balance within a living organism, and these can be impacted by oxidative stress. Excessive reactive oxygen and nitrogen species (RONS) during oxidative stress can modify biological molecules and directly cause DNA damage, which can lead to altered signal transduction pathways (Hughson, Helm & Durante, 2018; Lehtinen & Bonni, 2006; Nagane et al., 2021; Ping et al., 2020; Ramadan et al., 2021; Schmidt-Ullrich et al., 2000; Soloviev & Kizub, 2019; Wang, Boerma & Zhou, 2016; Venkatesulu et al., 2018; Zhang et al., 2016). Different cell types can express distinct cellular pathways that can have varied response to an increase in oxidative stress. For example, oxidative stress in endothelial cells has been shown to inhibit the insulin-like growth factor 1 receptor (IGF-1R) and phosphatidylinositol-3-kinase/protein kinase B (PI3K/Akt) pathway and to activate the mitogen-activated protein kinase (MAPK) pathway, which can then have downstream detrimental effects (Ping et al., 2020). The MAPK family pathway is also activated in the central nervous system (CNS) in response to oxidative stress through calcium-induced phosphorylation of several kinases. These include phosphoinositide 3-kinase (PI3K), protein kinase A (PKA) and protein kinase C (PKC) and calcium/calmodulin-dependent protein kinase II (CaMKII) (Lehtinen & Bonni, 2006; Li et al., 2013; Ramalingam & Kim, 2012). Oxidative stress in bone cells can lead to increased expression of the receptor activator of nuclear factor kappa B ligand (RANKL) and Nrf2 activation (Tahimic & Globus, 2017; Tian et al., 2017). Following activation, Nrf2 then interferes with the activation of runt-related transcription factor 2 (Runx2), and depending on the level of oxidative stress, this may result in altered bone cell function (Kook et al., 2015).

Evidence Supporting this KER

Overall weight of evidence: High

Biological Plausibility

Many reviews describe the role of oxidative stress in altered signaling. The mechanisms through which oxidative stress can contribute to changes in various signaling pathways are well-described. For example, oxidative stress can directly alter signaling pathways through protein oxidation (Ping et al., 2020; Schmidt-Ullrich et al., 2000; Valerie et al., 2007). Oxidation of cysteine and methionine residues, which are particularly sensitive to oxidation, can cause conformational change, protein expansion, and degradation, leading to changes in the protein levels of signaling pathways (Ping et al., 2020). Furthermore, oxidation of key residues in signaling proteins can alter their function, resulting in altered signaling. For example, oxidation of methionine 281 and 282 in the Ca^{2+}/calmodulin binding domain of Ca^{2+}/calmodulin-dependent protein kinase II (CaMKII) leads to constitutive activation of its kinase activity and subsequent downstream alterations in signaling pathways (Li et al., 2013; Ping et al., 2020). Similarly, during oxidative stress, tyrosine phosphatases can be inhibited by oxidation of a catalytic cysteine residue, resulting in increased phosphorylation of proteins in various signaling pathways (Schmidt-Ullrich et al., 2000; Valerie et al., 2007). Particularly relevant to this are the MAPK pathways. For example, the extracellular signal-regulated kinase (ERK) pathway is activated by upstream tyrosine kinases and relies on tyrosine phosphatases for deactivation (Lehtinen & Bonni, 2006; Valerie et al., 2007).

Furthermore, oxidative stress can indirectly influence signaling pathways through oxidative DNA damage which can lead to mutations or changes in the gene expression of proteins in signaling pathways (Ping et al., 2020; Schmidt-Ullrich et al., 2000; Valerie et al., 2007). DNA damage surveillance proteins like ataxia telangiectasia mutated (ATM) kinase and ATM/Rad3-related (ATR) protein kinase phosphorylate over 700 proteins, leading to changes in downstream signaling (Nagane et al., 2021; Schmidt-Ullrich et al., 2000; Valerie et al., 2007). For example, ATM, activated by oxidative DNA damage, phosphorylates many proteins in the ERK, p38, and Jun N-terminal kinase (JNK) MAPK pathways, leading to various downstream effects (Nagane et al., 2021; Schmidt-Ullrich et al., 2000).

The response of oxidative stress on signaling pathways has been studied extensively in various diseases. Herein presented are examples relevant to a few cell types related to vascular disease, impaired learning and memory, and bone loss. Many other pathways are plausible but available research has highlighted these to be critical to disease.

Endothelial cells: Endothelial cells can normally produce ROS. Antioxidant enzymes and the glutathione redox buffer control the redox state of vascular tissues. However, the dysregulation of signaling pathways can occur in the endothelium when oxidative stress is favored (Soloviev & Kizub, 2019). Oxidative stress can activate the acidic sphingomyelinase (ASMase)/ceramide pathway, the MAPK pathways, the p53/p21 pathway, and the signaling proteins p16 and p21, as well as inhibit the PI3K/Akt pathway (Hughson, Helm & Durante, 2018; Nagane et al., 2021; Ping et al., 2020; Ramadan et al., 2021; Soloviev & Kizub, 2019; Wang, Boerma & Zhou, 2016).

Bone cells: oxidative stress can induce signaling changes in the Wnt/β-catenin pathway, the RANK/RANKL pathway, the Nrf2/HO-1 pathway, and the MAPK pathways (Domazetovic et al., 2017; Manolagas & Almeida, 2007; Tian et al., 2017).

Brain cells: oxidative stress can induce alterations to various pathways such as the PI3K/Akt pathway, cAMP response element-binding protein (CREB) pathway, the p53/p21 pathway, as well as the MAPK family pathways, including JNK, ERK and p38 (Lehtinen & Bonni, 2006; Ramalingam & Kim, 2012).

Additionally, the electron transport chain in the mitochondria is an important source of ROS, which can damage mitochondria by inducing mutations in mitochondrial DNA. These mutations lead to mitochondrial dysfunction due to alterations in cellular respiration mechanisms that perpetuates oxidative stress and can then induce the release of signaling molecules related to apoptosis from the mitochondria. Pro-apoptotic markers (Bax, Bak and Bad) and anti-apoptotic markers (Bcl-2 and Bcl-xL) can regulate the caspase pathway that ultimately mediate apoptosis (Annunziato et al., 2003; Wang & Michaelis, 2010; Wu et al., 2019).

The mechanisms of oxidative stress leading to altered signaling may be different for each pathway. For example, although both the PI3K/Akt and MAPK pathways can be regulated by insulin-like growth factor (IGF)-1, ROS results in selective inhibition of the IGF-1R/PI3K/Akt pathway by inhibiting the IGF-1 receptor (IGF-1R) activation of IRS1 (Ping et al., 2020). Additionally, ROS-induced MAPK activation can be done through Ras-dependent signaling. Firstly, oxygen radicals mediate the phosphorylation of upstream epidermal growth factor receptors (EGFRs) on tyrosine residues, resulting in increased binding of growth factor receptor-bound protein 2 (Grb2) and subsequent activation of Ras signaling (Lehtinen & Bonni, 2006). Direct inhibition of MAPK phosphatases with hydroxyl radicals also activates this pathway (Li et al., 2013). In another mechanism, ROS competitively inhibit the Wnt/β-catenin pathway through the activation of forkhead box O (FoxO), which are involved in the antioxidant response and require binding of β-catenin for transcriptional activity (Tian et al., 2017).

Empirical Evidence

Evidence for this relationship was collected from studies using *in vivo* mouse, rat, and pig models, as well as *in vitro* mouse-derived, rat-derived, bovine-derived, and human-derived models. The stressors used to support this relationship include gamma rays, X rays, microgravity, hydrogen peroxide, chronic cold stress, heavy ion radiation, simulated ischemic stroke and growth differentiation factor (GDF) 15 overexpression. These stressors were shown to increase levels of oxidative stress and induce changes within relevant signaling pathways (Azimzadeh et al., 2021; Azimzadeh et al., 2015; Fan et al., 2017; Xu et al., 2019; Suman et al., 2013; Limoli et al., 2004; Tian et al., 2020; Hladik et al., 2020; Diao et al., 2018; Hasan, Radwan & Galal, 2019; Xin et al., 2015; El-Missiry et al., 2018; Kenchegowda et al., 2018; Kook et al., 2015; Sun et al., 2013; Yoo, Han & Kim, 2016, Zhao et al., 2013; Bai et al., 2020; Chen et al., 2009; Carvour et al., 2008; Wortel et al., 2019; Azimzadeh et al., 2017; Park et al., 2016; Sakata et al., 2015; Ruffels et al., 2004; Crossthwaite et al., 2002).

Incidence concordance

A few studies demonstrate greater changes to oxidative stress than to altered signaling. Human umbilical vein endothelial cells (HUVECs) irradiated with 10 Gy of X-rays showed a 20-fold increase in ROS and a 0.5-fold decrease in the ratio of p-Akt/Akt (Sakata et al., 2015). Microgravity exposure to preosteoblast cells showed a 0.24-fold decrease to the antioxidant Cu/Zn-superoxide dismutase (SOD) and a 0.36-fold decrease to p-Akt (Yoo, Han & Kim, 2016). It was also shown in rats that MDA levels increased by 1.5-fold while angiotensin and aldosterone increased by 1.4-fold after 6 Gy of gamma rays (Hasan, Radwan & Galal, 2020). Bai et al. (2020) demonstrated with multiple endpoints that ROS levels increased, and antioxidant enzyme levels decreased more than signaling pathways were altered.

Dose Concordance

Many studies demonstrate dose concordance for this relationship, at the same doses. Low-dose (0.5 Gy) X-ray irradiation of human coronary artery endothelial cells (HCAECs) show increased protein carbonylation with decreased glutathione S-transferase omega-1 (GSTO1) antioxidant levels and a simultaneous alteration of signaling proteins Rho GDP-dissociation inhibitor (RhoGDI), p16, and p21 (Azimzadeh et al., 2017). A dose of about 2 Gy of gamma rays showed decreased antioxidants as well as decreased protein levels and activation of the PI3K/Akt pathway in pig cardiac tissue (Kenchegowda et al., 2018). Similarly, gamma irradiation at 6 Gy resulted in reduced levels of the antioxidant glutathione (GSH) and increased levels of the lipid peroxidation marker MDA as well as an increase in the renin angiotensin aldosterone system (RAAS) measured in rat heart tissue and blood serum, respectively (Hasan, Radwan & Galal, 2020). HUVECs irradiated with 10 Gy of X-rays demonstrated increased ROS while p-Akt decreased and p-ERK1/2 increased (Sakata et al., 2015). Gamma radiation at 15 Gy led to both increased ROS as well as attenuated p38 MAPK and Nrf2 signaling pathways in murine cardiac tissue (Fan et al., 2017). In contrast, 16 Gy X-ray exposure led to decreased levels of the antioxidant SOD, increased MDA as well as increased MAPK signaling in murine heart tissue (Azimzadeh et al., 2021). After simulated microgravity, changes to signaling pathways, increased ROS and MDA, and decreased antioxidants were found both in *in vitro* mouse-derived bone cells and in *in vivo* rat femurs. Increased ROS levels and decreased antioxidants were found with changes in the RANK/RANKL pathway, Wnt/β-catenin pathway, Runx2, PI3K/Akt pathway, and MAPK pathways (Diao et al., 2018; Sun et al., 2013; Xin et al., 2015; Yoo, Han & Kim, 2016).

A few studies also find that oxidative stress often occurs at lower doses than altered signaling pathways. Bai et al. (2020) measured oxidative stress, shown by increased ROS and decreased antioxidant expression, at 2, 5, and 10 Gy of gamma rays. They also found Runx2 increased at the same doses, but the p53/p21 pathway was only significantly altered at 5 and 10 Gy (Bai et al., 2020). At similar doses, X-ray irradiated mouse osteoblast-like cell line MC3T3-E1 cells showed increased ROS and decreased antioxidants both 4 and 8 Gy (Kook et al., 2015). While HO-1 also increased at both 4 and 8 Gy, Nrf2 and Runx2 were measured altered at 8 Gy (Kook et al., 2015). In another study, X-ray irradiation at 16 Gy resulted in decreased SOD and increased MDA and protein carbonylation, which were associated with decreased PI3K/Akt pathway activity and protein levels, decreased ERK activity and protein levels, increased p38 activity, and increased p16 and p21 protein levels in heart tissue (Azimzadeh et al., 2015). Azimzadeh et al. (2015) also showed that at 8 Gy oxidative stress was still observed, but fewer signaling molecule levels and activity were altered at this. Particularly, no changes to MAPK pathways were observed.

Within the rat hippocampus, El-Missiry et al. (2018) demonstrated that exposure to 4 Gy of X-irradiation results in increased 4-HNE (oxidative stress marker) levels, reduced antioxidant activity and an increase in p53 expression. In the cerebral cortex of mice, Suman et al. (2013) reported that 1.6 Gy of ^{56}Fe and 2 Gy of gamma rays increased ROS levels, consequently increased p21 and p53 levels. Limoli et al. (2004) also reported increased ROS levels in mice and rat neural precursor cells after exposure to X-irradiation (1-10 Gy), accompanied by increased expression of p21 and p53. Hladik et al. (2020) exposed female mice to 0.063, 0.125 or 0.5 Gy of gamma-radiation, which resulted in increases of protein carbonylation, as well as increased phosphorylation of CREB, ERK1/2 and p38. Radiation-induced changes in apoptotic markers were also reported. More specifically, there was a significant rise in pro-apoptotic markers Bax and caspase 3, with significant reduction in anti-apoptotic marker Bcl-xL (Hladik et al., 2020). Furthermore, middle cerebral artery occlusion (MCAO) surgery known to simulate ischemic stroke in C57BL/6J mice was shown to increase ROS levels, as well as the phosphorylation of ERK1/2, p38 and JNK (Tian et al., 2020).

Other studies that have used hydrogen peroxide (H_2O_2) to induce oxidative stress within cell cultures, have also observed alterations in signaling pathways. Zhao et al. (2013) exposed mouse hippocampal-derived HT22 cells to varying concentrations of H_2O_2 and found a dose-dependent increase in ROS production from 250-1000 µM. Additionally, treating the cells to H_2O_2 resulted in a concentration-dependent increase of ERK1/2, JNK1/2 and p38 phosphorylation. Ruffels et al. (2004) incubated human neuroblastoma cells (SH-SY5Y) to varying concentrations of H_2O_2 that ranged from 0.5-1.25 mM and found a dose-dependent increase in JNK1/2, ERK1/2 and Akt phosphorylation. Another study exposed SH-SY5Y and rat pheochromocytoma (PC12) cells to 0.05-2 mM H_2O_2 and found a dose-dependent increase in ROS from 0-1 mM in SH-SY5Y cells, and from 0-2 mM in PC12 cells with a concentration-dependent increase in ERK1/2, p38 and JNK phosphorylation (Chen et al., 2009). Furthermore, Crossthwaite et al. (2002) incubated neuronal cultures from 15- to 16-day-old Swiss mice to 100, 300 and 1000 µm H_2O_2 and showed increased levels of ROS. A corresponding increase in ERK1/2 and Akt activation was observed at 100-300 µm, and for JNK1/2 the observation was observed at 1000 µm. Carvour et al. (2008) treated N27 cells (rat dopaminergic cell line) to 3-30 µM H_2O_2 and measured increased ROS levels, as well as increased apoptotic signaling molecules caspase 3 and proapoptotic kinase protein kinase C-δ (PKCδ) cleavage.

Time Concordance

Limited evidence shows that oxidative stress leads to altered signaling pathways in a time concordant manner. When irradiated with X-rays, HCAECs, BAECs and MCT3T3-E1 osteoblast-like cells show increase in ROS or levels of protein carbonylation, or a decrease in the levels of superoxide dismutase (SOD), catalase (CAT), GSTO1 or GSH at earlier timepoints than alterations in the signaling molecules p16, p21, Ceramide, Runx2, and HO-1 (Azimzadeh et al., 2017; Kook et al., 2015; Wortel et al., 2019). As the key events are both molecular-level changes, both can occur quickly after irradiation. Wortel et al. (2019) found that increased hydrogen peroxide levels could be observed *in vitro* as early as 2 minutes post-irradiation, while ASMase activity and ceramide levels were only increased 5 minutes post-irradiation.

When exposed to H_2O_2, PC12 cells show an increase production of ROS with a corresponding increase in phosphorylation of MAPK proteins in a time-dependent fashion. An increase in ERK1/2, JNK and p38 phosphorylation was observed within 5-15 minutes and sustained for over 2 hours (Chen et al., 2009). When exposed to cold stress for 1, 2 and 3 weeks, MDA levels increased in a time-dependent manner from 1-3 weeks within the brain tissue isolated from C57BL/6 mice. The expressions of JNK, ERK and p38 phosphorylation levels were all also significantly upregulated in chronic cold-stressed groups for all time-points (Xu et al., 2019). After gamma irradiation (2 Gy), ROS increased 2 months post-irradiation, while increased p21 and decreased Bcl-2 were only observed at 12 months (Suman et al., 2013). However, other signaling molecules were increased at both times.

Essentiality

Several studies have investigated the essentiality of the relationship, where the blocking or attenuation of the upstream KE causes a change in frequency of the downstream KE. The increase in oxidative stress can be modulated by certain drugs, antioxidants and media. L-carnitine injections decreased ROS and increased p-p38/p38 and p-Nrf2/Nrf2 signaling (Fan et al., 2017). Fenofibrate was found to return SOD, phosphorylated MAPK signaling proteins and increase Nrf2 levels (Azimzadeh et al., 2021). Antioxidants (N-acetyl cysteine, curcumin) were shown to restore or reduce ROS levels closer to control levels following radiation or microgravity exposure, respectively. Signaling proteins in the Nrf2/HO-1 pathway and the RANKL/osteoprotegerin (OPG) ratio were decreased and brought closer to control levels (Kook et al., 2015; Xin et al., 2015). Hydrogen rich medium showed reduced ROS with restoration of OPG and RANKL signaling levels to controls (Sun et al., 2013). Polyphenol S3 (60 mg/kg/d) treatment was found to reverse the effect of microgravity on CAT, SOD and MDA, returning the levels to near control values. Meanwhile, Runx2 mRNA levels and β-catenin/β-actin levels increased following treatment (Diao et al., 2018). Sildenafil is another drug that was found to reduce ROS generation by inhibiting O_2^- production and intracellular peroxynitrite levels in bovine aortic endothelial cells (BAECs) after gamma irradiation. As well, ASMase activity and ceramide levels were inhibited by sildenafil (Wortel et al., 2019).

Within brain cells, several antioxidants have been found to attenuate oxidative stress-induced alterations in signaling pathways. These antioxidants include Melandrii Herba extract, N-acetyl-L-cysteine (NAC), gallocatechin gallate/epigallocatechin-3-gallate, Cornus officinalis (CC) and fermented CC (FCC), L-165041, fucoxanthin, and edaravone. These antioxidants were shown to reduce ROS and subsequently decrease phosphorylation of MAPKs such as ERK1/2, JNK1/2 and p38 after exposure to radiation, H2O2 or LPS (Lee et al., 2017; Deng et al., 2012; Park et al., 2021; Tian et al., 2020; Schnegg et al., 2012; Zhao et al., 2017; Zhao et al., 2013; El-Missiry et al., 2018). Another documented modulator is mesenchymal stem-cell conditioned medium (MSC-CM), which was able to alleviate oxidative stress in HT22 cells and restore levels of p53 (Huang et al., 2021).

Uncertainties and Inconsistencies

- MAPK pathways can exhibit varied responses after exposure to oxidative stress. The expected response is an increase in the activity of the ERK, JNK, and p38 pathways as protein phosphatases, involved in the inactivation of MAPK pathways, are deactivated by oxidative stress (Valerie et al., 2007). Although some studies observe this (Azimzadeh et al., 2021; Sakata et al., 2015), others show a decrease (Fan et al., 2017; Yoo, Han & Kim, 2016) or varying changes (Azimzadeh et al., 2015) in the MAPK pathways.

Quantitative Understanding of the Linkage

The tables below provide representative examples of quantitative linkages between the two key events. It was difficult to identify a general trend across all the studies due to differences in experimental design and reporting of the data. All data that is represented is statistically significant unless otherwise indicated.

Response-response relationship

Dose/Incidence Concordance

Reference	Experiment Description	Result
Azimzadeh et al., 2017	*In vitro*. HCAECs were irradiated with 0.5 Gy of X-rays (0.5 Gy/min). Protein carbonylation and GSTO1 antioxidant levels were measured with a carbonylation assay and immunoblotting, respectively. Proteins from various signaling pathways including RhoGDI, p16, and p21 were measured with immunoblotting.	After 0.5 Gy, carbonyl content increased a maximum of 1.2-fold and GSTO1 decreased a maximum of 0.78-fold. After 0.5 Gy, p-RhoGDI decreased a maximum of 0.7-fold, p16 increased a maximum of 1.5-fold, and p21 increased a maximum of 1.2-fold.
Kenchegowda	*In vivo*. Male 3- to 5-month-old Gottingen minipigs and Sinclair minipigs were whole-body irradiated with 1.7-2.3 Gy of ^{60}Co gamma rays (0.6 Gy/min). Both survivors (n=23) and euthanized moribund animals (n=17) had measurements taken for	Compared to survivors, radiation induced a 2.1-fold increase in p67, 0.87-fold decrease in SOD, and a 0.83-fold decrease in CAT (non-significant, ns) in the deceased group.

et al., 2018	oxidative stress and altered signaling taken from the heart. SOD, CAT, and p67 (subunit of NADPH oxidase/NOX, involved in producing superoxide) levels were determined with western blot. ELISA and western blot were used to measure altered signaling in the IGF/PI3K/Akt pathway.	Compared to survivors, the ratio of activated (phosphorylated) to total IGF-1R and the ratio of activated (phosphorylated) to total Akt both decreased 0.5-fold in the deceased group.
Kook et al., 2015	*In vitro*. MC3T3-E1 osteoblast-like cells were irradiated with 2, 4, and 8 Gy of X-rays (1.5 Gy/min). ROS were measured with a fluorescent probe, and SOD, CAT, and GSH antioxidant activities were determined with assay kits. Protein levels in the Nrf2/HO-1 signaling pathway were determined by either western blot or RT-PCR.	ROS increased linearly at 2 and 4 Gy up to 1.4-fold at 8 Gy (significant changes at 4 Gy and 8 Gy). GSH and SOD were decreased 0.7-fold at 4 Gy and 0.5-fold at 8 Gy (insignificant increases at 2 Gy). CAT was also decreased but not significantly. HO-1 increased 3.3-fold after 4 Gy and 4.9-fold after 8 Gy (insignificant increase at 2 Gy). Nrf2 increased 2.3-fold after 8 Gy. Runx2 mRNA was decreased 0.5-fold after 8 Gy.
Bai et al., 2020	*In vitro*. Rat-derived bone marrow-derived mesenchymal stem cells (bmMSCs) were irradiated with 2, 5, and 10 Gy of ^{137}Cs gamma rays. Mitochondrial and cellular ROS levels were determined with fluorescent probes. RT-qPCR was performed to measure antioxidant enzyme expression. Protein expression in various signaling pathways was measured by western blot.	Mitochondrial ROS increased 1.6-fold at 2 Gy (non-significant), 2-fold at 5 Gy, and 2.3-fold at 10 Gy. Cellular ROS increased 1.2-fold at 2 Gy, 1.5-fold at 5 Gy, and 2.1-fold at 10 Gy. Antioxidants SOD1, SOD2, and CAT all decreased about 0.9-fold (ns for SOD2) after 2 Gy, 0.8- to 0.7-fold at 5 Gy, and 0.7- to 0.4-fold at 10 Gy. Runx2 decreased 0.9-fold at 2 and 5 Gy and 0.6-fold at 10 Gy. p21 increased 1.6-fold at 5 Gy and 2.5-fold at 10 Gy. p53 increased 1.6-fold at 5 Gy and 1.7-fold at 10 Gy. p16 remained unchanged.
Fan et al., 2017	*In vivo*. 10-week-old male C57BL/6J mice were irradiated with ^{60}Co gamma rays at 3 Gy/day for 5 days. Left ventricular cardiac tissue was harvested for analysis. ROS was detected by dihydroethidium (DHE) staining. MAPK and Nrf2 signaling molecules were measured by western blot.	Following irradiation, ROS production increased by 3.6-fold. p-p38/p38 decreased by 0.36-fold and p-Nrf2/Nrf2 decreased by 0.14-fold.
Hasan, Radwan & Galal, 2020	*In vivo*. 6-week-old male Wistar rats were irradiated with 6 Gy ^{137}Cs gamma rays. Oxidative stress was measured by MDA and GSH in heart tissue. Angiotensin II (AngII) and aldosterone, key molecules in the RAAS pathway, were measured with ELISA kits in serum.	Following irradiation, MDA levels increased by 1.5-fold and GSH levels decreased by 0.5-fold. AngII and aldosterone increased 1.4-fold compared to control.
Azimzadeh et al., 2015	*In vivo*. Male 10-week-old C57BL/6 mice were irradiated with 8 and 16 Gy of X-rays. SOD, MDA, and protein carbonylation levels were determined with immunoblotting, lipid peroxidation, and protein carbonylation assays, respectively, in heart tissue. Proteins in various signaling pathways were measured with immunoblotting in heart tissue.	SOD decreased 0.7-fold at both 8 and 16 Gy and MDA increased 1.4-fold after 8 Gy and 2.1-fold after 16 Gy. Protein carbonylation increased 1.4-fold after 16 Gy. Levels and activity of proteins in the PI3K/Akt pathway were decreased between 0.5- and 0.1-fold at both 8 and 16 Gy. The ERK/MAPK pathway was found decreased 0.5-fold at 16 Gy and the p38/MAPK pathway was found increased 1.3-fold at 16 Gy. p16 was increased 1.6-fold at both 8 and 16 Gy. p21 was increased 2.4-fold at both 8 and 16 Gy.
Sakata et al., 2015	*In vitro*. HUVECs were irradiated with 10 Gy X-rays at a dose rate of 5 Gy/min. Measurements were performed 0-72 h post-irradiation. ROS were detected by fluorescence microscopy. MAPK, Akt, p-p38, JNK and ERK1/2 signaling molecules were measured by western blot.	Following 10 Gy irradiation, the intensity representing ROS generation increased 20- and 30-fold at the 24 and 72 h timepoints, respectively. MAPK, p38 and JNK remained unchanged for the 72 h measured following 10 Gy irradiation. p-Akt/Akt in HUVECs after 10 Gy irradiation showed an initial decrease at 5 min and a delayed decrease of 0.5-fold at 6-24 h. p-ERK1/2 decreased at 5 min then increased to a maximum 1.75-fold change.
Wortel et al., 2019	*In vitro*. BAECs were irradiated with 10 Gy ^{137}Cs gamma rays at a rate of 1.66 Gy/min. Extracellular H2O2 was measured by Amplex Red Assay, intracellular H_2O_2 levels were determined by HyPer sensor and peroxynitrite was quantified by chemiluminescence assay. Superoxide levels were quantified by luminescence after treatment with	Following 10 Gy irradiation, intracellular H_2O_2 increased to a maximum 1.35-fold. Extracellular H_2O_2 increased by 1.75-fold. Peroxynitrite increased by 2.86-fold after 10 Gy (Fig 5). Superoxide levels increased over 350% at 2 minutes after 10 Gy irradiation. ASMase activity increased to a maximum 5.6-fold at 5 min after irradiation, then decreased and remained

	Diogenes Complete Enhancer Solution. The activation of the ASMase enzyme and the levels of ceramide were quantified by radioenzymatic assay to deter mine the changes on the ASMase/ceramide pathway.	unchanged until the 30 min time-point. Ceramide increased from -500 to over 3000 pmol/106 cells. The significance of these changes was not indicated against a control.
Azimzadeh et al., 2021	*In vivo*. Male C57BL/6J mice 8 weeks of age were irradiated with 16 Gy of X-rays to the heart. SOD antioxidant activity and MDA in heart tissue were determined with an assay kit and lipid peroxidation assay, respectively. The level of proteins in MAPK pathways were determined by ELISA in heart tissue.	After 16 Gy, SOD decreased 0.8-fold and MDA increased 1.3-fold. After 16 Gy, p-ERK increased 1.5-fold, p-p38 increased 1.3-fold, and p-JNK increased 1.3-fold.
Xin et al., 2015	*In vitro* and *in vivo*. *In vitro*. MC3T3-E1 osteoblast-like cells were exposed to microgravity for 96 hours. ROS were determined with a fluorescent probe and the RANK/RANKL pathway was measured using RANKL and OPG assay kits. *In vivo*. Male 8-week-old Sprague-Dawley rats were exposed to hind-limb suspension for 6 weeks. Femur and plasma MDA and femur sulfhydryl levels were measured with assay kits and the RANK/RANKL pathway was measured in the femur using RANKL and OPG assay kits.	*In vitro*. ROS increased 1.5-fold and the RANKL/OPG ratio increased 1.6-fold. *In vivo*. Serum and femur MDA increased 1.4-fold and femur sulfhydryl decreased 0.6-fold. The RANKL/OPG ratio increased 3.5-fold.
Sun et al., 2013	*In vitro*. MC3T3-E1 osteoblast-like cells were exposed to microgravity (0.01G) for 96 hours. ROS production was measured by a fluorescent probe. The RANKL/OPG ratio was determined by assay kit and Runx2 mRNA expression was determined by RT-qPCR	ROS increased 1.5-fold. The RANKL/OPG ratio increased 1.6-fold. Runx2 expression decreased 0.4-fold.
Yoo, Han & Kim, 2016	*In vitro*. Preosteoblast MC3T3-E1 cells were exposed to microgravity conditions by a 3D clinostat at a speed from 1-10 rpm. Oxidative stress was measured by Cu/Zn-SOD, Mn-SOD and catalase activity. Signaling molecules, p-Akt, phosphorylation of the mechanistic target of rapamycin p-(mTOR), and p-ERK were measured by western blot.	Following microgravity exposure, Cu/Zn-SOD and Mn-SOD levels decreased by 0.24 and 0.65-fold, respectively. Signaling molecules p-Akt decreased by 0.36-fold. p-mTOR and p-ERK decreased by 0.58-fold.
Diao et al., 2018	*In vivo*. The left femur of rats was studied after exposure to simulated microgravity. Oxidative stress was measured by MDA, SOD, and CAT levels. RANK/RANKL signaling pathway was measured in rat femur by enzyme-linked immunoassay detection of OPG/RANKL molecules. Signaling molecule, Runx2, mRNA levels were measured by quantitative real time PCR. The Wnt/β-catenin pathway was measured by western blot for β-catenin protein levels.	MDA increased by 1.4-fold. SOD and CAT levels decreased by 0.4-fold. OPG/RANKL decreased by 0.6-fold. Runx2 mRNA levels decreased 0.04-fold (Fig 8d). β-catenin decreased 0.6-fold.
El-Missiry et al., 2018	*In vivo*. Male Wistar rats were irradiated with gamma rays (^{137}Cs source, 4 Gy, 0.695 cGy/s) and measurements were taken from the hippocampus. Assay kits were used to assess levels of oxidative stress for marker 4-HNE (4-hydroxy-2-nonenal) and antioxidant markers GSH, glutathione peroxidase (GPx) and glutathione reductase (GR). Levels of p53 were determined using an assay kit.	After 4 Gy, 4-HNE increased 2.4-fold, protein carbonylation increased 3.2-fold, GSH decreased 0.4-fold, GPx decreased 0.3-fold, GR decreased 0.2-fold, and p53 increased 2.7-fold.
Suman et al., 2013	*In vivo*. Female adult C57BL/6J mice were irradiated with 1.6 Gy of ^{56}Fe or 2 Gy of ^{137}Cs gamma irradiation at 1 Gy/min, then measurements were taken from the cerebral cortex. ROS levels were determined with flow cytometry and 4-HNE levels were assessed with immunohistochemical staining. p21 and p53 levels were determined with immunoblotting.	ROS increased a maximum of 1.2-fold after gamma rays and 1.4-fold after ^{56}Fe radiation. The number of 4-HNE+ cells increased a maximum of 4.4-fold after gamma radiation and 14-fold after ^{56}Fe radiation. p21 increased a maximum of 1.5-fold after gamma rays and 3-fold after ^{56}Fe radiation. p53 increased a maximum of 8.4-fold after gamma rays and 9-fold after ^{56}Fe radiation.

Limoli et al., 2004	*In vivo*. Adult male C57BL/6J mice were irradiated with 1-10 Gy of X-ray at 1.75 Gy/min. MDA levels in the hippocampus were measured using an assay kit and western blot was used to determine p53 and p21 levels. *In vitro*. Neural precursor cells from the rat hippocampus were irradiated with 1-10 Gy of X-ray at 4.5 Gy/min. ROS levels were measured using CM-H2DCFDA dye and Western blot was used to measure p53 and p21 levels.	MDA levels increased about 30% at 10 Gy. ROS increased a maximum of 31% at 1 Gy and 35% at 5 Gy, after 24 and 12 hours, respectively. At 5 Gy, p53 levels increased a maximum of 4-fold, while p- p21 also increased at this dose.
Tian et al., 2020	*In vivo*. C57BL/6J mice (including miR-137-/- and Src-/- models) underwent middle cerebral artery occlusion (MCAO) to simulate ischemic stroke and measurements were taken 7 days later in the cerebral cortex. ROS levels were measured with DCFH-DA fluorescent dye. Signaling molecules were measured with western blotting or RT-qPCR.	ROS increased 1.8-fold. ERK1/2, p38 and JNK mRNA increased 2- to 3- fold. The ratios of phosphorylated to total ERK1/2, p38 and JNK increased 2- to 3- fold as well.
Hladik et al., 2020	*In vivo*. Female B6C3F1 mice were exposed to total body ^{60}Co gamma irradiation at 0.063, 0.125, or 0.5 Gy and at a dose rate of 0.063 Gy/min. Measurements from the hippocampus were taken up to 24 months post-irradiation. Protein levels in various signaling pathways (CREB, p38, ERK1/2, pro-apoptotic Bax and cleaved caspase 3, anti-apoptotic Bcl-xL) were determined with immunoblotting.	Carbonylated proteins (indicative of ROS levels) were elevated in the 0.125 and 0.5 Gy group by approximately 25% and 30%, respectively. CREB phosphorylation increased by approximately 20% and 25% at 0.063 and 0.125 Gy, respectively. Phosphorylated p38 increased by approximately 100% and 80% at 0.063 and 0.125 Gy, respectively. Phosphorylated ERK1/2 increased by approximately 100% and 90% at 0.063 and 0.125 Gy, respectively. Anti-apoptotic BCL-xL decreased by 1.7-fold at 0.5 Gy, whereas pro-apoptotic Bax increased by approximately 2-fold at this dose. Caspase 3 also increased by approximately 2-fold at 0.5 Gy.
Carvour et al., 2008	*In vitro*. Mesencephalic dopaminergic neuronal cell line (N27) derived from rat mesencephalon were exposed to 3, 10, or 30 µM of H_2O_2. ROS levels were detected using dihydroethidine dye and flow cytometry. Western blot was used to detect cleaved PKCδ and Sytox fluorescence was used to measure caspase-3 enzyme activity.	Exposure to 10 and 30 µM of H_2O_2 resulted in 34 and 58% increases in ROS production, respectively, compared to untreated N27 cells. Exposure to 3, 10, and 30 µM hydrogen peroxide resulted in 2-, 10-, and 9-fold increases in caspase-3 enzyme activity. Lastly, exposure to 10 and 30 µM of H_2O_2 dose-dependently induced proteolytic cleavage of PKCδ.
Chen et al., 2009	*In vitro*. PC12 and SH-SY5Y human cells were incubated with H_2O_2. The production of ROS was measured by detecting the fluorescent intensity of oxidant-sensitive probe CM-H2DCFDA. Western blot analysis was used to assess activation of MAPKs.	Treatment with H_2O_2 for 24 h resulted in a concentration-dependent increase of ROS production at the concentrations of 0–1 mM in PC12 and SH-SY5Y cells. In comparison with PC12, SH-SY5Y cells appeared to be more sensitive to H_2O_2, thereby showing a decreased ROS production at 2 mM. Additionally, treatment of PC12 cells with H_2O_2 for 2 h increased phosphorylation of Erk1/2 and p38 in a concentration-dependent manner. Noticeably, H_2O_2-activation of JNK resulted in a robust (5–10-fold) increase of protein expression and phosphorylation of c-Jun at 0.3–1 mM. Similar results were also seen in SH-SY5Y cells (data not shown).

Time-scale

Time Concordance

Reference	Experiment Description	Result
Azimzadeh et al., 2017	*In vitro*. HCAECs were irradiated with 0.5 Gy of X-rays (0.5 Gy/min). Protein carbonylation and GSTO1 antioxidant level were measured with a carbonylation assay and immunoblotting, respectively. Proteins from various signaling pathways including RhoGDI, p16 and p21 were measured with immunoblotting. Measurements	After 7 and 14 days, carbonyl content increased 1.2-fold (insignificant increase at 1 day post-irradiation). After 1-14 days, GSTO1 decreased 0.78-fold (significant decreases at all timepoints). After 1 and 7 days, p-RhoGDI decreased 0.7-fold (non-significant decrease at 14 days post-irradiation). p16 increased 1.2-fold after 7 days and 1.5-fold after 14 days (non-significant increase at 1 day post-

	were taken at 1, 7, and 14 days after irradiation.	irradiation). p21 increased 1.2-fold after 7 and 14 days (insignificant increase at 1 day post-irradiation).
Wortel et al., 2019	*In vitro*. BAECs were irradiated with 10 Gy ^{137}Cs gamma rays at a rate of 1.66 Gy/min. Superoxide levels were quantified by luminescence after treatment with Diogenes Complete Enhancer Solution. The activation of the ASMase enzyme and the levels of ceramide were quantified by radioenzymatic assay to deter mine the changes on the ASMase/ceramide pathway.	Superoxide increased by over 350% at 2 minutes post-irradiation. ASMase activity increased to a maximum 5.6-fold at 5 min post-irradiation. Ceramide increased from -500 to over 3000 pmol/106 cells at 5 minutes post-irradiation. The significance of these changes was not indicated against a control.
Kook et al., 2015	*In vitro*. MC3T3-E1 osteoblast-like cells were irradiated with X-rays (1.5 Gy/min). ROS were measured with a fluorescent probe, and SOD, CAT, and GSH antioxidant activities were determined with assay kits. Protein levels in the Nrf2/HO-1 signaling pathway were determined by either western blot or RT-PCR.	After 1 day and 8 Gy, ROS increased 1.4-fold, GSH decreased 0.5-fold, and SOD decreased 0.5-fold. CAT was also decreased but not significantly. After 1 day and 8 Gy, Nrf2 increased 2.3-fold. After 2 days and 8 Gy, HO-1 increased 4.9-fold. After 3 days and 8 Gy, Runx2 mRNA was decreased 0.5-fold.
Suman et al., 2013	*In vivo*. Female adult C57BL/6J mice were irradiated with 1.6 Gy of ^{56}Fe or 2 Gy of 137Cs gamma irradiation at 1 Gy/min, then measurements were taken from the cerebral cortex until up to 12 months. ROS levels were determined with flow cytometry and 4-HNE levels were determined with immunohistochemical staining. p21 and p53 levels were determined with immunoblotting.	All changes after ^{56}Fe radiation were found after both 2 and 12 months post-irradiation. Most endpoints were also increased at both time points following gamma irradiation, however, p21 only increased at 12 months by 3-fold, but not 2 months, while oxidative stress was shown at 2 months (0.2-fold increase).
Xu et al., 2019	*In vitro*. Adult male C57BL/6 mice experienced chronic cold stress for various lengths (1, 2 and 3 weeks). Brain tissue was then collected, and Western blot was used to measure MDA and proteins of MAPK (JNK, ERK and p38).	MDA levels increased in a time-dependent manner. At 1 week, there was an approximate 3-fold increase, at 2 weeks was an approx. 4-fold increase and for 3 weeks, there was an approx. 5-fold increase in response to cold stress. Phosphorylated JNK increased by ~10% (1 week) and ~30% at 2 and 3 weeks compared to room temperature control. Phosphorylated ERK increased by ~60% at 1 week, ~150% at 2 weeks and ~140% at 3 weeks. Phosphorylated p38 increased by ~50% at 1 week, ~100% at 2 weeks and ~150% at 3 weeks.
Chen et al., 2009	*In vitro*. PC12 and SH-SY5Y human cells were incubated with hydrogen peroxide. The production of ROS was measured by detecting the fluorescent intensity of oxidant-sensitive probe CM-H2DCFDA. Western blot analysis was used to assess activation of MAPKs.	They observed that H_2O_2 induced phosphorylation of MAPKs in a time-dependent fashion. Within 5–15 min, H_2O_2 increased phosphorylation of Erk1/2, JNK and p38, and such phosphorylation was sustained for over 2 h. Consistently, high levels of c-Jun and phospho-c-Jun were induced.

Known modulating factors

Modulating factor	Details	Effects on the KER	References
Drug	Fenofibrate (PPARα activator, PPARα is a transcription factor that can activate antioxidant response)	Treatment of mice with 100 mg/kg of body weight daily for 2 weeks before and 2 weeks after radiation restored SOD activity, returned the level of phosphorylated MAPK proteins and increased Nrf2 levels.	Azimzadeh et al., 2021
Drug	L-carnitine (antioxidant)	L-carnitine injections (100 mg/kg) following irradiation resulted in decreased DHE staining, indicating ROS, and increased p-p38/p38 and p-Nrf2/Nrf2.	Fan et al., 2017
Drug	N-acetyl cysteine (antioxidant)	Treatment of osteoblast-like cells with 5 mM restored ROS levels, SOD activity, and the level of proteins in the Nrf2/HO-1 pathway.	Kook et al., 2015
Drug	Curcumin (antioxidant)	Treatment of osteoblast-like cells with 4 μM reduced ROS levels and the RANKL/OPG ratio. Treatment of rats with 40 mg/kg of body weight reduced oxidative stress and the RANKL/OPG ratio.	Xin et al., 2015
Drug	Bradykinin potentiating factor (BFP) (antioxidant)	Treatment with BFP (1ug/g) after irradiation showed decreased AngII and aldosterone levels compared to irradiation alone.	Hasan, Radwan & Galal, 2020
Media	Hydrogen-rich (antioxidant)	Osteoblasts in a medium consisting of 75% H2, 20% O2, and 5% CO_2 (vol/vol/vol) showed a reduction in ROS production and restoration of	Sun et al.,

		normal signaling.	2013
Drug	Melatonin (antioxidant)	Treatment with 200 nM melatonin reversed the effect of microgravity on Cu/Zn-SOD and Mn-SOD to control levels.	Yoo, Han & Kim, 2016
Drug	Polyphenol S3	Polyphenol S3 treatment reverses the effect of microgravity on CAT, SOD and MDA, returning the levels to near control values when S3 is used at high dose (60mg/kg/d). Runx2 mRNA levels and β-catenin/β-actin levels increased following treatment and simulated microgravity.	Diao et al., 2018
Drug	Sildenafil	Sildenafil (5 uM) inhibits O2- production and attenuates intracellular peroxynitrite in BAECs after 10 Gy irradiation. As well, ASMase activity and ceramide generation was inhibited.	Wortel et al., 2019
Drug	DPI (NOX-inhibitor)	Inhibits O_2^- production and intracellular H_2O_2 in BAECs after 10 Gy irradiation.	Wortel et al., 2019
Drug	Edaravone (EDA) which acts as a free radical scavenger	EDA treatment was able to reduce the levels of ROS and consequently decrease the expression levels of phosphorylated JNK, p38 and ERK1/2.	Zhao et al., 2013
Drug	Melandrii Herba extract (antioxidant)	The extract was able to reduce the H_2O_2-induced phosphorylation of ERK1/2, JNK1/2 and p38 in human neuroblastoma SH-SY5Y cells.	Lee et al., 2017
Drug	N-acetyl-L-cysteine (NAC) (antioxidant)	Attenuated the effects of H_2O_2 in BV-2 murine microglial cells as treatment with NAC reduced c-Jun and ERK1/2 phosphorylation.	Deng et al., 2012
Drug	Gallocatechin gallate (GCG) or epigallocatechin-3-gallate (EGCG), both of which have antioxidant properties	GCG and EGCG inhibits ROS accumulation in mouse hippocampal-derived HT22 cells and Wistar rats, respectively. This consequently reduced glutamate-induced phosphorylation of MAPKs (ERK and JNK) and returned p53 to control levels.	Park et al., 2021; El-Missiry et al., 2018
Drug	Cornus officinalis (CC) and fermented CC (FCC), both of which have antioxidant properties	Both CC and FCC were able to reduce intracellular ROS generation in H2O2-induced neurotoxicity in SH-SY5Y human neuroblastoma cells. This was accompanied with a decrease in ERK1/2, JNK and p38 phosphorylation.	Tian et al., 2020
Drug	L-165041, a PPARδ agonist (PPARα is a transcription factor that can activate antioxidant response).	10 Gy of ^{137}Cs irradiation resulted in an increase in intracellular ROS and c-Jun, MEK1/2 and ERK1/2 phosphorylation in BV-2 cells, all of which were attenuated with L-165041 treatment.	Schnegg et al., 2012
Drug	Fucoxanthin (antioxidant)	Fucoxanthin was able to inhibit the LPS-induced increase in intracellular ROS and phosphorylation of JNK, ERK and p38.	Zhao et al., 2017
Media	Mesenchymal stem-cell conditioned medium (MSC-CM)	MSC-CM was able to inhibit the X-ray-induced increase in ROS and MDA levels and decrease in SOD and GSH levels, resulting in activation of PI3/Akt.	Huang et al., 2021

Known Feedforward/Feedback loops influencing this KER

ROS can upregulate protein kinase C, which stimulates the production of ceramide from sphingomyelinase. Ceramide activates NADPH oxidase, which can then produce more ROS (Soloviev & Kizub, 2019). Another feedback loop exists between the Nrf2/HO-1 signaling pathway and oxidative stress. The Nrf2/HO-1 signaling pathway is involved in negative feedback of oxidative stress, activating transcription of anti-oxidative enzymes to regulate cellular ROS and maintain a redox balance (Tahimic & Globus, 2017; Tian et al., 2017). Lastly, the MAPK pathway also exhibits a feedback loop. ERK can regulate ROS levels indirectly through p22phox, which increases ROS and upregulates antioxidants by Nrf2 activation. JNK activation can lead to FoxO activation, thereby resulting in antioxidant production (Arfin et al., 2021; Essers et al., 2004).

References

Annunziato, L. (2003), "Apoptosis induced in neuronal cells by oxidative stress: role played by caspases and intracellular calcium ions", *Toxicology Letters*, Vol. 139/2–3, https://doi.org/10.1016/S0378-4274(02)00427-7.

Arfin, S. et al. (2021), “Oxidative Stress in Cancer Cell Metabolism”, *Antioxidants 2021*, Vol. 10/5, MDPI, Basel, https://doi.org/10.3390/ANTIOX10050642

Azimzadeh, O. et al. (2021), "Activation of pparα by fenofibrate attenuates the effect of local heart high dose irradiation on the mouse cardiac proteome", *Biomedicines*, Vol. 9/12, MDPI, Basel, https://doi.org/10.3390/biomedicines9121845

Azimzadeh, O. et al. (2017), "Proteome analysis of irradiated endothelial cells reveals persistent alteration in protein degradation and the RhoGDI and NO signalling pathways", *International Journal of Radiation Biology*, Vol. 93/9, Informa, London, https://doi.org/10.1080/09553002.2017.1339332

Azimzadeh, O. et al. (2015), "Integrative proteomics and targeted transcriptomics analyses in cardiac endothelial cells unravel mechanisms of long-term radiation-induced vascular dysfunction", *Journal of Proteome Research*, Vol. 14/2, American Chemical Society, Washington, https://doi.org/10.1021/pr501141b

Bai, J. et al. (2020), "Irradiation-induced senescence of bone marrow mesenchymal stem cells aggravates osteogenic differentiation dysfunction via paracrine signaling", *American Journal of Physiology - Cell Physiology*, Vol. 318/5, American Physiological Society, https://doi.org/10.1152/ajpcell.00520.2019

Boyce, B. F. and L. Xing. (2007), "The RANKL/RANK/OPG pathway", *Current Osteoporosis Reports*, Vol. 5/3, https://doi.org/10.1007/s11914-007-0024-y

Cabrera, M. P. and R. H. Chihuailaf. (2011), "Antioxidants and the Integrity of Ocular Tissues", *Veterinary Medicine International*, Vol. 2011, Hindawi, London, https://doi.org/10.4061/2011/905153

Carvour, M. et al. (2008), "Chronic Low-Dose Oxidative Stress Induces Caspase-3-Dependent PKCδ Proteolytic Activation and Apoptosis in a Cell Culture Model of Dopaminergic Neurodegeneration", *Annals of the New York Academy of Sciences*, Vol. 1139/1, https://doi.org/10.1196/annals.1432.020.

Chen, L. et al. (2009), "Hydrogen peroxide-induced neuronal apoptosis is associated with inhibition of protein phosphatase 2A and 5, leading to activation of MAPK pathway", *The International Journal of Biochemistry & Cell Biology*, Vol. 41/6, Elsevier, Amsterdam, https://doi.org/10.1016/j.biocel.2008.10.029.

Crossthwaite, A. J., S. Hasan and R. J. Williams. (2002), "Hydrogen peroxide-mediated phosphorylation of ERK1/2, Akt/PKB and JNK in cortical neurones: dependence on Ca2+ and PI3-kinase", *Journal of Neurochemistry*, Vol. 80/1, John Wiley & Sons, Hoboken, https://doi.org/10.1046/j.0022-3042.2001.00637.x.

Deng, Z. et al. (2012), "Radiation-Induced c-Jun Activation Depends on MEK1-ERK1/2 Signaling Pathway in Microglial Cells", (I. Ulasov, Ed.) *PLoS ONE*, Vol. 7/5, https://doi.org/10.1371/journal.pone.0036739.

Diao, Y. et al. (2018), "Polyphenols (S3) Isolated from Cone Scales of Pinus koraiensis Alleviate Decreased Bone Formation in Rat under Simulated Microgravity", *Scientific Reports*, Vol. 8/1, Nature, https://doi.org/10.1038/s41598-018-30992-8

Domazetovic, V. et al. (2017), "Oxidative stress in bone remodeling: role of antioxidants", *Clinical cases in mineral and bone metabolism*, Vol. 14/2, pp. 209-216

El-Missiry, M. A. et al. (2018), "Neuroprotective effect of epigallocatechin-3-gallate (EGCG) on radiation-induced damage and apoptosis in the rat hippocampus", *International Journal of Radiation Biology*, Vol. 94/9, https://doi.org/10.1080/09553002.2018.1492755.

Fan, Z. et al. (2017), "L-carnitine preserves cardiac function by activating p38 MAPK/Nrf2 signalling in hearts exposed to irradiation", *European Journal of Pharmacology*, Vol. 804, Elsevier, Amsterdam, https://doi.org/10.1016/j.ejphar.2017.04.003

Hasan, H. F., R. R. Radwan and S. M. Galal. (2020), "Bradykinin-potentiating factor isolated from Leiurus quinquestriatus scorpion venom alleviates cardiomyopathy in irradiated rats via remodelling of the RAAS pathway", *Clinical and Experimental Pharmacology and Physiology*, Vol. 47/2, Wiley, https://doi.org/10.1111/1440-1681.13202

Hladik, D. et al. (2020), "CREB Signaling Mediates Dose-Dependent Radiation Response in the Murine Hippocampus Two Years after Total Body Exposure", *Journal of Proteome Research*, Vol. 19/1, https://doi.org/10.1021/acs.jproteome.9b00552.

Huang, Y. et al. (2021), "Mesenchymal Stem Cell-Conditioned Medium Protects Hippocampal Neurons From Radiation Damage by Suppressing Oxidative Stress and Apoptosis", *Dose-Response*, Vol. 19/1, https://doi.org/10.1177/1559325820984944.

Hughson, R. L., A. Helm and M. Durante. (2018), "Heart in space: Effect of the extraterrestrial environment on the cardiovascular system", *Nature Reviews Cardiology*, Vol. 15/3, Nature, https://doi.org/10.1038/nrcardio.2017.157

Kenchegowda, D. et al. (2018), "Selective Insulin-like Growth Factor Resistance Associated with Heart Hemorrhages and Poor Prognosis in a Novel Preclinical Model of the Hematopoietic Acute Radiation Syndrome", *Radiation Research*, Vol. 190/2, BioOne, https://doi.org/10.1667/RR14993.1

Kook, S. H. et al. (2015), "Irradiation inhibits the maturation and mineralization of osteoblasts via the activation of Nrf2/HO-1 pathway", *Molecular and Cellular Biochemistry*, Vol. 410/1–2, Nature, https://doi.org/10.1007/s11010-015-2559-z

Kozbenko, T. et al. (2022), “Deploying elements of scoping review methods for adverse outcome pathway development: a space travel case example”, *International Journal of Radiation Biology*, Vol. 98/12. https://doi.org/10.1080/09553002.2022.2110306

Lee, K., A. Lee and I. Choi. (2017), "Melandrii Herba Extract Attenuates H2O2-Induced Neurotoxicity in Human Neuroblastoma SH-SY5Y Cells and Scopolamine-Induced Memory Impairment in Mice", *Molecules*, Vol. 22/10, MDPI, Basel, https://doi.org/10.3390/molecules22101646.

Lehtinen, M. and A. Bonni. (2006), "Modeling Oxidative Stress in the Central Nervous System", *Current Molecular Medicine*, Vol. 6/8, https://doi.org/10.2174/156652406779010786.

Li, J. et al. (2013), "Oxidative Stress and Neurodegenerative Disorders", *International Journal of Molecular Sciences*, Vol. 14/12, https://doi.org/10.3390/ijms141224438.

Limoli, C. L. et al. (2004), "Radiation Response of Neural Precursor Cells: Linking Cellular Sensitivity to Cell Cycle Checkpoints, Apoptosis and Oxidative Stress", *Radiation Research*, Vol. 161/1, https://doi.org/10.1667/RR3112.

Manolagas, S. C. and M. Almeida. (2007), "Gone with the Wnts: β-Catenin, T-Cell Factor, Forkhead Box O, and Oxidative Stress in Age-Dependent Diseases of Bone, Lipid, and Glucose Metabolism", *Molecular Endocrinology*, Vol. 21/11, Oxford University Press, Oxford, https://doi.org/10.1210/me.2007-0259

Essers, M. A. et al. (2004), “FOXO transcription factor activation by oxidative stress mediated by the small GTPase Ral and JNK”. *The EMBO journal*, Vol. 23/24, EMBO, https://doi.org/10.1038/sj.emboj.7600476

Nagane, M. et al. (2021), "DNA damage response in vascular endothelial senescence: Implication for radiation-induced cardiovascular diseases", *Journal of Radiation Research*, Vol. 62/4, Oxford University Press, Oxford, https://doi.org/10.1093/jrr/rrab032

Park, H. et al. (2016), "GDF15 contributes to radiation-induced senescence through the ROS-mediated p16 pathway in human endothelial cells", *Oncotarget*, Vol. 7/9, https://doi.org/10.18632/oncotarget.7457

Park, D. H. et al. (2021), "Neuroprotective Effect of Gallocatechin Gallate on Glutamate-Induced Oxidative Stress in Hippocampal HT22 Cells", *Molecules*, Vol. 26/5, MDPI, Basel, https://doi.org/10.3390/molecules26051387.

Ping, Z. et al. (2020), "Oxidative Stress in Radiation-Induced Cardiotoxicity", *Oxidative Medicine and Cellular Longevity*, Vol. 2020, Hindawi, London, https://doi.org/10.1155/2020/3579143

Ramadan, R. et al. (2021), "The role of connexin proteins and their channels in radiation-induced atherosclerosis", *Cellular and Molecular Life Sciences*, Vol. 78, Nature, https://doi.org/10.1007/s00018-020-03716-3

Ramalingam, M. and S.-J. Kim. (2012), "Reactive oxygen/nitrogen species and their functional correlations in neurodegenerative diseases", *Journal of Neural Transmission*, Vol. 119/8, Springer Nature, Berlin, https://doi.org/10.1007/s00702-011-0758-7.

Ruffels, J., M. Griffin and J. M. Dickenson. (2004), "Activation of ERK1/2, JNK and PKB by hydrogen peroxide in human SH-SY5Y neuroblastoma cells: role of ERK1/2 in H2O2-induced cell death", *European Journal of Pharmacology*, Vol. 483/2–3, Elsevier, Amsterdam https://doi.org/10.1016/j.ejphar.2003.10.032.

Sakata, K. et al. (2015), "Roles of ROS and PKC-βII in ionizing radiation-induced eNOS activation in human vascular endothelial cells", *Vascular Pharmacology*, Vol. 70, Elsevier, Amsterdam, https://doi.org/10.1016/j.vph.2015.03.016

Schmidt-Ullrich, R. K. et al. (2000), "Signal transduction and cellular radiation responses.", *Radiation research*, Vol. 153/3, BioOne, https://doi.org/10.1667/0033-7587(2000)153[0245:stacrr]2.0.co;2

Schnegg, C. I. et al. (2012), "PPARδ prevents radiation-induced proinflammatory responses in microglia via transrepression of NF-κB and inhibition of the PKCα/MEK1/2/ERK1/2/AP-1 pathway", *Free Radical Biology and Medicine*, Vol. 52/9, https://doi.org/10.1016/j.freeradbiomed.2012.02.032.

Soloviev, A. I. and I. V. Kizub. (2019), "Mechanisms of vascular dysfunction evoked by ionizing radiation and possible targets for its pharmacological correction", *Biochemical Pharmacology*, Vol. 159, Elsevier, Amsterdam, https://doi.org/10.1016/j.bcp.2018.11.019

Suman, S. et al. (2013), "Therapeutic and space radiation exposure of mouse brain causes impaired DNA repair response and premature senescence by chronic oxidant production", *Aging*, Vol. 5/8, https://doi.org/10.18632/aging.100587.

Sun, Y. et al. (2013), "Treatment of hydrogen molecule abates oxidative stress and alleviates bone loss induced by modeled microgravity in rats", *Osteoporosis International*, Vol. 24/3, Nature, https://doi.org/10.1007/s00198-012-2028-4

Tahimic, C. G. T. and R. K. Globus. (2017), “Redox Signaling and Its Impact on Skeletal and Vascular Responses to Spaceflight”, *International Journal of Molecular Sciences*, Vol. 18/10, MDPI, Basel, https://doi.org/10.3390/IJMS18102153

Tian, Y. et al. (2017), "The impact of oxidative stress on the bone system in response to the space special environment", *International Journal of Molecular Sciences*, Vol. 18/10, MDPI, Basel, https://doi.org/10.3390/ijms18102132

Tian, W. et al. (2019), "Neuroprotective Effects of Cornus officinalis on Stress-Induced Hippocampal Deficits in Rats and H2O2-Induced Neurotoxicity in SH-SY5Y Neuroblastoma Cells", *Antioxidants*, Vol. 9/1, MDPI, Basel, https://doi.org/10.3390/antiox9010027.

Tian, R. et al. (2020), "miR-137 prevents inflammatory response, oxidative stress, neuronal injury and cognitive impairment via blockade of Src-mediated MAPK signaling pathway in ischemic stroke", *Aging*, Vol. 12/11, https://doi.org/10.18632/aging.103301.

Valerie, K. et al. (2007), "Radiation-induced cell signaling: inside-out and outside-in", *Molecular Cancer Therapeutics*, Vol. 6/3, American Association for Cancer Research, https://doi.org/10.1158/1535-7163.MCT-06-0596

Venkatesulu, B. P. et al. (2018), “Radiation-Induced Endothelial Vascular Injury: A Review of Possible Mechanisms”, *JACC: Basic to translational science*, Vol. 3/4, Elsevier, Amsterdam, https://doi.org/10.1016/j.jacbts.2018.01.014.

Wang. (2010), "Selective neuronal vulnerability to oxidative stress in the brain", *Frontiers in Aging Neuroscience*, https://doi.org/10.3389/fnagi.2010.00012.

Wang, Y., M. Boerma and D. Zhou. (2016), "Ionizing Radiation-Induced Endothelial Cell Senescence and Cardiovascular Diseases", *Radiation Research*, Vol. 186/2, BioOne, https://doi.org/10.1667/RR14445.1

Wortel, R. C. et al. (2019), "Sildenafil Protects Endothelial Cells From Radiation-Induced Oxidative Stress", *The Journal of Sexual Medicine*, Vol. 16/11, Elsevier, Amsterdam, https://doi.org/10.1016/j.jsxm.2019.08.015

Wu, Y., M. Chen and J. Jiang. (2019), "Mitochondrial dysfunction in neurodegenerative diseases and drug targets via apoptotic signaling", *Mitochondrion*, Vol. 49, https://doi.org/10.1016/j.mito.2019.07.003.

Xin, M. et al. (2015), "Attenuation of hind-limb suspension-induced bone loss by curcumin is associated with reduced oxidative stress and increased vitamin D receptor expression", *Osteoporosis International*, Vol. 26/11, Nature, https://doi.org/10.1007/s00198-015-3153-7

Xu, B. et al. (2019), "Oxidation Stress-Mediated MAPK Signaling Pathway Activation Induces Neuronal Loss in the CA1 and CA3 Regions of the Hippocampus of Mice Following Chronic Cold Exposure", *Brain Sciences*, Vol. 9/10, MDPI, Basel, https://doi.org/10.3390/brainsci9100273.

Yoo, Y. M., T. Y. Han and H. S. Kim. (2016), "Melatonin suppresses autophagy induced by clinostat in preosteoblast MC3T3-E1 cells", *International Journal of Molecular Sciences*, Vol. 17/4, MDPI, Basel, https://doi.org/10.3390/ijms17040526

Zhao, Z.-Y. et al. (2013), "Edaravone Protects HT22 Neurons from H 2 O 2 -induced Apoptosis by Inhibiting the MAPK Signaling Pathway", *CNS Neuroscience & Therapeutics*, Vol. 19/3, John Wiley & Sons, Hoboken, https://doi.org/10.1111/cns.12044.

Zhao, D. et al. (2017), "Anti-Neuroinflammatory Effects of Fucoxanthin via Inhibition of Akt/NF-κB and MAPKs/AP-1 Pathways and Activation of PKA/CREB Pathway in Lipopolysaccharide-Activated BV-2 Microglial Cells", *Neurochemical Research*, Vol. 42/2, Springer Nature, Berlin, https://doi.org/10.1007/s11064-016-2123-6.

Relationship: 2772: Oxidative Stress leads to Increased pro-inflammatory mediators

AOPs Referencing Relationship

AOP Name	Adjacency	Weight of Evidence	Quantitative Understanding
Deposition of energy leads to vascular remodeling	adjacent	Moderate	Moderate

Evidence Supporting Applicability of this Relationship

Taxonomic Applicability

Term	Scientific Term	Evidence	Links
human	Homo sapiens	Low	NCBI
mouse	Mus musculus	High	NCBI
rat	Rattus norvegicus	Moderate	NCBI

Life Stage Applicability

Life Stage	Evidence
Juvenile	Low
Adult	Low
Not Otherwise Specified	Moderate

Sex Applicability

Sex	Evidence
Male	High
Female	Low
Unspecific	Low

Most evidence defining the relationship is derived from mice or rat models. A low number of *in-vitro* human studies were available. Males have been studied more often than females. The age of the models remained unspecified in several studies, while a few studies reported evidence from adult and adolescent models.

Key Event Relationship Description

The increase in reactive oxygen species (ROS) and reactive nitrogen species (RNS) during a state of oxidative stress can stimulate an increase in pro-inflammatory mediators. Reactive oxygen and nitrogen species (RONS) cause cellular damage, which leads to the production of pro-inflammatory mediators (Slezak et al., 2015; Sylvester et al., 2018; Wang et al., 2019a). In addition, ROS can act as second messenger signalling molecules in activating pro-inflammatory transcription factor nuclear factor kappa B (NF-κB),

resulting in increased production of pro-inflammatory cytokines and adhesion factors (Ping et al., 2020; Slezak et al., 2017; Slezak et al., 2015; Sylvester et al., 2018; Venkatesulu et al., 2018; Wang et al., 2019a). The inflammatory state induced by RONS will further increase RONS, leading to a cycle of chronic inflammation and oxidative stress (Venkatesulu et al., 2018; Wang et al., 2019a).

Evidence Supporting this KER

Overall weight of evidence: Moderate

Biological Plausibility

The biological plausibility of the linkage between oxidative stress and pro-inflammatory mediators is strongly supported by review papers on the subject (Ping et al., 2020; Ramadan et al., 2021; Slezak et al., 2017; Slezak et al., 2015; Sylvester et al., 2018; Venkatesulu et al., 2018; Wang et al., 2019a). Pro-inflammatory mediators are released in instances of cell damage to recruit macrophages, monocytes, and other scavengers to ingest and degrade dead and damaged cells. As a major pathway of cell damage, oxidative stress causes upregulation of pro-inflammatory mediators including NF-κB, transforming growth factor-β (TGF-β), tumour necrosis factor-α (TNF-α), interleukin-1 (IL-1), and interleukin-6 (IL-6) (Ping et al., 2020; Slezak et al., 2017; Slezak et al., 2015; Sylvester et al., 2018; Venkatesulu et al., 2018; Wang et al., 2019a). Oxidative stress also stimulates a rise in pro-inflammatory adhesion factors, such as E-selectin, intercellular adhesion molecule-1 (ICAM1), and vascular cell adhesion molecule-1 (VCAM1), which facilitate inflammation by assisting the entrance of inflammatory cells into tissues and recruiting macrophages (Ping et al., 2020; Slezak et al., 2017; Slezak et al., 2015; Sylvester et al., 2018; Venkatesulu et al., 2018; Wang et al., 2019a).

Once antioxidant levels become exhausted in a state of oxidative stress, ROS are present in higher concentrations and can therefore act more effectively as second messenger signalling molecules in activating pro-inflammatory transcription factors, such as NF-κB, and stimulating production of pro-inflammatory cytokines, such as IL-1, IL-6 and TNF-α (Ping et al., 2020; Sylvester et al., 2018; Wang et al., 2019a). NF-κB is normally kept in an inactive state through formation of a complex with the IkB family of inhibitor proteins but is activated by oxidative stress through nuclear translocation of the complex to the promoter areas of inflammation regulatory genes (Ping et al., 2020; Slezak et al., 2017). The macrophages that are recruited in the resulting inflammatory response can also produce ROS and activate the pro-inflammatory mediator, TGF-β, forming a positive feedback loop (Venkatesulu et al., 2018). Another positive feedback loop is formed by ROS and NF-κB, as ROS activates NF-κB, resulting in the expression of the genes cyclooxygenase-2 (COX-2) and 5-lipoxygenase (5-LPO), which are responsible for ROS production (Ping et al., 2020). In addition, NF-κB is also involved in the production of the pro-inflammatory adhesion factors ICAM and VCAM (Ping et al., 2020; Slezak et al., 2017; Slezak et al., 2015).

Oxidative stress may also result in oxidation of low-density lipoproteins, allowing the lipoproteins to be ingested by macrophages. This could initiate the atherosclerotic process (plaque build-up in the arteries) and subsequently lead to lipid cells secreting pro-inflammatory cytokines, such as IL-1β and TGF-β (Ramadan et al., 2021; Slezak et al., 2017; Sylvester et al., 2018; Ping et al., 2020; Venkatesulu et al., 2018).

Empirical Evidence

The empirical evidence relevant to this KER provides moderate support for the linkage between increases in oxidative stress and increases in pro-inflammatory mediators. The evidence to support this relationship comes from studies examining the effects of ionizing radiation, such as ^{137}Cs gamma-rays, on the cardiovascular system. There is moderate evidence for a dose- and time-dependent relationship between oxidative stress and pro-inflammatory mediators (Abdel-Magied & Shedid, 2019; Chen et al., 2019; Cho et al., 2017; Ismail et al., 2015; Ismail et al., 2016; Karam et al., 2019; Philipp et al., 2020; Wang et al., 2019a).

Dose Concordance

Current literature on the dose-dependent relationship between oxidative stress and increases in pro-inflammatory mediators is moderate. Chen et al. (2019) exposed male Sprague Dawley rats to simulated microgravity for 7 and 21 days and measured levels of the oxidative stress marker H_2O_2 along with the pro-inflammatory mediators, IL-6, interferon-gamma (IFN-γ), and TNF-α. Their finding provided evidence of dose concordance between oxidative stress and pro-inflammatory mediators, as the study observed more significant changes to H2O2 levels at 7 days than 21 days, while IL-6, IFN-γ, and TNF-α levels were more significantly affected at day 21 than day 7 (Chen et al., 2019). Philipp et al. (2020) irradiated human telomerase-immortalized coronary artery endothelial cells (TICAE cells) with 0.25, 0.5, 2, and 10 Gy of 137Cs gamma rays. They found that superoxide dismutase (SOD) decreased consistently at 2 Gy, while pro-inflammatory mediators showed consistent increases at 2 or 10 Gy, but not at lower doses. Other studies using gamma rays show levels of oxidative stress markers increase with subsequent increases to pro-inflammatory mediators following exposure to high doses (>2 Gy), with some markers being significantly affected at low doses (<2 Gy) (Abdel-Magied & Shedid, 2019; Cho et al., 2017; Ismail et al., 2016; Ismail et al., 2015; Karam et al., 2019). However, not all studies demonstrated dose concordance. Wang et al. (2019b) irradiated human endothelial cells with various doses of gamma rays. They found pro-inflammatory mediators significantly increased at lower doses (0.2-5Gy) than oxidative stress (5 Gy only), although this could be due to the sensitivity of the assays.

Time Concordance

Current literature on the time-dependent relationship between oxidative stress and increases in pro-inflammatory mediators is low. Cho et al. (2017) irradiated male C57BL/6 mice and measured levels of superoxide and the pro-inflammatory mediators TNF-α and monocyte chemoattractant protein (MCP-1), at 4, 8, and 24 hours post-irradiation. Oxidative stress and pro-inflammatory mediators demonstrated a time concordant relationship, as ROS levels were significantly increased at 4 hours post-irradiation, while both pro-inflammatory mediators did not significantly change until 8 hours (Cho et al., 2017). Philipp et al. (2020) irradiated telomerase immortalized human coronary artery endothelial cells and measured levels of the antioxidant, SOD1, and the pro-inflammatory adhesion factor, ICAM1, at 4 hours, 24 hours, 48 hours, and 1 week post-irradiation. Neither SOD1 nor ICAM1 followed consistent changes over time across all doses. However, the earliest decrease in SOD1 and the earliest increase in ICAM1 were both found at 4 hours (Philipp et al., 2020).

Incidence concordance

Few studies demonstrated incidence concordance between oxidative stress and increased pro-inflammatory mediators. In human TICAE cells irradiated with 2 Gy of gamma rays, SOD1 was decreased 0.5-fold at 24h post-irradiation, while ICAM1 was increased 1.1-fold at this dose and time (Philipp et al., 2020).

Essentiality

Studies that treated models with countermeasures to suppress the increase in oxidative stress caused by ionizing radiation exposure found that subsequent increases in pro-inflammatory mediators were also significantly attenuated (Abdel-Magied & Shedid, 2019; Karam et al., 2019). Blocking ionizing radiation effect on oxidative stress (upstream KE) and analyzing the subsequent effect on pro-inflammatory mediators (downstream KE) provided evidence for essentiality between the KEs.

Treatment of irradiated albino rat heart tissue with the antidiabetic drug, metformin (50 mg/kg daily for 2 weeks), provided evidence for its efficacy as an antioxidant and anti-inflammatory drug. Metformin treatment following irradiation resulted in a recovery of SOD and catalase (CAT) activity to 90% and 44%, respectively, compared to irradiated groups. In addition to attenuating ionizing radiation effect on oxidative stress, metformin mitigated increases to NF-κB, TNF-α, and IL-6 levels, as well as reduced elevated E-selectin, ICAM, and VCAM levels by 0.5-, 0.55-, and 0.6-fold, respectively (Karam et al., 2019).

Irradiated Wistar albino rats were treated with the food and drug additive ZnO-NP (10 mg/kg daily for 2 weeks), which has antioxidant effects. Treatment with ZnO-NPs attenuated all IR-induced changes to oxidative and inflammatory markers. Compared to the irradiated group, ZnO-NP treatment resulted in restoration of CAT, SOD, glutathione (GSH), and glutathione peroxidase (GPx) levels by ~104%, ~73%, ~91%, and ~73%, respectively. Elevated levels of ICAM, TNF-α, IL-18, and C-reactive protein (CRP) were reduced by ~44%, ~46%, ~45%, and ~42%, respectively, compared to irradiated groups (Abdel-Magied & Shedid, 2019).

Irradiated Wistar rats were treated with flaxseed oil (FSO) (500 mg/kg-bw daily for 7 days), which has a uniquely high content of the antioxidant lignans. Treatment with FSO significantly reduced IR-induced changes to both antioxidants and pro-inflammatory mediators. IR-induced reductions to the activity of the antioxidants SOD, CAT, and GSH-Px were significantly alleviated back to levels statistically similar to the controls. Reduced levels of pro-inflammatory mediators, TNF-α, IL-1β, and IL-6, back to control levels was also observed (Ismail et al., 2016).

Uncertainties and Inconsistencies

- Chen et al. (2019) found that levels of the pro-inflammatory mediators, IL-6, IFN-γ, and TNF-α, decreased following 7 and 21 days of microgravity exposure, contrary to the trend generally observed following ionizing radiation exposure (Chen et al., 2019).

Quantitative Understanding of the Linkage

Several examples of studies that provide quantitative understanding of the relationship are summarized. All data represented is statistically significant unless otherwise indicated.

Response-response relationship

Dose/Incidence Concordance

Reference	Experiment Description	Result
	In vivo. Adult male albino rats underwent whole-body	

Karam et al., 2019	*In vivo*. Adult male albino rats underwent whole-body irradiation with 5 Gy of ^{137}Cs gamma rays at a rate of 0.665 cGy/s. Measurements of oxidative stress markers, including levels of the antioxidants SOD and CAT, were taken from the heart tissue of the rats, along with measurements of inflammatory markers, including nuclear factor kappa B (NF-κB), tumour necrosis factor-α (TNF-α), and interleukin-6 (IL-6), as well as the pro-inflammatory adhesion factors, E-selectin, ICAM, and VCAM.	Compared to non-irradiated controls, activity levels of SOD and CAT decreased significantly by 57% and 43%, respectively. This was accompanied by significant increases to inflammatory markers by 96%, 335%, and 292% to NF-κB, TNF-α, and IL-6, respectively. There were also similarly significant increases in the endothelial adhesion molecules, E-selectin, ICAM, and VCAM, by 287%, 234%, and 207%, respectively.
Wang et al., 2019b	*In vitro*. Human umbilical vein endothelial cells (HUVECs) were irradiated with 0.2, 0.5, 1, 2, and 5 Gy of ^{137}Cs gamma rays. ROS levels were measured as a marker for oxidative stress, along with pro-inflammatory cytokines, IL-6 and TNF-α.	Although ROS levels increased in a dose-dependent fashion from 0.5-5 Gy, they did not change significantly until a ~36% increase at 5 Gy. IL-6 levels significant changed at doses >0.2 Gy. IL-6 levels increased from 0 Gy to 0.2 Gy, decreased from 0.2 Gy to 0.5 Gy, and gradually increased again from 0.5 Gy until a maximum increase of ~50% at 5 Gy. TNF-α levels did not change significantly until 2 Gy. TNF-α levels increased by ~25% at 2 Gy and 5 Gy.
Philipp et al., 2020	*In vitro*. Human TICAE cells were irradiated with 0.25, 0.5, 2, and 10 Gy of ^{137}Cs gamma rays at a rate of 0.4 Gy/min. Levels of the antioxidant, SOD1, were measured along with the inflammatory marker, ICAM1, and pro-inflammatory transcription factor STAT1, at 4 hours, 24 hours, 48 hours, and 1 week post-irradiation to assess oxidative stress and pro-inflammatory mediators, respectively.	SOD1 levels did not follow a dose-dependent pattern of change at any time point. SOD1 levels had a maximum decrease of 0.5-fold at 2 Gy. ICAM1 levels had maximum increases of 1.4-fold at 10 Gy. The earliest increase in STAT1 occurred after 2 Gy.
Abdel-Magied & Shedid, 2019	*In vivo*. Adult, male, Wistar albino rats underwent whole body irradiation with 8 Gy of ^{137}Cs gamma rays at a rate of 0.4092 Gy/min. The antioxidants SOD, CAT, GSH, and GPx were measured to assess IR-induced oxidative stress. The inflammatory markers ICAM1, TNF-α, IL-18, and CRP were measured to examine subsequent changes in pro-inflammatory mediators.	Compared to non-irradiated controls, SOD, CAT, GSH, and GPx decreased by 53%, 62%, 56%, and 51%, respectively. Compared to non-irradiated controls, ICAM1, TNF-α, IL-18, and CRP increased by ~138%, ~132%, ~150%, and ~116%, respectively.
Cho et al., 2017	*In vivo*. 10-week-old, male, C57BL/6 mice were irradiated with fractionated doses of 40, 60, and 106.7 Gy of ^{137}Cs gamma rays over the course of 4 weeks. Levels of superoxide anion were measured along with the protein expression of the pro-inflammatory mediators TNF-α and MCP-1.	ROS levels increased to a maximum of 6.3-fold compared to the control at 4 hours post-irradiation. Protein expression of TNF-α and MCP-1 both had a maximum increase of 18.4-fold and 5.8-fold, respectively, at 8 hours post-irradiation.
Ismail et al., 2016	*In vivo*. Female Wistar rats underwent whole-body irradiation with 7 Gy of ^{137}Cs gamma rays at a rate of 0.456 Gy/min. Levels of the antioxidants SOD, CAT, and GSH-Px were measured following irradiation, along with levels of the pro-inflammatory cytokines TNF-α, IL-1β, IL-6, and TGF- β1.	Following irradiation, the activity of antioxidant enzymes significantly decreased following irradiation (19% for SOD, 33% for CAT, and 19% for GSH-Px). This increase in oxidative stress was accompanied by an increase in pro-inflammatory cytokine levels of 199%, 429%, 142%, and 147% for TNF-α, IL-1β, IL-6, and TGF- β1, respectively.
Ismail et al., 2015	*In vivo*. Female Wistar rats underwent whole-body irradiation with 7 Gy of ^{137}Cs gamma rays at a rate of 0.456 Gy/min. Levels of the antioxidants SOD, CAT, and GSH-Px were measured following irradiation, along with levels of the pro-inflammatory cytokines TNF-α, IL-1β, IL-6, and TGF- β1.	Following irradiation, the activity of antioxidant enzymes significantly decreased following irradiation (~19% for SOD, ~34% for CAT, and ~16% for GSH-Px). This increase in oxidative stress was accompanied by an increase in pro-inflammatory cytokine levels of ~257%, ~150%, and ~160% for TNF-α, IL-6, and TGF- β1, respectively.
Chen et al., 2019	*In vivo*. Male Sprague Dawley rats underwent 7 and 21 days of tail suspension to simulate microgravity conditions. Levels of H_2O_2 were measured to analyze microgravity oxidative stress. Levels of IL-6, IFN-γ, and TNF-α were measured to analyze associated changes to pro-inflammatory mediators.	After 7 days of simulated microgravity, H_2O_2 levels increased by ~39-75% compared to the control depending on the region of tissue analyzed. After 21 days of simulated microgravity, expression of IL-6, IFN-γ, and TNF-α decreased by ~32-52%, ~39-40%, and ~24-42%, respectively.

Time-scale

Time Concordance

Reference	Experiment Description	Result
	In vitro. Human TICAE cells were irradiated with 0.25, 0.5, 2, and 10 Gy	

Philipp et al., 2020	of ^{137}Cs gamma rays at a rate of 400 mGy/min. Levels of the antioxidant SOD1 were measured along with the inflammatory marker ICAM1 at 4 hours, 24 hours, 48 hours, and 1 week post-irradiation to assess oxidative stress and pro-inflammatory mediators, respectively.	TICAE cells that were irradiated with 10 Gy showed ~1.2-fold increases in SOD1 levels at 24 and 48 hours, a decrease of ~0.2-fold at 1 week, and no change at 4 hours. ICAM1 levels increased by ~1.2-fold at 4 hours, ~1.15 at 24 hours, ~1.1-fold at 48 hours, and ~1.4-fold at 1 week).
Cho et al., 2017	*In vivo*. Male C57BL/6 mice were irradiated with fractionated doses of 40, 60, and 106.7 Gy of ^{137}Cs gamma rays over the course of 4 weeks. Levels of superoxide anion were measured along with the protein expression of the pro-inflammatory mediators and MCP-1 at 4, 8, and 24 hours post-irradiation.	ROS levels were significantly increased at 4, 8, and 24 hours. ROS generation was highest at 4 hours post-irradiation (6.3-fold increase compared to control) before decreasing by 59% from 4 hours to 8 hours (2.6-fold increase compared to control) and maintaining the same level at 24 hours (2.6-fold increase compared to control). Protein expression of TNF-α and MCP-1 both increased in a time-dependent manner from 0 hours to 8 hours before a significant reduction from 8 hours to 24 hours. Both pro-inflammatory mediators saw their first significant changes at 8 hours, but only TNF-α experienced another significant increase at 24 hours post-irradiation while MCP-1 did not.

Known modulating factors

Modulating factor	Details	Effects on the KER	References
Drug	Metformin (antidiabetic drug)	50 mg/kg daily for 2 weeks restored SOD and CAT levels while reducing various pro-inflammatory mediators after irradiation	Karam et al., 2019
Drug	ZnO-NPs (antioxidant properties)	10 mg/kg daily for 2 weeks attenuated all radiation-induced changes to oxidative stress and pro-inflammatory markers	Abdel-Magied & Shedid, 2019
Drug	FSO (contains antioxidants)	CAT, SOD, GSh and GPx levels were restored, and reduced pro-inflammatory mediator levels	Ismail et al., 2016

Known Feedforward/Feedback loops influencing this KER

- Positive feedback loop: oxidative stress upregulates production of pro-inflammatory cytokines, which in turn upregulate ROS production. The macrophages that are recruited in an oxidative stress-induced inflammatory response can also produce ROS and activate the pro-inflammatory mediator, TGF-β (Venkatesulu et al., 2018). Another positive feedback loop is formed by ROS and NF-κB, as ROS activates NF-κB, resulting in expression of the genes, COX-2 and 5-LPO, which are responsible for ROS production (Ping et al., 2020).

References

Abdel-Magied, N. and S. M. Shedid (2019), “Impact of zinc oxide nanoparticles on thioredoxin-interacting protein and asymmetric dimethylarginine as biochemical indicators of cardiovascular disorders in gamma-irradiated rats”, *Environmental Toxicology*, Vol. 35, John Wiley & Sons, Ltd., Hoboken, https://doi.org/10.1002/tox.22879

Chen, B. et al. (2019), “The Impacts of Simulated Microgravity on Rat Brain Depended on Durations and Regions”, *Biomedical and Environmental Sciences*, Vol. 32/7, Elsevier, Amsterdam, https://doi.org/10.3967/bes2019.067

Cho, H. J. et al. (2017), “Role of NADPH oxidase in radiation-induced pro-oxidative and pro-inflammatory pathways in mouse brain”, *International Journal of Radiation Biology*, Vol. 93/11, Informa, London, https://doi.org/10.1080/09553002.2017.1377360

Ismail, A. F. M., F.S.M. Moawed and M. A. Mohamed (2015), “Protective mechanism of grape seed oil on carbon tetrachloride-induced brain damage in γ-irradiated rats”, *Journal of Photochemistry and Photobiology B: Biology*, Vol. 153, Elsevier, Amsterdam, https://doi.org/10.1016/j.jphotobiol.2015.10.005

Ismail, A. F. M., A. A. M. Salem and M. M. T. Eassawy (2016), “Modulation of gamma-irradiation and carbon tetrachloride induced oxidative stress in the brain of female rats by flaxseed oil”, *Journal of Photochemistry and Photobiology B: Biology*, Vol. 161, Elsevier, Amsterdam, https://doi.org/10.1016/j.jphotobiol.2016.04.031

Karam, H. M. and R. R. Radwan (2019), “Metformin modulates cardiac endothelial dysfunction, oxidative stress and inflammation in irradiated rats: A new perspective of an antidiabetic drug”, *Clinical and Experimental Pharmacology and Physiology*, Vol. 46/12, Wiley-Blackwell, Hoboken, https://doi.org/10.1111/1440-1681.13148

Kozbenko, T. et al. (2022), “Deploying elements of scoping review methods for adverse outcome pathway development: a space travel case example”, *International Journal of Radiation Biology*, Vol. 98/12. https://doi.org/10.1080/09553002.2022.2110306

Philipp, J. et al. (2020), “Radiation Response of Human Cardiac Endothelial Cells Reveals a Central Role of the cGAS-STING Pathway in the Development of Inflammation”, *Proteomes*, Multidisciplinary Digital Publishing Institute, Basel, https://doi.org/10.3390/proteomes8040030

Ping, Z. et al. (2020), “Review Article Oxidative Stress in Radiation-Induced Cardiotoxicity”, *Oxidative Medicine and Cellular*

Longevity, Vol. 2020, Hindawi, London, https://doi.org/10.1155/2020/3579143

Ramadan, R. et al. (2021), "The role of connexin proteins and their channels in radiation-induced atherosclerosis", *Cellular and molecular life sciences: CMLS*, Vol. 78/7, Springer, London, https://doi.org/10.1007/s00018-020-03716-3

Slezak, J. et al. (2017), "Potential markers and metabolic processes involved in the mechanism of radiation-induced heart injury", *Canadian Journal of Physiology and Pharmacology*, Vol. 95/10, Canadian Science Publishing, Ottawa, https://doi.org/10.1139/cjpp-2017-0121.

Slezak, J. et al. (2015), "Mechanisms of cardiac radiation injury and potential preventive approaches", *Canadian Journal of Physiology and Pharmacology*, Vol. 93/9, Canadian Science Publishing, Ottawa, https://doi.org/10.1139/CJPP-2015-0006

Sylvester, C. B. et al. (2018), "Radiation-induced Cardiovascular Disease: Mechanisms and importance of Linear energy Transfer", *Frontiers in Cardiovascular Medicine*, Vol. 5, Frontiers Media SA, Lausanne, https://doi.org/10.3389/fcvm.2018.00005

Venkatesulu, B. P. et al. (2018), "Radiation-Induced Endothelial Vascular Injury: A Review of Possible Mechanisms", *JACC: Basic to translational science*, Vol. 3/4, Elsevier, Amsterdam, https://doi.org/10.1016/j.jacbts.2018.01.014

Wang, H. et al. (2019a), "Radiation-induced heart disease: a review of classification, mechanism and prevention", *International Journal of Biological Sciences*, Vol. 15/10, Ivyspring International Publisher, Sydney, https://doi.org/10.7150/ijbs.35460

Wang, H. et al. (2019b), "Gamma Radiation-Induced Disruption of Cellular Junctions in HUVECs Is Mediated through Affecting MAPK/NF-κB Inflammatory Pathways", *Oxidative medicine and cellular longevity*, Vol. 2019, Hindawi, London, https://doi.org/10.1155/2019/1486232.

Relationship: 2773: Altered Signaling leads to Altered, Nitric Oxide Levels

AOPs Referencing Relationship

AOP Name	Adjacency	Weight of Evidence	Quantitative Understanding
Deposition of energy leads to vascular remodeling	adjacent	Moderate	Low

Evidence Supporting Applicability of this Relationship

Taxonomic Applicability

Term	Scientific Term	Evidence	Links
human	Homo sapiens	Low	NCBI
mouse	Mus musculus	Moderate	NCBI
rat	Rattus norvegicus	Moderate	NCBI

Life Stage Applicability

Life Stage	Evidence
Adult	Low
Not Otherwise Specified	Moderate

Sex Applicability

Sex	Evidence
Male	Low
Female	Low
Unspecific	Moderate

The majority of the evidence for this KER is from rat and mouse models. Most evidence regarding sex and lifestage is unspecified with a small amount of evidence from adult models.

Key Event Relationship Description

Multiple signaling pathways can regulate nitric oxide (NO) levels. The phosphatidylinositol 3-kinase (PI3K)/Akt pathway can activate nitric oxide synthase (NOS), an enzyme that produces NO, through phosphorylation (Hemmings & Restuccia 2012; Nagane et al., 2021). The RhoA/Rho kinase (ROCK) pathway inhibits both the expression and phosphorylation of NOS (Yao et al., 2010). Furthermore, the renin-angiotensin-aldosterone system (RAAS) can both inhibit NOS to reduce vasodilation and activate NOS as a countermeasure for vasoconstriction (Millatt, Abdel-Rahman & Siragy, 1999). The extracellular signal-regulated protein kinase 5

(ERK5)/kruppel-like factor 2 (KLF2) pathway can increase transcription of endothelial NOS (eNOS), which results in increased NO levels (Paudel, Fusi & Schmidt, 2021). Lastly, the acidic sphingomyelinase/ceramide pathway can activate NADPH oxidase (NOX) production of reactive oxygen species (ROS) that react with NO, resulting in lower NO levels (Soloviev & Kizub, 2019). Alterations in these pathways will result in altered NO levels.

Evidence Supporting this KER

Overall weight of evidence: Moderate

Biological Plausibility

The biological plausibility surrounding the connection between altered signaling pathways and altered NO levels is well-supported by the literature. Studies have shown that altered signaling pathways lead to altered NO levels (Azimzadeh et al., 2015; Azimzadeh et al., 2017; Hasan, Radwan & Galal, 2019; Shi et al., 2012; Siamwala et al., 2010).

Multiple signaling pathways can influence NO levels. Under normal physiological conditions, the PI3K/Akt pathway is regulated by various growth factors and other signaling molecules to modulate eNOS phosphorylation and therefore NO production (Hemmings & Restuccia, 2012). Phosphorylation of eNOS can affect its function. Phosphorylation at Ser1177 activates the enzyme, while phosphorylation at Thr495 acts in reverse and decreases enzymatic activity instead (Forstermann, 2010; Nagane et al., 2021). In endothelial cells, Thr495 is constitutively phosphorylated by kinases like protein kinase C (PKC) (Forstermann, 2010). Following Akt activation, eNOS is phosphorylated on Ser1177 to activate the enzyme and thus NO production is upregulated (Karar & Maity, 2011). Although peroxisome proliferator-activated receptor α (PPARα) can increase eNOS directly through transcription, it can also increase vascular endothelial growth factor (VEGF) (Du, Wagner & Wagner, 2020), which can activate the PI3K pathway to activate eNOS (Hicklin & Ellis, 2005). Alternatively, activation of the RhoA/ROCK pathway leads to a decrease in NO bioavailability (Yao et al., 2010). The RhoA/ROCK pathway causes eNOS mRNA destabilization and prevents Ser1177 eNOS phosphorylation by Akt (Yao et al., 2010). However, phosphorylation of RhoGDI, a regulator in the RhoA/ROCK pathway, causes increased affinity to GTP-RhoA, sequestering the active form of RhoA and preventing eNOS inhibition (Dovas & Couchman, 2005). The RAAS pathway results in the production of angiotensin II (AngII) which can cause various downstream effects on vascular homeostasis, including inducing vasoconstriction (Millatt, Abdel-Rahman & Siragy, 1999). AngII can downregulate eNOS Ser1177 phosphorylation to prevent vasodilation (Ding et al., 2020; Millatt, Abdel-Rahman & Siragy, 1999), or activate eNOS as a corrective measure (Millatt, Abdel-Rahman & Siragy, 1999). As a result, depending on the mechanism, NO levels can either increase or decrease after AngII stimulation. The ERK5/KLF2 pathway results in activation of the KLF2 transcription factor, which increases transcription of eNOS (Paudel, Fusi & Schmidt, 2021).

Empirical Evidence

The empirical evidence to support this KER is provided by *in vivo* mouse and rat models and *in vitro* models of human coronary artery endothelial cell (HCAECs), human umbilical vein endothelial cells (HUVECs), and EA.hy96 cells (a hybrid of HUVECs and A549 cells). The effects of altered signaling pathways on the levels of NO as well as inducible NOS (iNOS) and eNOS have been investigated. These studies examined levels of signaling molecules in insulin-dependent PI3K/Akt pathway such as IGFR1, PPARα, PI3K, Akt, and the phosphorylated versions of each (Azimzadeh et al., 2015; Azimzadeh et al., 2021; Shi et al., 2012), RAAS pathway indicator, AngII (Hasan, Radwan & Galal, 2019), phosphorylated Rho GDP-dissociation inhibitor (p-RhoGDI) in the RhoA/ROCK pathway (Azimzadeh et al., 2017), ERK5 and KLF2 (Sadhukhan et al., 2020), and the effect they have on NO. The studies used stressors such as X-rays (Azimzadeh et al., 2015; Azimzadeh et al., 2017; Azimzadeh et al., 2021), gamma rays (Hasan, Radwan & Galal, 2019; Sadhukhan et al., 2020) and altered gravity (Shi et al., 2012; Siamwala et al., 2010).

Dose Concordance

There is moderate evidence to demonstrate dose concordance between altered signaling pathways leading to altered NO levels. Activated RhoA reduces the activity and abundance of eNOS (Yao et al., 2010). HCAECs irradiated with 0.5 Gy demonstrated a 0.7-fold decrease in p-RhoGDI, a 0.6-fold decrease in p-eNOS and a 0.8-fold decrease in cellular NO, 7 days after exposure (Azimzadeh et al., 2017). The decrease in p-RhoGDI, involved in the RhoA/ROCK pathway, was correlated with a decrease in p-eNOS and NO (Azimzadeh et al., 2017). HSP90, a protein that binds to and activates eNOS (Karar & Maity, 2011), decreased 0.8-fold following 0.5 Gy X-ray irradiation (Azimzadeh et al., 2017).

High doses (>2 Gy) also show dose concordance between altered signaling pathways and altered NO levels. X-ray irradiation of BAECs and HUVECs caused a 5.6-fold increase in p-Akt/Akt after 6 Gy (Sonveaux et al., 2003). eNOS increased 3-fold after 6 Gy, while p-eNOS increased 1.2-fold after 2 Gy and 1.7-fold after 6 Gy (Sonveaux et al., 2003). Although the p-Akt/Akt ratio was not significantly increased after 2 Gy, p-Akt alone had increased, indicating changes in the PI3K/Akt pathway had occurred at 2 Gy. Therefore, a decrease in PI3K/Akt pathway proteins, such as p-IGFR1, p-Akt and p-PI3K are correlated with decreases in p-eNOS and NO (Azimzadeh et al., 2015), while an increase in p-Akt correlates with increases in eNOS and p-eNOS (Shi et al., 2012; Sonveaux et al., 2003). In rat blood serum, 6 Gy gamma ray irradiation led to a 1.4-fold increase in AngII and aldosterone levels and a 3.3-fold increase in iNOS expression indicating that a change in the RAAS pathway can lead to altered NO levels (Hasan, Radwan & Galal, 2019).

Mice that received high dose (8 or 16 Gy) X-ray irradiation on the heart showed alterations in the levels of signalling proteins involved in the PI3K/Akt pathway, including a 0.4 and 0.3-fold decrease of p-IGFR1, a 0.5-fold decrease of PI3K, a 0.2 and 0.1-fold decrease of p-Akt and a 0.6 and 0.2-fold decrease of p-eNOS at 8 Gy and 16 Gy, respectively (Azimzadeh et al., 2015).

Concurrently to changes to PI3K/Akt pathway signaling molecules, the level of serum NO decreased 0.3-fold and 0.3-fold following 8 Gy and 16 Gy X-ray irradiation, respectively (Azimzadeh et al., 2015). As well, following X-ray irradiation, the ERK/MAPK pathway decreased 0.5-fold at 16 Gy and the p38/MAPK pathway increased 1.3-fold at 16 Gy (Azimzadeh et al., 2015). X-ray irradiation in mice at 16 Gy also inhibited PPARα resulting in decreased activity and phosphorylation of eNOS through the PI3K/Akt pathway and decreased NO levels (Azimzadeh et al., 2021). This study also showed an increase in p-ERK, and p-p38 at 16 Gy (Azimzadeh et al., 2021). After irradiation of HUVECs with 10 or 12 Gy, p-ERK5, KLF2 and eNOS were all found to decrease after fractionated doses, while KLF2 and eNOS both decreased after acute doses (Sadhukhan et al., 2020).

Microgravity in HUVEC-C was simulated by a clinostat using rotation at a slow speed to negate centrifugal force. Following clinorotation, levels of eNOS and p-eNOS expression were significantly increased by 5.2-fold and 5.5-fold, respectively. As well, p-Akt increased by 2.9-fold after exposure to simulated microgravity in HUVEC-C (Shi et al., 2012).

Time Concordance

There is some evidence to demonstrate time concordance between altered signaling pathways leading to altered NO levels. After 0.5 Gy X-ray of HCAECs, p-Rho-GDI significantly decreased after 1 day, while NO was not significantly lower after 1 day (Azimzadeh et al., 2017). After 24 h, p-Akt was increased, while eNOS was increased 24 and 48 h after X-ray irradiation of BAECs and HUVECs (Sonveaux et al., 2003). After 7 days, p-Rho-GDI decreased further and NO showed a significant decrease. HUVECs irradiated with 10 or 12 Gy acute or fractionated X-rays showed decreased levels of p-ERK5, KLF2 and eNOS at 4 h, and decreased KLF2 and eNOS at 24 h after irradiation (Sadhukhan et al., 2020).

Incidence Concordance

The evidence of incidence concordance for this relationship is moderate, as a few studies demonstrated incidence concordance. In mice hearts irradiated with X-rays, p-Akt, the direct upstream activator of eNOS, decreased 0.2-fold after 8 Gy and 0.1-fold after 16 Gy, while NO decreased 0.3-fold after 8 Gy and 0.2-fold after 16 Gy (Azimzadeh et al., 2015). Similarly, after 0.5 Gy X-ray irradiation of HCAECs, p-RhoGDI decreased 0.7-fold while NO decreased 0.8-fold (Azimzadeh et al., 2017). X-ray irradiation of BAECs and HUVECs at 6 Gy resulted in a 5.6-fold increase in the ratio of p-Akt/Akt and a 3-fold increase to p-eNOS (Sonveaux et al., 2003).

Essentiality

Several studies have investigated the essentiality of various signalling pathways in altering NO levels. Under normal conditions, the phosphorylation of eNOS by the PI3K/Akt pathway activates NOS, resulting in NO production. LY294002 treatment, a PI3K inhibitor, led to significant decreases in eNOS and p-eNOS levels in HUVEC-C samples (Shi et al., 2012). After exposure to simulated microgravity by clinorotation, LY294002 treatment led to decreased p-Akt levels to below control levels (Shi et al., 2012). The inhibition of the PI3K/Akt pathway with wortmanin, another PI3K inhibitor, also led to a 0.3-fold decrease in NO production (Siamwala et al., 2010). Irradiation inhibited PPARα and eNOS, while treatment with fenofibrate, a PPARα activator, kept both p-PPARα and NO at control levels (Azimzadeh et al., 2021).

Bradykinin-potentiating factor (BPF) is implicated in muscle contraction, inflammatory responses and angiotensin-converting enzyme (ACE) inhibition. ACE in endothelial cells converts AngI to AngII. Irradiation at 6 Gy led to increased iNOS, AngII, and aldosterone, while the subsequent treatment with BPF decreased all endpoints measured following irradiation, including the levels of iNOS, AngII, and aldosterone. The recovery of iNOS serum levels in 6 Gy gamma irradiated rats following BPF treatment indicates that the signaling pathways play a role in NO levels (Hasan, Radwan & Galal, 2019). In addition, bradykinin signaling through bradykinin receptor 2 (B2R) activates eNOS (Ancion et al., 2019). Nitrite concentration was found to increase after both microgravity and treatment with bradykinin (Siamwala et al., 2010).

Various inhibitors of the mevalonate pathway were used to recover KLF2 levels after irradiation, which resulted in increased KLF2 and eNOS levels (Sadhukhan et al., 2020).

Uncertainties and Inconsistencies

- Due to the high reactivity of NO, it can be difficult to obtain its direct measures (Luiking, Engelen & Deutz, 2010). The inconsistencies in NO levels may be attributed to the challenges in measuring NO. Directionality of NO changes cannot be compared between studies due to a variety of experimental conditions like stressor type, dose, dose rate, model and time course of the experiment.

Quantitative Understanding of the Linkage

The following are a few examples of quantitative understanding of the relationship. All data that is represented is statistically significant unless otherwise indicated.

Response-response relationship

Dose/Incidence Concordance

Reference	Experiment Description	Result
Shi et al., 2012	*In vitro*. Microgravity was stimulated with a clinostat using rotation at a slow speed to negate centrifugal force and simulate weightlessness. eNOS expression and Akt phosphorylation in HUVEC-C were measured by western blot.	After clinorotation, eNOS and p-eNOS expression increased by 5.2-fold and 5.5-fold respectively. p-Akt increased by 2.9-fold, while there was no significant change in Akt after clinorotation in HUVEC-C.
Hasan, Radwan & Galal, 2019	*In vivo*. Rat heart serum were exposed to irradiation by 6 Gy Gamma rays. iNOS levels were measured by ELISA. RAAS indices, AngII and aldosterone, were also measured in serum by ELISA.	Irradiation with 6 Gy led to a 3.3-fold increase in iNOS expression, ~1.4-fold increase in AngII and aldosterone.
Azimzadeh et al., 2015	*In vivo*. Mice were exposed to heart X-ray irradiation at either 8 or 16 Gy. Levels of proteins in the insulin-dependent PI3K/Akt pathway with and without phosphorylation were determined along with levels of NO and eNOS. Protein levels in various signaling pathways were measured using immunoblotting, and NO was measured using an ELISA assay.	Many key proteins in each pathway showed significant changes in abundance and phosphorylation after 8 and 16 Gy irradiation. For example, phosphorylation of the insulin receptor IGFR1 decreased 0.4-fold after 8 Gy and 0.2-fold after 16 Gy. Similarly, p-Akt decreased 0.2-fold at 8 Gy and 0.1-fold at 16 Gy. p-eNOS decreased 0.6-fold after 8 Gy and 0.2-fold after 16 Gy. The ERK/MAPK pathway was found decreased 0.5-fold at 16 Gy and the p38/MAPK pathway was found increased 1.3-fold at 16 Gy. NO decreased 0.3-fold after 8 Gy and 0.2-fold after 16 Gy.
Azimzadeh et al., 2017	*In vitro*. HCAECs were irradiated with 0.5 Gy X-ray irradiation over 1 minute. Phosphorylated RhoGDI and eNOS levels were determined using immunoblotting, and NO levels were determined using ELISA assay.	p-RhoGDI decreased 0.7-fold, p-eNOS decreased 0.6-fold, HSP90 (positive regulator of eNOS) decreased 0.8-fold and NO decreased 0.8-fold after 0.5 Gy irradiation.
Sonveaux et al., 2003	*In vitro*. Following X-ray irradiation of BAECs and HUVECs, levels of eNOS, p-eNOS, Akt, and p-Akt were measured with immunoblotting at various doses (0.86 Gy/min).	Compared to control, 24 h after irradiation, the ratio of p-Akt/Akt increased 1.3-fold after 2 Gy (not significant) and 5.6-fold after 6 Gy. eNOS increased 1.3-fold after 2 Gy (not significant), 2.1-fold after 4 Gy (not significant), 3-fold after 6 and 8 Gy, 4.3-fold after 10 Gy and 3.4-fold after 20 Gy. Compared to control, 24 h after irradiation, p-eNOS increased 1.2-fold after 2 Gy and 1.7-fold after 6 Gy.
Azimzadeh et al., 2021	*In vivo*. Male C57BL/6J were irradiated with an acute dose of 16 Gy X-rays. Activation of the PI3K-Akt pathway was determined through p-PPARα (deactivated) levels from Ponceau S staining. eNOS activity and NO were measured using fluorometric assay and Griess assay, respectively. The level of proteins in MAPK pathways were determined by ELISA in heart tissue.	After 16 Gy, p-PPARα increased 1.3-fold. After 16 Gy, p-ERK increased 1.5-fold, and p-p38 increased 1.3-fold, eNOS was unchanged, p-eNOS decreased 0.8-fold and NO decreased to 65% of control levels.
Sadhukhan et al., 2020	*In vitro*. HUVECs were irradiated with various regimens and doses of gamma radiation. Signaling from the ERK5/KLF2 pathway was determined through KLF2 and p-ERK5 levels from western blot. eNOS levels were determined by western blot. Fractionated doses were separated by 24 h.	p-ERK5 decreased 0.6-fold after 5 doses of 2 Gy, increased 1.5-fold after acute 10 Gy, decreased 0.5-fold after 5 doses of 2.5 Gy, and increased 1.3-fold after acute 12.5 Gy. KLF2 and eNOS showed similar responses and were often slightly decreased after acute doses.

Time-scale

Time Concordance

Reference	Experiment Description	Result
Azimzadeh.et al., 2017	*In vitro*. AECs were irradiated with 0.5 Gy X-rays over 1 minute. Phosphorylated RhoGDI and eNOS levels were determined using immunoblotting, and NO levels were determined using ELISA assay. Measurements were taken after 1, 7 or 14 days.	p-RhoGDI significantly decreased after 1 day, while NO only significantly decreased after 7 days. However, p-eNOS significantly decreased after 1 day.
Sonveaux et al., 2003	*In vitro*. Levels of eNOS, p-eNOS, Akt, and p-Akt after X-ray irradiation of BAECs and HUVECs were measured with	p-Akt was significantly increased 24 h after irradiation, while eNOS was significantly increased after 12, 24, and 48 h and p-eNOS was significantly

	immunoblotting at various doses (0.86 Gy/min).	increased after 24 h.
Sadhukhan et al., 2020	*In vitro*. HUVECs were irradiated with various regimens and doses of gamma radiation. Fractionated doses were separated by 24 h. Signaling from the ERK5/KLF2 pathway was determined through KLF2 and p-ERK5 levels from western blot. eNOS levels were determined by western blot. Measurements were taken 4 or 24 h post-irradiation.	After 4 h, p-ERK5 decreased 0.6-fold after 5 doses of 2 Gy, increased 1.5-fold after acute 10 Gy, decreased 0.5-fold after 5 doses of 2.5 Gy, and increased 1.3-fold after acute 12.5 Gy. Both KLF2 and eNOS decreased similar to p-ERK5 after 4 h and were slightly decreased after 24 h.

Known modulating factors

Modulating factor	Details	Effects on the KER	References
Drug	BPF (ACE inhibitor)	BPF treatment led to decreased iNOS, angiotensin II and aldosterone following irradiation.	Hasan, Radwan & Galal, 2019
Drug	LY294002 (PI3K inhibitor)	LY294002 treatment led to reduced phosphorylation of both Akt and eNOS.	Shi et al., 2012;
Drug	Wortmanin (PI3K inhibitor)	Wortmanin decreased NO production.	Siamwala et al., 2010
Drug	Fenofibrate (PPARα activator)	Treatment with PPARα prevented the decrease in eNOS levels after irradiation.	Azimzadeh et al., 2021
Drug	Atorvastatin (HMG-CoA reductase inhibitor)	Treatment with atorvastatin increased KLF2 and eNOS levels slightly.	Sadhukhan et al., 2020
Drug	Gamma tocotrienol (HMG-CoA reductase inhibitor)	Treatment with gamma tocotrienol prevented the radiation-induced decrease in KLF2 and eNOS levels.	Sadhukhan et al., 2020
Drug	Geranylgeranyltransferase I inhibitor 298	Treatment with Geranylgeranyltransferase I inhibitor 298 prevented the radiation-induced decrease in KLF2 and eNOS levels.	Sadhukhan et al., 2020

Known Feedforward/Feedback loops influencing this KER

Not identified

References

Ancion, A. et al. (2019), “A Review of the Role of Bradykinin and Nitric Oxide in the Cardioprotective Action of Angiotensin-Converting Enzyme Inhibitors: Focus on Perindopril”, *Cardiology and Therapy*, Vol. 8/2, Springer, London, https://doi.org/10.1007/S40119-019-00150-W

Azimzadeh, O. et al. (2021), “Activation of pparα by fenofibrate attenuates the effect of local heart high dose irradiation on the mouse cardiac proteome”, *Biomedicines*, Vol. 9/12, Multidisciplinary Digital Publishing Institute, Basel, https://doi.org/10.3390/biomedicines9121845.

Azimzadeh, O. et al. (2017), “Proteome analysis of irradiated endothelial cells reveals persistent alteration in protein degradation and the RhoGDI and NO signalling pathways”, *International Journal of Radiation Biology*, Vol. 93/9, Informa, London, https://doi.org/10.1080/09553002.2017.1339332

Azimzadeh, O. et al. (2015), “Integrative Proteomics and Targeted Transcriptomics Analyses in Cardiac Endothelial Cells Unravel Mechanisms of Long-Term Radiation-Induced Vascular Dysfunction”, *Journal of Proteome Research*, Vol. 14/2, American Chemical Society, Washington, https://doi.org/10.1021/pr501141b

Ding, J. et al. (2020), “Angiotensin II Decreases Endothelial Nitric Oxide Synthase Phosphorylation *via* AT1R Nox/ROS/PP2A Pathway”, *Frontiers in physiology*, Vol.11, Frontiers Media SA, Lausanne, https://doi.org/10.3389/fphys.2020.566410

Dovas, A. and J. R. Couchman (2005), “RhoGDI: multiple functions in the regulation of Rho family GTPase activities”, *Biochemical Journal*, Vol. 390, Portland Press, London, https://doi.org/10.1042/BJ20050104

Du, S., N. Wagner and K. D. Wagner (2020), “The Emerging Role of PPAR Beta/Delta in Tumor Angiogenesis”, *PPAR*

Research, Vol. 2020, Hindawi, London, https://doi.org/10.1155/2020/3608315.

Förstermann, U. (2010), "Nitric oxide and oxidative stress in vascular disease", *Pflugers Archiv : European journal of physiology*, Vol. 459/6, Springer, London, https://doi.org/10.1007/s00424-010-0808-2

Hasan, H. F., R. R. Radwan and S. M. Galal (2019), "Bradykinin-potentiating factor isolated from Leiurus quinquestriatus scorpion venom alleviates cardiomyopathy in irradiated rats via remodelling of the RAAS pathway", *Clinical and Experimental Pharmacology and Physiology*, Vol. 47/2, Wiley-Blackwell, Hoboken, https://doi.org/10.1111/1440-1681.13202

Hemmings, B. A. and D. F. Restuccia (2012), "PI3K-PKB/Akt Pathway", *Cold Spring Harbor Perspectives in Biology*, Vol. 4/9, Cold Spring Harbor Laboratory Press, Cold Spring Harbor, https://doi.org/10.1101/CSHPERSPECT.A011189

Hicklin, D. J. and L. M. Ellis (2005), "Role of the Vascular Endothelial Growth Factor Pathway in Tumor Growth and Angiogenesis", *Journal of Clinical Oncology*, Vol. 23/5, American Society of Clinical Oncology, Virginia, https://doi.org/10.1200/JCO.2005.06.081.

Karar, J. and A. Maity (2011), "PI3K/AKT/mTOR Pathway in Angiogenesis", *Frontiers in Molecular Neuroscience*, Vol. 4, Frontiers Media SA, Lausanne, https://doi.org/10.3389/FNMOL.2011.00051

Kozbenko, T. et al. (2022), "Deploying elements of scoping review methods for adverse outcome pathway development: a space travel case example", *International Journal of Radiation Biology*, Vol. 98/12. https://doi.org/10.1080/09553002.2022.2110306

Luiking, Y. C., M. P. Engelen and N. E. Deutz (2010), "Regulation of nitric oxide production in health and disease", *Current Opinion in Clinical Nutrition and Metabolic Care*, Vol. 13/1, Lippincott Williams and Wilkins Ltd., Philadelphia, https://doi.org/10.1097/MCO.0b013e328332f99d

Millatt, L. J., E. M. Abdel-Rahman and H. M. Siragy (1999), "Angiotensin II and nitric oxide: a question of balance", *Regulatory Peptides*, Vol. 81/1-3, Elsevier, Amsterdam, https://doi.org/10.1016/S0167-0115(99)00027-0

Nagane, M. et al. (2021), "DNA damage response in vascular endothelial senescence: Implication for radiation-induced cardiovascular diseases", *Journal of Radiation Research*, Vol. 62/4, Oxford University Press, Oxford, https://doi.org/10.1093/JRR/RRAB032

Paudel, R., L. Fusi and M. Schmidt (2021), "The MEK5/ERK5 Pathway in Health and Disease", *International Journal of Molecular Sciences*, Vol. 22/14, Multidisciplinary Digital Publishing Institute, Basel, https://doi.org/10.3390/ijms22147594.

Sadhukhan, R. et al. (2020), "Fractionated radiation suppresses Kruppel-like factor 2 pathway to a greater extent than by single exposure to the same total dose", *Scientific Reports*, Vol. 10/1, Springer, London, https://doi.org/10.1038/s41598-020-64672-3.

Shi, F. et al. (2012), "Effects of Simulated Microgravity on Human Umbilical Vein Endothelial Cell Angiogenesis and Role of the PI3K-Akt-eNOS Signal Pathway", *PLoS ONE*, Vol. 7/7, PLOS, San Francisco, https://doi.org/10.1371/journal.pone.0040365

Siamwala, J. H. et al. (2010), "Simulated microgravity perturbs actin polymerization to promote nitric oxide-associated migration in human immortalized Eahy926 cells", *Protoplasma*, Vol. 242/1, Springer, London, https://doi.org/10.1007/S00709-010-0114-Z

Soloviev, A. I. and I.V. Kizub (2019), "Mechanisms of vascular dysfunction evoked by ionizing radiation and possible targets for its pharmacological correction", *Biochemical pharmacology*, Vol. 159, Elsevier, Amsterdam, https://doi.org/10.1016/j.bcp.2018.11.019

Sonveaux, P. et al. (2003), "Irradiation-induced Angiogenesis through the Up-Regulation of the Nitric Oxide Pathway: Implications for Tumor Radiotherapy", *Cancer Research*, Vol. 63/5, American Association for Cancer Research, Philadelphia, https://aacrjournals.org/cancerres/article/63/5/1012/511021/Irradiation-induced-Angiogenesis-through-the-Up

Yao, L. et al. (2010), "The role of RhoA/Rho kinase pathway in endothelial dysfunction", *Journal of Cardiovascular Disease Research*, Vol. 1/4, Elsevier, Amsterdam, https://doi.org/10.4103/0975-3583.74258

Relationship: 2774: Oxidative Stress leads to Altered, Nitric Oxide Levels

AOPs Referencing Relationship

AOP Name	Adjacency	Weight of Evidence	Quantitative Understanding
Deposition of energy leads to vascular remodeling	adjacent	Moderate	Low

Evidence Supporting Applicability of this Relationship

Taxonomic Applicability

Term	Scientific Term	Evidence	Links
human	Homo sapiens	Low	NCBI
rat	Rattus norvegicus	High	NCBI

Life Stage Applicability

Life Stage	Evidence
Adult	Moderate
Juvenile	Low

Sex Applicability

Sex	Evidence
Male	Moderate
Female	Low
Unspecific	Low

The evidence for the taxonomic applicability to humans is low as evidence comes from *in vitro* human cell-derived models. Many studies use *in vivo* rat models, predominately males. Occasionally, animal age is not specified in studies; most studies indicate the animals are adult or adolescent. In addition, the relationship is also plausible in preadolescent animals.

Key Event Relationship Description

The increased production of reactive oxygen species (ROS) and reactive nitrogen species (RNS) during oxidative stress can lead to altered nitric oxide (NO) levels, specifically a reduction in its bioavailability.

Although RNS can also interfere with NO levels, most studies focus on ROS and not RNS (Nagane et al., 2021). Oxidative stress influences the production and activity of endothelial nitric oxide synthase (eNOS), thereby altering and reducing NO levels and its bioavailability. eNOS, otherwise known as NOS3, is an enzyme that catalyzes NO production from the amino acid L-arginine in vascular endothelial cells. NO mediates vascular tone and blood flow via the activation of soluble guanylate cyclase (sGC) within the vascular smooth muscle (Chen, Pittman and & Popel, 2008). A form of ROS known as superoxide anion (O_2^-) causes increased NO degradation (Incalza et al., 2018), converting NO into the RNS peroxynitrite. In addition, ROS can uncouple eNOS by oxidation of the enzyme's cofactor, BH4 (Matsubara et al., 2015; Forstermann, 2010). Uncoupled eNOS produces ROS instead of NO, which can further convert existing NO into peroxynitrite (Forstermann, 2010).

Evidence Supporting this KER

Overall weight of evidence: Moderate

Biological Plausibility

The biological rationale for the relationship between increased oxidative stress and altered NO levels is well-supported by the literature, validated by many studies presented in this area of research. The biological mechanism of this relationship is well-known and widely accepted. The reaction between NO and free radicals leads to the creation of peroxynitrite, which results in reduced NO bioavailability (Incalza et al., 2018; Mitchell et al., 2019; Nagane et al., 2021; Soloviev & Kizub, 2019; Wang, Boerma & Zhou, 2016). In addition, in vascular tissues, increased levels of O2- or peroxynitrite can oxidize BH4 and lead to uncoupled eNOS (Forstermann, 2010; Matsubara et al., 2015; Soloviev & Kizub, 2019). When uncoupled, eNOS transfers electrons to O2- rather than L-arginine, causing O2- production instead of NO production, further reducing NO bioavailability. Although much of the biological plausibility indicates that NO decreases with oxidative stress, ROS have been associated with increased NO as well (Nagane et al., 2021; Soloviev & Kizub, 2019). This is likely due to the complexity of NO regulation in signaling pathways, upregulation of inducible nitric oxide synthase (iNOS), as well as variations in stressors, doses, dose rates, models, duration of study and diseases present in studies (Nagane et al., 2021).

Empirical Evidence

The empirical data for this KER somewhat supports the relationship of increased oxidative stress eventuating in altered NO levels. The evidence was gathered from both *in vivo* and *in vitro* models. Gamma rays (Abdel-Magied & Shedid, 2020; Hasan, Radwan & Galal, 2019; Soucy et al., 2010), X-rays (Cervelli et al., 2017; Yan et al., 2020), altered gravity (Zhang et al., 2009) and heavy ions (Soucy et al., 2011) were used as stressors with dose levels ranging from 0.25 to 10 Gy. Direct and indirect measures of NO, including iNOS, eNOS and nitrite levels, were used as endpoints to investigate the effect of increased oxidative stress on NO levels. Evidence from radiation sources that induce oxidative stress in human umbilical vein endothelial cells (HUVECs) or rat aorta have demonstrated a change in NO levels (Abdel-Magied & Shedid, 2020; Cervelli et al., 2017; Hasan, Radwan & Galal, 2019; Soucy et al., 2010; Soucy et al., 2011; Yan et al., 2020; Zhang et al., 2009).

Dose Concordance

Moderate evidence is available within current literature that demonstrates dose-concordance between increased oxidative stress and altered NO levels. Elevations in the production of ROS have been reported with exposure to altered gravity and different doses (0.25 Gy, 1 Gy, 4 Gy, 5 Gy, and 10 Gy) of radiation in HUVECs and rat aorta/tissue models, and provide supporting evidence that an increase in oxidative stress can lead to subsequent alterations in NO levels (Abdel-Magied & Shedeed, 2020; Cervelli et al., 2017; Hasan, Radwan & Galal, 2019; Sakata et al., 2015; Soucy et al., 2010; Soucy et al., 2011; Yan et al., 2020; Zhang et al., 2009). For example, a study involving HUVEC X-ray irradiation at 0.25 Gy found increases in both ROS and nitrite/nitrate levels (Cervelli et al., 2017). As well, a study involving 1 Gy of iron ions demonstrated elevations in ROS production with accompanying reductions in NO levels using the DAF-FM DA fluorescent probe (Soucy et al., 2011).

At high doses (>2 Gy), dose concordance between increased oxidative stress and altered nitric oxide can be observed. For example, 5 Gy gamma irradiation leads to increased ROS production with decreased NO levels measured using the DAF-FM DA fluorescent probe (Soucy et al., 2010) Gamma irradiation of rats with 6 Gy led to changes in oxidative stress indices that showed an increase in ROS, while iNOS levels were also increased (Hasan, Radwan & Galal, 2019). Rat cardiac tissue exposed to 8 Gy gamma irradiation also showed an increase in ROS through oxidative stress indices and an increase in nitrite/nitrate content (Abdel-Magied & Shedid, 2020). A study investigating HUVECs and rat aorta/tissue responses to 10 Gy and 4 Gy X-ray radiation, respectively, showed reduced eNOS dimerization and nitrite levels with elevations in ROS production in both models (Yan et al., 2020). Also in HUVECs, 10 Gy X-rays resulted in increased ROS, increased p-eNOS (Ser1177), decreased p-eNOS (Thr495), increased citrulline and increased NOx (nitrite and nitrate, NO proxies) (Sakata et al., 2015). NOx was also significantly increased after 20 Gy (Sakata et al., 2015).

Simulated microgravity showed increased eNOS and iNOS in rats, while superoxide levels, although not quantitatively shown, increased following altered gravity (Zhang et al., 2009). Although, the authors state that the increase in NOS would likely cause decreased NO production because of NOS uncoupling and peroxynitrite production (Zhang et al., 2009).

Time Concordance

Very few studies demonstrate time concordance of this relationship. In HUVECs irradiated with 0.25 Gy of X-rays, ROS levels increased after 45 minutes, while nitrite and nitrate levels increased after 24 hours. In rats exposed to 6 Gy of gamma rays, both oxidative stress indices and iNOS increased 4 weeks post-irradiation (Hasan, Radwan & Galal, 2019).

Incidence concordance

There is moderate evidence of incidence concordance for this relationship. Yan et al. (2020) showed both *in vivo* in a rat model irradiated with 4 Gy of X-rays and *in vitro* in HUVECs irradiated with 10 Gy of X-rays that superoxide levels increased more than NO and eNOS were decreased following irradiation. Rats irradiated with 1 Gy of ^{56}Fe ions showed a 1.8-fold increase in ROS and just a 0.8-fold decrease in NO levels (Soucy et al., 2011). Similarly, gamma irradiation of rats at 5 Gy resulted in a 1.7-fold increase in ROS and a 0.7-fold decrease in NO levels (Soucy et al., 2010). In HUVECs irradiated with 10 Gy of X-rays, ROS increased 15.5-fold while NOx levels increased just 10-fold (Sakata et al., 2015).

Essentiality

Studies scrutinizing the usefulness of antioxidants in inhibiting oxidative stress show a moderately supported relationship between elevated oxidative stress and altered NO levels. Antioxidants have been implicated in the activation of the NOS family of enzymes by preventing BH4 oxidation, thereby increasing NO bioavailability (Kojsova et al., 2006). One study observed that treatment with bradykinin potentiating factor (BPF), which can affect eNOS regulation through the renin aldosterone angiotensin system, contributed to elevations in the antioxidant glutathione (GSH) and a marker of antioxidant potential, ferric reducing antioxidant power (FRAP) (Hasan, Radwan & Galal, 2019). BPF contributed to reductions in malondialdehyde (MDA), a biomarker for oxidative stress, while also increasing iNOS levels (Hasan, Radwan & Galal, 2019).

Another study demonstrated that a composition of antioxidants (resveratrol, extramel, seleno-L-methionine, Curcuma longa, reduced glutathione, and vitamin C (RiduROS) inhibited increases in ROS while restoring NO levels (Cervelli et al., 2017). Furthermore, rat mesenteric arteries and HUVECs treated with 2,4-diamino-6-hydroxypyrimidine (DAHP), an inhibitor of Gch1 that is important for BH4 synthesis, lowered both the dimer:monomer eNOS ratio and the nitrite (measure of NO) concentration, and increased superoxide following irradiation (Yan et al., 2020). The notable elevation in O2- demonstrates that inhibiting Gch1 and limiting BH4 activity can prevent eNOS activity and elevate ROS Levels (Yan et al., 2020).

In addition, two studies demonstrated that treatment with oxypurinol (OXP), a xanthine oxidase (XO) inhibitor where XO is responsible for generating cardiac ROS, led to reductions in ROS well under the control level whereas NO increased to control levels demonstrating that oxidative damage contributes to a decrease in NO bioavailability (Soucy et al., 2010; Soucy et al., 2011).

Zinc oxide nanoparticles (ZnO-NPs) can act as antioxidants; Abdel-Magied & Shedid (2020) found that low concentrations (10 mg/kg ZnO-NPs) decreased oxidation and NO levels in rats after gamma irradiation. Angiotensin II type 1 (AT1) receptors are able to regulate NOS levels. Treatment with losartan, an AT1 receptor antagonist, led to a decrease in O2- , iNOS and eNOS levels, demonstrating that the increase in NOS and ROS can be prevented by blocking AT1 receptors (Zhang et al., 2009). Biotin was found to increase GSH content, superoxide dismutase (SOD), catalase (CAT) activity and return NOx levels to near control values following irradiation in hippocampus (Abdel-Magied & Shedid, 2020).

Uncertainties and Inconsistencies

- The directionality of changes to NO is inconsistent between studies, as some studies show increased NO levels and other studies show decreased NO levels. Improved methods are needed to assess NO levels directly, which may facilitate an understanding of the relationship (Cervelli et al., 2017, Hasan, Radwan & Galal, 2019). This, along with variation in experimental conditions, can account for the inconsistencies in NO changes between studies.

Quantitative Understanding of the Linkage

The following are a few examples of quantitative understanding of the relationship. All data that is represented is statistically significant unless otherwise indicated.

Response-response relationship

Dose/Incidence Concordance

Reference	Experiment Description	Result
Cervelli et al., 2017	*In vitro*. HUVECs were irradiated with 0.25 Gy X-rays. Levels of ROS as well as nitrite and nitrate (NO markers) were determined using a fluorescent probe and Griess assay, respectively.	The irradiated samples had a 2.8-fold increase in ROS (not significant) and a 1.6-fold increase in nitrite/nitrate compared to controls.
Yan et al., 2020	*In vitro* and *in vivo*. Rat arteries were irradiated with 4 Gy abdominal X-ray radiation. HUVEC were irradiated by 10 Gy X-rays. Oxidative stress was indicated by superoxide anions. Nitrite and eNOS levels were measured by NO assay kit and SDS-PAGE.	Following 4 Gy irradiation of rats, O2- levels increased by 2.1-fold. Nitrite (NO metabolite and marker) and eNOS ratio decreased by 0.6-fold. Following 10 Gy irradiation of HUVEC, O2- levels increased by 3.6-fold and nitrite along with eNOS decreased 0.5 and 0.6-fold respectively.
Soucy et al., 2011	*In vivo*. Male rats irradiated with 1 Gy ^{56}Fe ions. ROS and NO levels in rat aorta were measured using fluorescence rates of dihydroethidium and diaminofluorescein, respectively.	Iron ion irradiation at 1 Gy produced a 1.8-fold increase in ROS levels and 0.8-fold decrease in NO levels compared to controls.
Soucy et al., 2010	*In vivo*. 4-month-old rats were irradiated with 5 Gy ^{137}Cs gamma radiation. ROS and NO levels in rat aorta were measured using fluorescence rates of dihydroethidium and diaminofluorescein, respectively.	After 5 Gy, ROS increased 1.7-fold. NO production decreased 0.7-fold compared to controls.
Hasan, Radwan & Galal, 2019	*In vivo*. Rats were irradiated by 6 Gy ^{137}Cs gamma rays and serum was collected. Oxidative damage biomarker MDA ROS-clearing enzyme reduced GSH and FRAP were measured using various assays.	Irradiation with 6 Gy led to a 1.4-fold increase in MDA, a 0.5-fold decrease in GSH and a 0.4-fold decrease in FRAP. A 3.3-fold increase in iNOS levels was observed.
Zhang et al., 2009	*In vivo*. Hindlimb unweighted (HU) rats had superoxide and NOS levels measured in carotid arteries. Western blot was used to measure eNOS and iNOS levels, while dihydroethidium fluorescence was used to measure superoxide.	In HU rats, eNOS levels increased 2-fold in carotid arteries. A 4.2- and 3.3-fold increase in iNOS in carotid and cerebral arteries, respectively, was found in HU rats. Superoxide levels were not quantitatively shown but increased greatly after altered gravity.
Abdel-Magied & Shedid, 2020	*In vivo*. Male rats were irradiated with 8 Gy ^{137}Cs gamma irradiation at 0.4092 Gy/min. Oxidative damage biomarker MDA and ROS-clearing enzymes SOD, CAT and glutathione peroxidase (GPx) activities and GSH were measured using respective assay kits. Total nitrite/nitrate content was measured with nitrite/nitrite assay kit. The oxidative damage biomarker and ROS-clearing enzymes were measured in heart tissue and nitrite/nitrate was measured in heart tissue and blood serum.	Irradiated cardiac tissue showed a 1.8-fold increase in MDA levels, 0.4-fold decrease in GSH levels, 0.4-fold decrease in CAT activity, 0.5-fold decrease in SOD activity and a 0.5-fold decrease in GPx activity compared to control. XO levels increased 2-fold. Irradiated heart tissue showed a 2-fold increase in nitrite/nitrate content, while irradiated blood serum showed a 1.8-fold increase in nitrite/nitrate content compared to the control.
Sakata et al., 2015	*In vitro*. HUVECs were irradiated with various doses of X-rays. eNOS, p-eNOS (Ser1177 & Thr495), iNOS, citrulline (produced by NOS with NO) and NOx levels were measured with western blots for proteins and various assay kits for molecules. ROS intensity was measured using fluorescence	At maximum after 10 Gy, ROS increased 15.5-fold, eNOS expression did not significantly change, p-eNOS (Ser1177) increased 1.8-fold, p-eNOS (Thr495) decreased 0.3-fold, iNOS showed a non-significant 1.4-fold increase and citrulline increased 1.3-fold. NOx increased consistently from 1-20 Gy with significant

	microscopy.	fold changes at 10 and 20 Gy and a maximum 10-fold increase after 10 Gy.

Time-scale

Time Concordance

Reference	Experiment Description	Result
Cervelli et al., 2017	*In vitro*. HUVECs were irradiated with 0.25 Gy X-rays. Levels of ROS as well as nitrite and nitrate (NO markers) were determined using a fluorescent probe and Griess assay, respectively.	The irradiated samples had a 2.8-fold increase in ROS (not significant) measured after 45 minutes and a 1.6-fold increase in nitrite/nitrate measured after 24 hours.
Hasan, Radwan & Galal, 2019	*In vivo*. Rats were exposed to irradiation by 6 Gy ^{137}Cs gamma rays and serum was collected. Oxidative damage biomarker MDA, ROS-clearing enzyme reduced GSH and FRAP were measured using various assays.	Irradiation with 6 Gy led to a 1.4-fold increase in MDA, a 0.5-fold decrease in GSH and a 0.4-fold decrease in FRAP all measured after 4 weeks. A 3.3-fold increase in iNOS levels was observed after 4 weeks as well.

Known modulating factors

Modulating factor	Details	Effects on the KER	References
Drug	BPF (ACE inhibitor)	BPF treatment led to decreased iNOS, angiotensin II and aldosterone following irradiation. Oxidative stress indices returned closer to control levels.	Hasan, Radwan & Galal, 2019
Drug	OXP (XO inhibitor)	OXP can increase NO levels and decrease ROS after irradiation.	Soucy et al., 2010; Soucy et al., 2011
Drug	RiduROS (A combination of antioxidants resveratrol, extramel, seleno-L-methionine, Curcuma longa, reduced L-glutathione, vitamin C)	RiduROS led to decreased ROS and NO production after irradiation.	Cervelli et al., 2017
Drug	DAHP (Gch1 inhibitor which is involved in BH4 synthesis)	DAHP can decrease ROS production and increase NO production after irradiation.	Yan et al., 2020
Drug	Losartan (AT1 receptor antagonist)	Treatment with Losartan after microgravity decreased superoxide production and returned eNOS and iNOS to control levels.	Zhang et al., 2009
Drug	ZnO-NPs (Zinc oxide nanoparticles that act as antioxidants)	Treatment with ZnO-NPs returned serum and cardiac NO levels and ROS indicators closer to control levels after irradiation.	Abdel-Magied & Shedid, 2020
Drug	Biotin	Biotin (6mg) increased GSH content, SOD activity, and CAT activity closer to control levels following irradiation in hippocampus. NOx levels also returned to near control values.	Abdel-Magied & Shedid, 2020

Known Feedforward/Feedback loops influencing this KER

Not Identified.

References

Abdel-Magied, N. and S. M. Shedid (2020), “Impact of zinc oxide nanoparticles on thioredoxin-interacting protein and asymmetric dimethylarginine as biochemical indicators of cardiovascular disorders in gamma-irradiated rats”, *Environmental Toxicology*, Vol. 35, Wiley, https://doi.org/10.1002/tox.22879.

Cervelli, T. et al. (2017), “A new natural antioxidant mixture protects against oxidative and DNA damage in endothelial cell exposed to low-dose irradiation”, *Oxidative Medicine and Cellular Longevity*, Vol. 2017, Hindawi, London, https://doi.org/10.1155/2017/9085947.

Chen, K., R. N. Pittman and A. S. Popel (2008), “Nitric oxide in the vasculature: where does it come from and where does it go? A quantitative perspective”, *Antioxidants & redox signaling*, Vol. 10/7, Mary Ann Liebert, Inc., Larchmont, https://doi.org/10.1089/ars.2007.1959.

Förstermann, U. (2010), “Nitric oxide and oxidative stress in vascular disease”, *Pflugers Archiv : European journal of physiology*, Vol. 459/6, Springer, Berlin, https://doi.org/10.1007/s00424-010-0808-2.

Hasan, H. F., R. R. Radwan and S. M. Galal (2019), “Bradykinin-potentiating factor isolated from Leiurus quinquestriatus scorpion

venom alleviates cardiomyopathy in irradiated rats via remodelling of the RAAS pathway", *Clinical and Experimental Pharmacology and Physiology*, Vol. 47/2, Wiley-Blackwell, Hoboken, https://doi.org/10.1111/1440-1681.13202.

Incalza, M. A. et al. (2018), "Oxidative stress and reactive oxygen species in endothelial dysfunction associated with cardiovascular and metabolic diseases", *Vascular pharmacology*, Vol. 100, Elsevier, Amsterdam, https://doi.org/10.1016/j.vph.2017.05.005.

Kojsová, S. et al. (2006), "The effect of different antioxidants on nitric oxide production in hypertensive rats", *Physiological research*, Vol. 55, Czech Academy of Sciences, Prague, https://doi.org/10.33549/physiolres.930000.55.S1.3.

Kozbenko, T. et al. (2022), "Deploying elements of scoping review methods for adverse outcome pathway development: a space travel case example", *International Journal of Radiation Biology*, Vol. 98/12. https://doi.org/10.1080/09553002.2022.2110306

Matsubara, K. et al. (2015), "Nitric oxide and reactive oxygen species in the pathogenesis of preeclampsia", *International journal of molecular sciences*, Vol. 16/3, Multidisciplinary Digital Publishing Institute, Basel, https://doi.org/10.3390/ijms16034600.

Mitchell, A. et al. (2019), "Cardiovascular effects of space radiation: implications for future human deep space exploration", *European Journal of Preventive Cardiology*, Vol. 26/16, SAGE Publishing, Thousand Oaks, https://doi.org/10.1177/2047487319831497.

Nagane, M. et al. (2021), "DNA damage response in vascular endothelial senescence: Implication for radiation-induced cardiovascular diseases", *Journal of Radiation Research*, Vol. 62/4, Oxford University Press, Oxford, https://doi.org/10.1093/JRR/RRAB032.

Sakata, K. et al. (2015). "Roles of ROS and PKC-βII in ionizing radiation-induced eNOS activation in human vascular endothelial cells", *Vascular Pharmacology*, Vol. 70, Elsevier, Amsterdam, https://doi.org/10.1016/j.vph.2015.03.016.

Soloviev, A. I. and I.V. Kizub (2019), "Mechanisms of vascular dysfunction evoked by ionizing radiation and possible targets for its pharmacological correction", *Biochemical pharmacology*, Vol. 159, Elsevier, Amsterdam, https://doi.org/10.1016/j.bcp.2018.11.019.

Soucy, K. G. et al. (2011), "HZE 56Fe-ion irradiation induces endothelial dysfunction in rat aorta: Role of xanthine oxidase", *Radiation Research*, Vol. 176/4, Radiation Research Society, Bozeman, https://doi.org/10.1667/RR2598.1.

Soucy, K. G. et al. (2010), "Dietary inhibition of xanthine oxidase attenuates radiation-induced endothelial dysfunction in rat aorta", *Journal of Applied Physiology*, Vol. 108/5, American Physiological Society, Rockville, https://doi.org/10.1152/japplphysiol.00946.2009.

Wang, Y., M. Boerma and D. Zhou (2016), "Ionizing Radiation-Induced Endothelial Cell Senescence and Cardiovascular Diseases", *Radiation research*, Vol. 186/2, Radiation Research Society, Bozeman, https://doi.org/10.1667/RR14445.1.

Yan, T. et al. (2020), "Ionizing radiation induces BH4 deficiency by downregulating GTP-cyclohydrolase 1, a novel target for preventing and treating radiation enteritis", *Biochemical Pharmacology*, Vol. 180, Elsevier, Amsterdam, https://doi.org/10.1016/j.bcp.2020.114102.

Zhang, R. et al. (2009), "Blockade of AT1 receptor partially restores vasoreactivity, NOS expression, and superoxide levels in cerebral and carotid arteries of hindlimb unweighting rats", *Journal of applied physiology*, Vol. 106/1, American Physiological Society, Rockville, https://doi.org/10.1152/japplphysiol.01278.2007.

Relationship: 2775: Altered Signaling leads to Increase, Endothelial Dysfunction

AOPs Referencing Relationship

AOP Name	Adjacency	Weight of Evidence	Quantitative Understanding
Deposition of energy leads to vascular remodeling	adjacent	Moderate	Low

Evidence Supporting Applicability of this Relationship

Taxonomic Applicability

Term	Scientific Term	Evidence	Links
human	Homo sapiens	Low	NCBI
rat	Rattus norvegicus	Moderate	NCBI

Life Stage Applicability

Life Stage	Evidence
Adult	Moderate
Juvenile	Low

Sex Applicability

Sex	Evidence
Male	Moderate
Female	Low
Unspecific	Low

Evidence for this KER is supported through *in vivo* rat and *in vitro* human studies. The in vivo studies were conducted in male animals, although the relationship is still plausible in females. The in vivo studies were undertaken in adolescent and adult rats.

Key Event Relationship Description

Altered signaling pathways can disrupt cellular homeostasis and induce endothelial dysfunction, characterized by a prolonged state of endothelial activation (Deanfield et al., 2007). Signaling pathways involved in triggering endothelial dysfunction include the p53-p21 pathway, the Akt/phosphtidylinositol-3-kinase (PI3K)/mechanistic target of rapamycin (mTOR) pathway, the RhoA-Rho-kinase pathway, and the acid sphingomyelinase (ASM)/ceramide (Cer) pathway (Venkatsulu et al., 2018; Soloviev et al., 2019; Wang et al., 2016). Activation of the signaling molecule p53 by phosphorylation enhances its stability, leading to cell cycle arrest and premature senescence in endothelial cells and can alternatively lead to a caspase cascade resulting in cellular apoptosis. Activation of the sphingomyelinase ceramide pathway can also contribute to endothelial apoptosis through production of ceramide that activates mitogen-activated protein kinase (MAPK) and extracellular-signal-regulated kinase (ERK). Signaling molecules MAPK and ERK can also be activated as a direct response to a stressor and prompt a cascade of events resulting in endothelial cell apoptosis. Impairment of the Akt/PI3K/mTOR pathway can lead to apoptosis by preventing cell survival signaling and can also lead to downregulation of Rho cytoskeletal proteins for senescence of endothelial cells (Venkatesulu et al., 2018; Soloviev et al., 2019; Nagane et al., 2021; Ramadan et al., 2021; Hughson et al., 2018).

Evidence Supporting this KER

Overall weight of evidence: Moderate

Biological Plausibility

The biological plausibility of the connection between altered signaling pathways leading to an increase in endothelial dysfunction is well-supported by literature and the mechanisms are generally understood. Multiple signaling pathways influence endothelial function.

Modulation of the Akt/PI3K/mTOR pathway downregulates downstream Rho cytoskeletal proteins, which leads to partial-to-full senescence of endothelial cells, resulting in increased vascular permeability and endothelial dysfunction (Venkatsulu et al., 2018). Modulation of the Akt/PI3K/mTOR pathway also acts upstream of the p53-p21 pathway to mediate endothelial cell senescence (Wang et al., 2016). Unlike in other cell types, in endothelial cells the p53-p21 pathway is more important than the p16-Rb pathway for induction of cell senescence (Wang et al., 2016). Senescent endothelial cells show changes in cell morphology, cell-cycle arrest, and increased senescence-associated β-galactosidase (SA-β-gal) staining. These changes lead to endothelial dysfunction, which results in dysregulation of vasodilation (Wang et al., 2016; Hughson et al., 2018; Ramadan et al., 2021). Phosphorylation of p53 is another important moderator of apoptosis in endothelial cells, as well as the ASM/Cer pathway, where the production of ceramide mediates endothelial apoptosis through sphingomyelinase, activating MAPK and ERK, which prompt a cascade of events culminating in endothelial cell apoptosis, another cellular marker for endothelial dysfunction (Venkatsulu et al., 2018; Soloviev et al., 2019).

Empirical Evidence

Empirical Evidence

The empirical evidence supporting this KER was gathered from research utilizing both *in vivo* and *in vitro* models. Many in vitro studies have examined the relationship using endothelial cell cultures. Endothelial dysfunction due to altered signaling can be measured by premature endothelial cell senescence, apoptosis and impaired contractile response (Korpela & Liu, 2014). Levels of signaling molecules in pathways such as the Akt/PI3K/mTOR, RhoA-Rho-kinase, and ASM/Cer pathways, and the effect they have on endothelial dysfunction as characterized by endothelial cellular senescence, apoptosis and contractile response, was examined in these studies (Chang et al., 2017; Cheng et al., 2017; Su et al., 2020; Summers et al., 2008; Yentrapalli et al., 2013a; Yentrapalli et al., 2013b).

Dose Concordance

Studies have used *in vitro* models with acute and chronic doses of radiation administered from 0.23 to 10 Gy to show that the dose at which significant alterations in signaling pathways occurs is concordant with doses at which endothelial dysfunction occurs. Alterations in various signaling pathways, including decreases in the Akt/PI3K/mTOR pathway and increases in the p53-p21 pathway, both occurred at 2.4 and 4 Gy; endothelial cell senescence was found only at 4 Gy (Yentrapalli et al., 2013a). Another study using 4.1 mGy/h chronic gamma irradiation found significant changes in the p53-p21 and ERK signaling pathways after both

2.1 and 4.1 Gy (Yentrapalli et al., 2013b). These changes were associated with an increase in endothelial dysfunction at both doses as well, with only a slight increase in cell senescence after 2.1 Gy (Yentrapalli et al., 2013b). Endothelial cells exposed to a single dose of 10 Gy of X-rays showed an increase in Akt and p-Akt that was correlated with an increase in endothelial dysfunction indicated by a 5-fold increase in apoptosis (Chang et al., 2017).

Various studies also showed that altered signaling and endothelial dysfunction can occur at the same stressor severity during hindlimb unloading (HU). Rats exposed to microgravity for 20 days showed both decreased RhoA signaling molecule and impaired vasodilation (Summers et al., 2008). Two studies observing the effects of microgravity for 4 weeks in rats found that a decrease in the ASM/Cer pathway resulted in better endothelial function, while an increase in the pathway resulted in endothelial dysfunction (Cheng et al., 2017; Su et al., 2020).

Time Concordance

There is limited evidence to suggest a time concordance between altered signaling pathways and endothelial dysfunction. In a study using gamma irradiation in vitro, the p53-p21 and ERK signaling pathways were altered after 3 weeks of chronic gamma irradiation, while cell senescence was increased only slightly after 3 weeks, and increased more after 6 weeks (Yentrapalli et al., 2013b). In a similar study, alterations in various signaling pathways including decreases in the Akt/PI3K/mTOR pathway were found as early as 1 week during chronic gamma irradiation (Yentrapalli et al., 2013a). The earliest significant increase in cellular senescence occurred after 10 weeks (Yentrapalli et al., 2013a).

Incidence Concordance

There is limited support in current literature for an incidence concordance relationship between altered signaling and endothelial dysfunction. One out of the 6 primary research studies used to support this KER demonstrated an average change to endpoints of altered signaling that was greater or equal to that of endothelial dysfunction (Cheng et al., 2017; Yentrapalli et al., 2013b). After 6 weeks of gamma irradiation of HUVECs, altered signaling marker, p21, was increased by 3.5-fold, compared to the 3-fold increase in SA-β-gal staining, a marker for endothelial cell senescence (Yentrapalli et al., 2013b).

Essentiality

Changes in endothelial signaling pathways can trigger endothelial dysfunction. Therefore, in the absence of altered signaling endothelial dysfunction is not expected. Through the use of signaling molecule inhibitors such as Y27632 and dpm, altered signaling can be suppressed which results in reduced endothelial dysfunction (Venkatsulu et al., 2018; Soloviev et al., 2019; Wang et al., 2016). A study observing the effects of Y27632, a Rho kinase inhibitor, found that when rat abdominal aortas were incubated with Y27632 the contractile response, which was hindered by HU, was returned to control levels (Summers et al., 2008). Similar results have been shown by other groups that have looked at endothelial cells incubated in mesenchymal stem cell conditioned media (MSC-CM), which is thought to exhibit therapeutic potential for microvascular injury through angiogenic cytokines. MSC-CM prevented an increase in cleaved capsase-3 and increased both Akt and p-Akt, which was associated with a substantial decrease in apoptosis (Chang et al., 2017). It has also been found that enhancing the ASM/Cer pathway with C6-ceramide increases downstream caspase-3 and endothelial dysfunction, measured by apoptosis, while ASM inhibitors dpm and DOX partially decreased both caspase-3 and apoptosis (Su et al., 2020; Cheng et al., 2017).

Uncertainties and Inconsistencies

- Much of the evidence for this relationship comes from *in vitro* studies; further work is needed to determine the certainty of the relationship at the tissue level.

Quantitative Understanding of the Linkage

The following are a few examples of quantitative understanding of the relationship. All data that is represented is statistically significant unless otherwise indicated.

Response-response relationship

Dose/incidence concordance

Reference	Experiment Description	Result
Yentrapalli et al., 2013a	*In vitro*. Human umbilical vein endothelial cells (HUVECs) were irradiated with ^{137}Cs gamma radiation at 1.4 mGy/h or 2.4 mGy/h dose rates over a period of 12 weeks. Signaling molecules were used as measures of	1.4 mGy/h dose rate: This dose rate led to alterations in the Akt/PI3K/mTOR pathway including a 3-fold increase in p21, a 0.7-fold decrease in p-Akt and PI3K, and a 0.8-fold decrease in mTOR. However, this dose rate did not induce endothelial dysfunction (no significant changes in SA-β-gal staining). 2.4 mGy/h dose rate: This dose rate led to alterations in the Akt/PI3K/mTOR pathway including a 3-fold increase in p21, a 1.5-fold increase in Akt, a 0.7-fold

	altered signaling. Cell senescence was used as a measure of endothelial dysfunction.	decrease in p-Akt and PI3K, a 0.8-fold decrease in mTOR and a 0.5-fold decrease in p-ERK. This dose rate induced endothelial dysfunction as indicated by a 2-fold increase in SA-β-gal staining, a marker for endothelial cell senescence.
Yentrapalli et al., 2013b	*In vitro*. HUVECs were irradiated with ^{137}Cs gamma radiation at a 4.1 mGy/h dose rate over the course of 6 weeks. Signaling molecules were used as measures of altered signaling. Cell senescence was used as a measure of endothelial dysfunction.	Chronic irradiation led to a 2.5-fold increase in p-p53, a key signaling molecule in initiating endothelial cell senescence, after week 6 (4.13 Gy). There was no significant change in total p53 or p-ERK2 at any time point, while total ERK2 showed a 0.5-fold decrease after 3 weeks (2.07 Gy). p21, which acts downstream of p53, increased 3.5-fold by week 6 (4.13 Gy). Alterations in the above signaling molecules correlated with an increase in endothelial dysfunction as indicated by a 1.5-fold increase in SA-β-gal staining, a marker for endothelial cell senescence, after 3 weeks and 3-fold after 6 weeks (4.13 Gy).
Chang et al., 2017	*In vitro*. HUVECs were irradiated with 10 Gy of X-rays. Signaling molecules were used as measures of altered signaling. Apoptosis was used as a measure of endothelial dysfunction.	A 2-fold increase in cleaved caspase-3, part of the apoptosis signaling cascade, in the irradiated endothelial cells was correlated with an increase in endothelial dysfunction indicated by a 4-fold increase in the percentage of apoptotic cells.
Summers et al., 2008	*In vivo*. Adult male Wistar rats underwent 20-day HU after which abdominal aortas were harvested. Signaling molecules were used as measures of altered signaling. Contractile response was used as a measure of endothelial dysfunction.	Following HU, signaling molecule RhoA decreased by 0.5-fold and endothelial dysfunction was induced in the form of reduced contractile response to phenylephrine by 0.5-fold.
Su et al., 2020	*In vivo*. Sprague-Dawley male rats underwent 4 weeks of HU, following which cerebral and mesenteric arteries were harvested. Signaling molecules were used as measures of altered signaling. Apoptosis was used as a measure of endothelial dysfunction.	Simulated microgravity revealed a decrease in signaling molecules ASM and Cer in cerebral arteries but an increase in mesenteric arteries of rats. Caspase-3, a signaling molecule in the apoptosis cascade, decreased 0.5-fold in cerebral arteries and increased 2-fold in mesenteric arteries. This was associated with an increase in endothelial function in cerebral arteries by decreasing apoptosis 0.3-fold and an increase in endothelial dysfunction in mesenteric arteries by increasing apoptosis 2-fold.
Cheng et al., 2017	*In vivo*. Sprague-Dawley male rats underwent 4 weeks of hindlimb unloading following which carotid arteries were harvested. Signaling molecules were used as measures of altered signaling. Apoptosis was used as a measure of endothelial dysfunction.	2 weeks of simulated microgravity resulted in a 0.6-fold decrease in signaling molecules ASM and caspase-3, which led to a decrease of endothelial dysfunction indicated by 0.5-fold reduced apoptosis in the carotid arteries of rats.

Time-scale

Time concordance

Reference	Experiment Description	Result
Yentrapalli et al., 2013a	*In vitro*. HUVECs were irradiated with ^{137}Cs gamma radiation at 1.4 mGy/h or 2.4 mGy/h dose rates over a period of 10 weeks. Signaling molecules were used as measures of altered signaling. Cell senescence was used as a measure of endothelial dysfunction.	1.4 mGy/h dose rate: This dose rate led to alterations in the Akt/PI3K/mTOR pathway including a 3-fold increase in p21 after 10 weeks, a 0.7-fold decrease in p-Akt and PI3K after 6 and 10 weeks, and a 0.8-fold decrease in mTOR after 10 weeks. However, this dose rate did not induce endothelial dysfunction (no significant changes in SA-β-gal staining at any timepoint). 2.4 mGy/h dose rate: This dose rate caused alterations in the Akt/PI3K/mTOR pathway including a 3-fold increase in p21 after 10 weeks, a 1.5-fold increase in Akt after 1 week, a 0.7-fold decrease in p-Akt and PI3K after 6 and 10 weeks, a 0.8-fold decrease in mTOR and a 0.5-fold decrease in p-ERK after 10 weeks. This dose rate induced endothelial dysfunction indicated by a 2-fold increase in SA-β-gal staining, after 12 weeks.
Yentrapalli et al., 2013b	*In vitro*. HUVECs were irradiated with ^{137}Cs gamma radiation at a 4.1 mGy/h dose rate over the course of 6 weeks. Signaling molecules were used as measures of altered signaling. Cell senescence was used	Chronic irradiation led to a 2.5-fold increase in p-p53, a key signaling molecule in initiating endothelial cell senescence, after week 6 (4.13 Gy). There was no significant change in total p53 or p-ERK2 at any time point, while total ERK2 showed a 0.5-fold decrease after 3 weeks (2.07 Gy). p21, which acts downstream of p53, increased 3.5-fold by week 6 (4.13 Gy). Alterations in the above signaling molecules correlated with an increase in endothelial dysfunction

	as a measure of endothelial dysfunction.	as indicated by a 1.5-fold increase in SA-β-gal staining after 3 weeks and 3-fold after 6 weeks (4.13 Gy).

Known modulating factors

Modulating factor	Details	Effects on the KER	References
Drug	Ceramide-6 (Cer-6)	Increases downstream caspase-3 and apoptosis	(Cheng et al., 2017; Su et al., 2020)
Media	Mesenchymal stem cell conditioned media	Prevented an increase in cleaved capsase-3, increased both Akt and p-Akt, and decreased apoptosis	(Chang et al., 2017)
Drug	Y27632 (Rho kinase inhibitor)	Recovered contractile response that was attenuated by HU	(Summers et al., 2008)
Drug	Desipramine (dpm) (ASM inhibitor)	Partially decreased caspase-3 and apoptosis	(Cheng et al., 2017; Su et al., 2020)
Drug	Dopexin hydrochloride (DOX) (ASM inhibitor)	Partially decreased caspase-3 and apoptosis	(Cheng et al., 2017; Su et al., 2020)

Known Feedforward/Feedback loops influencing this KER

Not identified.

References

Chang, P. Y. et al. (2017), “MSC-derived cytokines repair radiation-induced intra-villi microvascular injury”, *Oncotarget*, Vol. 8/50, Impact Journals, Orchard Park, https://doi.org/10.18632/oncotarget.21236.

Cheng, Y. P. et al. (2017), “Acid sphingomyelinase/ceramide regulates carotid intima-media thickness in simulated weightless rats”, *Pflugers Archiv European Journal of Physiology*, Vol. 469, Springer, New York, https://doi.org/10.1007/s00424-017-1969-z

Deanfield, J.E., J. P. Halcox and T. J. Rabelink (2007), “Endothelial function and dysfunction: Testing and clinical relevance”, *Circulation*, Vol. 115/10, Lippincott Williams & Wilkins, Philadelphia, https://doi.org/10.1161/CIRCULATIONAHA.106.652859

Hughson, R.L., A. Helm and M. Durante (2018), “Heart in space: Effect of the extraterrestrial environment on the cardiovascular system”, *Nature Reviews Cardiology*, Vol. 15/3, Nature Portfolio, London, https://doi.org/10.1038/nrcardio.2017.157

Korpela, E., and S. K. Liu (2014), “Endothelial perturbations and therapeutic strategies in normal tissue radiation damage”, *Radiation oncology,* Vol. 9, BioMed Central, London, https://doi.org/10.1186/s13014-014-0266-7

Kozbenko, T. et al. (2022), “Deploying elements of scoping review methods for adverse outcome pathway development: a space travel case example”, *International Journal of Radiation Biology*, Vol. 98/12. https://doi.org/10.1080/09553002.2022.2110306

Nagane, M. et al. (2021), “DNA damage response in vascular endothelial senescence: Implication for radiation-induced cardiovascular diseases”, *Journal of Radiation Research*, Vol. 62/4, Oxford University Press, Oxford, https://doi.org/10.1093/JRR/RRAB032

Ramadan, R. et al. (2021), “The role of connexin proteins and their channels in radiation-induced atherosclerosis”, *Cellular and molecular life sciences: CMLS*, Vol. 78/7, Springer, New York, https://doi.org/10.1007/s00018-020-03716-3

Soloviev, A. I. and I. V. Kizub (2019), “Mechanisms of vascular dysfunction evoked by ionizing radiation and possible targets for its pharmacological correction”, *Biochemical pharmacology*, Vol. 159, Elsevier, Amsterdam, https://doi.org/10.1016/j.bcp.2018.11.019

Su, Y. T. et al. (2020), “Acid sphingomyelinase/ceramide mediates structural remodeling of cerebral artery and small mesenteric artery in simulated weightless rats”, *Life sciences*, Vol. 243, Elsevier, Amsterdam, https://doi.org/10.1016/j.lfs.2019.117253

Summers, S. M., S. V. Nguyen, and R. E. Purdy (2008), “Hindlimb unweighting induces changes in the RhoA-Rho-kinase pathway of the rat abdominal aorta”, *Vascular pharmacology*, Vol. 48/4-6, Elsevier, Amsterdam, https://doi.org/10.1016/j.vph.2008.03.006

Venkatesulu, B. P. et al. (2018), “Radiation-Induced Endothelial Vascular Injury: A Review of Possible Mechanisms”, *JACC: Basic to translational science*, Vol. 3/4, Elsevier, Amsterdam, https://doi.org/10.1016/j.jacbts.2018.01.014

Wang, Y., M. Boerma and D. Zhou (2016), “Ionizing Radiation-Induced Endothelial Cell Senescence and Cardiovascular Diseases”, *Radiation research*, Vol. 186/2, Radiation Research Society, Bozeman, https://doi.org/10.1667/RR14445.1.

Yentrapalli, R. et al. (2013a), “The PI3K/Akt/mTOR pathway is implicated in the premature senescence of primary human endothelial cells exposed to chronic radiation”, *PloS one*, Vol. 8/8, PLOS, San Francisco,

https://doi.org/10.1371/journal.pone.0070024

Yentrapalli, R. et al. (2013b), “Quantitative proteomic analysis reveals induction of premature senescence in human umbilical vein endothelial cells exposed to chronic low-dose rate gamma radiation”, *Proteomics*, Vol. 13/7, John Wiley & Sons, Ltd., Hoboken, https://doi.org/10.1002/pmic.201200463

Relationship: 2777: Increased pro-inflammatory mediators leads to Increase, Endothelial Dysfunction

AOPs Referencing Relationship

AOP Name	Adjacency	Weight of Evidence	Quantitative Understanding
Deposition of energy leads to vascular remodeling	adjacent	Moderate	Low

Evidence Supporting Applicability of this Relationship

Taxonomic Applicability

Term	Scientific Term	Evidence	Links
human	Homo sapiens	Low	NCBI
mouse	Mus musculus	Moderate	NCBI
rat	Rattus norvegicus	Low	NCBI

Life Stage Applicability

Life Stage	Evidence
Adult	Low
Juvenile	Moderate

Sex Applicability

Sex	Evidence
Male	Moderate
Female	Low
Unspecific	Low

The majority of the evidence is derived from *in vitro* studies, and a single *in vivo* study in male pre-adolescent mice.

Key Event Relationship Description

An increase in pro-inflammatory mediators including the cytokines tumor necrosis factor-α (TNF-α), interleukin 1 beta and 6 (IL-1β, IL-6), chemokines monocyte chemoattractant protein 1 (MCP-1) and intercellular adhesion molecule 1 (ICAM-1) can lead to inflammatory response which can disrupt cellular homeostasis and if persistent can lead to eventual endothelial dysfunction (Venkatesulu et al., 2018; Korpela & Liu, 2014). Normally, an inflammatory response provides a protective effect to the endothelium but if prolonged (over months) it can exhaust this protective inflammatory effect, as a result, endothelial cells may become senescent or apoptotic, leading to endothelial dysfunction (Deanfield et al., 2007; Bonetti et al., 2003, Wang et al., 2016; Hughson et al., 2018; Ramadan et al., 2021).

Evidence Supporting this KER

Overall weight of evidence: Moderate

Biological Plausibility

The biological plausibility connecting increased pro-inflammatory mediators to increased endothelial dysfunction is well-supported by literature (Bonetti et al., 2003; Deanfield et al., 2007; Hughson et al., 2018; Ramadan et al., 2021; Wang et al., 2019; Wang et al., 2016), and has been demonstrated in animal studies and human cell models (Shen et al., 2018; Chang et al., 2017; Baselet et al., 2017; Ramadan et al., 2020; Ungvari et al., 2013).

Inflammation can initially provide a protective effect to the endothelium, but chronic inflammation can exhaust this protective inflammatory effect resulting in loss of endothelial integrity and resident cells becoming senescent or apoptotic, leading to endothelial dysfunction (Deanfield et al., 2007; Bonetti et al., 2003). Senescent endothelial cells show changes in cell morphology, cell-cycle arrest, and increased senescence-associated β-galactosidase (SA-β-gal) staining. These changes lead to endothelial dysfunction, which also leads to dysregulation of vasodilation (Wang et al., 2016; Hughson et al., 2018; Ramadan et al., 2021). The

inflammatory response is regulated by a balance between pro-inflammatory and anti-inflammatory mediators, and specific cytokine profiles are dependent on parameters of the stressor/exposure/insult (Wang et al., 2019). The pro-inflammatory cytokines TNF-α and IL-1 play a critical role by triggering a cytokine cascade, which initiates an inflammatory response to promote healing and restore tissue function. TNF-α is able to induce apoptotic cell death, which is implicated in endothelial dysfunction. Nuclear factor kappa B (NF-κB) is also activated, which targets multiple genes coding for vascular cell adhesion proteins (VCAM), intercellular adhesion molecule (ICAM), and IL-1, as well as prothrombotic markers (Slezak et al., 2017). NF-κB mediates a pro-survival and pro-inflammatory state. Inflammation persisting for months leads to prolonged chronic inflammation, which causes an ineffective healing process that is further worsened by a decrease in endothelium-dependent relaxation. This causes endothelial dysfunction, making vasculature more vulnerable to damage from non-laminar flow (Sylvester et al., 2018). Senescent cells also have a pro-inflammatory secretory phenotype, which further contributes to negative effects on the endothelium. Increased pro-inflammatory mediators may be due to increased expression but may also be attributed to increased permeability of the endothelium as seen after irradiation in animal models, which results in increased transmigration of inflammatory cells into the endothelium and can lead to eventual dysfunction (Hughson et al., 2018).

Empirical Evidence

The empirical evidence supporting this KER is gathered from research utilizing both *in vivo* and *in vitro* models. Many *in vitro* studies have examined the relationship using endothelial cell cultures. Levels of pro-inflammatory mediators such as TNF-α, IL-1β, IL-6, IL-8, MCP-1 and ICAM-1, and the effect they have on endothelial dysfunction, as characterized by endothelial cellular senescence and apoptosis, have been examined in these studies. The evidence is derived from stressors of gamma and X-ray radiation in the range of 0.05-18 Gy (Shen et al., 2018; Baselet et al., 2017; Ramadan et al., 2020; Ungvari et al., 2013; Chang et al., 2017).

Dose Concordance

There is moderate evidence to demonstrate dose concordance between an increase in pro-inflammatory mediators and endothelial dysfunction. Most studies do not show statistically significant effects across all doses; however, biological trends across multiple doses have been included to support this relationship.

Studies examining a range of doses from 0.05 Gy to 18 Gy using predominantly X-rays as the source of stressor support the relationship between increased pro-inflammatory mediators and endothelial dysfunction. An *in vitro* study using X-ray irradiation on human endothelial cells showed an increase in pro-inflammatory cytokines IL-6 and CCL2 at a dose as low as 0.05 Gy. Though the increase was not statistically significant, there was a biological trend showing significant increases at higher doses. All doses demonstrated a correlation to endothelial dysfunction (Baselet et al., 2017). Another study using human endothelial cells exposed to X-rays showed similar results with increases in pro-inflammatory mediators, including IL-6, VCAM-1, and IL-8, as well as SA-β-gal activity at 5 Gy (Ramadan et al., 2020).

A gamma ray study that exposed rat endothelial cells to a 6 Gy dose showed an increase in pro-inflammatory mediators IL-6, IL-1α, IL-1β, and MCP-1 associated with an increase in endothelial cell senescence (Ungvari et al., 2013). Another single dose X-ray study at 10 Gy also revealed increases in pro-inflammatory mediators with a 1.2-fold increase in IL-1α, and a 6-fold increase in IL-6 and TNF-α. This was associated with an increase in endothelial dysfunction, indicated by a 5-fold increase in apoptotic cells (Chang et al., 2017). A study using X-rays on mouse aortas found that there was a 2-fold increase in the pro-inflammatory mediators TNF-α and ICAM-1 after 18 Gy, and a 5-fold increase in endothelial apoptosis, which is a defined marker for endothelial dysfunction (Shen et al., 2018).

Time Concordance

There is limited evidence to suggest a time concordance between increased pro-inflammatory mediators and endothelial dysfunction. An *in vitro* study using 5 Gy of X-rays found that pro-inflammatory mediators, including IL-6, VCAM-1, TNF-α, ICAM-1, IL-1β and MCP-1, increased as soon as 1 day post-irradiation. SA-β-gal, a marker for cellular senescence, showed the first increase 7 days post-irradiation (Ramadan et al., 2020). A study using 18 Gy of X-rays examined mouse aortas after 3-84 days post-irradiation and found an increase in both pro-inflammatory mediators and endothelial dysfunction as early as 3 days post-irradiation (Shen et al., 2018).

Incidence concordance

Few studies demonstrated incidence concordance. In an *in vitro* study using human endothelial cells irradiated with X-rays, incidence concordance was demonstrated at both 0.5 and 2 Gy as pro-inflammatory mediators IL-6 and CCL2 were increased 2-fold or greater while SA-β-gal increased a maximum of 1.5-fold (Baselet et al., 2017). Similarly, 5 Gy of X-rays resulted in increases to multiple pro-inflammatory mediators (IL-1β, IL-6, IL-8, MCP-1, and VCAM) between 1.5- and 4-fold, while SA-β-gal activity increased 1.5-fold in human endothelial cells (Ramadan et al., 2020).

Essentiality

An increase in inflammation can trigger endothelial dysfunction. Therefore, in the absence of an increase in pro-inflammatory mediators endothelial dysfunction is not expected. Through the use of certain treatments, such as TAT-Gap19 and mesenchymal stem cells, the increase in pro-inflammatory mediators can be greatly supressed, but not fully blocked, which results in reduced but not completely prevented endothelial dysfunction such as apoptosis and cellular senescence (Venkatsulu et al., 2018; Soloviev et al., 2019; Wang et al., 2016). These treatments demonstrate the essentiality of the relationship and are described below; however, the available empirical data supporting essentiality for this KER is limited.

A study observing the effects of TAT-Gap19, a connexin43 hemichannel blocker, found the increase in pro-inflammatory mediators

seen following the stressor was largely, though not fully in all mediators, prevented. This was also associated with a decrease in SA-β-gal, a marker of endothelial cell senescence and dysfunction, compared to the irradiated group (Ramadan et al., 2020). Similar results have been shown by other groups that have examined human endothelial cells incubated in mesenchymal stem cell conditioned media (MSC-CM), which is thought to exhibit therapeutic potential for microvascular injury through angiogenic cytokines. This study revealed a significant but not complete prevention of pro-inflammatory mediators IL-1α, IL-6 and TNF-α. The same pattern was seen in endothelial dysfunction, where apoptosis was significantly prevented but was still slightly above control levels (Chang et al., 2017).

Uncertainties and Inconsistencies

- Much of the evidence for this relationship comes from *in vitro* studies; further work is needed to determine the certainty of the relationship at the tissue level.
- Although studies often measure pro-inflammatory mediators at a few specific time points, chronic inflammation is what contributes to endothelial dysfunction. More human studies should examine the temporal concordance of this relationship to identify whether the inflammation is chronic.

Quantitative Understanding of the Linkage

The following are a few examples of quantitative understanding of the relationship. All data that is represented is statistically significant unless otherwise indicated.

Response-response relationship

Dose/Incidence Concordance

Reference	Experiment Description	Result
Baselet et al., 2017	*In vitro*. Telomerase immortalized human coronary artery endothelial cells (TICAE) were irradiated with X-rays in the range of 0.05-2 Gy at a dose rate of 0.50 Gy/min.	Pro-inflammatory mediators CCL2 and IL-6 show a slight but non-significant increase at 0.05 and 0.1 Gy. SA-β-gal, a marker for endothelial dysfunction, increased 1.2-fold after 0.05 Gy and 1.5-fold after 0.1 Gy. IL-6 and CCL2 increased 2-fold after 0.5 Gy, while SA-β-gal had a 1.5-fold increase. After 2 Gy IL-6 increased 3-fold, CCL2 increased 4-fold and SA-β-gal had a 1.5-fold increase.
Shen et al., 2018	*In vivo*. Male mice were irradiated with 18 Gy of X-rays. Endpoints were assessed in the aorta.	TNF-α and ICAM-1 increased 2-fold following irradiation. Apoptosis, a marker of endothelial dysfunction, increased 5-fold.
Chang et al., 2017	*In vitro*. Human endothelial cells were irradiated with 10 Gy of X-rays at a dose rate of 1.5 Gy/min.	IL-8 increased 4-fold following irradiation. IL-1α, IL-6, and TNF-α were also increased but significance was not indicated. Apoptosis increased 5-fold.
Ungvari et al., 2013	*In vitro*. Primary rat endothelial cells were irradiated with 6 Gy of ^{137}Cs gamma rays.	IL-6 secretion increased 1.8-fold, IL-1α increased 1.6-fold, MCP-1 increased 1.4-fold, and IL-1β increased 1.6-fold. SA-β-gal positive cells increased from 0% at control to ~30%.
Ramadan et al., 2020	*In vitro*. Human endothelial cells were irradiated with either 0.1 or 5 Gy of X-rays at a dose rate of 0.5 Gy/min.	At 5 Gy, MCP-1 increased 4-fold, IL-1β increased 1.5-fold, IL-8 and VCAM-1 increased 2-fold, and IL-6 increased 3-fold. SA-β-gal activity increased by 1.5-fold.

Time-scale

Time Concordance

Reference	Experiment Description	Result
Shen et al., 2018	*In vivo*. Male mice were irradiated with 18 Gy of X-rays. Endpoints were assessed in the aorta.	3 days post irradiation ICAM-1 increased by 1.25-fold and apoptosis increased 3-fold. After 7 days ICAM-1 and TNF-α both reached a peak with a 2-fold increase while apoptosis also reached a peak with a 5-fold increase. Both pro-inflammatory and endothelial dysfunction markers showed a linear decrease from day 14 to 84 post-irradiation.
Ramadan et al., 2020	*In vitro*. Human endothelial cells were irradiated with 5 Gy of X-rays at a dose rate of 0.5 Gy/min.	Pro-inflammatory mediators were significantly increased as soon as 24 hours post-irradiation. After 7 days MCP-1 increased 4-fold, IL-1β increased 1.5-fold, IL-8 and VCAM-1 increased 2-fold, and IL-6 increased 3-fold. SA-β-gal activity increased by 1.5-fold.

Known modulating factors

Modulating factor	Details	Effects on the KER	References
Drug	TAT-Gap19 (connexin 43	Attenuated the radiation-induced increase of many pro-	(Ramadan et

	hemichannel blocker)	inflammatory mediators and SA-β-gal activity.	al., 2020)
Media	Mesenchymal stem cell conditioned media	The increase in various pro-inflammatory mediators and apoptosis was reduced.	(Chang et al., 2017)

Known Feedforward/Feedback loops influencing this KER

Pro-inflammatory mediators can induce endothelial cell senescence and subsequent endothelial dysfunction. Senescent endothelial cells can secrete many pro-inflammatory cytokines and chemokines, contributing to further senescence of other endothelial cells and further endothelial dysfunction (Hughson et al., 2018; Wang et al., 2016).

References

Baselet, B. et al. (2017), “Functional Gene Analysis Reveals Cell Cycle Changes and Inflammation in Endothelial Cells Irradiated with a Single X-ray Dose”, *Frontiers in pharmacology*, Vol. 8, Frontiers Media SA, Lausanne, https://doi.org/10.3389/fphar.2017.00213

Bonetti, P. O., L. O. Lerman and A. Lerman (2003), “Endothelial dysfunction: a marker of atherosclerotic risk”, *Arteriosclerosis, thrombosis, and vascular biology*, Vol. 23/2, Lippincott Williams & Wilkins, Philadelphia, https://doi.org/10.1161/01.atv.0000051384.43104.fc

Chang, P. Y. et al. (2017), “MSC-derived cytokines repair radiation-induced intra-villi microvascular injury”, *Oncotarget*, Vol. 8/50, Impact Journals, Buffalo, https://doi.org/10.18632/oncotarget.21236

Deanfield, J. E., J. P. Halcox and T. J. Rabelink. (2007), “Endothelial Function and Dysfunction”, *Circulation*, Vol. 115/10, Lippincott Williams & Wilkins, Philadelphia, https://doi.org/10.1161/CIRCULATIONAHA.106.652859

Hughson, R. L., A. Helm and M. Durante. (2018), “Heart in space: Effect of the extraterrestrial environment on the cardiovascular system”, *Nature Reviews Cardiology*, Vol. 15/3, Nature Portfolio, London, https://doi.org/10.1038/nrcardio.2017.157

Kozbenko, T. et al. (2022), “Deploying elements of scoping review methods for adverse outcome pathway development: a space travel case example”, *International Journal of Radiation Biology*, Vol. 98/12. https://doi.org/10.1080/09553002.2022.2110306

Ramadan, R. et al. (2021), “The role of connexin proteins and their channels in radiation-induced atherosclerosis”, *Cellular and molecular life sciences: CMLS*, Vol. 78/7, Springer, New York, https://doi.org/10.1007/s00018-020-03716-3

Ramadan, R. et al. (2020), “Connexin43 Hemichannel Targeting With TAT-Gap19 Alleviates Radiation-Induced Endothelial Cell Damage”, *Frontiers in pharmacology*, Vol. 11, Frontiers Media SA, Lausanne, https://doi.org/10.3389/fphar.2020.00212

Shen, Y. et al. (2018), “Transplantation of Bone Marrow Mesenchymal Stem Cells Prevents Radiation-Induced Artery Injury by Suppressing Oxidative Stress and Inflammation”, *Oxidative medicine and cellular longevity*, Vol. 2018, Hindawi, London, https://doi.org/10.1155/2018/5942916

Slezak, J. et al. (2017), “Potential markers and metabolic processes involved in the mechanism of radiation-induced heart injury”, *Canadian journal of physiology and pharmacology*, Vol. 95/10, Canadian Science Publishing, Ottawa, https://doi.org/10.1139/cjpp-2017-0121

Sylvester, C. B. et al. (2018), “Radiation-Induced Cardiovascular Disease: Mechanisms and Importance of Linear Energy Transfer”, *Frontiers in Cardiovascular Medicine*, Vol. 5, Frontiers Media SA, Lausanne, https://doi.org/10.3389/fcvm.2018.00005

Soloviev, A. I. and I.V. Kizub (2019), “Mechanisms of vascular dysfunction evoked by ionizing radiation and possible targets for its pharmacological correction”, *Biochemical pharmacology*, Vol. 159, Elsevier, Amsterdam, https://doi.org/10.1016/j.bcp.2018.11.019

Ungvari, Z. et al. (2013), “Ionizing Radiation Promotes the Acquisition of a Senescence-Associated Secretory Phenotype and Impairs Angiogenic Capacity in Cerebromicrovascular Endothelial Cells: Role of Increased DNA Damage and Decreased DNA Repair Capacity in Microvascular Radiosensitivity”, *The Journals of Gerontology Series A: Biological Sciences and Medical Sciences*, Vol. 68/12, Oxford University Press, Oxford, https://doi.org/10.1093/gerona/glt057

Venkatesulu, B. P. et al. (2018), “Radiation-Induced Endothelial Vascular Injury: A Review of Possible Mechanisms”, *JACC: Basic to translational science*, Vol. 3/4, Elsevier, Amsterdam, https://doi.org/10.1016/j.jacbts.2018.01.014

Wang, H. et al. (2019), “Radiation-induced heart disease: a review of classification, mechanism and prevention”, *International Journal of Biological Sciences,* Vol. 15/10, Ivyspring International Publisher, Sydney, https://doi.org/10.7150/ijbs.35460

Wang, Y., M. Boerma and D. Zhou (2016), “Ionizing Radiation-Induced Endothelial Cell Senescence and Cardiovascular Diseases”, *Radiation research*, Vol. 186/2, Radiation Research Society, Bozeman, https://doi.org/10.1667/RR14445.1.

Relationship: 2784: Increase, Endothelial Dysfunction leads to Occurrence, Vascular Remodeling

AOPs Referencing Relationship

AOP Name	Adjacency	Weight of Evidence	Quantitative Understanding
Deposition of energy leads to vascular remodeling	adjacent	Moderate	Low

Evidence Supporting Applicability of this Relationship

Taxonomic Applicability

Term	Scientific Term	Evidence	Links
human	Homo sapiens	Moderate	NCBI
mouse	Mus musculus	Moderate	NCBI
rat	Rattus norvegicus	High	NCBI

Life Stage Applicability

Life Stage	Evidence
Adult	Moderate
Juvenile	Low
Not Otherwise Specified	Moderate

Sex Applicability

Sex	Evidence
Male	High
Female	Moderate

There is a substantial amount of evidence for this KER from *in vivo* rodent models and from human studies. The sex applicability is high for males and moderate for females as many studies were done only using male animals. Most studies indicated that the animals used were adult.

Key Event Relationship Description

Proper endothelial activation is a key step in the growth of new vessels through the process of angiogenesis, a process also affected by a dysfunctional endothelium (Rajashekhar et al., 2006). Regional responses to stressors are also possible, with mechanical stressors differentially affecting pressure in vessels above (superior to) and below (inferior to) the heart (Hargens & Watenpaugh, 1996; Zhang, 2001). The endothelial layer is responsive to these variations in mechanical stresses and can adapt through altering the balance between hypertrophic and hypotrophic remodeling in smooth vessel cells lining vasculature (Baeyens et al., 2016) in part through altering the progression of the acid sphingomyelinase (ASM)/ceramide (Cer) pathway (Cheng et al., 2017).

Evidence Supporting this KER

Overall weight of evidence: Moderate

Biological Plausibility

The relationship between endothelial function and vascular remodeling is well supported through a number of in-depth reviews about the mechanisms behind the connection. In a functional endothelial layer, the endothelial cells both contribute and react to the high levels of bioavailable nitric oxide (NO). The result is a vasomotive balance primed for vasodilation and an elevated ratio of antioxidant to pro-oxidant species (Deanfield et al., 2007). Endothelial cells can become activated through various signals, including vascular endothelial growth factor (VEGF), that subsequently induce angiogenesis (Carmeliet & Jain, 2011). Lastly, the endothelial cells form tight junctions and together with pericytes form a basement membrane in tight control of vessel and cell permeability (Carmeliet & Jain, 2011).

Initial endothelial tissue injury can lead to premature cellular senescence resulting in endothelial dysfunction (Hughson et al., 2018). Cell death in the vessels can lead to overall cell loss and reduced vascular density. Although recovery in the form of revascularization following the decrease in vascular density occurs, it is complicated in cases of continuous exposure as it negatively impacts the angiogenic process (Hughson et al., 2018). Stressors such as radiation are thought to disturb angiogenesis through decreasing VEGF secretion causing a decrease in tubule formation (Sylvester et al., 2018). Following the initial tissue injury, the body's ability to heal is also compromised, in part due to the prolonged state of oxidative stress and simultaneous decrease in endothelium-dependent vasorelaxation leading to increase in non-laminar blood flow. To compensate for the damage

caused by this turbulent flow, there is intima-media thickening and potential for eventual atherosclerosis (Bonetti et al., 2003; Hughson et al., 2018; Slezak et al., 2017; Sylvester et al., 2018). Continued injury also leaves the vessels vulnerable to maladaptive repair and ensuing fibrosis (Hsu et al., 2019).

When activated within healthy limits, endothelial cells loosen at their junction and the presence of VEGF induces increased vessel permeability allowing for the vessels to expand and undergo angiogenesis (Carmeliet & Jain, 2011). However, prolonged increase in permeability is also a marker of dysfunction, where increases in adhesion proteins, and elevated levels of cell senescence accompany this change (Demontis et al., 2017; Hughson et al., 2018). Disruption of endothelial integrity can also lead to cell detachment from the basement membrane; with cardiovascular deconditioning following bedrest leading to significantly elevated levels of circulating endothelial cells in microcirculation (Zhang, 2013). In addition to vessel permeability, there are changes to permeability of endothelial cells themselves, which is shown to increase and not recover following removal of the stressor (Baran et al., 2021).

The elevated bioavailability of NO associated with proper endothelial function correlates with a decrease in prothrombotic factors, while a dysfunction in the endothelium creates a pro-thrombotic environment (Krüger-Genge et al., 2019). This is also true in the case of certain kinds of vascular damage, where a dysfunctional endothelial layer following stressor exposure has been shown to lead to lymphocyte adhesion and thrombus formation. This pro-thrombotic environment causes vessel occlusion and a decrease in capillary and vascular density, which in turn results in increased vascular resistance requiring further vascular remodeling as compensation (Slezak et al., 2017). Cell senescence following damage also induces monocyte adhesion and can further contribute to creating a pro-atherosclerotic environment (Hughson et al., 2018).

There is also evidence that the relationship between endothelial function and vascular remodeling is regionally affected following the exposure to localized varied mechanical stressors such as microgravity. Under microgravity conditions (and in simulated microgravity models such as hindlimb unloading (HU)), there is a cephalic shift in blood and fluid resulting in a change of transmural pressure, increasing pressure in vessels above the heart and decreasing in those below (Hargens & Watenpaugh, 1996; Zhang, 2001). The heart continues to pump as usual; however, above the heart the arterial flow is no longer pushing against gravity resulting in increased arterial vascular pressure, while venous return is simultaneously slowed without gravitational assistance. This results in changes such distended veins and arteries in the upper body, increased carotid intima-media thickness and vascular stiffness (Garrett-Bakelman et al., 2019). In the lower limb, the opposite is true as arterial perfusion is decreased and venous return is increased resulting in muscle atrophy. Blood pressure and related fluid shear stress act as important mechanical input for the mechanosensing endothelial cells, which translate these forces into biochemical signals that guide vascular remodeling through affecting the balance between vascular smooth muscle cell proliferation and apoptosis (Baeyens et al., 2016). Above the heart, remodeling presents as hypertrophy and increase in vasoreactivity, while below the heart there is hypotrophy and decrease in myogenic tone and vasoreactivity (Zhang, 2013). This trend has been observed by various reviews and studies; a review examining studies using HU rats summarized that the models studied showed both a decrease in response to drugs inducing vasodilation and constriction and a subsequent increased stiffness in the aorta and carotid arteries (Platts et al., 2014). In humans, bedrest study participants showed both a decrease in endothelium-dependent vasodilation and an increase in circulating endothelial cells – both markers of endothelial dysfunction. Additional bedrest studies also show a decrease in vessel diameter and intimal-medial thickness in arteries below the heart while those above the heart remain unaffected (Zhang, 2013). Ultrasound measurements of cosmonauts having travelled aboard Mir and Salyut-7 showed that after spaceflight, blood supply to the brain remained stable while below the heart vascular tone and arterial resistance was severely compromised (Zhang, 2013).

Research comparing the changes in vascular structure and vasodilation response between the various muscle resistance arteries following HU also showed changes to regionally vary between the vessels studied (Delp et al., 2000; Zhang, 2013). Additionally, HU models showed differences in the arterial response to vasoconstrictors and changes to artery diameter in cutaneous versus skeletal muscle arteries (Tarasova et al., 2020). The ASM and Cer pathway has been investigated for its role in remodeling. The work of Cheng et al. (2017) and Su et al. (2020) both found that a decrease in ASM activity and subsequent Cer production was linked to a decrease in apoptosis levels and a resulting thickening of vessel structure (Cheng et al., 2017; Su et al., 2020). It is important to note that some of the vascular changes following microgravity are protective adaptations that serve to safeguard the cardiovascular system in altered gravity conditions. Under continued microgravity conditions, these changes maintain their protective purpose and are thought not to contribute to adverse outcome progression. The problem arises upon return to earth when the vessels that have adapted to microgravity blood distribution are faced with earth conditions and issues like a decreased orthostatic tolerance surface.

Empirical Evidence

Dose Concordance

There is some evidence in the literature supporting dose concordance between endothelial dysfunction and vascular remodeling. For example, gamma irradiation at 0.5 Gy led to a 9% decrease in endothelium-dependent vasodilation and no significant changes to vascular stiffness, while a 1 Gy dose led to 13% decrease in vasodilation corresponding to a 16% increase in vascular stiffness (Soucy et al., 2011). A dose of 5 Gy gamma rays significantly attenuated endothelium-dependent vasodilation, while simultaneously increasing vascular stiffness compared to a non-irradiated control (Soucy et al., 2010). Work exploring apoptosis as a measure of endothelial dysfunction demonstrated that an 18 Gy dose of X-rays increased the number of cells with apoptotic DNA fragmentation

~4.5-fold and increased aortic thickness ~1.5 fold compared to control (Shen et al., 2018).

Studies in rat models of HU by Su et al. (2020), Delp et al. (2000), and Cheng et al. (2017) all demonstrate the regional effects of changes in pressure on resulting vascular adaptation and remodeling. Su et al. (2020) compared the effects of 4-week unloading on the cerebral versus mesenteric artery, showing the balance moving towards cell proliferation above the heart (cerebral artery) with a decrease in apoptosis and increase in intima-media thickness and cross-sectional area. Meanwhile, below the heart (mesenteric artery) apoptosis increased and intima-media thickness and cross-sectional area decreased (Su et al., 2020). This agrees with a similar study that found apoptosis decreased and intima-media thickness of the carotid artery increased following HU (Cheng et al., 2017). Delp et al. (2000) showed that regional adaptations to changes in pressure following HU are also affected by how this change in pressure manifests. Vascular structure changes and endothelium-dependent vasodilation were observed in the gastrocnemius and soleus primary arterioles. Both vessels are in the hindlimbs of mice and therefore are subject to a decrease in pressure following cephalic shift in fluid in 2-week HU. In the gastrocnemius muscle, which saw a decrease in transmural pressure, the decrease in vessel cross sectional area (CSA) was due to muscle atrophy shown by a drop in media thickness but no change in outer media perimeter. In contrast, the soleus muscle experienced a drop in wall shear stress and saw a drop in vessel perimeter with no change in media thickness. Simultaneously, arterioles in the gastrocnemius muscle saw no change in acetylcholine (ACh) response, while those in soleus muscles saw a 50% decrease following the unloading and recovery to control levels at the 4-week time point (Delp et al., 2000).

Time Concordance

There is limited evidence supporting the time concordance of endothelial dysfunction and vascular remodeling. Aortic relaxation response to ACh in Sprague-Dawley rats was found to decrease 20-30% 2 weeks after gamma irradiation with an increase in vascular stiffness measured by pulse-wave velocity (PWV) from around 3.9 m/s to 4.9 m/s (Soucy et al., 2010; Soucy et al., 2007). Shen et al. (2018) demonstrated that endothelial dysfunction assessed via apoptosis became significant 3 days after 18 Gy X-rays in a mouse model, then had a linear decrease which tapered off by day 84. Aortic wall thickness, in turn, showed no significant increase on day 3 post-irradiation, only reaching maximal increase on day 7 before also decreasing linearly to day 84 (Shen et al., 2018). At 4 and 8 months post- ^{56}Fe-ion irradiation, Wistar rats had 13% and 16% decreased endothelial relaxation response respectively. As well, PWV increased from 4.03 m/s to 4.45 m/s at 4 months and 4.53 m/s to 5.06 m/s at 8 months post-irradiation (Soucy et al., 2011).

Incidence concordance

Incidence concordance is moderate in this KER, as multiple studies demonstrate greater changes to endothelial dysfunction than to vascular remodeling. Three studies by Soucy et al. (2011, 2010, 2007) in rats demonstrate greater changes to vasodilation than to vascular stiffness after 5 Gy of gamma rays or 1 Gy of iron ions. In addition, 18 Gy X-ray irradiation of mice showed a 4.5-fold increase in apoptosis and a 1.4-fold increase in aortic thickness (Shen et al., 2018). Following 1 or 4 weeks of HU, greater changes to apoptosis were observed compared to changes in vascular remodeling in the cerebral and small mesenteric arteries of rats (Su et al., 2020).

Essentiality

Human bone marrow-derived mesenchymal stem cells (hBMSCs) can prevent endothelial dysfunction and vascular remodeling via their antioxidant and anti-inflammatory properties. While a radiation dose of 18 Gy X-rays in a mouse model increased both the amount of apoptosis in the aorta (indicating endothelial dysfunction) and aortic wall thickness, treatment with hBMSCs reversed these changes. TUNEL positive cells decreased but remained elevated above the control, while aortic wall thickness returned to control levels (Shen et al., 2018).

In work exploring the role of the ASM/Cer pathway, a decrease in the ASM activity and resulting Cer production corresponded to a decrease in apoptosis and increase in cell-proliferation in rat models of simulated microgravity (Cheng et al., 2017; Su et al., 2020). Incubation with permeable Cer (C6-Cer) returned apoptosis to control levels. Treatment with the ASM inhibitor desipramine (dpm) led to an overall decrease in apoptosis in all arteries tested, while treatment with doxepin hydrochloride (DOX) led to significant increases in cell proliferation and subsequent intima medial thickness (IMT) and cross-sectional areas (CSA) (Su et al., 2020).

Uncertainties and Inconsistencies

- Lower doses (0.5 Gy and 1.6 Gy) did not show changes in vasomotion compared to control, but vascular stiffness increased at these doses (Soucy et al., 2007).
- Tarasova et al. (2020) showed differences in the vascular remodeling and vasoconstriction responses between skeletal and cutaneous arteries. While the two groups demonstrated differences, all vessels followed different trends showing no clear relationship between KEs.

- Studies exploring vasoreactivity, vascular structure and vessel stiffness endpoints in humans (Lee et al., 2020) and mice (Sofronova et al., 2015) flown in space, found changes in these endpoints to be inconsistent and/or changes were not statistically significant.
- C6-Cer incubation in cerebral arteries showed increased apoptosis with HU in the study by Cheng et al. (2017); however, in Su et al. (2020), there was a slight decrease in apoptosis, measured by TUNEL.

Quantitative Understanding of the Linkage

The following are a few examples of quantitative understanding of the relationship. All data that is represented is statistically significant unless otherwise indicated.

Response-response relationship

Dose/Incidence Concordance

Reference	Experiment Description	Result
Soucy et al., 2007	*In vivo*. Sprague-Dawley rats were whole-body irradiated with ^{137}Cs gamma radiation at 0.5 Gy, 1.6 Gy and 5 Gy. Vasodilation response to ACh was used to evaluate endothelial function. Vascular stiffness was measured by PWV.	No changes in endothelial relaxation were observed after 0.5 or 1.6 Gy, but relaxation decreased about 20 percentage points at 5 Gy. At 0.5 and 1.6 Gy, PWV increased from 3.9 m/s (before irradiation) to 4.2 m/s. At 5 Gy PWV increased to 4.6 m/s.
Soucy et al., 2010	*In vivo*. Sprague-Dawley rats were whole-body irradiated with ^{137}Cs gamma radiation at 5 Gy. Aortic relaxation response to ACh and PWV were measured.	Relaxation decreased about 30 percentage points after 5 Gy. PWV increased to 4.93 m/s from 4.06 m/s (control) after 5 Gy.
Soucy et al., 2011	*In vivo*. Wistar rats were exposed to 0.5 and 1 Gy doses of ^{56}Fe-ion radiation. ACh-induced vasodilation response was measured. PWV was measured with Doppler probe and electrocardiogram (ECG) while aortic wall thickness:lumen diameter ratio was measured by histological analysis.	0.5 Gy dose – 9% (non-significant) decrease in endothelium-dependent vasodilation and no significant change in PWV. 1 Gy dose - 13% decrease in endothelium-dependent vasodilation and PWV increased by 0.42 m/s. Neither dose showed changes to aortic wall thickness:lumen diameter.
Shen et al., 2018	*In vivo*. Male mice were irradiated with 18 Gy X-rays. Endothelial dysfunction was determined through a TUNEL apoptosis assay. To measure vascular remodeling, aortic thickness was determined at various times using hematoxylin and eosin (HE) staining, and the accumulation of collagen was measured using Sirius red staining.	Irradiation with 18 Gy caused a ~4.5-fold maximum increase in TUNEL positive cells and a maximum increase of 1.4-fold in aortic thickness and collagen content compared to controls.
Su et al., 2020	*In vivo*. The effects of simulated microgravity by 0 day, 3 day, 1 week, 2 week or 4 week HU on cerebral and small mesenteric rat arteries were studied. Apoptosis was used as a measure of endothelial dysfunction by TUNEL assay and IMT and media CSA were used as measures of vascular remodeling.	Significant changes occurred in small mesenteric artery following 1 week of HU with a ~2-fold increase in apoptosis, ~0.8-fold decrease in IMT and ~0.6-fold decrease in CSA. Rat cerebral artery exhibited significant changes following 4 weeks of HU at which point there was a 0.3-fold decrease in apoptosis, a ~2-fold increase in IMT, and a ~2.1-fold increase in CSA.
Delp et al., 2000	*In vivo*. Male Sprague-Dawley rats had 2 arteries and 2 arterioles analyzed after 2-week HU. Endothelial dysfunction was measured through the relaxation response to ACh and remodeling was	2-week HU led to the following changes: Soleus muscle feed artery – Cross sectional area decreased 0.5-fold, media thickness did not change, outer-media perimeter decreased 0.7-fold. Response to ACh (i.e. endothelium-dependent vasodilation) in arterioles decreased 50% after 2-week HU, but no change was observed after 4-week HU.

	determined through media cross-sectional area, wall thickness and perimeter.	Gastrocnemius muscle feed artery – Cross sectional area decreased 0.5-fold, media thickness decreased 0.6-fold and outer-media perimeter did not significantly change. Response to ACh (i.e. endothelium-dependent vasodilation) in arterioles did not significantly change.
Tarasova et al., 2020	*In vivo*. Male Wistar rats' skin and skeletal muscle arteries were analyzed after 2-week HU. Endothelial dysfunction was determined through contractile response to noradrenaline and serotonin vasoconstrictors, and remodeling was determined through vessel inner diameter.	Following 2-week HU, the following changes occurred: Forelimb arteries - Brachial artery: Inner artery diameter increased 22.5%, active tension response to noradrenaline increased ~2-fold while response to serotonin increased ~1.5-fold. Median artery: Inner artery diameter increased 10%, no significant changes in noradrenaline or serotonin responses. Hindlimb arteries - Sural artery: Inner artery diameter decreased 16.8%, ~0.7-fold decrease in active tension response for both noradrenaline and serotonin. Saphenous artery: Inner artery diameter showed no significant change, and active tension response following noradrenaline and serotonin was elevated above the control but this increase was not significant across all doses studied.
Cheng et al., 2017	*In vivo*. Male rat carotid arteries were studied with HU. Apoptosis, measured by a TUNEL assay, was used as a measure of endothelial dysfunction. IMT and CSA were markers of vascular remodeling using HE staining.	Following HU, IMT in the carotid artery increased 1.8-fold and intima-media area increased 2.1-fold. Apoptosis decreased by 0.5-fold after HU.
Lee et al., 2020	*In vivo*. Ten male and three female astronauts who participated in various durations of spaceflight (189 ± 61 days). Irradiation measurements showed the crew experienced an average of 0.048 ± 0.018 Gy from 0.031 to 0.077 Gy. Endothelial dysfunction was measured through flow-mediated vasodilation of the brachial artery. Vascular remodeling was measured through intima-media area and vascular stiffness.	No changes in endothelium-dependent or -independent vasodilation were observed from preflight to postflight. From preflight to postflight, intima-media area increased by 1.04 mm2 and stiffness increased by 4.4 arbitrary units. However, none of the changes were significant.
Sofronova et al., 2015	*In vivo*. Male mice were placed under microgravity environment to study the properties of cerebral arteries, including endothelial dysfunction measured by vascular tension, vessels response to ACh (vasodilator) and vascular remodeling determined by elastin-collagen content using staining tissue with Verhoeff-van Gieson.	Spaceflight mice (SF) showed a 30% decrease in relaxation response of basilar arteries to ACh compared to habitat control (HC) group. No significant changes in elastin or elastin-collagen ratio were observed between HC, vivarium control (VC) and SF mice. There was a 5% collagen content increase in VC mice compared to HC and SF groups.

Time-scale

Time concordance

Reference	Experiment Description	Result
Soucy et al., 2007	*In vivo*. Sprague-Dawley rats were whole-body irradiated with ^{137}Cs gamma radiation at 50, 160 and 500 cGy. Relaxation response to ACh was used to evaluate endothelial function. Vascular stiffness was measured by PWV at various times.	Relaxation decreased a maximum of about 20 percentage points and PWV increased from 3.9 m/s to a maximum of 4.6 m/s 2 weeks after irradiation.

Soucy et al., 2010	*In vivo*. Sprague-Dawley rats were whole-body irradiated with ^{137}Cs gamma radiation at 5 Gy. Aortic relaxation response to ACh and PWV were measured after 2 weeks.	Relaxation decreased about 30 percentage points and PWV increased to 4.93 m/s from 4.06 m/s (control) after 2 weeks.
Soucy et al., 2011	*In vivo*. Wistar rats were exposed to 0.5 and 1 Gy doses of ^{56}Fe-ion radiation. ACh-induced vasodilation response was measured. PWV was measured with Doppler probe and ECG while aortic wall thickness:lumen diameter ratio was measured by histological analysis. Relaxation and PWV were measured at 4 and 8 months post-irradiation.	At 4 months, endothelial relaxation decreased 13 percentage points and PWV increased from 4.03 to 4.45 m/s. At 8 months, endothelial relaxation decreased about 16 percentage points and PWV increased from 4.53 to 5.06 m/s. No changes in wall thickness:lumen diameter were observed.
Shen et al., 2018	*In vivo*. Male mice were irradiated with 18 Gy X-rays. Endothelial dysfunction was determined through a TUNEL apoptosis assay. To measure vascular remodeling, aortic thickness was determined at various times using hematoxylin and eosin (HE) staining, and the accumulation of collagen was measured using Sirius red staining. Measurements were taken at various times between 3 and 84 days.	Irradiation showed a significant increase in TUNEL positive cells at 3, 7, 14, 28, and 84 days, with a ~4.5-fold maximum increase at day 7. Irradiation also showed a 1.4-fold increase in collagen after 14, 28 and 84 days. Aortic thickness was significantly increased after 7, 14 and 28 days, with a maximum 1.4-fold increase after 7 days.

Known modulating factors

Modulating factor	Details	Effects on the KER	References
Drug	Oxp (xanthine oxidase inhibitor)	Treatment with Oxp after irradiation led to increased vasodilation and decreased PWV	Soucy et al., 2007; Soucy et al., 2010; Soucy et al., 2011
Drug	hBMSCs (protect against vascular damage)	Treatment with hBMSCs after irradiation led to decreased apoptosis and aortic thickness	Shen et al., 2018
Drug	C6-Cer (activates the ASM/Cer pathway)	Treatment with C6-Cer after microgravity caused increased apoptosis along with a return of proliferation to control levels	Cheng et al., 2017; Su et al., 2020
Drug	dpm (ASM inhibitor)	dpm treatment showed apoptosis and proliferation levels returned to control after microgravity	Su et al., 2020
Drug	DOX (ASM inhibitor)	Treatment with DOX after microgravity showed decreased apoptosis and increased IMT in rat carotid arteries	Su et al., 2020

References

Baeyens, N. et al. (2016), “Endothelial fluid shear stress sensing in vascular health and disease”, *The Journal of Clinical Investigation*, Vol. 126/3, American Society for Clinical Investigation, Ann Arbor, https://doi.org/10.1172/JCI83083.

Baran, R. et al. (2022), “The Cardiovascular System in Space: Focus on In Vivo and In Vitro Studies”, *Biomedicines*, Vol. 10/1, Multidisciplinary Digital Publishing Institute, Basel, https://doi.org/10.3390/BIOMEDICINES10010059.

Bonetti, P.O., L. O. Lerman and A. Lerman (2003), “Endothelial dysfunction: A marker of atherosclerotic risk”, *Arteriosclerosis, Thrombosis, and Vascular Biology*, Vol. 23/2, Lippincott Williams & Wilkins, Philadelphia, https://doi.org/10.1161/01.ATV.0000051384.43104.FC.

Carmeliet, P. and R. K. Jain. (2011), “Molecular mechanisms and clinical applications of angiogenesis”, *Nature*, Vol.473, Nature Portfolio, London, https://doi.org/10.1038/nature10144.

Cheng, Y. P. et al. (2017), “Acid sphingomyelinase/ceramide regulates carotid intima-media thickness in simulated weightless rats”, *Pflugers Archiv European Journal of Physiology*, Vol. 469, Springer, New York, https://doi.org/10.1007/s00424-017-1969-z.

Deanfield, J.E., J. P. Halcox and T. J. Rabelink (2007), “Endothelial function and dysfunction: Testing and clinical relevance”, *Circulation*, Vol. 115/10, Lippincott Williams & Wilkins, Philadelphia, https://doi.org/10.1161/CIRCULATIONAHA.106.652859.

Delp, M.D. et al. (2000), “Structural and functional remodeling of skeletal muscle microvasculature is induced by simulated microgravity”, *American Journal of Physiology - Heart and Circulatory Physiology*, Vol. 278, American Physiological Society, Rockville, https://doi.org/10.1152/ajpheart.2000.278.6.h1866.

Demontis, G.C. et al. (2017), “Human Pathophysiological Adaptations to the Space Environment”, *Frontiers in Physiology*, Vol. 8, Frontiers Media SA, Lausanne, https://doi.org/10.3389/fphys.2017.00547.

Garrett-Bakelman, F. E. et al. (2019) “The NASA Twins Study: A multidimensional analysis of year-long human spaceflight”, *Science*, Vol. 364/6436, American Association for the Advancement of Science, Washington, D.C., https://doi.org/10.1126/science.aau8650

Hargens, A.R. and D. E. Watenpaugh (1996), “Cardiovascular adaptation to spaceflight”, *Medicine & Science in Sports & Exercise*, Vol. 28/8, Lippincott Williams & Wilkins, Piladelphia, https://doi.org/10.1097/00005768-199608000-00007.

Hsu, T., H. H. Nguyen-Tran and M. Trojanowska (2019), “Active roles of dysfunctional vascular endothelium in fibrosis and cancer”, *Journal of Biomedical Science*, Vol. 26/1, BioMed Central, London, https://doi.org/10.1186/S12929-019-0580-3.

Hughson, R.L., A. Helm and M. Durante. (2018), “Heart in space: Effect of the extraterrestrial environment on the cardiovascular system”, *Nature Reviews Cardiology*, Vol. 15, Nature Portfolio, London, https://doi.org/10.1038/nrcardio.2017.157

Kozbenko, T. et al. (2022), “Deploying elements of scoping review methods for adverse outcome pathway development: a space travel case example”, *International Journal of Radiation Biology*, Vol. 98/12. https://doi.org/10.1080/09553002.2022.2110306

Krüger-Genge, A. et al. (2019), “Vascular Endothelial Cell Biology: An Update”, *International Journal of Molecular Sciences*, Vol. 20/18, Multidisciplinary Digital Publishing Institute, Basel, https://doi.org/10.3390/ijms20184411.

Lee, S. M. C. et al. (2020), “Arterial structure and function during and after long-duration spaceflight”, *Journal of Applied Physiology*, Vol. 129, American Physiological Society, Rockville, https://doi.org/10.1152/japplphysiol.00550.2019.

Platts, S.H. et al. (2014), “Effects of sex and gender on adaptation to space: Cardiovascular alterations”, *Journal of Women’s Health*, Vol. 23/11, Mary Ann Liebert, Larchmont, https://doi.org/10.1089/jwh.2014.4912.

Rajashekhar, G. et al. (2006), “Continuous Endothelial Cell Activation Increases Angiogenesis: Evidence for the Direct Role of Endothelium Linking Angiogenesis and Inflammation”, *Journal of Vascular Research*, Vol. 43/2, Karger Publishers, Berlin, https://doi.org/10.1159/000090949.

Shen, Y. et al. (2018), “Transplantation of bone marrow mesenchymal stem cells prevents radiation-induced artery injury by suppressing oxidative stress and inflammation”, *Oxidative Medicine and Cellular Longevity*, Vol. 2018, Hindawi, London, https://doi.org/10.1155/2018/5942916.

Slezak, J. et al. (2017), “Potential markers and metabolic processes involved in the mechanism of Radiation-Induced heart injury”, *Canadian Journal of Physiology and Pharmacology*, Vol. 95/10, Canadian Science Publishing, Ottawa, https://doi.org/10.1139/cjpp-2017-0121.

Sofronova, S. I. et al. (2015), “Spaceflight on the Bion-M1 biosatellite alters cerebral artery vasomotor and mechanical properties in mice”, *Journal of Applied Physiology*, Vol. 118/7, American Physiological Society, Rockville, https://doi.org/10.1152/japplphysiol.00976.2014.

Soucy, K. G. et al. (2011), “HZE ^{56}Fe-ion irradiation induces endothelial dysfunction in rat aorta: Role of xanthine oxidase”, *Radiation Research*, Vol. 176/4, Radiation Research Society, Bozeman, https://doi.org/10.1667/RR2598.1.

Soucy, K. G. et al. (2010), “Dietary inhibition of xanthine oxidase attenuates radiation-induced endothelial dysfunction in rat aorta”, *Journal of Applied Physiology*, Vol. 108/5, American Physiological Society, Rockville, https://doi.org/10.1152/japplphysiol.00946.2009.

Soucy, K. G. et al. (2007), “Single exposure gamma-irradiation amplifies xanthine oxidase activity and induces endothelial dysfunction in rat aorta”, *Radiation and Environmental Biophysics*, Vol. 46, Springer, New York, https://doi.org/10.1007/s00411-006-0090-z.

Su, Y. T. et al. (2020), “Acid sphingomyelinase/ceramide mediates structural remodeling of cerebral artery and small mesenteric artery in simulated weightless rats”, *Life Sciences*, Vol. 243, Elsevier, Amsterdam, https://doi.org/10.1016/j.lfs.2019.117253.

Sylvester, C. B. et al. (2018), “Radiation-Induced Cardiovascular Disease: Mechanisms and Importance of Linear Energy Transfer”, *Frontiers in Cardiovascular Medicine*, Vol. 5/5, Frontiers Media SA, Lausanne, https://doi.org/10.3389/fcvm.2018.00005.

Tarasova, O. S. et al. (2020), “Simulated Microgravity Induces Regionally Distinct Neurovascular and Structural Remodeling of Skeletal Muscle and Cutaneous Arteries in the Rat”, *Frontiers in Physiology*, Vol. 11, Frontiers Media SA, Lausanne, https://doi.org/10.3389/fphys.2020.00675.

Zhang, L. F. (2013), “Region-specific vascular remodeling and its prevention by artificial gravity in weightless environment”, *European Journal of Applied Physiology*, Vol. 113, American Physiological Society, Rockville, https://doi.org/10.1007/s00421-013-2597-8.

Zhang, L. F. (2001), “Vascular adaptation to microgravity: What have we learned?”, *Journal of Applied Physiology*, Vol. 91/6, American Physiological Society, Rockville, https://doi.org/10.1152/jappl.2001.91.6.2415.

Relationship: 2789: Altered, Nitric Oxide Levels leads to Increase, Endothelial Dysfunction

AOPs Referencing Relationship

AOP Name	Adjacency	Weight of Evidence	Quantitative Understanding
Deposition of energy leads to vascular remodeling	adjacent	Moderate	Low

Evidence Supporting Applicability of this Relationship

Taxonomic Applicability

Term	Scientific Term	Evidence	Links
human	Homo sapiens	Low	NCBI
rat	Rattus norvegicus	Moderate	NCBI
rabbit	Oryctolagus cuniculus	Low	NCBI

Life Stage Applicability

Life Stage	Evidence
Adult	Low
Not Otherwise Specified	Moderate

Sex Applicability

Sex	Evidence
Male	Moderate
Female	Low
Unspecific	Low

The majority of the evidence is derived from *in vivo* rat models. A limited number of studies were in human and rabbit models. The relationship has been more commonly shown *in vivo* in male animals, specifically in adult male rodents.

Key Event Relationship Description

Altered nitric oxide (NO) levels can lead to endothelial dysfunction (Soloviev & Kizub, 2019). In a functional endothelium, NO is bioavailable and is involved in preventing inflammation, proliferation and thrombosis (Deanfield, Halcox & Rabelink, 2007; Kruger-Genge et al., 2019). An increase in reactive oxygen species (ROS) along with increased NO can drive cellular senescence in endothelial cells (ECs) and catalyze endothelial dysfunction (Nagane et al., 2021; Wang, Boerma & Zhou, 2016). Another driver of endothelial dysfunction is reduced vasomotion. In a functional state, the endothelium requires a balance of vasoconstrictors and vasodilators (like NO); an interruption of this balance can lead to dysfunction (Deanfield, Halcox & Rabelink, 2007; Marti et al., 2012; Nagane et al., 2021; Schulz, Gori & Münzel, 2011; Soloviev & Kizub, 2019). Decreased NO due to direct reactions with ROS or uncoupling of NOS enzymes will lead to a reduced ability of smooth muscle cells (SMCs) to relax (Soloviev & Kizub, 2019).

Evidence Supporting this KER

Overall weight of evidence: Moderate

Biological Plausibility

The biological plausibility surrounding the connection between altered NO levels leading to endothelial dysfunction is well-supported by literature. NO is synthesized from L-arginine and oxygen with the aid of enzymes and cofactors (Nagane et al., 2021). NO regulates ECs by binding to soluble guanylyl cyclase (sGC) to create cGMP and activate protein kinase G (PKG), leading to activation of Ca^{2+}-dependent vasodilation and smooth muscle relaxation (Nagane et al., 2021; Soloviev & Kizub 2019). NOS isoforms, such as inducible NO synthase (iNOS) and endothelial NO synthase (eNOS) that synthesize NO are indirect measures of NO. Lower NO reduces the ability of SMCs relaxation and dilates the blood vessel leading to an inability to control vasodilation, a component of endothelial dysfunction (Soloviev & Kizub 2019).

Increased expression of NOS enzymes can result in reduced NO levels in the case of insufficient L-arginine substrate or BH4 cofactor leading to ROS production instead of NO (Zhang et al., 2009). ROS can decrease NO bioavailability by uncoupling/downregulating eNOS or converting NO to peroxynitrite (Mitchel et al 2019; Schulz, Gori & Münzel, 2011; Soloviev & Kizub 2019; Wang, Boerma & Zhou, 2016). A further decrease in NO occurs as peroxynitrite oxidizes BH4 to BH2 and induces eNOS to produce ROS, continuing the uncoupling of more NOS enzymes (Hong et al., 2013; Soloviev & Kizub, 2019; Zhang et al., 2009). A reduction in NO bioavailability due to ROS is an important mediator of endothelial dysfunction (Schulz, Gori & Münzel, 2011).

Another component of endothelial dysfunction influenced by NO levels is cellular senescence (Nagane et al., 2021). iNOS expression increases following an increase in oxidative stress (Nathan & Xie, 1994). In the presence of oxidative stress, NO is converted to peroxynitrite, which is a reactive nitrogen species (RNS) that can modify proteins and lead to cellular senescence

(Hong et al., 2013; Nagane et al., 2021; Soloviev & Kizub, 2019). Although NO can increase at first and cause cell senescence, senescent ECs show downregulation and/or uncoupling of eNOS that contributes to a decrease of NO in the endothelium (Wang, Boerma & Zhou, 2016). These changes in senescent ECs lead to endothelial dysfunction.

Empirical Evidence

The empirical evidence to support this KER was gathered from research that utilized *in vivo* rat and rabbit models (Soucy et al., 2010; Soucy et al., 2011; Hong et al., 2013; Yan et al., 2020; Zhang et al., 2009), *ex vivo* rabbit models and *in vitro* HUVEC models (Hong et al., 2013). Stressors used to alter NO levels and increase endothelial dysfunction include ^{56}Fe ions (Soucy et al., 2011), X-rays (Hong et al., 2013; Yan et al., 2020), gamma rays (Soucy et al., 2010) and altered gravity by hindlimb unweighting (HU) (Zhang et al., 2009). Irradiation dose levels ranged from 0.5 Gy to 16 Gy (Hong et al., 2013; Soucy et al., 2010; Soucy et al., 2011; Yan et al., 2020). Studies used various endpoints to measure NO levels while endothelial function was consistently determined through relaxation response to acetylcholine (ACh). Methods to measure NO included DAF-FM DA fluorescent probe (Soucy et al., 2010; Soucy et al., 2011), Griess reagent NO assay kit (Yan et al., 2020), eNOS dimer to monomer ratio (Yan et al., 2020), and NOS protein and mRNA levels (Hong et al., 2013; Zhang et al., 2009).

Dose Concordance

There is moderate evidence to demonstrate dose concordance between a decrease in nitric oxide and endothelial dysfunction. ^{56}Fe ion irradiation in rat aorta showed a decrease in both NO levels and endothelial relaxation at 1 Gy. However, endothelial relaxation did not significantly decrease at a lower dose of 0.5 Gy (Soucy et al., 2011). After 5 Gy gamma irradiation, NO production and endothelial relaxation both decreased 0.7-fold in rat aorta (Soucy et al., 2010). Increased NOS levels can cause further NO decreases due to uncoupling and production of more peroxynitrite, which is the result of NO reacting with ROS and can therefore, be used to determine NO levels (Hong et al., 2013; Zhang et al., 2009). In rat mesenteric arteries, NO levels decreased 0.6-fold after 4 Gy X-ray irradiation, while endothelial relaxation decreased 0.1-fold compared to non-irradiated arteries (Yan et al., 2020). X-ray irradiated human umbilical vein endothelial cells (HUVECs) showed significantly increased iNOS and peroxynitrite after 4 Gy, and X-ray irradiated rabbit carotid arteries had decreased relaxation after 8 and 16 Gy (Hong et al., 2013). Hong et al (2013) also showed that endothelial relaxation was lower after 16 Gy than 8 Gy ex vivo.

Altered gravity resulted in an increase of eNOS and increase of iNOS in carotid arteries (Zhang et al., 2009). Increases in eNOS and iNOS corresponded to a decrease in carotid artery relaxation from 64% to 33% at the same level of HU (Zhang et al., 2009). These studies showed increases in NOS isoforms and corresponding decreases in endothelial function, such as increased vasoconstriction and impaired vasodilation following altered gravity.

Time Concordance

Evidence of time concordance between altered NO levels and endothelial dysfunction is limited from the studies cited. HUVECs irradiated with 4 Gy X-rays displayed an increase in nitrotyrosine (peroxynitrite biomarker indicating reduced NO) after 6 hours post-irradiation (Hong et al., 2013). Rabbit carotid arteries *in vivo* and *ex vivo* irradiated with 8 or 16 Gy X-rays showed decreased ACh-induced endothelial relaxation only after 20 hours post-irradiation (Hong et al., 2013).

Incidence Concordance

There is limited support in current literature for an incidence concordance relationship between altered NO and endothelial dysfunction. A primary research study that supports this AOP demonstrated an average change to endpoints of altered NO that was greater or equal to that of endothelial dysfunction (Zhang et al., 2009).

Essentiality

Many studies show the essentiality of decreased NO levels in endothelial dysfunction. After stressors like irradiation, xanthine oxidase (XO) can produce cardiac ROS that can react with NO and decrease its concentration or oxidize BH4 and uncouple eNOS. Oxypurinol (Oxp), an inhibitor of XO, has been shown to reverse these effects and reduce ROS levels, restore NO levels, and increase endothelial relaxation following irradiation (Soucy et al., 2010; Soucy et al., 2011). L-nitroarginine (L-NA, general NOS inhibitor) and aminoguanidine (AG, specific iNOS inhibitor) together were able to reduce relaxation of rabbit carotid arteries, suggesting that reduced NO levels are a key cause to endothelial dysfunction (Hong et al., 2013). In addition, L-NA and AG were able to reduce iNOS and nitrotyrosine (peroxynitrite biomarker) levels after irradiation (Hong et al., 2013). Gch1 is an enzyme involved in the synthesis of BH4, a cofactor for eNOS coupling. DAHP, a Gch1 inhibitor, caused the ratio of coupled-to-uncoupled eNOS to decrease and endothelial relaxation to also decrease, showing how coupled eNOS is necessary for endothelial function (Yan et al., 2020). Angiotensin II (AngII) type 1 (AT1) receptor activation can activate NOS. HU rats treated with losartan, an AT1 receptor antagonist, show reduced NOS levels and increased endothelial relaxation (Zhang et al., 2009).

Uncertainties and Inconsistencies

- Directionality of NO changes cannot be compared between studies due to a variety of experimental conditions like stressor type, dose, dose rate, model and time course of the experiment.
- Irradiating in vivo rabbit carotid arteries with X-rays showed that endothelial dysfunction was higher after 8 Gy than 16 Gy (Hong et al., 2013). This was inconsistent with the ex vivo model, where endothelial dysfunction was highest after 16 Gy (Hong et al., 2013). Endothelial dysfunction was shown through a relaxation response to ACh.

Quantitative Understanding of the Linkage

The following are a few examples of quantitative understanding of the relationship. All data that is represented is statistically significant unless otherwise indicated.

Response-response relationship

Dose/Incidence Concordance

Reference	Experiment Description	Result
Soucy et al., 2011	*In vivo*. 3-4 months-old rats were irradiated with 1 Gy ^{56}Fe ions. Endothelial NO levels from male rat aorta were measured with a DAF-FM DA fluorescent probe in response to ACh-induced relaxation. Vascular tension response to ACh was measured in male rat aorta after 0, 0.5 and 1 Gy ^{56}Fe ion irradiation. Doses were given at 0.5 Gy/min.	Iron ion irradiation at 1 Gy produced a decrease of 0.8-fold in NO levels compared to aorta without irradiation. At 10-5 M ACh, aorta without irradiation relaxed by 88%, while aorta with 1 Gy irradiation had significantly lower relaxation of 75%. No significant changes were observed at 0.5 Gy.
Hong et al., 2013	*In vivo*, *in vitro* and *ex vivo*. HUVECs were irradiated with 4 Gy X-rays (2.7 Gy/min) and amounts of eNOS, iNOS and nitrotyrosine (a biomarker for peroxynitrite) were determined by western blot. Rabbit carotid arteries were irradiated with 8 or 16 Gy X-rays. In vivo arteries were irradiated at 4.1 Gy/min, and ex vivo arteries were irradiated at 3.9 Gy/min. Arteries were contracted with phenylephrine then relaxed with ACh to determine vascular responsiveness, which was measured with a computerized automated isometric transducer system.	In 4 Gy irradiated HUVECs, iNOS was increased 6.6-fold and nitrotyrosine was increased 6.4-fold. eNOS expression did not change. The responsiveness of the *ex vivo* carotid artery to ACh-induced relaxation was 77.4% without irradiation, 65.7% with 8 Gy and 60.1% with 16 Gy. The *in vivo* irradiated carotid artery also showed decreased ACh-induced relaxation, but relaxation was lowest after 8 Gy.
Zhang et al., 2009	*In vivo*. HU rats were exposed to altered gravity conditions as a stressor. Western blot was used to measure eNOS and iNOS protein in arteries. Endothelial dysfunction was determined by vasodilation.	Following HU, there was a 2-fold increase of eNOS in carotid arteries compared to control. A 4.3- and 3.3-fold increase in iNOS in carotid and cerebral arteries, respectively, was found in HU rats. Vasodilation was reduced by ~30% in the ACh induced relaxation of basilar arteries in HU rats. Vasoconstriction was increased in HU rats by 1.6 and 1.8-fold in the basilar artery in response to KCl (100 mmol/L) and 5-hydroxytryptamine (5-HT), respectively, and 1.2 and 1.3-fold in the carotid artery in response to KCl and phenylephrine (PE) respectively
Soucy et al., 2010	*In vivo*. In 4-month-old rats were irradiated with 0 or 5 Gy ^{137}Cs gamma radiation. Altered NO levels and endothelial function were investigated through fluorescent measurements of NO and vascular tension dose responses.	After 5 Gy NO production decreased 0.7-fold. There was a 0.7-fold decrease of relaxation response to ACh after 5 Gy compared to control.
Yan et al., 2020	*In vivo*. Rats were irradiated with 4 Gy abdominal X-ray radiation. Nitrite and eNOS levels were measured by NO assay kit and western blot, respectively. Endothelial dysfunction was determined by changes in vasodilation.	After radiation nitrite (NO metabolite and marker) levels and the eNOS ratio decreased 0.6-fold. With increasing ACh concentration the control group dropped to ~7% constriction while the irradiated group remained at ~75% constricted.

Time-scale

Time Concordance

Reference	Experiment Description	Result
Hong et al., 2013	*In vivo* and *ex vivo*. HUVECs were irradiated with 4 Gy X-rays (2.7 Gy/min) and amounts of iNOS and nitrotyrosine (a biomarker for peroxynitrite) were determined by western blot at various times over 6 hours. Rabbit carotid arteries were irradiated with 0, 8 or 16 Gy X-rays and the contraction was measured every 2 minutes for 10 minutes. In vivo arteries were irradiated at 4.1 Gy/min, and ex vivo arteries were irradiated at 3.9	After 4 Gy X-ray irradiation, iNOS levels in HUVECs increased consistently over 6 hours, while nitrotyrosine did not change at the 1.5- or 3-hour timepoint, but then increased at 6 hours. 20 hours after irradiation, relaxation with ACh was increased in the irradiated arteries

	Gy/min. Arteries were contracted with phenylephrine then relaxed with ACh to determine vascular responsiveness, which was measured with a computerized automated isometric transducer system.	compared to the non-irradiated arteries. This occurred in both the *in vivo* and *ex vivo* models.

Known modulating factors

Modulating factor	Details	Effects on the KER	References
Drug	AG (selective iNOS inhibitor)	AG treatment prevented radiation-induced increase in peroxynitrite and endothelial dysfunction along with L-NA treatment.	Hong et al., 2013
Drug	L-NA (general NOS inhibitor)	L-NA treatment prevented radiation-induced increase in peroxynitrite and endothelial dysfunction	Hong et al., 2013
Drug	DAHP (Gch1 inhibitor to inhibit BH4 synthesis)	DAHP (100 mg/kg/body weight) further decreased eNOS, nitrite concentration and endothelial relaxation after irradiation.	Yan et al., 2020
Drug	Losartan (AT1 receptor antagonist)	Losartan restored the levels eNOS and iNOS expression and improved endothelial relaxation after HU.	Zhang et al., 2009
Drug	Oxp (XO inhibitor)	Oxp increased NO levels and endothelial relaxation.	Soucy et al., 2010, 2011

Known Feedforward/Feedback loops influencing this KER

Not identified

References

Deanfield, J.E., J. P. Halcox and T. J. Rabelink (2007), “Endothelial function and dysfunction: Testing and clinical relevance”, *Circulation*, Vol. 115/10, Lippincott Williams & Wilkins, Philadelphia, https://doi.org/10.1161/CIRCULATIONAHA.106.652859.

Hong, C. W. et al. (2013), “Involvement of inducible nitric oxide synthase in radiation-induced vascular endothelial damage”, *Journal of Radiation Research*, Vol. 54/6, Oxford University Press, Oxford, https://doi.org/10.1093/JRR/RRT066.

Kozbenko, T. et al. (2022), “Deploying elements of scoping review methods for adverse outcome pathway development: a space travel case example”, *International Journal of Radiation Biology*, Vol. 98/12. https://doi.org/10.1080/09553002.2022.2110306

Krüger-Genge, A. et al. (2019), “Vascular Endothelial Cell Biology: An Update”, *International Journal of Molecular Sciences*, Vol. 20/18, Multidisciplinary Digital Publishing Institute, Basel, https://doi.org/10.3390/ijms20184411.

Marti, C. N. et al. (2012), “Endothelial dysfunction, arterial stiffness, and heart failure”, *Journal of the American College of Cardiology*, Vol. 60/16, Elsevier, Amsterdam, https://doi.org/10.1016/J.JACC.2011.11.082.

Mitchell, A. et al. (2019), “Cardiovascular effects of space radiation: implications for future human deep space exploration”, *European Journal of Preventive Cardiology*, Vol. 26/16, SAGE Publishing, Thousand Oaks, https://doi.org/10.1177/2047487319831497.

Nagane, M. et al. (2021), “DNA damage response in vascular endothelial senescence: Implication for radiation-induced cardiovascular diseases”, *Journal of Radiation Research*, Vol. 62/4, Oxford University Press, Oxford, https://doi.org/10.1093/JRR/RRAB032

Nathan, C. and Q. W. Xie (1994), “Regulation of biosynthesis of nitric oxide”, *Journal of Biological Chemistry*, Vol. 269/19, American Society for Biochemistry and Molecular Biology, Rockville, https://doi.org/10.1016/S0021-9258(17)36703-0

Schulz, E., T. Gori and T. Münzel (2011), “Oxidative stress and endothelial dysfunction in hypertension”, *Hypertension Research*, Vol. 34/6, Nature Portfolio, London, https://doi.org/10.1038/hr.2011.39

Soloviev, A. I. and I.V. Kizub (2019), “Mechanisms of vascular dysfunction evoked by ionizing radiation and possible targets for its pharmacological correction”, *Biochemical pharmacology*, Vol. 159, Elsevier, Amsterdam, https://doi.org/10.1016/j.bcp.2018.11.019.

Soucy, K. G. et al. (2011), “HZE 56Fe-ion irradiation induces endothelial dysfunction in rat aorta: Role of xanthine oxidase”, *Radiation Research*, Vol. 176/4, Radiation Research Society, Bozeman, https://doi.org/10.1667/RR2598.1.

Soucy, K. G. et al. (2010), “Dietary inhibition of xanthine oxidase attenuates radiation-induced endothelial dysfunction in rat aorta”, *Journal of Applied Physiology*, Vol. 108/5, American Physiological Society, Rockville, https://doi.org/10.1152/japplphysiol.00946.2009.

Wang, Y., M. Boerma and D. Zhou. (2016), “Ionizing Radiation-Induced Endothelial Cell Senescence and Cardiovascular Diseases”, *Radiation research*, Vol. 186/2, Radiation Research Society, Bozeman, https://doi.org/10.1667/RR14445.1.

Yan, T., et al. (2020), “Ionizing radiation induces BH4 deficiency by downregulating GTP-cyclohydrolase 1, a novel target for preventing and treating radiation enteritis”, *Biochemical Pharmacology*, Vol. 180, Elsevier, Amsterdam, https://doi.org/10.1016/J.BCP.2020.114102.

Zhang, R. et al. (2009), “Blockade of AT1 receptor partially restores vasoreactivity, NOS expression, and superoxide levels in cerebral and carotid arteries of hindlimb unweighting rats”, *Journal of Applied Physiology*, Vol. 106/1, American Physiological Society, Rockville, https://doi.org/10.1152/japplphysiol.01278.2007.

List of Non Adjacent Key Event Relationships

Relationship: 2779: Energy Deposition leads to Altered, Nitric Oxide Levels

AOPs Referencing Relationship

AOP Name	Adjacency	Weight of Evidence	Quantitative Understanding
Deposition of energy leads to vascular remodeling	non-adjacent	High	Low

Evidence Supporting Applicability of this Relationship

Taxonomic Applicability

Term	Scientific Term	Evidence	Links
human	Homo sapiens	Low	NCBI
mouse	Mus musculus	High	NCBI
rat	Rattus norvegicus	Moderate	NCBI

Life Stage Applicability

Life Stage	Evidence
Adult	Moderate
Juvenile	Moderate

Sex Applicability

Sex	Evidence
Male	Moderate
Female	Low
Unspecific	Low

The evidence for the taxonomic applicability to humans is low as evidence comes from *in vitro* human cell-derived models. The relationship has been shown *in vivo* in mice and rats, with considerable evidence in mice. The relationship has been shown *in vivo* in males and is likely in females. Most *in vivo* studies indicate adult or adolescent animal models used. In addition, the relationship is also likely in preadolescent animals.

Key Event Relationship Description

Deposition of energy from irradiation can affect nitric oxide (NO), a diffusible signaling molecule responsible for vasodilation (Dong et al., 2020; Mitchell et al., 2019; Soloviev & Kizub, 2019; Wang, Boerma & Zhou, 2016). NO activity is regulated by nitric oxide synthase (NOS) enzymes, which can be affected by NOS protein concentrations and cofactors tetrahydobiopterin (BH4), nicotinamide adenine dinucleotide phosphate (NADPH) and Ca^{2+} (Luiking, Engelen & Deutz, 2010). The deposition of energy can alter certain pathways involving NO and therefore indirectly alter NO levels. The phosphatidylinositol 3-kinase (PI3K)/Akt pathway, the RhoA/Rho kinase (ROCK) pathway, the renin-angiotensin-aldosterone system (RAAS), and the acidic sphingomyelinase/ceramide pathway can influence NO levels (Hemmings & Restuccia 2012; Millatt, Abdel-Rahman & Siragy, 1999; Nagane et al., 2021; Soloviev & Kizub, 2019; Yao et al., 2010).

Deposition of energy can alter NO levels through radiolysis and the direct formation of reactive oxygen species (ROS) (Azzam, Jay-Gerin & Pain, 2013). An increase in ROS and reactive nitrogen species (RNS) can influence NO levels; however, the involvement of RNS in NO production has not been strongly demonstrated in literature (Nagane et al., 2021). ROS acts as a modulator for the relationship between energy deposition leading to altered NO levels. Following ionizing radiation (IR) exposure, there are various enzymes and immune cells involved with indirectly increasing ROS, thereby influencing NO levels (Powers & Jackson, 2008; Soloviev & Kizub, 2019; Vargas-Mendoza et al., 2021).

Evidence Supporting this KER

Overall weight of evidence: High

Biological Plausibility

The biological plausibility surrounding the connection between deposition of energy and altered NO levels is well-supported by reviews in the literature and mechanistic understanding. NO is a diffusible molecule produced by endothelial cells (Soloviev & Kizub, 2019; Wang, Boerma & Zhou, 2016). The enzyme NOS produces NO and can be used as a proxy to measure NO levels. eNOS and iNOS are common endpoints for assessing NO levels. Changes in eNOS phosphorylation (p-eNOS) can also indicate NO levels, with phosphorylation at serine 1177 increasing eNOS activity and phosphorylation at threonine 495 decreasing eNOS activity (Nagane et al., 2021). The deposition of energy from IR can indirectly lead to changes in NO levels through various pathways (Nagane et al., 2021; Soloviev & Kizub, 2019).

NO levels can be altered by deposition of energy through ROS. ROS can be produced directly through the radiolysis of water or indirectly through the mitochondrial electron transport chain (ETC) and various enzymes and immune cells (Azzam, Jay-Gerin & Pain, 2013; Powers & Jackson, 2008; Soloviev & Kizub, 2019; Vargas-Mendoza et al., 2021). NO bioavailability is reduced through the molecule's reaction with ROS that produces peroxynitrite, or oxidation of the NOS cofactor BH4. This uncouples NOS causing it to produce ROS instead of NO, further driving down NO bioavailability (Forrester et al., 2019; Soloviev & Kizub, 2019). NO can also increase as a result of deposition of energy through activation of iNOS during oxidative stress (Nathan & Xie, 1994). However, this additional NO reacts with ROS to form peroxynitrite (Nagane et al., 2021; Soloviev & Kizub, 2019). The reaction of ROS with NO produces the RNS peroxynitrite, which can also further oxidize BH4 and uncouple NOS, resulting in further NO reduction (Soloviev & Kizub, 2019).

Deposition of energy can also alter NO levels by activating signaling pathways involved in NO regulation. Under normal conditions, the PI3K/Akt pathway can activate NOS through phosphorylation (Hemmings & Restuccia 2012; Nagane et al., 2021). The RhoA/ROCK pathway prevents both the expression and phosphorylation of NOS (Yao et al., 2010). Furthermore, the RAAS pathway can increase the production of ROS through NADPH oxidase (NOX), which causes decreased NO (Nguyen Dinh Cat et al., 2013). Additionally, the RAAS pathway can activate NOS as a countermeasure for vasoconstriction (Millatt, Abdel-Rahman & Siragy, 1999). Lastly, the acidic sphingomyelinase/ceramide pathway can also activate NOX, resulting in lower NO levels (Soloviev & Kizub, 2019). Deposition of energy from IR can change these pathways through oxidative stress and changes in protein expression, which results in altered NO levels (Schmidt-Ullrich et al., 2000).

Empirical Evidence

The empirical evidence supporting this KER was collected from research using both *in vivo* and *in vitro* models. The use of X-rays and gamma rays as stressors with doses ranging from 0.05 Gy to 60 Gy demonstrates the relationship between deposition of energy and altered NO levels. The dose, dose rate, and radiation type will all influence the level of energy deposition and therefore of NO production, but insufficient evidence exists to quantify the relationship between these factors and NO production. Human coronary artery endothelial cells (HCAECs) (Azimzadeh et al. 2017), human aortic endothelial cells (HAoECs) (Azimzadeh et al., 2021), human umbilical vein endothelial cells (HUVECs) (Hong et al. 2013; Sakata et al., 2015; Sonveaux et al., 2003), bovine aortic endothelial cells (BAECs) (Hirakawa et al., 2002; Sonveaux et al., 2003), tumor models (Sonveaux et al., 2003), cardiac microvascular endothelial cells and serum (Azimzadeh et al. 2015), as well as *in vivo* rat pulmonary arterioles (Fuji et al., 2016), Wistar albino rat heart tissue and serum (Abdel-Mageid & Shedid, 2019), B6J mice aortic endothelium (Hamada et al., 2020; Hamada et al., 2021), WAG/RijCmcr rat heart tissue (Baker et al., 2009), and serum from the abdominal inferior vena cava (Ohta et al., 2007) were the models used in these studies. Both direct NO measures, such as ELISA assay, and indirect NO measures, such as eNOS, iNOS, citrulline (NOS product) and NOx (nitrite and nitrate, NO metabolites) levels and activity, were used to determine changes in NO levels following energy deposition.

Dose Concordance

Evidence shows concordant changes in NO levels and deposition of energy. The study by Dias et al. (2018) showed varying changes to eNOS after chronic gamma irradiation, with a general trend of decreasing eNOS expression with increasing energy deposition (i.e., at 0.5, 1, and 2 Gy). Similarly, HUVECs exposed to gamma irradiation showed slightly lower eNOS levels at 12.5 Gy than at 10 Gy (Sadhukhan et al., 2020). X-ray irradiation of mouse cardiac microvascular endothelial cells showed 0.6 and 0.2-fold decreases in p-eNOS at 8 and 16 Gy, respectively (Azimzadeh et al., 2015). X-ray irradiation of mouse blood serum showed NO decreased 0.3-fold and 0.2-fold following 8 Gy and 16 Gy X-ray irradiation, respectively (Azimzadeh et al., 2015).

In contrast, BAECs and HUVECs irradiated with X-rays showed a trend of increasing eNOS expression and activation from 2 to 20 Gy (Sonveaux et al., 2003). Using similar doses of X-rays also showed that NOx increased dose-dependently from 1 to 20 Gy and reached a maximum increase of 10-fold (Sakata et al., 2015). Other high X-ray doses from 19.6 to 31.5 Gy on mice showed about a 2-fold increase in serum nitrate concentration, which had a general increasing trend at larger doses (Ohta et al., 2017). In BAECs, eNOS expression did not significantly change from 1 to 60 Gy of X-rays, while iNOS expression increased to 6% of GAPDH expression after 1 Gy, 26% after 2 Gy and remained around 40% of GAPDH expression from 10 to 60 Gy (Hirakawa et al., 2002).

Many studies do not examine this relationship at multiple doses. After 0.5 Gy X-ray irradiation of HCAECs, p-eNOS and NO were both decreased (Azimzadeh et al., 2017). HUVECs irradiated with 4 Gy X-rays showed increases in iNOS and nitrotyrosine (peroxynitrite biomarker) levels (Hong et al., 2013). eNOS levels decreased in mouse aortic endothelial cells when exposed to 5 Gy gamma and X-ray irradiation at various acute and chronic regimens (Hamada et al., 2020; Hamada et al., 2021; Hamada et al., 2021). Rat cardiac and serum NOx increased as a response to 8 Gy gamma irradiation (Abdel-Mageid & Shedid, 2019). Total body irradiation (TBI) of rats with 10 Gy X-rays resulted in a decrease in eNOS, iNOS and NOx levels (Baker et al., 2009). Both cardiac eNOS and serum NO decreased to 73% and 63%, respectively, following 16 Gy X-ray irradiation (Azimzadeh et al., 2021).

Time Concordance

There is evidence that a change in NO levels occurs after energy deposition (i.e., irradiation) occurred. HUVECs irradiated with 4 Gy X-rays displayed an increase in nitrotyrosine (peroxynitrite biomarker) at 6 hours post-irradiation (Hong et al., 2013). They also showed increased iNOS after 1.5, 3, and 6 hours (Hong et al., 2013). Following a 26 Gy X-ray irradiation of mice, serum nitrate concentration showed a maximum increase after 3h, followed by a return to pre-irradiation levels at 12 h and 24 h post-irradiation (Ohta et al., 2007). As well, in HUVECs, 10 and 12 Gy gamma rays led to decreased eNOS levels after 4 and 24 h (Sadhukhan et al., 2020). BAECs and HUVECs irradiated with 6 Gy X-rays did not exhibit significant changes in eNOS 1-6 h post-irradiation, but eNOS increased after 12, 24, and 48 hours (Sonveaux et al., 2003)

HUVECs irradiated with 10 Gy X-rays also had no change in eNOS levels over 72 h, while p-eNOS (Ser1177) increased consistently over 72 h, p-eNOS (Thr495) decreased after 6 h and returned to initial levels after 72 h, iNOS did not change other than a non-significant increased after 24 h, citrulline increased after 6 h and remained the same for 72 h and NOx increased over 72 h (Sakata et al., 2015). After 2 Gy X-ray irradiation of BAECs, eNOS expression did not significantly change from 0-120 h, iNOS expression increased to a maximum 6 h post-irradiation and NO increased to a maximum 12 h (Hirakawa et al., 2002).

Following 0.5 Gy X-ray irradiation of HCAECs, NO was not significantly lower after 1 day, while the 7 and 14 day time-points showed significant decreases (Azimzadeh et al., 2017). In human aortic endothelial cells, acute gamma radiation consistently showed decreased eNOS at each time-point up to 16 days after irradiation, while chronic irradiation decreased eNOS levels 1 and 4 days post-irradiation (Dias et al., 2018).

Finally, eNOS expression was lower 1, 3, and 6 months post-irradiation of mice aortic endothelial cells with 5 Gy gamma rays (Hamada et al., 2020).

Essentiality

Altered NO levels can occur due to a deposition of energy in the form of ionizing radiation. Since deposited energy initiates events immediately, the removal of deposited energy also supports the essentiality of the key event. Studies that do not deposit energy are observed to have no downstream effects. Deposition of energy cannot be blocked by chemicals, but radiation could be shielded. Currently, no studies show the effect of shielding on this relationship.

Uncertainties and Inconsistencies

- Due to the high reactivity of NO, it can be difficult to directly measure it (Luiking, Engelen & Deutz, 2010). The inconsistencies in NO levels may be attributed to the challenges in measuring NO, such as its availability in cell (Azimzadeh et al., 2017; Hirakawa et al., 2002; Hong et al., 2013; Sakata et al., 2015; Sonveaux et al., 2003), serum (Abdel-Magied & Shedid,. 2019; Azimzadeh et al. 2015; Ohta et al., 2007) or tissue (Abdel-Magied & Shedid, 2019; Baker et al., 2009; Fuji et al., 2016; Hamada et al., 2020), its homeostasis with ROS, and its relationship to nitrosylation as accumulated damage and whether p-eNOS/eNOS is being measured.

Quantitative Understanding of the Linkage

Examples of quantitative understanding of the relationship are provided. All data that is represented is statistically significant unless otherwise indicated.

Response-response relationship

Dose Concordance

Reference	Experiment Description	Result
Azimzadeh et al., 2015	*In vivo*. 10-week-old mice were exposed to X-ray irradiation at either 8 or 16 Gy. Cardiac levels of NO, eNOS and p-eNOS were determined. Protein levels were measured using immunoblotting, and NO was measured using an ELISA assay.	p-eNOS decreased 0.6-fold after 8 Gy and 0.2-fold after 16 Gy. NO decreased 0.3-fold after 8 Gy and 0.2-fold after 16 Gy. eNOS levels did not change.
Azimzadeh et al., 2017	*In vitro*. HCAECs were irradiated with 0.5 Gy X-ray irradiation over 1 minute. Phosphorylated and total eNOS levels were determined using immunoblotting, and NO levels were determined using ELISA assay. Measurements were taken after 1, 7, and 14 days.	p-eNOS/total eNOS was 0.7-fold lower than control and NO was 0.8-fold lower than control after 14 days.
Hong et al., 2013	*In vitro*. HUVECs were irradiated with 4 Gy X-rays (2.7 Gy/min) and amounts of eNOS, iNOS and nitrotyrosine (a biomarker for peroxynitrite) were determined by western blot. Measurements were taken after 1.5, 3, and 6 hours.	In 4 Gy irradiated HUVECs, iNOS was increased 6.6-fold and nitrotyrosine was increased 6.4-fold after 6 h. eNOS expression did not change.
	In vivo. eNOS levels in the smooth muscle layer of 4-week-old	

Fuji et al., 2016	rat pulmonary arteries were determined using immunohistochemical staining after irradiation (dose not specified). A 6.5 GeV electron beam was converted into monochromatic X-rays. Measurements were taken after 2 weeks.	eNOS levels decreased 0.6-fold compared to control.
Abdel-Magied & Shedid, 2019	*In vivo*. Adult male rats were irradiated with 8 Gy ^{137}Cs gamma irradiation (0.4092 Gy/min). Serum and heart total NOx was determined with a NOx assay kit. Measurements were taken after 14 days.	Cardiac and serum NOx increased 2 and 1.8-fold after exposure to 8 Gy, respectively.
Hamada et al., 2022	In vivo. 8-week-old mice were irradiated with 5 Gy 260 kVp X-rays at 0.5 Gy/min delivered in 25 or 100 daily fractions over 42 or 152 days, respectively, or delivered as an acute single dose. As well, chronic ^{137}Cs gamma rays (<1.4 mGy/h for 153 days) were delivered in another regimen. eNOS levels were determined by immunofluorescence.	At 6 months after the start of irradiation, eNOS decreased 0.3-fold, 0.4-fold, and 0.4-fold following single dose irradiation, 25 fraction regimens, and 100 fraction regimens, respectively. eNOS also decreased 0.8-fold after chronic gamma ray irradiation. At 12 months after the start of irradiation, eNOS decreased 0.7-fold, 0.8-fold and 0.8-fold following acute, 25 fraction and 100 fraction regimens, respectively.
Hamada et al., 2020	*In vivo*. 8-week-old male mice were irradiated by 5 Gy ^{137}Cs gamma rays (0.5 Gy/min). Immunofluorescence was used to determine eNOS levels. Measurements were taken after 1, 3, and 6 months.	6 months post-irradiation of 5 Gy, eNOS decreased by 0.3- fold.
Baker et al., 2009	*In vivo*. Male rats were irradiated with 10 Gy X-rays (1.95 Gy/min). Western blotting was used to determine eNOS and iNOS. NOx content was determined using ozone chemiluminescence. Measurements were taken after 120 days.	Rats exposed to 10 Gy of TBI experienced a 27% decrease in eNOS, a 29% decrease in iNOS protein, and a 20% decrease in NOx (index of NO activity).
Sonveaux et al., 2003	*In vitro*. Levels of eNOS and p-eNOS after X-ray irradiation of BAECs and HUVECs were measured with immunoblotting at various doses (0.86 Gy/min). eNOS mRNA was also measured with RT-qPCR before and after 2 Gy-irradiated human tumour cells.	Compared to controls, 24 h after irradiation, eNOS increased 1.3-fold after 2 Gy (not significant), 2.1-fold after 4 Gy (not significant), 3-fold after 6 and 8 Gy, 4.3-fold after 10 Gy and 3.4-fold after 20 Gy. Compared to controls, 24 h after irradiation, p-eNOS increased 1.2-fold after 2 Gy and 1.7-fold after 6 Gy. eNOS increased in human tumor cells in every patient after 2 Gy irradiation.
Hirakawa et al., 2002	*In vitro*. BAECs were irradiated with X-rays at various doses. eNOS and iNOS were measured with semiquantitative RT-PCR and western blot. NO was measured through DAF-2, a NO-sensitive fluorescent dye after treatment with L-arginine.	eNOS expression did not significantly change from 1-60 Gy. iNOS expression did not occur in non-irradiated samples, but increased to 6% of GAPDH expression after 1 Gy, 26% after 2 Gy and remained around 40% of GAPDH expression from 10-60 Gy. NO increased a maximum of 5.2-fold 12h after 2 Gy irradiation.
Sakata et al., 2015	*In vitro*. HUVECs were irradiated with various doses of X-rays. eNOS, p-eNOS (Ser1177 & Thr495), iNOS, citrulline (produced by NOS with NO) and NOx levels were measured with western blots for proteins and various assay kits for molecules.	For maximum changes after 10 Gy, eNOS expression did not significantly change, p-eNOS (Ser1177) increased 1.8-fold, p-eNOS (Thr495) decreased 0.3-fold, iNOS showed a non-significant 1.4-fold increase and citrulline increased 1.3-fold. NOx increased consistently from 1-20 Gy and showed a maximum 10-fold increase after 10 Gy.
Ohta et al., 2007	*In vivo*. Levels of nitrate in mouse serum were measured by Griess assay after a whole-body X-ray irradiation of 6-week-old mice using various doses from 19.6 to 31.5 Gy.	Serum nitrate concentrations increased about 2-fold from 0-31.5 Gy.
Hamada et al., 2021	*In vivo*. Either acute or chronic doses of X-rays and ^{137}Cs gamma rays were given to 8-week-old B6J mice, to a total 5 Gy dose. X-rays were given as a single acute dose, 25 fractions of 0.2 Gy/fraction spread over 42 days or 100 fractions of 0.05 Gy/fraction spread over 153 days all given at 0.5 Gy/min. Gamma rays were given as a single acute dose at 0.5 Gy/min or chronically at <1.4 mGy/h for 153 days. eNOS was measured through immunofluorescence.	All regimens of X-rays and acute gamma rays led to a 0.3- to 0.4-fold decrease in eNOS levels. Chronic gamma rays led to a 0.8-fold (nonsignificant) decrease in eNOS levels.
Azimzadeh et al., 2021	*In vivo*. 8-week-old male C57BL/6J were irradiated with an acute dose of 16 Gy X-rays. eNOS activity and NO were measured using fluorometric and Griess assays, respectively.	16 Gy resulted in a decrease in eNOS activity to 73% in heart tissue. NO levels decreased to 63% in serum.
Sadhukhan et al., 2020	*In vitro*. HUVECs were irradiated with various regimens and doses of ^{137}Cs gamma radiation. eNOS levels were determined by western blot. Fractionated doses were	At 5 doses of 2 Gy, eNOS decreased 0.2-fold. At 5 doses of 2.5 Gy, eNOS decreased 0.3-fold. At a single dose of 10 Gy, eNOS decreased 0.8-fold. At a single

	separated by 24 h.	dose of 12 Gy, eNOS decreased 0.7-fold.
Dias et al., 2018	*In vitro*. HAoECs were irradiated with various regimens of ^{60}Co gamma radiation. Acute radiation was given at 1 Gy/min, while chronic radiation was given at 6 mGy/h eNOS mRNA level was determined using qPCR. Each dose was measured at different times after irradiation.	An acute dose of 0.05 Gy led to a 0.6-fold decrease in eNOS while the chronic dose led to a 1.6-fold increase. At 0.5 Gy, the acute dose did not significantly change eNOS, while the chronic dose increased it 1.6-fold. Acute 1 Gy caused eNOS to decrease 0.5-fold without significant changes chronically. Acute 2 Gy caused a 0.3-fold decrease in eNOS without significant changes chronically.

Time-scale

Time Concordance

Reference	Experiment Description	Result
Azimzadeh et al., 2017	*In vitro*. HCAECs were irradiated with 0.5 Gy X-ray irradiation over 1 minute. Phosphorylated and total eNOS levels were determined using immunoblotting, and NO levels were determined using ELISA assay. Measurements were taken after 1, 7 or 14 days.	1 day after 0.5 Gy irradiation, p-eNOS/total eNOS was 0.8-fold lower than control and NO did not change. After 7 days, p-eNOS/total eNOS was 0.6-fold lower than control and NO was 0.8-fold lower than control. After 14 days, p-eNOS/total eNOS was 0.7-fold lower than control and NO was 0.8-fold lower than control.
Hong et al., 2013	*In vitro*. HUVECs were irradiated with 4 Gy X-rays (2.7 Gy/min) and amounts of iNOS and nitrotyrosine (a biomarker for peroxynitrite) were determined by western blot at various times over 6 hours.	1.5 h after 4 Gy irradiation, iNOS 1.9-fold higher than control and nitrotyrosine did not change. After 3 h, iNOS was 2.8-fold higher than control and nitrotyrosine did not change. After 6 h, iNOS was 6.6-fold higher than control and nitrotyrosine was 6.3-fold higher than control.
Hamada et al., 2020	*In vivo*. 8-week-old male mice were irradiated by 5 Gy ^{137}Cs gamma rays (0.5 Gy/min). Immunofluorescence was used to determine eNOS levels. Measurements were taken after 1, 3 and 6 months.	eNOS levels decreased 0.5-fold at 1-month post-irradiation, 0.4-fold at 3 months post-irradiation and a maximal fold decrease of 0.3-fold 6 months post-irradiation.
Sonveaux et al., 2003	*In vitro*. Level of eNOS after X-ray irradiation of BAECs and HUVECs was measured with immunoblotting at various times.	At 6 Gy, eNOS did not significantly change 1-6 h post-irradiation, but increased 1.8-fold after 12 h, 2-fold after 24 h and 1.5-fold after 48 h.
Hirakawa et al., 2002	*In vitro*. BAECs were irradiated with 2 Gy X-rays at various times. eNOS and iNOS were measured with semiquantitative RT-PCR and western blotting. NO was measured through DAF-2, a NO-sensitive fluorescent dye after treatment with L-arginine.	eNOS expression did not significantly change from 0-120 h post-irradiation. iNOS expression did not occur in non-irradiated samples but increased to a maximum 26% of GAPDH expression 6 h post-irradiation, and slowly decreased to 16% after 120 h. Similarly, NO increased a maximum of 5.2-fold after 12 h, while NO levels slowly returned after 120 h.
Sakata et al., 2015	*In vitro*. HUVECs were irradiated with 10 Gy X-rays at various times. eNOS, p-eNOS (Ser1177 & Thr495), iNOS, citrulline (produced by NOS with NO) and NOx levels were measured with western blots for proteins and various assay kits for molecules.	eNOS expression did not significantly change over 72 h, p-eNOS (Ser1177) increased 1.8-fold over 72 h, p-eNOS (Thr495) decreased 0.3-fold after 6 h and returned to initial levels after 72 h, iNOS did not change other than a nonsignificant 1.4-fold increased after 24 h. Citrulline increased 1.3-fold after 6 h and remained the same for 72 h. NOx increased 3.7-fold after 6 h and 5-fold after 72 h.
Ohta et al., 2007	*In vivo*. Levels of nitrate in mouse serum were measured by Griess assay at various times after a whole-body 26 Gy X-ray irradiation of 6-week-old mice.	Serum nitrate concentration showed a maximum increase of 2.1-fold after 3 h, followed by a return to pre-irradiation levels at 12 h and 24 h post-irradiation.
Sadhukhan et al., 2020	*In vitro*. HUVECs were irradiated with various regimens and doses of ^{137}Cs gamma radiation. eNOS levels were determined by western blot 4 and 24 h after irradiation. Fractionated doses were separated by 24 h.	After the 10 Gy doses, eNOS was lowest at 4 h, but after 12 Gy it was the same at both 4 and 24 h.
Dias et al., 2018	*In vitro*. HAoECs were irradiated with various regimens of ^{60}Co gamma radiation. Acute radiation was given at 1 Gy/min, while chronic radiation was given at 6 mGy/h. eNOS mRNA level was determined using qPCR up to 16 days	An acute dose of 0.05 Gy led to a 0.6-fold decrease in eNOS while the chronic dose led to a 1.6-fold increase 1 day post-irradiation. At 0.5 Gy, the acute dose did not significantly change eNOS, while the chronic dose increased it 1.6-fold 4 days post-irradiation. Acute 1 Gy caused eNOS to decrease 0.5-fold without significant changes chronically 8 days post-irradiation. Acute 2 Gy caused a 0.3-fold decrease in eNOS without

	after irradiation. Each timepoint used a different dose.	significant changes chronically 16 days post-irradiation.

Known modulating factors

Modulating factor	Details	Effects on the KER	References
Drug	ZnO-NPs (Zinc oxide nanoparticles that act as antioxidants)	Treatment with ZnO-NPs after irradiation returned nitrite/nitrate levels closer to control	Abdel-Magied & Shedid, 2019
Drug	Fenofibrate (PPARα agonist)	Treatment with Fenofibrate eliminated the radiation-induced decrease in NO levels.	Azimzadeh et al., 2021
Drug	Atorvastatin	Treatment significantly increased eNOS levels	Sadhukhan et al., 2020
Drug	Gamma tocotrienol	Treatment eliminated the radiation-induced decrease in eNOS levels.	Sadhukhan et al., 2020
Drug	Geranylgeranyl transferase I inhibitor 298	Treatment eliminated the radiation-induced decrease in eNOS levels.	Sadhukhan et al., 2020

Known Feedforward/Feedback loops influencing this KER

Not identified

References

Abdel-Magied, N. and S. M. Shedid (2019), “Impact of zinc oxide nanoparticles on thioredoxin-interacting protein and asymmetric dimethylarginine as biochemical indicators of cardiovascular disorders in gamma-irradiated rats”, *Environmental Toxicology*, Vol. 35, John Wiley & Sons, Ltd., Hoboken, https://doi.org/10.1002/tox.22879.

Azimzadeh, O. et al. (2021), “Activation of PPARα by feno fibrate attenuates the effect of local heart high dose irradiation on the mouse cardiac proteome”, *Biomedicines*, Vol. 9/12, Multidisciplinary Digital Publishing Institute, Basel, https://doi.org/10.3390/biomedicines9121845.

Azimzadeh, O. et al. (2017), “Proteome analysis of irradiated endothelial cells reveals persistent alteration in protein degradation and the RhoGDI and NO signalling pathways”, *International Journal of Radiation Biology*, Vol. 93/9, Informa, London, https://doi.org/10.1080/09553002.2017.1339332.

Azimzadeh, O. et al. (2015), “Integrative proteomics and targeted transcriptomics analyses in cardiac endothelial cells unravel mechanisms of long-term radiation-induced vascular dysfunction”, *Journal of Proteome Research*, Vol. 14/2, American Chemical Society, Washington, https://doi.org/10.1021/pr501141b.

Azzam, E. I., J. P. Jay-Gerin and D. Pain (2012), “Ionizing radiation-induced metabolic oxidative stress and prolonged cell injury”, *Cancer Letters*, Vol. 327, Elsevier, Amsterdam, https://doi.org/10.1016/j.canlet.2011.12.012.

Baker, J. E. et al. (2009), “10 Gy total body irradiation increases risk of coronary sclerosis, degeneration of heart structure and function in a rat model”, *International Journal of Radiation Biology*, Vol. 85/12, Informa, London, https://doi.org/10.3109/09553000903264473

Dias, J. et al. (2018), “Gamma Low- Dose-Rate Ionizing Radiation Stimulates Adaptive Functional and Molecular Response in Human Aortic Endothelial Cells in a Threshold-, Dose-, and Dose Rate–Dependent Manner”, *Dose-Response*, Vol. 16/1, SAGE Publications, Thousand Oaks, https://doi.org/10.1177/1559325818755238.

Dong, S. et al. (2020), “Oxidative stress: A critical hint in ionizing radiation induced pyroptosis”, *Radiation Medicine and Protection*, Vol. 1/4, National Institute of Radiological Protection, https://doi.org/10.1016/j.radmp.2020.10.001.

Forrester, S. J. et al. (2018), “Reactive Oxygen Species in Metabolic and Inflammatory Signaling”, *Circulation Research*, Vol. 122/6, Lippincot Williams & Wilkins, Philadelphia, https://doi.org/10.1161/CIRCRESAHA.117.311401.

Fuji, S. et al. (2016), “Association between endothelial function and micro-vascular remodeling measured by synchrotron radiation pulmonary micro-angiography in pulmonary arterial hypertension”, *General Thoracic and Cardiovascular Surgery*, Vol. 64, Springer, New York, https://doi.org/10.1007/s11748-016-0684-6.

Hamada, N. et al. (2022), “Temporal Changes in Sparing and Enhancing Dose Protraction Effects of Ionizing Irradiation for Aortic Damage in Wild-Type Mice”, Cancers, Vol. 14/14, MDPI, Basel, https://doi.org/10.3390/cancers14143319

Hamada, N. et al. (2021), “Vascular damage in the aorta of wild-type mice exposed to ionizing radiation: Sparing and enhancing effects of dose protraction”, *Cancers*, Vol.13/21, Multidisciplinary Digital Publishing Institute, Basel, https://doi.org/10.3390/cancers13215344.

Hamada, N. et al. (2020), “Ionizing Irradiation Induces Vascular Damage in the Aorta of Wild-Type Mice”, *Cancers*, Vol. 12/10, Multidisciplinary Digital Publishing Institute, Basel, https://doi.org/10.3390/CANCERS12103030.

Hemmings, B. A. and D. F. Restuccia (2012). “PI3K-PKB/Akt Pathway”, *Cold Spring Harbor Perspectives in Biology*, Vol. 4/9, Cold Spring Harbor Laboratory Press, Cold Spring Harbor, https://doi.org/10.1101/CSHPERSPECT.A011189.

Hirakawa, M. et al. (2002), “Tumor Cell Apoptosis by Irradiation-induced Nitric Oxide Production in Vascular Endothelium”, *Cancer Research,* Vol. 62/5, American Association for Cancer Research, Philadelphia, pp. 1450–1457.

Hong, C. W. et al. (2013), “Involvement of inducible nitric oxide synthase in radiation-induced vascular endothelial damage”, *Journal of Radiation Research*, Vol. 54/6, Oxford University Press, Oxford, https://doi.org/10.1093/JRR/RRT066.

Ježek, P. and L. Hlavatá (2005), “Mitochondria in homeostasis of reactive oxygen species in cell, tissues, and organism”, *The International Journal of Biochemistry & Cell Biology*, Vol. 37/12, Elsevier, Amsterdam, https://doi.org/10.1016/j.biocel.2005.05.013.

Kozbenko, T. et al. (2022), “Deploying elements of scoping review methods for adverse outcome pathway development: a space travel case example”, *International Journal of Radiation Biology*, Vol. 98/12. https://doi.org/10.1080/09553002.2022.2110306

Luiking, Y. C., M. P. Engelen and N. E. Deutz (2010), “Regulation of nitric oxide production in health and disease”, *Current Opinion in Clinical Nutrition and Metabolic Care*, Vol. 13/1, Lippincott Williams and Wilkins Ltd, Philadelphia, https://doi.org/10.1097/MCO.0b013e328332f99d.

Millatt, L. J., E. M. Abdel-Rahman and H. M. Siragy (1999), “Angiotensin II and nitric oxide: a question of balance”, *Regulatory Peptides*, Vol. 81/1-3, Elsevier, Amsterdam, https://doi.org/10.1016/S0167-0115(99)00027-0.

Mitchell, A. et al. (2019), “Cardiovascular effects of space radiation: implications for future human deep space exploration”, *European Journal of Preventive Cardiology* Vol. 26/16, SAGE Publishing, Thousand Oaks, https://doi.org/10.1177/2047487319831497.

Nagane, M. et al. (2021), “DNA damage response in vascular endothelial senescence: Implication for radiation-induced cardiovascular diseases”, *Journal of Radiation Research*, Vol. 62/4, Oxford University Press, Oxford, https://doi.org/10.1093/JRR/RRAB032.

Nathan, C. and Q. W. Xie (1994), “Regulation of biosynthesis of nitric oxide”, *Journal of Biological Chemistry*, Vol. 269/19, American Society for Biochemistry and Molecular Biology, Rockville, https://doi.org/10.1016/S0021-9258(17)36703-0.

Nguyen Dinh Cat, A. et al. (2013), “Angiotensin II, NADPH Oxidase, and Redox Signaling in the Vasculature”, *Antioxidants & Redox Signaling*, Vol. 19/10, Mary Ann Liebert, Inc., Larchmont, https://doi.org/10.1089/ARS.2012.4641.

Ohta, S. et al. (2007), “The Role of Nitric Oxide in Radiation Damage”, *Biological and Pharmaceutical Bulletin*, Vol. 30/6, Pharmaceutical Society of Japan, Tokyo, https://doi.org/10.1248/bpb.30.1102.

Powers, S. K. and M. J. Jackson (2008), “Exercise-Induced Oxidative Stress: Cellular Mechanisms and Impact on Muscle Force Production”, *Physiological Reviews*, Vol. 88/4, The American Physiological Society, Rockville, https://doi.org/10.1152/physrev.00031.2007

Sadhukhan, R. et al. (2020), “Fractionated radiation suppresses Kruppel-like factor 2 pathway to a greater extent than by single exposure to the same total dose”, *Scientific Reports*, Vol. 10/1, Nature Portfolio, London, https://doi.org/10.1038/s41598-020-64672-3.

Sakata, K. et al. (2015), “Roles of ROS and PKC-βII in ionizing radiation-induced eNOS activation in human vascular endothelial cells”, *Vascular Pharmacology*, Vol. 70, Elsevier, Amsterdam, https://doi.org/10.1016/j.vph.2015.03.016.

Schmidt-Ullrich, R. K. et al. (2000), “Signal Transduction and Cellular Radiation Responses”, *Radiation Research*, Vol. 153, Radiation Research Society, Bozeman, https://doi.org/10.1667/0033-7587(2000)153[0245:STACRR]2.0.CO;2.

Soloviev, A. I. and I.V. Kizub (2019), “Mechanisms of vascular dysfunction evoked by ionizing radiation and possible targets for its pharmacological correction”, *Biochemical pharmacology*, Vol. 159, Elsevier, Amsterdam, https://doi.org/10.1016/j.bcp.2018.11.019.

Sonveaux, P. et al. (2003), “Irradiation-induced Angiogenesis through the Up-Regulation of the Nitric Oxide Pathway: Implications for Tumor Radiotherapy”, *Cancer Research*, Vol. 63/5, American Association for Cancer Research, Philadelphia, pp. 1012–1019.

Vargas-Mendoza, N. et al. (2021), “Oxidative Stress, Mitochondrial Function and Adaptation to Exercise: New Perspectives in Nutrition”, *Life*, Vol. 11/11, Multidisciplinary Digital Publishing Institute, Basel, https://doi.org/10.3390/life11111269.

Wang, Y., M. Boerma and D. Zhou (2016), “Ionizing Radiation-Induced Endothelial Cell Senescence and Cardiovascular Diseases”, *Radiation research*, Vol. 186/2, Radiation Research Society, Bozeman, https://doi.org/10.1667/RR14445.1.

Yao, L. et al. (2010), “The role of RhoA/Rho kinase pathway in endothelial dysfunction”, *Journal of Cardiovascular Disease*

Research, Vol. 1/4, Elsevier, Amsterdam, https://doi.org/10.4103/0975-3583.74258.

Relationship: 2780: Energy Deposition leads to Increase, Endothelial Dysfunction

AOPs Referencing Relationship

AOP Name	Adjacency	Weight of Evidence	Quantitative Understanding
Deposition of energy leads to vascular remodeling	non-adjacent	Moderate	Low

Evidence Supporting Applicability of this Relationship

Taxonomic Applicability

Term	Scientific Term	Evidence	Links
human	Homo sapiens	Low	NCBI
mouse	Mus musculus	Moderate	NCBI
rat	Rattus norvegicus	Moderate	NCBI
rabbit	Oryctolagus cuniculus	Moderate	NCBI

Life Stage Applicability

Life Stage	Evidence
Adult	Moderate
Juvenile	Low
Not Otherwise Specified	Moderate

Sex Applicability

Sex	Evidence
Male	Moderate
Female	Moderate
Unspecific	Low

The evidence for the taxonomic applicability to humans is low as the majority of the evidence is from *in vitro* human-derived cells. The relationship is supported by both sexes of mouse, rat, and rabbit models. The *in vivo* studies were mostly undertaken in adolescent or adult rats and mice. In addition, the relationship is likely at any life stage.

Key Event Relationship Description

Energy deposition can lead to ionization events that can directly interact with molecules within the cell and can subsequently lead to biological changes such as the formation of free radicals and the initiation of DNA damage repair mechanisms. Different radiation types have different physical properties and as a result the biological effects on cells may differ. Dose and dose rate of the deposited energy also play a role as these factors affect the amount and rate of energy deposited (Donaubauer et al., 2020). Repeated or prolonged exposure to radiation can exhaust the protective effect of the endothelium and lead to endothelial dysfunction (Baselet et al., 2019). Consequently, cells within the vascular endothelium may lose their integrity and become senescent or apoptotic via alterations to signaling pathways related to cell survival, leading to dysregulation of vasodilation and eventual endothelial dysfunction (Deanfield et al., 2007; Bonetti et al., 2003). Activation of the endothelium, consisting of inflammation, proliferation, thrombosis and low nitric oxide, occurs as a normal response to pathological conditions and oxidative stress from deposited energy (Krüger-Genge et al., 2019).

Evidence Supporting this KER

Overall weight of evidence: Moderate

Biological Plausibility

The biological plausibility surrounding the connection between deposition of energy leading to endothelial dysfunction is well-supported by reviews in the literature and mechanistic understanding. The impact on endothelial dysfunction from deposited energy onto cells may vary with the radiation source and associated parameters of dose, dose rate, and type, which can influence the amount of energy absorbed, among other factors such as tissue type.

Radiation types such as gamma rays, X-rays, and charged particles at doses ranging from 0.05-18 Gy and dose rates as low as 2.4 mGy/h induce endothelial dysfunction through an increase in cellular markers of apoptosis and cellular senescence in human cell and animal models as well as diminished relaxation response of vessels in animal models (Yentrepalli et al., 2013a; Yentrepalli et al., 2013b; Soucy et al., 2011; On et al., 2001; Hatoum et al., 2006; Soucy et al., 2010; Soloviev et al., 2003; Baselet et al., 2017; Shen et al., 2017). Following irradiation, endothelial cells may lose their integrity and become senescent or apoptotic via alterations to signaling pathways related to cell survival, leading to endothelial dysfunction (Deanfield et al., 2007; Bonetti et al., 2003). Senescent endothelial cells show changes in cell morphology, cell-cycle arrest, and increased senescence-associated β-galactosidase (SA-β-gal) staining. They also have a pro-inflammatory secretory phenotype, which further contributes to negative effects. These changes lead to endothelial dysfunction, which results in dysregulation of vasodilation (Wang et al., 2016; Hughson et al., 2018; Ramadan et al., 2021). Prolonged chronic inflammation following irradiation causes an ineffective healing process, further worsened by a decrease in endothelium-dependent relaxation. This leads to endothelial dysfunction, making the vasculature more vulnerable to damage from non-laminar flow (Sylvester et al., 2018). Since the endothelium is largely responsible for controlling fluid flow, dysfunctions in the endothelium can lead to fluid imbalance, blood pressure changes, and blood clot formation (Konukoglu & Uzun, 2017; Korpela & Liu, 2014; Verma et al., 2003).

Empirical Evidence

The empirical evidence supporting this KER is gathered from research utilizing both *in vivo* and *in vitro* models. Many *in vitro* studies have examined this relationship using human endothelial cell cultures, such as telomerase-immortalized coronary artery endothelial cells (TICAE) and human umbilical vein endothelial cells (HUVECs) (Baselet et al., 2017; Yentrapalli et al., 2013b). *In vivo* studies analyzed changes in murine aorta, white rabbit thoracic aorta, and rat aorta and microvessels (Hatoum et al., 2006; Shen et al., 2018; Soloviev et al., 2003; Soucy et al., 2010; Soucy et al., 2011). The evidence includes use of gamma, X-ray, and heavy ion radiation in the dose range of 0.05-18 Gy. SA-β-gal, a marker for cellular senescence, and therefore endothelial dysfunction, relaxation in response to acetylcholine (ACh) and apoptosis were examined in these studies (Baselet et al., 2017; Hatoum et al., 2006; Shen et al., 2018; Soloviev et al., 2003; Soucy et al., 2010; Soucy et al., 2011; Yentrapalli et al., 2013).

Dose Concordance

Studies using *in vitro* and *in vivo* models have shown that deposition of energy as produced by acute and chronic doses of ionizing radiation administered from 0.05-18 Gy, with dose rates ranging from 2.4 mGy/h to 2.43 Gy/min, cause endothelial dysfunction as indicated by cellular markers such as cellular senescence and apoptosis as well as decreased maximum relaxation response of vessels in response to ACh.

For example, chronic gamma irradiation of human endothelial cells at a dose rate as low as 2.4 mGy/h led to an increase of 2-fold in SA-β-gal staining (Yentrapalli et al., 2013a). A similar study showed that 4.1 mGy/h chronic gamma irradiation caused no significant changes after 0.69 Gy, but there was a 2-fold increase in SA-β-gal at 2.07 Gy and a 3-fold increase after 4.13 Gy (Yentrapalli et al., 2013b). Another study also looking at SA-β-gal found a 1.7-fold maximum increase in SA-β-gal after irradiating human endothelial cells with 0.05-2 Gy X-rays (Baselet et al., 2017). A study measuring radiation-induced apoptosis in mouse aorta found a 5-fold increase in the number of apoptotic cells after 18 Gy X-ray irradiation (Shen et al., 2018).

Many studies have measured endothelial dysfunction through the relaxation response of vessels in response to ACh. After rabbit thoracic aortas were irradiated with 6 Gy gamma rays, there was a 0.5-fold decrease in maximum relaxation response to ACh, with a linear decrease in relaxation from 0, 1, 2, and 4 Gy gamma rays (Soloviev et al., 2003). A study that irradiated rat aorta with 0.5 and 1 Gy ^{56}Fe ions found a 0.8-fold decrease in maximum relaxation response to ACh (Soucy et al., 2011). Microvessels from rat intestines irradiated with 2250 cGy of fractionated X-rays showed an ACh-induced maximum dilation of 3%, while controls showed a maximum dilation of 87%. A significant decrease was seen after only three doses of 250 cGy (Hatoum et al., 2006). Gamma ray irradiation of rat aorta at 5 Gy showed a 0.6-fold decrease in relaxation response to ACh (Soucy et al., 2010). Similar results were found in a study using 10 Gy gamma rays on rat aortas, which showed a 9% maximum relaxation response to ACh compared to the 48% maximum relaxation in the control group (On et al., 2001).

Time Concordance

There is moderate evidence to suggest a time concordance between the deposition of energy and endothelial dysfunction. A chronic gamma irradiation study at a dose rate of 2.4 mGy/h examined human endothelial cells *in vitro* after 1, 6, 10 and 12 weeks and showed an increase in SA-β-gal as early as 10 weeks, with levels remaining significantly increased at 12 weeks (Yentrapalli et al., 2013a). A study by the same group also looked at the effects of 4.1 mGy/h gamma rays on human endothelial cells *in vitro*, but at 1, 3 and 6 weeks of chronic irradiation, revealing an increase in cellular senescence, indicated by increased SA-β-gal, as soon as 3 weeks, with levels remaining significantly increased at 6 weeks (Yentrepalli et al., 2013b). After mouse aorta were irradiated with 18 Gy X-rays, the number of apoptotic cells were determined over 84 days. The number of apoptotic cells was significantly higher than the controls after 3, 7, 14, 28, and 84 days, but was highest (5-fold higher than control) after 7 days followed by a linear decrease (Shen et al., 2018).

Similarly, rabbit thoracic aortas irradiated with 6 Gy gamma rays and exposed to ACh showed a 0.5-fold decrease in maximum

relaxation after both 9 and 30 days (Soloviev et al., 2003). When rats were irradiated with 1 Gy ^{56}Fe ions, ACh-induced relaxation in the aorta decreased 0.25-fold compared to controls 4 months after irradiation, and went from a 67.5% relaxation response in the control group to 59% in the irradiated group after 6 months (although this change was not statistically significant). Relaxation response to ACh remained non-significant at 8 months post-irradiation (Soucy et al., 2011).

Essentiality

Endothelial dysfunction can be triggered in response to an injury or a stressor. Therefore, with a reduction in stressor severity, there should be less endothelial dysfunction. As deposition of energy is a physical stressor, it cannot be blocked/decreased using chemicals; however, it can be shielded, though currently no available data used shielding of radiation and measured the impact on endothelial dysfunction. Since deposited energy initiates events immediately, the removal of deposited energy also supports the essentiality of the key event. Studies that do not deposit energy are observed to have no downstream effects.

Uncertainties and Inconsistencies

Much evidence for this relationship comes from high dose studies (>2 Gy); further work is needed at varying doses and dose rates to better understand the relationship.

Quantitative Understanding of the Linkage

Examples of quantitative understanding of the relationship are shown in the table below. All data represented is statistically significant unless otherwise indicated.

Response-response relationship

Dose Concordance

Reference	Experiment Description	Result
Baselet et al., 2017	*In vitro*. X-ray radiation was delivered to human endothelial cells at a dose rate of 0.5 Gy/min for total doses of 0.05, 0.1, 0.5 and 2 Gy. SA-β-gal activity was used as a marker for senescence and endothelial dysfunction and was measured 14 days post exposure.	SA-β-gal activity for all radiation doses was significantly elevated above the non-irradiated control and increased with an increase in radiation dose. At the highest dose of 2 Gy, there was a 1.7-fold increase compared to control.
Soucy et al., 2011	*In vivo*. 3-4 months-old rats were whole body irradiated with 0.5 or 1 Gy of ^{56}Fe ions before their aortas were harvested and the endothelium dependent vasodilation response to ACh was evaluated at 4 months post-irradiation.	A 0.5 Gy dose did not show significant changes to maximum relaxation response to ACh compared to non-irradiated control. Following a 1 Gy dose there was a 0.8-fold decrease in maximum relaxation response to ACh compared to non-irradiated control.
Soucy et al., 2010	*In vivo*. 4-months-old rats were irradiated with 5 Gy of ^{137}Cs, and the endothelium dependent vasodilation response to ACh of harvested aortas was evaluated.	There was a 0.6-fold decrease in maximum relaxation response to ACh in the aorta compared to the non-irradiated control.
Soloviev et al., 2003	*In vivo*. The endothelium dependent vasorelaxation response to ACh of aortas from rabbits exposed to 6 Gy of ^{60}Co whole body irradiation was evaluated 9 days post exposure. Furthermore, endothelium dependent relaxation response following exposure to 1, 2, and 4 Gy on the 7th day post exposure were also evaluated.	9 days after exposure to 6 Gy, there was a 0.5-fold decrease in maximum relaxation response to ACh. At 7 days post irradiation, maximum relaxation response to ACh decreased with an increase in radiation dose, with 60% maximum relaxation at 0 Gy dropping down to 30% after 4 Gy.
Shen et al., 2018	*In vivo*. 18 Gy of X-ray radiation was delivered to 8-week-old mice. Apoptosis was evaluated using TUNEL assays at 3-, 7-, 14-, 28- and 84-days post irradiation.	Apoptosis levels in 18 Gy irradiated groups were significantly elevated above sham irradiated control at all time points tested. The difference peaked 7-days post irradiation at a 5-fold increase compared to control.
Hatoum et al., 2006	*In vivo*. Rats were whole body irradiated with up to 2250 cGy via 9 fractions of 250 cGy X-rays at a dose rate of 243 cGy/min. Endothelium dependent vasodilation response to ACh of harvested submucosal vessels was evaluated at various radiation doses.	After the final dose (total 22.5 Gy) there was a 0.03-fold decrease in maximum relaxation response to ACh in irradiated rat microvessels compared to non-irradiated controls. Following dose 1 and 2 (250 cGy and 500 cGy total dose), maximum dilation remained similar to non-irradiated control (~90% maximum dilation). However, following the third dose (750 cGy total), maximum dilation dropped

		below 10% and remained significantly below non-irradiated control levels for all remaining doses tested.

Time-scale

Time Concordance

Reference	Experiment Description	Result
Yentrapalli et al., 2013a	*In vitro*. Chronic gamma irradiation (^{137}Cs) was delivered to human umbilical vein endothelial cells (HUVECs) at a dose rate of 1.4 mGy/h or 2.4 mGy/h. SA-β-gal activity was used as a marker for premature endothelial cell senescence and was evaluated at 1-, 3-, 6-, 10- and 12-weeks post irradiation.	Between 1 to 6 weeks post irradiation no significant differences were observed between either of the irradiated groups and the sham irradiated control. At the 10- and 12-week time points, the 1.4 mGy/h exposure continued to show no significant changes from control, while the 2.4 mGy/h group showed a 1.7-fold increase at 10-weeks and 1.9-fold increase at 12-weeks.
Yentrapalli et al., 2013b	*In vitro*. Chronic gamma (^{137}Cs) of HUVECs at a dose rate of 4.1 mGy/h for up to 6 weeks for final doses of 0.69, 2.07 and 4.13 Gy. SA-β-gal activity was used as a marker for premature endothelial cell senescence and was evaluated at 1-, 3- and 6-weeks post exposure.	No significant changes in SA-β-gal activity were observed between irradiated and sham irradiated groups in the first week. SA-β-gal activity was significantly elevated in irradiated HUVECs at the 3- and 6-week timepoints, showing a 2-fold and 3-fold elevation above control respectively.
Soucy et al., 2011	*In vivo*. 3-4 months-old rats were whole body irradiated with 0.5 or 1 Gy of ^{56}Fe ions before their aortas were harvested and the endothelium dependent vasodilation response to ACh was evaluated.	At 4 months post radiation there was a 0.8-fold decrease in maximum relaxation response to ACh with a return to control levels by 6 months.
Soloviev et al., 2003	*In vivo*. The maximum endothelium dependent vasorelaxation response to ACh of aortas from rabbits having been whole body irradiated to 6 Gy ^{60}Co gamma-rays was evaluated 9- and 30-days post exposure.	At both 9- and 30-days post-irradiation there was a ~0.5-fold decrease in maximum relaxation response to ACh compared to non-irradiated control. There was no significant difference in maximum relaxation between the 9- and 30-day timepoints.
Shen et al., 2018	*In vivo*. 18 Gy of X-ray radiation was delivered to 8-week-old mice with apoptosis levels being measured for up to 84 days post-irradiation in the aorta.	There was a significant increase of 3-fold in apoptosis as soon as 3 days post-irradiation with a peak of 7-fold after 7 days. There was a gradual return to a 3-fold increase by 84 days.

Known modulating factors

Modulating factor	Details	Effects on the KER	References
Drug	Oxypurinol (Oxp) (a xanthine oxidase inhibitor)	Treatment led to increased endothelial relaxation response to ACh after irradiation.	(Soucy et al., 2011)
Drug	Vitamin C	Treatment increased the relaxation response to ACh after irradiation.	(On et al., 2001)
Drug	MnTBAP	Treatment restored vasodilation ability after irradiation.	(Hatoum et al., 2006)
Drug	Tempol	Treatment restored vasodilation ability after irradiation.	(Hatoum et al., 2006)
Drug	Human bone marrow stem cells	Both low and high doses decreased apoptosis after irradiation.	(Shen et al., 2018)

Known Feedforward/Feedback loops influencing this KER

Not identified.

References

Baselet, B. et al. (2019), “Pathological effects of ionizing radiation: endothelial activation and dysfunction”, Cellular and Molecular Life Science, Vol. 76, Springer, New York, https://doi.org/10.1007/s00018-018-2956-z.

Baselet, B. et al. (2017), “Functional Gene Analysis Reveals Cell Cycle Changes and Inflammation in Endothelial Cells Irradiated with a Single X-ray Dose”, *Frontiers in pharmacology*, Vol. 8, Frontiers Media SA, Lausanne, https://doi.org/10.3389/fphar.2017.00213

Boerma, M. et al. (2015), “Space radiation and cardiovascular disease risk”, *World Journal of Cardiology*, Vol. 7/12, Baishideng Publishing Group, Pleasanton, https://doi.org/10.4330/wjc.v7.i12.882

Bonetti, P. O., L. O. Lerman and A. Lerman (2003), “Endothelial dysfunction: a marker of atherosclerotic risk”, *Arteriosclerosis, thrombosis, and vascular biology*, Vol. 23/2, Lippincott Williams & Wilkins, Philadelphia, https://doi.org/10.1161/01.atv.0000051384.43104.fc

Deanfield, J. E., J. P. Halcox and T. J. Rabelink (2007), “Endothelial Function and Dysfunction”, *Circulation*, Vol. 115/10, Lippincott Williams & Wilkins, Philadelphia, https://doi.org/10.1161/CIRCULATIONAHA.106.652859.

Donaubauer, A. J. et al. (2020), “The Influence of Radiation on Bone and Bone Cells-Differential Effects on Osteoclasts and Osteoblasts”, *International journal of molecular sciences*, Vol. 21/7, Multidisciplinary Digital Publishing Institute, Basel, https://doi.org/10.3390/ijms21176377.

Finch, W., K. Shamsa, M. S. Lee (2014), “Cardiovascular complications of radiation exposure”, *Reviews in Cardiovascular Medicine*, Vol. 15/3, IMR Press, https://doi.org/10.3909/ricm0689

Hatoum, O. A. et al. (2006), “Radiation Induces Endothelial Dysfunction in Murine Intestinal Arterioles via Enhanced Production of Reactive Oxygen Species”, *Arteriosclerosis, Thrombosis, and Vascular Biology*, Vol. 26/2, Lippincott Williams & Wilkins, Philadelphia, https://doi.org/10.1161/01.ATV.0000198399.40584.8c

Hughson, R.L., A. Helm and M. Durante (2018), “Heart in space: Effect of the extraterrestrial environment on the cardiovascular system”, *Nature Reviews Cardiology*, Vol. 15/3, Nature Portfolio, London, https://doi.org/10.1038/nrcardio.2017.157.

Konukoglu, D., and H. Uzun (2017), “Endothelial Dysfunction and Hypertension”, *Advances in experimental medicine and biology*, Vol. 956, Springer, New York, https://doi.org/10.1007/5584_2016_90.

Korpela, E., and S. K. Liu (2014), “Endothelial perturbations and therapeutic strategies in normal tissue radiation damage”, *Radiation oncology,* Vol. 9, BioMed Central, London, https://doi.org/10.1186/s13014-014-0266-7.

Kozbenko, T. et al. (2022), “Deploying elements of scoping review methods for adverse outcome pathway development: a space travel case example”, *International Journal of Radiation Biology*, Vol. 98/12. https://doi.org/10.1080/09553002.2022.2110306

Krüger-Genge, A. et al. (2019), “Vascular Endothelial Cell Biology: An Update”, *International Journal of Molecular Sciences*, Vol. 20/18, Multidisciplinary Digital Publishing Institute, Basel, https://doi.org/10.3390/IJMS20184411.

On, Y. K. et al. (2001), “Vitamin C prevents radiation-induced endothelium-dependent vasomotor dysfunction and de-endothelialization by inhibiting oxidative damage in the rat”, *Clinical and experimental pharmacology & physiology*, Vol. 28/10, Wiley-Blackwell, Hoboken, https://doi.org/10.1046/j.1440-1681.2001.03528.x.

Ramadan, R. et al. (2021), “The role of connexin proteins and their channels in radiation-induced atherosclerosis”, *Cellular and molecular life sciences: CMLS*, Vol. 78/7, Springer, New York, https://doi.org/10.1007/s00018-020-03716-3.

Shen, Y. et al. (2018), “Transplantation of bone marrow mesenchymal stem cells prevents radiation-induced artery injury by suppressing oxidative stress and inflammation”, *Oxidative Medicine and Cellular Longevity*, Vol. 2018, Hindawi, London, https://doi.org/10.1155/2018/5942916.

Soloviev, A. I. et al. (2003), “Mechanisms of endothelial dysfunction after ionized radiation: selective impairment of the nitric oxide component of endothelium-dependent vasodilation”, *British journal of pharmacology*, Vol. 138/5, Wiley, https://doi.org/10.1038/sj.bjp.0705079

Soucy, K. G. et al. (2011), “HZE 56Fe-Ion Irradiation Induces Endothelial Dysfunction in Rat Aorta: Role of Xanthine Oxidase”, *Radiation Research*, Vol. 176/4, Radiation Research Society, Bozeman, https://doi.org/10.1667/RR2598.1.

Soucy, K. G. et al. (2010), “Dietary inhibition of xanthine oxidase attenuates radiation-induced endothelial dysfunction in rat aorta”, *Journal of Applied Physiology*, Vol. 108/5, American Physiological Society, Rockville, https://doi.org/10.1152/japplphysiol.00946.2009.

Sylvester, C. B. et al. (2018), “Radiation-Induced Cardiovascular Disease: Mechanisms and Importance of Linear Energy Transfer”, *Frontiers in Cardiovascular Medicine*, Vol. 5, Frontiers Media SA, Lausanne, https://doi.org/10.3389/fcvm.2018.00005.

Verma, S., M. R. Buchanan and T. J. Anderson (2003), “Endothelial function testing as a biomarker of vascular disease”, *Circulation*, Vol. 108/17, Lippincott Williams & Wilkins, Philadelphia, https://doi.org/10.1161/01.CIR.0000089191.72957.ED.

Wang, Y., M. Boerma and D. Zhou (2016), “Ionizing Radiation-Induced Endothelial Cell Senescence and Cardiovascular Diseases”, *Radiation research*, Vol. 186/2, Radiation Research Society, Bozeman, https://doi.org/10.1667/RR14445.1.

Yentrapalli, R. et al. (2013a), “The PI3K/Akt/mTOR pathway is implicated in the premature senescence of primary human endothelial cells exposed to chronic radiation”, *PloS one*, Vol. 8/8, PLOS, San Francisco, https://doi.org/10.1371/journal.pone.0070024.

Yentrapalli, R. et al. (2013b), “Quantitative proteomic analysis reveals induction of premature senescence in human umbilical vein endothelial cells exposed to chronic low-dose rate gamma radiation”, *Proteomics*, Vol. 13/7, John Wiley & Sons, Ltd.,

Hoboken, https://doi.org/10.1002/pmic.201200463.

Relationship: 2785: Energy Deposition leads to Occurrence, Vascular Remodeling

AOPs Referencing Relationship

AOP Name	Adjacency	Weight of Evidence	Quantitative Understanding
Deposition of energy leads to vascular remodeling	non-adjacent	High	Low

Evidence Supporting Applicability of this Relationship

Taxonomic Applicability

Term	Scientific Term	Evidence	Links
human	Homo sapiens	High	NCBI
mouse	Mus musculus	Moderate	NCBI
rat	Rattus norvegicus	High	NCBI

Life Stage Applicability

Life Stage	Evidence
Juvenile	Moderate
Adult	High

Sex Applicability

Sex	Evidence
Male	High
Female	High

The relationship has been shown *in vivo* in mice and rats and *ex vivo* in human models. Majority of studies used males. Evidence came from either adult or adolescent animals. However, the relationship is plausible at any life stage.

Key Event Relationship Description

Deposition of energy can trigger vascular remodeling through many pathways (Tapio, 2016) including changes to vessel structure and blood flow (Patel, 2020; Sylvester et al., 2018). Pro-inflammatory mediators can be increased, which can result in a low level of inflammation causing intimal thickening (Sylvester et al., 2018). Deposition of energy can generate reactive oxygen species (ROS) and highly reactive radicals sparsely from low- linear energy transfer (LET) radiation and densely from high-LET radiation, which can cause endothelial dysfunction and subsequent vascular remodeling (Boerma et al., 2015; Hughson, Helm & Durante, 2017; Slezak et al., 2017; Soloviev & Kizub, 2019; Sylvester et al., 2018). Increased production of ROS changes the bioavailability of nitric oxide (NO), a diffusible molecule responsible for vasodilation, which leads to inhibited vasomotion and cellular senescence as components of endothelial dysfunction (Patel, 2020; Soloviev & Kizub, 2019). Changes in the expression or activity of proteins in many signaling pathways can lead to endothelial dysfunction (Schmidt-Ullrich et al., 2000; Tapio, 2016). In addition, the increased pro-inflammatory mediators can lead to endothelial dysfunction and therefore, vascular remodeling (Tapio, 2016). Another possible vascular remodeling change is age accelerated atherosclerosis (EPRI, 2020; Hamada et al., 2014). Studies using varying LET, delivered at acute and chronic dose-rates, have shown remodeling of the vasculature (reviewed in Tapio, 2016).

Evidence Supporting this KER

Overall weight of evidence: High

Biological Plausibility

The biological plausibility suggesting that deposition of energy leads to vascular remodeling is well-supported by reviews and mechanistic studies published in the literature. Vascular remodeling may occur due to aging and diet (Zieman, Melenovsky & Kass, 2005). However, the deposition of energy from ionizing radiation (IR) can accelerate vascular remodeling in the form of accelerated atherosclerosis (Boerma et al., 2015; Boerma et al., 2016; EPRI, 2020; Hamada et al., 2014; Hughson, Helm & Durante, 2017; Mitchell et al., 2019; Sylvester et al., 2018), which can be demonstrated by arterial thickening or the amount of oxidized low-density lipoprotein (oxLDL) (Poznyak et al., 2021). Remodeling normally allows adaptation to long-term hemodynamic changes but can also contribute to vascular diseases (Gibbons & Dzau, 1994). Various short-term post-spaceflight studies have shown vascular remodeling after deposition of energy from space IR (Patel, 2020).

Under physiological conditions, the body maintains a balance of ROS and NO levels. IR generates ROS that can react with NO and reduce its bioavailability, causing endothelial dysfunction and vascular stiffness (Patel, 2020). Similarly, signaling pathways can cause vascular remodeling through endothelial dysfunction and altered NO (Tapio, 2016). Increased ROS or altered signaling can cause a prolonged inflammatory response; this has been observed in animal models exposed to high-LET radiation (Hughson, Helm & Durante, 2017; Sylvester et al., 2018; Tapio, 2016). The low level of inflammation results in intimal thickening and inhibits tissue and vessel recovery (Sylvester et al., 2018). Microvascular injury and inflammation may cause angiogenesis, which prevents vascular resistance (Slezak et al., 2017). However, depending on the source, radiation may have different effects on angiogenesis (Grabham & Sharma, 2013). An increase in pro-angiogenic factors, such as vascular endothelial growth factor (VEGF), secreted as a consequence of photon irradiation can promote angiogenesis. Exposure to low-LET protons and high-LET heavy ion radiation can disturb angiogenesis due to decreased VEGF secretion and tubule formation (Grabham & Sharma, 2013; Sylvester et al., 2018). Matrix metalloproteinases (MPPs) are involved in remodeling of the extracellular matrix (ECM) and can affect various pathological processes after irradiation (Slezak et al., 2017). Following radiation, existing collagen in the heart may be remodeled, which indicates ECM remodeling (Shen et al., 2018; Sridharan et al., 2020; Zieman, Melenovsky & Kass, 2005). Thus, many mechanisms exist via which the deposition of energy can lead to vascular remodeling; these are generally well understood and described in the literature, leading to a strong weight of evidence for the biological plausibility of this KER.

Empirical Evidence

There is moderate empirical evidence supporting the connection between deposition of energy leading to vascular remodeling. The evidence was gathered from studies using *in vivo* rat and mouse models, as well as *in vitro* models of human vessels and *ex vivo* human vessel biopsies (Grabham et al., 2011; Hamada et al., 2020; Hamada et al., 2021; Hamada et al., 2022; Russel et al., 2009; Sarkozy et al., 2019; Shen et al., 2018; Soucy et al., 2007; Soucy et al., 2010; Soucy et al., 2011; Sridharan et al., 2020; Yu et al., 2011). The models used stressors such as iron ions (^{56}Fe) (Soucy et al., 2011; Yu et al., 2011), gamma rays (Hamada et al., 2020; Hamada et al., 2021; Hamada et al., 2022; Soucy et al., 2007; Soucy et al., 2010), X-rays (Hamada et al., 2021; Hamada et al., 2022; Shen et al., 2018), electrons (Sarkozy et al., 2019), protons and oxygen ions (^{16}O) (Sridharan et al., 2020). Vascular stiffness measured by pulse wave velocity (PWV) and vascular composition (Hamada et al., 2020; Hamada et al., 2021; Hamada et al., 2022; Shen et al., 2018; Soucy et al., 2007; Soucy et al., 2010; Soucy et al., 2011; Sridharan et al., 2020), vessel thickness/diameter measured directly (Sarkozy et al., 2019; Shen et al., 2018; Soucy et al., 2011; Sridharan et al., 2020; Yu et al., 2011) and other morphological changes (Hamada et al., 2020; Hamada et al., 2021; Hamada et al., 2022) were used as endpoints for vascular remodeling.

Dose Concordance

PWV is often measured to determine vascular stiffness and therefore remodeling, where PWV is quadratically proportional to Young's modulus (measure of a material's stiffness) (Pereira, Correia & Cardoso, 2015; Soucy et al., 2011). The PWV of irradiated rats increased with an increase in radiation dose. Across several studies, 0.5, 1, 1.6, and 5 Gy doses were tested, with responses of 1.1 to 1.2-fold changes to PWV (Soucy et al., 2007, 2010, 2011). PWV is also quadratically proportional to the vessel diameter and inversely quadratically proportional to the vessel wall thickness. However, Soucy et al. (2011) found no significant change in the aortic wall thickness:lumen diameter ratio, indicating the change in PWV was due to changes in vessel composition and not geometric remodeling. Collagen composition in the membrane was also measured to determine vascular composition and therefore remodeling, with increased collagen indicating stiffness (Zieman, Melenovsky & Kass, 2005). Collagen accumulation increased 1.4-fold after 18 Gy X-ray irradiation (Shen et al., 2018) and 1.5-fold after various regiments of 5 Gy X-rays (Hamada et al., 2021; Hamada et al., 2022) in mice. Following 12 months of 16O exposure, the tissue content of collagen type III peptide increased 2.3-fold and 2-fold at 0.05 Gy and 0.25 Gy, respectively (Sridharan et al, 2020). VE-cadherin, a marker for adherens junctions, decreased 0.2- to 0.3-fold in mice after various regimens of 5 Gy gamma and X-rays, with a high decrease in the acute and fractionated doses and no change after chronic gamma rays (Hamada et al., 2022; Hamada et al., 2021; Hamada et al., 2020). oxLDL increased in mice after X-ray irradiation at both 8 and 16 Gy; however, the increase was not greater at 16 Gy relative to 8 Gy (Azimzadeh et al., 2015).

Vessel thickness was also measured in various studies. Aortic thickness increased 1.4-fold after 18 Gy X-ray irradiation of mice (Shen et al., 2018). Iron ion irradiation on apolipoprotein E (apoE)-deficient mice, a model for atherosclerosis, at both 2 and 5 Gy showed a 1.4-fold increase in carotid artery intima thickness compared to sham-irradiated apoE-deficient mice (Yu et al., 2011). Markers of vascular remodeling, anterior and inferior wall thicknesses in systole (AWTs and IWTs) and diastole (AWTd and IWTd) were measured after a high dose of 50 Gy electrons. AWTs increased 1.3-fold, IWTs increased 1.1-fold, AWTd increased 1.5-fold and IWTd increased 1.2-fold (Sarkozy et al., 2019). In turn, patients having undergone radiation treatment for head and neck or breast cancer with radiation doses totaling 66 Gy and 49 Gy, respectively, observed increased intima-media ratios (IMR) of 1.5- and 1.4-fold, respectively (Russel et al., 2009). Mice that did not show endothelial detachments before irradiation showed high frequencies of detachments after acute doses of 5 Gy gamma and X-rays (Hamada et al., 2020; Hamada et al., 2021). Vascular permeability was also significantly increased after 5 Gy gamma rays in mice (Hamada et al., 2020).

Radiation type can affect the nature of vascular remodeling following exposure. A study using 3D vessel models of endothelial cells in a gel matrix showed that high-LET iron-ions reduces vessel length in both mature and developing vessels after only 0.8 Gy. In

contrast, low-LET protons only inhibited growth in developing vessels at 0.8 Gy and required a dose of 3.2 Gy to affect mature vessels. Gamma radiation required a dose of 0.8 Gy to inhibit vessel growth and 6.4 Gy for any significant breakdown of mature vessels (Grabham et al., 2011).

Time Concordance

In rats irradiated with 5 Gy gamma rays, PWV as a measure of arterial stiffness increased from 3.9 m/s before irradiation to around 4.5 m/s after 1 day, 1 week and 2 weeks (Soucy et al., 2007). Under the same conditions, PWV increased from 4.1 m/s before irradiation to 4.6 m/s after 1 day, 4.9 m/s after 1 week, and 4.8 after 2 weeks in a separate study by the same authors (Soucy et al., 2010). Using 1 Gy iron ions instead, PWV increased by 0.5 m/s both 4 months and 8 months post-irradiation (Soucy et al., 2011). Mice irradiated with 18 Gy X-rays showed significantly increased aortic thickness 1.4-fold after 7 days and 1.3-fold after 14 and 28 days, while collagen accumulation increased 1.4-fold after 14, 28 and 84 days (Shen et al., 2018). ApoE-deficient mice that were irradiated with both 2 and 5 Gy iron ions showed a 1.4-fold increase in carotid artery intima thickness after 13 weeks compared to controls (Yu et al., 2011). Mice irradiated with 8 and 16 Gy of X-rays showed increased oxLDL levels at 16 weeks post-irradiation (Azimzadeh et al., 2015). Ventricular posterior wall thickness decreased at 3- and 5-months post-irradiation, and PWV increased at 12 months post-irradiation with ^{16}O irradiation (Sridharan et al., 2020). The results suggest that ^{16}O irradiation may lead to long-term vascular dysfunction in rats similar to iron ions in the studies by Soucy et al. (2011) and Yu et al. (2011). Collagen type III increased 2.4-fold after 12 months of 0.5 Gy proton irradiation (Sridharan et al., 2020). CD2, CD4 and CD8 markers for the T-protein lymphocytes that are thought to be involved with promoting hypertension and microvascular remodeling increased in rat hearts 6 months after a 0.1 Gy dose of 16O, and 12 months after a single 0.5 Gy dose of ^{16}O (Sridharan et al., 2020). Mice irradiated with 5 Gy gamma rays showed increased endothelial detachments, increased vascular permeability and VE-cadherin expression at 1, 3 and 6 months after irradiation (Hamada et al., 2020; Hamada et al., 2021). VE-cadherin was also increased 12 months after irradiation, but endothelial detachments were no longer present (Hamada et al., 2022).

Essentiality

Vascular remodeling such as arterial stiffness occurs naturally with aging, but deposition of energy can accelerate this process (Zieman, Melenovsky & Kass, 2005). Since deposited energy initiates events immediately, the removal of deposited energy also supports the essentiality of the key event. Studies that do not deposit energy are observed to have no downstream effects.

Uncertainties and Inconsistencies

- Not all results show the expected dose-response. For example, total collagen and collagen type III peptide levels studied in Sridharan et al. (2020) did not consistently increase with increasing dose. Similarly, oxLDL levels were higher at the 8 Gy dose compared to the 16 Gy dose (Azimzadeh et al., 2015).
- Yu et al. (2011) showed that intimal thickness increased at 13 weeks after iron ion irradiation of apoE-deficient mice. At 40 weeks post-irradiation, intimal thickness remained at similar levels, but the level was no longer statistically significant because the sham-irradiated group showed higher intimal thickness.

Quantitative Understanding of the Linkage

The following are a few examples of quantitative understanding of the relationship. All data that is represented is statistically significant unless otherwise indicated.

Response-response relationship

Dose Concordance

Reference	Experimental Description	Result
Sridharan et al., 2020	*In vivo*. In study B, male rats were exposed to oxygen ions (0.01-0.25 Gy). Heart tissue analysis was performed 6-7 and 12 months after radiation using histology and western blots.	Study B: At 12 months after ^{16}O exposure, the tissue content of the 75 kDa collagen type III peptide increased 2.3-fold and 2-fold at 0.05 Gy and 0.25 Gy respectively.
Soucy et al., 2007	*In vivo*. Sprague-Dawley rats were irradiated with ^{137}Cs gamma rays (0.5, 1.6, 5 Gy). Vascular stiffness was calculated using PWV with an ECG and doppler probe.	At 0.5 and 1.6 Gy, PWV increased from 3.9 m/s (before irradiation) to 4.2 m/s. At 5 Gy PWV increased to 4.6 m/s.
	In vitro. 3D models of human vessels were created using human endothelial cells in gel matrix. Mature and developing vessel models were exposed to iron-ion (1 GeV/nucleon; LET	In mature vessels, iron-ion exposure reduced vessel length significant starting after 0.8 Gy with a 44% decrease in length after 1.6 Gy. Proton exposure

Grabham et al., 2011	151 keV/um) and proton (1 GeV/nucleon; LET 0.22 keV/um) radiation at a 0.1-1 Gy/min dose rate or ^{137}Cs gamma radiation at 85 cGy/min dose rate. Vessel length as determined by length of capillary with lumen per cell was evaluated by DTAF staining for proteins and propidium iodide for nuclei.	produced no significant change, while gamma exposure required a dose of 6.4 Gy for significant vessel length breakdown. In developing vessels iron-ion exposure of 0.8 Gy decreased length by 50%, proton exposure of 0.4 Gy inhibited development and 0.8 Gy decreased length by 60%, while gamma exposure of 0.8 Gy inhibited vessel growth, and 6.4 Gy was required to reduce vessel length.
Soucy et al., 2011	*In vivo*. ^{56}Fe ions were used to irradiate rats at 0.5 or 1 Gy (0.5 Gy/min). PWV measured with Doppler probe and ECG and aortic wall thickness:lumen diameter ratio measured with histological analysis were used to determine vascular remodeling.	After 0.5 Gy, there was no significant change in PWV, but at 1 Gy there was a significant 1.1-fold increase in PWV. No change in aortic wall thickness:lumen diameter was observed after either dose.
Yu et al., 2011	*In vivo*. ^{56}Fe ions were irradiated onto apoE-/- mice, and intima thickness of the carotid artery was measured using hematoxylin and eosin staining at 0, 2 and 5 Gy doses and a 13- and 40-weeks post-irradiation.	13-weeks post irradiation, both 2 and 5 Gy doses showed a maximum 1.5-fold elevation in thickness compared to controls. 40-weeks post irradiation there was no significant difference between the control, 2 Gy, and 5 Gy groups.
Soucy et al., 2010	*In vivo*. Rats were irradiated with 5 Gy ^{137}Cs gamma radiation and PWV, measured with Doppler probe and ECG was used as a measure of aortic stiffness and vascular remodeling.	After 5 Gy, maximum PWV increased 1.2-fold compared to PWV pre-irradiation.
Hamada et al., 2020	*In vivo*. Male mice were irradiated by 5 Gy ^{137}Cs gamma rays (0.5 Gy/min) and compared to 0 Gy control. Vascular remodeling was measured through a Miles assay to show vascular permeability, vascular endothelial cadherin (VE-cadherin, a marker for adherens junctions) levels and number of endothelial detachments.	Vascular permeability increased to a maximum of 16-fold as shown by staining intensity; VE-cadherin decreased to a maximum of 0.2-fold and percent of mice with total endothelial detachments increased from 0 to 90% at the maximum response.
Hamada et al., 2021	*In vivo*. Either acute or chronic doses of X-rays and ^{137}Cs gamma rays were given to B6J mice, all resulting in a total 5 Gy dose. X-rays were given as a single acute dose, 25 fractions of 0.2 Gy/fraction spread over 42 days or 100 fractions of 0.05 Gy/fraction spread over 153 days all given at 0.5 Gy/min. Gamma rays were given as a single acute dose at 0.5 Gy/min or chronically at <1.4 mGy/h for 153 days. Vascular remodeling was measured by IMT, collagen content (aniline blue staining), VE-cadherin levels and number of mice with detachments 6 months post-irradiation.	IMT in the aorta increased about 2-fold after all X-ray treatments, but chronic gamma rays did not cause a change and acute gamma rays were not measured. Stained intensity to show collagen content increased about 1.5-fold for both the acute and 25 fractions X-ray regimens, but not in others. VE-cadherin decreased after acute gamma rays (0.2-fold) and all X-ray doses (0.2- to 0.3-fold). After acute gamma and X-rays and 25 fraction X-rays the percent of mice with a detachment went from 0 to a maximum of 100%.
Hamada et al., 2022	*In vivo*. Either acute or chronic doses of X-rays and ^{137}Cs gamma rays were given to B6J mice, all resulting in a total 5 Gy dose. X-rays were given as a single acute dose, 25 fractions of 0.2 Gy/fraction spread over 42 days or 100 fractions of 0.05 Gy/fraction spread over 153 days all given at 0.5 Gy/min. Gamma rays were given chronically at <1.4 mGy/h for 153 days. Vascular remodeling was measured by IMT, collagen content (aniline blue staining), VE-cadherin levels and number of mice with detachments 12 months post-irradiation.	IMT in the aorta increased about 1.3-fold after X-rays in acute or 25 fraction regimens, but not after other regimens. Collagen content increased about 1.1-fold for all regimens except X-rays at 100 fractions. VE-cadherin decreased after all X-ray doses (maximum 0.5-fold). No mice were observed to have a detachment.
Azimzadeh et al., 2015	*In vivo*. 10-week-old male C57Bl/6 mice received cardiac irradiation at 8 or 16 Gy with X-rays. Serum oxLDL was measured using ELISA.	oxLDL increased 1.2-fold after 8 Gy and 1.1-fold after 16 Gy compared to 0 Gy control.
Shen et	*In vivo*. Male mice irradiated with 18 Gy X-rays had measurements of aortic thickness determined at various times using hematoxylin and eosin staining. The	Sham-irradiated control: Thickness and collagen accumulation remained unchanged throughout the timepoints tested. 18 Gy irradiated:

al., 2018	accumulation of collagen was measured using Sirius red staining. Endpoints were evaluated at 3-, 7-, 14-, 28- and 84-days post exposure and compared to a sham-irradiated control group.	Thickness and collagen accumulation were elevated above control at all time points tested. Thickness peaked 7-days post exposure with a 1.4-fold increase compared to controls. Collagen accumulation peaked at 14-days post exposure with a 1.4-fold increase above controls.
Sarkozy et al., 2019	*In vivo*. Rats were irradiated with 50 Gy electrons (5 Gy/min). Various markers of vascular remodeling, anterior and inferior wall thicknesses in systole (AWTs and IWTs) and diastole (AWTd and IWTd) were measured with an echocardiograph. Endpoints were evaluated at 1, 3 and 19-weeks post-irradiation.	All three timepoints tested showed significant differences in cardiac structure measures between 50 Gy irradiated and 0 Gy control groups. By week 19, AWTs increased 1.3-fold, IWTs increased 1.1-fold, AWTd increased 1.5-fold and IWTd increased 1.2-fold.
Russel et al., 2009	*Ex vivo*. Recipient arteries from 147 patients receiving reconstructive surgery following treatment for head and neck cancer (H&N) or breast cancer (BC) were studied. H&N treatment group received 66 Gy (standard deviation 7 Gy) dose of radiation, while BC group received 49 Gy (standard deviation 3 Gy). Intimal-medial thickness in the form of intima-media ratio (IMR) was assessed through histology and proteoglycan and collagen content were scored. Analysis compared irradiated vessels, unirradiated vessels from the same patient as well as donor controls.	In the H&N group the IMR was 1.5-fold greater without correction for the control artery. In the BC group the IMR increased 1.4-fold after correction for the control artery at a mean of 4 years following irradiation. There was an increase in the proteoglycan content of the intima of the irradiated IMA vessels, from 65% to 73%.

Time-scale

Time concordance

Reference	Experiment Description	Result
Sridharan et al., 2020	*In vivo*. Male rats were exposed to oxygen ions and whole-body protons (0.5 Gy) to measure cardiac function and blood flow in study A. Measurements were taken at 3, 5, 9 and 12 months after radiation. Ultrasound, histology and Western blots were used as measurement methods. In study B, male rats were exposed to oxygen ions (0.01-0.25 Gy). Heart tissue analysis was performed 6-7 and 12 months after radiation using histology and western blots.	Study A: At 3 and 5 months after proton and oxygen ion radiation, there was a significant decrease in left ventricular posterior wall thickness. 12 months after oxygen ion exposures, velocity measures of pulsed wave Doppler of abdominal aorta increased. Cardiac volume increased at all time points in proton exposed rats, with a significance at 3 and 9 months. Collagen type III increased 2.4-fold after 12 months of 0.5 Gy protons radiation. Protein T lymphocyte markers CD2, CD4 and CD8 content in the rat hearts increased 6 months after a dose of ^{16}O at 0.1 Gy. CD2, CD4 and CD8 increased 1.4-fold 12 months after ^{16}O at 0.5 Gy.
Soucy et al., 2007	*In vivo*. Sprague-Dawley rat aorta was irradiated with 0.5, 1.6 and 5 Gy ^{137}Cs gamma rays. A measure of vascular stiffness and vascular remodeling was calculated using PWV and measurements taken with an ECG and doppler probe.	At 1 day post irradiation in each group PWV significantly increased. At 1- and 2-weeks levels remained similar to the 1-day results, but slightly increased in the 500 cGy group and slightly decreased in the 50 and 160 cGy groups.
Soucy et al., 2011	*In vivo*. ^{56}Fe ions were used to irradiate rats (0.5 Gy/min). PWV measured with Doppler probe and ECG was used to determine vascular remodeling.	At 4 months after irradiation with 1 Gy, PWV increased by ~0.5 m/s. At 8 months, PWV remained at a 0.5 m/s increase over control.
Yu et al., 2011	*In vivo*. 2 and 5 Gy ^{56}Fe ions were irradiated onto apoE-/- mice, and intima thickness of the carotid artery was measured using hematoxylin and eosin staining after 13 and 40 weeks.	At both doses, after 13 weeks, intima thickness increased 1.4-fold. Intima thickness was the same as control after 40 weeks.
	In vivo. Rats were irradiated with 5 Gy ^{137}Cs gamma	

Soucy et al., 2010	*In vivo*. Rats were irradiated with 5 Gy ^{137}Cs gamma radiation and PWV, measured with Doppler probe and electrocardiogram (ECG) over 2 weeks, was used as a measure of aortic stiffness and vascular remodeling.	PWV increased 1.1-fold (not significant) after 1 day, 1.2-fold after 1 week and 1.2-fold after 2 weeks.
Hamada et al., 2020	*In vivo*. Male mice were irradiated by 5 Gy ^{137}Cs gamma rays (0.5 Gy/min). Vascular remodeling was measured after 1, 3 and 6 months through a Miles assay to show vascular permeability, vascular endothelial cadherin (VE-cadherin, a marker for adherens junctions) levels and number of endothelial detachments.	Vascular permeability increased 8-fold at 1 month, 16-fold at 3 months and 5-fold at 6 months shown by staining intensity. VE-cadherin decreased about 0.2-fold after 1, 3, and 6 months. Percent of mice with total endothelial detachments increased from 0 to 20% at 1 month, 34% at 3 months and 90% at 6 months post-irradiation.
Shen et al., 2018	*In vivo*. Male mice irradiated with 18 Gy X-rays had measurements of aortic thickness determined from 3 to 84 days post-irradiation using hematoxylin and eosin staining. The accumulation of collagen was measured using Sirius red staining from 3 to 84 days.	Aortic thickness increased 1.1-fold after 3 days (ns), 1.4-fold after 7 days, 1.3-fold after 14 and 28 days and 1.2-fold (ns) after 84 days. Collagen increased 1.4-fold 14-, 28- and 84- days post-irradiation.
Azimzadeh et al., 2015	*In vivo*. 10-week-old male C57Bl/6 mice received cardiac irradiation at 8 or 16 Gy with X-rays. Serum oxLDL was measured using ELISA 16 weeks post-irradiation.	After 16 weeks, oxLDL increased 1.2-fold after 8 Gy and 1.1-fold after 16 Gy compared to 0 Gy control.

Known modulating factors

Modulating factor	Details	Effects on the KER	References
Drug	Oxypurinol (Oxp, a xanthine oxidase (XO) inhibitor to prevent ROS production)	Oxp treatment reduced PWV after irradiation through reduced oxidative stress	(Soucy et al., 2010; Soucy et al., 2011)
Drug	hBMSCs (human bone marrow mesenchymal stem cells, assist in repairing vascular injuries)	Treatment with hBMSCs reduced aortic thickness after irradiation	(Shen et al., 2018)
Sex	Epidemiology and pathophysiology of vascular remodeling related to CVD progression differs between the sexes.	Sex hormones are thought to play a role in several remodeling mechanisms such as hypertrophy, inflammation, fibrosis and apoptosis. Sex-specific genetic components are also involved in the variation of remodelling between sexes.	(Winham, de Andrade & Miller, 2015; Kessler et al., 2019)
Age	Increased age increases the occurrence and severity of vascular remodelling	Advanced age is linked to vascular changes such as luminal enlargement with wall thickening and decrease of endothelial function with related increase in vessel stiffness. The effect of radiation exposure is sometimes referred to as an acceleration of age-related cardio-pathology. Additionally, age-related changes in sex hormones are modulators of vascular structure.	(North & Sinclair, 2012; Harvey, Montezano, & Touyz, 2015; Ungvari et al., 2018; Kessler et al., 2019)
Genetics	CVD progression (of which vascular remodelling is part) are complex traits with genetic	Traits such as baseline carotid intima-medial thickness (CIMT), vascular stiffness and prevalence of coronary calcification have been found to have a hereditary component and some are shown to vary by ethnicity. Sex-specific genetics also play a role in genetic modulation with some genes relaxed to hypertension and adverse cardiac remodeling processes found on the Y chromosome. Additionally, X chromosome inactivation is implicated in remodelling.	(Berk & Korshunov, 2006; Winham, de Andrade & Miller, 2015)

Known Feedforward/Feedback loops influencing this KER

None exist

References

Andreassi, M. G. et al. (2015), “Subclinical Carotid Atherosclerosis and Early Vascular Aging From Long-Term Low-Dose Ionizing Radiation Exposure: A Genetic, Telomere, and Vascular Ultrasound Study in Cardiac Catheterization Laboratory Staff”, *JACC: Cardiovascular Interventions*, Vol. 8/4, Elsevier, Amsterdam, https://doi.org/10.1016/j.jcin.2014.12.233

Azimzadeh, O. et al. (2015), “Integrative Proteomics and Targeted Transcriptomics Analyses in Cardiac Endothelial Cells Unravel Mechanisms of Long-Term Radiation-Induced Vascular Dysfunction”, *Journal of Proteome Research*, Vol. 14/2, American Chemical Society, Washington, https://doi.org/10.1021/pr501141b

Berk, B. C. and V. A. Korshunov (2006), “Genetic determinants of vascular remodelling”, *The Candian Journal of Cardiology*, Vol. 22, Elsevier, Amsterdam, https://doi.org/10.1016/s0828-282x(06)70980-1

Boerma, M. et al. (2016), “Effects of ionizing radiation on the heart”, *Mutation Research/Reviews in Mutation Research*, Vol. 770, Elsevier, Amsterdam, https://doi.org/10.1016/j.mrrev.2016.07.003

Boerma, M. et al. (2015), “Space radiation and cardiovascular disease risk”, *World Journal of Cardiology*, Vol. 7/12, Baishideng Publishing Group, Pleasanton, https://doi.org/10.4330/wjc.v7.i12.882

Dorresteijn, L. D. A. et al. (2005), “Increased carotid wall thickening after radiotherapy on the neck”, *European Journal of Cancer*, Vol. 41/7, Elsevier, Amsterdam, https://doi.org/10.1016/j.ejca.2005.01.020

EPRI. (2020). *Cardiovascular Risks from Low Dose Radiation Exposure: Review and Scientific Appraisal of the Literature*

Gianicolo, M. E. et al. (2010), “Effects of external irradiation of the neck region on intima media thickness of the common carotid artery”, *Cardiovascular Ultrasound*, Vol. 8, Nature, https://doi.org/10.1186/1476-7120-8-8

Gibbons, G. H., and V. J. Dzau (1994), “The Emerging Concept of Vascular Remodeling”, *New England Journal of Medicine*, Vol. 330/20, Massachusetts Medical Society, Waltham, https://doi.org/10.1056/NEJM199405193302008.

Grabham, P. et al. (2011), “Effects of ionizing radiation on three-dimensional human vessel models: differential effects according to radiation quality and cellular development”, *Radiation Research,* Vol. 175, BioOne, https://doi.org/10.1667/RR2289.1

Grabham, P. and P. Sharma (2013), “The effects of radiation on angiogenesis”, *Vascular Cell*, Vol. 5/1, Publiverse Online S.R.L., Bucharest, https://doi.org/10.1186/2045-824X-5-19.

Hamada, N. et al. (2022), “Temporal Changes in Sparing and Enhancing Dose Protraction Effects of Ionizing Irradiation for Aortic Damage in Wild-Type Mice”, Cancers, Vol. 14/14, MDPI, Basel, https://doi.org/10.3390/cancers14143319

Hamada, N. et al. (2021), “Vascular damage in the aorta of wild-type mice exposed to ionizing radiation: Sparing and enhancing effects of dose protraction”, *Cancers*, Vol.13/21, Multidisciplinary Digital Publishing Institute, Basel, https://doi.org/10.3390/cancers13215344.

Hamada, N. et al. (2020), “Ionizing Irradiation Induces Vascular Damage in the Aorta of Wild-Type Mice”, *Cancers*, Vol. 12/10, Multidisciplinary Digital Publishing Institute, Basel, https://doi.org/10.3390/CANCERS12103030.

Hamada, N. et al. (2014), “Emerging issues in radiogenic cataracts and cardiovascular disease”, *Journal of radiation research*, Vol. 55/5, Oxford University Press. https://doi.org/10.1093/jrr/rru036

Harvey, A., A. C. Montezano and R. M. Touyz (2015), “Vascular biology of ageing—Implications in hypertension”, *Journal of Molecular and Cellular Cardiology*, Vol. 83, Elsevier, Amsterdam, https://doi.org/10.1016/j.yjmcc.2015.04.011

Hughson, R.L., A. Helm and M. Durante (2017), “Heart in space: Effect of the extraterrestrial environment on the cardiovascular system”, *Nature Reviews Cardiology*, Vol. 15/3, Nature Portfolio, London, https://doi.org/10.1038/nrcardio.2017.157.

Kessler, E. L. et al. (2019), “Sex-specific influence on cardiac structural remodeling and therapy in cardiovascular disease”, *Biology of Sex Differences*, Vol. 10/7, BioMed Central, London, https://doi.org/10.1186/s13293-019-0223-0

King, L. J. et al. (1999), “Asymptomatic carotid arterial disease in young patients following neck radiation therapy for Hodgkin lymphoma”, *Radiology*, Vol. 213/1, Radiological Society of North America, https://doi.org/10.1148/radiology.213.1.r99oc07167

Kozbenko, T. et al. (2022), “Deploying elements of scoping review methods for adverse outcome pathway development: a space travel case example”, *International Journal of Radiation Biology*, Vol. 98/12. https://doi.org/10.1080/09553002.2022.2110306

Mitchell, A. et al. (2019), “Cardiovascular effects of space radiation: implications for future human deep space exploration”, *European Journal of Preventive Cardiology*, Vol. 26/16, SAGE Publishing, Thousand Oaks, https://doi.org/10.1177/2047487319831497

North, B. J. and D. A. Sinclair (2012), “The Intersection Between Aging and Cardiovascular Disease”, *Circulation Research*, Vol. 110/8, Lippincott Williams & Wilkins, Philadelphia, https://doi.org/10.1161/CIRCRESAHA.111.246876

Patel, S. (2020), “The effects of microgravity and space radiation on cardiovascular health: From low-Earth orbit and beyond”, *IJC Heart and Vasculature,* Vol. 30, Elsevier, Amsterdam, https://doi.org/10.1016/j.ijcha.2020.100595.

Pereira, T., C. Correia and J. Cardoso (2015), “Novel Methods for Pulse Wave Velocity Measurement”, *Journal of Medical and Biological Engineering*, Vol. 35/5, Springer, New York, https://doi.org/10.1007/s40846-015-0086-8.

Poznyak, A. V. et al. (2021), “Overview of OxLDL and Its Impact on Cardiovascular Health: Focus on Atherosclerosis”, *Frontiers in Pharmacology*, Vol. 11, Frontiers, https://doi.org/10.3389/fphar.2020.613780

Russel et al., (2009), “Novel insights into pathological changes in muscular arteries of radiotherapy patients”, *Radiotherapy and Oncology*, Vol. 92, Elsevier, Amsterdam, https://doi.org/10.1016/j.radonc.2009.05.021

Sárközy, M. et al. (2019), “Selective heart irradiation induces cardiac overexpression of the pro-hypertrophic miR-212”, *Frontiers in Oncology,* Vol. 9, Frontiers Media SA, Lausanne, https://doi.org/10.3389/fonc.2019.00598

Shen, Y. et al. (2018), “Transplantation of bone marrow mesenchymal stem cells prevents radiation-induced artery injury by suppressing oxidative stress and inflammation”, *Oxidative Medicine and Cellular Longevity*, Vol. 2018, Hindawi, London, https://doi.org/10.1155/2018/5942916.

Schmidt-Ullrich, R. K. et al. (2000), “Signal Transduction and Cellular Radiation Responses”, *Radiation Research*, Vol. 153, Radiation Research Society, Bozeman, https://doi.org/10.1667/0033-7587(2000)153[0245:STACRR]2.0.CO;2

Slezak, J. et al. (2017), “Potential markers and metabolic processes involved in the mechanism of radiation-induced heart injury”, *Canadian journal of physiology and pharmacology*, Vol. 95/10, Canadian Science Publishing, Ottawa, https://doi.org/10.1139/cjpp-2017-0121

Soloviev, A. I. and I.V. Kizub (2019), “Mechanisms of vascular dysfunction evoked by ionizing radiation and possible targets for its pharmacological correction”, *Biochemical pharmacology*, Vol. 159, Elsevier, Amsterdam, https://doi.org/10.1016/j.bcp.2018.11.019

Soucy, K. G. et al. (2011), “HZE 56Fe-Ion Irradiation Induces Endothelial Dysfunction in Rat Aorta: Role of Xanthine Oxidase”, *Radiation Research*, Vol. 176/4, Radiation Research Society, Bozeman, https://doi.org/10.1667/RR2598.1

Soucy, K. G. et al. (2010), “Dietary inhibition of xanthine oxidase attenuates radiation-induced endothelial dysfunction in rat aorta”, *Journal of Applied Physiology*, Vol. 108/5, American Physiological Society, Rockville, https://doi.org/10.1152/japplphysiol.00946.2009

Soucy, K. G. et al. (2007), “Single exposure gamma-irradiation amplifies xanthine oxidase activity and induces endothelial dysfunction in rat aorta”, *Radiation and Environmental Biophysics*, Vol. 46/2, Springer, New York, https://doi.org/10.1007/s00411-006-0090-z.

Sridharan, V. et al. (2020), “Effects of single-dose protons or oxygen ions on function and structure of the cardiovascular system in male Long Evans rats”, *Life Sciences in Space Research*, Vol. 26, Elsevier, Amsterdam, https://doi.org/10.1016/j.lssr.2020.04.002

Sylvester, C. B. et al. (2018), “Radiation-induced Cardiovascular Disease: Mechanisms and importance of Linear energy Transfer”, *Frontiers in Cardiovascular Medicine*, Vol. 5, Frontiers Media SA, Lausanne, https://doi.org/10.3389/fcvm.2018.00005.

Tapio, S. (2016), “Pathology and biology of radiation-induced cardiac disease”, *Journal of Radiation Research*, Vol. 57/5, Oxford University Press, Oxford, https://doi.org/10.1093/jrr/rrw064.

Ungvari, Z. et al. (2018), “Mechanisms of Vascular Aging”, *Circulation Research*, Vol. 123/7, Lippincott Williams & Wilkins, Philadelphia, https://doi.org/10.1161/CIRCRESAHA.118.31137

Winham, S. J., M. de Andrade and V. M. Miller (2015), “Genetics of cardiovascular disease: Importance of sex and ethnicity”, *Atherosclerosis,* Vol. 241/1, Elsevier, Amsterdam, https://doi.org/10.1016/j.atherosclerosis.2015.03.021

Yu, T. et al. (2011), “Iron-ion radiation accelerates atherosclerosis in apolipoprotein E-Deficient mice”, *Radiation Research*, Vol. 175/6, Radiation Research Society, Bozeman, https://doi.org/10.1667/RR2482.1.

Zieman, S. J., V. Melenovsky and D. A. Kass (2005), “Mechanisms, Pathophysiology, and Therapy of Arterial Stiffness”, *Arteriosclerosis, Thrombosis, and Vascular Biology*, Vol. 25/5, Lippincott Williams & Wilkins, Philadelphia, https://doi.org/10.1161/01.ATV.0000160548.78317.29

Relationship: 2776: Oxidative Stress leads to Increase, Endothelial Dysfunction

AOPs Referencing Relationship

AOP Name	Adjacency	Weight of Evidence	Quantitative Understanding
Deposition of energy leads to vascular remodeling	non-adjacent	Moderate	Low

Evidence Supporting Applicability of this Relationship

Taxonomic Applicability

Term	Scientific Term	Evidence	Links
human	Homo sapiens	Low	NCBI
mouse	Mus musculus	Moderate	NCBI
rat	Rattus norvegicus	High	NCBI
pigs	Sus scrofa	Low	NCBI

Life Stage Applicability

Life Stage	Evidence
Adult	Moderate
Not Otherwise Specified	Low

Sex Applicability

Sex	Evidence
Male	High
Female	Low
Unspecific	Low

The evidence is derived from rat *in vivo* and *in vitro* models. Mice cell-derived studies were also available but less *in-vivo* evidence was available from this species. There was a low number of studies containing human or pig models to support this KER. Males have been studied more often than females. There are a few studies with unspecified lifestage of models, while the studies with a defined age typically used adult models.

Key Event Relationship Description

Oxidative stress describes the imbalances in reactive oxygen and reactive nitrogen species (RONS) radical formation as well as antioxidants and reactive oxygen species (ROS) scavengers (Beckhauser et al., 2016; Elahi et al., 2009; Ray et al., 2012). Oxidative stress can lead to endothelial dysfunction. Within the cardiovascular system, every vessel is lined with a single layer of endothelial cells (Augustin et al., 1994; Fishman, 1982). This endothelial layer plays a crucial role in the regulation of vascular homeostasis through controlling various factors such as vascular permeability, vasomotion, and immune response (Baran et al., 2021; Bonetti et al., 2003; Hughson et al., 2018; Slezak et al., 2017; Sylvester et al., 2018). Of the vascular wall components, the endothelium is also the most vulnerable to damage from ROS (Soloviev & Kizub, 2018). Endothelial cells normally exist in a quiescent state characterized by high nitric oxide (NO) bioavailability (Carmeliet & Jain, 2011); however, cells can become activated as part of a normal host-defence response following tissue injury or oxidative stress (Deanfield et al., 2007; Krüger-Genge et al., 2019). Sustained activation leads to the pathological state of endothelial dysfunction which is defined by decreased NO bioavailability, increased vessel permeability, altered vasomotion, and a pro-thrombotic and inflammatory environment (Baran et al., 2021; Bonetti et al., 2003; Deanfield et al., 2007; Schiffrin, 2008).

Shifting redox balance towards oxidation is known to indirectly lead to endothelial dysfunction through various mechanisms (Hughson et al., 2018; Ramadan et al., 2020; Soloviev & Kizub, 2018). There are several ways through which imbalanced ROS can affect endothelium function, including decreasing NO bioavailability through direct scavenging, which forms the RNS peroxynitrite ($ONOO^-$) (Hatoum et al., 2006; Li et al., 2002; Schiffrin, 2008; Soloviev & Kizub, 2018; Venkatesulu et al., 2018), as well as impeding NO production and diffusion (Hatoum et al., 2006; Li et al., 2002; Schiffrin, 2008; Soloviev & Kizub, 2018; Venkatesulu et al., 2018; Schiffrin, 2008; Soloviev & Kizub, 2018). Additionally, elevated ROS contribute to introducing a pro-inflammatory and pro-thrombotic milieu characteristic of dysfunction (Hughson et al., 2018; Schiffrin, 2008; Slezak et al., 2017; Tapio, 2016; Venkatesulu et al., 2018). It is also linked to decreased vasomotion (Schiffrin, 2008; Soloviev & Kizub, 2018; Venkatesulu et al., 2018) and finally the onset of endothelial cell apoptosis and premature senescence (Borghini et al., 2013; Hughson et al., 2018; Tapio, 2016; Wang et al., 2016).

Evidence Supporting this KER

Overall weight of evidence: Moderate

Biological Plausibility

Mechanisms for oxidative stress leading to endothelial dysfunction are outlined in various reviews on the topic (Hughson et al., 2018; Nagane et al., 2021; Slezak et al., 2017; Soloviev & Kizub, 2018; Venkatesulu et al., 2018; Wang et al., 2016).

Elevated ROS can indirectly lead to endothelial dysfunction by causing an imbalance of NO, specifically the decrease in NO bioavailability. Firstly, ROS can react with NO directly; if quenching outpaces NO production, it will cause reduced NO bioavailability underlying endothelial dysfunction (Hatoum et al., 2006; Li et al., 2002; Soloviev & Kizub, 2018). In particular, the superoxide anion ($\bullet O^-_2$) reacts with NO to form peroxynitrite, both reducing available NO and further accelerating NO degradation (Li et al., 2002;

Soloviev & Kizub, 2018). In addition, superoxide and peroxynitrite can uncouple eNOS which produces more ROS instead of NO (Soloviev & Kizub, 2018). Peroxynitrite can cause cellular senescence as a part of endothelial dysfunction (Nagane et al., 2021). eNOS downregulation and subsequent drop in NO levels are caused in part by increased endothelin-1 (ET-1), a vasoconstrictor with enhanced secretion during an oxidative stress state (Marasciulo, Montagnani & Potenza, 2006; Ramadan et al., 2020). ROS is also involved in perturbing NO diffusion from the endothelial cells (Soloviev & Kizub, 2018). Overall, the decreased NO bioavailability causes reduced vasodilation and endothelial dysfunction (Soloviev & Kizub, 2018).

Oxidative stress also affects endothelial function through inhibition of endothelium-dependent vasodilation (Soloviev & Kizub, 2018; Venkatesulu et al., 2018). ROS in both endothelial cells and surrounding vascular smooth muscle cells (VSMCs) act as second messengers to many cellular pathways that mediate VSMC contractility and endothelial permeability and function, causing disruption to these endothelial functions (Hughson et al., 2018; Li et al., 2002; Ramadan et al., 2020; Soloviev & Kizub, 2018; Ungvari et al., 2013; Venkatesulu et al., 2018). Specifically, impaired endothelium-dependent vasomotion following radiation (Venkatesulu et al., 2018) was suggested to be due to the loss of PGF2α inhibition and therefore, vasoconstriction (Li et al., 2002).

Oxidative stress is also involved in inducing the pro-thrombotic and inflammatory environment of endothelial dysfunction. In the case of radiation induced endothelial injury, radiation type, fraction size used, and endothelial cell model used all influence the resulting downstream endpoints (Venkatesulu et al., 2018). Possible changes to the endothelial milieu include alterations of cell adhesion molecule levels, creation of pro-thrombotic environment, endothelial cell apoptosis and inflammation (Hughson et al., 2018; Nagane et al., 2021; Slezak et al., 2017; Tapio, 2016; Venkatesulu et al., 2018). When induced by oxidative stress, nuclear factor kappa B (NF-κB) can target genes involved with the upregulation of prothrombotic markers associated with endothelial dysfunction (Slezak et al., 2017). Free radicals produced by macrophages have also been shown to stimulate TGF-β, thus accelerating the creation of a profibrotic milieu (Venkatesulu et al., 2018). ROS can also oxidize low-density lipoproteins (LDL) resulting in structural complications as oxidized LDL accumulates in blood circulation due to decreased cell uptake (Nagane et al., 2021; Slezak et al., 2017). Furthermore, endothelial cells can undergo morphological changes following oxidative injury, as the cells become enlarged, and form fibrin networks, showing increased levels of activated platelets and leukocytes with membrane protrusions and pseudopodial extensions, which are all indicative of an inflammatory and pro-thrombotic state (Li et al., 2002).

Furthermore, ROS can induce premature endothelial cell senescence, which in turn contributes to overall endothelial dysfunction (Hughson et al., 2018; Nagane et al., 2021; Tapio, 2016). In contrast to replicative senescence attributed to telomere dysfunction, oxidative stress is one of several injuries causing stress-induced premature senescence (Nagane et al., 2021). This is thought to occur through oxidative stress causing the induction of the p53/p21 pathway which regulates cell senescence (Borghini et al., 2013; Wang et al., 2016). Once senescent, the endothelial cells contribute to dysfunction in multiple ways. Firstly, senescence can stimulate a pro-inflammatory response and trigger apoptosis through decreased cell repair (Nagane et al., 2021; Ramadan et al., 2020). Additionally, senescent cells themselves are sources of ROS, furthering both genomic instability causing additional senescence in neighbouring cells and endothelial dysfunction itself (Tapio, 2016; Wang et al., 2016). Senescent cells also lack proper endothelial cell function, contributing to changing the environment to a dysfunctional one (Hughson et al., 2018; Tapio, 2016). This lack of function includes a decrease in NO production, increased monocyte adhesion, and loss of cell barrier integrity paired with increased levels of ET-1 (Hughson et al., 2018; Nagane et al., 2021; Tapio, 2016).

Finally, oxidative stress has been shown to lead to mitochondrial dysfunction and dysregulation, which is thought to play an important role in the development of endothelial dysfunction (Borghini et al., 2013; Hughson et al., 2018; Nagane et al., 2021; Slezak et al., 2017).

Empirical Evidence

Empirical evidence provides a moderate level of support to this KER. Examples of this evidence are summarized here and further in attached tables.The evidence to support the relationship between oxidative stress leading to endothelial dysfunction was gathered from studies using *in vitro* and *in vivo* rat and mice models (Delp et al., 2016; Hatoum et al., 2006; Shen et al., 2018; Soucy et al., 2007; Soucy et al., 2010; Soucy et al., 2011; Ungvari et al., 2013), *in vivo* pig models (Li et al., 2002) and human *in vitro* cells (Ramadan et al., 2020). Various stressors were applied, including X-rays, hindlimb unloading (HU), heavy ions (^{56}Fe ions and ^{32}P) and gamma rays with a dose range of 0.1 to 22.5 Gy. To determine the effect of oxidative stress on endothelial dysfunction, various assays and end-points were measured. Senescence-associated β-galactosidase (SA -gal), insulin-like growth factor-binding protein-7 (IGFBP-7) and growth differentiation factor 15 (GDF-15) as senescence markers, caspase 3/7 activity as an apoptosis marker, endothelin-1 levels for the ratio of apoptotic to normal cells, 4-hydroxynonenal (4-HNE) and 3-nitrotyrosine (3-NT) as aortic oxidative damage markers, superoxide production, vascular tension, and ROS detection via xanthine oxidase (XO) activity, and fluorescent dyes, such as dihydroethidium fluorescence were all used as end-point measures.

Dose Concordance

Dose concordance between the two key events is supported by numerous studies. Hatoum et al. (2006) explored the effect of 3 to 9 cumulative X-ray doses of 0.25 Gy on murine intestinal arterioles. The study found that superoxide and hydrogen peroxide generation was increased, while at the same doses vasodilation in response to acetylcholine (ACh) was decreased (Hatoum et al., 2006). Another study using various doses on cerebral microvascular endothelial cells found a significant change in cellular peroxide and mitochondrial oxidative stress following the 4 Gy dose, while SA β-gal showed the first large increase at 4 Gy (Ungvari et al., 2013).

Ramadan et al. (2020) used X-ray irradiation in multiple types of human endothelial cells has shown that ROS production is significantly higher in both the 0.1 Gy and 5 Gy compared to the control. These changes were correlated to endothelial dysfunction as SA β-gal activity and endothelial apoptosis were also affected, showing a response of greater magnitude following the 5 Gy dose compared to 0.1 Gy (Ramadan et al., 2020).

Exposure of mice to 18 Gy X-rays led to a ~1.8-fold and ~2.2-fold decrease in 4-HNE and 3-NT respectively, both being markers of aortic oxidative damage. Simultaneously, the 18 Gy dose caused a ~5-fold increase in aortic apoptosis, a marker of endothelial dysfunction (Shen et al., 2018). Two studies (Soucy et al., 2007; Soucy et al., 2010) found that varying doses (0.5 and 5 Gy) of gamma radiation led to significant increases in ROS levels in rat aorta. Subsequently, endothelial function was affected with a 0.5 Gy dose resulting in a ~30% decrease in ACh-induced vasodilation response (Soucy et al., 2007), and a 5 Gy dose leading to a ~13-15% decrease in ACh-induced vasodilation (Soucy et al., 2010).

Iron ion irradiation resulted in oxidative stress and endothelial dysfunction both occurring after 1 Gy (Soucy et al., 2011). Similarly, Delp et al. (2016) showed total body ^{56}Fe irradiation at 1 Gy led to a ~2-fold increase in XO activity and a ~10% decrease in ACh response in mice (Delp et al., 2016). Delp et al. (2016) also explored the effects of HU on mice and found no significant changes to XO activity or ACh response following 2-week HU, while HU in combination with 1 Gy ^{56}Fe radiation led to a ~2.2-fold increase in XO activity and the same ~10% decrease in ACh response. Li et al. (2002) showed ~3.5-fold increase in superoxide anion production and a ~25-80% decrease in vasoconstriction and vasodilation response to various vasomotive substances following 20 Gy ^{32}P radiation in pig coronary arteries.

Time Concordance

There is some evidence of time concordance between oxidative stress and endothelial dysfunction. Ramadan et al. (2020) used human endothelial cells and showed ROS production first increased 45 minutes after 5 Gy X-ray exposure before returning to baseline levels after 2 hours. Apoptosis markers Annexin V and Caspase 3/7 were first increased after 4 hours. Cellular senescence evaluated with the SA-β-gal activity was first measured only after 7 days (Ramadan et al., 2020). ROS production and dilation response to ACh after irradiation were measured at various times as cumulative doses were given, which showed increased ROS and decreased dilation of rat intestinal microvessels both after 5 days of cumulative 0.25 Gy X-ray doses (Hatoum et al., 2006). Work using 4-HNE and 3-NT as biomarkers of oxidative stress in mice aorta following 18 Gy 6MV X-ray at 3, 7, 14, 28, and 84 days after irradiation showed both markers to be significantly elevated starting after 3 days. Exposure also led to significantly increased apoptosis, indicating endothelial dysfunction after 3 days (Shen et al., 2018).

Incidence Concordance

There is moderate support in current literature for an incidence concordance relationship between oxidative stress and endothelial dysfunction. Three of the primary research studies used to support this AOP demonstrated an average change to endpoints of oxidative stress that was greater or equal to that of endothelial dysfunction (Soucy et al., 2011; Soucy et al., 2010; Soucy et al., 2007).

Essentiality

Essentiality in the relationship was demonstrated in the following studies. Studies by Soucy et al. (2007, 2010, 2011) explored the relationship between radiation exposure, ROS levels and endothelial function, all focusing on the role of XO. Soucy et al. (2007) incubated aortic rings from irradiated rats in the XO inhibitor oxypurinol (Oxp) and saw this treatment result in recovery of ACh vasodilation response. Soucy et al. (2010) showed that administration of allopurinol (a superoxide scavenger) following irradiation led to significantly decreased ROS levels. Additionally, the latter two studies showed that XO inhibition by dietary administration of Oxp significantly decreased XO activity and ROS levels while simultaneously recovering ACh response (Soucy et al., 2010, 2011). Similar results were observed when treatment with manganese tetrakis (4-benzoic acid) porphyrin chloride (MnTBAP), a SOD mimetic, returned peroxide and superoxide levels and significantly improved ACh response irradiated rats (Hatoum et al., 2006). Dietary treatment with Tempol, a water-soluble SOD-mimetic likewise increased vasomotion and decreased superoxide levels (Hatoum et al., 2006).

Human bone marrow mesenchymal stem cells (hBMSCs) have also been studied for their ability to prevent radiation-induced aortic injury. Both high and low doses of hBMSCs were shown to increase catalase and heme oxygenase 1 (HO-1) antioxidant activity, and decrease levels of the aortic oxidative damage markers 4-HNE and 3-NT. Subsequently, this treatment also significantly decreased levels of apoptosis in the aorta (Shen et al., 2018). Finally, blocking Connexin43 hemichannels using TAT-Gap19 peptide also significantly reduced oxidative stress and resultant cell senescence and death, suggesting the role of intracellular communication in mediating radiation response (Ramadan et al., 2020).

Studies have also shown that transgenic mice overexpressing superoxide dismutase (SOD) have a twofold reduction in aortic lesions following X-ray exposure compared to control (Hughson et al., 2018). Overexpression of SOD also mitigates atherosclerotic plaque formation, further outlining the relationship between oxidative stress and the pathological environment of endothelial dysfunction (Tapio, 2016).

Uncertainties and Inconsistencies

Work by Ramadan et al. (2020) explored the use of TAT-Gap19 to block endothelial intracellular communication in order to modulate radiation response of intercellular connexin proteins. Overall, TAT-Gap19 was shown to reduce ROS production and subsequent senescence (SA β-gal activity) and apoptosis (Annexin V and Caspase 3/7) markers. However, treatment with TAT-Gap19 led to an increase in SA β-gal in non-irradiated control at the 9-day point. Additionally, the 0.1 Gy irradiated group showed persistent SA β-gal activity at all time points studied, while the 5 Gy group demonstrated an unexpected decrease before day 14.

Quantitative Understanding of the Linkage

The following are a few examples of quantitative understanding of the relationship. All data that is represented is statistically significant unless otherwise indicated.

Response-response relationship

Dose/incidence concordance

Reference	Experiment Description	Result
Soucy et al. 2007	*In vivo*. Sprague-Dawley rats were whole-body irradiated with ^{137}Cs gamma radiation at 50, 160 and 500 cGy. XO is a primary source of cardiac ROS and was used as a measure of oxidative stress. Vasodilation response to ACh was used to evaluate endothelial function.	At 500 cGy, XO activity was found to be 2-fold elevated compared to control, and there was also an increase in XO quantity. Simultaneously, there was endothelial dysfunction as seen with a ~30 percentage point decrease in vasodilation response to ACh.
Soucy et al. 2010	*In vivo*. In Sprague-Dawley rats were whole-body irradiated with ^{137}Cs gamma radiation at 5 Gy. ROS were measured using dihydroethidium fluorescence. Aortic relaxation response to ACh was also measured.	After 5 Gy, ROS increased 1.7-fold and relaxation decreased 0.7-fold.
Soucy et al. 2011	*In vivo*. Wistar rats were exposed to 0.5 and 1 Gy doses of ^{56}Fe-ion radiation. ROS production rates were evaluated using dihydroethidium fluorescence. ACh-induced vasodilation responses were measured.	^{56}Fe irradiation at 1 Gy produced a 1.8-fold increase in ROS levels. At 10^{-5} M ACh, aorta without irradiation relaxed by 87%, while aorta with 1 Gy irradiation had significantly lower relaxation of 76%.
Li et al. 2002	*In vivo*. Surgically exposed coronary arteries of yucatan pigs were irradiated with 20 Gy ^{32}P β-irradiation. Oxidative stress was evaluated through superoxide production. Endothelial function was evaluated through endothelial-dependent vasomotor response and morphological changes.	Superoxide production increased 3.5-fold between the control and 20 Gy irradiated groups. Contractile response to KCl dropped over 50% in the irradiated group. Morphological changes were also observed, with irradiated arteries seeing enlarged endothelial cells, formation of fibrin networks, activated platelets, leukocytes exhibiting membrane protrusions and pseudopodial extensions all indicative of an inflammatory and pro-thrombotic state of endothelial dysfunction.
Shen et al. 2018	*In vivo*. Male mice were irradiated with 18 Gy X-rays. Oxidative stress was measured with 4-HNE and 3-NE oxidative damage markers and antioxidant enzymes catalase and HO-1, measured by immunohistological	4-HNE showed a maximum increase of ~1.8-fold, and 3-NT showed a maximum increase of ~2.2-fold. Apoptosis levels peaked at a ~5-fold increase above control levels.

	staining. Endothelial dysfunction was determined through apoptosis.	
Ramadan et al. 2020	*In vitro*. Telomerase-immortalized human Coronary Artery and Microvascular Endothelial cells (TICAE) and Telomerase Immortalized human Microvascular Endothelial cells (TIME) were exposed to X-rays (0.1 and 5 Gy). ROS production was measured using CM-H2DCFDA combined with Incucyte live cell imaging. Endothelial dysfunction was evaluated through: endothelial apoptosis • Annexin V and Caspase 3/7 marker levels • Dextran fluorescein dye uptake level by necrotic cells cell senescence • SA β-gal activity • IGFBP-7 and GDF-15 senescence marker levels	ROS production was increased in TIME cells after 0.1 and 5 Gy dose. In both coronary and endothelial cells, apoptosis mainly occurred after 5 Gy radiation. With coronary cells demonstrating an increase in Annexin V and Caspase 3/7 markers and endothelial cells showing elevated Annexin V and membrane leakage. SA β-gal activity significantly increased for both 0.1 and 5 Gy doses. IGFBP-7 and GDF-15 levels were also elevated in both cell types; GDF-15 increasing at both 0.1 and 5 Gy doses, while IGFBP-7 only showed significant elevation at the 5 Gy dose. With the 0.1 Gy dose, there was a significant increase in SA β-gal activity of ~3-fold, while at 5 Gy the activity increased ~5-fold. Endothelin-1 was found to be significantly elevated following 5 Gy irradiation in both cell types.
Ungvari et al. 2013	*In vitro*. Cerebral microvascular endothelial cells (CMVECs) from F344×BN rats were harvested and cultured. Following culture, cells were irradiated with ^{137}Cs gamma radiation in doses between 2-8 Gy. Oxidative stress was evaluated through cellular peroxide and superoxide production. Endothelial dysfunction was evaluated through cell senescence via SA-β-gal presence, and apoptosis via caspase 3/7 maker and ratio of apoptotic:viable cells.	Oxidative stress increased in a dose-dependent manner following irradiation. Change of ROS became significant after 4 Gy at a ~1.5-fold increase and reached ~3-fold increase at the highest studied dose of 8 Gy. Mitochondrial oxidative stress also became significant after 4 Gy and increased linearly for a peak of a ~1.5-fold increase at 8 Gy. Endothelial cell senescence and apoptosis were similarly found to increase in a dose dependent manner. With ~30% of cells being SA-β-gal positive after 8 Gy irradiation, signalling premature senescence. Ratio of dead cells peaked at 10% and Caspase 3/7 peaking at a ~5.5-fold change following 18h post irradiation.
Hatoum et al. 2006	*In vivo*. Effect of cumulative	After the final cumulative dose of

	radiation doses on rat gut microvessels was studied. Rats were exposed to 1 to 9 fractions of 250 cGy for a total dose of up to 2250 cGy. Following exposure, the animals were euthanized, and submucosal vessels isolated. Oxidative stress was measured through superoxide and peroxide levels. Endothelial function was assessed through ACh vasodilation response.	2250 cGy, superoxide was ~1.6-fold elevated and peroxides were ~1.7-fold elevated compared to non-irradiated controls. ROS levels increased sharply after the second dose, immediately preceding drop in ACh vasodilation response. Max dilation dropped from 87% to 3% between pre-irradiation and post-final radiation dose. ACh response remained within control levels following fractions 1 and 2, however following fraction 3, response dropped below 30% for all remaining doses.
Delp et al. 2016	*In vivo*. The effects of HU and 1 Gy dose of ^{56}Fe radiation of the gastrocnemius muscle feed arteries and coronary arteries of C57BL/6 mice was studied. Xanthine oxidase (XO) levels were used as a measure of ROS production and therefore oxidative stress. Endothelial function was evaluated through vasodilation response to ACh.	Following 2-week HU, there were no significant changes to XO levels or vasomotor response. Following total body irradiation with 1 Gy, there was a ~2-fold increase in XO activity in both gastrocnemius muscle feed and coronary arteries. Vasodilation response subsequently decreased ~10 percentage points. Combined HU and total body irradiation led to a ~2.2-fold increase in XO activity in both artery types and vasodilation response decrease of ~10 percentage points.

Time-scale

Time concordance

Reference	Experiment Description	Result
Soucy et al. 2007	*In vivo*. Sprague-Dawley rats were whole-body irradiated with ^{137}Cs gamma radiation at various doses. 2 weeks after irradiation, the animals were euthanized, and aortas were harvested. XO was used as a measure of oxidative stress. Dose-dependent vasodilation response to ACh was used to evaluate endothelial function.	XO activity was elevated 2-fold compared to control, and there was also an increase in XO quantity. Simultaneously, endothelial dysfunction was seen with a ~30% decrease in vasodilation response to ACh.
Soucy et al. 2010	*In vitro*. Sprague-Dawley rats were whole-body irradiated with ^{137}Cs gamma radiation. 2 weeks after receiving radiation dose, the animals were euthanized and aortas were harvested. ROS were measured using dihydroethidium fluorescence. Aortic relaxation response to ACh was also measured.	ROS increased 1.7-fold and relaxation simultaneously decreased 0.7-fold.
Soucy et al. 2011	*In vivo*. Wistar rats were exposed to ^{56}Fe-ion radiation. Rats were euthanized at 4 months post-irradiation and aorta was harvested. ROS production rates evaluated using dihydroethidium along the ACh-induced vasodilation response were measured.	ROS levels increased by 75% 4 months post-irradiation. ACh vasodilation response decreased by 13%.
		Exposure to 18 Gy caused increased 4-HNE and 3-

Shen et al. 2018	*In vivo*. Male mice were irradiated with 18 Gy X-rays. Immunohistochemical staining assessed oxidative stress using 4-HNE and 3-NE as markers for oxidative damage. Endothelial dysfunction was determined through apoptosis.	NT levels. 4-HNE showed a maximum ~1.8-fold increase at 14-days post radiation, and 3-NT showed a maximum ~2.3-fold increase 7 days post radiation. Apoptosis levels peaked at 7 days post-irradiation with a ~5-fold increase above control levels.
Ramadan et al. 2020	*In vitro*. TICAE and TIME cells were exposed to X-rays (0.1 and 5 Gy). Oxidative stress was evaluated through intracellular ROS production. Endothelial dysfunction was evaluated through: endothelial apoptosis • Annexin V and Caspase 3/7 marker levels • Dextran fluorescein dye uptake level by necrotic cells cell senescence • SA β-gal activity • IGFBP-7 and GDF-15 senescence marker levels Endothelin-1 levels	Highest response was observed for both doses at 45 minutes after irradiation followed by a decline at the 2- and 3-hour time points but remaining elevated above non-irradiated control levels. Endothelial cells studied produced more ROS than the coronary cells. Caspase 3/7 and annexin V increased linearly until 100h. SA β-gal activity significantly increased at 7 and 9 days. GDF-15 and IGFBP-7 were increased after 7 days. Endothelin-1 was found to be significantly elevated after 7 days.
Ungvari et al. 2013	*In vitro*. Cerebral microvascular endothelial cells (CMVECs) from F344×BN rats were harvested and cultured. Following culture, cells were irradiated with ^{137}Cs gamma radiation. Oxidative stress was evaluated through cellular peroxide and superoxide production. Endothelial dysfunction was evaluated through cell senescence via SA-β-gal presence, and apoptosis via caspase 3/7 maker and ratio of apoptotic:viable cells.	Superoxide and peroxide increased 1 day but not 14 days post-irradiation ~30% of cells were SA-β-gal positive after 8 Gy irradiation, measured 7 days post-irradiation. 24 h after irradiation, 10% of cells were dead. Caspase 3/7 increased from 2 to 18 h, peaking at a ~5.5-fold change following 18 h post-irradiation but decreased at 24 h.
Hatoum et al. 2006	*In vivo*. Effect of cumulative radiation doses on rat gut microvessels was studied. Rats were exposed to 1 to 9 cGy in 3 fractions per week on alternate days for 3 successive weeks for a total dose of up to 2250 cGy over a total time of 19 days. Oxidative stress was measured through superoxide and peroxide levels from various fluorescent markers. Endothelial function was assessed through ACh vasodilation response.	After 19 days, superoxide was ~1.6-fold elevated and peroxides were ~1.7-fold elevated compared to non-irradiated controls. ROS levels increased at day 5, at the same time as a drop in ACh vasodilation response. Max dilation dropped from 87% to 3% between day 1 and day 19.

Known modulating factors

Modulating factor	Details	Effects on the KER	References
Drug	MnTBAP (a superoxide dismutase mimetic)	Treatment with MnTBAP after irradiation was able to reduce superoxide and peroxide levels and restore vasodilation ability	(Hatoum et al., 2006)
Drug	Tempol (a superoxide dismutase mimetic)	Treatment with tempol after	(Hatoum et al., 2006)

		irradiation was able to restore vasodilation ability	
Drug	TAT-Gap19 (inhibitor of connexin 43 which is associated with atherogenesis and endothelial stiffness)	Treatment with TAT-Gap19 led to a decrease in ROS and SA β-gal levels after irradiation	(Ramadan et al., 2020)
Drug	hBMSCs (protect against vascular damage through antioxidant properties)	Treatment with hBMSCs after irradiation caused increased catalase and HO-1, as well as decreased oxidative damage and apoptosis	(Shen et al., 2018)
Drug	Oxp (can inhibit XO, a source of ROS)	Treatment with Oxp showed decreased XO activity and ROS production along with increased vasodilation after irradiation	(Soucy et al., 2007; Soucy et al., 2010; Soucy et al., 2011)

References

References

Augustin, H. G., D. H. Kozian and R. C. Johnson (1994), “Differentiation of endothelial cells: Analysis of the constitutive and activated endothelial cell phenotypes”, *BioEssays*, Vol. 16/12, Wiley, Hoboken, https://doi.org/10.1002/bies.950161208.

Baran, R. et al. (2021), “The Cardiovascular System in Space: Focus on In Vivo and In Vitro Studies”, *Biomedicines*, Vol. 10/1, Multidisciplinary Digital Publishing Institute, Basel, https://doi.org/10.3390/biomedicines10010059.

Beckhauser, T. F., J. Francis-Oliveira and R. De Pasquale (2016), “Reactive Oxygen Species: Physiological and Physiopathological Effects on Synaptic Plasticity”, *Journal of Experimental Neuroscience*, Vol. 10, SAGE Publishing, Thousand Oaks, https://doi.org/10.4137/JEN.S39887.

Bonetti, P. O., L. O. Lerman and A. Lerman (2003), “Endothelial Dysfunction: a marker of atherosclerotic risk”, *Arteriosclerosis, Thrombosis, and Vascular Biology*, Vol. 23/2, Lippincott Williams & Wilkins, Philadelphia, https://doi.org/10.1161/01.ATV.0000051384.43104.FC.

Borghini, A. et al. (2013), “Ionizing radiation and atherosclerosis: Current knowledge and future challenges”, *Atherosclerosis*, Vol. 230/1, Elsevier, Amsterdam, https://doi.org/10.1016/j.atherosclerosis.2013.06.010.

Carmeliet, P., and R. K. Jain. (2011), “Molecular mechanisms and clinical applications of angiogenesis”, *Nature*, Vol. 473/7347, Nature Portfolio, London, https://doi.org/10.1038/nature10144.

Deanfield, J. E., J. P. Halcox and T. J. Rabelink (2007), “Endothelial Function and Dysfunction”, *Circulation*, Vol. 115/10, Lippincott Williams & Wilkins, Philadelphia, https://doi.org/10.1161/CIRCULATIONAHA.106.652859.

Delp, M. D. et al. (2016), “Apollo Lunar Astronauts Show Higher Cardiovascular Disease Mortality: Possible Deep Space Radiation Effects on the Vascular Endothelium”, *Scientific Reports*, Vol. 316/23, Nature Portfolio, London, https://doi.org/10.1038/SREP29901.

Elahi, M. M., Y. X. Kong and B. M. Matata (2009), “Oxidative Stress as a Mediator of Cardiovascular Disease”, *Oxidative Medicine and Cellular Longevity*, Vol. 2/5, Hindawi, London, https://doi.org/10.4161/oxim.2.5.9441.

Fishman, A. P. (1982), “ENDOTHELIUM: A DISTRIBUTED ORGAN OF DIVERSE CAPABILITIES”, *Annals of the New York Academy of Sciences*, Vol. 401/1, Wiley-Blackwell, Hoboken, https://doi.org/10.1111/j.1749-6632.1982.tb25702.x.

Hatoum, O. A. et al. (2006), “Radiation Induces Endothelial Dysfunction in Murine Intestinal Arterioles via Enhanced Production of Reactive Oxygen Species”, *Arteriosclerosis, Thrombosis, and Vascular Biology*, Vol. 26/2, Lippincott Williams & Wilkins, Philadelphia, https://doi.org/10.1161/01.ATV.0000198399.40584.8c.

Hughson, R.L., A. Helm and M. Durante (2018), “Heart in space: Effect of the extraterrestrial environment on the cardiovascular system”, *Nature Reviews Cardiology*, Vol. 15/3, Nature Portfolio, London, https://doi.org/10.1038/nrcardio.2017.157.

Kozbenko, T. et al. (2022), “Deploying elements of scoping review methods for adverse outcome pathway development: a space travel case example”, *International Journal of Radiation Biology*, Vol. 98/12.

https://doi.org/10.1080/09553002.2022.2110306

Krüger-Genge, A. et al. (2019), “Vascular Endothelial Cell Biology: An Update”, *International Journal of Molecular Sciences*, Vol. 20/18, Multidisciplinary Digital Publishing Institute, Basel, https://doi.org/10.3390/IJMS20184411.

Li, J. et al. (2002), “Endovascular irradiation impairs vascular functional responses in noninjured pig coronary arteries”, *Cardiovascular Radiation Medicine*, Vol. 3/3–4, Elsevier, Amsterdam, https://doi.org/10.1016/S1522-1865(03)00096-9.

Marasciulo, F., M. Montagnani and M. Potenza (2006), “Endothelin-1: The Yin and Yang on Vascular Function”, *Current Medicinal Chemistry*, Vol. 13/14, Bentham Science Publishers, Sharjah, https://doi.org/10.2174/092986706777441968.

Nagane, M. et al. (2021), “DNA damage response in vascular endothelial senescence: Implication for radiation-induced cardiovascular diseases”, *Journal of Radiation Research*, Vol. 62/4, Oxford University Press, Oxford, https://doi.org/10.1093/JRR/RRAB032.

Ramadan, R. et al. (2020), “Connexin43 Hemichannel Targeting With TAT-Gap19 Alleviates Radiation-Induced Endothelial Cell Damage”, *Frontiers in Pharmacology*, Vol. 11, Frontiers Media SA, Lausanne, https://doi.org/10.3389/fphar.2020.00212.

Ray, P. D., B. W. Huang and Y. Tsuji (2012), “Reactive oxygen species (ROS) homeostasis and redox regulation in cellular signaling”, *Cellular Signalling*, Vol. 24/5, Elsevier, Amsterdam, https://doi.org/10.1016/j.cellsig.2012.01.008.

Schiffrin, E. L. (2008), “Oxidative Stress, Nitric Oxide Synthase, and Superoxide Dismutase”, *Hypertension*, Vol. 51/1, Lippincott Williams & Wilkins, Philadelphia, https://doi.org/10.1161/HYPERTENSIONAHA.107.103226.

Shen, Y. et al. (2018), “Transplantation of bone marrow mesenchymal stem cells prevents radiation-induced artery injury by suppressing oxidative stress and inflammation”, *Oxidative Medicine and Cellular Longevity*, Vol. 2018, Hindawi, London, https://doi.org/10.1155/2018/5942916.

Slezak, J. et al. (2017), “Potential markers and metabolic processes involved in the mechanism of radiation-induced heart injury”, *Canadian Journal of Physiology and Pharmacology*, Vol. 95/10, Canadian Science Publishing, Ottawa, https://doi.org/10.1139/cjpp-2017-0121.

Soloviev, A. I. and I.V. Kizub (2019), “Mechanisms of vascular dysfunction evoked by ionizing radiation and possible targets for its pharmacological correction”, *Biochemical pharmacology*, Vol. 159, Elsevier, Amsterdam, https://doi.org/10.1016/j.bcp.2018.11.019.

Soucy, K. G. et al. (2011), “HZE 56Fe-Ion Irradiation Induces Endothelial Dysfunction in Rat Aorta: Role of Xanthine Oxidase”, *Radiation Research*, Vol. 176/4, Radiation Research Society, Bozeman, https://doi.org/10.1667/RR2598.1.

Soucy, K. G. et al. (2010), “Dietary inhibition of xanthine oxidase attenuates radiation-induced endothelial dysfunction in rat aorta”, *Journal of Applied Physiology*, Vol. 108/5, American Physiological Society, Rockville, https://doi.org/10.1152/japplphysiol.00946.2009.

Soucy, K. G. et al. (2007), “Single exposure gamma-irradiation amplifies xanthine oxidase activity and induces endothelial dysfunction in rat aorta”, *Radiation and Environmental Biophysics*, Vol. 46/2, Springer, New York, https://doi.org/10.1007/s00411-006-0090-z.

Sylvester, C. B. et al. (2018), “Radiation-Induced Cardiovascular Disease: Mechanisms and Importance of Linear Energy Transfer”, *Frontiers in Cardiovascular Medicine*, Vol. 5, Frontiers Media SA, Lausanne, https://doi.org/10.3389/fcvm.2018.00005.

Tapio, S. (2016), “Pathology and biology of radiation-induced cardiac disease”, *Journal of Radiation Research*, Vol. 57/5, Oxford University Press, Oxford, https://doi.org/10.1093/jrr/rrw064.

Ungvari, Z. et al. (2013), “Ionizing Radiation Promotes the Acquisition of a Senescence-Associated Secretory Phenotype and Impairs Angiogenic Capacity in Cerebromicrovascular Endothelial Cells: Role of Increased DNA Damage and Decreased DNA Repair Capacity in Microvascular Radiosensitivity”, *The Journals of Gerontology Series A: Biological Sciences and Medical Sciences*, Vol. 68/12, Oxford University Press, Oxford, https://doi.org/10.1093/gerona/glt057.

Venkatesulu, B. P. et al. (2018), “Radiation-Induced Endothelial Vascular Injury”, *JACC: Basic to Translational Science*, Vol. 3/4, Elsevier, Amsterdam, https://doi.org/10.1016/j.jacbts.2018.01.014.

Wang, Y., M. Boerma and D. Zhou (2016), “Ionizing Radiation-Induced Endothelial Cell Senescence and Cardiovascular Diseases”, *Radiation research*, Vol. 186/2, Radiation Research Society, Bozeman, https://doi.org/10.1667/RR14445.1.